

Development of Copper and Cobalt-Catalyzed Electrophilic C–H Amination Reactions

A Thesis Submitted to
Jadavpur University

For the Award of the Degree of
Doctor of Philosophy

In

Chemical Sciences

By

Hasina Mamataj Begam

(Index No: 156/18/Chem./26)

Under the Guidance of

Dr. Ranjan Jana



**Organic & Medicinal Chemistry Division
Indian Institute of Chemical Biology
(Council of Scientific & Industrial Research)
4, Raja S.C. Mullick Road,
Kolkata, West Bengal, India, PIN -700 032**

May, 2022



सी.एस.आई.आर-भारतीय रासायनिक जीवविज्ञान संस्थान

वैज्ञानिक तथा औद्योगिक अनुसंधान परिषद की एक इकाई
विज्ञान एवं प्रौद्योगिकी मंत्रालय के अधीन, एक स्वायत्त निकाय, भारत सरकार
4, राजा एस. सी. मल्लिक रोड, यादवपुर, कोलकाता - 700 032



CSIR - INDIAN INSTITUTE OF CHEMICAL BIOLOGY

A Unit of Council of Scientific & Industrial Research
An Autonomous Body, under Ministry of Science & Technology, Government of India
4, Raja S. C. Mullick Road, Jadavpur, Kolkata-700 032

From:

Ranjan Jana, M.Sc., Ph.D.

Principal Scientist

Organic and Medicinal Chemistry Division

CSIR-Indian Institute of Chemical Biology

4 Raja S. C. Mullick Rd, Kolkata – 700 032

Phone +91 (033) 24995819

Fax +91 (033) 24735197

Email rjana@iicb.res.in, janaegra@gmail.com

CERTIFICATE FROM THE SUPERVISOR

This is to certify that the thesis entitled “**Development of Copper and Cobalt-Catalyzed Electrophilic C–H Amination Reactions**” submitted by Miss Hasina Mamataj Begam who got her name registered on 30.08.2018 for the award of Ph. D. (Science) degree of Jadavpur University, is absolutely based upon her own work under my supervision and that neither this thesis nor any part of it has been submitted for either any degree / diploma or any other academic award anywhere before.

Jana 23/05/2022



DR. RANJAN JANA

Principal Scientist

Organic and Medicinal Chemistry Division

CSIR-Indian Institute of Chemical Biology

4, Raja, S. C. Mullick Road, Kolkata-32



Dedicated to my Mother

*“Winners are not those who never fail but those
who never quite.”*

-A.P.J.Abdul Kalam

ACKNOWLEDGEMENT

First of all, thanks to Almighty Allah (SWT) for giving me the opportunity to have little glimpses of the excellent world of science and also for giving me the strength and ability to understand, learn and complete my Ph.D. research. With the divine grace of Almighty Allah, I must say, it is the moment when I am going to submit my thesis for the fulfilment of my Ph.D. degree I have many people to thank with open arms who helped me to sustain through the years of ups and downs and probably words will fall short.

It is a genuine pleasure to express my deep sense of thanks and gratitude to my mentor, philosopher and guide Dr. Ranjan Jana, Principal Scientist, CSIR-Indian Institute of Chemical Biology, for giving me the opportunity to pursue Ph.D. under his guidance. Without his supervision, support and criticism it won't be possible for me to accomplish the research work described herein. His timely advice, meticulous scrutiny, scholarly advice and scientific approach have also helped me to a very great extent to accomplish this task. His dedication towards research, concern for every single research activity obviously made me motivated towards work. I am thankful to Dr. Enakshi Dinda for her caring attitude, encourage and support during my research period.

I am grateful to our present director Dr. Arun Bandyopadhyay and former director of IICB Prof. Samit Chattopadhyay for giving me an opportunity to work in Organic & Medicinal Chemistry Division, CSIR-IICB and providing all infrastructural supports.

I am thankful to my RAC members Prof. Swapan Kumar Bhattacharya, Head of the Chemistry Department, Jadavpur University and Dr. Samit Guha for their valuable suggestions to improve my research work.

I would like to acknowledge my research institute CSIR-Indian Institute of Chemical Biology for providing me the platform and infrastructure to work. I am also thankful to CSIR, New Delhi, for awarding me J.R.F. and S.R.F and providing corresponding fellowships throughout my doctoral studies.

I am indebted to the faculty members of our institute Dr. P. Jaisankar, Dr. C. Chowdhury, Dr. B. Banerji, Dr. I. Das, Dr. S. Dutta, Dr. A. Talukdar, Dr. R. Natarajan and Dr. I. B. Deb and also their corresponding group members for helping me in various aspects during my research work.

I am also thankful to all the non-teaching staffs of CSIR-IICB for their timely help during my research work at IICB. I am very much grateful to Dr. Tapas Sarkar, Dr. E. Padmanban, Shahfiaz Khan, Gautam Karmakar for recording NMR, Diptendu Bhattacharya, Sandip Chowdhury, Soumik Laha, and Santu Paul for mass analysis, Sandip Kundu for XRD. It would be really difficult to complete my thesis work without their spontaneous help and support.

I express my earnest respect and gratitude to every single teacher of my life who made the path for me to reach in this position today. My mother, the first teacher of my life shaped my mind at the early stage to dream bigger and work hard to fulfil it. The interest in Chemistry developed by the excellent teaching skill of my H.S. chemistry teacher Subrata Mukerjee. I also sincerely express my gratitude to my B.Sc. teachers Abul Hasan, Dr. Dilip Debnath, Deepak Kumar, Dr. Subhankar Choudhury, Dr. Suranjan Sikdar and Narendra Nath Ghosh. I am also highly obliged to my M.Sc. teachers of department of Chemistry, University of Gour Banga, Dr. Sougata Pal, Dr. Mohabul Alam Mondal, Dr. Tanmay Ghorai, Dr. Samit Guha, Dr. Subhamoy Chowdhury and Dr. Sadananda Mandal for their excellent teaching and motivation for doing research.

I am thankful to my lab seniors Dr. Ashok Behera, Dr. Suvankar Das, Dr. Krishnendu Bera, Dr. Bijaya Kumar Singh, Dr. Asik Hossian, Dr. Manash Kumar Manna, Dr. Samir Kumar Bhunia, Dr. Arghya Polley and Gurupada Bairy for their mentorship and support. Their criticism and guidance certainly made my path smooth. I am blessed with very helpful fellow lab mates and wonderful juniors. I record my sincere thanks to my fellow lab mates Pritha Das, Kartic Manna, Shantanu Nandi, Kasarla Varalaxmi and to my juniors Raj Kumar Avunuri, Sharyu Kesharwani, Rajarshee Choudhury, Arijit Nandi, Subhodeep Das, Shuvam Mondol, Kangkan Pradhan, Abdur Rahaman, Animesh Pal and Antara De for their pleasant company and coordination during my research period. They have all been a continuous source of help and enjoyment throughout these years.

I like to convey my deepest thankfulness to all of my family members. I express my utmost love and gratitude to my parents. I specially thank my mother for being such positive role model who never stopped trying to understand just what it was I was studying, gave inspiration to work harder and comforted continuously whenever I failed or things were not working in laboratory. Whatever I have achieved so far is the result of their love, support and sacrifice. I express my deep sense of thank to my dearest friend Israful Hoque, for his help

during my NET preparation, otherwise it couldn't be possible for me to come in the field of research. He also remained a constant source of motivation throughout this journey. I like to thank my brother and sisters for their sustained help and pleasant association in my entire academic and personal endeavors.

May, 2022

Jadavpur, Kolkata

Hasina Mamataj Begam

ABBREVIATIONS

| | |
|--|--|
| CDCl ₃ | Deuterated chloroform |
| DMF | <i>N, N'</i> -dimethylformamide |
| DMSO | Dimethylsulphoxide |
| DMSO-d ₆ | Deuterated Dimethyl sulfoxide |
| NMR | Nuclear Magnetic Resonance |
| FTIR | Fourier transform infrared |
| 1, 10-Phen | 1, 10-Phenanthroline |
| DMAP | 4-Dimethylaminopyridine |
| MeCN | Acetonitrile |
| THF | Tetrahydrofuran |
| HFIP | 1,1,1,3,3,3-Hexafluoro-2-propanol |
| TFE | 2,2,2-Trifluoroethanol |
| DCM | Dichloromethane |
| K ₂ S ₂ O ₈ | Potassium persulfate |
| TBHP | <i>tert</i> -Butyl hydroperoxide |
| Bz ₂ O ₂ | Benzoyl peroxide |
| AcOH | Acetic Acid |
| TEMPO | (2, 2, 6, 6-Tetramethylpiperidin-1-yl)oxyl |

TABLE OF CONTENTS

| Contents | Pages |
|--|-------|
| Chapter I - Transition metal catalysed C-H amination or C-H amination/ cyclisation cascade using different electrophilic aminating reagents | |
| I.1 Introduction | 1-2 |
| I.2. Transition-metal catalysed C-N cross-coupling reactions | 2-3 |
| I.3. C-N cross-coupling vs. C-H amination reactions | 4 |
| I.4. General mechanistic approaches for C-H amination reactions | 4 |
| I.5. Introduction to C-H amination using electrophilic aminating agents with umpolung of reactive N-centres | 5-6 |
| I.6. Commonly used electrophilic aminating agents | 6 |
| I.7. C-H amination using various electrophilic aminating reagents | 6 |
| I.7a. N-Chloramines/N-chlorocarbamates | 6-9 |
| I.7b. Hydroxylamine based electrophilic aminating reagents | 9 |
| I.7b.1. <i>O</i> -protected hydroxylamine-based carbamates | 9-14 |
| I.7b.2. <i>O</i> -protected 0°/1° amine-based hydroxylamines | 14-16 |
| I.7b.3. <i>O</i> -protected 2° amine-based hydroxylamines | 16-21 |
| I.7c. Organic azides | 21 |
| I.7d. N-Fluorobenzenesulfonimide (NFSI) | 22-23 |
| I.7e. Nitroso-compounds | 23-25 |
| I.7f. Oximes/oxime esters | 26-27 |
| I.7g. Anthranils (2,1-benzisooxazoles) | 27-31 |
| I.7h. Dioxazolones | 32 |
| I.8. C-H amination/cyclisation cascade using electrophilic amines for the synthesis of N-heterocycles | 33 |
| I.8a. C-H amination/cyclisation <i>via</i> Catellani-type reaction using <i>O</i> -protected hydroxylamines | 33-36 |

| | |
|---|---------|
| I.8b. C-H amination/cyclisation cascade using other electrophilic aminating agents | 36-43 |
| I.9. Conclusion | 44 |
| I.10. References | 44-49 |
| Chapter II – Copper-catalyzed electrophilic <i>ortho</i> C(sp²)-H amination of picolinamide protected aryl amines for the synthesis of 2-amino anilides with dramatic reactivity found in bicyclic system | 50 |
| II.1. Introduction | 51-52 |
| II. 2. Review | 52-59 |
| II. 3. Present work | 59-60 |
| II. 4. Results and discussion | 60-64 |
| II. 5. Reaction in aqueous media | 64-66 |
| II. 6. Investigation of the reaction mechanism | 67-69 |
| II.7. Deprotection of DG and product derivatisation | 69-70 |
| II.8. Conclusion | 70 |
| II.9. Experimental Section | 70-74 |
| II.10. Spectral data | 74-96 |
| II.11. ¹ H and ¹³ C NMR spectra | 96-114 |
| II.12. References | 115-116 |
| Chapter III – Directing group switch in copper-catalyzed electrophilic C-H amination/migratory annulation cascade: divergent access to benzimidazolone/benzimidazole | 117 |
| III.1. Introduction | 118-121 |
| III. 2. Review | 121-126 |
| III. 3. Present work | 126-127 |
| III. 4. Results and discussion | 127-137 |
| III. 5. Metal-free condition for benzimidazolone | 137-138 |
| III. 6. Investigation of the reaction mechanism | 138-143 |

| | |
|---|---------|
| III. 7. Deprotection of <i>N</i> -heteroaryl of the benzimidazolone product | 143 |
| III.8. Conclusion | 143-144 |
| III.9. Experimental section | 144-147 |
| III.10. X-ray crystallography data | 147-152 |
| III.11. Spectral data | 152-189 |
| III.12. ¹ H and ¹³ C NMR spectra | 190-203 |
| III.13. References | 204-207 |
| Chapter IV – Cobalt Catalysed Electrophilic C-H amination/Cyclisation cascade with <i>O</i>-benzyloxy primary amines using paraformaldehyde as C1 synthon: Direct access to naphthimidazoles using picolinamide as traceless directing group | 208 |
| IV.1. Introduction | 209-210 |
| IV. 2. Review | 210-216 |
| IV. 3. Present work | 216-217 |
| IV. 4. Results and discussion | 217-223 |
| IV. 5. Reaction mechanism | 223-224 |
| IV. 6. Product derivatisation | 224-225 |
| IV. 7. Conclusion | 225 |
| IV. 8. Experimental section | 225-227 |
| IV. 9. X-ray crystallography data | 227-230 |
| IV.10. Spectral data | 230-246 |
| IV.11. ¹ H and ¹³ C spectra | 246-260 |
| IV.12. References | 261-264 |
| List of Publications | 265 |
| List of attended conferences | 266 |

Chapter I

Transition metal catalysed C-H amination or C-H amination/cyclisation cascade using different electrophilic aminating reagents

I.1. Introduction

Nitrogen containing molecules are ubiquitously found in pharmaceutically active drugs, natural products, and functionalized materials and even in the basic unit of life i.e. amino acids.¹ Amongst all the nitrogen containing important compounds, *N*-heterocycles are much important in life science because they are abundant in nature, which are found as subunits in a variety of natural products such as vitamins, hormones and antibiotics.² The structural significance of nitrogen-based heterocycles in drug design and pharmaceutical engineering is revealed by the FDA database which shows that almost 59% small-molecule drugs comprise a nitrogen heterocycle.³ Besides *N*-heterocycles, acyclic amines having either C(sp²)-N or C(sp³)-N bonds are also privileged structural motifs which are seen in many biologically and pharmaceutically important compounds.⁴ For example, Plavix (an amino ester), is an antiplatelet drug which is used for inhibiting blood clots and in 2010, it was the second most prescribed drug.⁵ One of the examples of aryl amine containing drug is Abilify. This is an antipsychotic drug used to treat schizophrenia and bipolar disorder. Some *N*-heterocycle containing drugs are shown below (**Figure 1**). Therefore, an intense research has been dedicated for the C-N bond construction.

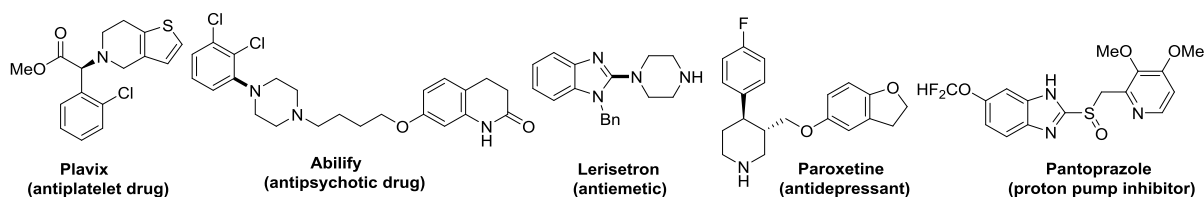
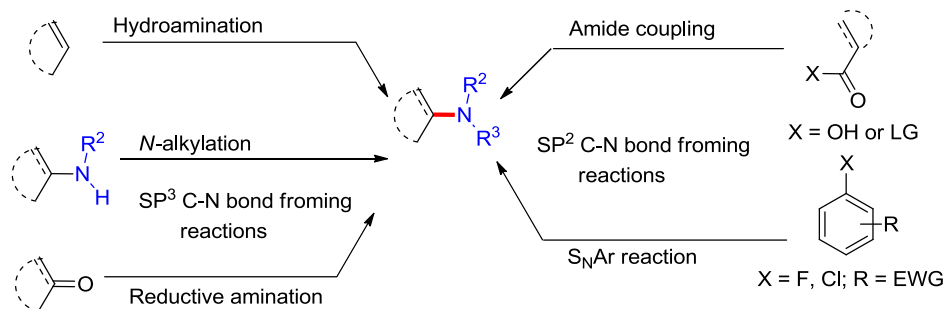


Figure 1. Some amino group/*N*-heterocycle containing FDA approved drugs

However, the conventional synthesis of sp³ C-N bond is accomplished via simple nucleophilic addition, reductive amination, hydroamination etc. Whereas, sp² C-N bond formation can be achieved by amide coupling, alkylation and mainly by S_NAr type reaction (**Scheme 1**). These conventional methods mainly rely on the inherent reactivity of functional groups present in the substrate and this is why they are incompatible towards late-stage functionalization and these reactions requires harsh reaction conditions. The development of transition metal catalysts has opened up new ways to form covalent bonds, allowing for the derivatization of raw chemicals with few functional groups into synthetically diverse compounds.⁶



Scheme 1. Conventional methods for the synthesis of C-N bonds

I.2. Transition-metal catalysed C-N cross-coupling reactions

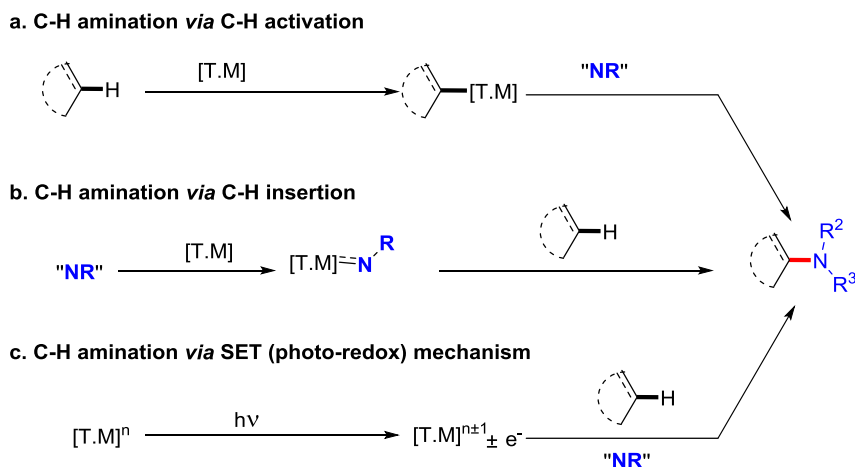
Transition metal catalysed/mediated cross-coupling reactions offered good flexibility and applicability to form C–N bonds that S_NAr reactions fails and also in a direct, cost-effective way.⁷ Chronological development of transition metal-catalysed C–N cross-coupling is depicted below (**Scheme 2**). In this chronology first comes Ullmann–Goldberg reaction (using stoichiometric copper) then Buchwald–Hartwig coupling using catalytic palladium along with various sophisticated phosphine ligands.⁸ Subsequently, this Buchwald–Hartwig coupling has been accomplished using inexpensive stoichiometric or catalytic copper along with various ligands. Alternatively, a mechanistically distinct Chan–Lam coupling with stoichiometric copper has also been developed.⁹ In lieu of the oxidative addition of low valent copper to the organohalides, the reaction starts with transmetallation with copper(II) salts. Further, catalytic version of this Chan-Lam coupling has been developed which occurs under mild conditions and find many medicinal chemistry applications.¹⁰ C-N cross coupling reactions with other metals such as Fe, Co and Ni have also been developed.¹¹ Recently, Photoredox-mediated C-N coupling reactions are now emerging.¹² In recent years, significant works on Ullmann–Goldberg reaction with catalytic copper (upto only 1 mol % loading) have been achieved *via* modified mechanisms.¹³ Modifications are made by using oxygen or nitrogen-based ligands for examples, diamines, aminoalcohols, diketones and diols. Following the Buchwald-Hartwig's palladium-catalyzed C–N bond formation from the corresponding aryl halides, an impressive array of transition-metal catalysed amination reactions has been

I.3. C-N cross-coupling vs. C-H amination reactions

Despite of significant importance of C-N cross-coupling reactions, still they suffer from some limitations such as the requirement of pre-functionalised substrates and generation of stoichiometric by-products. On the other hand, conversion of a C-H bond into a C-N bond is a straightforward method which has been appeared recently. It has unique ability to convert renewable feedstocks to pharmacophores omitting the production of stoichiometric by-products in a highly atom-efficient manner.

I.4. General mechanistic approaches for C-H amination reactions

The Chang group represented the C-H amination reactions in a review where they divided the mechanism of C-H amination reaction reported until 2016, into three categories.¹⁶ C-H amination may undergo *via* either of the three strategies C-H activation, C-H insertion or SET mechanism. According to 1st strategy transition metal activates C-H bond generating an organometallic intermediate with a metal-carbon bond. The corresponding metallacyclic complexes reacts with the nitrogen source available affording the amination product (**Scheme 3a**). In the 2nd strategy metal first forms metal-nitrenoid species which then interacts with a

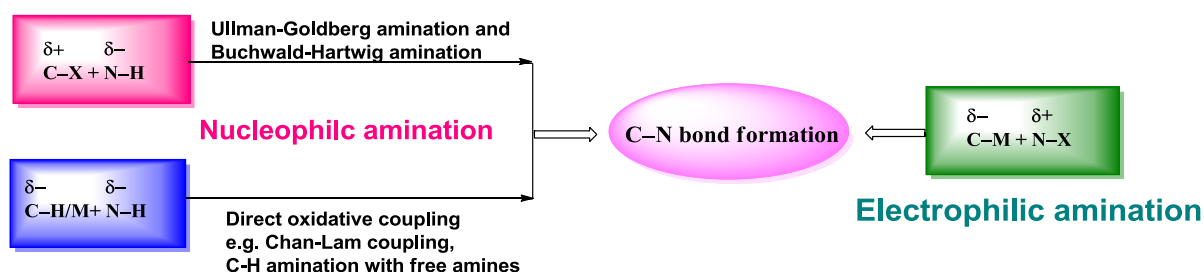


Scheme 3. Mechanistic approaches for C-H amination reactions

substrate either through concerted or a stepwise mechanism resulting the C-N bond (**Scheme 3b**). Benzylic, allylic, or tertiary C-H bonds are prone to undergo C-H amination *via* this mechanism. The third strategy works under photo-redox catalysis where an organoradical is generated *via* SET process that combines with other coupling partner affording the amination product (**Scheme 3c**).

I.5. Introduction to C–H amination using electrophilic aminating agents with umpolung of reactive *N*-centres

The carbon and nitrogen reactive centres in cases of Ullman-Goldberg or Buchwald-Hartwig amination are electrophilic and nucleophilic in nature respectively as shown below (**Scheme 4**) whereas in oxidative Chan-Lam coupling, carbon and nitrogen reacting centres are both nucleophilic in nature. In all of these cases the amine source is nucleophilic in nature. Despite the usefulness of the Buchwald-Hartwig and oxidative C–H/N–H C–N coupling type nucleophilic aminations, they have some limitations, such as harsh reaction conditions including high temperatures, strong oxidants, use of acidic or basic additives and higher catalyst loading probably due to catalyst inhibition by the free amines. And also most of the transition metal mediated aminations with nucleophilic amines are restricted to the synthesis of aryl amines. But there is another approach for transition metal-catalysed C–N bond formation where the amine nitrogen atom is electrophilic in nature i.e. electrophilic amination strategy with umpolung concept that is the reversal of polarity of the reacting *N*-atom of amines. Most of these amine sources the *N*-atom is attached to electronegative atoms such as O, F or Cl [In case of organic azides (N–N₂) although having N–N bond it is considered as electrophilic because metal can undergo oxidation by the cleavage of this N–N₂ bond]. This approach addresses many problems associated with nucleophilic amination strategies and has several advantages such as broad scope, milder conditions, lower catalysts loading and notably the ability to functionalize typically unreactive bonds. Another important advantage is that due to the weak N-heteroatom bond these reagents act as mild oxidants and most of the C–H amination reactions take place in overall redox-neutral conditions without using external strong metal oxidants.¹⁷ Due to these reasons significant efforts have been dedicated towards the development of this umpolung strategies with reversal of polarity of the amine nitrogen source

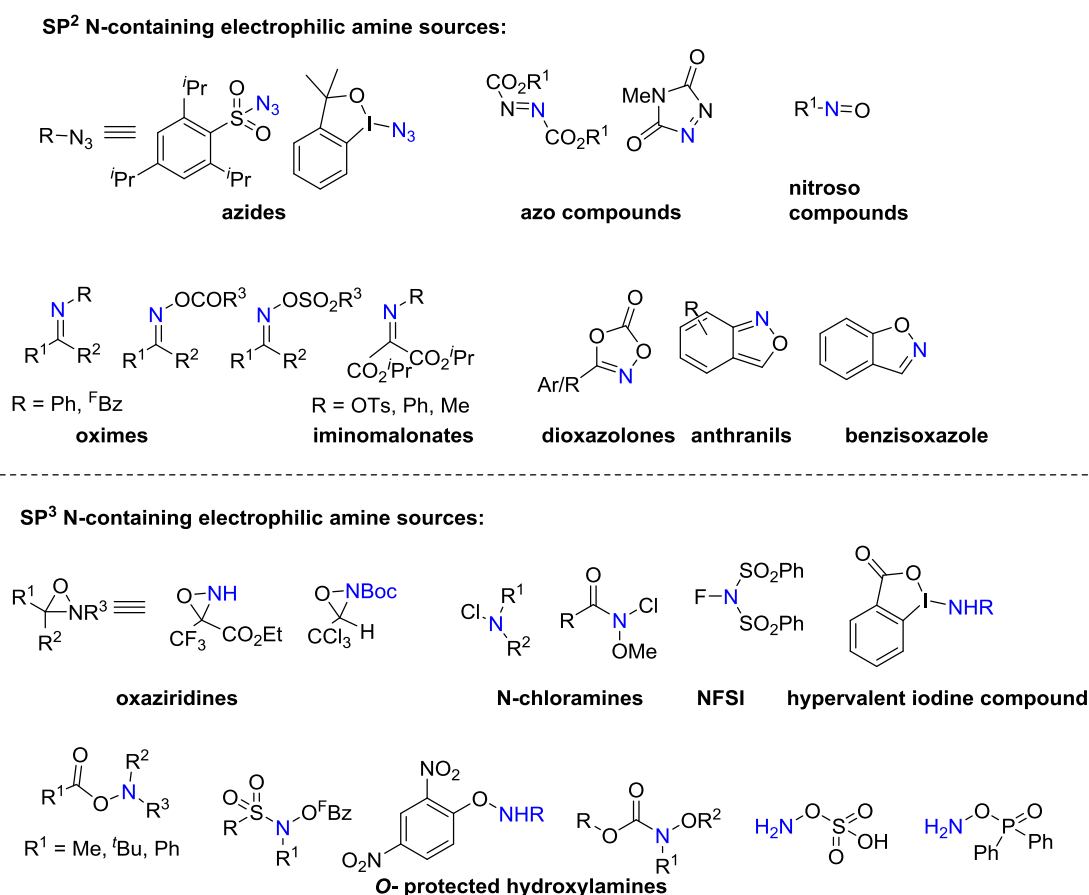


Scheme 4. Comparison of C/N reacting centres of nucleophilic vs. electrophilic amination reactions

(equivalents to the R_2N^+ synthon).¹⁸ Electrophilic aminations offer efficient methods for the synthesis of $C(sp^2)-N$ bonds as well as $C(sp^3)-N$ bonds.

I.6. Commonly used electrophilic aminating agents

Several $[NR_2]^+$ synthons have been developed for the progression of electrophilic amination methods.¹⁹ These reagents generally comprise an electron-withdrawing group bonded to the nitrogen which induces a partial positive charge on the nitrogen atom. Electrophilic aminating reagents can be divided into two groups sp^2 and sp^3 nitrogen-containing compounds which are shown below (**Scheme 5**).



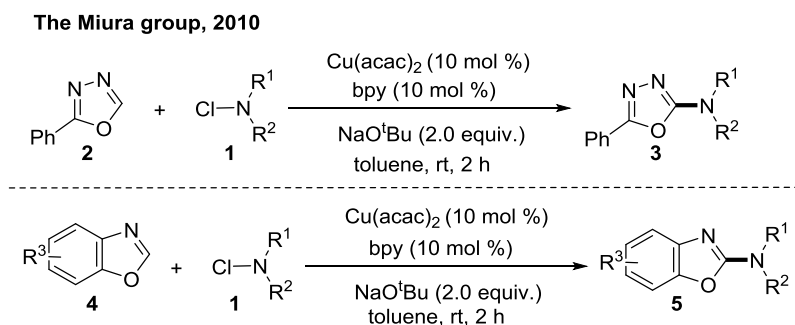
Scheme 5. Commonly used electrophilic aminating agents

Installation of primary, secondary or tertiary amine groups can be performed using the above electrophilic aminating reagents as per one's requirement.

I.7. C-H amination using various electrophilic aminating reagents

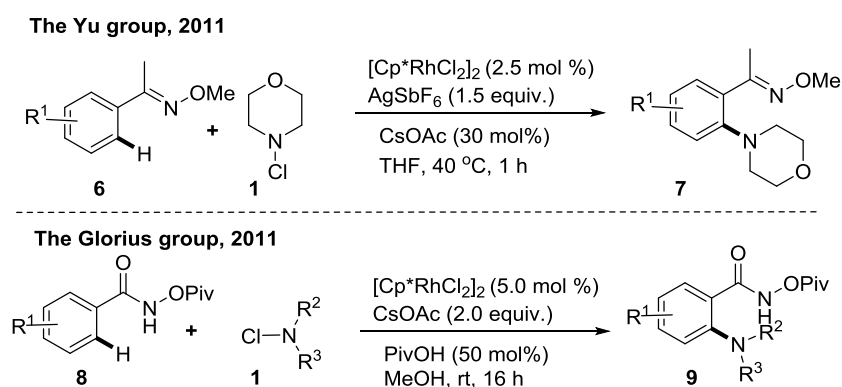
I.7a. N-Chloramines/N-chlorocarbamates

The Miura group first introduced chloramines for heteroaromatic C-H amination in 2010.²⁰ Chloramines are a readily available, efficient electrophilic sp^3 nitrogen source. This copper-catalysed C-H amination of azoles took place at room temperature affording variety of heteroarylamines which are quite important in biology and medicinal chemistry (**Scheme 6**).

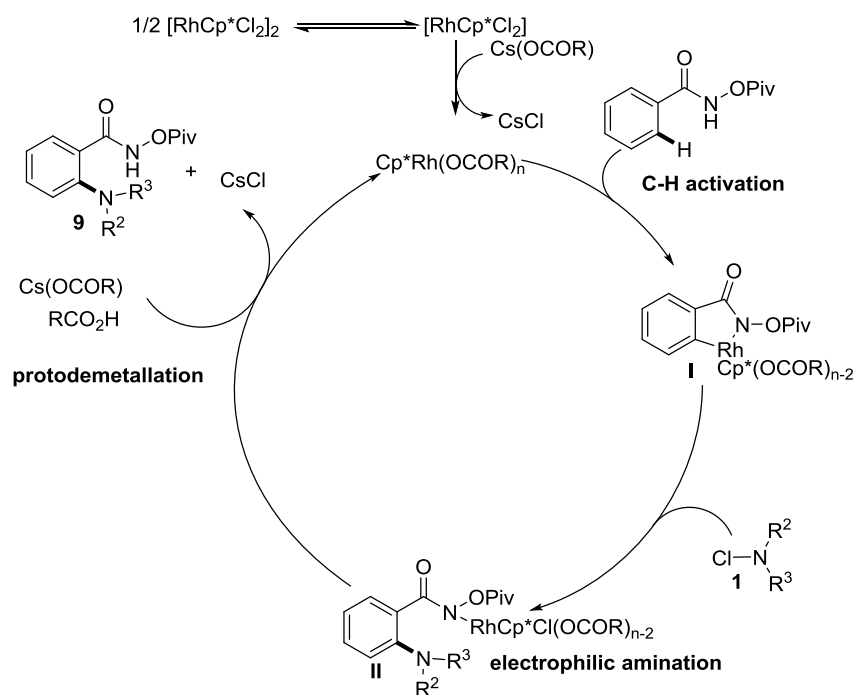


Scheme 6. Cu-catalysed C-H amination of oxazoles with chloramines

Then in 2011 the Yu and Glorius groups independently reported directed *ortho* C-H amination with chloramines under Rh-catalysis.²¹ They used ketoximes *and* *N*-pivaloyloxy benzamides as directing group respectively (**Scheme 7**). Both the conditions are very mild and showed very good functional group tolerance and broad scope. Reaction mechanism proposed by both the groups are almost similar, first the Rh-catalyst activates *ortho* C-H bond forming a rhodacycle **I**, then electrophilic amination with the aminating agent **1** followed by protodemetalation gives the product with regeneration of the catalyst (**Scheme 8**). In 2013 the Yu group developed *ortho* C-H amination of ketoximes with primary *N*-chloroalkylamines under almost similar conditions.²²

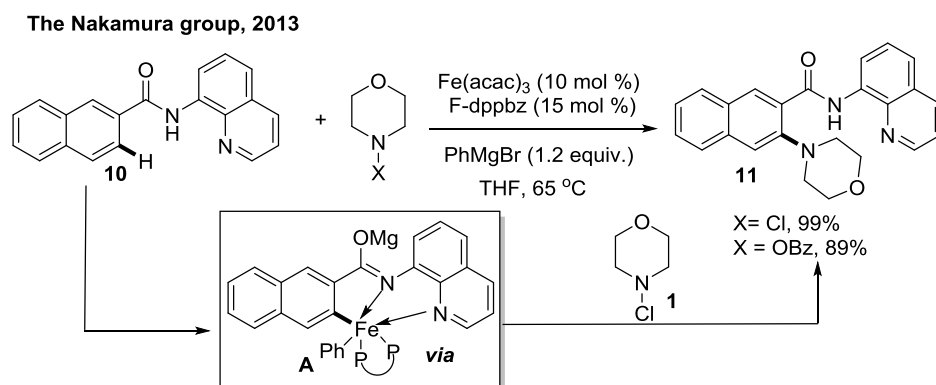


Scheme 7. Rh-catalysed C-H amination with chloramines



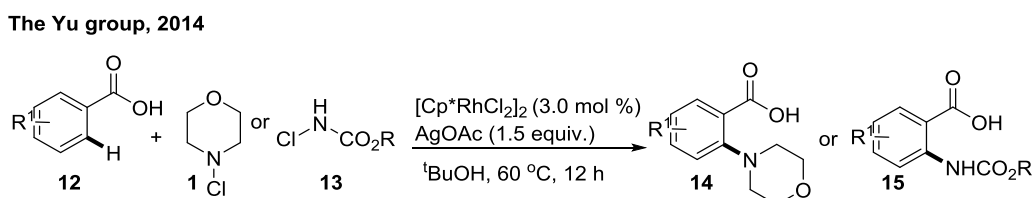
Scheme 8. Proposed mechanism of Rh-catalysed C-H amination of *N*-pivaloyloxy benzamides with chloramines

In 2013, the Nakamura group disclosed inexpensive and earth abundant Fe-catalysed directed C-H amination with *N*-chloramines.²³ Several screenings of different directing groups showed that amide of 8-aminoquinoline was acted as best DG. Comparative study of product yield (99% vs. 89% respectively) using *N*-chloramine and *O*-benzoyloxyamine suggested that *N*-chloramine was most suitable here as amine source. Though cheaper Fe-catalyst was used, stoichiometric amount of Grignard reagents are needed as reducing agent for catalyst regeneration. Stoichiometric reaction of substrate and iron-catalyst in absence of aminating agent followed by quenching with D₂O produced *ortho* deuterium incorporated product which suggests that organoiron species intermediate **A** was formed via C-H activation (**Scheme 9**).



Scheme 9. Fe-catalysed C-H amination of benzamides with chloramines

The Yu group in 2014 unveiled a carboxyl directed Rh-catalysed *ortho* C-H amidation or amination of benzoic acids using *N*-chlorocarbamates or *N*-chloromorpholines respectively.²⁴ This methodology afforded anthranilic acid derivatives in upto 85% yield with very good functional group tolerance. This methodology is more step economic which omits the requirement of extra steps for incorporation and removal of directing groups (**Scheme 10**).



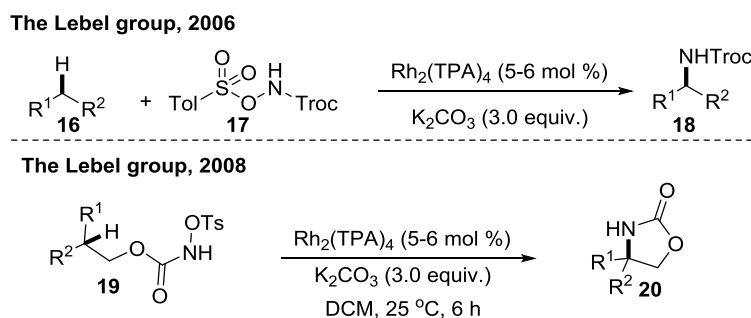
Scheme 10. Rh-catalysed C-H amination of benzoic acids with chloramines

I.7b. Hydroxylamine based electrophilic aminating reagents

Hydroxylamine based aminating agents in which OH is replaced with good leaving groups serve as very good electrophilic aminating agents delivering the amino group. Use of these reagents attracted attention because of their remarkable and versatile synthetic potential to provide different synthetic transformations *via* efficient electrophilic nitrene/amine transfer. These reagents can be synthesized very easily from commercially available low-cost starting materials. Because of the labile nature of the N–O bond of various *O*-protected hydroxylamines are mostly used for the electrophilic amination with different nucleophilic reagents *via* transition metal catalysis. There are now several excellent reviews covering the multitude of transformations that has been achieved using these electrophilic aminating reagents.²⁵ We will discuss on transition metal catalysed C-H amination reactions those are performed by these reagents.

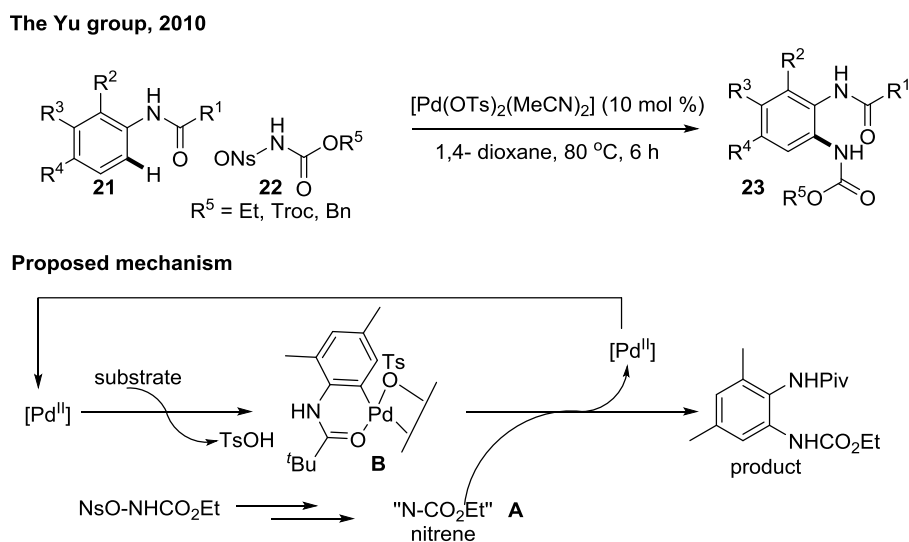
I.7b.1. *O*-protected hydroxylamine-based carbamates

The Lebel group first reported in 2006 an intermolecular (sp^3)C-H amination and in 2008 an intramolecular (sp^3)C-H amination using 2,2,2-trichloroethyl-*N*-tosyloxycarbamate as the electrophilic amine source under rhodium catalysis.²⁶ The first reaction proceeded in good to excellent yields affording a variety of Troc-protected amines (**Scheme 11**). Using chiral rhodium catalysts, they were also able to get an enantioselective version of this method. The starting material was very stable and easy to prepare and handle and also the reaction conditions were very mild. Various oxazolidinones were prepared in good yields through intramolecular C-H amination.²⁷



Scheme 11. Inter- and intramolecular (sp^3)C-H amination with trichloroethyl-N-tosylloxycarbamates

In 2010, the Yu group disclosed a Pd-catalyzed method for intermolecular C-H amidation of anilides using *N*-nosyloxycarbamate (**Scheme 12**).²⁸ The methodology showed high functional group tolerance, regioselectivity, and scope under relatively mild conditions. Based on their control experiments they proposed that the *N*-nosyloxycarbamate forms nitrene **A**, which then undergoes formal nitrene insertion to the cyclopalladated complex **B** via a metal-nitrene pathway. They have proposed another alternative pathway in which the C-N bond formation may proceed through the formation of a Pd(IV) or a dimeric Pd(III) complex and from which reductive elimination affords the product amide with catalyst re-generation.

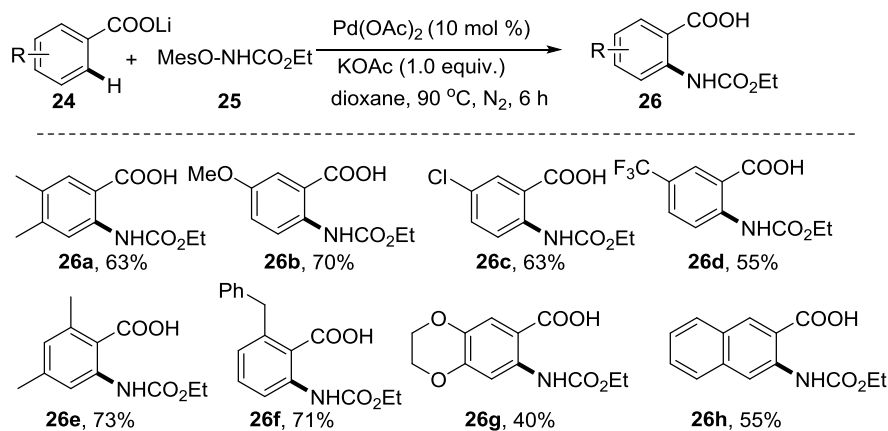


Scheme 12. *Ortho* (sp^2)C-H amidation of anilides with *N*-nosyloxycarbamates

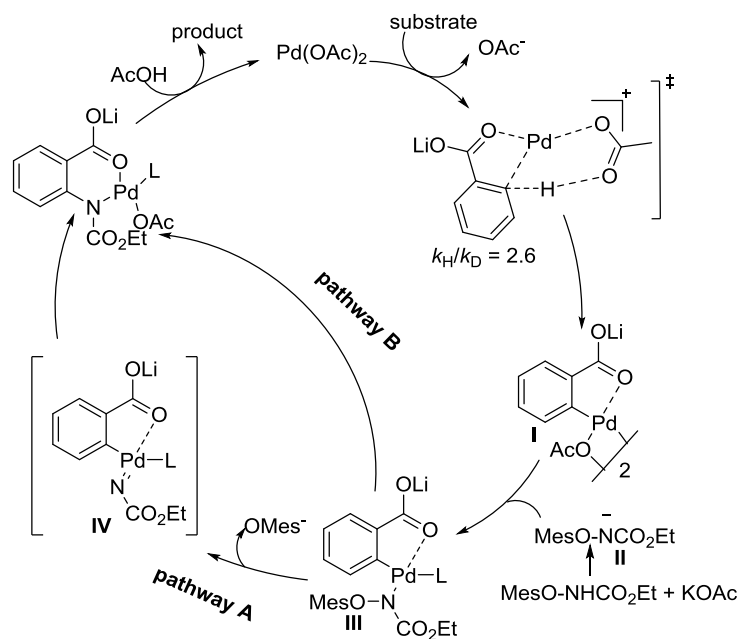
The same group in 2012 reported Pd-catalyzed direct *ortho* C-H amidation of benzoic acid derivatives (**Scheme 13**).²⁹ This direct amidation offered an expedient route to the synthesis of anthranilic acid derivatives, which serve as vital precursors to synthesise many medicinally important heterocycles. This protocol exhibited excellent regio-selectivity and

functional group tolerance. The high $k_H/k_D = 2.6$ value indicated that the formation of cyclopalladation complex may be the rate-limiting step in this amidation method.

The Yu group, 2012



Scheme 13. Carboxylate directed *ortho* (sp^2)C-H amination with *N*-mesityloxycarbamates

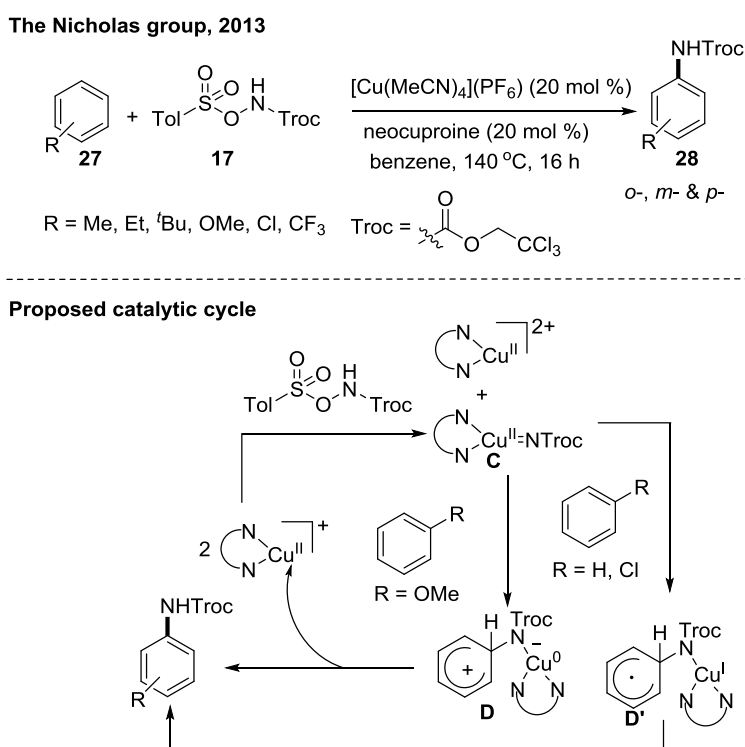


Scheme 14. Proposed catalytic cycle

They postulated that after cyclopalladation the amine source undergoes reversible deprotonation with KOAc affording the *N*-mesitylsulfonyloxycarbamate anion **II** (**Scheme 14**). The palladacyclic complex **I** then reacts with this anion to form a putative Pd-nitrene species **IV** (**pathway A**). Then C-N bond is formed through a migratory insertion followed by protonation. They also proposed an alternative pathway *via* concerted migration of aryl with the removal of the sulfonate group (**pathway B**).

The Emmert group in 2013 described a Pd-catalysed chemoselective synthesis of aniline derivatives *via* C-H amination of benzene in non-directed fashion, using hydroxylamine derivatives as electrophilic aminating agent.³⁰ They also systematically developed pyridine type ligands for this non-directed C-H amination methodology.

The Nicholas group in 2013 disclosed a C-H amidation protocol of unactivated arenes using *N*-tosyloxyltrichloroethylcarbamates as electrophilic amine source.³¹ Benzenes were selectively converted to aromatic amines (**Scheme 15**).

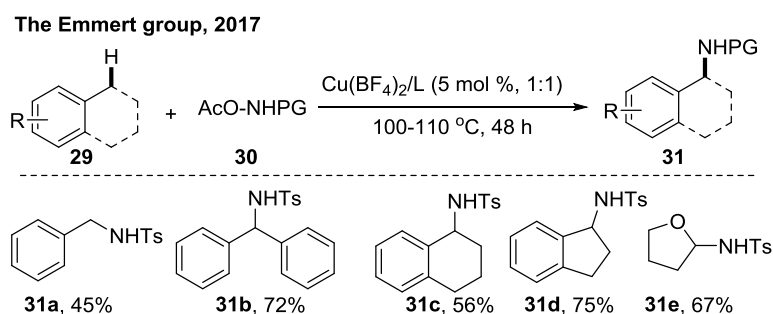


Scheme 15. Copper catalysed non-directed (sp^2)C-H amination of arenes with trichloroethyl-*N*-tosyloxycarbamates

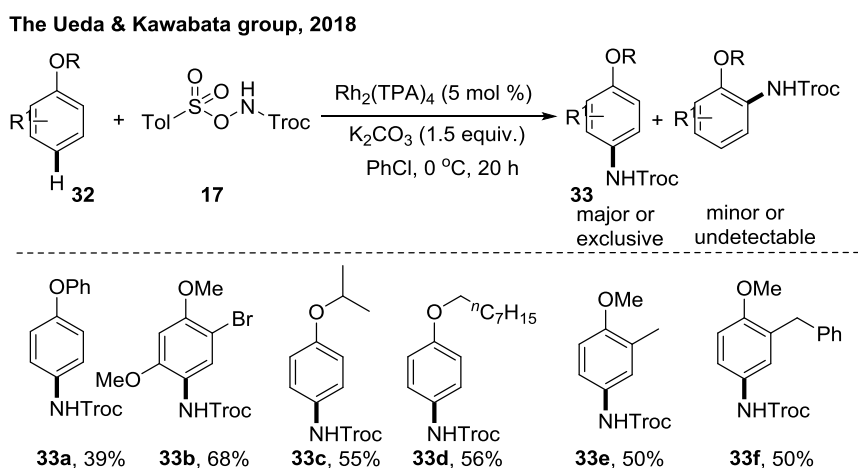
However, substituted arenes afforded mixture of regioisomeric products. Mechanistically, a Cu(II)-imido species **C** is formed *via* OA followed by redox disproportionation. Then this electrophilic radicaloid can react with the arene in two-way, either by electrophilic (two electron) attack to afford adduct **D** or by radical attack to generate **D'**, depending on the electronic nature of the arene and finally re-aromatization with (phen)Cu⁺ elimination gives the product.

In 2017 the Emmert group reported non-directed copper catalysed (sp^3)C-H amination using RSO₂NH-OAc, another hydroxylamine based electrophilic amine reagent.³² Various arene substrates containing weak, benzylic C-H bonds and also THF successfully underwent

the reaction under their optimized conditions (**Scheme 16**). They proposed based on their mechanistic studies that out of two possible pathways the C-H amination took place *via* a radical pathway.



Scheme 16. Copper catalyzed benzylic (sp^3)C-H amination with acyloxycarbamates

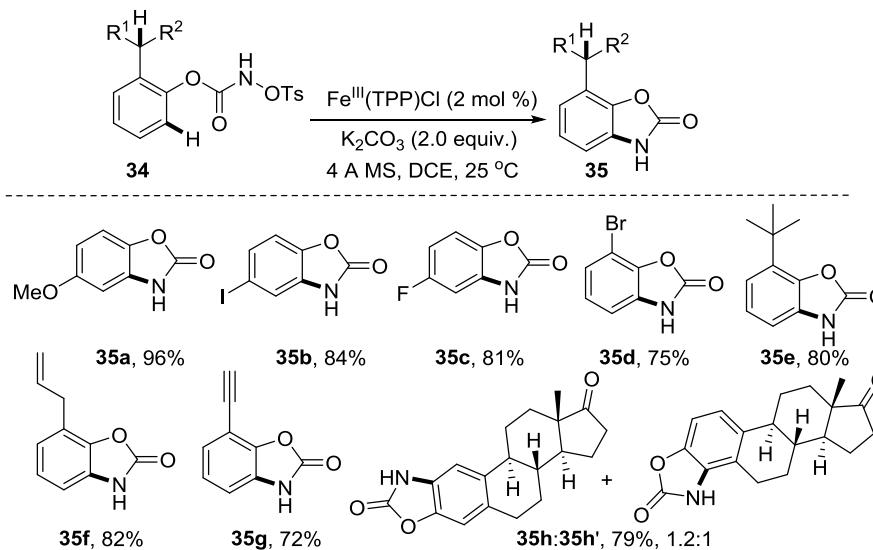


Scheme 17. Rh-catalyzed non-directed (sp^2)C-H amination of arenes with trichloroethyl-N-tosyloxycarbamates

The Ueda and Kawabata group in 2018 unveiled an intermolecular non-directed aromatic C-H amination endorsed by neutral rhodium nitrenoids (**Scheme 17**).³³ The reactions proceeded in various oxygen-substituted arenes in a chemo- and regioselective fashion. The C (sp^2)-H amination took place regioselectively at the *para* position of the ethereal groups in the presence of benzylic (sp^3)C-H bonds and or (sp^3)C-H bonds a to ethereal oxygen groups.

In 2018, the Singh group first time reported iron-porphyrine catalyzed intramolecular (sp^2)C-H amination through intramolecular C-H amination of *N*-tosyloxyarylcarbamate substrates for the synthesis of privileged scaffold benzoxazolones (**Scheme 18**).³⁴ Various functional groups were well tolerated under this conditions.

The Singh group, 2018



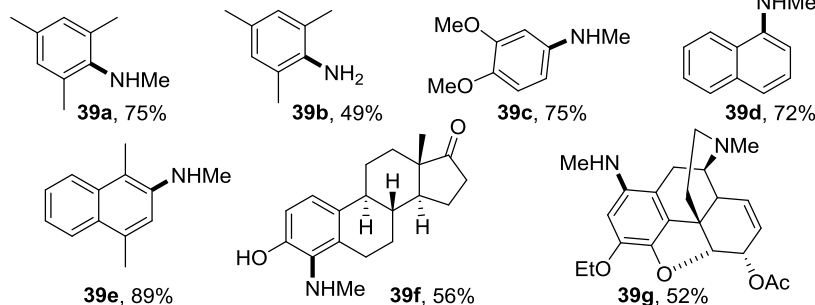
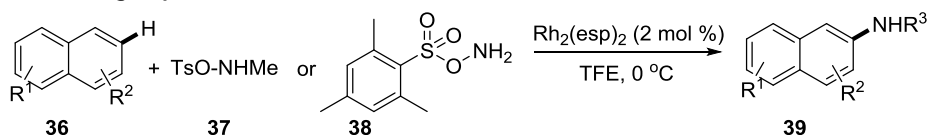
Scheme 18. Fe-catalysed intramolecular directed (sp^2)C-H amination

Terminal alkene and alkyne groups which generally don't survive under strong oxidising conditions were also remained unreacted. Low catalyst loading, use of earth-abundant metal catalyst along with a water-soluble side product formation made this method very useful.

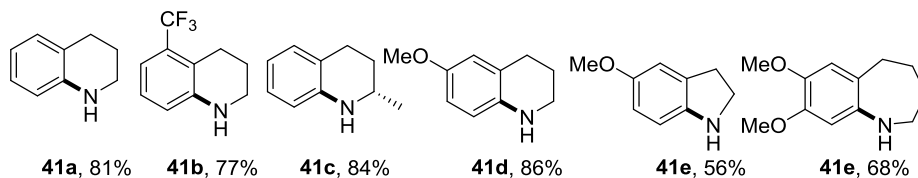
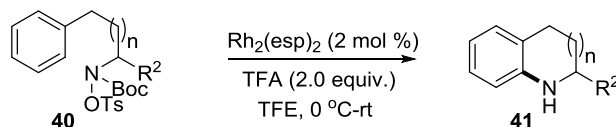
I.7b.2. *O*-protected $0^\circ/1^\circ$ amine-based hydroxylamines

The Falck group in 2016 reported an efficient method for direct C–H amination of variety of aromatic hydrocarbons under Rh-catalysis.³⁵ *N*-methyl-*O*-tosylhydroxylamine (TsONHMe) was used as the amine source in presence of $\text{Rh}_2(\text{esp})_2$ (DuBois catalyst) (Scheme 19). The weak N–O bond of the amine reagents acted as an internal oxidant omitting the requirement of external oxidant. Aryl sulfonic acid generated under the reaction conditions produced help to generate the aryl-amines in protected form so that the chance of catalyst inactivation was minimised. This methodology showed an extensive functional group tolerance such as bromo, hydroxyl, ether, silyl, carbonyl groups and many potentially sensitive groups including benzylic, tertiary and α -keto hydrogens. Epoxides and acetals were not tolerated under these reaction conditions. This versatile methodology offered a broad substrate scope with various electron-rich arenes. Late-stage C-H amination of steroids and phenanthrene has also been achieved using this protocol very efficiently. The methodology was also applicable to the intramolecular C-H amination reaction for making several azacycles in moderate to good yields.

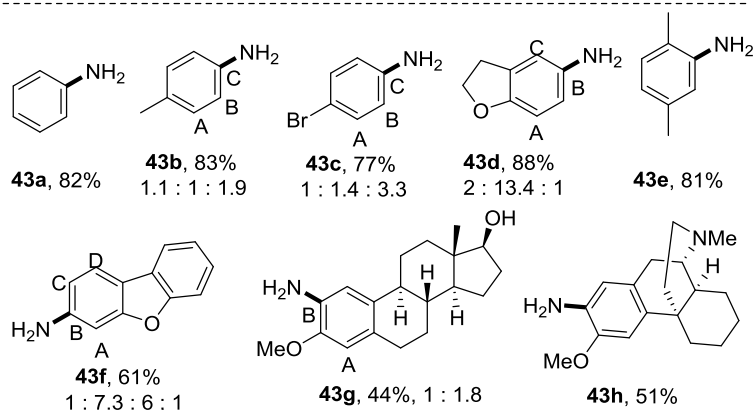
The Falck group, 2016



intramolecular C-H amination

Scheme 19. Rh-catalysed non-directed inter- and intramolecular (sp^2)C-H amination

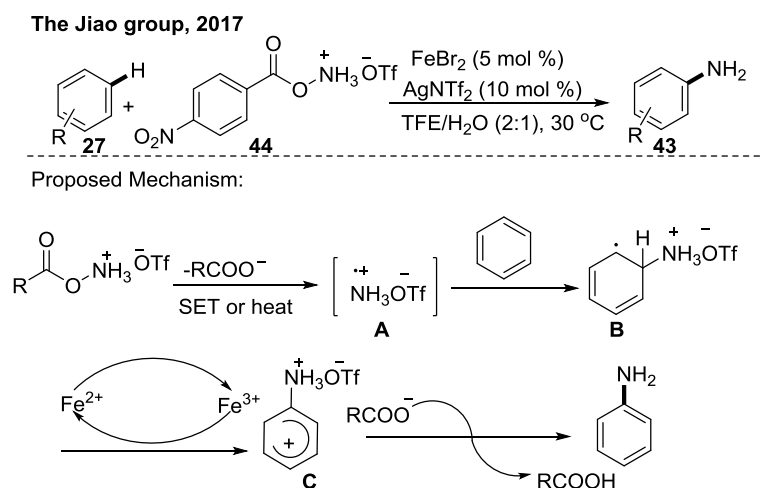
The Morandi group, 2016

Scheme 20. Fe-catalysed non-directed (sp^2)C-H amination affording anilines

The Morandi group in 2016 revealed an improved protocol for direct C–H amination of various arenes with very cheap iron catalyst, FeSO_4 (Scheme 20).³⁶ They synthesized primary anilines from mono-, di- and trisubstituted benzenes with a very stable amine source, MsONH_3OTf under mild reaction conditions. The protonated aminating agent not only

increased the electrophilicity of the aminium radical species formed under the conditions but also helpful in preventing over amination. Variety of functional groups hydroxy, halo, benzyl and amino and also various heteroarenes also underwent amination with high yields. This methodology was also applied for late stage amination of some bio-active compounds. Although the amination took place under very cost-effective way but regioselectivity issue in mono-substituted arenes affording regioisomeric mixtures slightly limits the methodology.

In 2017, the Jiao group disclosed similar methodology for C-H amination of arenes in non-directed fashion with Fe-catalyst (**Scheme 21**).³⁷ They synthesized many new *O*-substituted hydroxylamine reagents as electrophilic amine source and out of them they achieved the desired product using two equivalents of *O*-(*p*-nitrobenzoyl) hydroxylamine. Amination took place efficiently in many heterocyclic arenes such as indole, pyridine and thiophene. This methodology showed good functional group tolerance and was used for late-stage aminations. Based on their control experiment and preliminary EPR spectra they proposed that the reaction proceeds *via* a radical mechanism. Initially an *N*-centred radical cation **A** was formed by a SET from Fe²⁺ followed by the N–O bond cleavage. This radical then reacts with arenes to form the radical intermediate **B**. This upon oxidation by Fe³⁺ generates the cationic intermediate **C**. Finally, the deprotonation of the benzoate group affords the product.

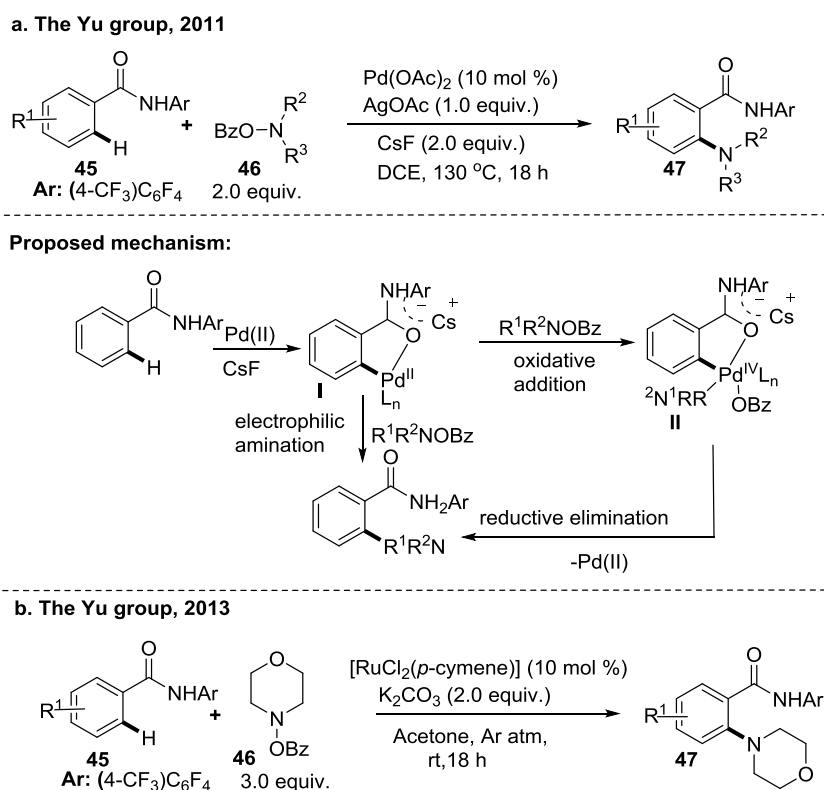


Scheme 21. Fe-catalysed non-directed (sp^2)C-H amination with *O*-(*p*-nitrobenzoyl) hydroxylamine

I.7b.3. *O*-protected 2^o amine-based hydroxylamines

O-Benzoylhydroxylamines are very important $[NR_2]^+$ synthons for electrophilic aminations. Large number of amination reactions utilizing these *O*-benzoylhydroxylamines have been

achieved with variety of organometallic reagents including organozincs, organolithium, organozirconium, organoaluminium, organomagnesium, organoboron and organosilicon reagents. Amination reactions of organometallics with *O*-benzoylhydroxylamines generally utilize transition metals e.g. copper or nickel for cleaving the N–O bond promoting the C–N bonds formation. Although most of these electrophilic aminations have been achieved using various organometallic reagents, significant advancement has also been accomplished via C–H functionalization.³⁸ Unlikely to the 0°/1° amine-based hydroxylamine reagents as discussed earlier which reacts mostly through metal-nitrenoid formation, with these *O*-benzoylhydroxylamines (2° amine-based hydroxylamines) most of the metals generally undergoes oxidative addition to the weak N–O bond generating a high-valent metal species which then transfers amine moiety to the arenes or alkanes affording the C–H amination products. Under Rh-catalysis these aminating reagents react *via* Rh-nitrenoid formation.



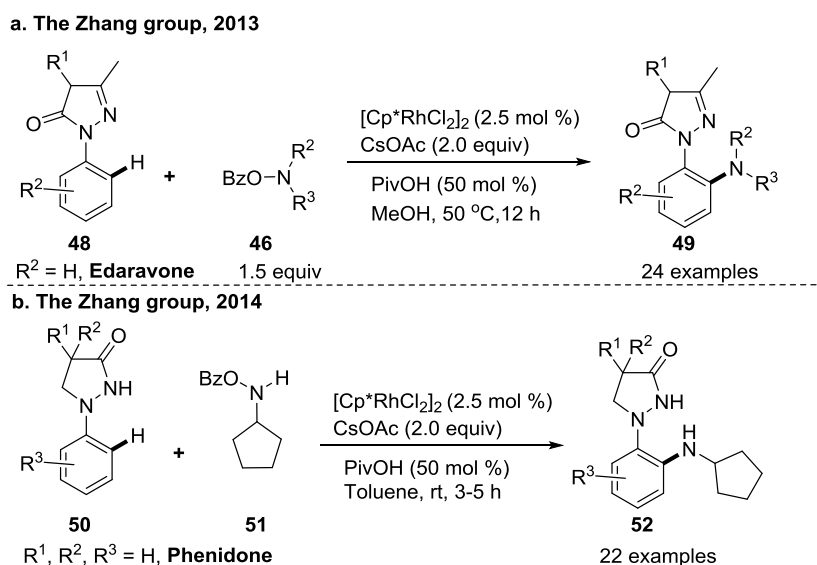
Scheme 22. Directed *ortho* (sp^2)C–H amination of benzamides under Pd or Ru catalysis

In 2011, a Pd-catalyzed *ortho* C(sp^2)–H amination of *N*-aryl benzamides with *O*-benzoylhydroxylamines was established by the Yu group (**Scheme 22a**).³⁹ The reaction was unsuccessful with *N*-chloroamine but both *O*-acetyl and *O*-benzoyl protected hydroxylamines were found as effective aminating reagents. They used *O*-benzoyl hydroxylamines for the reaction due to their ease of preparation. The scope of the reaction was with respect to

both benzoic acids and the secondary amines. Mechanistically, CsF or KF first deprotonates acidic amide proton giving the corresponding salt. The weak chelation of Pd(II) with the carbonyl moiety of the benzamide salt undergoes *ortho* C-H activation in a similar fashion to that of benzoic acid substrates. Then according to them the arylpalladium(II) intermediate **I** may undergo electrophilic amination affording the product or *via* oxidative addition to the N-O bond of the electrophilic aminating agent may generate the Pd(IV)-species **II**, which on reductive elimination affords the product with catalyst regeneration.

In 2013, the Yu group described a mild Ru(II) catalysed *ortho* amination of weakly coordinating benzamides with *O*-benzoyl hydroxylamines at room temperature.⁴⁰ Unlikely to the previous methods, this reaction took place very efficiently in numerous heterocyclic systems also. They proposed similar kind of catalytic cycle as mentioned above with Pd-catalysis (**Scheme 22b**).

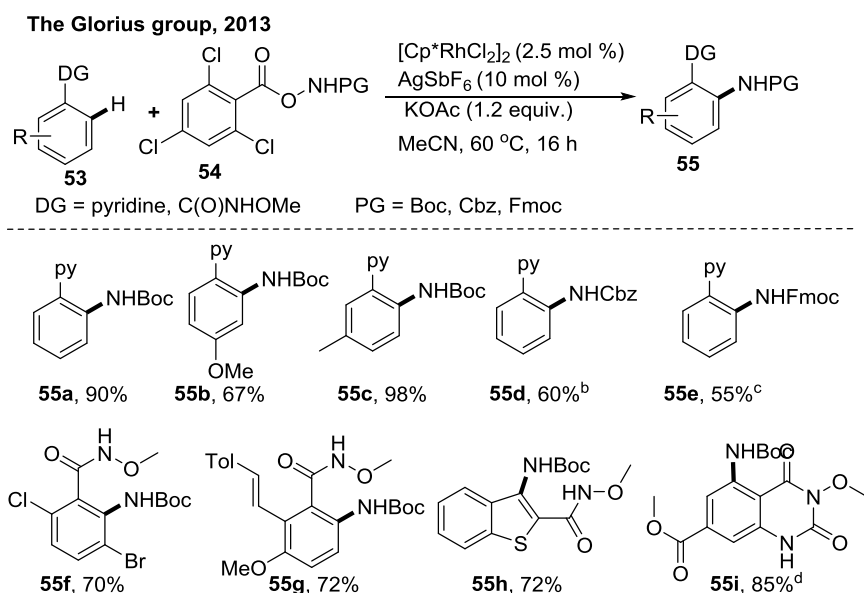
In the same year, the Zhang group reported a Rh(III) catalysed *ortho* C-H amination of 1-aryl-1H-pyrazol-5(4H)-ones with a broad range of *O*-protected hydroxylamines cyclic/acyclic secondary as well as primary amines (**Scheme 23a**).⁴¹ They have used an intrinsic functional group as directing group which afforded directly a library of new analogues of the existing neuroprotective drug marketed as Edaravone. The reaction conditions were relatively mild with very low catalyst loading. They also proposed similar kind of catalytic cycle as mentioned above by the Yu group above with Pd-catalysis and Glorius group with Rh-catalysis.



Scheme 23. Rh-catalysed *ortho* (sp^2)C-H amination using intrinsic directing groups

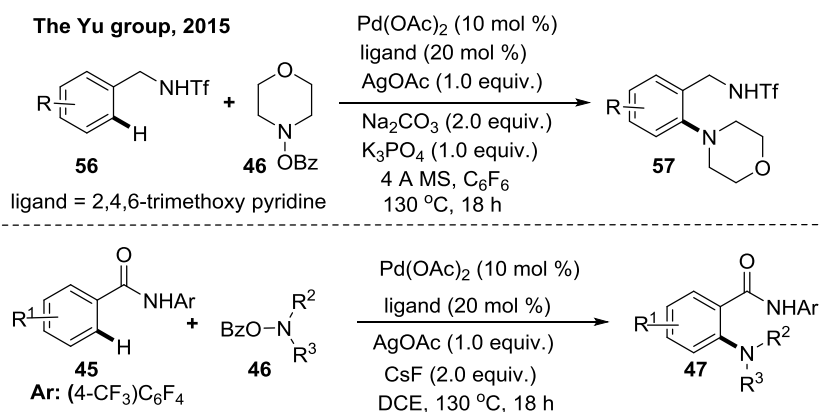
In 2014 the same group disclosed another Rh(III)-catalysed *ortho* C–H amination of substrates containing intrinsic functional group (cyclic hydrazine moiety) which is an essential part of substrate acting as directing group (**Scheme 23b**).⁴² This moiety is present in phenidones which are 5-lipoxygenase inhibitor. Thus this protocol provided a library of various *ortho* amino substituted phenidones.

In similar time, the Glorius group unveiled an amidation protocol of (sp²)C–H bonds using electron-deficient aryloxycarbamates as efficient electrophilic amide source under Rh(III)-catalysis (**Scheme 24**).⁴³ The reaction was progressed under mild conditions with good functional group tolerance. Pyridine and *O*-methyl hydroxamic acids acted as efficient directing groups affording valuable *N*-Boc protected arylamines.



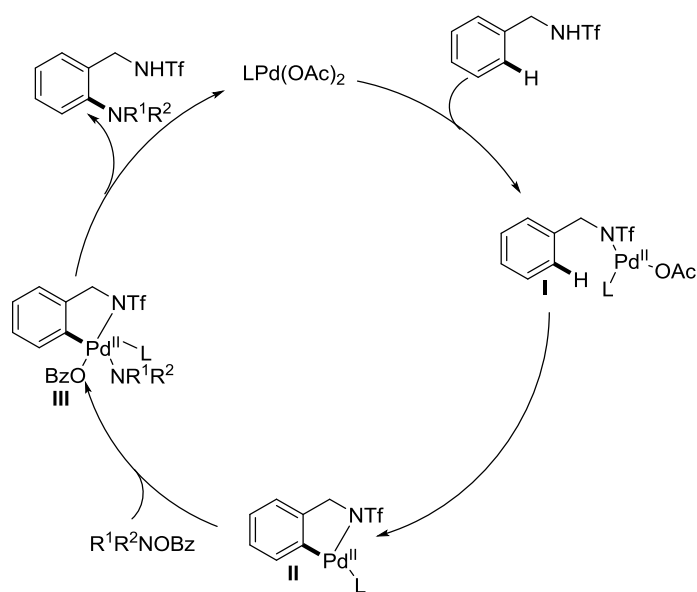
Scheme 24. Rh-catalysed directed (sp²)C–H amidation with electron-deficient aryloxycarbamates

Note: ^bamine source (1.2 equiv.), [RhCp*Cl₂]₂ (5 mol %), AgSbF₆ (20 mol %), 80 °C. ^c amine source (1.5 equiv.), KOAc (1.0 equiv), [RhCp*Cl₂]₂ (5 mol %), AgSbF₆ (20 mol %), 100 °C. ^damine source (2.5 equiv.), KOAc (4.0 equiv.), 80 °C, 16 h.



Scheme 25. Pd-catalysed *ortho* (sp^2)C-H amination of benzamides and benzylamines

In 2015, the Yu group described another efficient Pd-catalyzed *ortho* C-H amination of triflyl-protected benzylamines and benzamides by ligand promoted condition (**Scheme 25**).⁴⁴ After several screening of various pyridine based ligand they found 2,4,6-trimethoxy pyridine as the best one.

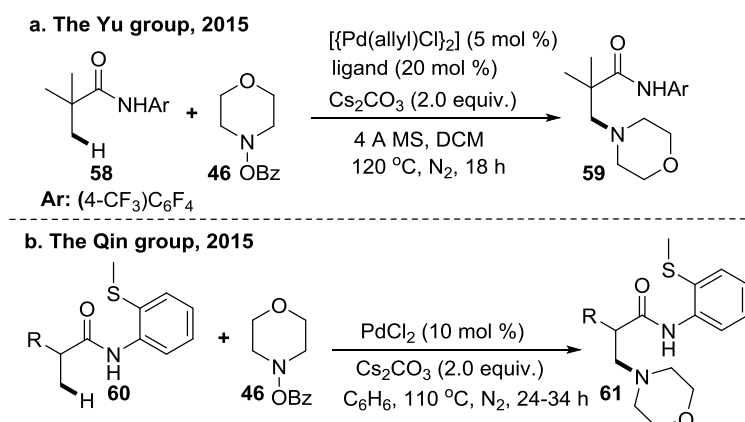


Scheme 26. Proposed catalytic cycle

Based on their control experiments, they proposed that substrate first undergoes chelation with the anionic triflamide to give **I** followed by C-H activation giving intermediate **II**. This is upon oxidative addition to the N-O bond forms a Pd(IV) species **III**. Finally, reductive elimination from **III** affords the amination product with Pd(II) regeneration (**Scheme 26**).

In spite of having numerous reports on (sp^2)C-H aminations with these aminating agents a limited number of (sp^3)C-H aminations has been explored. For example, in 2015, the Yu group described a Pd-catalysed intermolecular amination of β -(sp^3)C-H amination of aliphatic

acids which provided a library of β -amino acids (**Scheme 27a**).⁴⁵ In the same year, the Qin group also reported a Pd(II)-catalysed intermolecular amination of unactivated (sp^3)C-H bonds using 2-aminothioether as weak coordinating group (**Scheme 27b**).⁴⁶

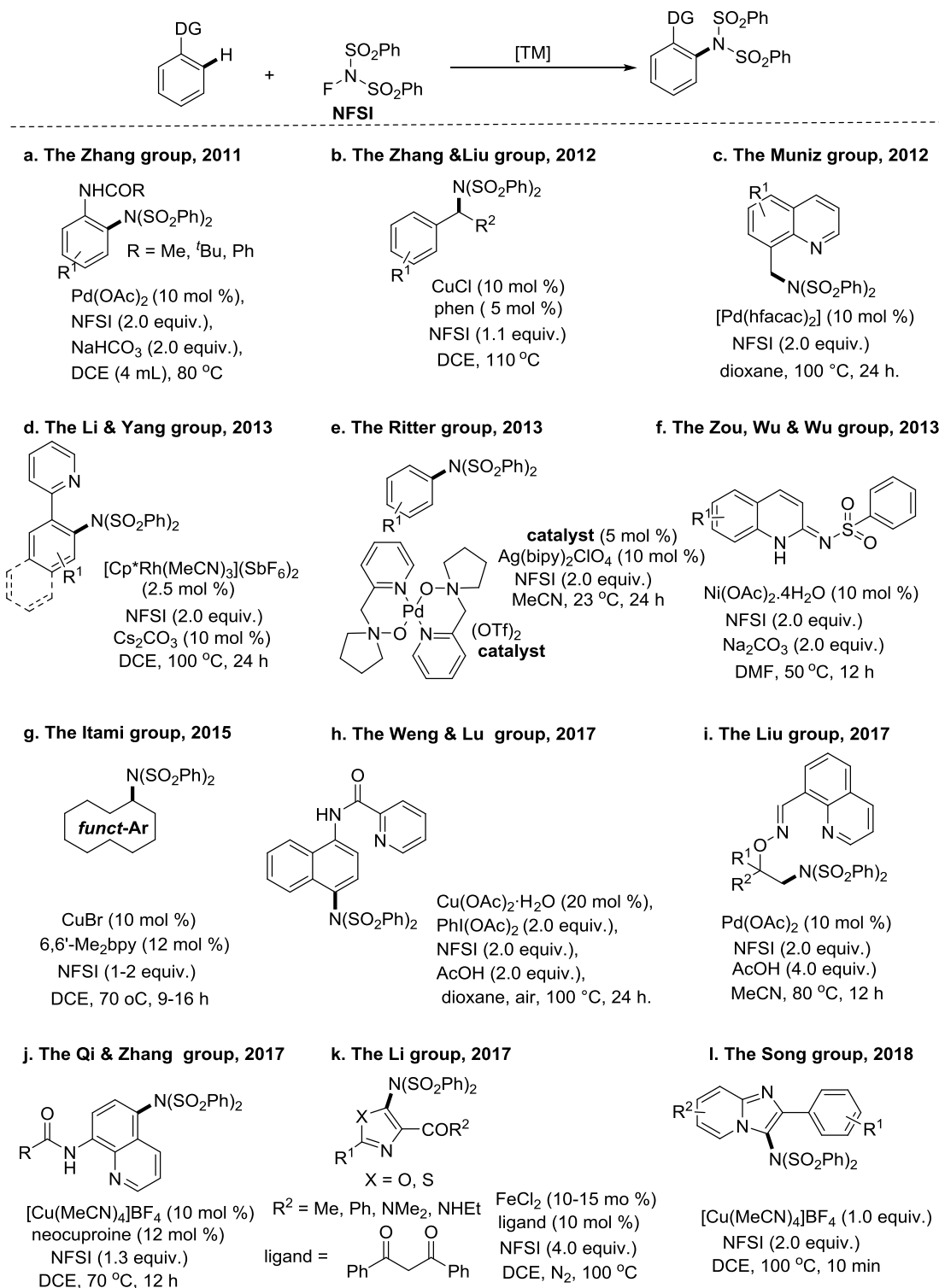


Scheme 27. Pd-catalysed β -(sp^3)C-H amination of aliphatic amides

I.7c. Organic azides

Organic azides are important class that fall in the category of electrophilic aminating agent. They are considered as an environmentally benevolent amine source and an additional advantage of using these azides is that a sole by-product is molecular nitrogen (N_2). More importantly, like hydroxyl amine based reagent they also act as internal oxidant via N– N_2 bond cleavage omitting the requirement of additional stoichiometric external oxidants. Most of these reactions are performed mostly under expensive Rh or Ir catalysis and some works under Ru or Co catalysis has also been achieved.⁴⁷ Besides activated aryl sulfonyl azides, aryl, alkyl even acyl azides also work well under those catalytic conditions.⁴⁸ Mechanistic investigations revealed that all these reactions proceed through a more or less similar catalytic cycle which consists of three steps: formation of metallacycle *via* C–H bond cleavage through chelation-assistance followed by formation of C–N bond through the *in situ* generated metal–nitrenoid intermediate and then the insertion of an imido moiety to the M–C bond and finally, formation of the product *via* protodemetalation with catalyst regeneration. Significant advances have been achieved in this field of C–H amination or C–H amination/annulation cascade to synthesize *N*-heterocycles using various organic azides which are excellently reviewed, so we will not further elaborate this topic.⁴⁹

Table 1. Transition metal-catalysed C-H amination achieved using NFSI (*N*-Fluorobenzenesulfonimide)



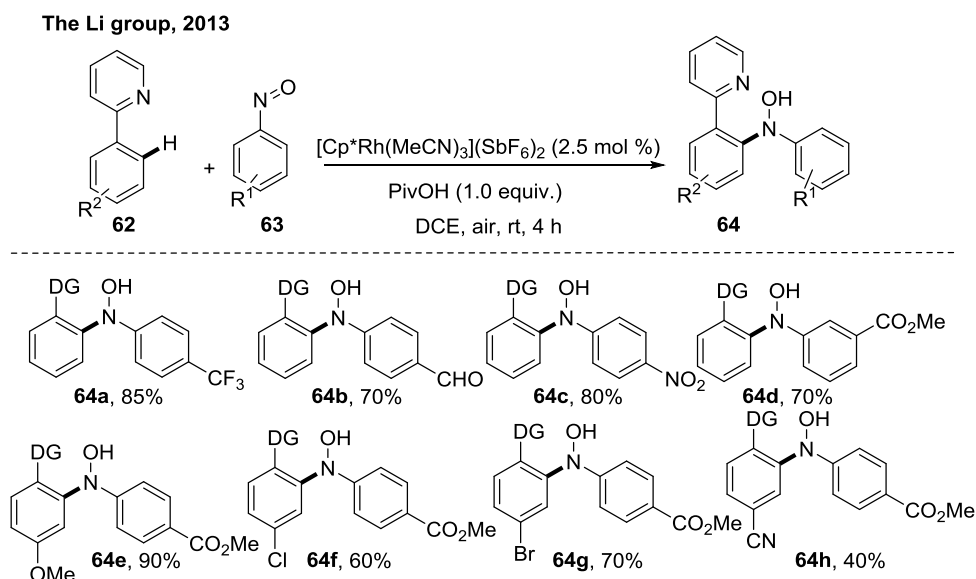
I.7d. *N*-Fluorobenzenesulfonimide (NFSI)

N-Fluorobenzenesulfonimide (NFSI) is one of the most popular commercially available N–F reagents which was first introduced as electrophilic fluorinating agent by Differding group in 1991.⁵⁰ This mild, stable, and highly soluble crystalline solid serves as a multipurpose reagent in various transformations of aliphatic and aromatic compounds such as an oxidant, safer radical fluorine source and an excellent electrophilic aminating agent. In last decade lots of C–H amination have been achieved using NFSI which are also reviewed.⁵¹ Some of those reactions are tabulated above (**Table 1**).

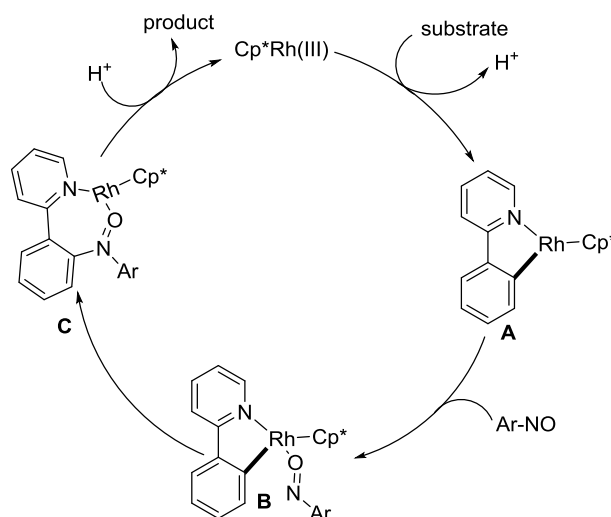
I.7e. Nitroso-compounds

Nitrosobenzene serves as electrophilic nitrogen or oxygen source in nitroso-aldol reactions affording aminoxylation or hydroxyamination products.⁵² Although C–N bond formation with various organometallic reagents has also been achieved but there is limited reports on C–H amination utilising these nitrosoarenes. Most of the nitrosoarenes are prepared by oxidising the anilines which have been directly used for C–H amination from many years. Though one extra step is needed for their preparation they have high potential to solve many problems associated with C–H amination using anilines such as i) catalyst inhibition can be minimised, ii) C–H amination with these more reactive amine source can be performed at very mild conditions. Their high reactivity can be attributed to the fact that so many C–H aminations have been achieved in metal free conditions also.⁵³

The Li group first reported C–H amination with nitrosoarenes in 2013 in 2-phenyl pyridine system under Rh-catalysis to give biaryl hydroxylamines (**Scheme 28**).⁵⁴ The reaction showed high functional group tolerance and took place at room temperature. These hydroxylamines can be converted to important biaryl amines one step reduction. Based on their control experiments they proposed that Rh-catalyst first undergoes chelation assisted *ortho* C–H bond activation providing rhodacycle **A**. Then coordination with nitroso to give **B**, followed by nucleophilic addition (or migratory insertion of N=O) may generate O–Rh species **C**. After protonation the hydroxylamine is formed with regeneration of catalyst (**Scheme 29**).

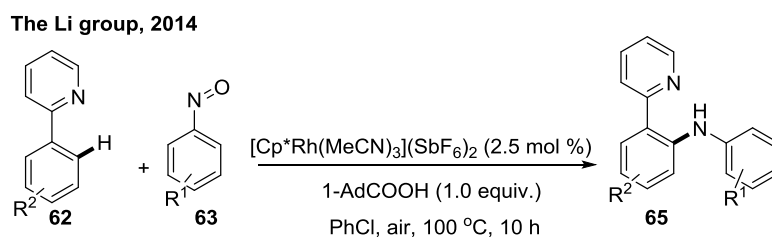


Scheme 28. Rh-catalysed directed *ortho* (sp^2)C-H amination using nitrosoarenes



Scheme 29. Proposed catalytic cycle

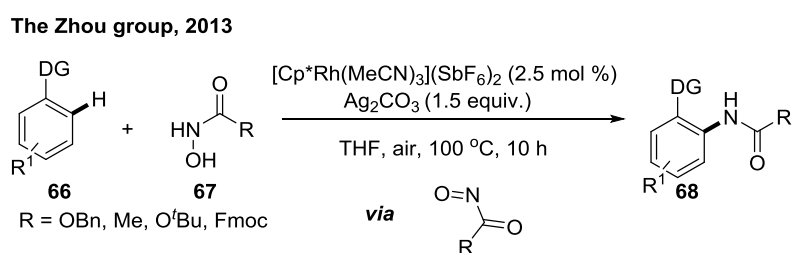
Then in 2014, the same group further re-optimised their catalytic condition to get the diarylamines in single step (**Scheme 30**).⁵⁵ Using 1-adamantanecarboxylic acid instead of pivalic acid, changing the solvent system from DCE to chlorobenzene and 100 °C reaction



Scheme 30. Rh-catalysed one-step synthesis of diarylamines using nitrosoarenes

temperature they were able to get the desired product in one sort. The reaction is scalable and worked well even with 1 mol % of catalyst loading.

N-hydroxycarbamates are also found promising for C-H amidation which under slightly oxidising conditions proceeds *via* formation of nitroso intermediates as reported the Zhou and Zhang groups.⁵⁶ The Zhou group in 2013, first disclosed C-H amidation of various substrates with different directing groups using numerous *N*-hydroxy carbamates under Rh-catalysis (**Scheme 31**). Their control experiments show that under air these *N*-hydroxy carbamates oxidised to nitroso compounds and the next C-H amidation follow the catalytic cycle as mentioned in the previous section.



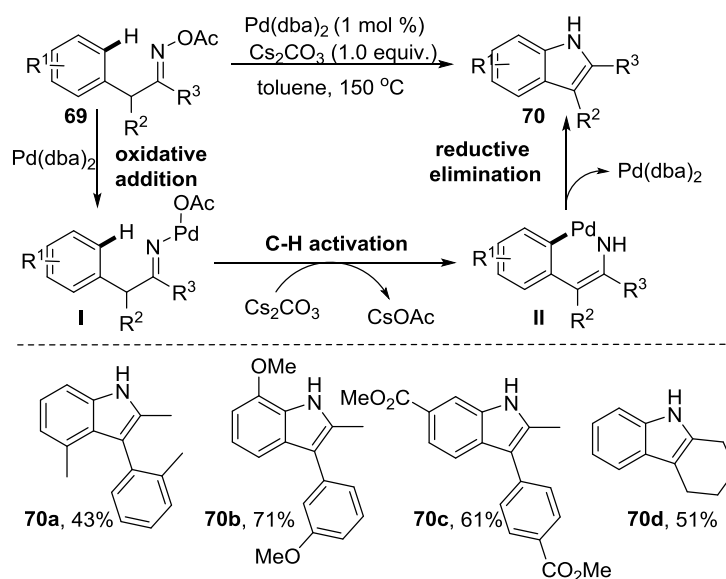
Scheme 31. Rh-catalysed directed *ortho* C-H amidation using *N*-hydroxycarbamates *via* nitrosoarenes

I.7f. Oximes/oxime esters

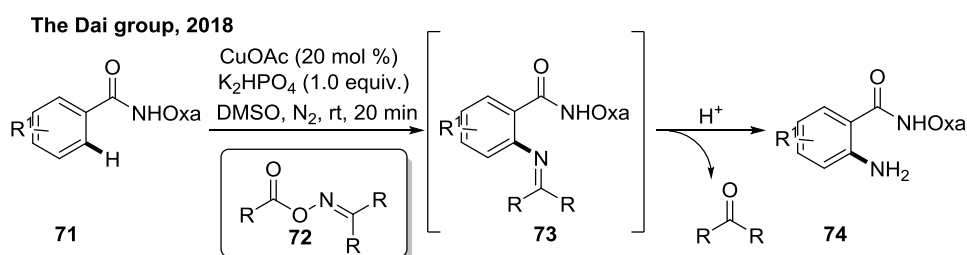
Oximes having weak N–O bond with an average energy of 57 kcal/mol much less than the energies of the C–X (X = C, N, O) (69–91 kcal/mol) sigma bonds are also important source of electrophilic amine to perform C-H amination. Significant advancement has been achieved for the synthesis of various heterocycles using oximes *via* Pd-catalysed intramolecular amino-Heck or Narasaka–Heck cyclization (most these reactions are C-H amination reactions) which are summarised in many reviews.⁵⁷ Reactive imino-Pd^{II} intermediate formed by the oxidative addition of Pd⁰ to N–O bond of the oximes was also trapped in many cases with external reaction partners as done by Neuville and Zhu group in 2009.⁵⁸ Many C-H amination reactions with oximes as electrophilic amine source have also been developed.

In 2010, the Hartwig group reported Pd-catalysed synthesis of indoles using oximes *via* an intramolecular C-H amination (**Scheme 32**).⁵⁹ The oxime moiety acted as directing group, oxidant and amine source. Mechanistically, Pd(0) on oxidative addition to the N–O bond of oxime generates intermediate **I** which after C-H activation gives **II**. This intermediate after reductive elimination affords the product.

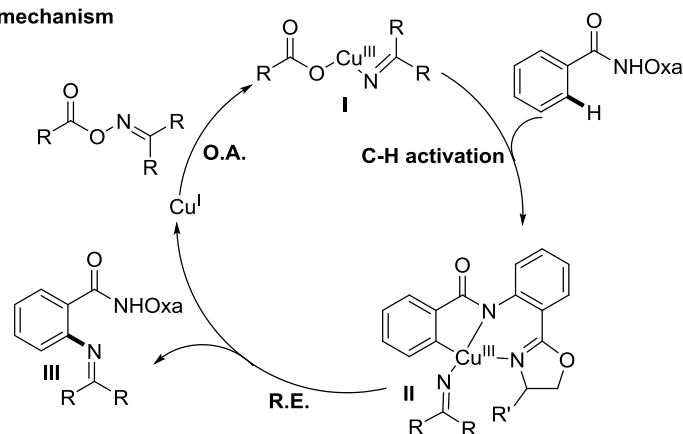
The Hartwig group, 2010



Scheme 32. Pd-catalysed intramolecular C-H amination of oximes for the synthesis of indoles

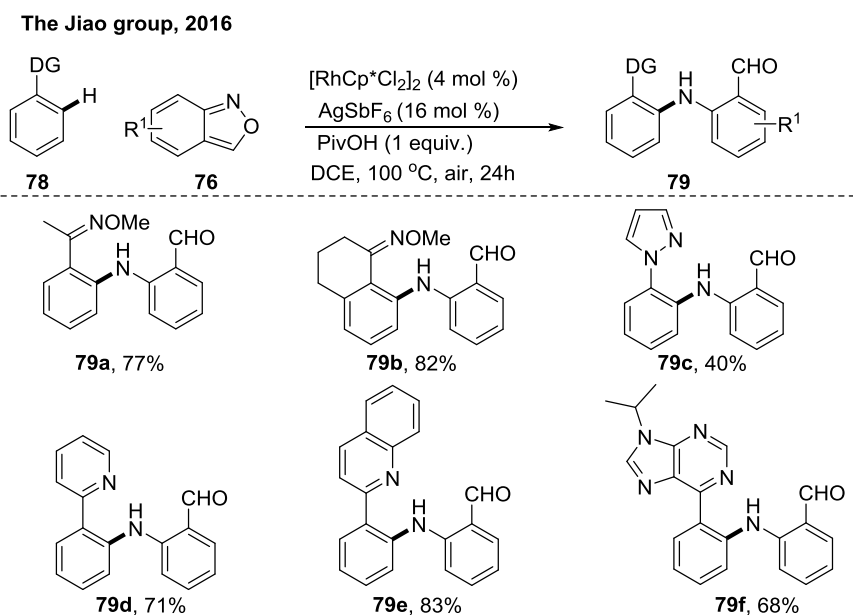


Proposed mechanism



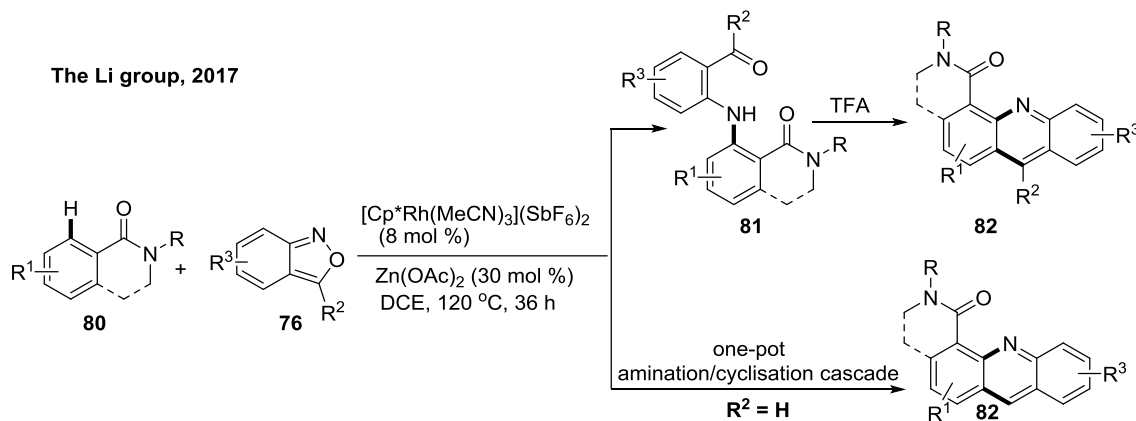
Scheme 33. Cu-catalysed C-H amination with oximes

The Dai group in 2018 introduced oxime for directed *ortho* (sp²)C-H amination to deliver primary amine under copper catalysis (Scheme 33).⁶⁰ The method showed functional group tolerance and this protocol was efficient for the amination of various heterocyclic molecules which is a major advantageous over the previous methods. Late-stage C-H amination has also been achieved using this strategy. Mechanistically, the Cu^I catalyst first generates a



Scheme 35. Rh-catalysed (sp^2)C-H amination with anthranils

In 2017, the Li group further disclosed a Rh(III)-catalysed C–H amination of benzamides and isoquinolones using anthranils (**Scheme 36**).⁶³ This methodology provided various bifunctionalized amination products **81**, which can then undergo cyclisation in presence of TFA to give acridines, **82**.

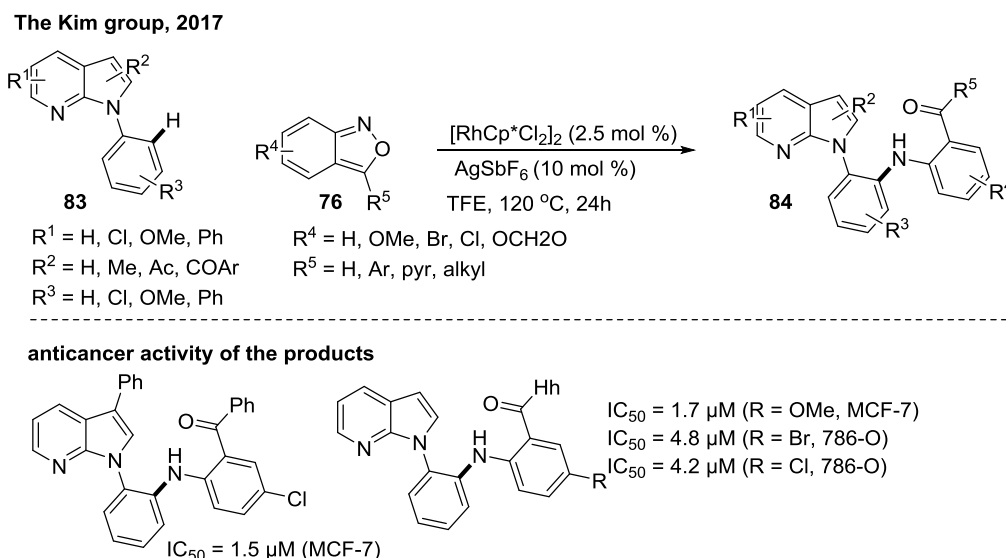


Scheme 36. Rh-catalysed (sp^2)C-H amination of benzamides and isoquinolones with anthranils

When 3-unsubstituted anthranils were used in this transformation, the corresponding acridine derivatives were obtained in one pot through C–H amination/cyclisation cascade reactions.

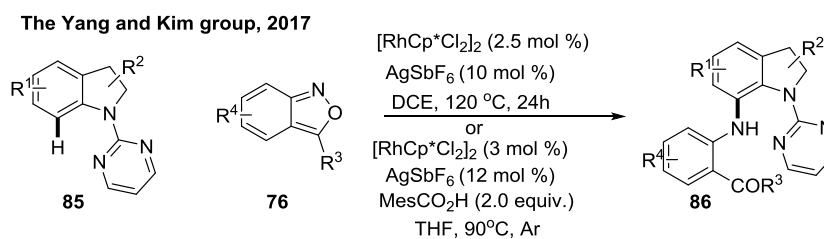
The site-selective C–H amination of 7-azaindoles with anthranils under Rh(III)-catalysis was reported by the Kim group (**Scheme 37**).⁶⁴ This transformation efficiently delivered a range of *ortho*-aminated *N*-aryl-7-azaindoles with excellent site-selectivity and functional group tolerance. The *ortho*-aminated 7-azaindoles hence made were readily

converted into biologically relevant heterocycles such as azaindoloacridine, azaindoloacridone and bis-indole compounds. The synthetic utility of this method was further demonstrated by good *in vitro* anticancer activity against human breast adenocarcinoma cells (MCF-7), human renal carcinoma cells (786-O), and human prostate adenocarcinoma cells (DU145).



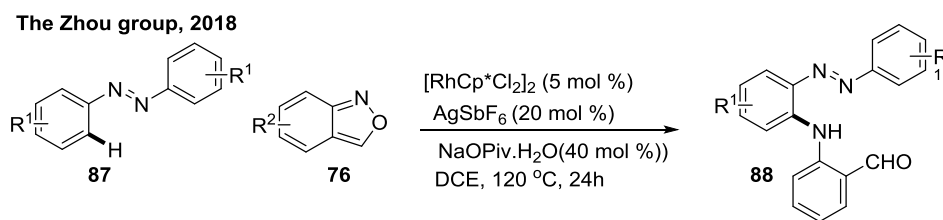
Scheme 37. Rh-catalysed (sp^2)C-H amination of 7-aza indoles with anthranils

The Yang and Kim groups reported independently Rh(III)-catalysed C-7 selective amination of indolines with *N*-pyrimidine DG. Amination took place selectively at the C-7 positions (**Scheme 38**).⁶⁵ Both methods afforded C-7 aminated indolines in good yields with excellent site-selectivity and functional group tolerance.

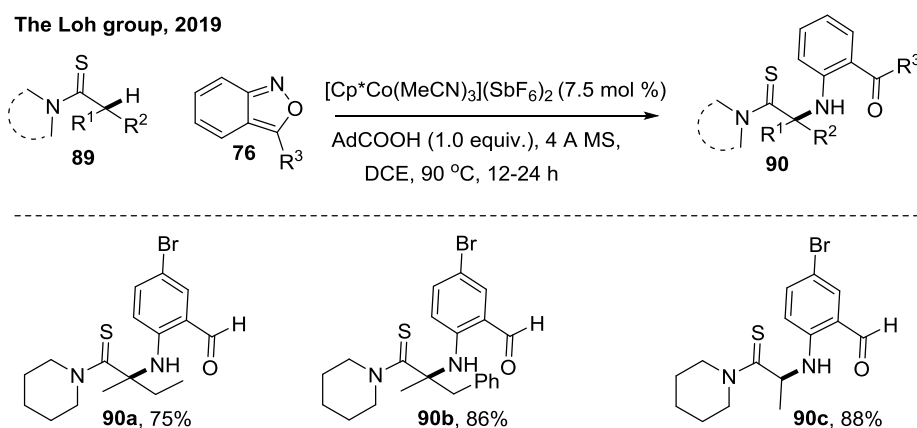


Scheme 38. Rh-catalysed selective C-7 (sp^2)C-H amination of indolines with anthranils

In 2018, the Zhou group reported a rhodium-catalysed *ortho* C–H amination of azobenzenes using anthranils (**Scheme 39**).⁶⁶ This reaction showed excellent functional group tolerance and wide variety of aminated products were obtained in good yields.

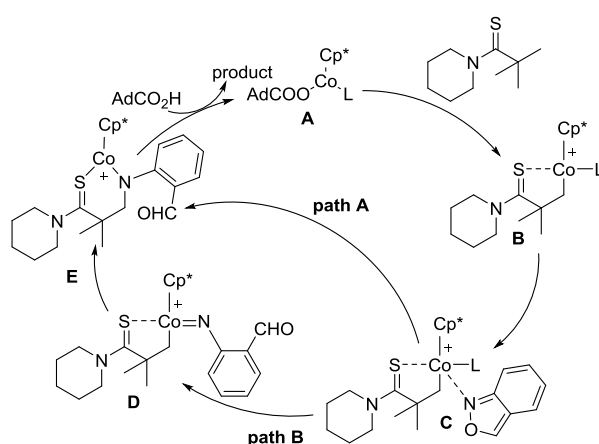


Scheme 39. Rh-catalysed *ortho* (sp^2)C-H amination of azo compounds with anthranils



Scheme 40. Co-catalysed thioamide directed (sp^3)C-H amination with anthranils

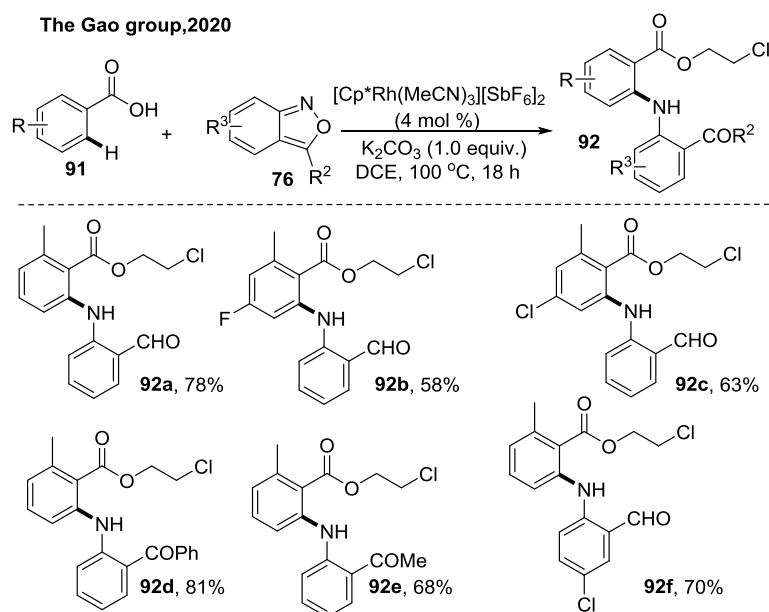
In 2019, a Co-catalysed (sp^3)C-H amination has been accomplished by the Loh group.⁶⁷ The excellent site-selectivity on primary β (sp^3)C-H bonds was observed for a various thioamides with very good functional group tolerance (**Scheme 40**). In 2020, the Li group also reported similar thioamide directed (sp^3)C-H amination with anthranils under cobalt catalysis.⁶⁸



Scheme 41. Proposed catalytic cycle of Co-catalysed thioamide directed (sp^3)C-H amination

Mechanistically, the cationic Co(III) species **A** undergoes chelation assisted C(sp^3)-H bond activation with the thioamide substrate forming a five-membered cobaltacycle **B**. The

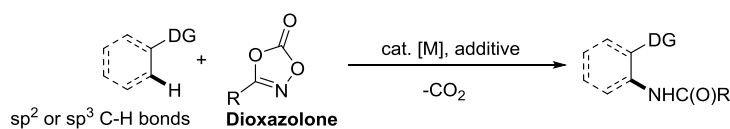
intermediate **B** may then undergo coordination with anthranil followed by migratory insertion *via* complex **C** generating Co(III)-amino species **E** (path A). Finally, **E** on protolysis with AdCO₂H furnished the product with the regeneration of the active Co(III) species **A**. Alternatively, a putative Co(V)-nitrenoid species **D** may be formed *via* an intramolecular N–O bond cleavage followed by nitrene insertion into the Co–C(sp³) bond forming the intermediate **E** (path B).



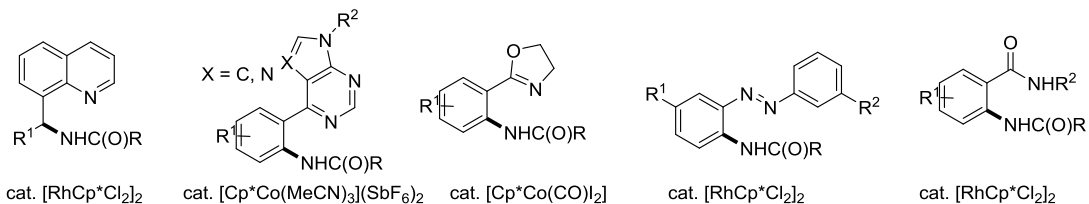
Scheme 42. Carboxylic acid directed Rh-catalysed *ortho* C-H amination with anthranils

The Gao group unveiled an efficient Rh(III)-catalysed *ortho* (sp²)C-H amination methodology of benzoic acids using anthranils was established for the quick synthesis of valued anthranilic acid derivatives (**Scheme 42**).⁶⁹ In this process COOH acted as weakly coordinating directing group and after amination the products were obtained as ester. This protocol is highly application for various functional group containing benzoic acid derivatives. The reaction proceeded through a general mechanism shown in **Scheme 34**.

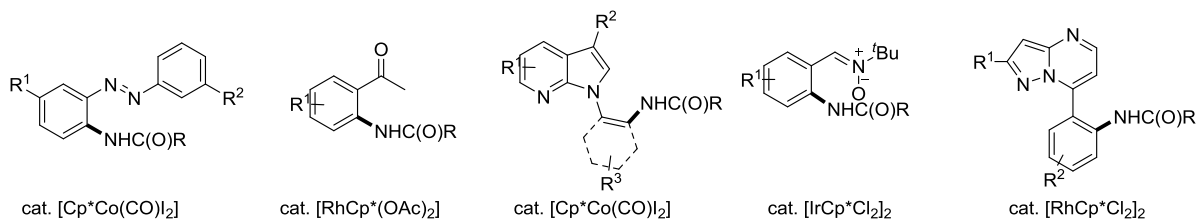
Table 2. C-H amidation achieved using various directing groups with dioxazolones



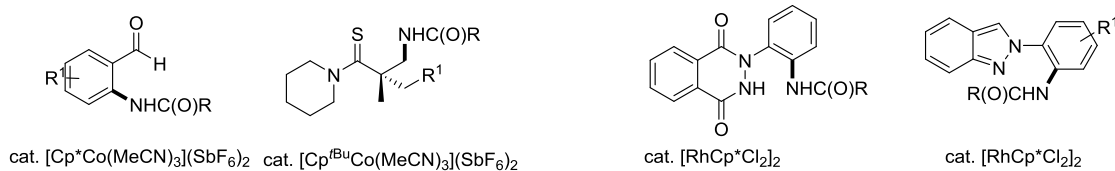
a. The Li group, 2015 b. The Jiao group, 2015 c. The Ackermann group, 2016 d. The Lee group, 2016 e. The Bolm group, 2017



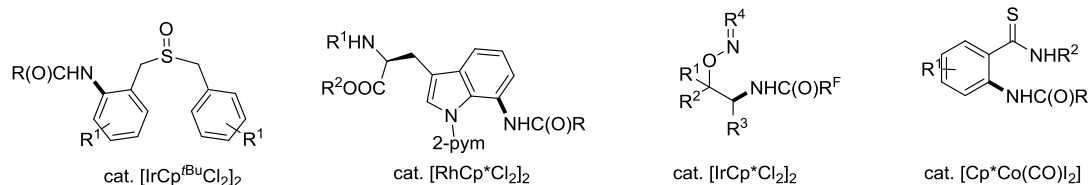
f. The Patel group, 2017 g. The Prabhu group, 2018 h. The Dong group, 2018 i. The Cui group, 2019 j. The Zou group, 2019



k. The Li & Wu group, 2019 l. The Matsunaga group, 2019 m. The Kim group, 2020 n. The Hajra group, 2020



o. The He group, 2020 p. The Ackermann group, 2020 q. The Baudoin group, 2021 r. The Zheng group, 2021



I.7h. Dioxazolones

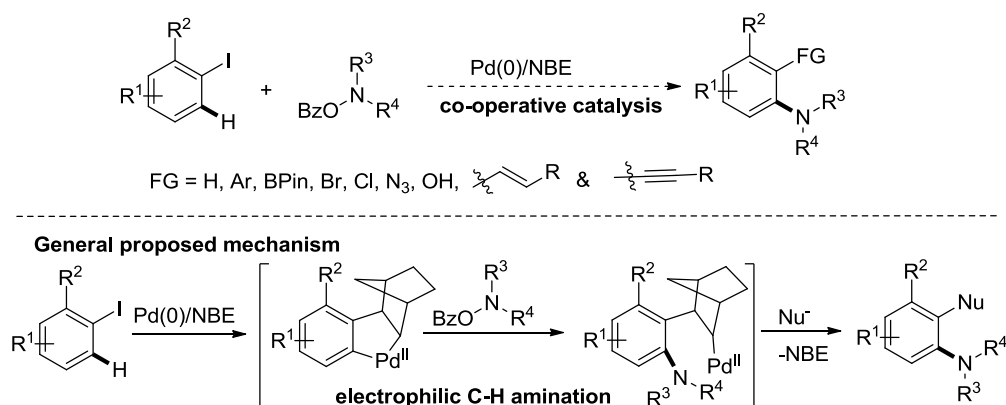
Dioxazolones are found to be a versatile nitrogen source in recent years for the transition metal catalysed C-H amidation using different directing groups by many research groups. Some of the examples are shown in **Table 2**. Mechanistically the reactions proceed via metal-acylnitrenoid intermediate formation through the decarboxylation of the dioxazolones.⁷⁰ The Sukbok chang group has significant contribution in this area. They have performed comparative studies of amidation reactions by dioxazolone under Ir, Rh and Co catalysis.⁷¹ The C-H amidation reactions achieved using dioxazolones are tabulated above and the amidation/cyclisation cascade reactions using dioxazolones are mentioned in **Scheme 55**.

I.8. C-H amination/cyclisation cascade using electrophilic amines for the synthesis of N-heterocycles

Development of cascade reactions having undeniable benefits including atom economy, and also economies of time, labour, resource management, and waste generation is upcoming field of research area. This is why cascade reactions are now considered to fall under the banner of “green chemistry”.⁷² Many one-pot C-H amination followed by cyclisation cascade reactions using various electrophilic aminating agents have been developed for the efficient synthesis of valuable *N*-heterocycles.

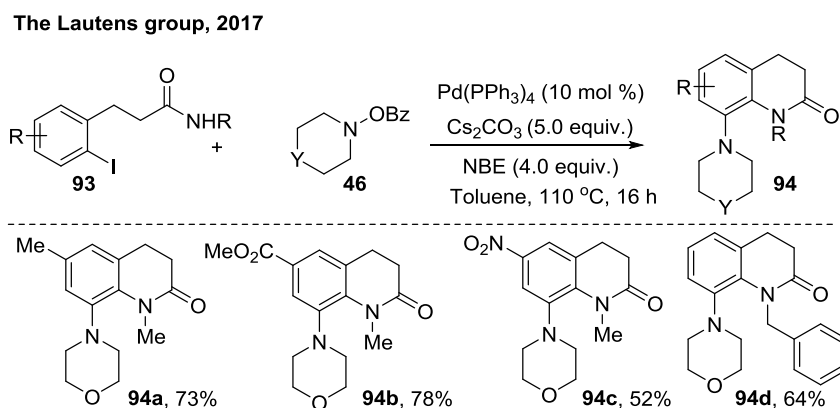
I.8a. C-H amination/cyclisation *via* Catellani-type reaction using *O*-protected hydroxylamines

Many bi- or tri-functionalisation of aryl halides under Pd(0)/NBE co-operative catalysis (Catellani reaction) including C-H aminations using *O*-benzoyloxyhydroxylamines have been achieved by several research groups which are also reviewed.⁷³ General proposed mechanism is shown below (**Scheme 43**).



Scheme 43. General mechanism electrophilic C-H amination through Catellani reaction

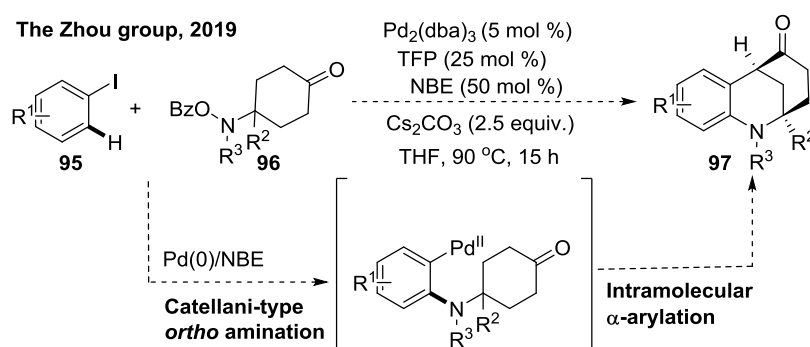
There are some examples of electrophilic C-H amination/cyclisation cascade reactions under Pd(0)/NBE co-operative catalysis for the synthesis of *N*-heterocycles.



Scheme 44. Synthesis of *ortho*-aminated dihydroquinolinones through *ortho*- and *ipso*- C–N bond-forming Catellani reaction

For example, the Lautens group in 2017, reported a palladium-catalyzed, norbornene-mediated *ortho*- and *ipso*- C–N bond-forming Catellani reaction (**Scheme 44**).⁷⁴ This reaction proceeds through a sequential intermolecular amination followed by intramolecular cyclization of the tethered amide to afford *ortho*-aminated dihydroquinolinones.

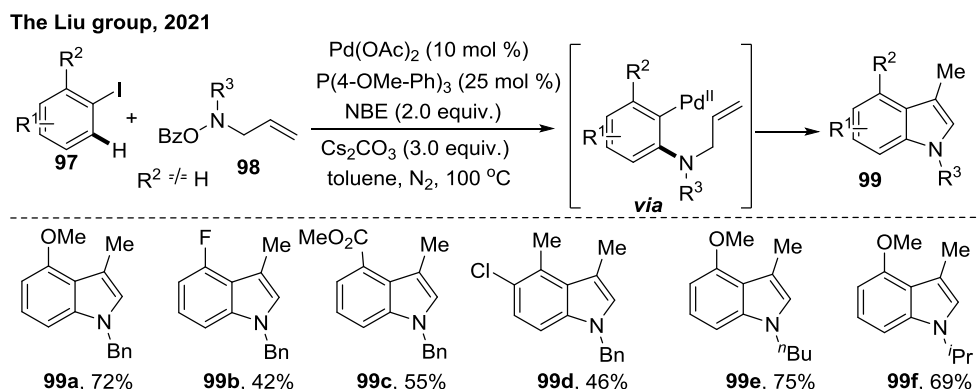
Then the Zhou group in 2019 disclosed an *ortho*-C–H amination using electrophilic amines followed by intramolecular Heck cascade between aryl iodides and functionalized amination reagents through Catellani-type reaction (**Scheme 45**).⁷⁵ Thus this protocol provided an efficient synthesis of unique *N*-containing bridged scaffolds called hexahydro-2,6-methano-1-benzazocines. This highly step-economic method also showed broad substrate scope with good chemoselectivity.



Scheme 45. Catellani-type *ortho* amination/intramolecular α -arylation for the synthesis of bridged azacycles

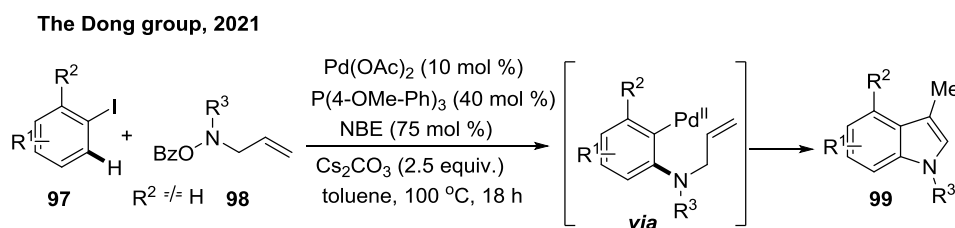
The Liu group in 2021 unveiled an efficient strategy for the synthesis of 3-methyl indole derivatives under the Catellani type reaction which involves electrophilic C–H amination followed by annulation through Heck coupling (**Scheme 46**).⁷⁶ *O*-benzoylhydroxylamine

containing an allyl group here is source of both electrophile and nucleophile under this Pd(0)/NBE co-operative catalysis providing the benzocyclic molecules.



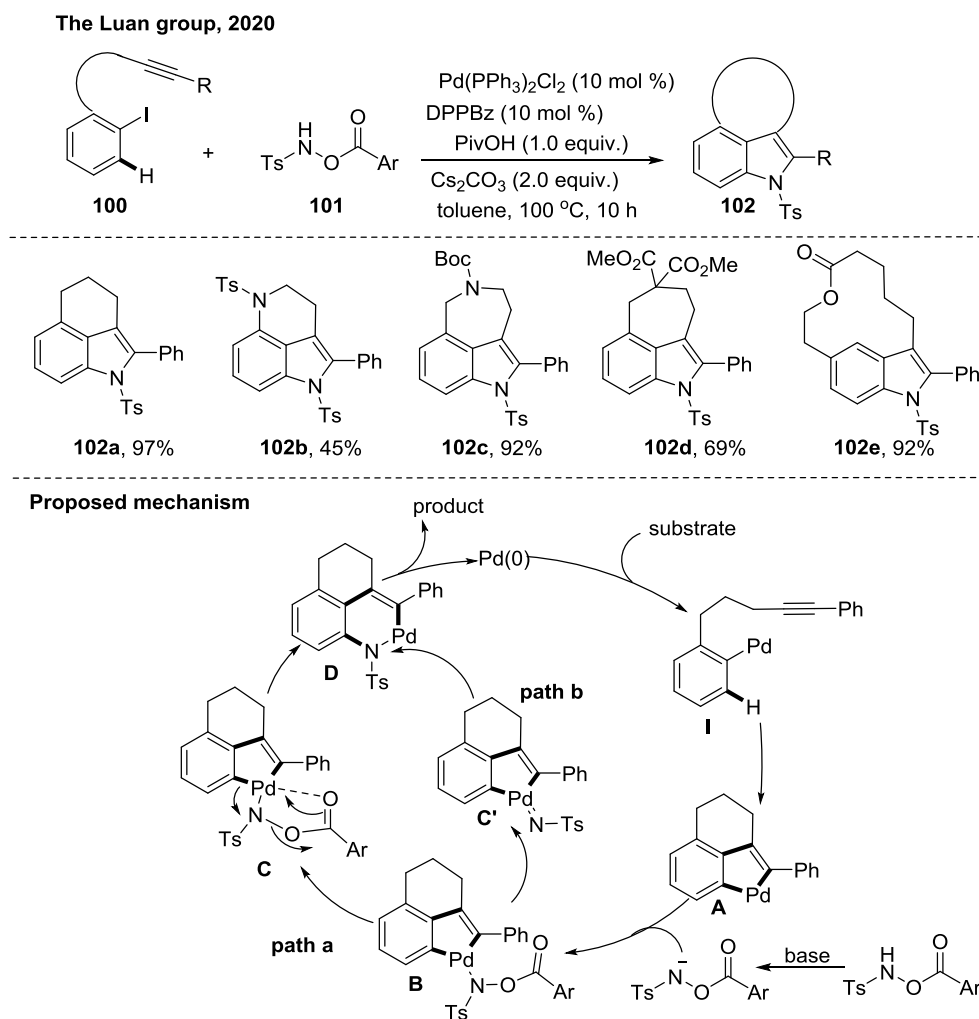
Scheme 46. Catellani-type *ortho* amination/intramolecular Heck reaction for the synthesis of 3-methyl indoles by the Liu group

Subsequently, in almost same time the Dong group also reported similar cascade reaction for the synthesis of 3-methyl indoles under Pd(0)/NBE co-operative catalysis (**Scheme 47**).⁷⁷



Scheme 47. Catellani-type *ortho* amination/intramolecular Heck reaction for the synthesis of 3-methyl indoles by the Dong group

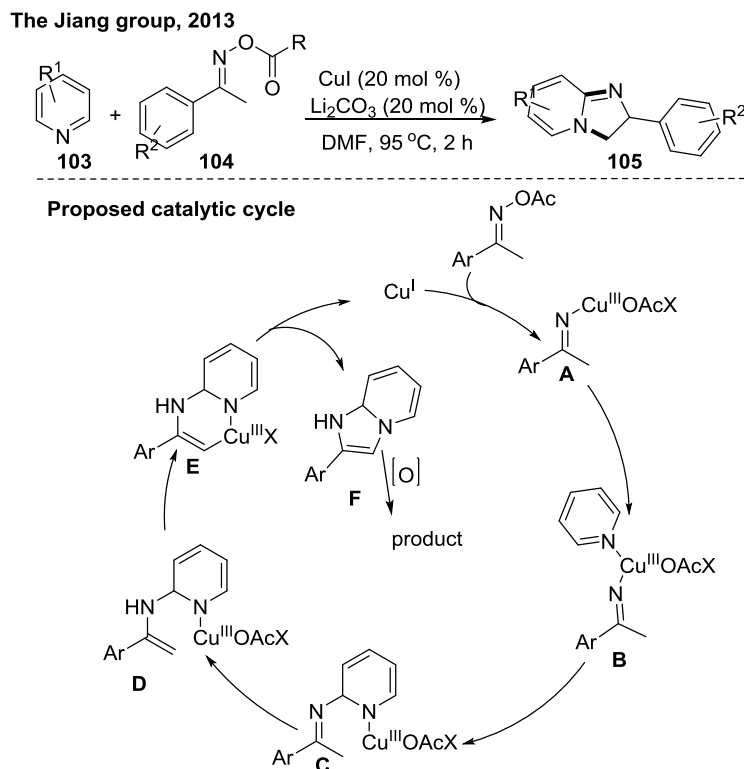
The Luan group in 2020 reported an efficient methodology through alkyne insertion/C–H activation/amination cascade using fine-tuned electrophilic amines for the rapid synthesis of a library of tricyclic indoles (**Scheme 48**).⁷⁸ This method afforded not only medium sized tricyclic indoles but a variety of macro-cyclised (20-membered) tricyclic indoles also in moderate to very good yields. Mechanistically, they proposed that Pd(0) first undergoes oxidative addition to generate a Pd^{II}-species **I** which then after carbopalladation (**A**) followed by chelation with the amine source gives intermediate **B**. This may undergo 1,2-aryl migration (*via C*, path a) or nitrene insertion (*via C'*, path b) to give **D** which after reductive elimination affords the product with catalyst regeneration.



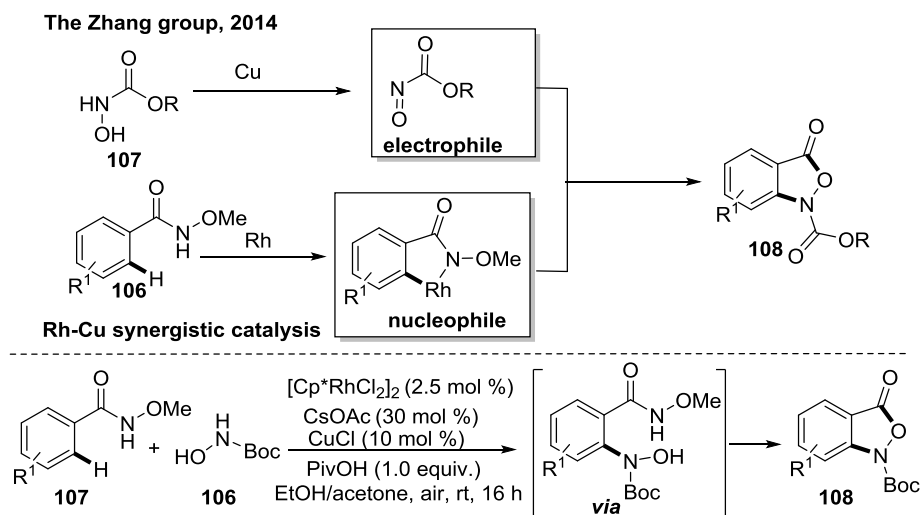
Scheme 48. Synthesis of tricyclic indoles alkyne insertion/C–H activation/amination cascade

I.8b. C–H amination/cyclisation cascade using other electrophilic aminating agents

The Jiang group in 2013 reported Cu-catalysed C–H amination followed by cyclisation of pyridines with oximes to give imidazo[1,2-*a*]pyridines (**Scheme 49**).⁷⁹ Based on their control experiments they proposed that Cu(I) undergoes oxidative addition to N–O bond of the oxime to generate a Cu(III)-species **A**. Then insertion of Cu–N bond of **B** takes place at the 1,2-positions of the pyridine ring. Then a cupracycle is formed after tautomerisation of **C** through **D**. Finally, reductive elimination followed by oxidative aromatization gives the final imidazo[1,2-*a*]pyridine product with regeneration of Cu(I).



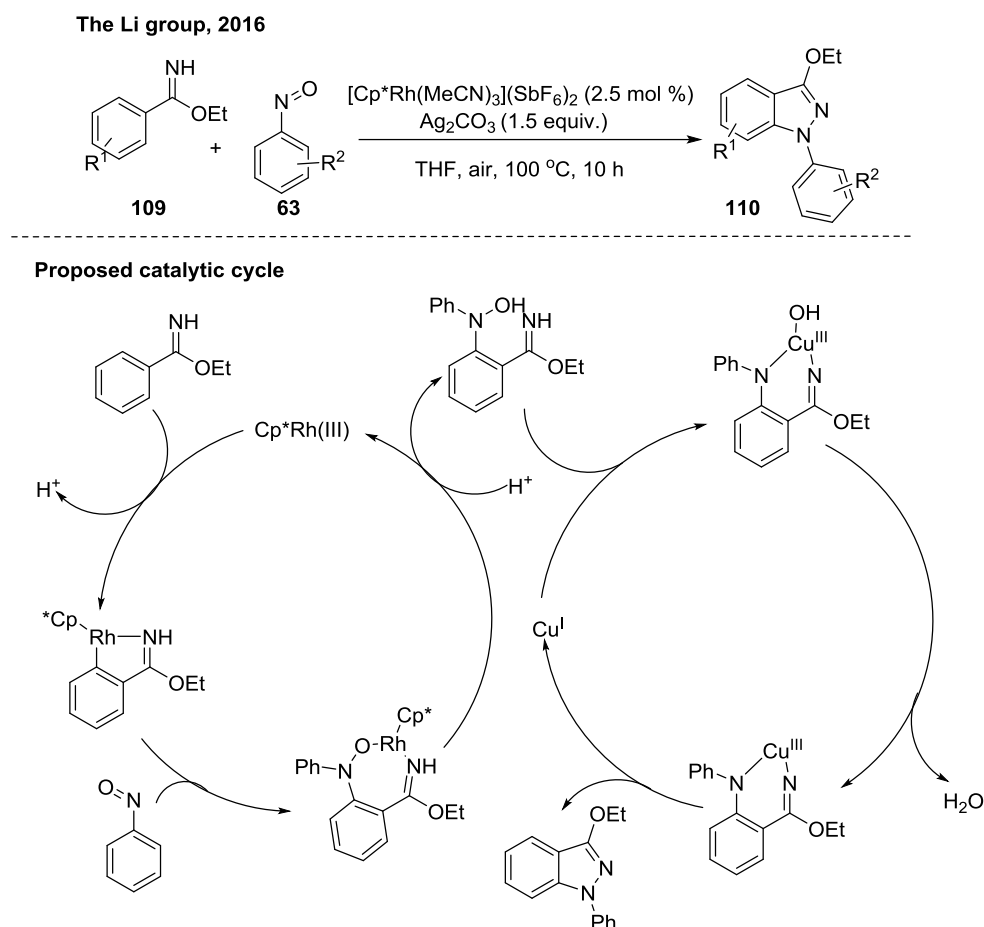
Scheme 49. Cu-catalysed synthesis of imidazo[1,2-a]pyridines through C-H amination/cyclisation cascade using oximes



Scheme 50. Rh-catalysed directed synthesis of benzo[c]isoxazoles using *N*-hydroxycarbamates *via* nitrosoarenes

In the similar time, the Zhang group reported directed C–H amination using *N*-Boc-hydroxyamine *via* synergistic combination of copper and rhodium catalysis (**Scheme 50**).^{56b} This protocol provided a library of valuable heterocycle benzo[c]isoxazole derivatives, which are the subunits of many natural products such as parnafungins A and B17 and other bioactive

complex molecules. In this synergistic approach the Rh catalyst was needed for C-H bond activation to generate the nucleophilic rhodacycle and copper catalyst with O₂ combination produced electrophilic nitroso compound.

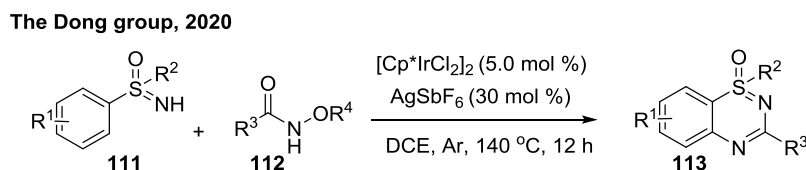


Scheme 51. Rh-catalysed directed synthesis of indazole using *N*-hydroxycarbamates *via* Rh-Cu co-operative catalysis

Then in 2016 the Li group unveiled a new strategy for the one-pot synthesis of indazole derivatives using nitrosobenzenes as a convenient nitrogen source for the C-H amination of arenes under Rh and Cu co-operative catalysis (**Scheme 51**).⁸⁰ The reaction conditions are very mild with broad substrate scope and very good functional group tolerance. Based on their control experiments they proposed similar catalytic cycle for C-H amination with nitrosoarenes as mentioned earlier to afford diaryhydroxylamines. Then in a sequential Cu-catalytic cycle Cu^I undergoes oxidative addition to the N-O bond forming a cupracycle. Then dehydration followed by reductive elimination gives the product with the regeneration of Cu^I catalyst.

In 2020 the Dong group first disclosed an example of Ir(III)-catalyzed C-H amidation followed by cyclization cascade reactions using *N*-alkoxyamides as amidation reagents (**Scheme**

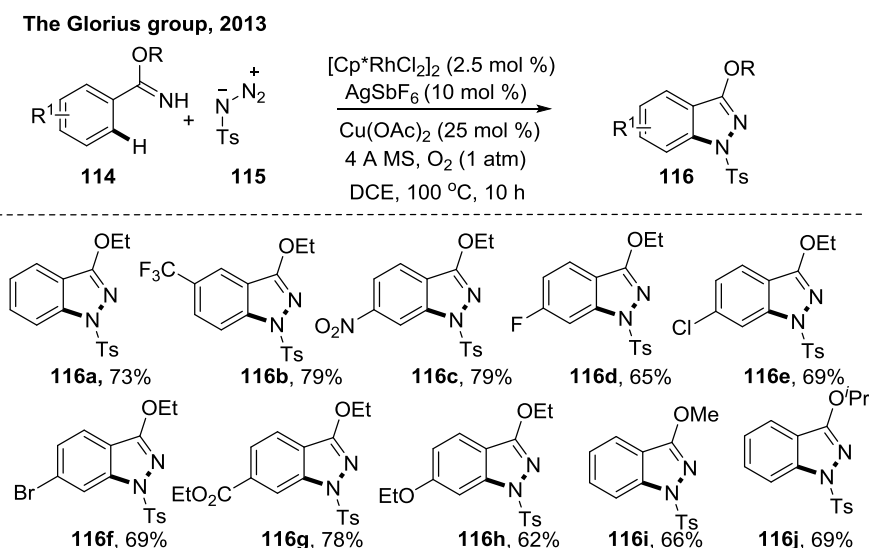
52).⁸¹ NH-sulfoximines was used as directing group and this protocol afforded wide range of thiadiazine 1-oxides.



Scheme 52. Ir-catalyzed (sp^2)C-H amidation/cyclisation cascade with *N*-alkoxyamides

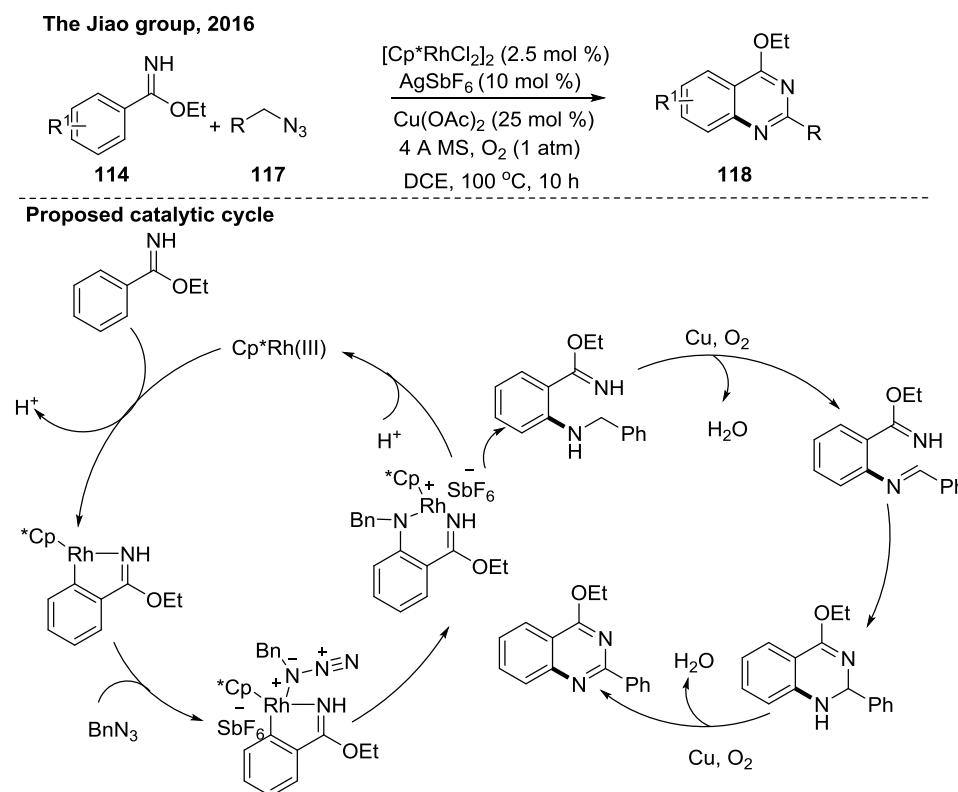
Synthesis of various *N*-heterocycles synthesis *via* C-H amination/cyclisation cascade reactions using organic azides are reported by many research groups which are also nicely reviewed recently by Hu group.^{49c} So without elaborately discussing we will mention some early findings on this type of reactions.

For example, the Glorius group in 2013 reported the synthesis of indazoles through a Rh^{III} -catalyzed C–H activation/C–N bond formation and Cu-catalyzed N–N bond formation cascade using organic azides as amine source and NH imidates as directing group (**Scheme 53**).⁸² They first introduced these N-H-imidates as directing groups in C–H activation. C-H amination product is formed through Rh-catalysed nitrenoid formation. After that the *ortho* C-H amination product undergoes a copper catalysed N-N bond formation furnishing the indazoles. The methodology showed good functional group tolerance with moderate to good yield of products.



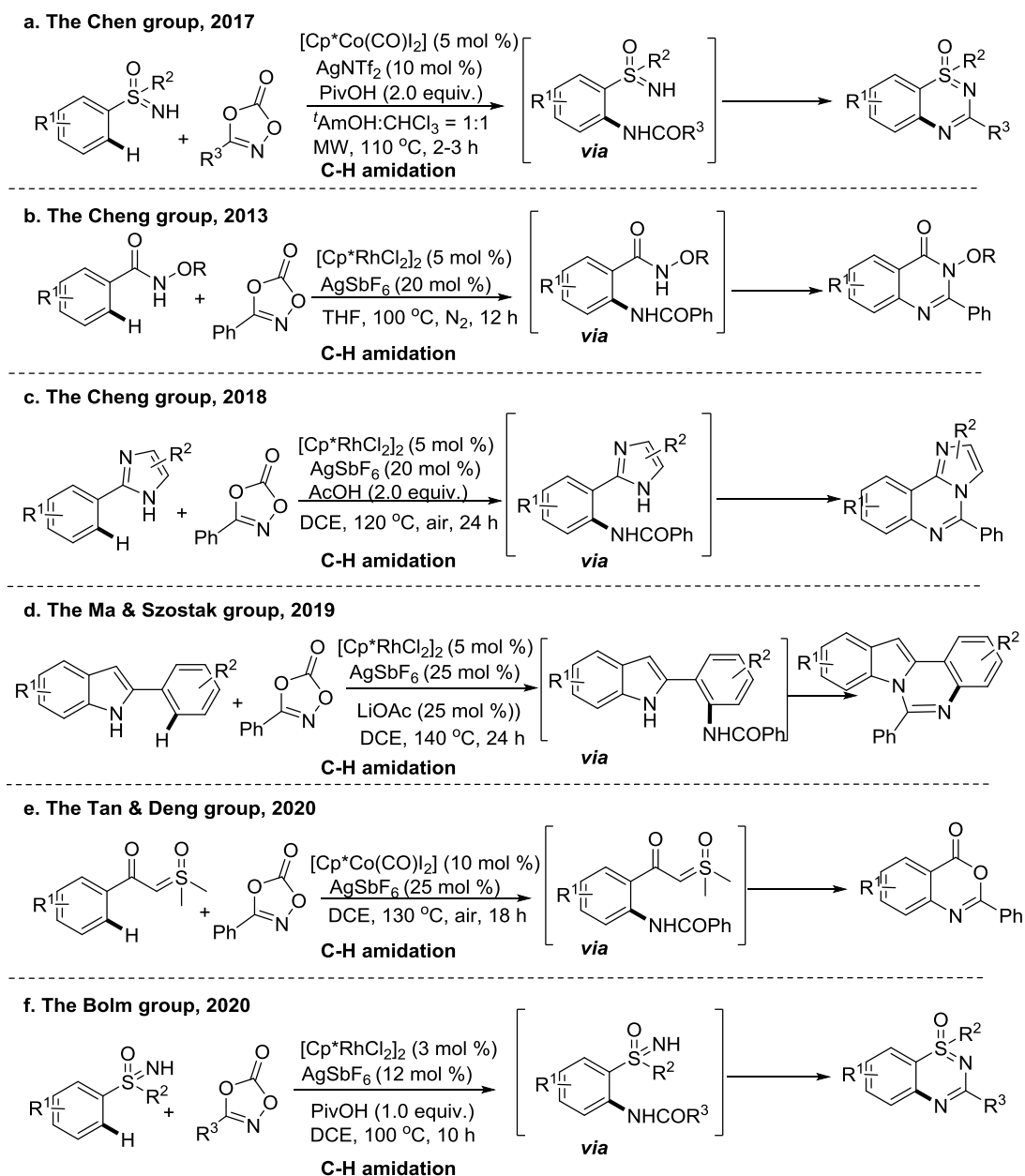
Scheme 53. Synthesis of indazoles through C–H amination/N-N bond formation cascade with azides

Then in 2016 the Jiao group disclosed a Rh^{III}-catalysed C-H amination with organic azides followed by a copper co-catalysed annulation cascade to afford a library of quinazoline derivatives (**Scheme 54**).⁸³ C-H amination follows the general catalytic cycle through Rh-nitrenoid formation. Then the *ortho* amination product undergoes Cu-catalysed oxidative annulation under O₂ atmosphere giving the cyclised product.



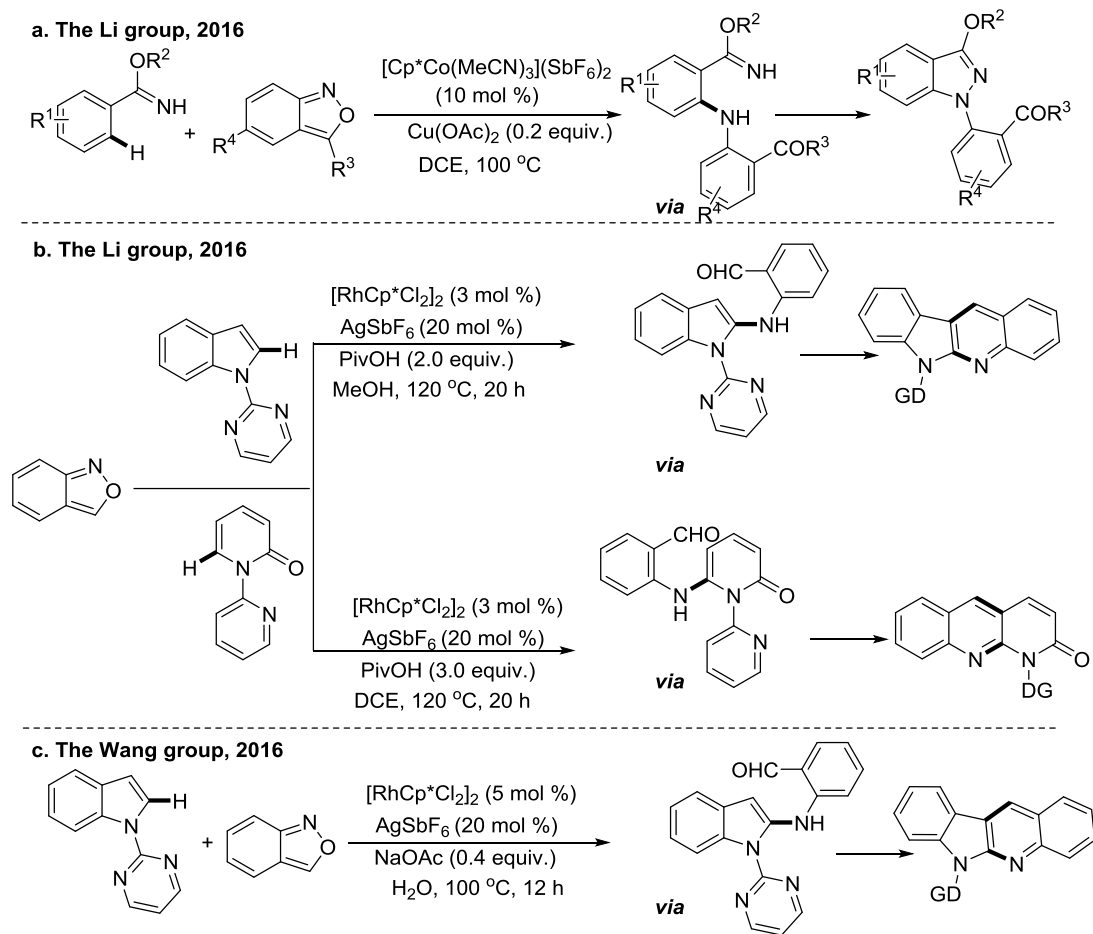
Scheme 54. Synthesis of quinazolines through C–H amination/oxidative cyclisation cascade

Dioxazolones are important C-H amidating agent which generates a tethered carbonyl of the amide after C-H amidation. This carbonyl can easily undergo cyclisation followed by condensation with many NH groups placed in suitable positions affording many valuable N-heterocycles.⁸⁴ Some of them are shown below (**Scheme 55**)



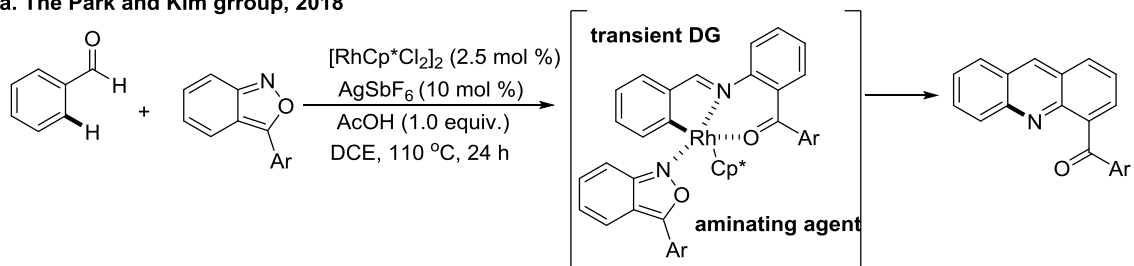
Scheme 55. Synthesis of various *N*-heterocycles through C–H amidation/cyclisation cascade using dioxazolones

Anthranils are also similarly leaves a tethered carbonyl after C-H amination. This carbonyl can easily undergo cyclisation followed by condensation with many N or carbon nucleophiles placed in suitable positions affording many valuable *N*-heterocycles.⁸⁵ Some of them are shown below (**Scheme 56-57**).

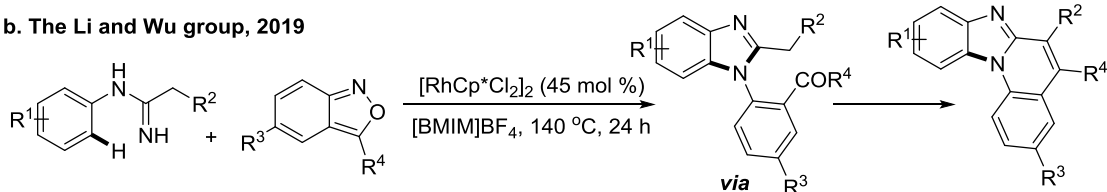


Scheme 56. Synthesis of various *N*-heterocycles through C–H amination/cyclisation cascade using antranils

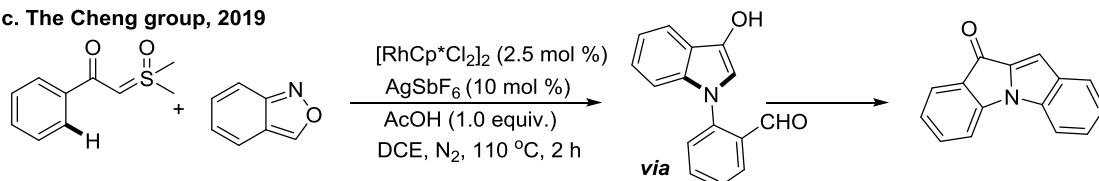
a. The Park and Kim group, 2018



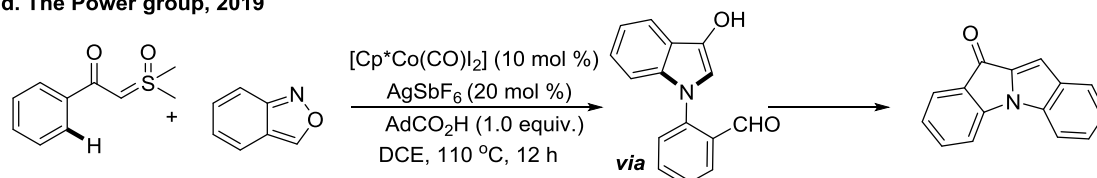
b. The Li and Wu group, 2019



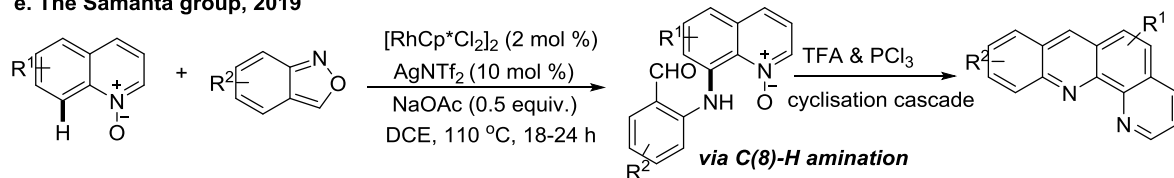
c. The Cheng group, 2019



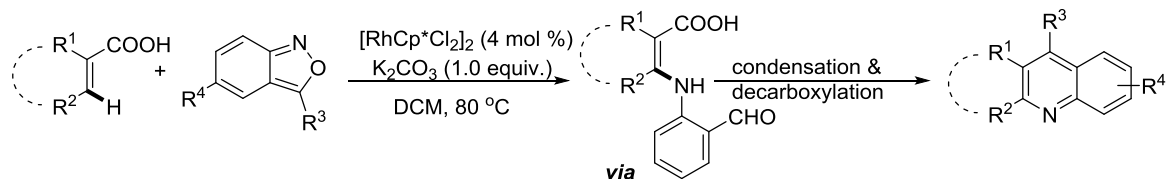
d. The Power group, 2019



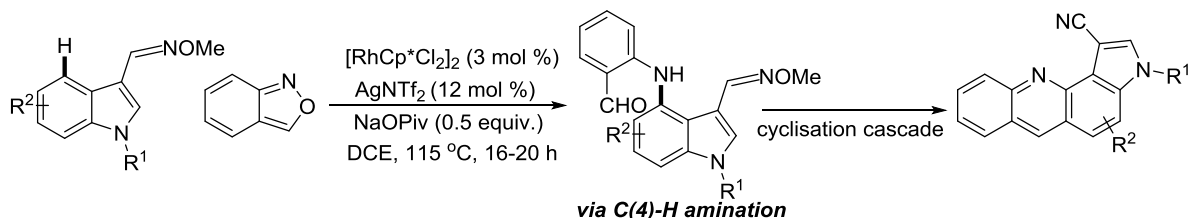
e. The Samanta group, 2019



f. The Gao and Hu group, 2020



g. The Samanta group, 2020



Scheme 57. Synthesis of other *N*-heterocycles through C–H amination/cyclisation cascade using anthranils

I.9. Conclusion

Development of transition-metal catalysed direct C–H amination of hydrocarbons has become an important synthetic tool enabling the direct introduction of amino functional groups at the desired position. In this direction, electrophilic amination strategy with umpolung concept addresses many problems associated with nucleophilic aminations with free amines offering several advantages such as broad scope, milder conditions, lower catalysts loading and notably the ability to functionalize typically unreactive bonds and these reagents act as mild oxidants and most of the C-H amination reactions take place in overall redox-neutral conditions without using external strong metal oxidants. This is why significant efforts have been dedicated towards the development of this umpolung strategy with reversal of polarity of the amine nitrogen source (equivalents to the R_2N^+ synthon). Beside single C-N bond forming reactions these electrophilic aminating reagents are able to furnish many valuable azacycles through C-H amination followed by cyclisation cascades. Although having remarkable progresses on this field using expensive second and third row transition metals, a limited number of works has been achieved under first row transition metal catalysis. So, the development of C-H amination protocols with these electrophilic amines using earth-abundant first-row transition metals is in high demand. Also it is envisioned that the scope of substrates in the direct C–H amination can be expanded from simple hydrocarbons to complex molecules enabling the late-stage introduction of amino functionality even in the presence of labile functional groups. Design, synthesis and application of more versatile electrophilic amino group surrogates that are convenient and environmentally friendly are highly desirable especially from a practical point of view.

I.10. References

1. N. Kerru, L. Gummidi, S. Maddila, K. K. Gangu, S. B. Jonnalagadda, *Molecules*, 2020, **25**, 1909.
2. a) M. M. Heravi, V. Zadsirjan, *RSC Adv.*, 2020, **10**, 44247-44311; b) P. Martins, J. Jesus, S. Santos, L. R. Raposo, C. Roma-Rodrigues, P. V. Baptista, A. R. Fernandes, *Molecules*, 2015, **20**, 16852-16891; c) G. Li Petri, M. V. Raimondi, V. Spanò, R. Holl, P. Barraja, A. Montalbano, *Top. Curr. Chem.*, 2021, **379**, 34.
3. E. Vitaku, D. T. Smith, J. T. Njardarson, *J. Med. Chem.*, 2014, **57**, 10257-10274.
4. G. Roman, *Eur. J. Med. Chem.*, 2015, **89**, 743-816.

5. D. T. Ko, H. M. Krumholz, J. V. Tu, P. C. Austin, T. A. Stukel, M. Koh, A. Chong, J. F. de Melo, C. A. Jackevicius, *Circulation: Cardiovascular Quality and Outcomes*, 2018, **11**, e004194.
6. a) G. Dyker, *Angew. Chem. Int. Ed.*, 1999, **38**, 1698-1712; b) J. Magano, J. R. Dunetz, *Chem. Rev.*, 2011, **111**, 2177-2250.
7. J. Bariwal, E. Van der Eycken, *Chem. Soc. Rev.*, 2013, **42**, 9283-9303.
8. B. Seifinoferest, A. Tanbakouchian, B. Larijani, M. Mahdavi, *Asian J. Org. Chem*, 2021, **10**, 1319-1344.
9. M. J. West, J. W. B. Fyfe, J. C. Vantourout, A. J. B. Watson, *Chem. Rev.*, 2019, **119**, 12491-12523.
10. I. Munir, A. F. Zahoor, N. Rasool, S. A. R. Naqvi, K. M. Zia, R. Ahmad, *Mol. Divers.*, 2019, **23**, 215-259.
11. a) S. K. Ghorai, V. G. Gopalsamuthiram, A. M. Jawalekar, R. E. Patre, S. Pal, *Tetrahedron*, 2017, **73**, 1769-1794; b) G. Cahiez, A. Moyeux, *Chem. Rev.*, 2010, **110**, 1435-1462; c) M. Marín, R. J. Rama, M. C. Nicasio, *Chem. Record*, 2016, **16**, 1819-1832.
12. a) J. Twilton, C. Le, P. Zhang, M. H. Shaw, R. W. Evans, D. W. C. MacMillan, *Nat. Rev. Chem.*, 2017, **1**, 0052; b) C. Cavedon, P. H. Seeberger, B. Pieber, *Eur. J. Org. Chem.*, 2020, **2020**, 1379-1392.
13. a) H. Lin, D. Sun, *Org. Prep. Proced. Int.*, 2013, **45**, 341-394; b) F. Monnier, M. Taillefer, *Angew. Chem. Int. Ed.*, 2009, **48**, 6954-6971; c) C. Sambigao, S. P. Marsden, A. J. Blacker, P. C. McGowan, *Chem. Soc. Rev.*, 2014, **43**, 3525-3550.
14. a) P. Ruiz-Castillo, S. L. Buchwald, *Chem. Rev.*, 2016, **116**, 12564-12649; b) R. Dorel, C. P. Grugel, A. M. Haydl, *Angew. Chem. Int. Ed.*, 2019, **58**, 17118-17129.
15. J.-Q. Chen, J.-H. Li, Z.-B. Dong, *Adv. Synth. Catal.*, 2020, **362**, 3311-3331.
16. Y. Park, Y. Kim, S. Chang, *Chem. Rev.*, 2017, **117**, 9247-9301.
17. a) X.-G. Liu, H. Gao, S.-S. Zhang, Q. Li, H. Wang, *ACS Catal.*, 2017, **7**, 5078-5086; b) H. Huang, X. Ji, W. Wu, H. Jiang, *Chem. Soc. Rev.*, 2015, **44**, 1155-1171; c) J. Mo, L. Wang, Y. Liu, X. Cui, *Synthesis*, 2015, **47**, 439-459; d) B. Liu, C. Song, C. Sun, S. Zhou, J. Zhu, *J. Am. Chem. Soc.*, 2013, **135**, 16625-16631; e) B. Qi, L. Fang, Q. Wang, S. Guo, P. Shi, B. Chu, J. Zhu, *Tet. Lett.*, 2020, **61**, 151771.
18. a) X. Yan, X. Yang, C. Xi, *Catal. Sci. Technol.*, 2014, **4**, 4169-4177; b) M. Corpet, C. Gosmini, *Synthesis*, 2014, **46**, 2258-2271.
19. L. G. O'Neil, J. F. Bower, *Angew. Chem. Int. Ed.*, 2021, **60**, 25640-25666.

20. T. Kawano, K. Hirano, T. Satoh, M. Miura, *J. Am. Chem. Soc.*, 2010, **132**, 6900-6901.
21. a) K.-H. Ng, Z. Zhou, W.-Y. Yu, *Org. Lett.*, 2012, **14**, 272-275; b) C. Grohmann, H. Wang, F. Glorius, *Org. Lett.*, 2012, **14**, 656-659.
22. K.-H. Ng, Z. Zhou, W.-Y. Yu, *Chem. Commun.*, 2013, **49**, 7031-7033.
23. T. Matsubara, S. Asako, L. Ilies, E. Nakamura, *J. Am. Chem. Soc.*, 2014, **136**, 646-649.
24. F.-N. Ng, Z. Zhou, W.-Y. Yu, *Chem. Eur. J.*, 2014, **20**, 4474-4480.
25. S. Sabir, G. Kumar, J. L. Jat, *Org. Biomol. Chem.*, 2018, **16**, 3314-3327.
26. H. Lebel, K. Huard, *Org. Lett.*, 2007, **9**, 639-642.
27. K. Huard, H. Lebel, *Chem. Eur. J.*, 2008, **14**, 6222-6230.
28. K.-H. Ng, A. S. C. Chan, W.-Y. Yu, *J. Am. Chem. Soc.*, 2010, **132**, 12862-12864.
29. K.-H. Ng, F.-N. Ng, W.-Y. Yu, *Chem. Commun.*, 2012, **48**, 11680-11682.
30. H. M. D. Bandara, D. Jin, M. A. Mantell, K. D. Field, A. Wang, R. P. Narayanan, N. A. Deskins, M. H. Emmert, *Catal. Sci. Technol.*, 2016, **6**, 5304-5310.
31. A. John, J. Byun, K. M. Nicholas, *Chem. Commun.*, 2013, **49**, 10965-10967.
32. A. Wang, N. J. Venditto, J. W. Darcy, M. H. Emmert, *Organometallics*, 2017, **36**, 1259-1268.
33. K. Arai, Y. Ueda, K. Morisaki, T. Furuta, T. Sasamori, N. Tokitoh, T. Kawabata, *Chem. Commun.*, 2018, **54**, 2264-2267.
34. A. V. G. Prasanthi, S. Begum, H. K. Srivastava, S. K. Tiwari, R. Singh, *ACS Catal.*, 2018, **8**, 8369-8375.
35. P. Paudyal Mahesh, M. Adebessin Adeniyi, R. Burt Scott, H. Ess Daniel, Z. Ma, L. Kürti, R. Falck John, *Science*, 2016, **353**, 1144-1147.
36. L. Legnani, G. Prina Cerai, B. Morandi, *ACS Catal.*, 2016, **6**, 8162-8165.
37. J. Liu, K. Wu, T. Shen, Y. Liang, M. Zou, Y. Zhu, X. Li, X. Li, N. Jiao, *Chem. Eur. J.*, 2017, **23**, 563-567.
38. X. Dong, Q. Liu, Y. Dong, H. Liu, *Chem. Eur. J.*, 2017, **23**, 2481-2511.
39. E. J. Yoo, S. Ma, T.-S. Mei, K. S. L. Chan, J.-Q. Yu, *J. Am. Chem. Soc.*, 2011, **133**, 7652-7655.
40. M. Shang, S.-Z. Sun, H.-X. Dai, J.-Q. Yu, *Org. Lett.*, 2014, **16**, 5666-5669.
41. K. Wu, Z. Fan, Y. Xue, Q. Yao, A. Zhang, *Org. Lett.*, 2014, **16**, 42-45.
42. Y. Xue, Z. Fan, X. Jiang, K. Wu, M. Wang, C. Ding, Q. Yao, A. Zhang, *Eur. J. Org. Chem.*, 2014, **2014**, 7481-7488.
43. C. Grohmann, H. Wang, F. Glorius, *Org. Lett.*, 2013, **15**, 3014-3017.

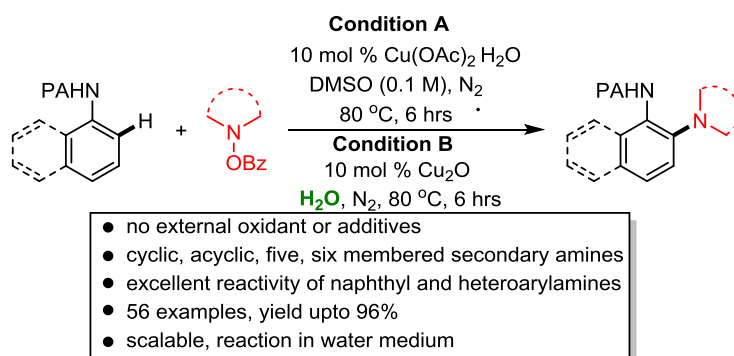
44. D. Zhu, G. Yang, J. He, L. Chu, G. Chen, W. Gong, K. Chen, M. D. Eastgate, J.-Q. Yu, *Angew. Chem. Int. Ed.*, 2015, **54**, 2497-2500.
45. J. He, T. Shigenari, J.-Q. Yu, *Angew. Chem. Int. Ed.*, 2015, **54**, 6545-6549.
46. Q. Gou, G. Liu, Z.-N. Liu, J. Qin, *Chem. Eur. J.*, 2015, **21**, 15491-15495.
47. Y. Shin, S. Han, U. De, J. Park, S. Sharma, N. K. Mishra, E.-K. Lee, Y. Lee, H. S. Kim, I. S. Kim, *J. Org. Chem.*, 2014, **79**, 9262-9271.
48. a) D. Lee, S. Chang, *Chem. Eur. J.*, 2015, **21**, 5364-5368; b) J. Ryu, K. Shin, S. H. Park, J. Y. Kim, S. Chang, *Angew. Chem. Int. Ed.*, 2012, **51**, 9904-9908; c) Y. Lian, J. R. Hummel, R. G. Bergman, J. A. Ellman, *J. Am. Chem. Soc.*, 2013, **135**, 12548-12551; d) H. Kim, G. Park, J. Park, S. Chang, *ACS Catal.*, 2016, **6**, 5922-5929; e) X. Dong, P. Ma, T. Zhang, H. B. Jalani, G. Li, H. Lu, *J. Org. Chem.*, 2020, **85**, 13096-13107.
49. a) K. Shin, H. Kim, S. Chang, *Acc. Chem. Res.*, 2015, **48**, 1040-1052; b) D. Intrieri, P. Zardi, A. Caselli, E. Gallo, *Chem. Commun.*, 2014, **50**, 11440-11453; c) Z.-K. Liu, Q.-Q. Zhao, Y. Gao, Y.-X. Hou, X.-Q. Hu, *Adv. Synth. Catal.*, 2021, **363**, 411-424.
50. a) E. Differding, H. Ofner, *Synlett*, 1991, **1991**, 187-189; b) A. Rostami, *Synlett*, 2007, **2007**, 2924-2925.
51. Q. Gu, E. Vessally, *RSC Adv.*, 2020, **10**, 16756-16768.
52. a) N. Momiyama, H. Yamamoto, *Angew. Chem. Int. Ed.*, 2002, **41**, 2986-2988; b) S. P. Brown, M. P. Brochu, C. J. Sinz, D. W. C. MacMillan, *J. Am. Chem. Soc.*, 2003, **125**, 10808-10809.
53. a) A. Purkait, S. K. Roy, H. K. Srivastava, C. K. Jana, *Org. Lett.*, 2017, **19**, 2540-2543; b) S. K. Roy, A. Tiwari, M. Saleem, C. K. Jana, *Chem. Commun.*, 2018, **54**, 14081-14084.
54. B. Zhou, J. Du, Y. Yang, H. Feng, Y. Li, *Org. Lett.*, 2013, **15**, 6302-6305.
55. J. Du, Y. Yang, H. Feng, Y. Li, B. Zhou, *Chem. Eur. J.*, 2014, **20**, 5727-5731.
56. a) B. Zhou, J. Du, Y. Yang, H. Feng, Y. Li, *Org. Lett.*, 2014, **16**, 592-595; b) W. Yang, J. Sun, X. Xu, Q. Zhang, Q. Liu, *Chem. Commun.*, 2014, **50**, 4420-4422.
57. a) M. Kitamura, K. Narasaka, *Chem. Record*, 2002, **2**, 268-277; b) K. Narasaka, M. Kitamura, *Eur. J. Org. Chem.*, 2005, **2005**, 4505-4519.
58. T. Gerfaud, L. Neuville, J. Zhu, *Angew. Chem. Int. Ed.*, 2009, **48**, 572-577.
59. Y. Tan, J. F. Hartwig, *J. Am. Chem. Soc.*, 2010, **132**, 3676-3677.
60. L.-L. Xu, X. Wang, B. Ma, M.-X. Yin, H.-X. Lin, H.-X. Dai, J.-Q. Yu, *Chem. Sci.*, 2018, **9**, 5160-5164.

61. a) C. Tang, M. Zou, J. Liu, X. Wen, X. Sun, Y. Zhang, N. Jiao, *Chem. Eur. J.*, 2016, **22**, 11165-11169; b) S. Yu, G. Tang, Y. Li, X. Zhou, Y. Lan, X. Li, *Angew. Chem. Int. Ed.*, 2016, **55**, 8696-8700.
62. M. Zou, J. Liu, C. Tang, N. Jiao, *Org. Lett.*, 2016, **18**, 3030-3033.
63. M. Wang, L. Kong, F. Wang, X. Li, *Adv. Synth. Catal.*, 2017, **359**, 4411-4416.
64. M. Jeon, J. Park, P. Dey, Y. Oh, H. Oh, S. Han, S. H. Um, H. S. Kim, N. K. Mishra, I. S. Kim, *Adv. Synth. Catal.*, 2017, **359**, 3471-3478.
65. a) H. Li, J. Jie, S. Wu, X. Yang, H. Xu, *Org. Chem. Front.*, 2017, **4**, 250-254; b) N. K. Mishra, M. Jeon, Y. Oh, H. Jo, J. Park, S. Han, S. Sharma, S. H. Han, Y. H. Jung, I. S. Kim, *Org. Chem. Front.*, 2017, **4**, 241-249.
66. T. Fu, J. Yang, H. Sun, C. Zhang, H. Xiang, X. Zhou, *Asian J. Org. Chem*, 2018, **7**, 1844-1848.
67. R.-H. Liu, Q.-C. Shan, X.-H. Hu, T.-P. Loh, *Chem. Commun.*, 2019, **55**, 5519-5522.
68. L. Liu, Z. Zhang, Y. Wang, Y. Zhang, J. Li, *Synthesis*, 2020, **52**, 3881-3890.
69. Y. Gao, J. Nie, Y. Li, G. Liao, Y. Huo, X.-Q. Hu, *ChemCatChem*, 2020, **12**, 2721-2725.
70. S. Y. Hong, Y. Hwang, M. Lee, S. Chang, *Acc. Chem. Res.*, 2021, **54**, 2683-2700.
71. J. Park, S. Chang, *Angew. Chem. Int. Ed.*, 2015, **54**, 14103-14107.
72. a) P. T. W. J. C. Anastas, *Green chemistry : theory and practice*, Oxford University Press, Oxford 1998; b) A. S. Matlack, *Introduction to green chemistry*, Marcel Dekker, New York, 2001.
73. a) N. Della Ca', M. Fontana, E. Motti, M. Catellani, *Acc. Chem. Res.*, 2016, **49**, 1389-1400; b) J. Wang, G. Dong, *Chem. Rev.*, 2019, **119**, 7478-7528.
74. A. Whyte, M. E. Olson, M. Lautens, *Org. Lett.*, 2018, **20**, 345-348.
75. Q. Gao, Z.-S. Liu, Y. Hua, L. Li, H.-G. Cheng, H. Cong, Q. Zhou, *Chem. Commun.*, 2019, **55**, 8816-8819.
76. J. Li, Y. Yang, Y. Liu, Q. Liu, L. Zhang, X. Li, Y. Dong, H. Liu, *Org. Lett.*, 2021, **23**, 2988-2993.
77. A. J. Rago, G. Dong, *Org. Lett.*, 2021, **23**, 3755-3760.
78. L. Fan, J. Hao, J. Yu, X. Ma, J. Liu, X. Luan, *J. Am. Chem. Soc.*, 2020, **142**, 6698-6707.
79. H. Huang, X. Ji, X. Tang, M. Zhang, X. Li, H. Jiang, *Org. Lett.*, 2013, **15**, 6254-6257.
80. Q. Wang, X. Li, *Org. Lett.*, 2016, **18**, 2102-2105.

81. H.-B. Xu, J.-H. Yang, X.-Y. Chai, Y.-Y. Zhu, L. Dong, *Org. Lett.*, 2020, **22**, 2060-2063.
82. D.-G. Yu, M. Suri, F. Glorius, *J. Am. Chem. Soc.*, 2013, **135**, 8802-8805.
83. Wang, N. Jiao, *Org. Lett.*, 2016, **18**, 2150-2153.
84. a) J. Huang, Y. Huang, T. Wang, Q. Huang, Z. Wang, Z. Chen, *Org. Lett.*, 2017, **19**, 1128-1131; b) H. Xiong, S. Xu, S. Sun, J. Cheng, *Org. Chem. Front.*, 2018, **5**, 2880-2884; c) X. Wu, S. Sun, S. Xu, J. Cheng, *Adv. Synth. Catal.*, 2018, **360**, 1111-1115; d) X. Wang, J. Zhang, D. Chen, B. Wang, X. Yang, Y. Ma, M. Szostak, *Org. Lett.*, 2019, **21**, 7038-7043; e) Y. Yu, Z. Xia, Q. Wu, D. Liu, L. Yu, Y. Xiao, Z. Tan, W. Deng, G. Zhu, *Chin. Chem. Lett.*, 2021, **32**, 1263-1266; f) P. Shi, Y. Tu, C. Wang, D. Kong, D. Ma, C. Bolm, *Org. Lett.*, 2020, **22**, 8842-8845.
85. a) S. Yu, Y. Li, X. Zhou, H. Wang, L. Kong, X. Li, *Org. Lett.*, 2016, **18**, 2812-2815; b) L. Shi, B. Wang, *Org. Lett.*, 2016, **18**, 2820-2823; c) S. Kim, S. H. Han, N. K. Mishra, R. Chun, Y. H. Jung, H. S. Kim, J. S. Park, I. S. Kim, *Org. Lett.*, 2018, **20**, 4010-4014; d) Y. Hu, T. Wang, Y. Liu, R. Nie, N. Yang, Q. Wang, G.-B. Li, Y. Wu, *Org. Lett.*, 2020, **22**, 501-504; e) X. Wu, Y. Xiao, S. Sun, J.-T. Yu, J. Cheng, *Org. Lett.*, 2019, **21**, 6653-6657; f) Y. N. Aher, A. B. Pawar, *Chem. Commun.*, 2021, **57**, 7164-7167; g) A. Biswas, S. Sarkar, R. Samanta, *Chem. Eur. J.*, 2019, **25**, 3000-3004; h) Y. Gao, J. Nie, Y. Li, X. Li, Q. Chen, Y. Huo, X.-Q. Hu, *Org. Lett.*, 2020, **22**, 2600-2605; i) A. Biswas, S. Bera, P. Poddar, D. Dhara, R. Samanta, *Chem. Commun.*, 2020, **56**, 1440-1443; j) L. Li, H. Wang, S. Yu, X. Yang, X. Li, *Org. Lett.*, 2016, **18**, 3662-3665.

Chapter II

Copper-Catalyzed Electrophilic *Ortho*-C(sp²)-H Amination of Aryl Amines: Dramatic Reactivity of Bicyclic System



Abstract: A practical copper-catalyzed, 2-picolinamide directed *ortho*-C–H amination of anilines with benzoyl protected hydroxylamines has been disclosed that proceeds smoothly without any external stoichiometric oxidant or additives. Remarkably, besides anilines, bicyclic naphthyl or heterocyclic amines furnished amination products with five- and six-membered cyclic and acyclic amines at the *ortho*-position selectively. This electrophilic C–H amination also proceeds smoothly in water under slightly modified reaction conditions.

H. M. Begam, R. Choudhury, A. Behera, R. Jana, *Org. Lett.* 2019, **21**, 4651–4656.

Copper-catalyzed electrophilic *ortho* C(sp²)–H amination of picolinamide protected aryl amines for the synthesis of 2-amino anilides with dramatic reactivity found in bicyclic system

II. 1. Introduction

2-Aminoanilide moiety is essential structural motif seen in many drug candidates which are used for the treatment of cancer, Alzheimer's disease, wet age-related macular degeneration (wet AMD) and infectious diseases.¹ Some 2-aminoanilide based bioactive compounds are shown below (**Figure 1**). The *ortho*-aminoanilines precursors were generally made by S_NAr reactions followed by reduction. But this method is limited in scope and also uses harsh reaction conditions. Therefore, development of novel methodology for the synthesis of structurally diverse this important scaffold is highly desirable.

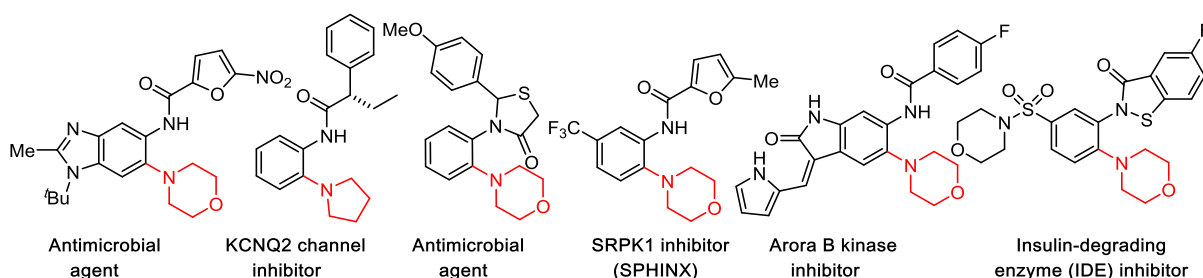
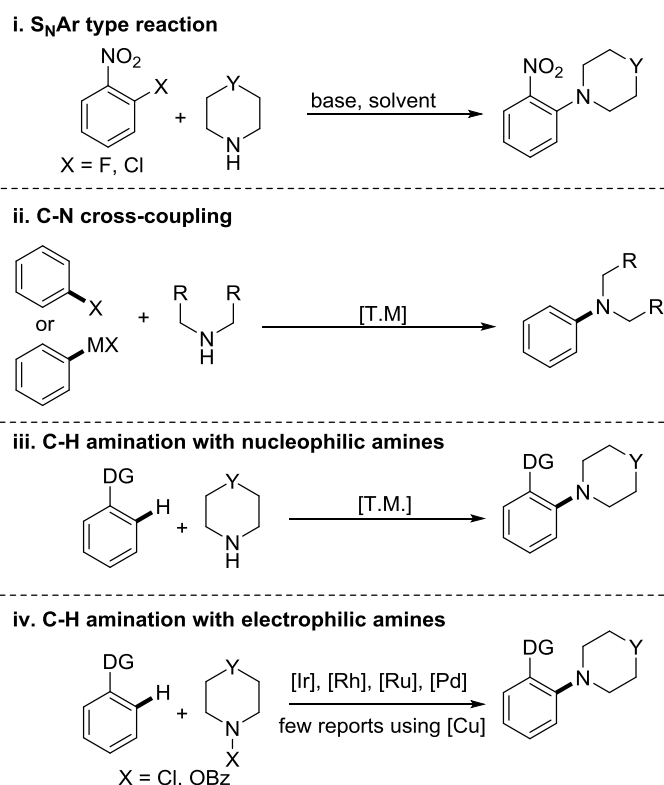


Figure 1. Some selected examples of 2-aminoanilide containing bio-active molecules

In this context, C-N bond forming cross-coupling reactions (Ullmann-Goldberg, Buchwald-Hartwig and Chan-Lam coupling) have been extensively used since last three decades.² As discussed in chapter I despite of their tremendous applications in the field of C-N bond formation they suffer from some limitations and to circumvent many of those problems C-H amination reactions came into the market. To get rapid access to a library *ortho*-aminoanilines for SAR studies C-H amination would be an excellent tool over the S_NAr or C-N cross-coupling reactions because here non-prefunctionalised hydrocarbons (C-H instead of C-X bonds) can undergo amination forming the C-N bond.³ Initially, C-H aminations have been extensively studied with nucleophilic free amines but later, researchers found that they suffer from many limitations, such as harsh reaction conditions that include high temperatures, strong oxidants, or acidic or basic additives and higher catalyst loading probably due to inhibition by the free amines. Later on another strategy with the reversal of polarity of the reacting *N*-centre i.e. with umpolung concept came out to solve many of the problems associated with nucleophilic amines. In most of these amine sources the N atom is attached to electronegative atoms such as O or Cl. Expensive second and third row metals such as Rh, Ir, Pd, Ru have been dominated the field of C-H aminations using these electrophilic amines.⁴ C-H amination

reactions achieved using these novel electrophilic aminating reagents are elaborately discussed in chapter I. Although having some examples of electrophilic C-H amination using copper, cobalt and iron catalysts, methods based on earth-abundant 3d transition metals are still in demand. Their demand is increasing not only for their cost effective and earth abundant nature but as they meet many principles of green chemistry.⁵ Although the C-H amination reactions with arylamines has been studied extensively, but installation of aliphatic amines through C-H activation is limited in number.⁶

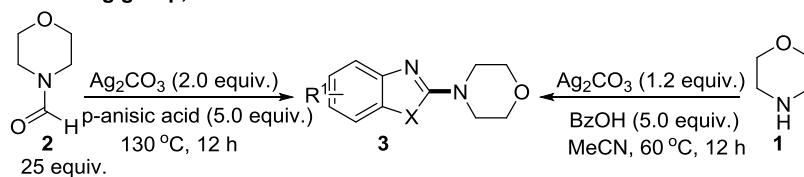


Scheme 1. Synthesis of aliphatic amino containing molecules

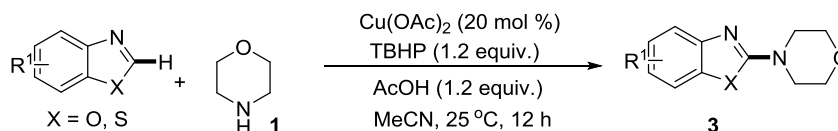
II. 2. Review

The Chang group in 2009 unveiled a silver-mediated decarbonylative C-H amination of benzoxazoles using formamide as amine source (**Scheme 2a**).⁷ This decarbonylative amination using formamide needed high temperature. However, the amination with parent amines took place under milder conditions affording 2-amino benzoxazoles. This method requires stoichiometric amount of silver salts which led the same group to develop a better protocol for this transformation. So, in 2010 the same group developed a new catalytic condition for C-H amination of azoles (**Scheme 2b**).⁸ The reaction took place under much milder conditions using 2 mol % Co(OAc)₂ only and tert-butyl hydroperoxide as oxidant with a broad range of substrate scope.

a. The Chang group, 2009



b. The Chang group, 2010

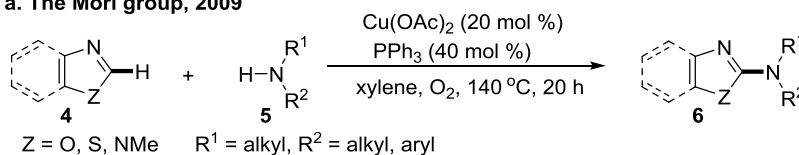


Scheme 2. Silver and copper catalyzed C-H amination of azoles

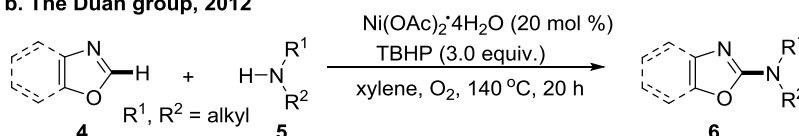
In the similar time the Mori group reported a copper catalysed amination of azoles with aliphatic amines but reaction worked at very high temperature only (**Scheme 3a**).⁹

The Duan group in 2012, reported a methodology for the C-H amination of benzoxazoles with aliphatic amines under Ni-catalysis using TBHP as oxidant for catalytic turnover (**Scheme 3b**).¹⁰ This reaction proceeded at lower temperature 70 °C. A library of differently substituted benzoxazol-2-amines were produced in medium to good yields.

a. The Mori group, 2009



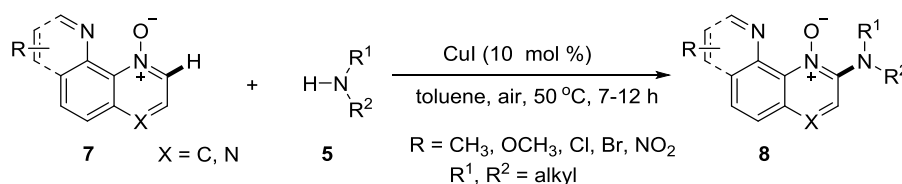
b. The Duan group, 2012



Scheme 3. Copper and nickel catalyzed C-H amination of azoles

Then in 2013, the Wu and Cui group developed an efficient protocol for a dehydrogenative amination of quinolone *N*-oxides with aliphatic amines under copper catalysis with excellent yields of the products (**Scheme 4**).¹¹

The Wu and Cui group, 2013

Scheme 4. Copper catalyzed C-H amination of quinoline *N*-oxides

In 2013, the Daugulis group reported *ortho* C(sp²)-H amination of amination of 8-aminoquinoline protected benzamides under copper-silver catalytic system (**Scheme 5a**).¹²

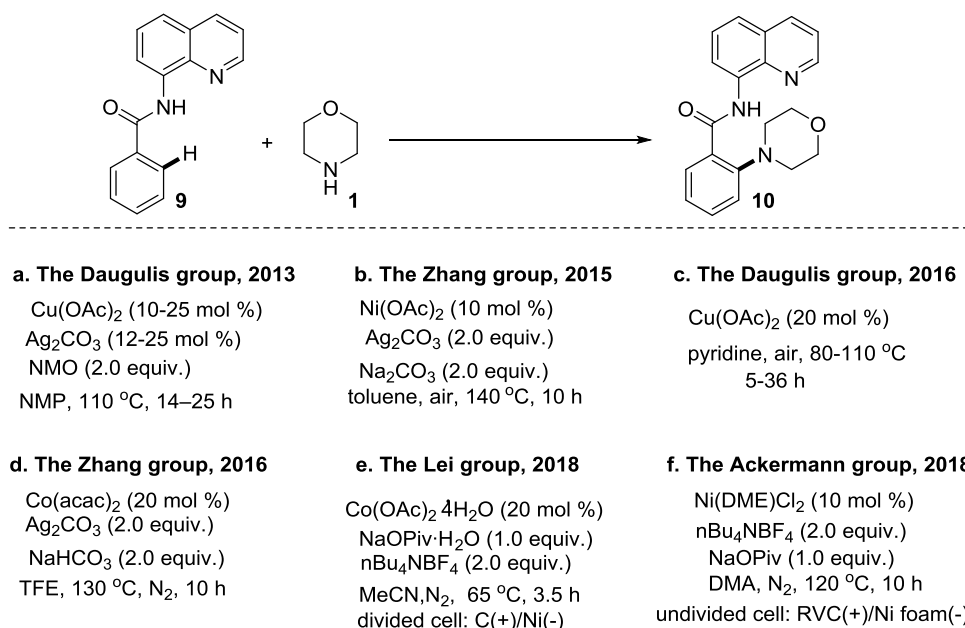
In 2015, the Zhang group a Ni-catalysed C(sp²) amination of the same substrate (**Scheme 5b**).¹³ The reaction underwent at very high temperature 140 °C and also the method required 2.0 equiv. of Ag-salt as oxidant. Their mechanistic studies suggested the involvement of Ni(II)/Ni(III) catalytic pathway.

In 2016, the Daugulis group established a general method for the same transformation under a copper catalysed condition (**Scheme 5c**).¹⁴ Therein atmospheric oxygen acted as terminal oxidant. The reaction proceeded smoothly with a variety of aliphatic primary, secondary as well as aryl amines. Many heterocycles including indoles, pyrazole, and carbazole, sulphonamides also worked well as aminating agent. One disadvantage associated with this method is that the reaction took place at very high temperature.

The Zhang group development a cobalt catalysed condition for the directed *ortho* C(sp²)-H amination of 8-aminoquinoline protected benzamides in the same year (**Scheme 5d**).¹⁵ Although this protocol offered a large number of *ortho*-amino benzamides but it used 2.0 equiv. of Ag-salt as oxidant and also the reaction took place at very high temperature.

The Lei group disclosed an efficient protocol for the same reaction under an environmentally benign cobalt catalysed electrooxidative condition in 2018 (**Scheme 5e**).¹⁶ This method underwent with very good efficacy without the need of any external oxidant offering a broad range of substrate scope with respect to both alkylamines and benzamides.

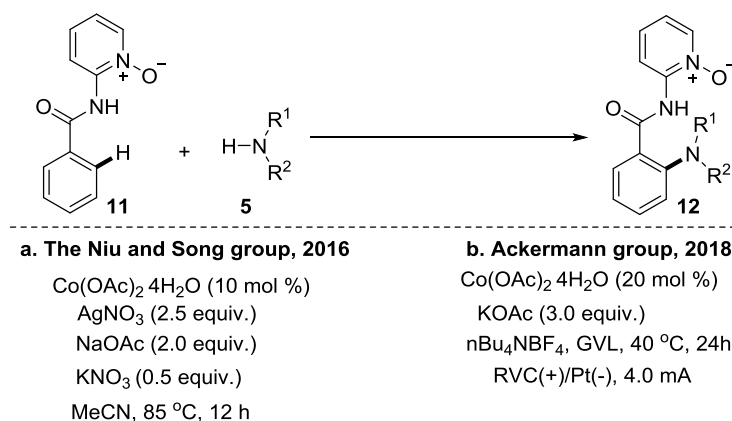
In the same year, the Ackermann group was successful to achieve the same transformation under a nickel catalysed electrochemical condition (**Scheme 5f**).¹⁷ Although this Ni-catalysed protocol afforded the products in almost similar yields but it was not efficient as cobalt catalysed method because it was performed at 120 °C. Their mechanistic studies delivered a supporting information for the involvement a nickel(II/III/IV) manifold in the catalytic cycle.



Scheme 5. First-row transition metal catalyzed C-H amination of benzamides

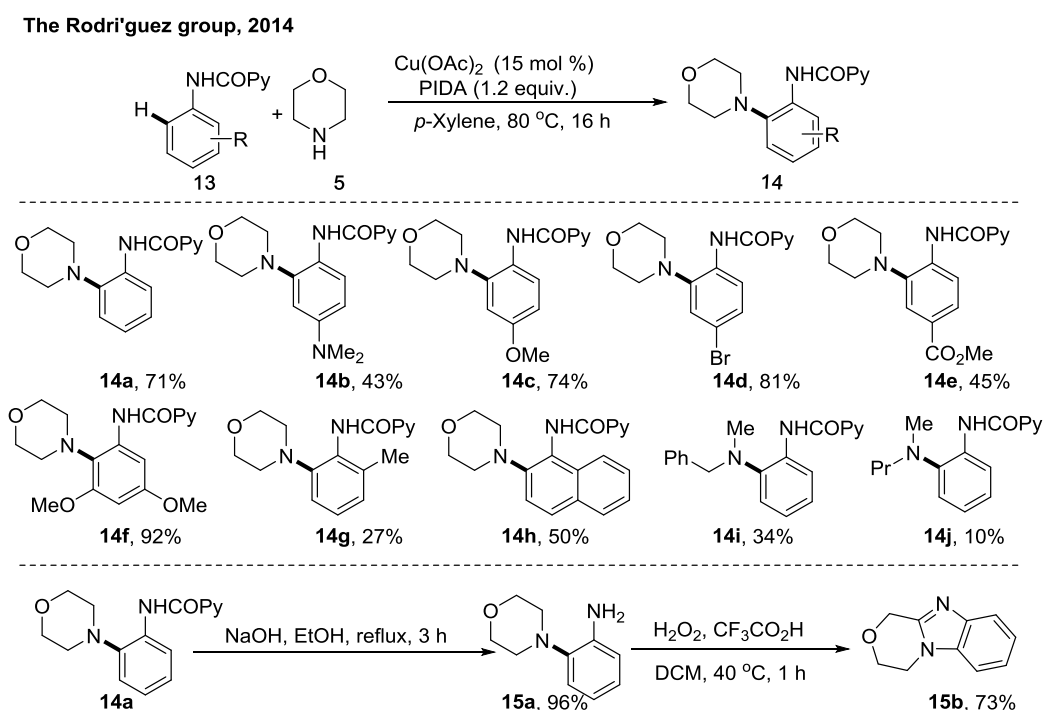
In 2016, the Niu and Song group reported a cobalt catalysed *ortho* C(sp²)-H amination of 2-benzamidopyridine 1-oxide (**Scheme 6a**).¹⁸ Using this method a variety of 2-amino substituted 2-benzamidopyridine 1-oxides were obtained. Although the reaction proceeded at lower temperature than the above method but this method required 2.5 equiv. of AgNO₃ as oxidant and two other additives (NaOAc and KNO₃) are needed in stoichiometric amount.

In 2018, the Ackermann group disclosed a proficient protocol for *ortho* C(sp²)-H amination of the same substrate under a cobalt catalysed electrochemical condition using γ -valerolactone (GVL) as renewable solvent (**Scheme 6b**).¹⁹ The reaction underwent efficiently at 40 °C without the use of any external oxidant and after the amination the catalytic regeneration was achieved by anodic oxidation.

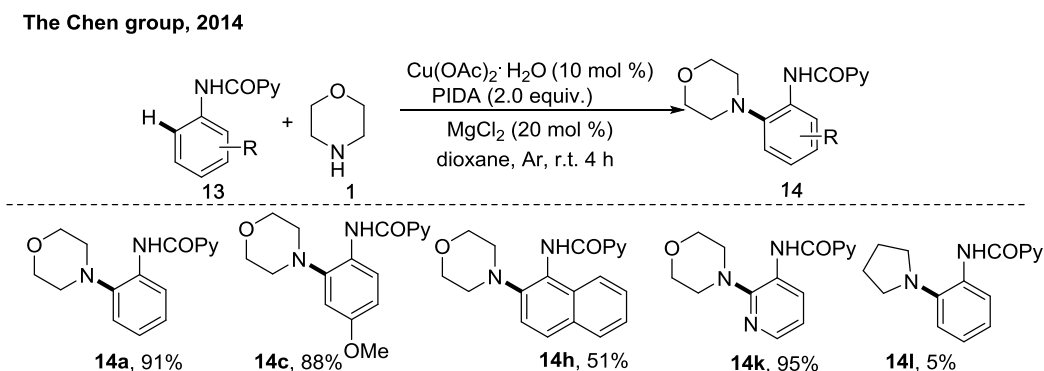


Scheme 6. Cobalt catalyzed C-H amination of 2-benzamidopyridine 1-oxides

In 2014, the Rodríguez group reported the synthesis 2-aminoanilides through copper catalyzed *ortho*-C-H amination of picolinamide protected anilines (**Scheme 7**).²⁰ They first screened various amide protections as directing group such as benzamide, picolinamide, acetamide and out of all only picolinamide protected aniline afforded the *ortho*-C-H amination product in reasonable yield. They have used 15 mol % of Cu(OAc)₂ and stoichiometric amount of expensive PhI(OAc)₂ as an oxidant which generates PhI as a byproduct. Although various *para*-, *meta*- substituted anilines gave the products in moderate yields the *ortho*- substituted anilines found to afford significantly lesser yield. They deprotected the amide and further functionalized to fused benzimidazole under acidic conditions. Bicyclic and heterocyclic systems were also found to be inferior substrates under their condition.



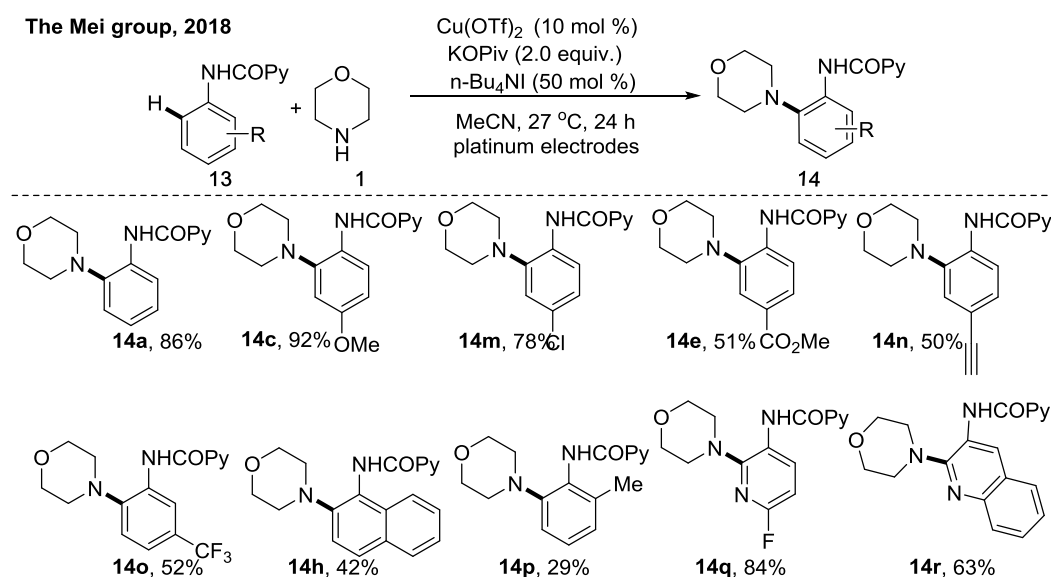
Scheme 7. Copper catalyzed *ortho* C-H amination of anilines



Scheme 8. Copper catalyzed *ortho* C-H amination of anilines at room temperature

In the same time the Chen group also independently disclosed *ortho*-C-H amination of picolinamide protected anilines with various alkylamines (**Scheme 8**).²¹ They also used 2.0 equiv. of expensive $\text{PhI}(\text{OAc})_2$ as an oxidant. The product yields were better than the previous one and worked well at room temperature. Variety of cyclic six-membered amines furnished the desired product in moderate to good yields but limitation of amination with five-membered or acyclic amines was not still overcome. Here also the bicyclic system didn't give the product in more than 51%.

In 2018, the Mei group disclosed a copper catalyzed an electrochemical procedure for *ortho* C-H amination of the same substrate using tetrabutylammonium iodide (TBAI) as a redox mediator (**Scheme 9**).²² The reaction was performed in an undivided cell at 27 °C. Unlike the previous methods this method didn't require stoichiometric external oxidants. Although the protocol offered broader substrates scope with respect to both anilines and amines, five-membered or acyclic amines were unsuccessful and bicyclic naphthylamines afforded poor yields. *Ortho*-substituted anilines were also inferior substrates.

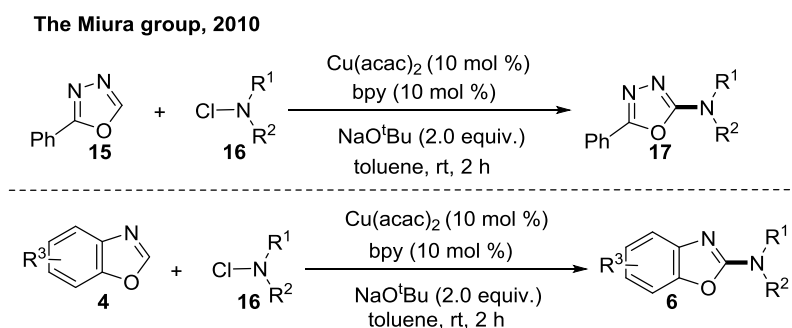


Scheme 9. Copper catalyzed electrochemical *ortho* C-H amination of anilines at room temperature

Development of a practically useful methodology for the *ortho*-C-H amination of anilines is still in need which excludes the use of stoichiometric amount of external oxidant. From green aspect of organic chemistry, development of a method for transition metal-catalysed cross-coupling or C-H functionalisation reactions in water, instead of organic solvents would afford a number of potential benefits in terms of cost, environmental impact, safety, and impurity

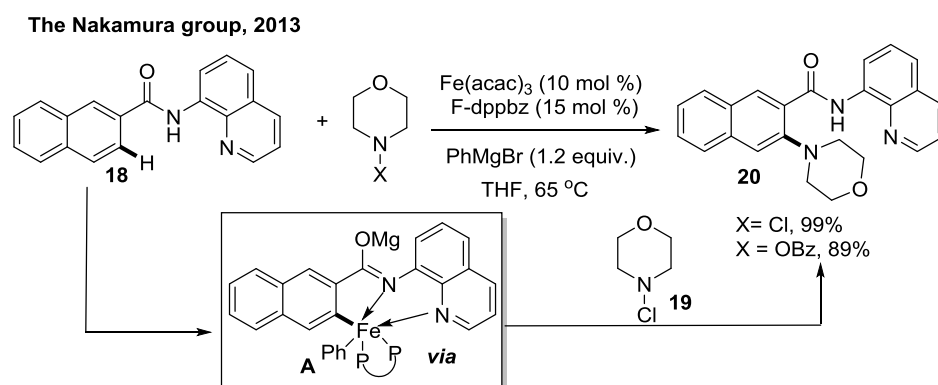
profiles. Since electrophilic amination strategy requires mild conditions with broader substrate scope we chose to utilise this strategy. In this direction, palladium, rhodium, ruthenium, and iron catalysis have been explored where a high-valent metal center is believed to be involved in the catalytic cycle. Although copper catalyzed electrophilic amination using organometallic reagents has been well-explored, electrophilic C–H amination by a copper catalyst is limited to a very few cases.

For example, the Miura group in 2010, first reported a copper catalysed heteroaromatic C–H amination with chloramines as electrophilic amine source (**Scheme 10**).²³ This copper-catalysed C–H amination of azoles took place at room temperature affording variety of heteroarylamines which are quite important in biological and medicinal chemistry.



Scheme 10. Copper catalyzed C–H amination with electrophilic chloramines

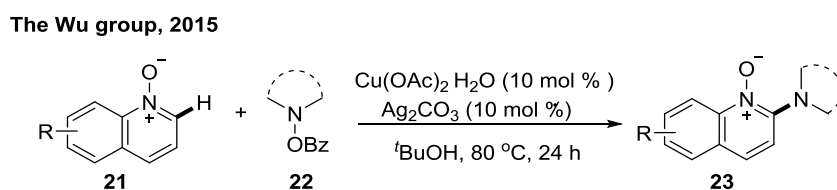
In 2013, the Nakamura group disclosed inexpensive and earth abundant Fe-catalysed directed C–H amination with *N*-chloramines.²⁴ Several screenings of different directing groups showed that amide of 8-aminoquinoline was acted as best DG. Comparative study of product yield (99% vs. 89% respectively) using *N*-chloramine and *O*-benzoyloxyhydroxylamine



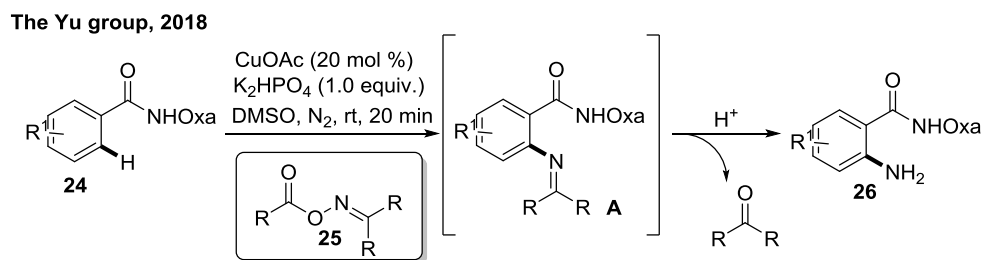
Scheme 11. Fe-catalysed C–H amination of benzamides with chloramines

suggested that *N*-chloramine was most suitable here as amine source. Though cheaper Fe-catalyst was used, stoichiometric amount of Grignard reagents are needed as reducing agent for catalyst re-generation. Stoichiometric reaction of substrate and iron-catalyst in absence of aminating agent followed by quenching with D₂O produced *ortho* deuterium incorporated product which suggest that organoiron species intermediate **A** was formed via C-H activation (**Scheme 11**).

The Wu group in 2015, reported *ortho* (sp²)C-H amination of quinoline *N*-oxides with *O*-benzoyloxyhydroxylamines under copper catalysis (**Scheme 12**).²⁵



Scheme 12. Copper catalyzed C-H amination with *O*-benzoyloxyhydroxylamines

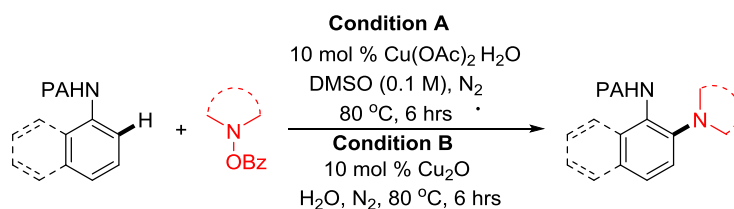


Scheme 13. Copper catalyzed C-H amination with oximes

In 2018, a copper-mediated electrophilic directed *ortho* (sp²)C-H amination with oximes to deliver primary amines was reported by the Yu group (**Scheme 13**).²⁶

II. 3. Present work

From the above literature reports we chose the electrophilic amination strategy to solve the problems associated with previous reports of C-H amination of anilines. Our hypothesis was that the weak N-O bond of the *N*-benzoate or the *N*-benzoyloxyamine of the corresponding amine may act as the internal oxidant omitting the requirement of external oxidants. We also hypothesized that cheap, non-toxic first row transition metal Cu(II) with *O*-benzoyloxyhydroxylamines can give a more practical and general method for the *ortho* C-H amination of anilines than the existing ones.

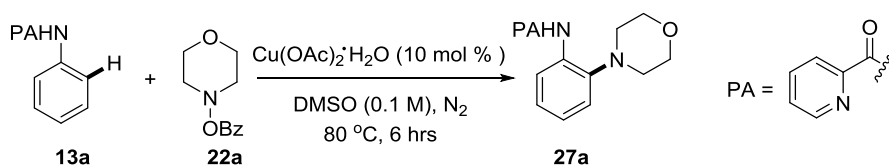


Scheme 14. Copper-catalyzed electrophilic *ortho* C(sp²)-H amination of aryl amines

II. 4. Result and discussions

To get an optimized reaction condition we started initially with 2-picolinamide protected aniline **13a** and *O*-benzoyl hydroxylmorpholine **22a**. The optimization results are concised in **Table 1**. After screenings of various solvents DMSO provided best yield. Other copper catalysts such as Cu(OTf)₂, Cu₂O afforded the product in lower yield. Without copper catalyst no product obtained. When **13a** was subjected to heating at 80 °C for 6 h under a N₂ atmosphere alongwith 2.5 equiv. of **22a** and 10 mol % of Cu(OAc)₂·H₂O in dry dimethylsulfoxide (DMSO), the expected *ortho* aminated product was obtained in 94% yield. Remarkably, low-cost metallic copper was also capable to deliver the amination product in 85% yield, signifying the better reactivity of the electrophilic amine source. Performing the reaction under an air or O₂ atmosphere, the yield was reduced, probably because of breakdown *via* over-oxidation of the amination product. The reaction at room temperature delivered the wanted product in 51% yield. The reaction using copper nanoparticle (~50 nm) in 5 mol % only gave product yield upto 70%.

Table 1. Optimisation of the Reaction Conditions ^{a, b}



| entry | deviation from optimized condition | yield (%) ^b |
|-------|--|------------------------|
| 1 | none | 94 |
| 2 | no Cu(OAc) ₂ ·H ₂ O | nr |
| 3 | Cu(OTf) ₂ instead of Cu(OAc) ₂ ·H ₂ O | 76 |
| 4 | CuOAc instead of Cu(OAc) ₂ ·H ₂ O | 84 |
| 5 | Cu ₂ O instead of Cu(OAc) ₂ ·H ₂ O | 78 |
| 6 | Cu powder instead of Cu(OAc) ₂ ·H ₂ O | 85 |
| 7 | O ₂ atm instead of N ₂ | 72 |

| | | |
|----|---|----|
| 8 | air instead of N ₂ | 65 |
| 9 | 25 °C instead of 80 °C | 51 |
| 10 | 1.0 equiv. of 22a | 40 |
| 11 | 3.5 equiv. of 22a | 95 |
| 12 | morpholine/Bz ₂ O ₂ instead of 22a | 50 |

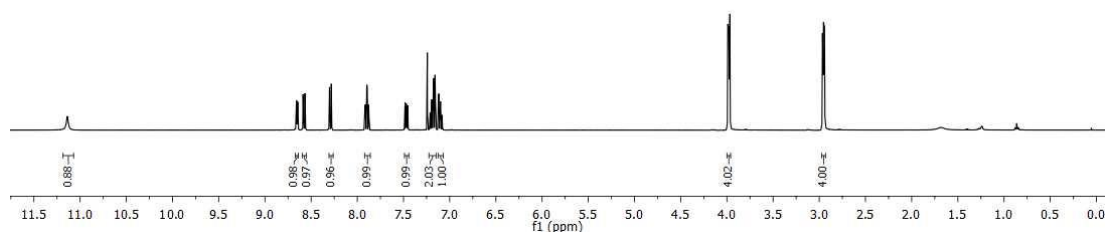
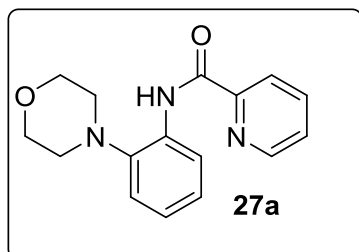
^aAll reactions were carried out in 0.2 mmol scale. ^bYields refer to the overall isolated yields.

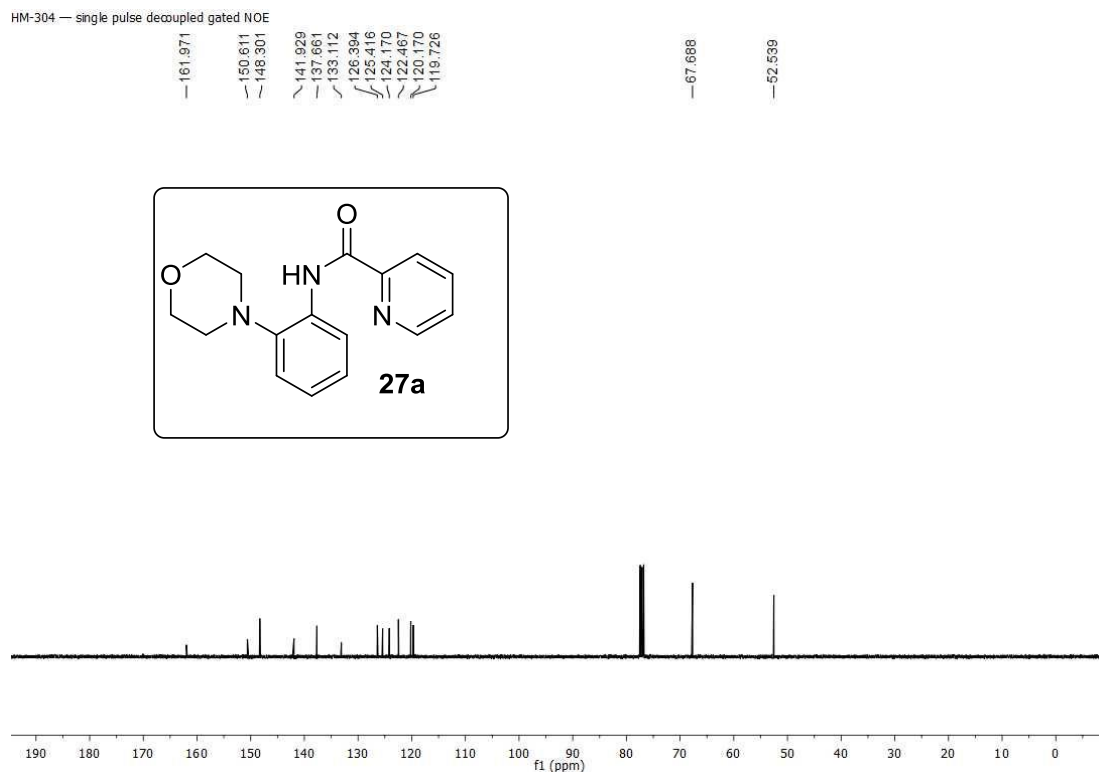
Characteristics peaks in ¹HNMR spectrum of compound **27a**

The four protons in the range of δ value 7.87-8.67 ppm correspond to the pyridine protons. One aromatic proton was vanished and two new peaks were appeared in the aliphatic region as triplets with integration value of 4 protons: δ 3.98 (t, J = 4.8 Hz, 4H) ppm, δ 2.95 (t, J = 4.4 Hz, 4H) ppm. This indicated the incorporation of morpholine moiety in the benzene ring of aniline.

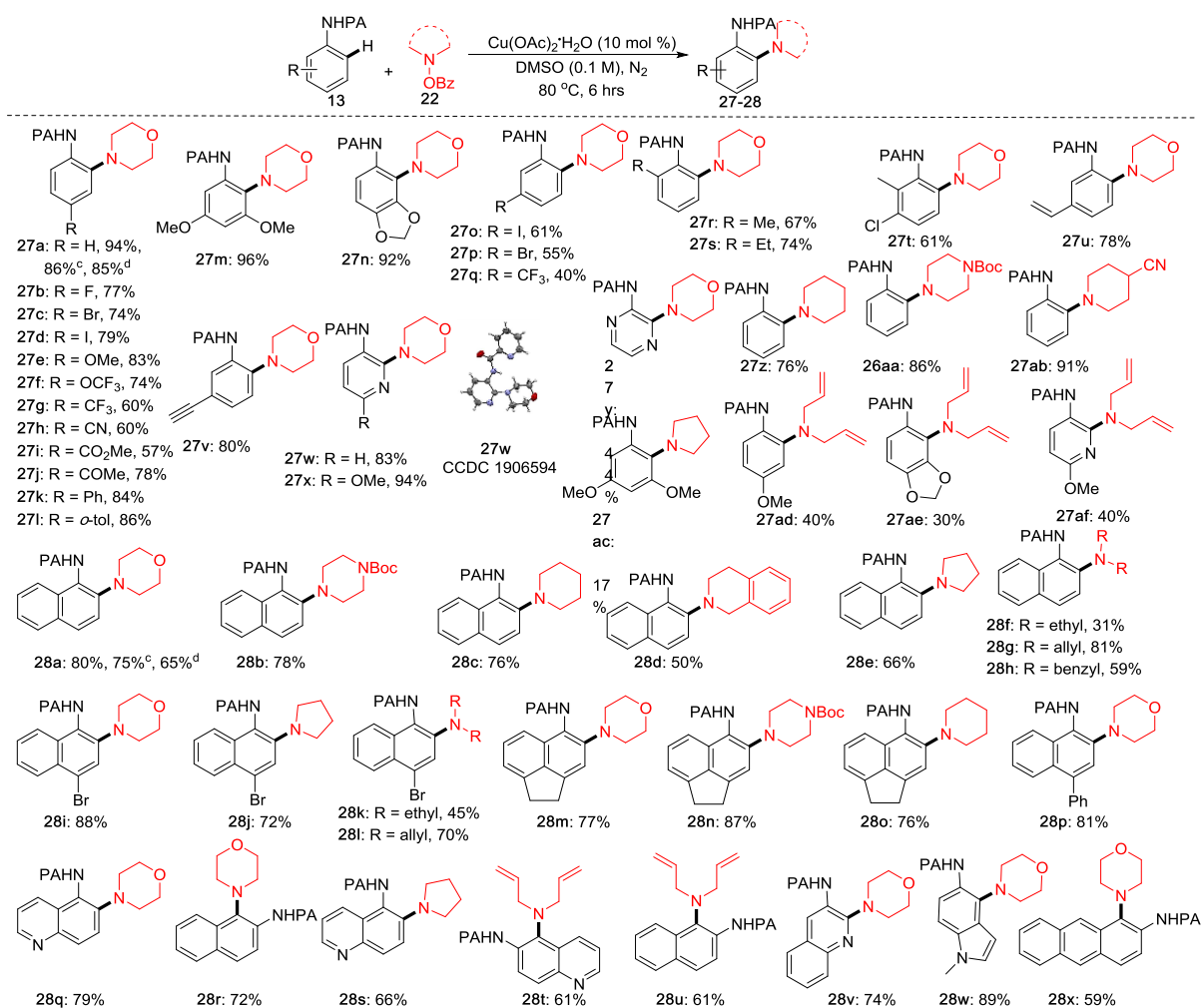
Characteristics peaks in ¹³CNMR spectrum of compound **27a**

Alongwith the substrate's peaks in ¹³C NMR spectrum two new peaks were appeared at δ 67.7 and 52.7 ppm corresponding to the carbon atoms attached to O and N atoms of the morpholine moiety respectively.





After getting the optimized condition we surveyed the substrate scope (**Scheme 15**). Aniline moieties holding fluoro, bromo, iodo groups at the *para* position (**27b–27d**) offered moderate yields under this optimized reaction conditions. Unsurprisingly, electron-rich substrates provided better yields compared to electron-deficient anilines. Electron-donating groups including methoxy, phenyl, *O*-tolyloxy at the *para* position (**27e**, **27k**, **27l**) delivered good yields. In contrast, electron-withdrawing groups such as $-\text{OCF}_3$, $-\text{CF}_3$, $-\text{CN}$ at the same location provided moderate yields (**27f–27h**). Ester as well as keto groups are tolerated under this condition, giving medium yields of the expected product (**27i–27j**). Methylene dioxy-, *meta*-dimethoxy- substituted anilines offered excellent yields (**27m**, **27n**). Iodo, bromo groups at the *meta* position gave inferior yields compared to their corresponding *para* substitution (**27o**, **27p**). Terminal alkyne as well as vinylic groups were also found to be survived furnishing very good yields (**27u**, **27v**). Extraordinarily, sterically crowded *ortho* -Me, -Et group containing anilines also provided moderate yields, which were inferior substrates in the earlier reports (**27r–27t**). Various heterocyclic amines proceeded smoothly using this protocol. For example, 3-amino pyridine substrates produced the desired product in superb yields (**27w**, **27x**) and the amination took place at the 2-position which was confirmed from X-ray crystallography (**27w**, CCDC 1906594).



Scheme 15. Substrate scope of electrophilic *ortho* C(sp²)-H amination of anilines and naphthylamines^{a,b}

Note: ^aReactions were performed in 0.2 mmol scale. ^bYields refer to isolated pure compounds. ^cReaction was performed in gram scale. ^d10 mol % Cu powder was used.

However, picolinamide protected 2-amino pyridine remained unsuccessful. Picolinamide protected 2-aminopyrazine also delivered amination product in moderate yield (**27y**). Other six-membered amines including piperidine, *N*-Boc-protected piperazine, 4-cyano-piperidine also delivered the products in good to superb yields (**27z–27ab**). Moreover, five-membered cyclic amines as well as many acyclic amines were successfully provide the products albeit in lower yields (**27ac–27af**).

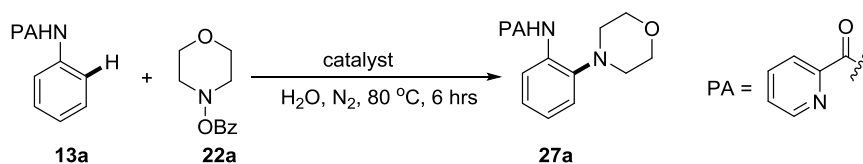
Next, we examined the scope of bicyclic naphthylamines which were poor substrates in the earlier reports (yields of ~50%). Delightfully, 1-naphthylamine provided of the *ortho* amination product in 80% yield under the same reaction condition (**28a**). Other six-membered amines also furnished the products in moderate to very good yields (**28b–28d**). Extraordinarily,

this bicyclic system exhibited excellent reactivity with five-membered pyrrolidine (**28e**, **28j**, **28s**) as well as many acyclic amines (**28f-28h**, **28k-28l**, **28t-28u**) affording good to high yields. Various groups containing naphthylamines (**28i-28p**) also furnished the products in comparable yields. Heterobicycles including quinoline (**28s**, **28v**) and indole (**28w**) were also recognized to be very good substrates. Tricyclic 2-amino anthracene yielded the amination product in 59% yield (**28x**).

II. 5. Reaction in aqueous media

Transition metal-catalyzed C–H functionalization in aqueous media has emerged as a growing research field with immense interest. The major problems associated to perform such reactions are the stability of the metal catalysts and ligands in water and the solubility issues of the organic compounds. In this direction Lu group first disclosed C-H amidation and amination reactions in water medium under rhodium and palladium catalysis.²⁷ To establish the practicability of this present protocol we re-optimized the reaction to achieve the amination reaction in water as an environmentally benevolent and green solvent. Satisfyingly, picolinamide-protected anilines as well as naphthalenes successfully gave the corresponding *ortho* amination products using catalytic Cu₂O instead of Cu(OAc)₂. The detailed optimization studies are shown in **Table 2**.

Table 2. Optimisation of the Reaction Conditions ^{a, b}

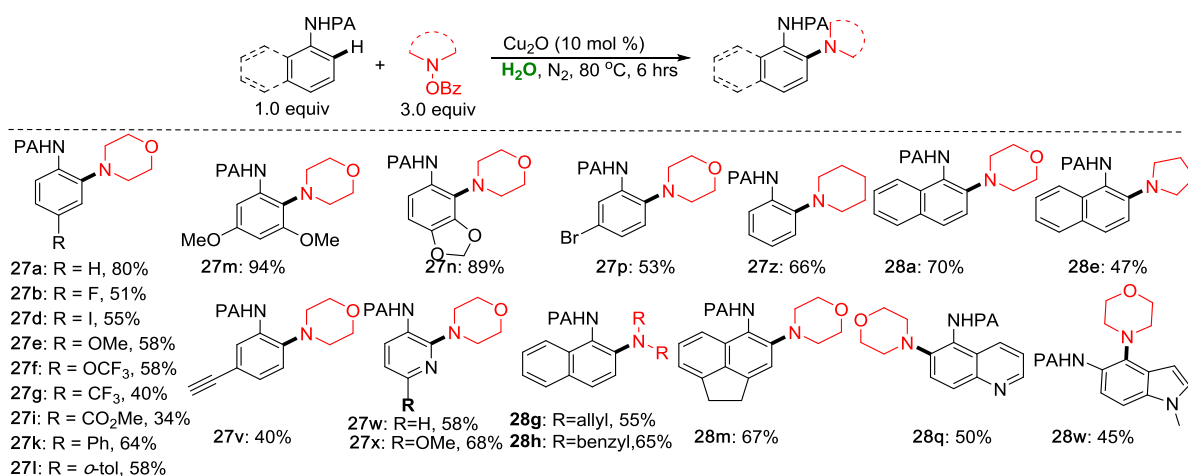


| Entry | Amount of <i>N</i> -OBz (equiv.) | Catalyst (mol %) | Additive/Oxidant (equiv.) | Solvent | Yield (%) |
|----------------|----------------------------------|------------------|---------------------------|------------------|-----------|
| 1 | 2.5 | Cu (10) | - | DMSO | 85 |
| 2 ^c | 2.5 | Cu (10) | PIDA (2.5) | DMSO | n.r |
| 3 | 2.5 | Cu (10) | - | H ₂ O | 64 |

| | | | | | |
|-----------------|------------|-----------------------------|---------------------------------|---------------------------------|-----------|
| 4 | 2.5 | Cu (10) | - | H ₂ O: DMSO (9:1) | 64 |
| 5 | 2.5 | Cu (10) | - | H ₂ O: DMSO (1:1) | 20 |
| 6 ^d | 2.5 | Cu (10) | - | H ₂ O | 64 |
| 7 ^e | 2.5 | Cu (10) | - | H ₂ O | 65 |
| 8 | 2.5 | Cu (10) | Na ₂ CO ₃ | H ₂ O | 51 |
| 9 | 3.5 | Cu (10) | - | H ₂ O | 66 |
| 10 | 2.5 | Cu (20) | - | H ₂ O | 64 |
| 11 | 2.5 | Cu (10) | - | Ethylene glycol | 35 |
| 12 ^f | 2.5 | Cu (10) | - | H ₂ O | 74 |
| 13 ^g | 2.5 | Cu (10) | - | H ₂ O | 64 |
| 14 ^h | 3.0 | Cu (10) | - | H ₂ O | 78 |
| 15 | 3.0 | Cu₂O (10) | - | H₂O | 81 |
| 16 | 3.0 | CuCl (10) | - | H ₂ O | 57 |
| 17 | 3.0 | CuBr (10) | - | H ₂ O | 61 |
| 18 | 3.0 | Cu ₂ O (10) | CTAB (1) | H ₂ O | 56 |
| 19 | 3.0 | Cu ₂ O (10) | TBAA (1) | H ₂ O | 56 |
| 20 | 3.0 | Cu ₂ O (10) | TBAC (1) | H ₂ O | 59 |
| 21 | 3.0 | Cu ₂ O (10) | TBAI (1) | H ₂ O | 5< |

| | | | | | |
|-----------------|-----|---|--|------------------|-----|
| 22 | 3.0 | Cu(OAc) ₂ ·2H ₂ O (10) | LiO ^t Bu (1) | H ₂ O | 40 |
| 23 ^c | 2.5 | Cu ₂ O (10) | K ₂ S ₂ O ₈ (2.5) | H ₂ O | n.r |
| 24 ^c | 2.5 | Cu(OAc) ₂ ·2H ₂ O (10) | K ₂ S ₂ O ₈ (2.5) | H ₂ O | n.r |
| 25 ^c | 2.5 | Cu(OAc) ₂ ·2H ₂ O (10) | PIDA (2.5) | H ₂ O | n.r |

^aAll reactions were carried out in 0.2 mmol scale. ^bYields refer to here are overall isolated yields. ^cFree amine was used. ^dReaction was continued to 22 hrs. ^eReaction was carried out at 100 °C. ^fAdditional 5 mol % Cu₂O was used. ^gAdditional 5 mol % CuO was used. ^hAdditional 5 mol % Cu₂O and 3.0 equiv. *N*-OBz were used.



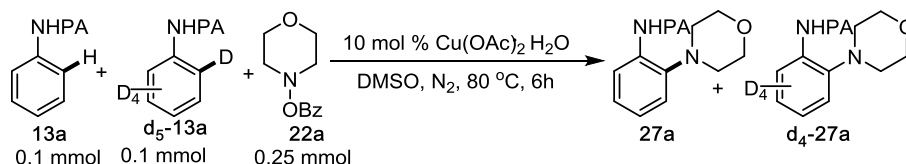
Scheme 16. Substrate scope of electrophilic *ortho* C(sp²)-H amination of anilines and naphthylamines in aqueous medium

Although electron rich group containing substrates (**27m**, **27n**; **Scheme 16**) supplied the products in comparable yields to DMSO, the electron-deficient substrates (**27g**, **27i**) gave moderate yields. Bicycles (**28a**, **28e**, **28g**, **28h**, **28m**) and many heterocycles (**28w**, **28x**, **28q**, **28w**) also successfully afforded the amination product in water in moderate to good yields. The nucleophilic-free amines were unproductive under this condition to offer the amination product.

II. 6. Investigation of reaction mechanism

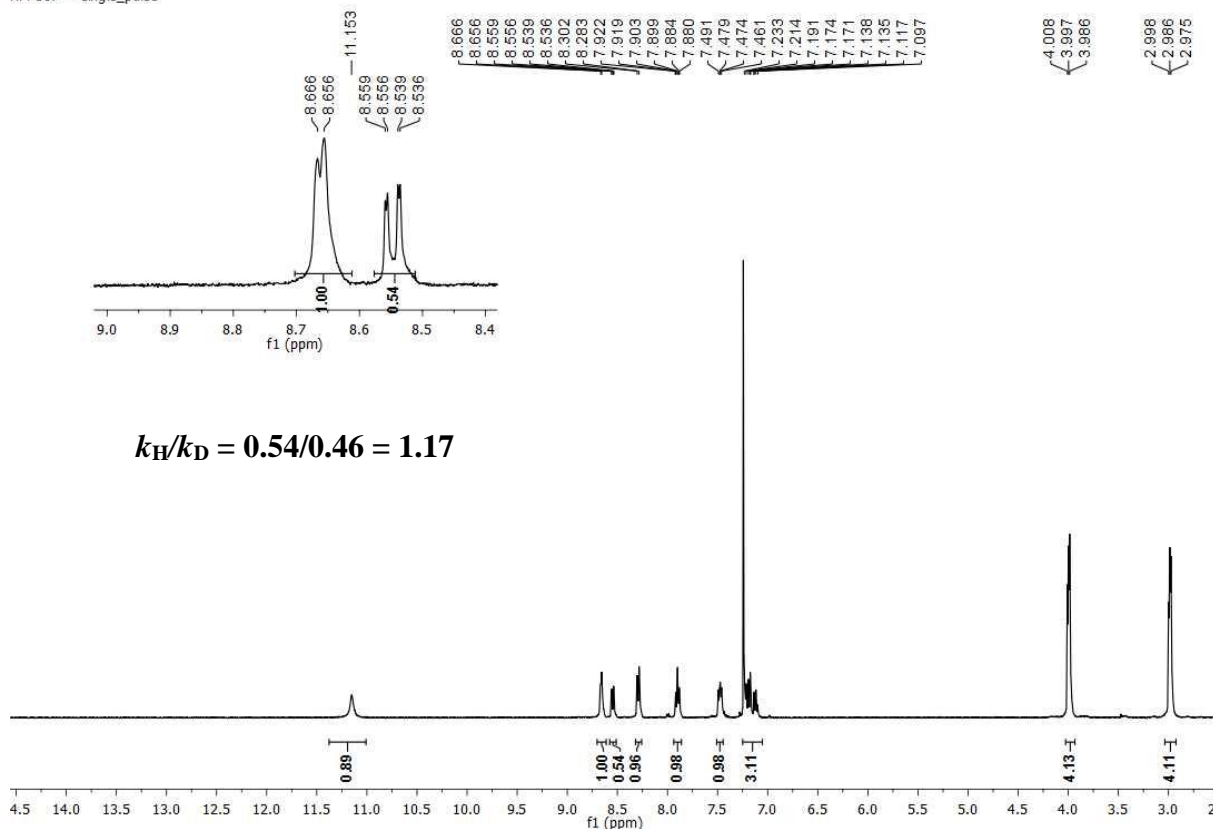
To gain an insight of the reaction mechanism of this reaction, we did a number of control experiments (**Scheme 17**). From a competition experiment between **13a** and **d₅-13a**, the primary kinetic isotope effect value k_H/k_D was calculated to be 1.17 suggesting that cleavage of C–H bond may not be the rate-limiting step (**Scheme 17a**). When substrate **13a** was exposed to the reaction conditions using additional 20.0 equiv. D₂O or CD₃COOD in presence or absence of the amine source, no *ortho* H–D exchange product was formed, indicating that no reversible *ortho* C–H insertion took place (**Scheme 17b**). The reaction in presence of radical scavengers such as 2.0 equiv. of TEMPO and BHT was suppressed significantly, signifying a plausible radical pathway (**Scheme 17c**). Moreover, when **13a** was underwent heating for 1 h in the presence of a catalytic Cu(OAc)₂·H₂O in DMSO and subsequent addition of an amine source, and stirring for 5 h the corresponding product was gained in comparable yields. But, the opposite addition sequence generated no product which suggests that first, chelation of substrate with copper catalyst occurs to generate complex-**I**. In reverse, oxidative addition followed by chelation may not be working here.

Competitive experiment for primary KIE study

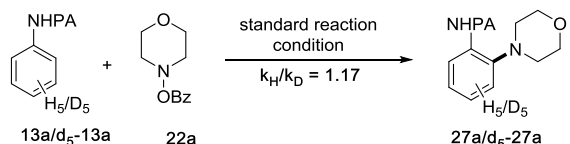


Similar to the previous amination procedure, picolinamide of aniline (0.1 mmol) **13a**, picolinamide of D₅-aniline (0.1 mmol) **d₅-13a**, *O*-benzoylhydroxylamine (0.5 mmol) and Cu(OAc)₂·H₂O (0.02 mmol) were taken in an oven dried sealed tube. Dry DMSO (2 mL) was then added and N₂ gas was purged for 2 minutes. The mixture was stirred at 80 °C for 90 minutes. Then the reaction mixture was cooled to room temperature. The mixture was then diluted with EtOAc (15 mL) and washed with saturated aq. NaHCO₃ solution (25 mL), followed by brine solution (25 mL) and dried over Na₂SO₄, and evaporated in *vacuo*. The crude mixture was loaded on a silica gel column chromatography and purified using (Hexane/EtOAc) to give the mixture of *ortho* aminated products (**27a** and **d₄-27a**). The ratio of **27a** and **d₄-27a**) was determined from ¹H NMR which give the k_H/k_D value of 1.17.

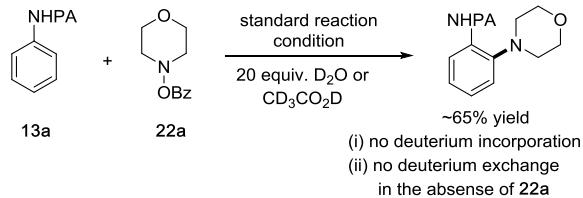
HM-567 — single_pulse



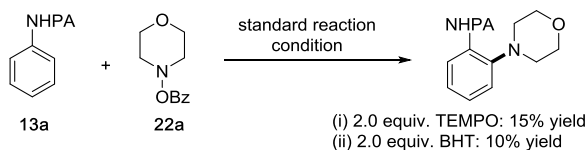
a) primary kinetic isotope experiment



b) deuterium exchange experiment



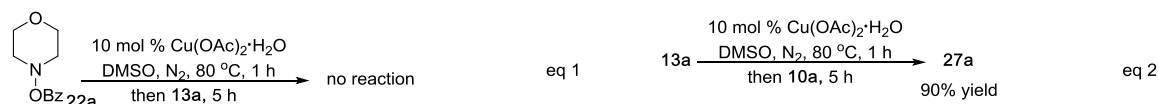
c) radical scavenger experiment



d) External oxidant experiment



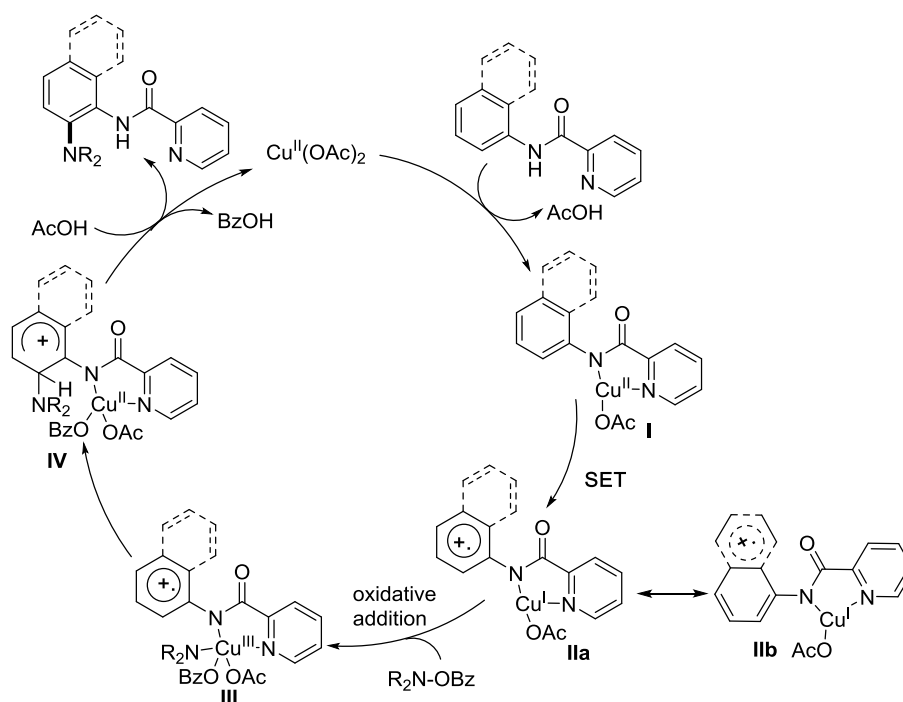
e) Sequence of addition experiment



Scheme 17. Control experiments to get into insight the mechanism

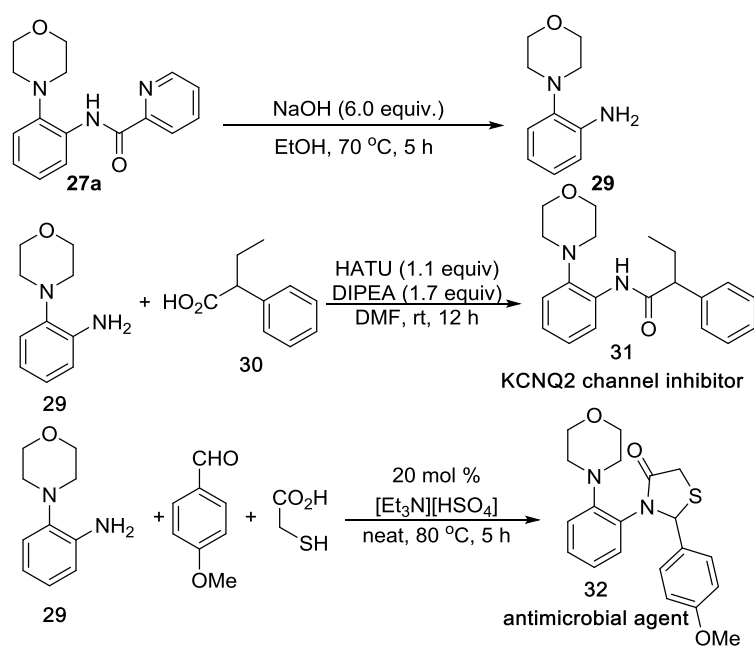
From the above control experiments and previous literature survey,²⁸ a plausible catalytic cycle is proposed in **Scheme 18**. Initially, copper catalyst undergoes chelation in a bidentate fashion with the substrate generating complex **I**. Next, complex **I** on single-electron reduction forms of copper(I) complex **II**, which is better resonance-stabilized in bicyclic naphthylamines. This Cu(I) complex undergoes oxidative addition with *O*-

benzoylhydroxylamines giving a high-valent Cu(III) species (**III**). Then amine transfer to the arenes and subsequent deprotonation, provides the desired C–H amination product with copper(II) regeneration for the next runs.



Scheme 18. Plausible catalytic cycle

II. 7. Deprotection of DG and product derivatisation



Scheme 19. Directing group deprotection and product derivatisation

This electrophilic amination protocol was also applicable for gram-scale synthesis. The 2-picolinamide DG was detached by using excess NaOH–ethanol under reflux condition to provide **29** (Scheme 19). By coupling this free diamine, **29** with **30** a KCNQ2 channel inhibitor, **31** was obtained. Additionally, a three-component reaction using this diamine in neat condition delivered an antimicrobial agent, **32**.

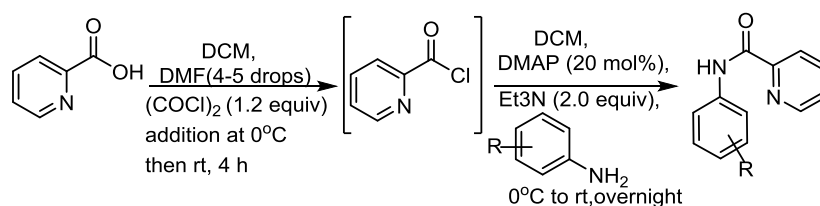
II. 8. Conclusion

In summary, we have successfully established a mild copper-catalysed 2-picolinamide directed electrophilic *ortho*-amination of anilines and naphthylamines using *O*-benzoylhydroxylamines as amine surrogate. The reaction takes place efficiently without using any external oxidants or additives. Remarkably, bicyclic anilines were also found to be effective substrates with a broad scope of dialkylamines under this proficient condition, which is an outstanding discovery, compared to the earlier methods. The amination can also be performed in water medium, affording an environmentally benevolent methodology. Thus, we antedate that this practical methodology will be highly applicable in academia as well as industrial research.

II. 9. Experimental section

Preparation of the starting materials

A. Preparation of picolinamides

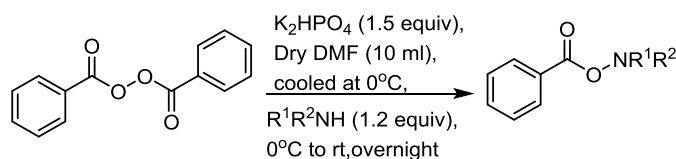


Scheme 14. General procedure for the preparation of picolinamides

To an oven dried round bottom flask was charged with pyridine-2-carboxylic acid (308 mg, 2.5 mmol), then DCM (5 mL) was added. 4-5 drops of DMF was added and the mixture was stirred at 0 °C for 5 minutes. Then oxalyl chloride (0.26 ml, 3 mmol) was added dropwise into the cooled solution of the acid which immediately formed rust-red color with the gas bubbling and then stirred at 0 °C for 10 minutes. The reaction mixture was stirred at room temperature for 4 hours. After completion, the excess oxalyl chloride was removed under *vacuum* to obtain crude acid chloride. Then, the crude pyridine chloride was dissolved in 5 mL DCM, and cooled

to 0 °C and DMAP (61 mg, 0.5 mmol), Et₃N (0.7 mL, 5 mmol) and the aniline (2.5 mmol) were successively added. Then the reaction mixture was stirred under room temperature for overnight. After completion as indicated by TLC, solvent was evaporated and extracted with ethyl acetate (40 mL). The reaction mixture was washed with 2N HCl (20 mL), brine solution (20 mL) and dried over Na₂SO₄. The solvent was evaporated under reduced pressure and finally the crude product was purified by column chromatography to afford the 2-picolinamide (50-85% yield).

B. Preparation of *O*-benzoylhydroxylamines



Scheme 14. General procedure for the preparation of *O*-benzoylhydroxylamines

As previously reported literature, a 50 mL, round-bottomed flask equipped with a teflon-coated magnetic stir bar was charged with benzoyl peroxide (1.21 g, 5.0 mmol), K₂HPO₄ (1.31 g, 7.5 mmol), and *N, N*-dimethyl formamide (10 mL). The suspension was stirred at 0 °C and the amine (6.0 mmol) was added via syringe in one portion. The suspension was stirred at ambient temperature for the indicated reaction time. Deionized water (25 mL) was added and the contents were stirred vigorously for several minutes until all solids were dissolved. The reaction mixture was transferred to a 125 mL separating funnel and extracted with 50 mL of ethyl acetate. The organic phase was collected and washed with two 25 mL portions of saturated aq. NaHCO₃ solution and then by 25 mL water, 25 mL of brine, dried over Na₂SO₄, and concentrated by rotary evaporation. The resulting crude product mixture was purified by column chromatography. The solid compounds were stored at room temperature under anhydrous conditions and liquid products were stored at 4 °C.

Experimental procedure for the *ortho* C-H amination

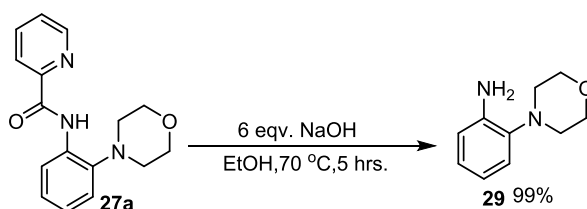
In an oven dried pressure tube containing a stir bar was added corresponding picolinamide (0.2 mmol, 1.0 equiv), *O*-benzoylhydroxylamine (0.5 mmol) and Cu(OAc)₂·H₂O (0.02 mmol). Dry DMSO (2mL) was then added and N₂ gas was purged for 2 minutes. The mixture was stirred at 80 °C for 6 hours. After allotted time the reaction mixture was cooled to room temperature. The mixture was diluted with EtOAc (15 mL) and washed with saturated aq. NaHCO₃ solution (25 mL), followed by brine solution (25 mL) and dried over Na₂SO₄, and evaporated in *vacuo*.

The crude mixture was loaded on a silica gel column chromatography and purified using (Hexane/EtOAc) to give the desired *ortho* aminated product.

Experimental procedure for the *ortho* C-H amination in water

In an oven dried pressure tube containing a stir bar was added corresponding picolinamide (0.2 mmol), *O*-benzoylhydroxylamine (0.5 mmol) and Cu₂O (0.02 mmol). HPLC water (2mL) was then added and N₂ gas was purged for few minutes. The mixture was stirred at 80 °C for 6 hours. After allotted time the reaction mixture was cooled to room temperature. The mixture was extracted with EtOAc (15 mL) and the organic part was then washed with saturated aq. NaHCO₃ solution (25mL), followed by brine (25 mL) and dried over Na₂SO₄, and evaporated in *vacuo*. The crude mixture was loaded on a silica gel column chromatography and purified using (Hexane/EtOAc) to give corresponding *ortho* aminated product.

Deprotection of the directing group



Ortho-morpholino picolinamide (708 mg, 2.5 mmol) was dissolved in 10 mL ethanol and excess amount of NaOH (700 mg, 7.0 equiv.) was added. Then the mixture was refluxed at 70 °C for 5 hours. After completion of the reaction as indicated by TLC solvent was evaporated and then poured into separating funnel with ethyl acetate. The organic layer was washed with water and then with brine solution and dried over Na₂SO₄. Solvent was evaporated under reduced pressure and then purified by silica-gel column chromatography with pet ether/ethyl acetate (80:20) which afforded 442 mg pale yellow solid product (99% yield).

¹H NMR (400 MHz, CDCl₃): δ 7.01-6.98 (m, 1H), 6.99-6.92 (m, 1H), 6.77-6.73 (m, 2H), 4.17 (brs, 2H), 3.87-3.84 (m, 4H), 2.95-2.91 (m, 4H); ¹³C NMR (100 MHz, CDCl₃): δ 141.5, 125.1, 119.1, 118.8, 115.5, 67.6, 51.7.

Product derivatization

1. Synthesis of KCNQ2 channel inhibitor (31)

To a mixture of racemic 2-phenyl butyric acid (50 mg, 0.304 mmol) and HATU (116 mg, 0.304 mmol) 2 mL dry DMF was added followed by DIPEA (0.079 mL, 0.456 mmol). Then *ortho* morpholino aniline (49 mg, 0.275 mmol) was added to this mixture and stirred overnight at rt. The reaction mixture was diluted with ethyl acetate and poured into separating funnel. The organic layer was washed with chilled water two times and dried over Na₂SO₄ and solvent was

evaporated using rotary evaporator. This crude product was then purified by column chromatography hexane/ethyl acetate as eluting solvent which afforded the desired product in 90% yield ⁵.

¹H NMR (400 MHz, CDCl₃): δ 8.38(d, *J* = 8.4 Hz, 2H), 7.38-7.27 (m, 5H), 7.14-7.09 (m, 1H), 7.07-6.98 (m, 2H), 3.49-3.43 (m, 5H), 2.58 (t, *J* = 4.8 Hz, 4H), 2.36-2.26 (m, 1H), 1.19-1.80 (m, 1H), 0.91 (t, *J* = 7.6 Hz, 3H); ¹³C NMR (100 MHz, CDCl₃): δ 171.6, 140.8, 139.9, 133.7, 129.2, 128.4, 127.7, 125.8, 123.8, 120.6, 119.6, 67.3, 56.5, 52.5, 26.1, 12.4.

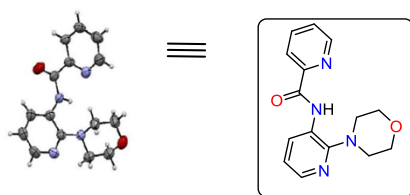
2. Synthesis of antimicrobial agent (32)

The acidic Bronsted ionic liquid [Et₃N][HSO₄] used for this reaction was prepared according to the literature reported procedure.²⁹ To a mixture of 2-morpholino aniline (178 mg, 1.0 mmol), *p*-anisaldehyde (0.122 mL, 1.0 mmol) and thioglycolic acid (0.070 mL, 1.0 mmol) the above mentioned ionic liquid (40 mg, 0.2 mmol) was added and heated to 80 °C for 5 hours. Then the reaction mixture was diluted with DCM and transferred into a separating funnel and organic layer was washed with water two times and dried over Na₂SO₄. The crude mixture was purified by column chromatography using pet ether/ethyl acetate as eluting solvent. The product was obtained as white crystalline solid in 50% yield.

¹H NMR (400 MHz, CDCl₃): δ 7.19-7.11 (m, 3H), 7.01 (d, *J* = 8.0 Hz, 1H), 6.95-6.88 (m, 2H), 6.73-6.69 (m, 2H), 6.57 (s, 1H), 4.00-3.93 (m, 3H), 3.88-3.83 (m, 2H), 3.77 (d, *J* = 15.6 Hz, 1H), 3.70 (s, 3H), 3.08-3.04 (m, 2H), 2.80-2.75 (m, 2H); ¹³C NMR (100 MHz, CDCl₃): δ 171.6, 159.9, 148.5, 131.4, 131.1, 129.2, 128.8, 124.4, 120.4, 113.9, 67.6, 62.7, 55.3, 52.3, 33.1; HRMS (ESI, *m/z*) calcd. For C₂₀H₂₃N₂O₃S [M+H]⁺: 371.1429; found: 371.1442.

Crystal structure of compound 27w

The crystals were grown in dichloromethane solvent. The pure compound was dissolved in dichloromethane slow evaporation led to the crystal **27w**. The crystal data was collected in X-ray spectroscopy (Bruker Kappa Apex-2, CCD Area Detector), and the data was analyzed using OLEX2 software. The structure is given below. The corresponding cif file has been uploaded separately as supporting information.

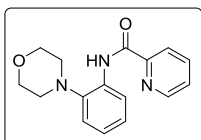


X-ray determined molecular structure of **27w**, CCDC: 1906594

| | |
|--|---|
| Identification code | HM-309 |
| Empirical formula | C ₁₅ H ₁₆ N ₄ O ₂ |
| Formula weight | 284.32 |
| Temperature/K | 298 K |
| Crystal system | orthorhombic |
| Space group | P 21 21 21 |
| a/Å | 7.1086(4) |
| b/Å | 11.7985(7) |
| c/Å | 17.0932(10) |
| a/° | 90 |
| b/° | 90 |
| g/° | 90 |
| Volume/Å ³ | 1433.62(14) |
| Z | 4 |
| R _{calc} /cm ³ | 1.317 |
| m/mm ⁻¹ | 0.091 |
| F(000) | 600 |
| Crystal size/mm ³ | 0.2 x 0.2 x 0.2 |
| Radiation | MoKα (λ = 0.71073) |
| 2θ range for data collection/° | 2.943 to 24.252 |
| Index ranges | -9 ≤ h ≤ 9, -15 ≤ k ≤ 15, -21 ≤ l ≤ 21 |
| Reflections collected / unique | 3247 / 2627 [R(int) = 0.061] |
| Data / restraints / parameters | 3247 / 0 / 190 |
| Goodness-of-fit on F ² | 1.065 |
| Final R indices [I > 2σ(I)] | R1 = 0.0426, wR2 = 0.0996 |
| R indices (all data) | R1 = 0.0547, wR2 = 0.1066 |
| Largest diff. peak and hole/ e Å ⁻³ | 0.144 and -0.253 |

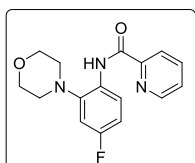
II.10. Spectral Data

N-(2-morpholinophenyl)picolinamide (**27a**)^{19, 20, 21}



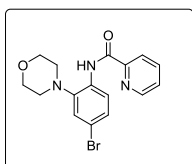
The same general procedure was followed. Column chromatography (SiO₂, eluting with 85:15 hexane/ethyl acetate) afforded the desired product as a white solid (53 mg, 94% yield). ¹H NMR (400 MHz, CDCl₃): δ 11.14 (s, 1H), 8.66-8.56 (m, 1H), 8.58 (dd, *J*₁ = 8.0 Hz, *J*₂ = 1.2 Hz, 1H), 8.29 (dt, *J*₁ = 8.0 Hz, *J*₂ = 0.8 Hz, 1H), 7.90 (td, *J*₁ = 7.6 Hz, *J*₂ = 1.6 Hz, 1H), 7.49-7.45 (m, 1H), 7.22-7.16 (m, 2H), 7.12-7.08 (m, 1H), 3.98 (t, *J* = 4.8 Hz, 4H), 2.95 (t, *J* = 4.4 Hz, 4H); ¹³C NMR (100 MHz, CDCl₃): δ 162.0, 150.6, 148.3, 141.9, 137.7, 133.1, 126.4, 125.4, 124.2, 122.5, 120.2, 119.7, 67.7, 52.5.

***N*-(4-fluoro-2-morpholinophenyl)picolinamide (27b)**¹⁹



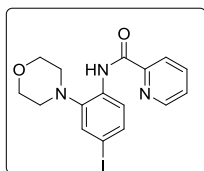
The same general procedure was followed. Column chromatography (SiO₂, eluting with 85:15 hexane/ethyl acetate) afforded the desired product as a white solid (46 mg, 77% yield). ¹H NMR (400 MHz, CDCl₃): δ 10.9 (s, 1H), 8.65-8.63 (m, 1H), 8.55-8.51 (m, 1H), 8.28 (dt, *J*₁ = 8.0 Hz, *J*₂ = 1.2 Hz, 1H), 7.90 (td, *J*₁ = 8.0 Hz, *J*₂ = 2.0 Hz, 1H), 7.49-7.46 (m, 1H), 6.91-6.85 (m, 2H), 3.97 (t, *J* = 4.4 Hz, 4H), 2.94 (t, *J* = 4.4 Hz, 4H); ¹³C NMR (100 MHz, CDCl₃): δ 161.8, 159.3 (d, *J* = 243.0 Hz), 150.4, 148.3, 143.5 (d, *J* = 7.6 Hz), 137.7, 129.07 (d, *J* = 3.1 Hz), 126.5, 122.4, 120.8 (d, *J* = 8.7 Hz), 120.7, 111.4 (d, *J* = 21.7 Hz), 107.7 (d, *J* = 23.1 Hz), 67.5, 52.3.

***N*-(4-bromo-2-morpholinophenyl)picolinamide (27c)**²⁰



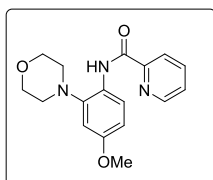
The same general procedure was followed. Column chromatography (SiO₂, eluting with 85:15 hexane/ethyl acetate) afforded the desired product as a white solid (53 mg, 74% yield). ¹H NMR (400 MHz, CDCl₃): δ 11.00 (s, 1H), 8.65-8.63 (m, 1H), 8.48 (d, *J* = 8.8 Hz, 1H), 8.28 (dt, *J*₁ = 7.6 Hz, *J*₂ = 1.2 Hz, 1H), 7.90 (td, *J*₁ = 7.6 Hz, *J*₂ = 1.6 Hz, 1H), 7.50-7.47 (m, 1H), 7.31 (dd, *J*₁ = 8.8 Hz, *J*₂ = 2.4 Hz, 1H), 7.25 (d, *J* = 2.4 Hz, 1H), 3.97 (t, *J* = 4.8 Hz, 4H), 2.94 (t, *J* = 4.4 Hz, 4H); ¹³C NMR (100 MHz, CDCl₃): δ 162.0, 150.2, 148.3, 143.2, 137.8, 132.1, 128.2, 126.6, 123.6, 122.5, 120.9, 116.5, 67.5, 52.4.

***N*-(4-iodo-2-morpholinophenyl)picolinamide (27d)**¹⁹



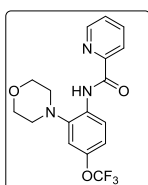
The same general procedure was followed. Column chromatography (SiO₂, eluting with 85:15 hexane/ethyl acetate) afforded the desired product as a white crystalline solid (65 mg, 79% yield). ¹H NMR (400 MHz, CDCl₃): δ 11.02 (s, 1H), 8.64-8.63 (m, 1H), 8.35-8.32 (m, 1H), 8.28-8.25 (m, 1H), 7.92-7.87 (m, 1H), 7.51-7.46 (m, 2H), 7.41 (d, *J* = 2.0 Hz, 1H), 3.91 (t, *J* = 4.8 Hz, 4H), 2.93 (t, *J* = 4.4 Hz, 4H); ¹³C NMR (100 MHz, CDCl₃): δ 161.9, 150.3, 148.3, 143.3, 137.8, 134.4, 132.9, 129.6, 126.6, 122.5, 121.3, 87.1, 67.5, 52.4.

***N*-(4-methoxy-2-morpholinophenyl)picolinamide (27e)**^{19, 21}



The same general procedure was followed. Column chromatography (SiO₂, eluting with 80:20 hexane/ethyl acetate) afforded the desired product as a white crystalline solid (52 mg, 83% yield). ¹H NMR (400 MHz, CDCl₃): δ 10.85 (s, 1H), 8.63-8.61 (m, 1H), 8.47 (m, 1H), 8.26 (dt, *J*₁ = 7.6 Hz, *J*₂ = 1.2 Hz, 1H), 7.87 (td, *J*₁ = 8.0 Hz, *J*₂ = 2.0 Hz, 1H), 7.46-7.42 (m, 1H), 6.72-6.69 (m, 2H), 3.95 (t, *J* = 4.4 Hz, 4H), 3.79 (s, 3H), 2.92 (t, *J* = 4.4 Hz, 4H); ¹³C NMR: (100 MHz, CDCl₃): δ 161.5, 156.4, 150.7, 148.3, 143.5, 137.6, 126.4, 126.2, 122.3, 120.7, 108.8, 107.3, 67.6, 55.6, 52.2;

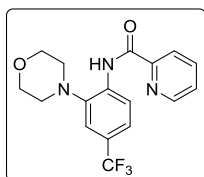
***N*-(2-morpholino-4-(trifluoromethoxy)phenyl)picolinamide (27f)**



The same general procedure was followed. Column chromatography (SiO₂, eluting with 85:15 hexane/ethyl acetate) afforded the desired product as a white solid (54 mg, 74% yield), mp 102-104°C. ¹H NMR (400 MHz, CDCl₃): δ 10.99 (s, 1H), 8.66-8.64 (m, 1H), 8.59 (d, *J* = 8.8 Hz, 1H), 8.28 (dt, *J*₁ = 7.6 Hz, *J*₂ = 1.2 Hz, 1H), 7.90 (td, *J*₁ = 7.6 Hz, *J*₂ = 1.6 Hz, 1H), 7.50-7.47 (m, 1H), 7.07-7.04 (m, 1H), 6.99 (d, *J* = 2.8 Hz, 1H), 3.98 (t, *J* = 4.4 Hz, 4H), 2.95 (t, *J* = 4.4 Hz, 4H); ¹³C NMR (100 MHz, CDCl₃): 162.0, 150.2, 148.3, 145.2, 143.1, 137.8, 131.7, 126.6, 122.6, 120.6 (q, *J* = 255.0 Hz), 120.4, 117.6, 113.6, 67.5, 52.3; IR (neat): ν_{max} 3303,

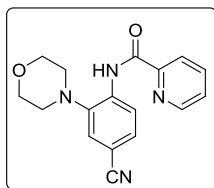
2960, 2921, 2855, 1686, 1519, 1423, 1246, 1216, 1157, 1114, 989, 746, 690 cm^{-1} ; HRMS (ESI, m/z) calcd. For $\text{C}_{17}\text{H}_{17}\text{F}_3\text{N}_3\text{O}_3$ [$\text{M}+\text{H}^+$: 368.1222; found: 368.1219.

***N*-(2-morpholino-4-(trifluoromethyl)phenyl)picolinamide (27g)**²¹



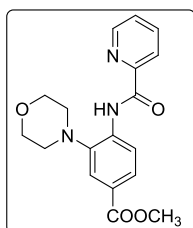
The same general procedure was followed. Column chromatography (SiO_2 , eluting with 85:15 hexane/ethyl acetate) afforded the desired product as a white solid (42 mg, 60% yield). ^1H NMR (400 MHz, CDCl_3): δ 11.21 (s, 1H), 8.70 (d, $J = 8.4$ Hz, 1H), 8.67-8.66 (m, 1H), 8.29 (dt, $J_1 = 7.6$ Hz, $J_2 = 1.2$ Hz, 1H), 7.92 (td, $J_1 = 8.0$ Hz, $J_2 = 2.0$ Hz, 1H), 7.52-7.49 (m, 1H), 7.45 (d, $J = 8.4$ Hz, 1H), 7.37 (d, $J = 0.8$ Hz, 1H), 3.99 (t, $J = 4.4$ Hz, 4H), 2.98 (t, $J = 4.4$ Hz, 4H); ^{13}C NMR (100 MHz, CDCl_3): δ 162.3, 150.1, 148.4, 141.9, 137.8, 136.1, 126.8, 125.8, (q, $J = 32.6$ Hz), 124.2 (q, $J = 270.0$ Hz), 122.6, 122.5 (q, $J = 3.7$ Hz), 117.2 (q, $J = 3.3$ Hz), 114.4, 67.5, 52.4.

***N*-(4-cyano-2-morpholinophenyl)picolinamide (27h)**²⁰



The same general procedure was followed. Column chromatography (SiO_2 , eluting with 80:20 hexane/ethyl acetate) afforded the desired product as a white solid (37 mg, 60% yield). ^1H NMR (400 MHz, CDCl_3): δ 11.26 (s, 1H), 8.71 (d, $J = 8.4$ Hz, 1H), 8.69-8.65 (m, 1H), 8.28 (dt, $J_1 = 7.6$ Hz, $J_2 = 1.2$ Hz, 1H), 7.93 (td, $J_1 = 7.6$ Hz, $J_2 = 1.6$ Hz, 1H), 7.53-7.48 (m, 2H), 7.40 (d, $J = 2.0$ Hz, 1H), 3.99 (t, $J = 4.4$ Hz, 4H), 2.95 (t, $J = 4.4$ Hz, 4H); ^{13}C NMR (100 MHz, CDCl_3): δ 162.4, 149.7, 148.4, 142.1, 137.9, 137.3, 129.9, 127.0, 124.0, 122.7, 119.7, 119.1, 106.9, 67.4, 52.3.

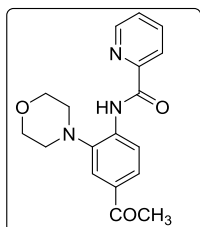
methyl 3-morpholino-4-(picolinamido)benzoate (27i)^{20, 21}



The same general procedure was followed. Column chromatography (SiO_2 , eluting with 75:25 hexane/ethyl acetate) afforded the desired product as a white solid (39 mg, 57% yield). ^1H

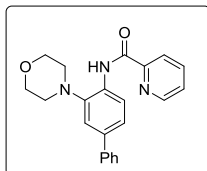
NMR (400 MHz, CDCl₃): δ 11.30 (s, 1H), 8.67-8.64 (m, 2H), 8.29 (dt, $J_1 = 8.0$ Hz, $J_2 = 0.8$ Hz, 1H), 7.93-7.87 (m, 2H), 7.84 (d, $J = 2.0$ Hz, 1H), 7.51-7.48 (m, 1H), 3.99 (t, $J = 4.4$ Hz, 4H), 3.89 (s, 3H), 2.98 (t, $J = 4.4$ Hz, 4H); ¹³C NMR (100 MHz, CDCl₃): δ 166.8, 162.3, 150.1, 148.4, 141.6, 137.8, 137.3, 127.4, 126.7, 125.5, 122.6, 121.7, 118.8, 67.6, 52.5, 52.1.

N-(4-acetyl-2-morpholinophenyl)picolinamide (27j)²⁰



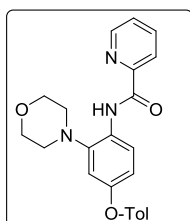
The same general procedure was followed. Column chromatography (SiO₂, eluting with 80:20 hexane/ethyl acetate) afforded the desired product as a white solid (51 mg, 78% yield). ¹H NMR (400 MHz, CDCl₃): δ 11.31 (s, 1H), 8.68-8.65 (m, 2H), 8.28 (dt, $J_1 = 8.0$ Hz, $J_2 = 1.2$ Hz, 1H), 7.91 (td, $J_1 = 8.0$ Hz, $J_2 = 2.0$ Hz, 1H), 7.81-7.77 (m, 2H), 7.52-7.48 (m, 1H), 3.99 (t, $J = 4.4$ Hz, 4H), 2.98 (t, $J = 4.4$ Hz, 4H); 2.58 (s, 3H); ¹³C NMR (100 MHz, CDCl₃): δ 197.0, 162.4, 150.1, 148.4, 141.9, 137.8, 137.5, 132.9, 126.9, 126.8, 122.7, 119.9, 118.7, 67.5, 52.5, 26.5.

N-(3-morpholino-[1,1'-biphenyl]-4-yl)picolinamide (27k)²¹



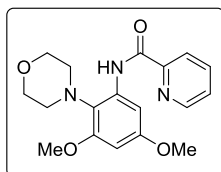
The same general procedure was followed. Column chromatography (SiO₂, eluting with 85:15 hexane/ethyl acetate) afforded the desired product as a white solid (60 mg, 84% yield). ¹H NMR (400 MHz, CDCl₃): δ 11.16 (s, 1H), 8.67-8.65 (m, 2H), 8.31 (dt, $J_1 = 7.6$ Hz, $J_2 = 0.8$ Hz, 1H), 7.90 (td, $J_1 = 7.6$ Hz, $J_2 = 1.6$ Hz, 1H), 7.60-7.58 (m, 2H), 7.49-7.46 (m, 1H), 7.45-7.41 (m, 3H), 7.39 (d, $J = 2.0$ Hz, 1H), 7.35-7.30 (m, 1H), 4.01 (t, $J = 4.4$ Hz, 4H), 3.02 (t, $J = 4.8$ Hz, 4H); ¹³C NMR (100 MHz, CDCl₃): δ 162.0, 150.6, 148.4, 142.5, 140.9, 137.7, 137.2, 132.3, 128.9, 127.3, 127.0, 126.5, 124.4, 122.5, 120.0, 119.0, 67.7, 52.6.

N-(2-morpholino-4-(p-tolyloxy)phenyl)picolinamide (26l)



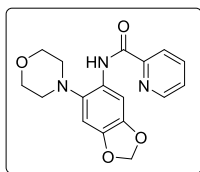
The same general procedure was followed. Column chromatography (SiO₂, eluting with 80:20 hexane/ethyl acetate) afforded the desired product as a white solid (67 mg, 86% yield), mp 133–135 °C. ¹H NMR (400 MHz, CDCl₃): δ 10.93 (s, 1H), 8.65-8.63 (m, 1H), 8.49 (d, *J* = 9.2 Hz, 1H), 8.28 (dt, *J*₁ = 7.6 Hz, *J*₂ = 1.2 Hz, 1H), 7.89 (td, *J*₁ = 7.6 Hz, *J*₂ = 1.6 Hz, 1H), 7.48-7.45 (m, 1H), 7.14-7.10 (m, 2H), 6.92-6.88 (m, 2H), 6.85 (d, *J* = 2.8 Hz, 1H), 6.78 (dd, *J*₁ = 9.2 Hz, *J*₂ = 2.8 Hz, 1H), 3.96 (t, *J* = 4.4 Hz, 4H), 2.92 (t, *J* = 4.4 Hz, 4H), 2.32 (s, 3H); ¹³C NMR (100 MHz, CDCl₃): δ 161.7, 155.1, 153.9, 150.6, 148.3, 143.5, 137.7, 132.8, 130.3, 128.3, 126.4, 122.4, 120.8, 118.6, 114.8, 111.2, 67.6, 52.4, 20.8; IR (neat): ν_{max} 3304, 2958, 2853, 1679, 1519, 1501, 1421, 1255, 1215, 1102, 980, 887, 813, 744, 689 cm⁻¹; HRMS (ESI, *m/z*) calcd. For C₂₃H₂₄N₃O₃ [M+H]⁺: 390.1818; found: 390.1814.

***N*-(3,5-dimethoxy-2-morpholinophenyl)picolinamide (27m)**^{19, 21}



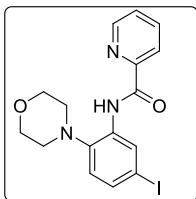
The same general procedure was followed. Column chromatography (SiO₂, eluting with 80:20 hexane/ethyl acetate) afforded the desired product as a white white solid (66 mg, 96% yield). ¹H NMR (400 MHz, CDCl₃): δ 11.83 (s, 1H), 8.65-8.63 (m, 1H), 8.25-8.22 (m, 1H), 7.93 (d, *J* = 2.4 Hz, 1H), 7.88-7.83 (m, 1H), 7.45-7.42 (m, 1H), 6.20 (d, *J* = 2.8 Hz, 1H), 3.94-3.88 (m, 4H), 3.82 (s, 3H), 3.78 (s, 3H), 3.63-3.55 (m, 2H), 2.58 (d, *J* = 11.6 Hz, 2H); ¹³C NMR (100 MHz, CDCl₃): δ 162.3, 159.0, 158.95, 150.7, 148.4, 137.6, 137.3, 126.3, 122.3, 121.6, 95.3, 95.2, 68.4, 55.6, 55.2, 50.7.

***N*-(6-morpholinobenzo[d][1,3]dioxol-5-yl)picolinamide (27n)**¹⁹



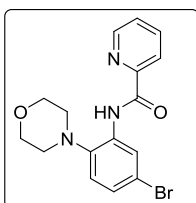
The same general procedure was followed. Column chromatography (SiO₂, eluting with 85:15 hexane/ethyl acetate) afforded the desired product as a yellow solid (60 mg, 92% yield). ¹H NMR (400 MHz, CDCl₃): δ 11.14 (s, 1H), 8.62-8.61 (m, 1H), 8.24 (dd, *J*₁ = 8.0 Hz, *J*₂ = 0.8 Hz, 1H), 8.19 (s, 1H), 7.86 (td, *J*₁ = 7.6 Hz, *J*₂ = 1.6 Hz, 1H), 7.45-7.42 (m, 1H), 6.73 (s, 1H), 5.91 (s, 2H), 3.93 (t, *J* = 4.8 Hz, 4H), 2.84 (t, *J* = 4.4 Hz, 4H); ¹³C NMR (100 MHz, CDCl₃): δ 161.5, 150.6, 148.3, 144.6, 143.6, 137.6, 135.7, 127.7, 126.3, 122.3, 102.0, 101.4, 101.3, 67.7, 52.9.

***N*-(5-iodo-2-morpholinophenyl)picolinamide (27o)**



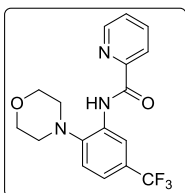
The same general procedure was followed. Column chromatography (SiO₂, eluting with 80:20 hexane/ethyl acetate) afforded the desired product as a white solid (50 mg, 61% yield), mp 177-179 °C. ¹H NMR (400 MHz, CDCl₃): δ 11.03 (s, 1H), 8.94 (d, *J* = 2.0 Hz, 1H), 8.65-8.63 (m, 1H), 8.26 (dt, *J*₁ = 7.6 Hz, *J*₂ = 1.2 Hz, 1H), 7.90 (td, *J*₁ = 7.6 Hz, *J*₂ = 1.2 Hz, 1H), 7.50-7.46 (m, 1H), 7.41 (dd, *J*₁ = 8.4 Hz, *J*₂ = 2.0 Hz, 1H), 6.87 (d, *J* = 8.4 Hz, 1H), 3.96 (t, *J* = 4.4 Hz, 4H), 2.91 (t, *J* = 4.4 Hz, 4H); ¹³C NMR (100 MHz, CDCl₃): δ 161.8, 150.2, 148.4, 141.6, 137.8, 134.3, 133.1, 128.2, 126.6, 122.5, 122.0, 89.4, 67.5, 52.3; HRMS (ESI, *m/z*) calcd. For C₁₆H₁₇IN₃O₃ [M+H]⁺: 410.0365; found: 410.0377.

***N*-(5-bromo-2-morpholinophenyl)picolinamide (27p)**¹⁹



The same general procedure was followed. Column chromatography (SiO₂, eluting with 80:20 hexane/ethyl acetate) afforded the desired product as a white solid (40 mg, 55% yield). ¹H NMR (400 MHz, CDCl₃): δ 11.09 (s, 1H), 8.78 (d, *J* = 2.4 Hz, 1H), 8.65-8.64 (m, 1H), 8.27 (dt, *J*₁ = 7.6 Hz, *J*₂ = 1.2 Hz, 1H), 7.90 (td, *J*₁ = 7.6 Hz, *J*₂ = 1.6 Hz, 1H), 7.50-7.47 (m, 1H), 7.21 (dd, *J*₁ = 8.4 Hz, *J*₂ = 2.0 Hz, 1H), 7.01 (d, *J* = 8.4 Hz, 1H), 3.96 (t, *J* = 4.4 Hz, 4H), 2.92 (t, *J* = 4.4 Hz, 4H); ¹³C NMR (100 MHz, CDCl₃): δ 162.0, 150.2, 148.4, 140.8, 137.8, 134.3, 126.9, 126.6, 122.6, 121.7, 118.6, 67.6, 52.4.

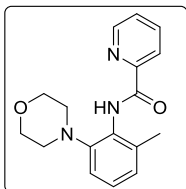
***N*-(2-morpholino-5-(trifluoromethyl)phenyl)picolinamide (27q)**^{19, 21}



The same general procedure was followed. Column chromatography (SiO₂, eluting with 80:20 hexane/ethyl acetate) afforded the desired product as a white solid (28 mg, 40% yield). ¹H NMR (400 MHz, CDCl₃): δ 11.05 (s, 1H), 8.95 (d, *J* = 2.0 Hz, 1H), 8.65 (d, *J* = 4.4 Hz, 1H), 8.28 (d, *J* = 8.0 Hz, 1H), 7.92 (td, *J*₁ = 7.6 Hz, *J*₂ = 1.6 Hz, 1H), 7.51-7.48 (m, 1H), 7.35 (dd, *J*₁

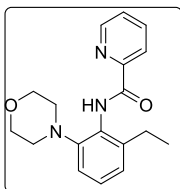
= 8.4 Hz, $J_2 = 1.6$ Hz, 1H), 7.21 (d, $J = 8.0$ Hz, 1H), 3.99 (t, $J = 4.8$ Hz, 4H), 2.98 (t, $J = 4.4$ Hz, 4H); ^{13}C NMR (100 MHz, CDCl_3): δ 162.2, 150.0, 148.4, 144.7, 137.9, 133.2, 127.2 (q, $J = 32.5$ Hz), 126.8, 124.2 (q, $J = 270.3$ Hz), 122.6, 121.04 (q, $J = 3.7$ Hz), 120.1, 116.7 (q, $J = 3.7$ Hz), 67.5, 52.2.

***N*-(2-methyl-6-morpholinophenyl)picolinamide (27r)**^{20, 21}



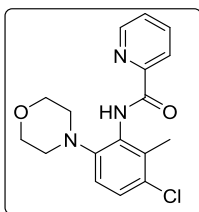
The same general procedure was followed. Column chromatography (SiO_2 , eluting with 90:10 hexane/ethyl acetate) afforded the desired product as a white solid (40 mg, 67% yield). ^1H NMR (400 MHz, CDCl_3): δ 10.03 (s, 1H), 8.68-8.66 (m, 1H), 8.27 (dt, $J_1 = 7.6$ Hz, $J_2 = 0.8$ Hz, 1H), 7.89 (td, $J_1 = 7.6$ Hz, $J_2 = 1.6$ Hz, 1H), 7.50-7.47 (m, 1H), 7.16 (t, $J = 8.0$ Hz, 1H), 7.03 (d, $J = 7.6$ Hz, 1H), 6.93 (d, $J = 8.0$ Hz, 1H), 3.75 (t, $J = 4.4$ Hz, 4H), 2.86 (t, $J = 4.4$ Hz, 4H), 2.33 (s, 3H); ^{13}C NMR (100 MHz, CDCl_3): δ 162.5, 150.2, 148.3, 137.6, 136.1, 130.2, 126.9, 126.6, 126.5, 122.7, 116.7, 67.4, 52.3, 19.6.

***N*-(2-ethyl-6-morpholinophenyl)picolinamide (27s)**



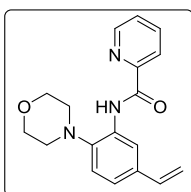
The same general procedure was followed. Column chromatography (SiO_2 , eluting with 90:10 hexane/ethyl acetate) afforded the desired product as a white crystalline solid (46 mg, 74% yield), mp 98-100 °C. ^1H NMR (400 MHz, CDCl_3): δ 9.95 (s, 1H), 8.66-8.65 (m, 1H), 8.27 (dt, $J_1 = 7.6$ Hz, $J_2 = 1.6$ Hz, 1H), 7.88 (td, $J_1 = 7.6$ Hz, $J_2 = 1.6$ Hz, 1H), 7.49-7.45 (m, 1H), 7.22 (t, $J = 7.6$ Hz, 1H), 7.08 (d, $J = 7.6$ Hz, 1H), 6.94 (d, $J = 7.6$ Hz, 1H), 3.71 (t, $J = 4.8$ Hz, 4H), 2.84 (t, $J = 4.4$ Hz, 4H), 2.72 (q, $J = 7.6$ Hz, 2H), 1.20 (t, $J = 7.6$ Hz, 3H); ^{13}C NMR (100 MHz, CDCl_3): δ 162.9, 150.1, 148.3, 147.6, 141.7, 137.6, 129.6, 127.3, 126.5, 124.4, 122.7, 116.9, 67.5, 52.4, 25.2, 14.1; IR (neat): ν_{max} 3313, 2961, 2853, 2820, 1682, 1499, 1408, 1236, 1114, 997, 952, 747, 695, 619 cm^{-1} ; HRMS (ESI, m/z) calcd. For $\text{C}_{18}\text{H}_{22}\text{N}_3\text{O}_2$ $[\text{M}+\text{H}]^+$: 312.1712; found: 312.1712.

***N*-(3-chloro-2-methyl-6-morpholinophenyl)picolinamide (27t)**



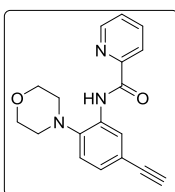
The same general procedure was followed. Column chromatography (SiO₂, eluting with 90:10 hexane/ethyl acetate) afforded the desired product as a white solid (40 mg, 61% yield), mp 148-150 °C. ¹H NMR (400 MHz, CDCl₃): δ 10.05 (s, 1H), 8.68-8.66 (m, 1H), 8.26 (d, *J* = 8.0 Hz, 1H), 7.90 (td, *J*₁ = 8.0 Hz, *J*₂ = 1.6 Hz, 1H), 7.52-7.49 (m, 1H), 7.27 (d, *J* = 8.4 Hz, 1H), 6.88 (d, *J* = 8.4 Hz, 1H), 3.74 (t, *J* = 4.4 Hz, 4H), 2.82 (t, *J* = 4.8 Hz, 4H), 2.33 (s, 3H); ¹³C NMR (100 MHz, CDCl₃): δ 162.7, 149.8, 148.4, 145.9, 137.7, 134.2, 131.6, 130.7, 127.5, 126.7, 122.8, 117.6, 67.4, 52.2, 17.3; HRMS (ESI, *m/z*) calcd. For C₁₇H₁₉ClN₃O₂ [M+H]⁺: 332.1166; found: 332.1167.

***N*-(2-morpholino-5-vinylphenyl)picolinamide (27u)**



The same general procedure was followed. Column chromatography (SiO₂, eluting with 80:20 hexane/ethyl acetate) afforded the desired product as a white solid (50 mg, 80% yield). mp 120-122 °C. ¹H NMR (400 MHz, CDCl₃): δ 11.13 (s, 1H), 8.66-8.64 (m, 1H), 8.54 (d, *J* = 8.4 Hz, 1H), 8.28 (dt, *J*₁ = 7.6 Hz, *J*₂ = 1.2 Hz, 1H), 7.89 (td, *J*₁ = 7.6 Hz, *J*₂ = 1.6 Hz, 1H), 7.48-7.45 (m, 1H), 7.24 (dd, *J*₁ = 8.0 Hz, *J*₂ = 1.6 Hz, 1H), 7.20 (d, *J* = 2.0 Hz, 1H), 6.67 (dd, *J*₁ = 17.6 Hz, *J*₂ = 10.8 Hz, 1H), 5.69 (dd, *J*₁ = 17.6 Hz, *J*₂ = 0.8 Hz, 1H), 5.20 (dd, *J*₁ = 10.8 Hz, *J*₂ = 0.8 Hz, 1H), 3.98 (t, *J* = 4.4 Hz, 4H), 2.97 (t, *J* = 4.4 Hz, 4H); ¹³C NMR (100 MHz, CDCl₃): δ 161.9, 150.5, 148.3, 142.1, 137.7, 136.5, 133.7, 132.7, 126.4, 123.5, 122.5, 119.6, 117.8, 113.0, 67.7, 52.5; IR (neat): ν_{max} 3297, 2957, 2852, 1682, 1519, 1477, 1461, 1113, 870, 816, 690 cm⁻¹; HRMS (ESI, *m/z*) calcd. For C₁₈H₁₉N₃NaO₂ [M+Na]⁺: 332.1375; found: 332.1375.

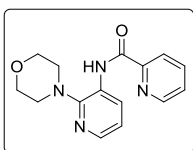
***N*-(5-ethynyl-2-morpholinophenyl)picolinamide (27v)**



The same general procedure was followed. Column chromatography (SiO₂, eluting with 80:20 hexane/ethyl acetate) afforded the desired product as a white solid (48 mg, 78% yield), mp

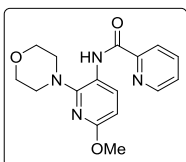
180–182 °C. ^1H NMR (400 MHz, CDCl_3): δ 11.00 (s, 1H), 8.73 (d, $J = 2.0$ Hz, 1H), 8.65–8.63 (m, 1H), 8.28 (dt, $J_1 = 8.0$ Hz, $J_2 = 1.2$ Hz, 1H), 7.90 (td, $J_1 = 7.6$ Hz, $J_2 = 1.6$ Hz, 1H), 7.50–7.46 (m, 1H), 7.23 (dd, $J_1 = 8.0$ Hz, $J_2 = 2.0$ Hz, 1H), 7.07 (d, $J = 8.0$ Hz, 1H), 3.97 (t, $J = 4.4$ Hz, 4H), 3.03 (s, 1H), 2.94 (t, $J = 4.4$ Hz, 4H); ^{13}C NMR (100 MHz, CDCl_3): δ 161.9, 150.3, 148.3, 142.5, 137.8, 132.8, 128.2, 126.6, 123.3, 122.6, 119.9, 118.9, 99.9, 83.6, 67.5, 52.3; IR (neat): ν_{max} 3290, 3225, 3060, 2969, 2916, 2853, 2831, 1676, 1570, 1528, 1477, 1457, 1231, 1113, 895, 818, 746, 691 cm^{-1} ; HRMS (ESI, m/z) calcd. For $\text{C}_{18}\text{H}_{18}\text{N}_3\text{O}_2$ $[\text{M}+\text{H}]^+$: 308.1399; found: 308.1400.

***N*-(2-morpholinopyridin-3-yl)picolinamide (27w)**^{19, 21}



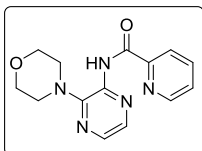
The same general procedure was followed. Column chromatography (SiO_2 , eluting with 75:25 hexane/ethyl acetate) afforded the desired product as white crystalline solid (47 mg, 83% yield). ^1H NMR (400 MHz, CDCl_3): 10.65 (s, 1H), 8.75 (dd, $J_1 = 8.0$ Hz, $J_2 = 1.6$ Hz, 1H), 8.65–8.63 (m, 1H), 8.26 (dt, $J_1 = 7.6$ Hz, $J_2 = 1.2$ Hz), 7.90 (td, $J_1 = 7.6$ Hz, $J_2 = 1.6$ Hz, 1H), 7.50–7.47 (m, 1H), 7.08–7.04 (m, 1H), 3.96 (t, $J = 4.8$ Hz, 4H), 3.13 (t, $J = 4.8$ Hz, 4H); ^{13}C NMR (100 MHz, CDCl_3): δ 162.4, 153.2, 150.0, 148.4, 142.8, 137.8, 127.3, 127.2, 126.8, 122.5, 120.0, 67.4, 50.5.

***N*-(6-methoxy-2-morpholinopyridin-3-yl)picolinamide (27x)**



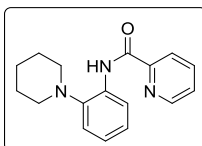
The same general procedure was followed. Column chromatography (SiO_2 , eluting with 75:25 hexane/ethyl acetate) afforded the desired product as a light brown crystalline solid (59 mg, 94% yield), mp 100–102 °C. ^1H NMR (400 MHz, CDCl_3): δ 10.29 (s, 1H), 8.61–8.59 (m, 2H), 8.23 (dt, $J_1 = 7.6$ Hz, $J_2 = 1.6$ Hz, 1H), 7.87 (td, $J_1 = 7.6$ Hz, $J_2 = 1.6$ Hz, 1H), 7.46–7.43 (m, 1H), 6.48 (d, $J = 8.4$ Hz, 1H), 3.91 (t, $J = 4.4$ Hz, 4H), 3.86 (s, 3H), 3.13 (t, $J = 4.8$ Hz, 4H); ^{13}C NMR (100 MHz, CDCl_3): δ 161.7, 159.9, 151.1, 150.1, 148.3, 137.7, 131.8, 126.5, 122.3, 119.9, 104.4, 67.3, 53.5, 50.2; HRMS (ESI, m/z) calcd. For $\text{C}_{16}\text{H}_{19}\text{N}_4\text{O}_3$ $[\text{M}+\text{H}]^+$: 315.1457; found: 315.1462.

***N*-(3-morpholinopyrazin-2-yl)picolinamide (27y)**



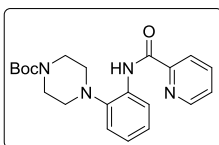
The same general procedure was followed. Column chromatography (SiO₂, eluting with 85:15 hexane/ethyl acetate) afforded the desired product as a brownish solid (27 mg, 44% yield), mp 156-158 °C. ¹H NMR (400 MHz, CDCl₃): δ 10.80 (s, 1H), 8.65-8.63 (m, 1H), 8.35-8.33 (m, 1H), 8.15 (d, *J* = 2.8 Hz, 1H), 8.02 (d, *J* = 2.8 Hz, 1H), 7.93 (td, *J*₁ = 7.6 Hz, *J*₂ = 1.6 Hz, 1H), 7.54-7.51 (m, 1H), 3.95 (t, *J* = 4.4 Hz, 4H), 3.23 (t, *J* = 4.8 Hz, 4H); ¹³C NMR (100 MHz, CDCl₃): δ 161.4, 149.7, 149.6, 148.3, 141.1, 137.9, 137.3, 136.9, 127.1, 123.1, 67.0, 49.6; IR (neat): ν_{max} 3310, 2916, 2851, 1710, 1499, 1438, 1115, 750 cm⁻¹; HRMS (ESI, *m/z*) calcd. For C₁₄H₁₆N₅O₂ [M+H]⁺: 286.1304; found: 286.1306.

***N*-(2-(piperidin-1-yl)phenyl)picolinamide (27z)**^{19, 20, 21}

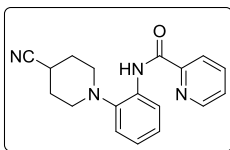


The same general procedure was followed. Column chromatography (SiO₂, eluting with 90:10 hexane/ethyl acetate) afforded the desired product as a white solid (43 mg, 76% yield). ¹H NMR (400 MHz, CDCl₃): δ 11.1 (s, 1H), 8.66-8.64 (m, 1H), 8.58-8.55 (m, 1H), 8.29 (dt, *J*₁ = 7.6 Hz, *J*₂ = 1.2 Hz, 1H), 8.88 (td, *J*₁ = 7.6 Hz, *J*₂ = 1.6 Hz, 1H), 7.46-7.42 (m, 1H), 7.17-7.13 (m, 2H), 7.09-7.05 (m, 1H), 2.87 (t, *J* = 4.4 Hz, 4H), 1.87-1.81 (m, 4H), 1.62 (brs, 2H); ¹³C NMR (100 MHz, CDCl₃): δ 162.1, 150.8, 148.3, 137.5, 133.1, 126.2, 124.7, 124.0, 122.4, 120.2, 119.5, 53.8, 26.8, 24.4.

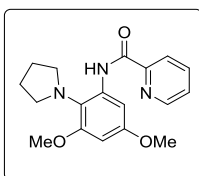
***tert*-butyl 4-(2-(picolinamido)phenyl)piperazine-1-carboxylate (27aa)**^{19, 20}



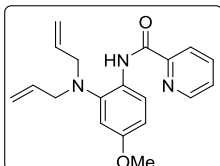
The same general procedure was followed. Column chromatography (SiO₂, eluting with 85:15 hexane/ethyl acetate) afforded the desired product as a white solid (66 mg, 86% yield). ¹H NMR (400 MHz, CDCl₃): δ 11.08 (s, 1H), 8.65-8.63 (m, 1H), 8.57 (dd, *J*₁ = 8.0 Hz, *J*₂ = 0.8 Hz, 1H), 8.29 (dt, *J*₁ = 8.0 Hz, *J*₂ = 0.8 Hz, 1H), 7.89 (td, *J*₁ = 7.6 Hz, *J*₂ = 1.6 Hz, 1H), 7.48-7.44 (m, 1H), 7.21-7.17 (m, 1H), 7.14-7.06 (m, 2H), 3.69 (brs, 4H), 2.89 (t, *J* = 4.8 Hz), 1.49 (s, 9H); ¹³C NMR (100 MHz, CDCl₃): δ 162.0, 154.8, 150.6, 148.4, 142.0, 137.7, 133.0, 126.4, 125.4, 124.1, 122.5, 120.2, 119.8, 80.0, 52.1, 28.6.

***N*-2-(4-cyanopiperidin-1-yl)phenylpicolinamide (27ab)**^{20, 21}

The same general procedure was followed. Column chromatography (SiO₂, eluting with 90:10 hexane/ethyl acetate) afforded the desired product as a white crystalline solid (56 mg, 91% yield). ¹H NMR (400 MHz, CDCl₃): δ 11.01 (s, 1H), 8.65-8.64 (m, 1H), 8.56 (dd, *J*₁ = 8.0 Hz, *J*₂ = 1.6 Hz, 1H), 8.29 (dt, *J*₁ = 8.0 Hz, *J*₂ = 0.8 Hz, 1H), 7.89 (td, *J*₁ = 7.6 Hz, *J*₂ = 1.6 Hz, 1H), 7.49-7.45 (m, 1H), 7.20-7.05 (m, 3H), 3.14-3.09 (m, 2H), 2.87-2.82 (m, 3H), 2.23-2.11 (m, 4H); ¹³C NMR (100 MHz, CDCl₃): δ 161.9, 150.5, 148.3, 142.1, 137.8, 133.0, 126.5, 125.5, 124.1, 122.5, 121.8, 120.3, 119.7, 50.8, 29.7, 26.2.

***N*-(3,5-dimethoxy-2-(pyrrolidin-1-yl)phenyl)picolinamide (27ac)**

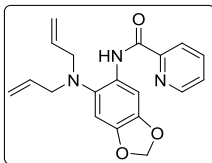
The same general procedure was followed. Column chromatography (SiO₂, eluting with 85:15 hexane/ethyl acetate) afforded the desired product as a gummy liquid (11 mg, 17% yield). ¹H NMR (400 MHz, CDCl₃): δ 11.62 (s, 1H), 8.62 (d, *J* = 4.4 Hz, 1H), 8.25 (dt, *J*₁ = 8.0 Hz, *J*₂ = 0.8 Hz, 1H), 7.96 (brs, 1H), 7.86 (td, *J*₁ = 8.0 Hz, *J*₂ = 2.0 Hz, 1H), 7.44-7.40 (m, 1H), 6.27 (s, 1H), 3.85 (s, 3H), 3.80 (s, 3H), 3.15 (brs, 4H), 2.01 (s, 4H); ¹³C NMR (100 MHz, CDCl₃): δ 158.7, 148.5, 137.4, 126.1, 122.4, 120.1, 55.7, 55.3, 26.1; HRMS (EI, *m/z*) calcd. For C₁₈H₂₂N₃O₃ [M+H]⁺: 328.1661; found: 328.1671.

***N*-(2-(diallylamino)-4-methoxyphenyl)picolinamide (27ad)**

The same general procedure was followed. Column chromatography (SiO₂, eluting with 90:10 hexane/ethyl acetate) afforded the desired product as a gummy liquid (26 mg, 40% yield). ¹H NMR (400 MHz, CDCl₃): δ 10.96 (s, 1H), 8.64-8.62 (m, 1H), 8.50 (d, *J* = 8.0 Hz, 1H), 8.28-8.26 (m, 1H), 7.86 (td, *J*₁ = 7.6 Hz, *J*₂ = 1.6 Hz, 1H), 7.44-7.41 (m, 1H), 6.72-6.69 (m, 2H), 5.91-5.81 (m, 2H), 5.22-5.17 (m, 2H), 5.11-5.08 (m, 2H), 3.78 (s, 3H), 3.58-3.56 (m, 4H); ¹³C NMR (100 MHz, CDCl₃): δ 161.7, 155.9, 150.8, 148.2, 142.0, 137.5, 134.7, 128.0, 126.1, 122.,

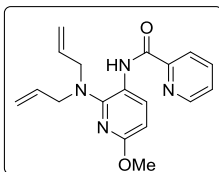
120.5, 118.0, 110.1, 109.2, 56.5, 55.5; IR (neat): ν_{\max} 3307, 2925, 2834, 1675, 1518, 1417, 1279, 1205, 1101, 997, 922, 812, 690 cm^{-1} ; HRMS (ESI, m/z) calcd. For $\text{C}_{19}\text{H}_{22}\text{N}_3\text{O}_2$ $[\text{M}+\text{H}]^+$: 324.1712; found: 324.1719.

***N*-(4-(diallylamino)benzo[d][1,3]dioxol-5-yl)picolinamide (27ae)**



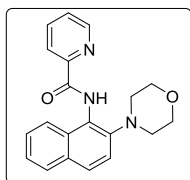
The same general procedure was followed. Column chromatography (SiO_2 , eluting with 90:10 hexane/ethyl acetate) afforded the desired product as a gummy liquid (20 mg, 30% yield). ^1H NMR (400 MHz, CDCl_3): δ 11.23 (s, 1H), 8.64-8.62 (m, 1H), 8.27-8.23 (m, 2H), 7.89-7.84 (m, 1H), 7.45-7.41 (m, 1H), 6.73 (s, 1H), 5.92 (s, 2H), 5.89-5.80 (m, 2H), 5.18 (d, $J = 18.0$ Hz, 2H), 5.07 (d, $J = 9.6$ Hz, 2H), 3.51 (d, $J = 6.0$ Hz, 4H); ^{13}C NMR (100 MHz, CDCl_3): δ 161.7, 150.8, 148.3, 144.7, 143.4, 137.5, 134.8, 134.1, 129.5, 126.1, 122.3, 118.0, 104.3, 101.2, 101.1, 57.6; IR (neat): ν_{\max} 3294, 2923, 2853, 1675, 1503, 1476, 1171, 1038, 925, 747, 694, 530 cm^{-1} ; HRMS (ESI, m/z) calcd. For $\text{C}_{19}\text{H}_{20}\text{N}_3\text{O}_3$ $[\text{M}+\text{H}]^+$: 338.1505; found: 338.1508.

***N*-(2-(diallylamino)-6-methoxypyridin-3-yl)picolinamide (27af)**



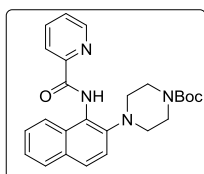
The same general procedure was followed. Column chromatography (SiO_2 , eluting with 90:10 hexane/ethyl acetate) afforded the desired product as a gummy liquid (26 mg, 40 % yield). ^1H NMR (400 MHz, CDCl_3): δ 10.25 (s, 1H), 8.63-8.61 (m, 1H), 8.53 (d, $J = 8.8$ Hz, 1H), 8.25 (dt, $J_1 = 8.0$ Hz, $J_2 = 0.8$ Hz, 1H), 7.87 (td, $J_1 = 7.6$ Hz, $J_2 = 1.6$ Hz, 1H), 7.46-7.43 (m, 1H), 6.45 (d, $J = 8.4$ Hz, 1H), 6.00-5.90 (m, 2H), 5.21 (q, $J = 1.6$ Hz), 5.17 (q, $J = 1.6$ Hz), 5.11 (q, $J = 1.2$ Hz), 5.08 (q, $J = 1.2$ Hz), 3.87 (s, 3H), 3.77 (t, $J = 0.8$ Hz), 3.75 (t, $J = 1.2$ Hz); ^{13}C NMR (100 MHz, CDCl_3): δ 162.2, 159.1, 151.1, 150.2, 148.2, 137.5, 135.3, 132.9, 126.3, 122.3, 120.1, 117.4, 104.2, 54.0, 53.5; IR (neat): ν_{\max} 3295, 3014, 2925, 2854, 1675, 1508, 1215, 749, 690, 667 cm^{-1} (HRMS (ESI, m/z) calcd. For $\text{C}_{18}\text{H}_{21}\text{N}_4\text{O}_2$ $[\text{M}+\text{H}]^+$: 325.1665; found: 325.1669.

***N*-(2-morpholinonaphthalen-1-yl)picolinamide (28a)**^{19, 20, 21}



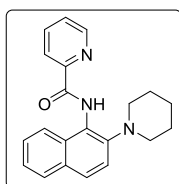
The same general procedure was followed. Column chromatography (SiO₂, eluting with 80:20 hexane/ethyl acetate) afforded the desired product as a light brown crystalline solid (53 mg, 80 % yield). ¹H NMR (400 MHz, CDCl₃): δ 10.28 (s, 1H), 8.72-8.70 (m, 1H), 8.34 (dt, *J*₁ = 8.0 Hz, *J*₂ = 0.8 Hz, 1H), 7.94-7.88 (m, 2H), 7.80 (d, *J* = 8.8 Hz, 2H), 7.53-7.46 (m, 2H), 7.42-7.38 (m, 1H), 7.36 (d, *J* = 8.8 Hz, 1H), 3.80 (t, *J* = 4.4 Hz, 4H), 2.99 (t, *J* = 4.4 Hz, 4H); ¹³C NMR (100 MHz, CDCl₃): δ 163.5, 150.0, 148.4, 144.2, 137.7, 131.3, 129.8, 128.1, 128.0, 126.7, 126.3, 126.2, 125.0, 124.6, 123.0, 118.7, 67.6, 52.2.

***tert*-butyl 4-(1-(picolinamido)naphthalen-2-yl)piperazine-1-carboxylate (28b)**¹⁹



The same general procedure was followed. Column chromatography (SiO₂, eluting with 80:20 hexane/ethyl acetate) afforded the desired product as a light brown solid (67 mg, 78% yield), mp 158-160 °C. ¹H NMR (400 MHz, CDCl₃): δ 10.26 (s, 1H), 8.71-8.69 (m, 1H), 8.34 (dt, *J*₁ = 8.0 Hz, *J*₂ = 0.8 Hz, 1H), 7.92 (td, *J*₁ = 7.6 Hz, *J*₂ = 1.6 Hz, 1H), 7.87 (d, *J* = 8.4 Hz, 1H), 7.79 (d, *J* = 8.8 Hz, 2H), 7.54-7.46 (m, 2H), 7.42-7.38 (m, 1H), 7.32 (d, *J* = 8.8 Hz, 1H), 3.52 (t, *J* = 4.8 Hz, 4H), 2.93 (t, *J* = 4.4 Hz, 4H), 1.44 (s, 9H); ¹³C NMR (100 MHz, CDCl₃): δ 163.5, 154.8, 150.0, 148.5, 144.2, 137.7, 131.3, 129.8, 128.1, 128.0, 126.7, 126.35, 126.29, 125.1, 124.6, 122.8, 118.7, 79.9, 51.8, 28.5; HRMS (ESI, *m/z*) calcd. For C₂₅H₂₈N₄NaO₃ [M+Na]⁺: 455.2059; found: 455.2072.

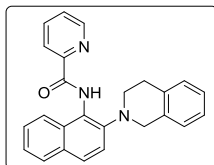
***N*-(2-(piperidin-1-yl)naphthalen-1-yl)picolinamide (28c)**



The same general procedure was followed. Column chromatography (SiO₂, eluting with 80:20 hexane/ethyl acetate) afforded the desired product as a gummy liquid (50 mg, 76% yield). ¹H NMR (400 MHz, CDCl₃): δ 10.26 (s, 1H), 8.72 (s, 1H), 8.35 (d, *J* = 8.0 Hz, 1H), 7.92 (td, *J*₁ = 8.0 Hz, *J*₂ = 2.0 Hz, 1H), 7.85 (d, *J* = 8.4 Hz, 1H), 7.79 (d, *J* = 7.6 Hz, 2H), 7.53-7.49 (m, 1H),

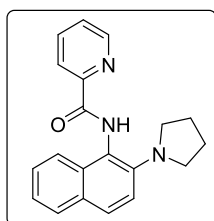
7.48-7.44 (m, 1H), 7.38 (brs, 2H), 2.92 (s, 3H), 1.65 (s, 4H), 1.53 (s, 3H); ^{13}C NMR (100 MHz, CDCl_3): δ 163.6, 150.2, 148.3, 145.8, 137.5, 130.9, 129.6, 127.9, 127.7, 126.4, 126.0, 125.9, 124.63, 124.56, 122.8, 119.1, 53.4, 26.7, 24.5; HRMS (ESI, m/z) calcd. For $\text{C}_{21}\text{H}_{22}\text{N}_3\text{O}$ $[\text{M}+\text{H}]^+$: 332.1763; found: 332.1771.

***N*-2-(3,4-dihydroisoquinolin-2(1H)-yl)naphthalen-1-yl)picolinamide (28d)**



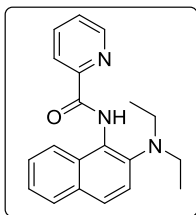
The same general procedure was followed. Column chromatography (SiO_2 , eluting with 80:20 hexane/ethyl acetate) afforded the desired product as a light yellow solid (38 mg, 50% yield), mp 136–138 °C. ^1H NMR (400 MHz, CDCl_3): δ 10.16 (s, 1H), 8.57-8.55 (m, 1H), 8.36 (dt, $J_1 = 8.0$ Hz, $J_2 = 0.8$ Hz, 1H), 7.91 (td, $J_1 = 8.0$ Hz, $J_2 = 2.0$ Hz, 1H), 7.86-7.79 (m, 3H), 7.50-7.44 (m, 3H), 7.42-7.38 (m, 1H), 7.18-7.08 (m, 3H), 7.04 (d, $J = 6.8$ Hz, 1H), 4.32 (s, 2H), 3.28 (t, $J = 5.6$ Hz, 2H), 2.88 (t, $J = 5.6$ Hz, 2H); ^{13}C NMR (100 MHz, CDCl_3): δ 163.8, 150.0, 148.3, 137.6, 134.8, 131.0, 130.1, 129.0, 128.1, 126.52, 126.46, 126.4, 126.3, 125.8, 125.5, 124.8, 124.3, 122.8, 119.0, 53.2, 51.1, 29.6; HRMS (ESI, m/z) calcd. For $\text{C}_{25}\text{H}_{22}\text{N}_3\text{O}$ $[\text{M}+\text{H}]^+$: 380.1763; found: 380.1753.

***N*-2-(pyrrolidin-1-yl)naphthalen-1-yl)picolinamide (28e)**



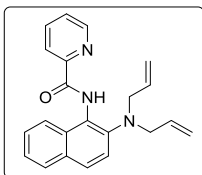
The same general procedure was followed. Column chromatography (SiO_2 , eluting with 70:30 hexane/ethyl acetate) afforded the desired product as a brownish foamy solid (42 mg, 66% yield). ^1H NMR (400 MHz, CDCl_3): δ 9.66 (s, 1H), 8.68-8.66 (m, 1H), 8.34 (dt, $J_1 = 8.0$ Hz, $J_2 = 0.8$ Hz, 1H), 7.90 (td, $J_1 = 7.6$ Hz, $J_2 = 1.6$ Hz, 1H), 7.72-7.67 (m, 3H), 7.51-7.48 (m, 1H), 7.39-7.35 (m, 1H), 7.24-7.20 (m, 2H), 3.44 (t, $J = 5.2$ Hz, 4H), 1.88 (t, $J = 6.0$ Hz, 4H); ^{13}C NMR (100 MHz, CDCl_3): δ 163.9, 150.2, 148.5, 144.9, 137.6, 132.4, 128.4, 128.12, 128.11, 126.9, 126.5, 122.9, 122.4, 121.6, 117.2, 114.8, 50.6, 25.8; HRMS (ESI, m/z) calcd. For $\text{C}_{20}\text{H}_{20}\text{N}_3\text{O}$ $[\text{M}+\text{H}]^+$: 318.1606; found: 318.1605.

***N*-2-(diethylamino)naphthalen-1-yl)picolinamide (28f)**



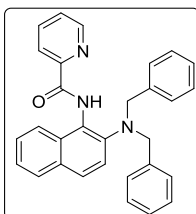
The same general procedure was followed. Column chromatography (SiO₂, eluting with 90:10 hexane/ethyl acetate) afforded the desired product as a light yellow gummy liquid (20 mg, 31% yield). ¹H NMR (400 MHz, CDCl₃): δ 10.29 (s, 1H), 8.71-8.69 (m, 1H), 8.35 (dt, *J*₁ = 8.0 Hz, *J*₂ = 0.8 Hz, 1H), 7.93-7.85 (m, 2H), 7.80 (d, *J* = 8.0 Hz, 1H), 7.76 (d, *J* = 8.8 Hz, 1H), 7.51-7.44 (m, 2H), 7.40 (t, *J* = 7.6 Hz, 2H), 3.06 (q, *J* = 7.2 Hz, 4H), 0.99 (t, *J* = 7.2 Hz, 6H); ¹³C NMR (100 MHz, CDCl₃): δ 163.5, 150.3, 148.4, 137.5, 131.3, 129.7, 128.6, 128.0, 127.3, 126.4, 126.0, 125.0, 122.8, 121.0, 48.0, 13.2; HRMS (ESI, *m/z*) calcd. For C₂₀H₂₂N₃O [M+H]⁺: 320.1763; found: 320.1763.

***N*-(2-(diallylamino)naphthalen-1-yl)picolinamide (28g)**



The same general procedure was followed. Column chromatography (SiO₂, eluting with 90:10 hexane/ethyl acetate) afforded the desired product as a light yellow gummy liquid (56 mg, 81% yield). ¹H NMR (400 MHz, CDCl₃): δ 10.17 (s, 1H), 8.71-8.69 (m, 1H), 8.34 (dt, *J*₁ = 8.0 Hz, *J*₂ = 0.8 Hz, 1H), 7.91 (td, *J*₁ = 7.6 Hz, *J*₂ = 1.6 Hz, 1H), 7.85 (d, *J* = 8.4 Hz, 1H), 7.78 (d, *J* = 8.4 Hz, 1H), 7.74 (d, *J* = 8.8 Hz, 1H), 7.51-7.44 (m, 2H), 7.40-7.35 (m, 2H), 5.83-5.73 (m, 2H), 5.16 (dd, *J*₁ = 17.2 Hz, *J*₂ = 1.6 Hz, 2H), 5.03 (dd, *J*₁ = 10.0 Hz, *J*₂ = 1.6 Hz, 2H), 3.67 (d, *J* = 6.0 Hz, 4H); ¹³C NMR (100 MHz, CDCl₃): δ 163.5, 150.2, 148.3, 137.6, 135.1, 131.0, 130.1, 127.9, 127.3, 126.54, 126.46, 126.2, 124.8, 124.4, 122.8, 121.3, 117.6, 55.9; HRMS (ESI, *m/z*) calcd. For C₂₂H₂₂N₃O [M+H]⁺: 344.1763; found: 344.1765.

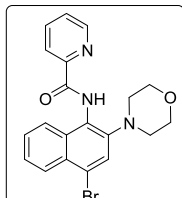
***N*-(2-(dibenzylamino)naphthalen-1-yl)picolinamide (28h)**



The same general procedure was followed. Column chromatography (SiO₂, eluting with 90:10 hexane/ethyl acetate) afforded the desired product as a light yellow gummy liquid (52 mg, 59% yield). ¹H NMR (400 MHz, CDCl₃): δ 10.31 (s, 1H), 8.76-8.74 (m, 1H), 8.32-8.29 (m, 1H),

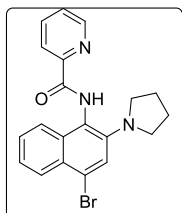
7.92-7.86 (m, 2H), 7.77 (d, $J = 8.0$ Hz, 1H), 7.70 (d, $J = 8.8$ Hz, 1H), 7.53-7.50 (m, 1H), 7.48-7.44 (m, 1H), 7.41-7.37 (m, 1H), 7.33-7.24 (m, 5H), 7.21-7.15 (m, 6H), 4.17 (s, 4H); ^{13}C NMR (100 MHz, CDCl_3): δ 163.4, 150.2, 148.2, 143.6, 138.1, 137.5, 131.4, 130.1, 128.8, 128.3, 127.9, 127.5, 127.3, 127.1, 126.4, 126.2, 125.1, 124.7, 122.8, 121.8, 57.3; HRMS (ESI, m/z) calcd. For $\text{C}_{30}\text{H}_{26}\text{N}_3\text{O}$ $[\text{M}+\text{H}]^+$: 444.2076; found: 444.2067.

***N*-(4-bromo-2-morpholinonaphthalen-1-yl)picolinamide (28i)**



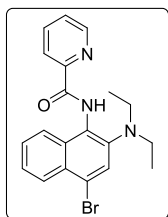
The same general procedure was followed. Column chromatography (SiO_2 , eluting with 80:20 hexane/ethyl acetate) afforded the desired product as a light brown solid (72 mg, 88% yield), mp 146–148 °C. ^1H NMR (400 MHz, CDCl_3): δ 10.20 (s, 1H), 8.73-8.71 (m, 1H), 8.33 (dt, $J_1 = 8.0$ Hz, $J_2 = 0.8$ Hz, 1H), 8.20-8.16 (m, 1H), 7.94 (td, $J_1 = 8.0$ Hz, $J_2 = 2.0$ Hz, 1H), 7.90-7.86 (m, 1H), 7.67 (s, 1H), 7.56-7.50 (m, 3H), 3.80 (t, $J = 4.4$ Hz, 4H), 2.99 (t, $J = 4.4$ Hz, 4H); ^{13}C NMR (100 MHz, CDCl_3): δ 163.6, 149.8, 148.4, 144.4, 137.8, 130.8, 129.7, 127.4, 127.1, 126.8, 126.4, 126.3, 124.9, 123.3, 122.9, 122.2, 67.4, 52.1; HRMS (ESI, m/z) calcd. For $\text{C}_{20}\text{H}_{19}\text{BrN}_3\text{O}_2$ $[\text{M}+\text{H}]^+$: 412.0661; found: 412.0662.

***N*-(4-bromo-2-(pyrrolidin-1-yl)naphthalen-1-yl)picolinamide (28j)**



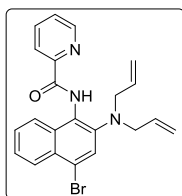
The same general procedure was followed. Column chromatography (SiO_2 , eluting with 80:20 hexane/ethyl acetate) afforded the desired product as a light brown gummy liquid (57 mg, 72% yield). ^1H NMR (400 MHz, CDCl_3): δ 9.63 (s, 1H), 8.68-8.66 (m, 1H), 8.32 (dt, $J_1 = 8.0$ Hz, $J_2 = 0.8$ Hz, 1H), 8.07 (d, $J = 8.4$ Hz, 1H), 7.92 (td, $J_1 = 7.6$ Hz, $J_2 = 1.6$ Hz, 1H), 7.68 (d, $J = 8.4$ Hz, 1H), 7.55-7.50 (m, 2H), 7.40 (t, $J = 7.2$ Hz, 1H), 7.32 (t, $J = 7.6$ Hz, 1H), 3.44 (s, 4H), 1.89 (t, $J = 5.6$ Hz, 4H); ^{13}C NMR (100 MHz, CDCl_3): δ 163.9, 149.9, 148.5, 137.7, 133.3, 127.7, 127.5, 126.7, 123.3, 122.9, 122.0, 121.3, 50.8, 25.8; HRMS (ESI, m/z) calcd. For $\text{C}_{20}\text{H}_{19}\text{BrN}_3\text{O}$ $[\text{M}+\text{H}]^+$: 396.0711; found: 396.0714.

***N*-(4-bromo-2-(diethylamino)naphthalen-1-yl)picolinamide (28k)**



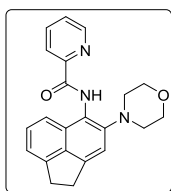
The same general procedure was followed. Column chromatography (SiO₂, eluting with 90:10 hexane/ethyl acetate) afforded the desired product as a brownish gummy liquid (36 mg, 45% yield). ¹H NMR (400 MHz, CDCl₃): δ 10.17 (s, 1H), 8.71-8.69 (m, 1H), 8.34-8.31 (m, 1H), 8.19-8.16 (m, 1H), 7.92 (td, *J*₁ = 8.0 Hz, *J*₂ = 2.0 Hz, 1H), 7.87-7.84 (m, 1H), 7.68 (s, 1H), 7.53-7.49 (m, 3H), 3.03 (q, *J* = 6.8 Hz, 4H), 0.99 (t, *J* = 6.8 Hz, 6H); ¹³C NMR (100 MHz, CDCl₃): δ 149.9, 148.1, 137.6, 130.7, 128.5, 127.3, 126.8, 126.3, 125.4, 125.0, 122.9, 99.5, 47.9, 13.2; IR (neat): ν_{max} 3339, 2968, 2926, 2852, 1689, 1589, 1492, 1463, 1431, 1379, 1326, 749, 699, 521 cm⁻¹ HRMS (ESI, m/z) calcd. For C₂₀H₂₁BrN₃O [M+H]⁺: 398.0868; found: 398.0868.

***N*-(4-bromo-2-(diallylamino)naphthalen-1-yl)picolinamide (28I)**



The same general procedure was followed. Column chromatography (SiO₂, eluting with 90:10 hexane/ethyl acetate) afforded the desired product as a light brown solid (59 mg, 70% yield), mp 102-104 °C. ¹H NMR (400 MHz, CDCl₃): δ 10.05 (s, 1H), 8.71-8.69 (m, 1H), 8.32 (dt, *J*₁ = 8.0 Hz, *J*₂ = 0.8 Hz, 1H), 8.18-8.14 (m, 1H), 7.92 (td, *J*₁ = 7.6 Hz, *J*₂ = 1.6 Hz, 1H), 7.86-7.82 (m, 1H), 7.65 (s, 1H), 7.53-7.47 (m, 3H), 5.81-5.71 (m, 2H), 5.19 (d, *J* = 1.6 Hz, 1H), 5.15 (d, *J* = 1.6 Hz, 1H), 5.07 (d, *J* = 1.2 Hz, 1H), 5.04 (d, *J* = 1.2 Hz, 1H), 3.65 (d, *J* = 6.0 Hz, 4H); ¹³C NMR (100 MHz, CDCl₃): δ 163.6, 149.9, 148.4, 137.6, 134.5, 131.1, 129.4, 127.4, 127.0, 126.6, 126.4, 126.2, 125.6, 124.7, 122.8, 121.7, 118.0, 77.4, 55.8; IR (neat): ν_{max} 3336, 3008, 2923, 2851, 1684, 1588, 1489, 1431, 997, 917, 903, 747, 694, 621, 580 cm⁻¹; HRMS (ESI, m/z) calcd. For C₂₂H₂₀BrN₃NaO [M+Na]⁺: 444.0687; found: 444.0683.

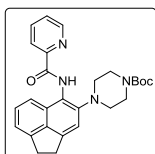
***N*-(4-morpholino-1,2-dihydroacenaphthylen-5-yl)picolinamide (28m)**



The same general procedure was followed. Column chromatography (SiO₂, eluting with 80:20 hexane/ethyl acetate) afforded the desired product as a yellow solid (55 mg, 77% yield), mp

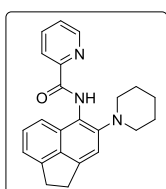
168–170 °C. ^1H NMR (400 MHz, CDCl_3): δ 10.35 (s, 1H), 8.71-8.69 (m, 1H), 8.35 (dt, $J_1 = 8.0$ Hz, $J_2 = 1.2$ Hz, 1H), 7.92 (td, $J_1 = 7.6$ Hz, $J_2 = 1.6$ Hz, 1H), 7.60 (d, $J = 8.4$ Hz, 1H), 7.51-7.43 (m, 2H), 7.21 (d, $J = 8.4$ Hz, 2H), 3.83 (t, $J = 4.4$ Hz, 4H), 3.37 (s, 4H), 2.98 (t, $J = 4.8$ Hz, 4H), ^{13}C NMR (100 MHz, CDCl_3): δ 163.9, 150.4, 148.3, 145.9, 145.7, 137.7, 136.9, 128.2, 127.4, 126.5, 122.82, 122.77, 120.7, 118.5, 112.3, 67.7, 52.5, 30.6, 30.3; HRMS (ESI, m/z) calcd. For $\text{C}_{22}\text{H}_{22}\text{N}_3\text{O}_2$ $[\text{M}+\text{H}]^+$: 360.1712; found: 360.1714.

***tert*-butyl 4-(5-(picolinamido)-1,2-dihydroacenaphthylen-4-yl)piperazine-1-carboxylate (28n)**



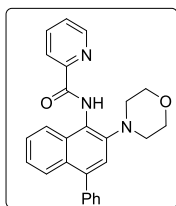
The same general procedure was followed. Column chromatography (SiO_2 , eluting with 80:20 hexane/ethyl acetate) afforded the desired product as a yellow solid (80 mg, 87% yield), mp 154–156 °C. ^1H NMR (400 MHz, CDCl_3): δ 10.30 (s, 1H), 8.70-8.68 (m, 1H), 8.35 (dt, $J_1 = 8.0$ Hz, $J_2 = 0.8$ Hz, 1H), 7.91 (td, $J_1 = 7.6$ Hz, $J_2 = 1.6$ Hz, 1H), 7.58 (d, $J = 8.4$ Hz, 1H), 7.51-7.42 (m, 2H), 7.21-7.15 (m, 2H), 3.54 (t, $J = 4.4$ Hz, 4H), 3.36 (brs, 4H), 2.92 (t, $J = 4.0$ Hz, 4H), 1.45 (s, 9H); ^{13}C NMR (100 MHz, CDCl_3): δ 162.9, 154.9, 150.3, 148.4, 145.90, 145.85, 145.7, 137.6, 136.9, 128.2, 127.4, 126.5, 122.8, 120.7, 118.6, 112.4, 79.9, 52.1, 30.6, 30.3, 28.5; HRMS (ESI, m/z) calcd. For $\text{C}_{22}\text{H}_{31}\text{N}_4\text{O}_3$ $[\text{M}+\text{H}]^+$: 459.2396; found: 459.2390.

***N*-(4-(piperidin-1-yl)-1,2-dihydroacenaphthylen-5-yl)picolinamide (28o)**



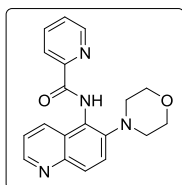
The same general procedure was followed. Column chromatography (SiO_2 , eluting with 90:10 hexane/ethyl acetate) afforded the desired product as a yellow solid (54 mg, 76% yield), mp 182–184 °C. ^1H NMR (400 MHz, CDCl_3): δ 10.34 (s, 1H), 8.71-8.69 (m, 1H), 8.37 (dt, $J_1 = 7.6$ Hz, $J_2 = 1.2$ Hz, 1H), 7.90 (td, $J_1 = 8.0$ Hz, $J_2 = 2.0$ Hz, 1H), 7.59 (dd, $J_1 = 8.4$ Hz, $J_2 = 0.4$ Hz, 1H), 7.49-7.42 (m, 2H), 7.21-7.17 (m, 2H), 3.36 (brs, 4H), 2.91 (t, $J = 5.2$ Hz, 4H), 1.71-1.66 (m, 4H), 1.57-1.51 (m, 2H); ^{13}C NMR (100 MHz, CDCl_3): δ 163.0, 150.5, 148.3, 147.5, 145.8, 145.3, 137.5, 136.6, 128.0, 127.3, 126.3, 122.7, 122.5, 120.7, 118.1, 112.7, 53.7, 30.6, 30.3, 26.8, 24.5; HRMS (ESI, m/z) calcd. For $\text{C}_{23}\text{H}_{24}\text{N}_3\text{O}$ $[\text{M}+\text{H}]^+$: 358.1919; found: 358.1918.

***N*-(2-morpholino-4-phenylnaphthalen-1-yl)picolinamide (28p)**



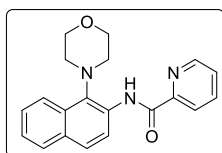
The same general procedure was followed. Column chromatography (SiO₂, eluting with 90:10 hexane/ethyl acetate) afforded the desired product as a white solid (66 mg, 81% yield), mp 234–236 °C. ¹H NMR (400 MHz, CDCl₃): δ 10.29 (s, 1H), 8.74–8.73 (m, 1H), 8.37 (dt, *J*₁ = 8.0 Hz, *J*₂ = 0.8 Hz, 1H), 7.97–7.93 (m, 2H), 8.27 (d, *J* = 7.6 Hz, 1H), 7.56–7.52 (m, 1H), 7.51–7.47 (m, 5H), 7.46–7.42 (m, 1H), 7.37–7.32 (m, 1H), 7.30 (s, 1H), 3.81 (t, *J* = 4.8 Hz, 4H), 3.03 (t, *J* = 4.4 Hz, 4H); ¹³C NMR (100 MHz, CDCl₃): δ 163.7, 150.1, 148.4, 143.7, 140.6, 137.7, 130.2, 130.1, 129.5, 128.4, 127.5, 126.7, 126.4, 126.3, 125.6, 125.1, 124.7, 122.9, 119.9, 67.6, 52.2; HRMS (ESI, *m/z*) calcd. For C₂₆H₂₄N₃O₂ [M+H]⁺: 410.1869; found: 410.1871.

***N*-(6-morpholinoquinolin-5-yl)picolinamide (28q)**



The same general procedure was followed. Column chromatography (SiO₂, eluting with 75:25 hexane/ethyl acetate) afforded the desired product as a light brown solid (53 mg, 79% yield), mp 148–150 °C. ¹H NMR (400 MHz, CDCl₃): δ 10.36 (s, 1H), 8.83 (dd, *J*₁ = 4.4 Hz, *J*₂ = 1.6 Hz, 1H), 8.76–8.71 (m, 1H), 8.32 (dt, *J*₁ = 7.6 Hz, *J*₂ = 1.2 Hz, 1H), 8.25–8.22 (m, 1H), 8.06 (d, *J* = 9.2 Hz, 1H), 8.94 (td, *J*₁ = 7.6 Hz, *J*₂ = 1.6 Hz, 1H), 7.59 (d, *J* = 9.2 Hz, 1H), 7.56–7.52 (m, 1H), 7.38 (q, *J* = 4.0 Hz, 1H), 3.82 (t, *J* = 4.4 Hz, 4H), 2.91 (t, *J* = 4.4 Hz, 4H); ¹³C NMR (100 MHz, CDCl₃): δ 163.5, 149.7, 149.5, 148.5, 145.6, 144.0, 137.8, 133.5, 129.3, 126.9, 125.9, 124.9, 122.9, 121.9, 120.9, 67.5, 51.9; HRMS (ESI, *m/z*) calcd. For C₁₉H₁₉N₄O₂ [M+H]⁺: 335.1508; found: 335.1507.

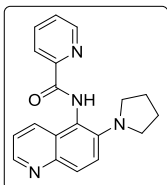
***N*-(1-morpholinonaphthalen-2-yl)picolinamide (28r)²⁰**



The same general procedure was followed. Column chromatography (SiO₂, eluting with 80:20 hexane/ethyl acetate) afforded the desired product as light yellow amorphous solid (48 mg, 72 % yield). ¹H NMR (400 MHz, CDCl₃): δ 11.98 (s, 1H), 8.90 (d, *J* = 8.8 Hz, 1H), 8.74–8.72 (m, 1H), 8.33 (dt, *J*₁ = 8.0 Hz, *J*₂ = 1.2 Hz, 1H), 8.11 (d, *J* = 8.8 Hz, 1H), 7.92 (td, *J*₁ = 7.6 Hz,

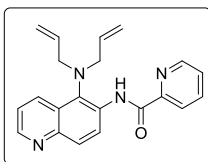
$J_2 = 1.6$ Hz, 1H), 7.85 (d, $J = 8.8$ Hz, 1H), 7.79 (d, $J = 8.8$ Hz, 1H), 7.52-7.46 (m, 2H), 7.40-7.36 (m, 1H), 4.19-4.13 (m, 2H), 4.03 (d, $J = 10.4$ Hz, 2H), 3.94-3.88 (m, 2H), 2.93 (d, $J = 12.4$ Hz, 2H); ^{13}C NMR (100 MHz, CDCl_3): δ 162.3, 150.7, 148.3, 137.7, 134.7, 133.3, 132.3, 131.6, 129.3, 127.9, 126.4, 126.1, 124.3, 123.4, 122.6, 118.9, 68.5, 51.1.

***N*-(6-(pyrrolidin-1-yl)quinolin-5-yl)picolinamide (28s)**



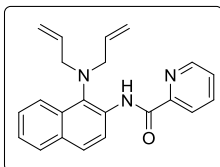
The same general procedure was followed. Column chromatography (SiO_2 , eluting with 80:20 hexane/ethyl acetate) afforded the desired product as yellow amorphous solid (42 mg, 66% yield), mp 144-146°C. ^1H NMR (600 MHz, CDCl_3): δ 9.63 (s, 1H), 8.66-8.64 (m, 1H), 8.62 (dd, $J_1 = 4.4$ Hz, $J_2 = 1.6$ Hz, 1H), 8.32 (dt, $J_1 = 7.6$ Hz, $J_2 = 1.2$ Hz, 1H), 7.97-7.89 (m, 3H), 7.52-7.49 (m, 1H), 7.40 (d, $J = 9.2$ Hz, 1H), 7.26-7.23 (m, 1H), 3.46-3.43 (m, 4H), 1.88-1.86 (m, 4H); ^{13}C NMR (150 MHz, CDCl_3): δ 164.1, 149.9, 148.5, 146.5, 144.5, 143.2, 137.7, 130.1, 129.7, 127.8, 126.7, 122.8, 121.6, 120.5, 113.4, 50.5, 25.8; HRMS (ESI, m/z) calcd. For $\text{C}_{19}\text{H}_{19}\text{N}_4\text{O}$ $[\text{M}+\text{H}]^+$: 319.1559; found: 319.1558.

***N*-(5-(diallylamino)quinolin-6-yl)picolinamide (28t)**



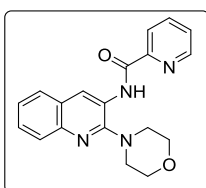
The same general procedure was followed. Column chromatography (SiO_2 , eluting with 80:20 hexane/ethyl acetate) afforded the desired product as a white solid (42 mg, 61% yield), mp 136-138 °C. ^1H NMR (400 MHz, CDCl_3): δ 11.58 (s, 1H), 9.96 (d, $J = 9.6$ Hz, 1H), 8.80 (dd, $J_1 = 4.0$ Hz, $J_2 = 1.6$ Hz, 1H), 8.69-8.67 (m, 1H), 8.33-8.28 (m, 2H), 8.03 (d, $J = 9.2$ Hz, 1H), 7.90 (td, $J_1 = 7.6$ Hz, $J_2 = 1.6$ Hz, 1H), 7.49-7.46 (m, 1H), 7.37 (q, $J = 4.4$ Hz, 1H), 6.02-5.92 (m, 2H), 5.15 (dd, $J_1 = 2.8$ Hz, $J_2 = 1.2$ Hz, 1H), 5.11 (dd, $J_1 = 2.8$ Hz, $J_2 = 1.6$ Hz, 1H), 5.02 (dd, $J_1 = 10.0$ Hz, $J_2 = 1.2$ Hz, 2H), 4.05-4.00 (m, 2H), 3.86-3.81 (m, 2H); ^{13}C NMR (100 MHz, CDCl_3): δ 162.4, 150.5, 148.5, 148.3, 146.4, 137.6, 135.9, 135.5, 132.9, 131.9, 128.8, 127.5, 126.6, 122.6, 122.5, 120.7, 117.8, 57.4; IR (neat): ν_{max} 3290, 3075, 2924, 2853, 1684, 1590, 1499, 1429, 814 cm^{-1} ; HRMS (ESI, m/z) calcd. For $\text{C}_{21}\text{H}_{21}\text{N}_4\text{O}$ $[\text{M}+\text{H}]^+$: 345.1715; found: 345.1715.

***N*-(1-(diallylamino)naphthalen-2-yl)picolinamide (28u)**



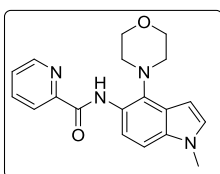
The same general procedure was followed. Column chromatography (SiO₂, eluting with 90:10 hexane/ethyl acetate) afforded the desired product as a white solid (42 mg, 61% yield); mp 126-128 °C. ¹H NMR (400 MHz, CDCl₃): δ 11.71 (s, 1H), 8.88 (d, *J* = 8.8 Hz, 1H), 8.70-8.69 (m, 1H), 8.33 (dt, *J*₁ = 8.0 Hz, *J*₂ = 0.8 Hz, 1H), 7.98 (d, *J* = 8.8 Hz, 1H), 7.91 (td, *J*₁ = 7.6 Hz, *J*₂ = 1.6 Hz, 1H), 7.84 (d, *J* = 8.0 Hz, 1H), 7.76 (d, *J* = 8.8 Hz, 1H), 7.50-7.46 (m, 2H), 7.40-7.36 (m, 1H), 6.02-5.98 (m, 2H), 5.17 (q, *J* = 1.6 Hz, 1H), 5.13 (q, *J* = 1.6 Hz, 1H), 5.03-4.99 (m, 2H), 4.08-4.04 (m, 2H), 3.91-3.85 (m, 2H); ¹³C NMR (100 MHz, CDCl₃): δ 162.3, 150.8, 148.3, 137.6, 136.1, 135.6, 133.4, 132.3, 131.8, 129.3, 127.4, 126.2, 126.0, 124.2, 123.7, 122.5, 119.1, 117.3, 57.5; HRMS (ESI, *m/z*) calcd. For C₂₂H₂₁N₃NaO [M+Na]⁺: 366.1582; found: 366.1572.

***N*-(2-morpholinoquinolin-3-yl)picolinamide (28v)**²¹



The same general procedure was followed. Column chromatography (SiO₂, eluting with 80:20 hexane/ethyl acetate) afforded the desired product as white solid (49 mg, 74% yield). ¹H NMR (400 MHz, CDCl₃): δ 11.31 (s, 1H), 10.08 (s, 1H), 8.71-8.69 (m, 1H), 8.32 (dt, *J*₁ = 7.6 Hz, *J*₂ = 1.2 Hz, 1H), 8.12-8.09 (m, 2H), 7.92 (td, *J*₁ = 7.6 Hz, *J*₂ = 1.6 Hz, 1H), 7.62-7.58 (m, 1H), 7.54-7.49 (m, 2H), 4.05 (t, *J* = 4.4 Hz, 4H), 3.35 (brs, 4H); ¹³C NMR (100 MHz, CDCl₃): δ 162.4, 149.9, 148.4, 146.8, 145.5, 141.6, 137.9, 130.8, 129.5, 127.8, 126.9, 126.8, 126.6, 123.4, 122.8, 68.2, 51.1.

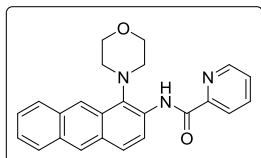
***N*-(1-methyl-4-morpholino-1H-indol-5-yl)picolinamide (28w)**



The same general procedure was followed. Column chromatography (SiO₂, eluting with 80:20 hexane/ethyl acetate) afforded the desired product as a gummy white solid (60 mg, 89% yield), mp 184-186 °C. ¹H NMR (400 MHz, CDCl₃): δ 11.62 (s, 1H), 8.69-8.67 (m, 1H), 8.63 (d, *J* = 8.8 Hz, 1H), 8.31 (dt, *J*₁ = 8.0 Hz, *J*₂ = 0.8 Hz, 1H), 7.88 (td, *J*₁ = 7.6 Hz, *J*₂ = 1.6 Hz, 1H), 7.46-

7.43 (m, 1H), 7.21 (d, $J = 8.8$ Hz, 1H), 7.03 (d, $J = 3.2$ Hz, 1H), 6.66 (dd, $J_1 = 3.2$ Hz, $J_2 = 0.4$ Hz, 1H), 4.03 (t, $J = 4.8$ Hz, 4H), 3.77 (s, 3H), 3.65-2.81 (brs, 4H); ^{13}C NMR (100 MHz, CDCl_3): δ 161.6, 151.3, 148.3, 137.6, 135.3, 132.2, 129.0, 127.6, 126.0, 124.3, 122.3, 114.5, 107.3, 99.4, 68.3, 51.8, 33.1; IR (neat): ν_{max} 3279, 2954, 2851, 1671, 1527, 1514, 1428, 1334, 1251, 1112, 872, 748, 691 cm^{-1} ; HRMS (ESI, m/z) calcd. For $\text{C}_{19}\text{H}_{21}\text{N}_4\text{O}_2$ $[\text{M}+\text{H}]^+$: 337.1665; found: 337.1667.

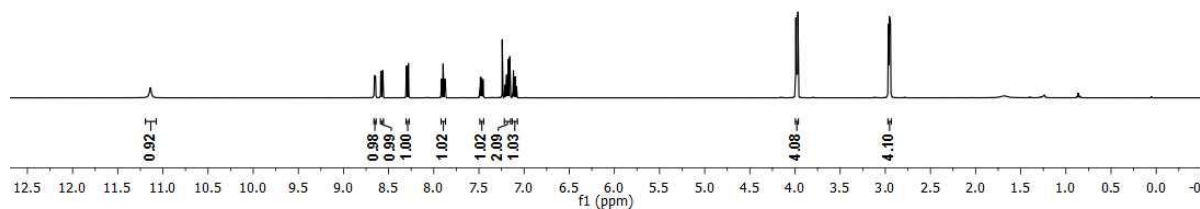
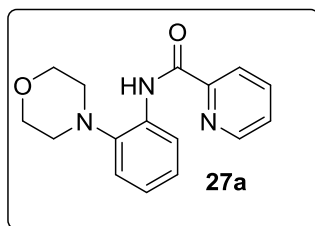
***N*-(1-morpholinoanthracen-2-yl)picolinamide (28x)**



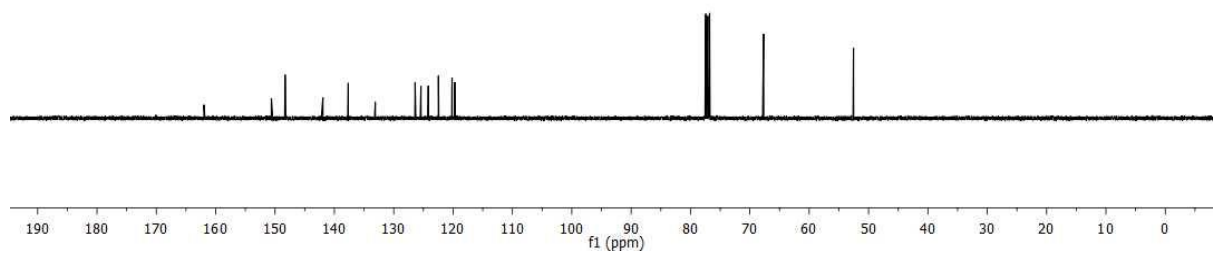
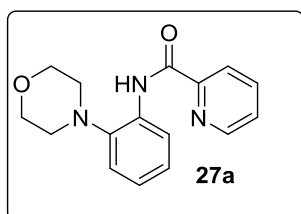
The same general procedure was followed. Column chromatography (SiO_2 , eluting with 90:10 hexane/ethyl acetate) afforded the desired product as light yellow amorphous solid (45 mg, 59% yield), mp 220-222 $^{\circ}\text{C}$. ^1H NMR (400 MHz, CDCl_3): δ 12.03 (s, 1H), 8.93 (d, $J = 9.2$ Hz, 1H), 8.75-8.73 (m, 1H), 8.62 (s, 1H), 8.43 (s, 1H), 8.35 (dt, $J_1 = 7.6$ Hz, $J_2 = 1.2$ Hz, 1H), 8.00-7.91 (m, 4H), 7.53-7.40 (m, 3H), 4.24-4.18 (m, 2H), 4.13-4.03 (m, 4H), 2.99 (d, $J = 11.2$ Hz, 2H); ^{13}C NMR (100 MHz, CDCl_3): δ 162.3, 150.8, 148.4, 137.7, 134.2, 132.2, 131.7, 130.48, 130.40, 128.3, 128.1, 127.8, 126.5, 126.0, 125.3, 122.6, 121.8, 119.4, 68.6, 51.1; HRMS (ESI, m/z) calcd. For $\text{C}_{24}\text{H}_{22}\text{N}_3\text{O}_2$ $[\text{M}+\text{H}]^+$: 384.1712; found: 384.1710.

II. 11. ^1H and ^{13}C NMR Spectra

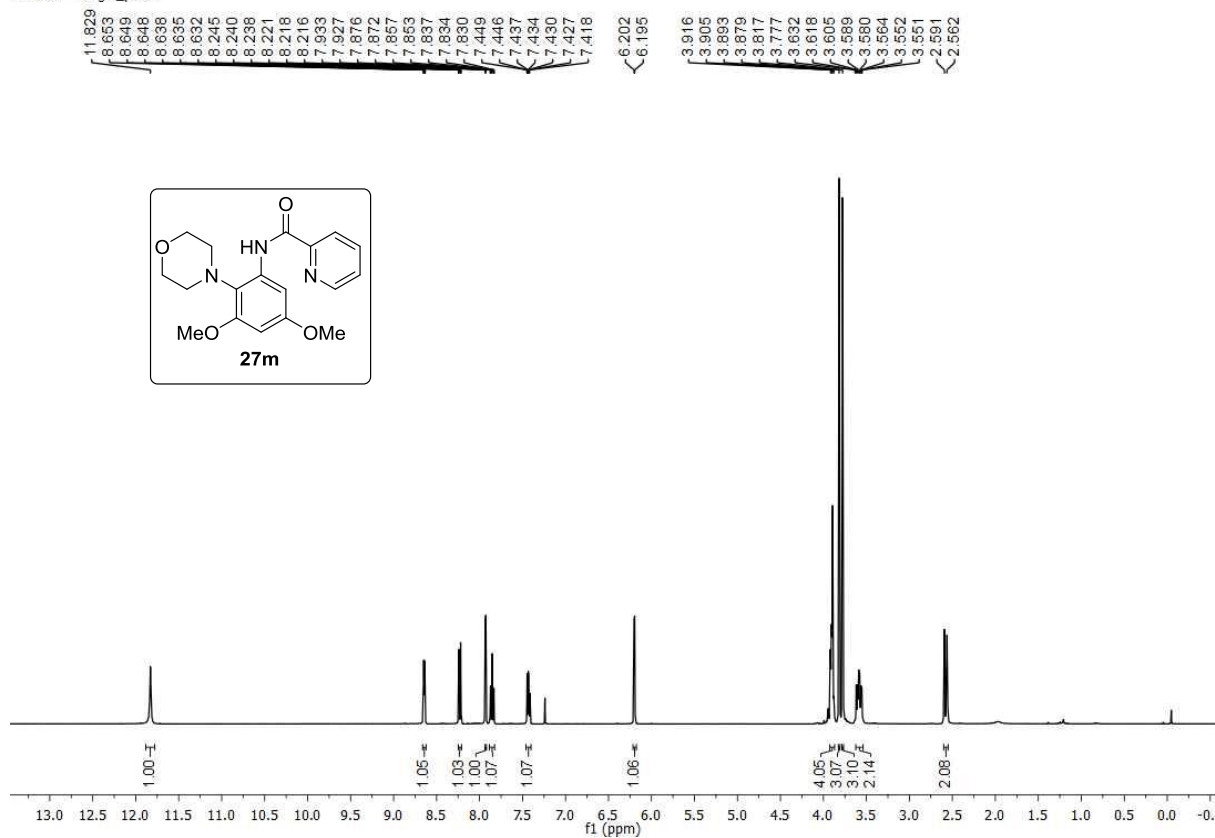
HM-304 — single_pulse



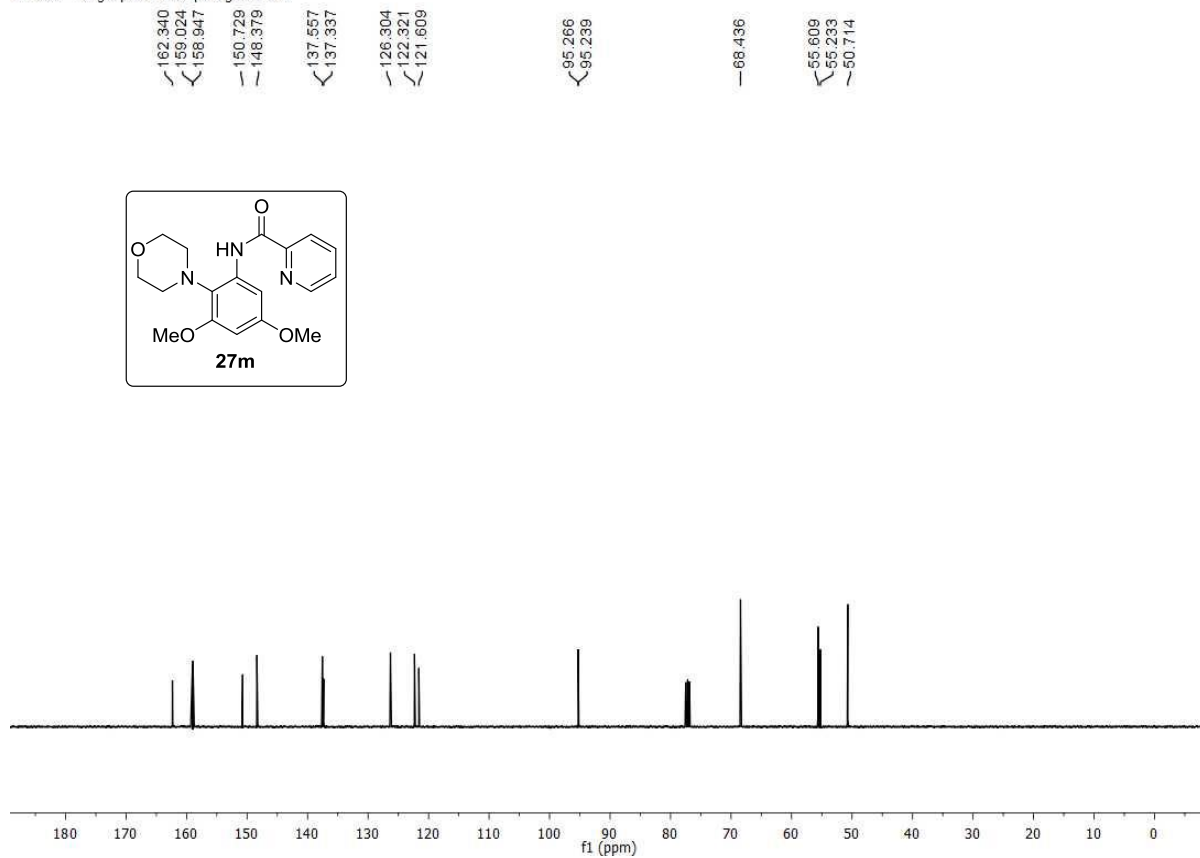
HM-304 — single pulse decoupled gated NOE



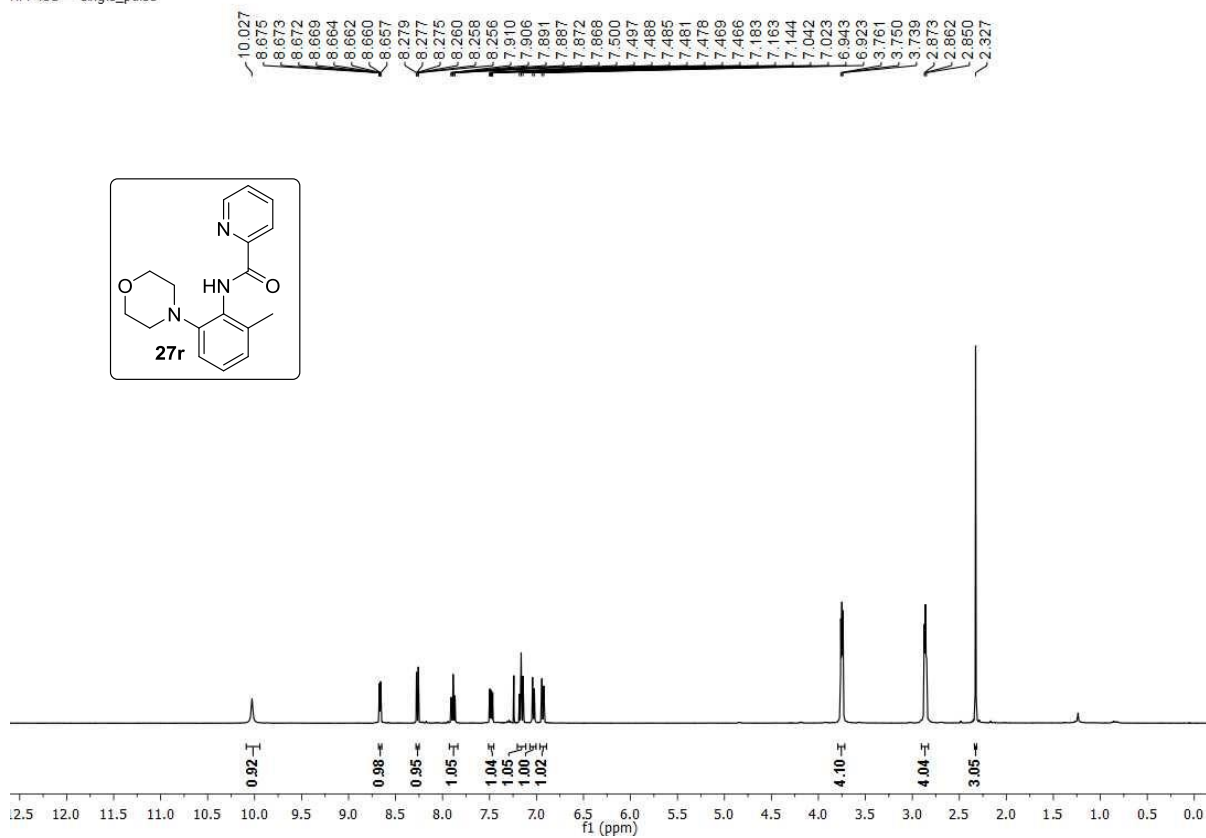
HM-290 — single_pulse



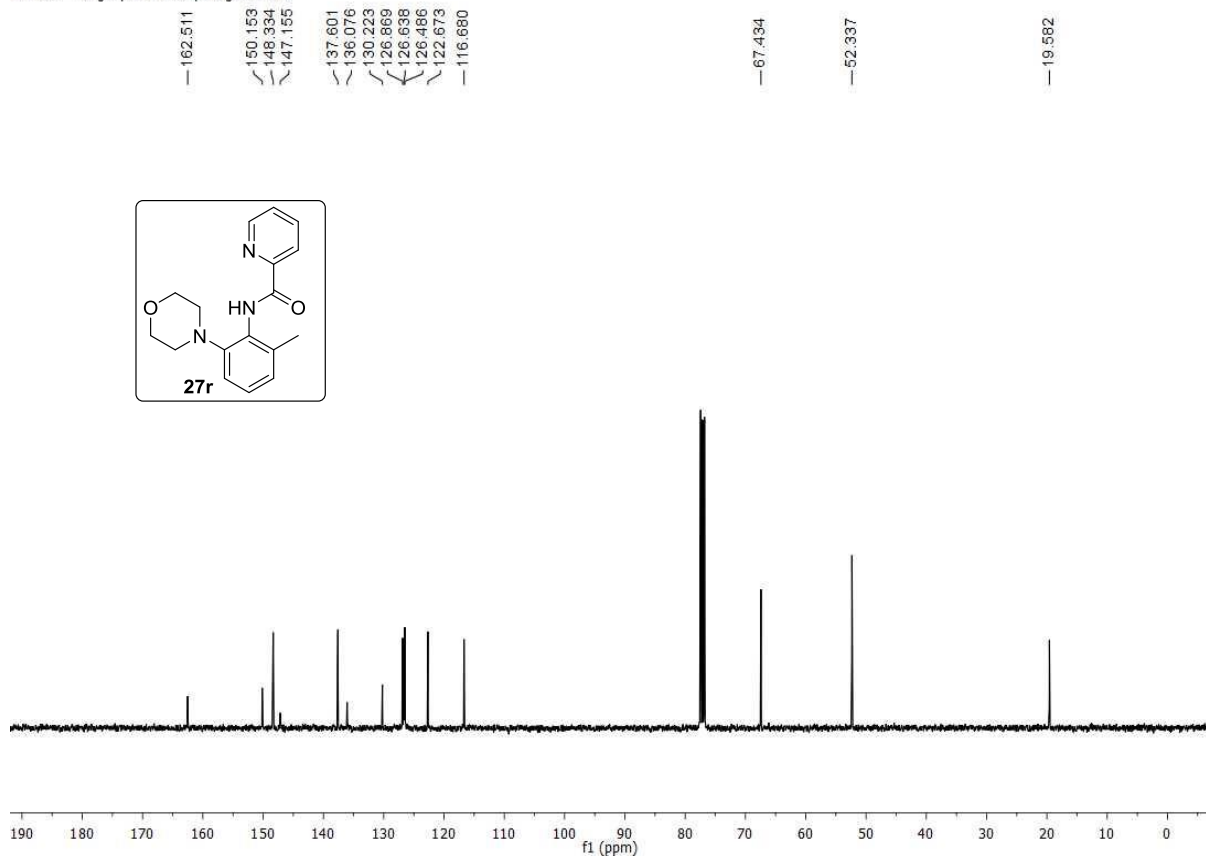
HM-290 — single pulse decoupled gated NOE



HM-451 — single_pulse

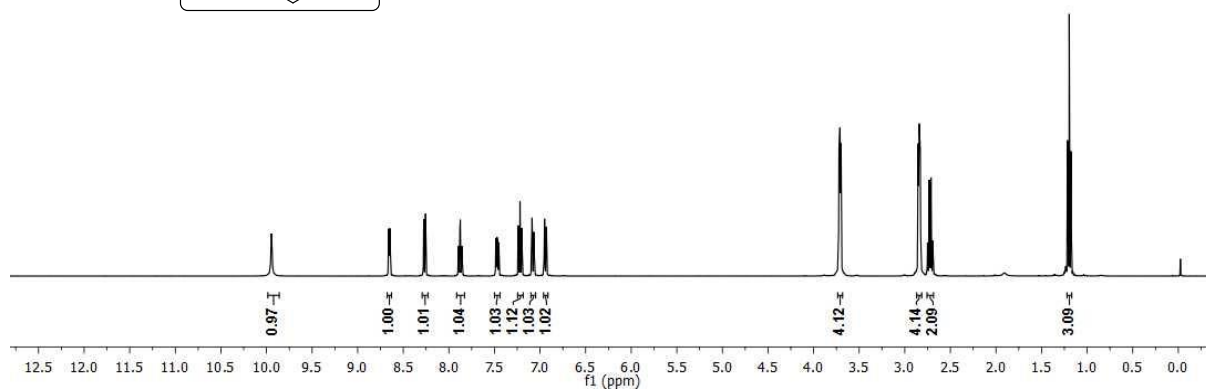
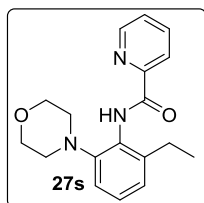


HM-451 — single pulse decoupled gated NOE



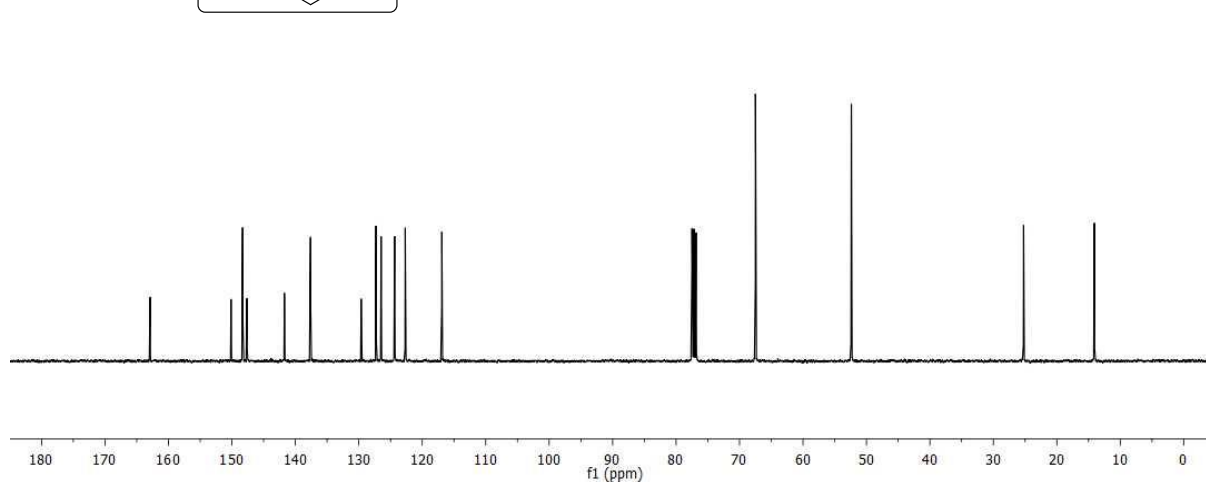
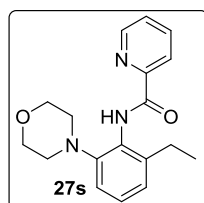
HM-319 — single_pulse

9.945
8.663
8.660
8.659
8.657
8.649
8.647
8.645
8.279
8.275
8.273
8.258
8.256
8.254
7.898
7.894
7.879
7.875
7.860
7.855
7.487
7.484
7.475
7.472
7.468
7.465
7.456
7.453
7.239
7.220
7.200
7.087
7.068
6.950
6.931
3.722
3.711
3.699
2.853
2.841
2.830
2.750
2.731
2.712
2.693



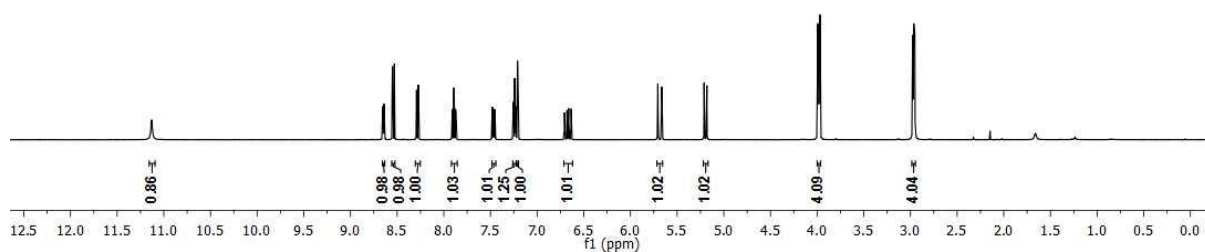
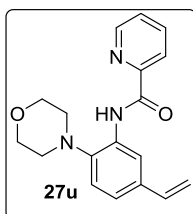
HM-319 — single pulse decoupled gated NOE

162.890
150.134
148.313
147.622
141.720
137.615
129.628
127.290
126.489
124.361
122.680
116.915
67.485
52.379
25.231
14.075



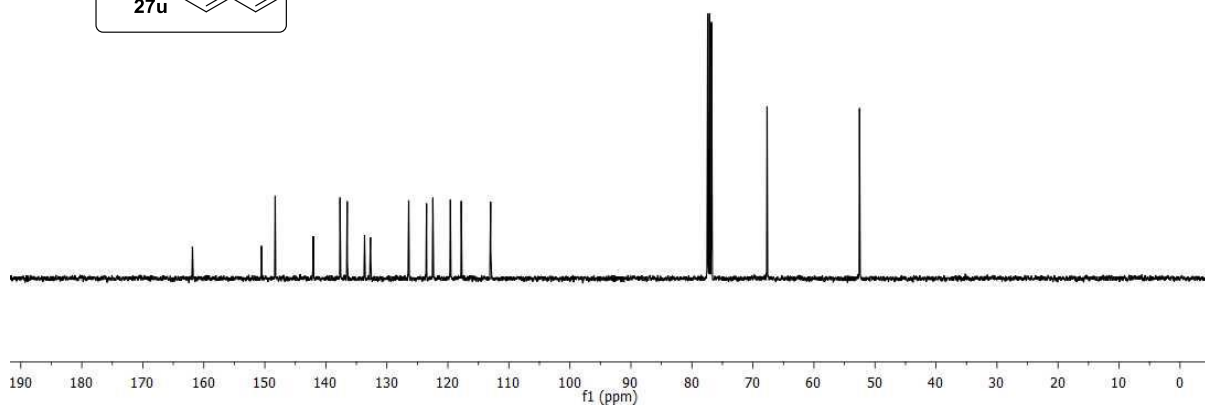
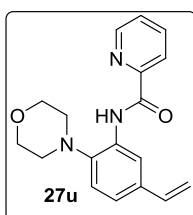
HM-393 — single_pulse

11.129
8.655
8.653
8.651
8.649
8.643
8.641
8.639
8.637
8.551
8.530
8.295
8.292
8.290
8.275
8.273
8.270
7.913
7.909
7.894
7.890
7.875
7.870
7.483
7.480
7.471
7.466
7.464
7.461
7.452
7.449
7.256
7.252
7.236
7.231
7.211
7.206
6.706
6.679
6.662
6.635
5.708
5.706
5.664
5.662
5.211
5.209
5.184
5.182
3.992
3.981
3.970
2.976
2.965
2.953

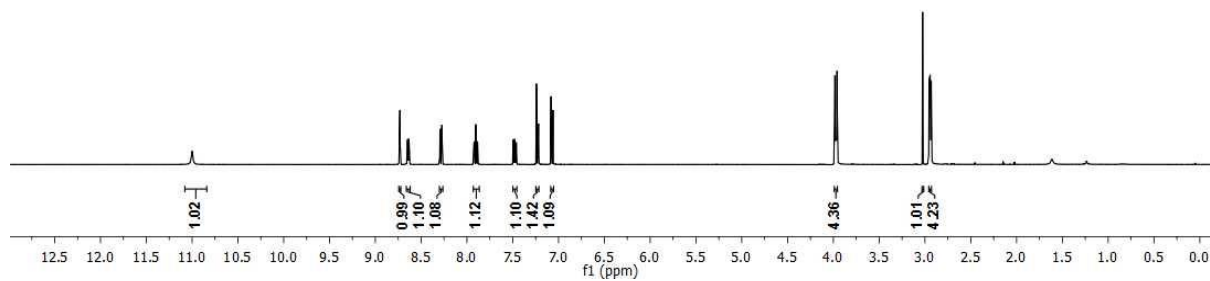
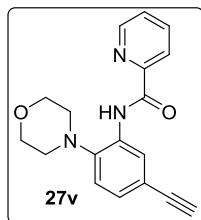


HM-393 — single pulse decoupled gated NOE

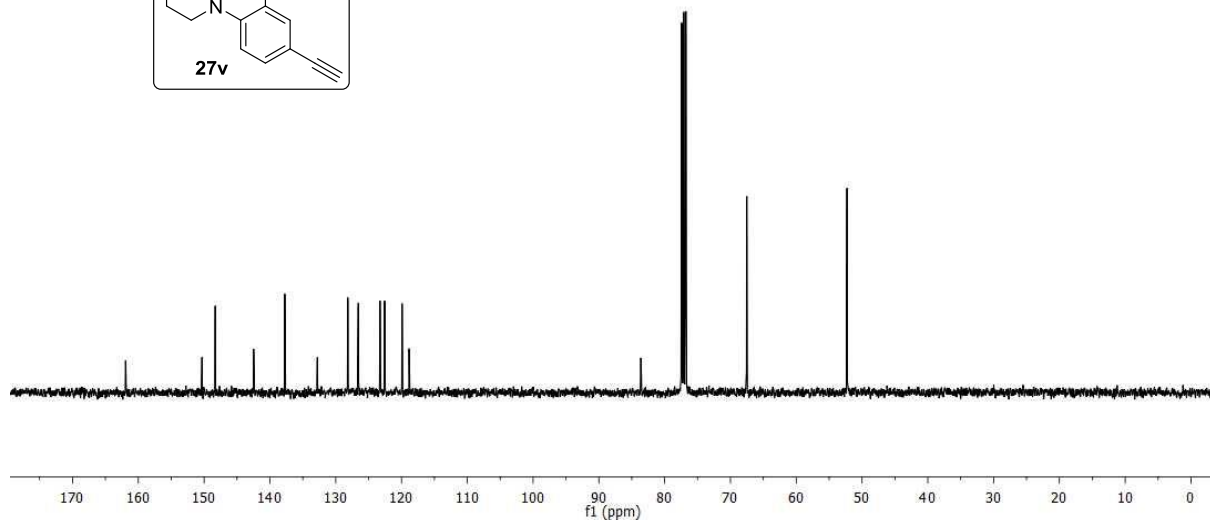
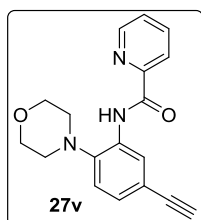
161.861
150.540
148.304
142.066
137.679
136.497
133.653
132.665
126.417
123.498
122.459
119.585
117.806
112.994
67.678
52.530



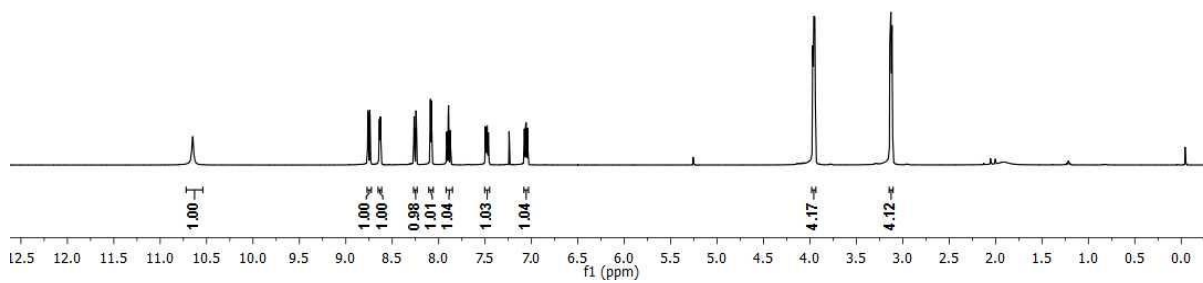
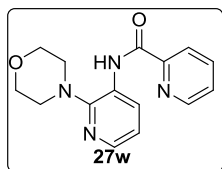
HM-392 — single_pulse



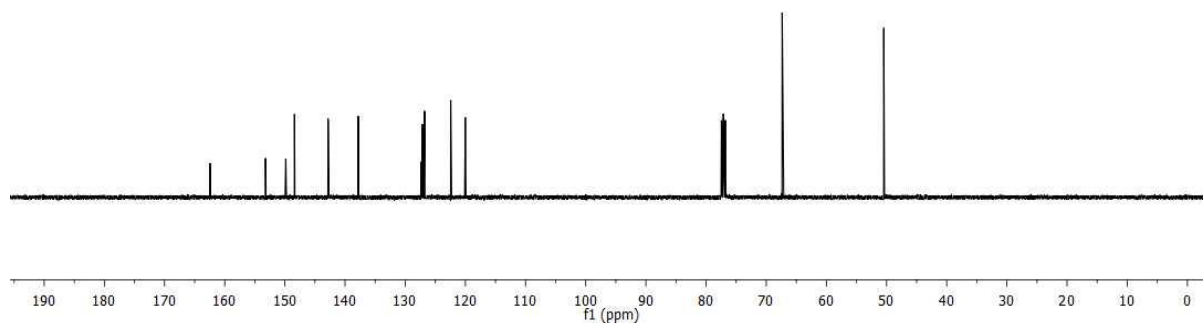
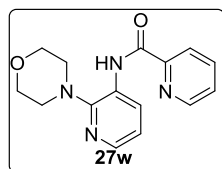
HM-392 — single pulse decoupled gated NOE



HM-309 — single_pulse

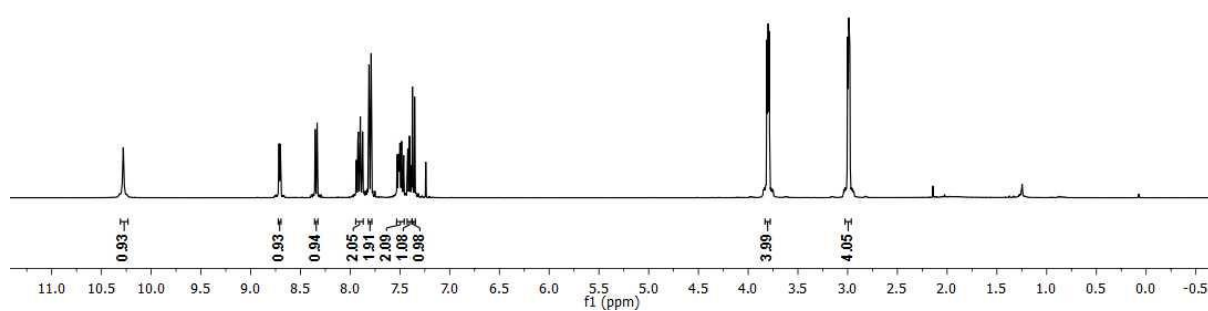
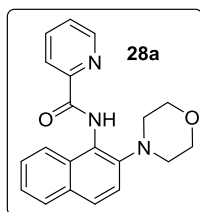


HM-309 — single pulse decoupled gated NOE



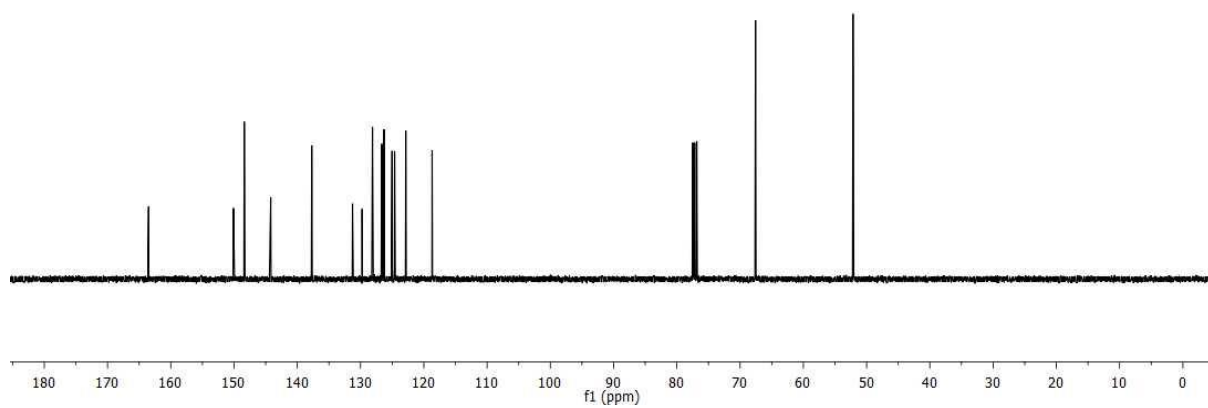
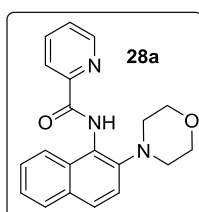
HM-273 — single_pulse

10.281
8.719
8.717
8.715
8.712
8.707
8.705
8.703
8.701
8.354
8.352
8.349
8.334
8.332
8.330
7.941
7.937
7.922
7.918
7.903
7.898
7.875
7.811
7.788
7.530
7.527
7.518
7.515
7.511
7.508
7.504
7.500
7.496
7.487
7.484
7.480
7.486
7.483
7.423
7.421
7.406
7.403
7.401
7.386
7.383
7.374
7.352
3.810
3.798
3.788
3.001
2.990
2.978



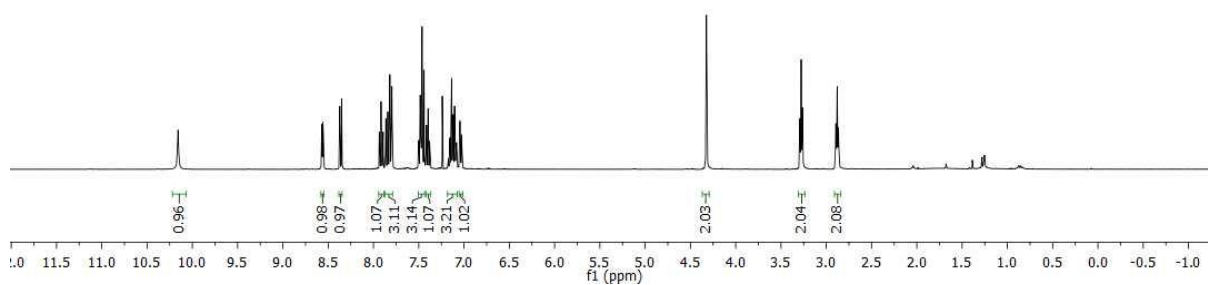
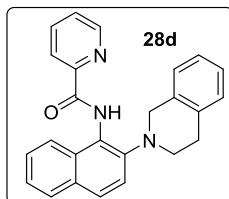
HM--273 — single_pulse decoupled gated NOE

163.506
150.086
148.382
144.203
137.719
131.271
129.759
128.115
128.052
128.651
126.304
126.278
125.018
124.620
122.853
118.688
-67.565
-52.150



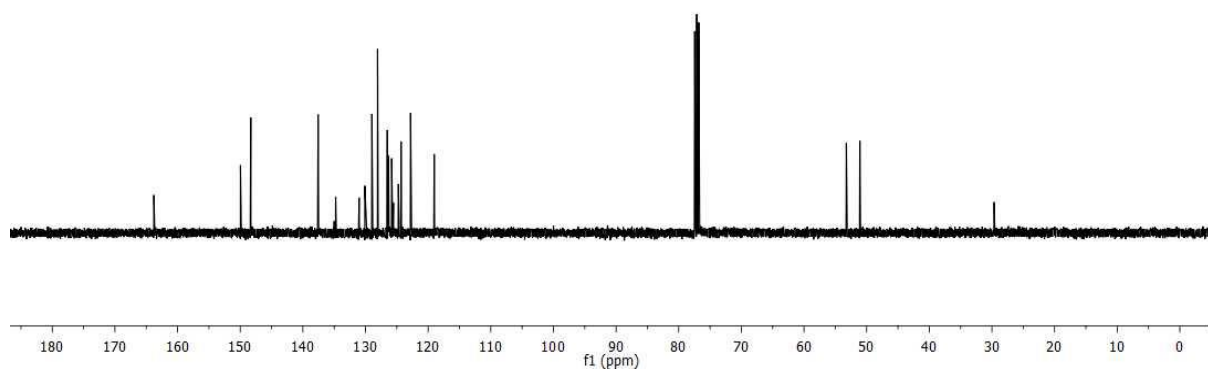
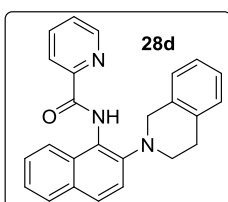
HM-325
single_pulse

10.158
8.573
8.570
8.569
8.566
8.561
8.558
8.557
8.554
8.373
8.371
8.368
8.364
8.351
8.349
7.936
7.931
7.916
7.912
7.897
7.893
7.884
7.863
7.843
7.841
7.819
7.796
7.500
7.487
7.484
7.480
7.476
7.472
7.468
7.463
7.459
7.457
7.454
7.441
7.417
7.415
7.400
7.397
7.394
7.380
7.377
7.177
7.173
7.159
7.155
7.142
7.137
7.135
7.130
7.105
7.085
7.044
7.007
4.823
3.302
3.277
3.263
2.894
2.880
2.866

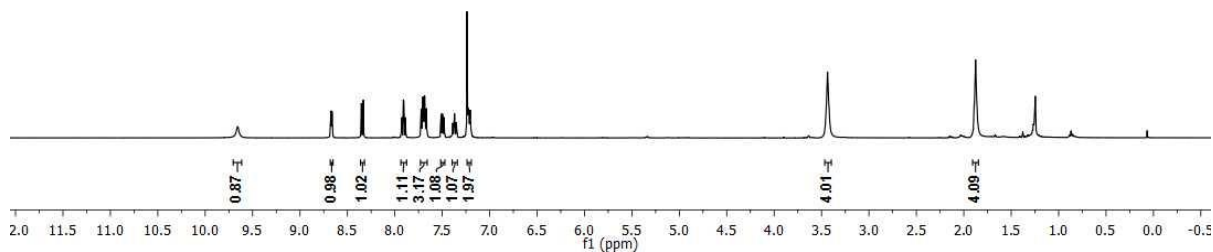
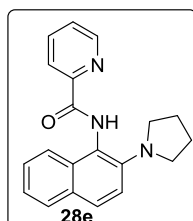
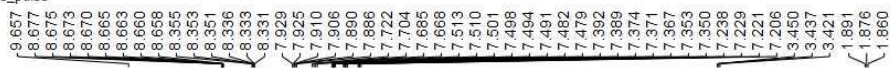


HM-325 — single pulse decoupled gated NOE

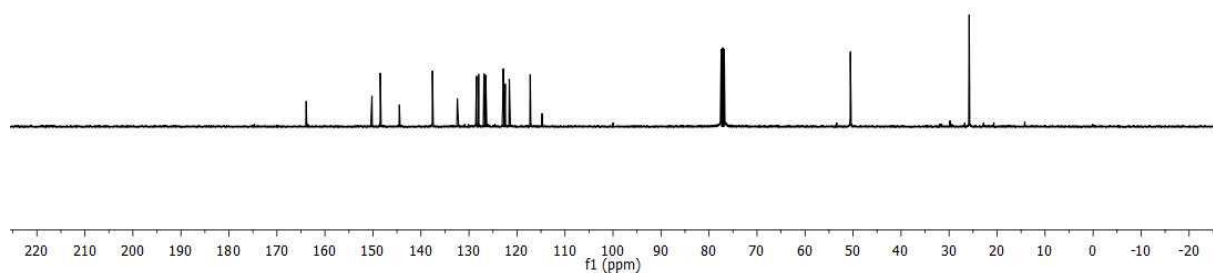
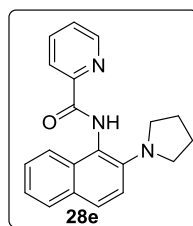
163.781
149.958
148.315
137.663
134.767
131.018
130.106
128.978
128.071
126.514
126.454
126.390
126.319
125.822
125.537
124.753
124.322
122.802
119.029
63.237
51.086
29.639



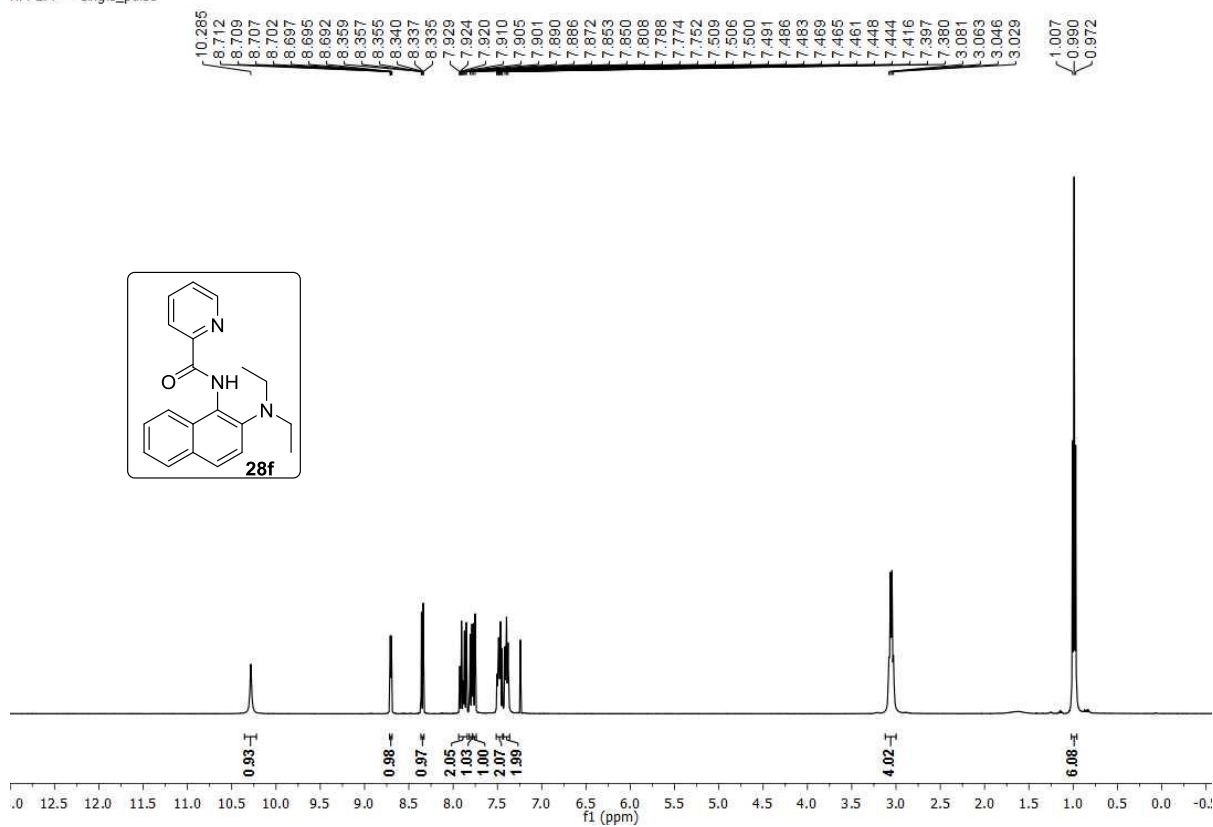
HM-276 — single_pulse



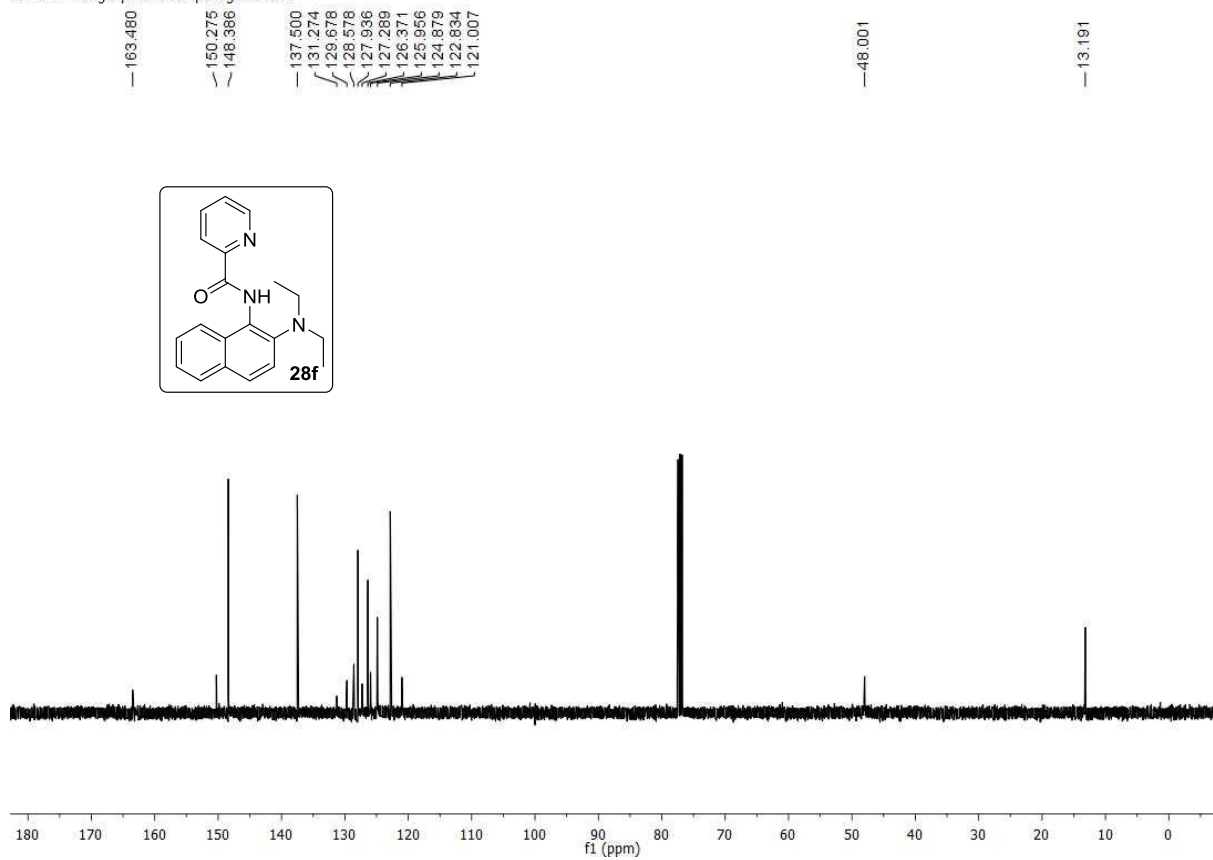
HM-276 — single pulse decoupled gated NOE



HM-277 — single_pulse

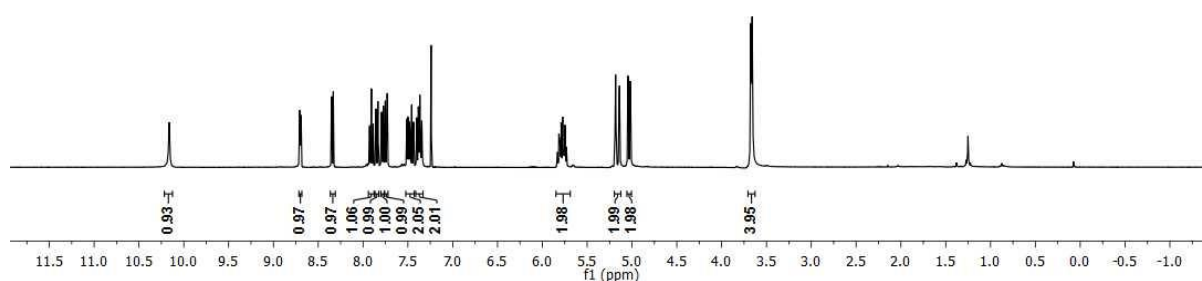
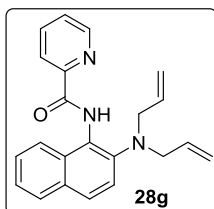


HM-277 — single pulse decoupled gated NOE



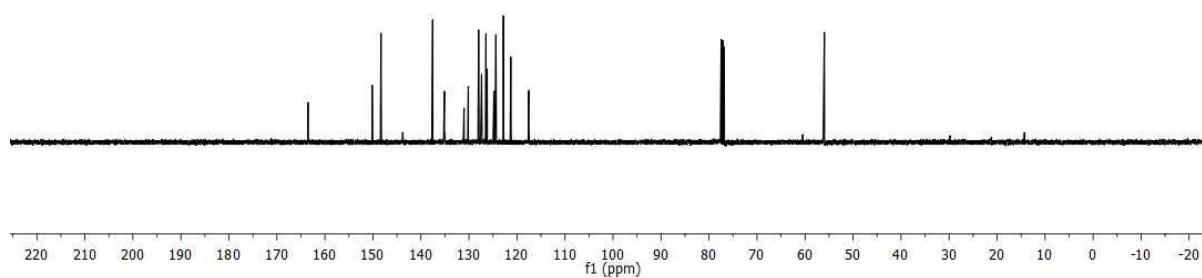
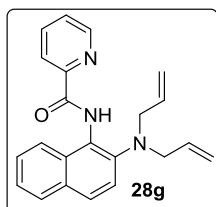
HM-331R — single_pulse

10.163
8.710
8.708
8.706
8.704
8.698
8.696
8.694
8.692
8.354
8.352
8.349
8.335
8.332
8.330
7.930
7.926
7.911
7.906
7.891
7.887
7.855
7.834
7.793
7.773
7.752
7.730
7.514
7.511
7.502
7.499
7.495
7.482
7.463
7.478
7.461
7.457
7.454
7.440
7.436
7.403
7.400
7.363
7.366
7.345
5.831
5.816
5.790
5.773
5.747
5.732
5.167
5.183
5.144
5.140
5.047
5.044
5.022
5.018
3.675
3.660

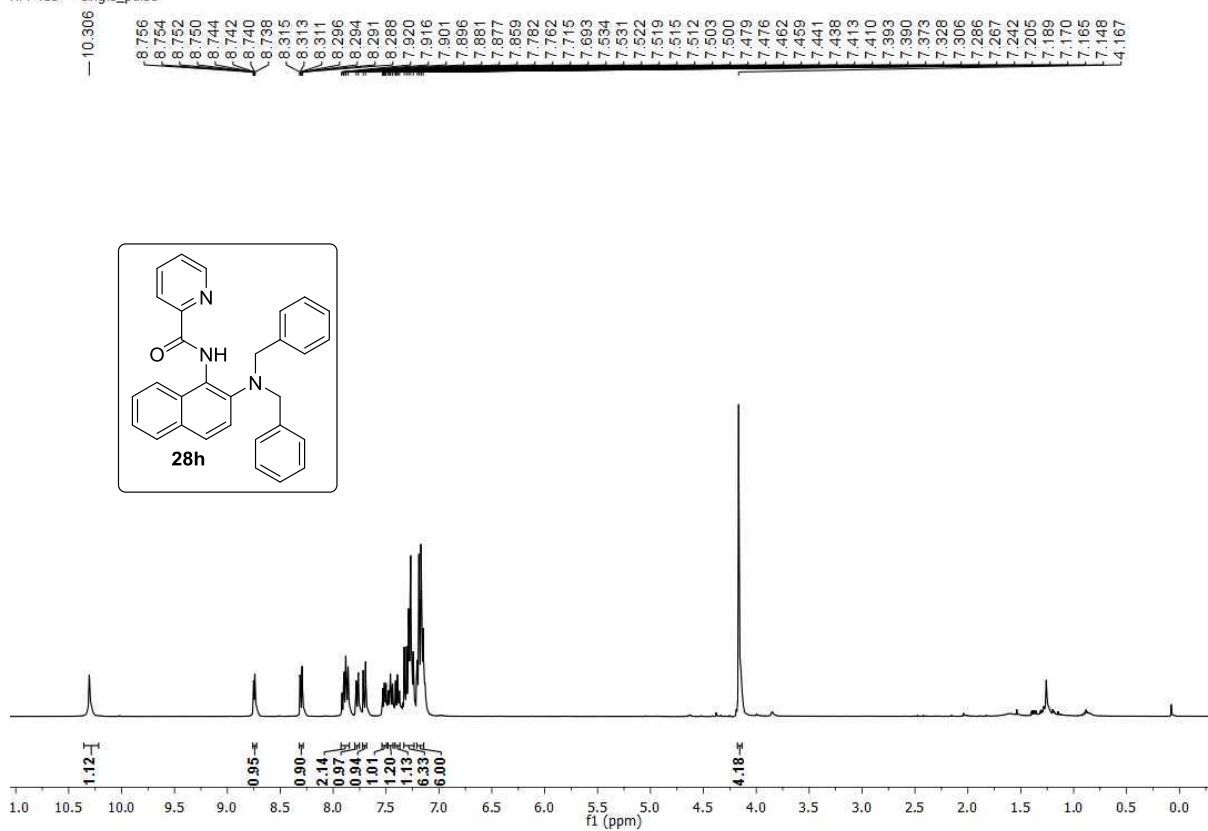


HM-331 — single pulse decoupled gated NOE

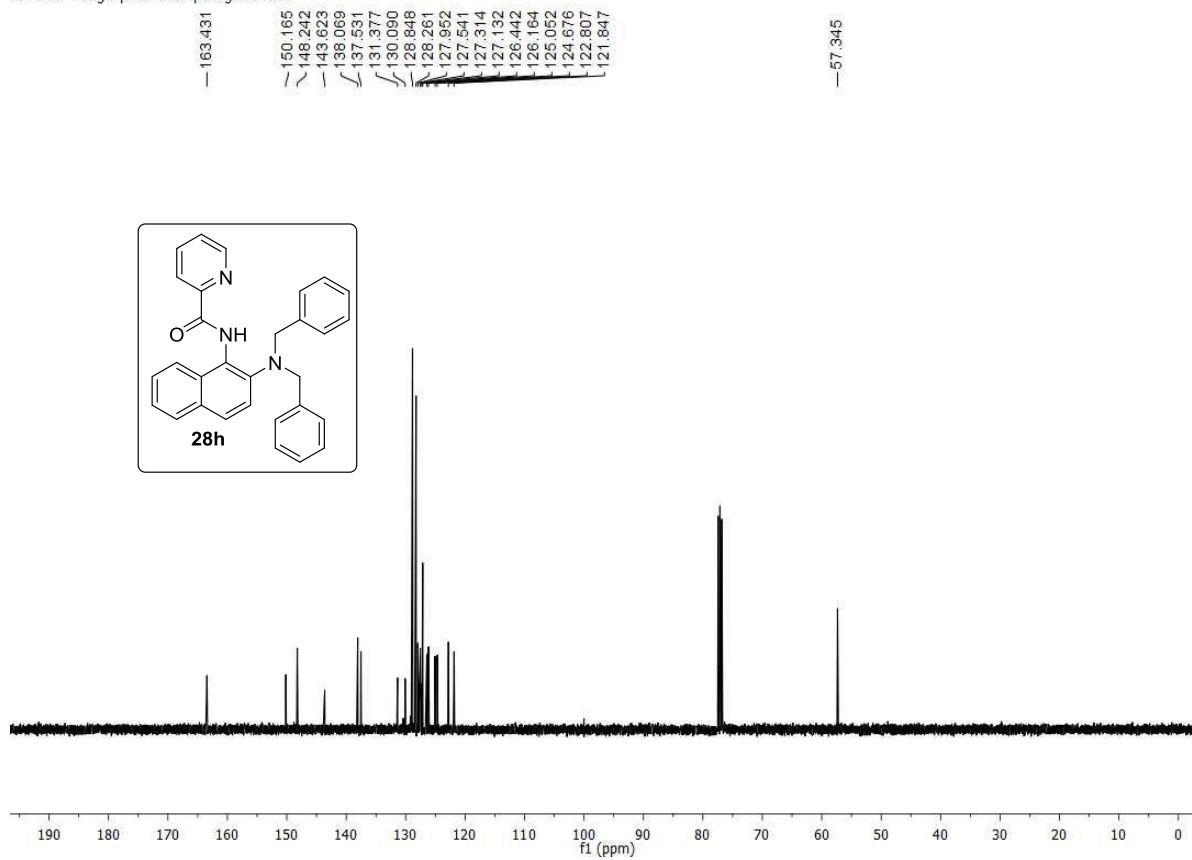
163.526
150.165
148.328
137.559
135.119
131.025
130.133
127.990
127.370
126.547
126.457
126.207
124.802
124.387
122.825
121.291
117.567
55.972



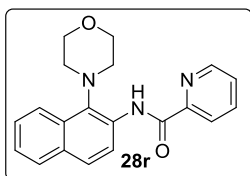
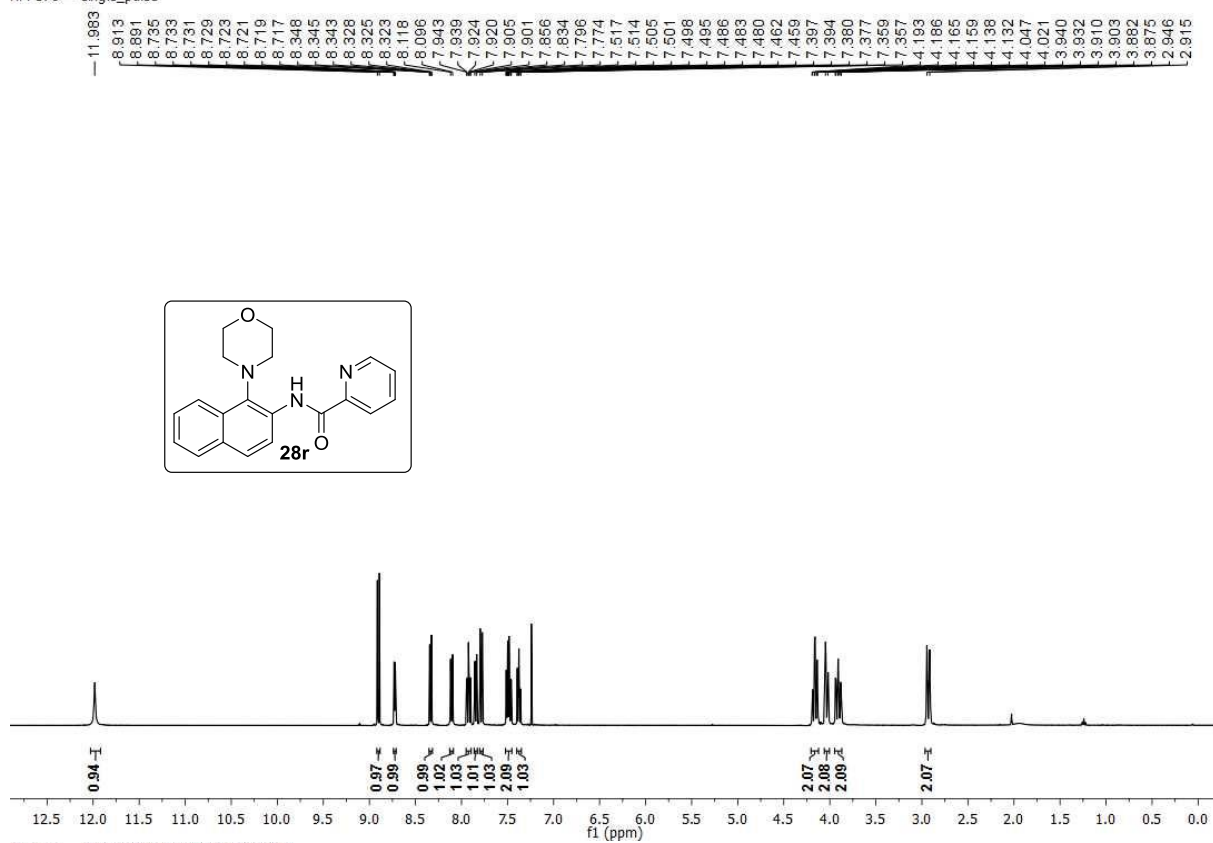
HM-415 — single_pulse



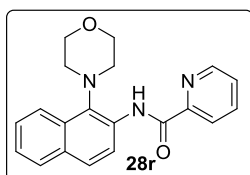
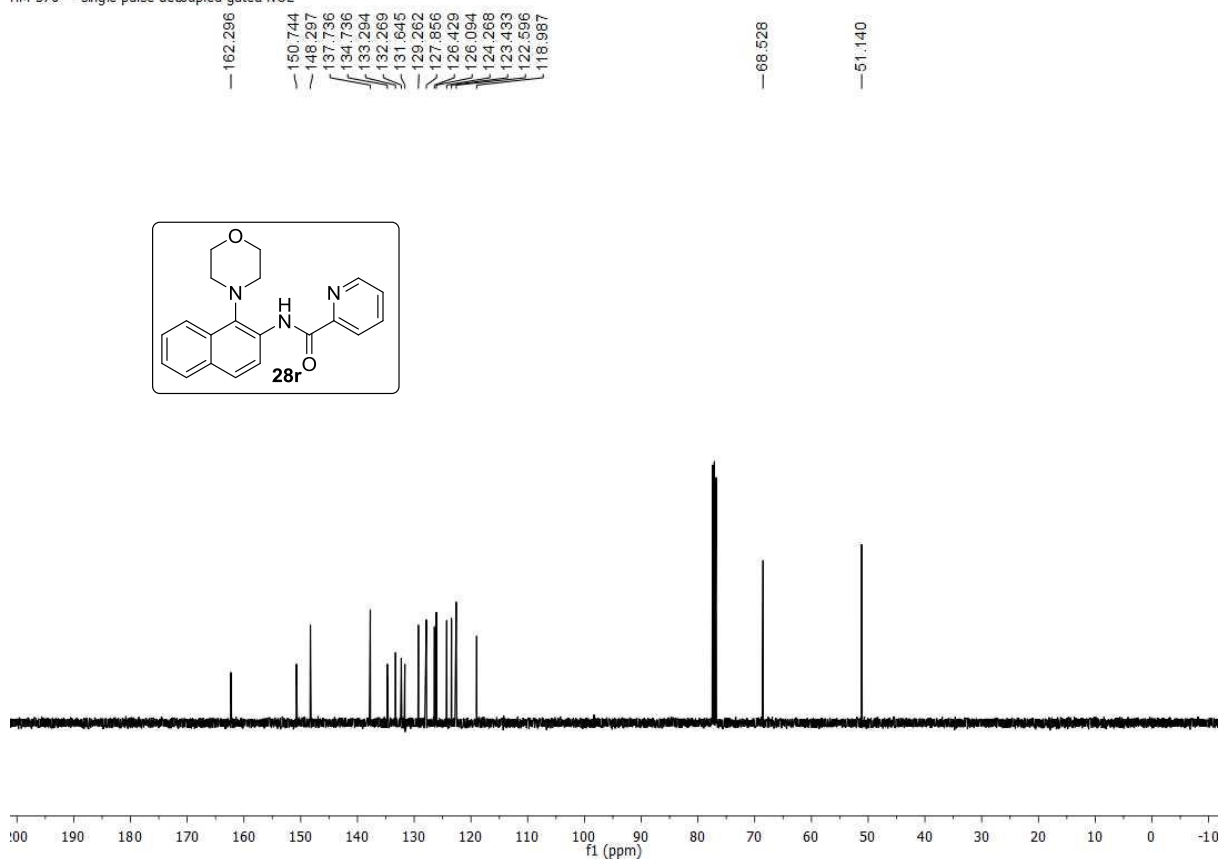
HM-415 — single pulse decoupled gated NOE

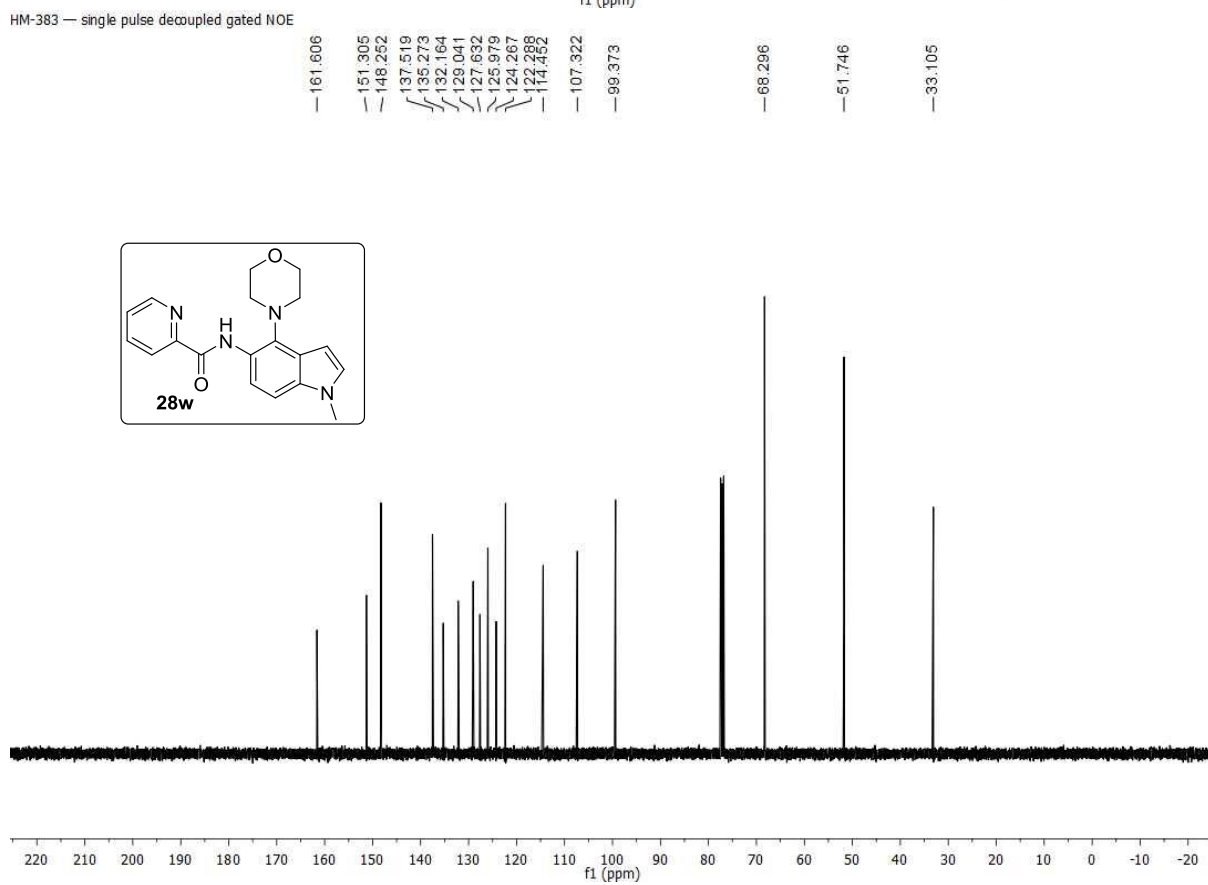
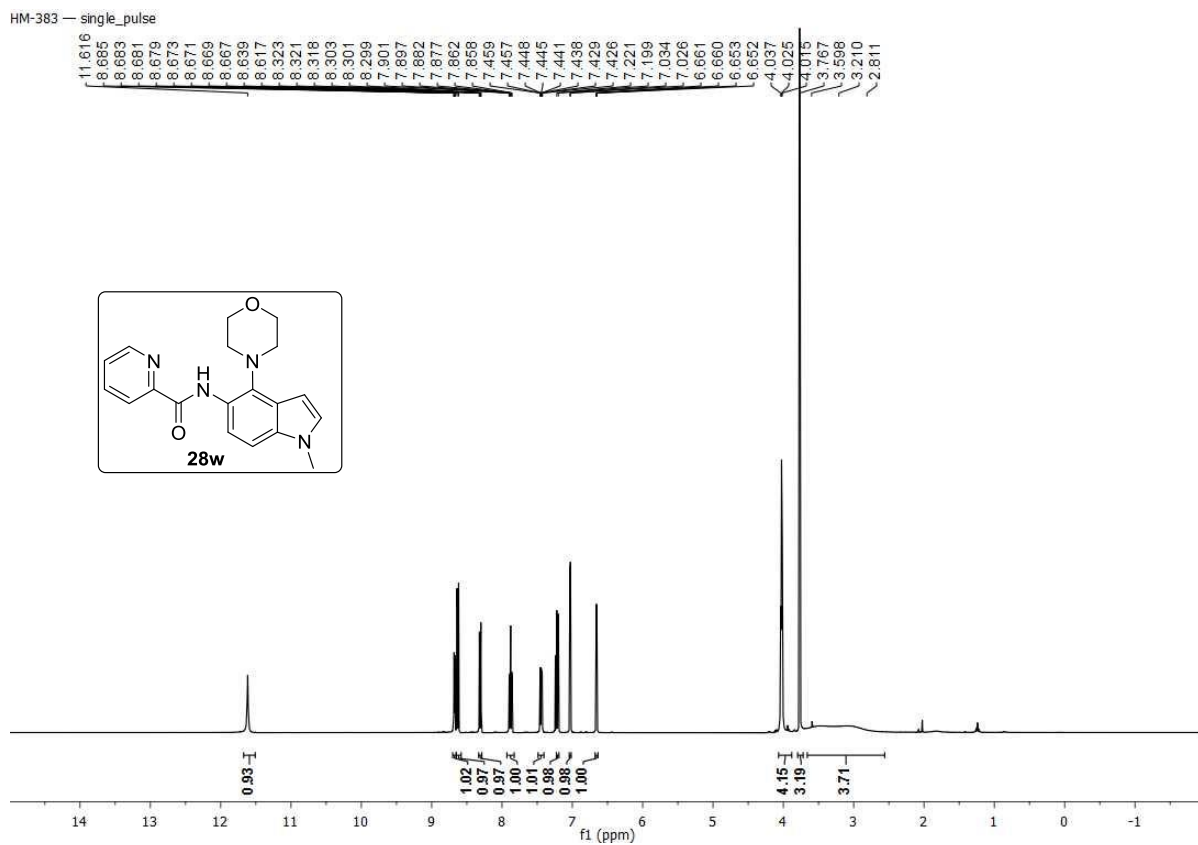


HM-576 — single_pulse



HM-576 — single pulse decoupled gated NOE



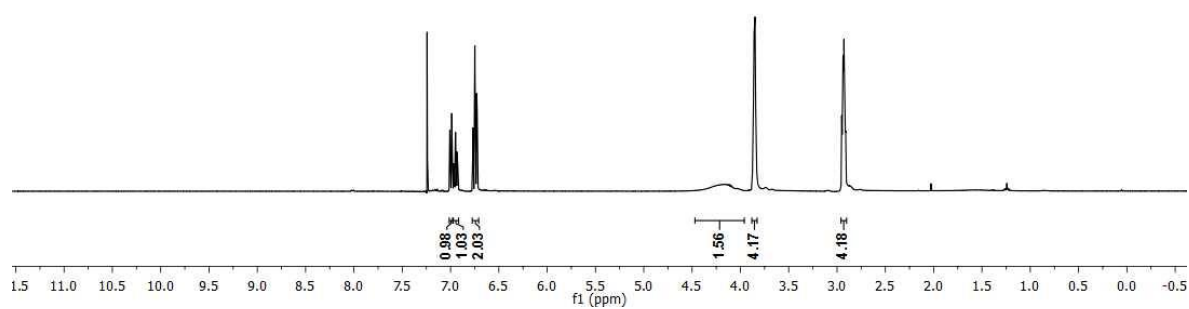
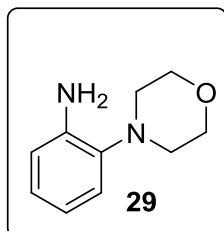


RC-17 — single_pulse

7.011
7.009
7.007
6.992
6.991
6.987
6.983
6.871
6.867
6.863
6.852
6.848
6.833
6.829
6.821
6.771
6.768
6.764
6.753
6.749
6.744
6.730
6.726

4.169
3.872
3.859
3.849
3.836

2.951
2.838
2.834
2.828
2.811



RC-17 — single pulse decoupled gated NOE

— 141.524

— 125.124

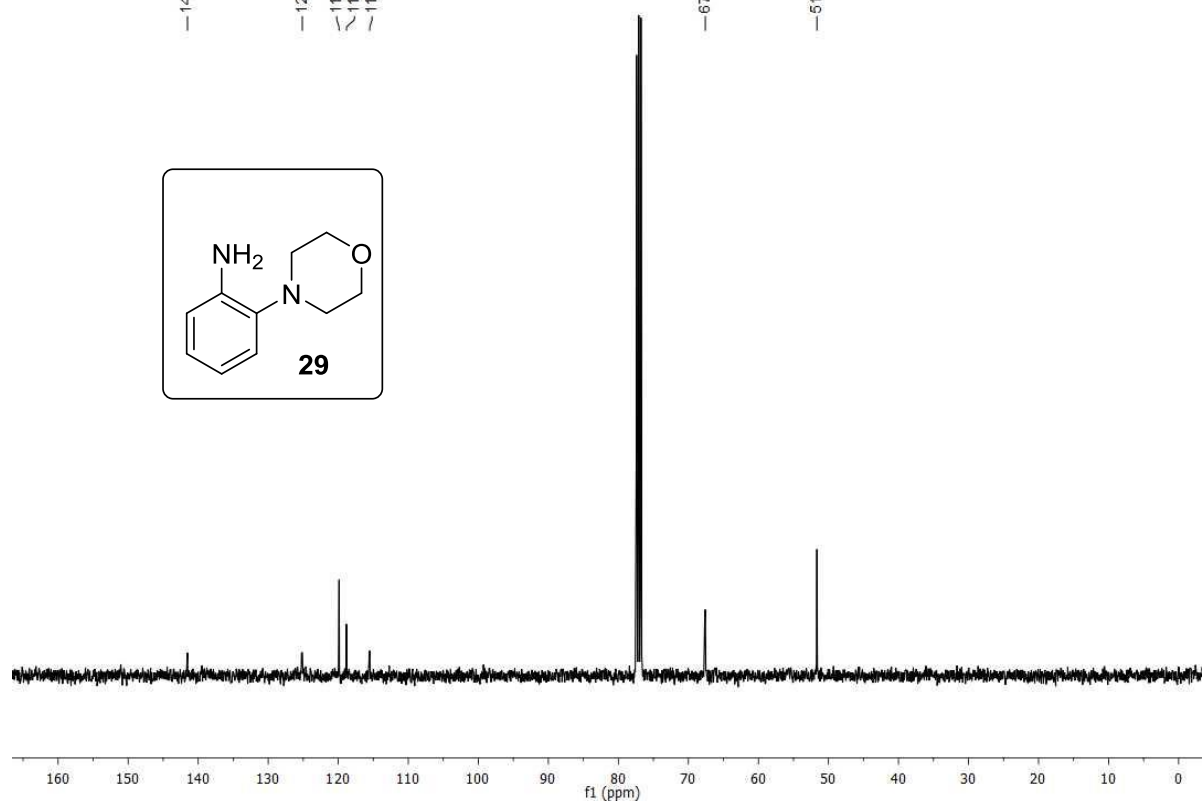
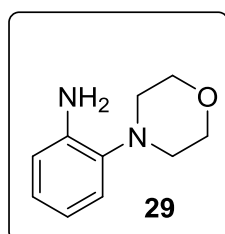
— 119.876

— 118.821

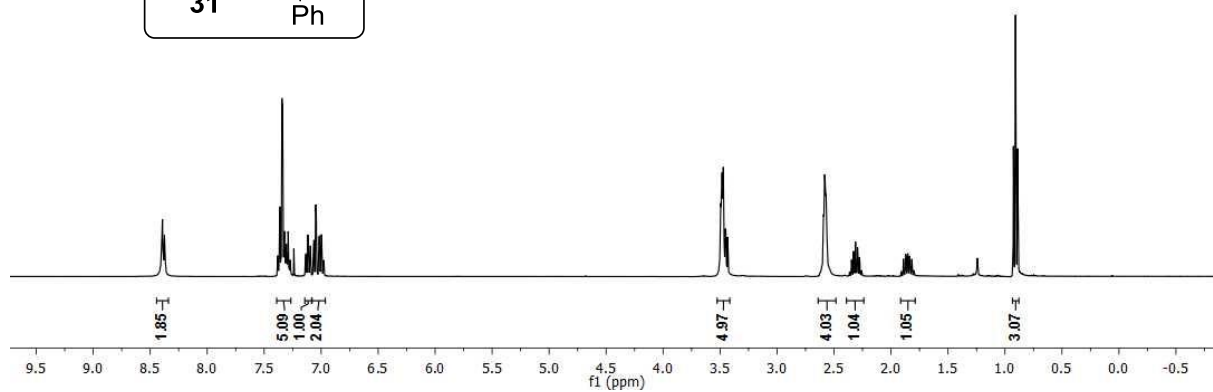
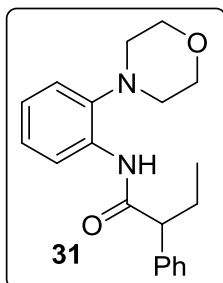
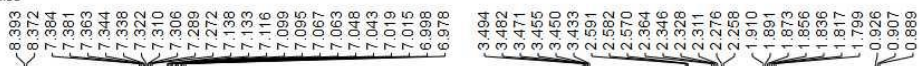
— 115.499

— 67.584

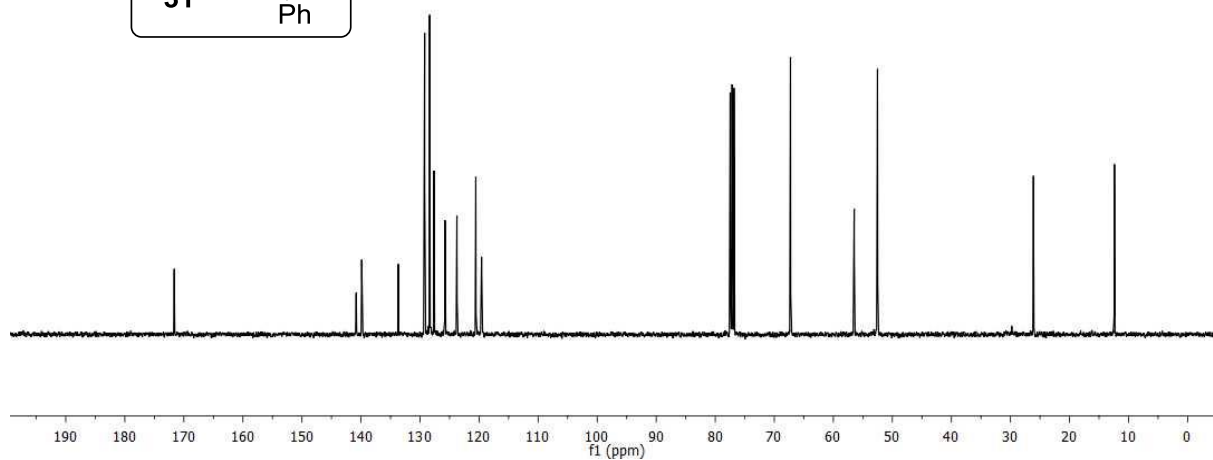
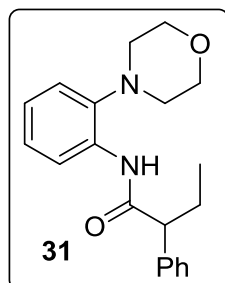
— 51.647



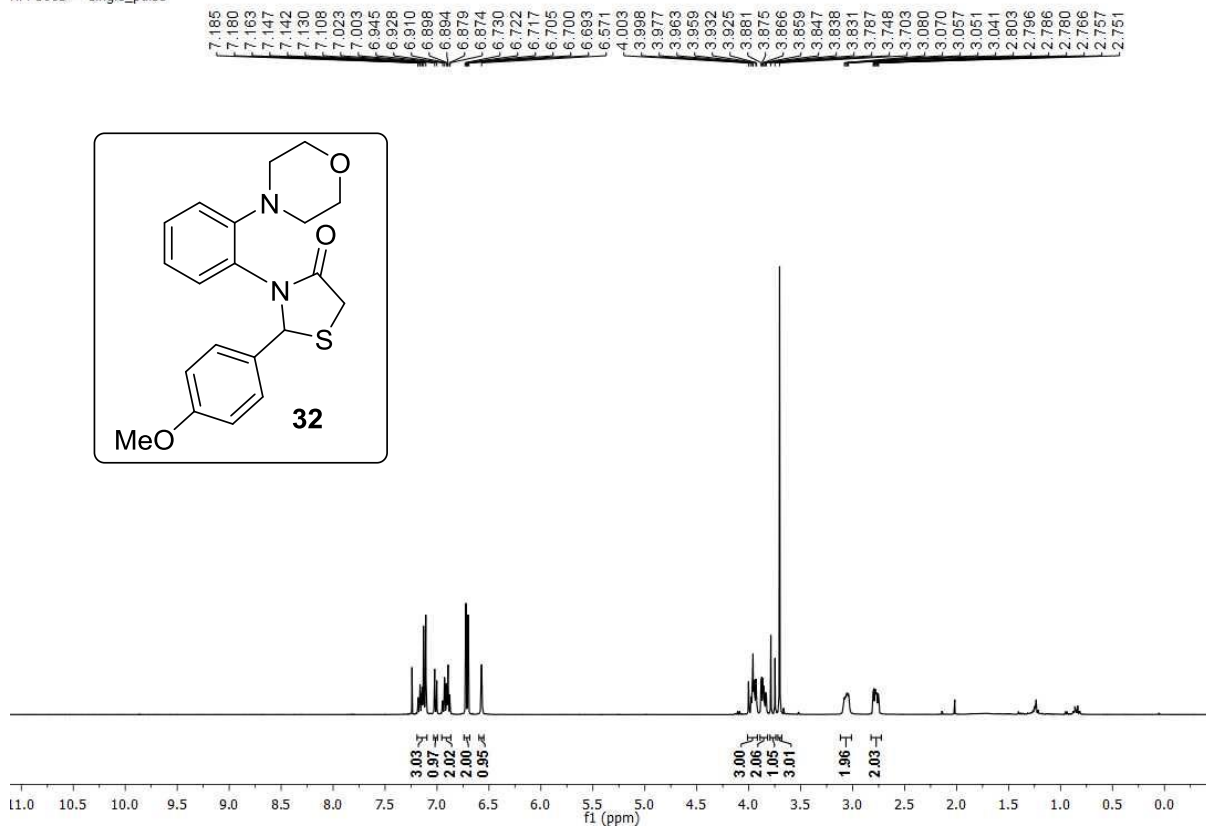
HM-496 — single_pulse



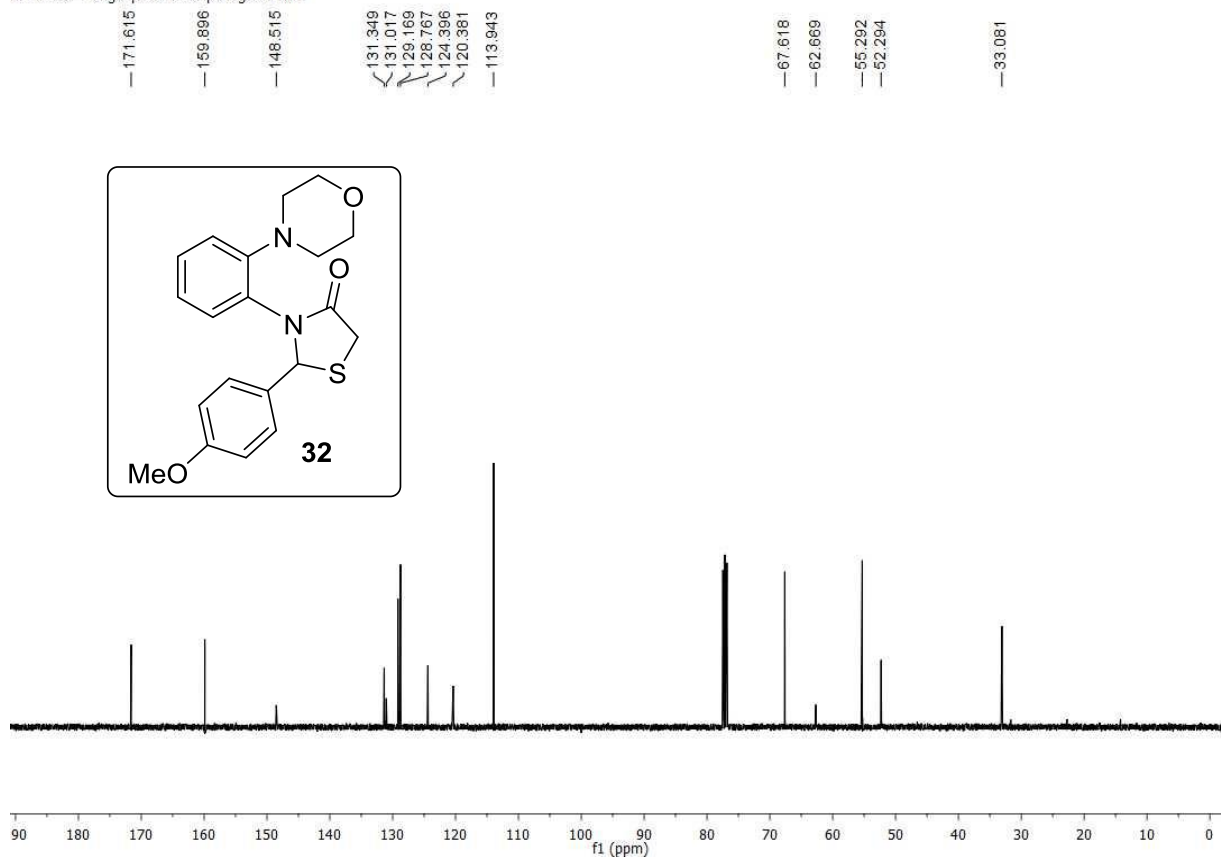
HM-496 — single pulse decoupled gated NOE



HM-566B — single_pulse



HM-566B — single pulse decoupled gated NOE



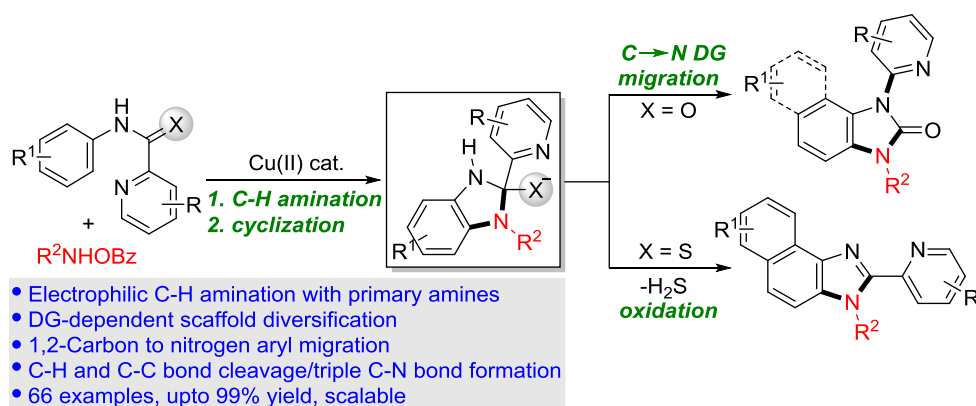
II.12. Refereneces

1. a) T. M. Doran, Y. Gao, S. Simanski, P. McEnaney, T. Kodadek, *Bioorg. Med. Chem. Lett.*, 2015, **25**, 4910-4917; b) S. O. Abdul-Hay, T. D. Bannister, H. Wang, M. D. Cameron, T. R. Caulfield, A. Masson, J. Bertrand, E. A. Howard, M. P. McGuire, U. Crisafulli, T. R. Rosenberry, C. L. Topper, C. R. Thompson, S. C. Schürer, F. Madoux, P. Hodder, M. A. Leissring, *ACS Chem. Biol.*, 2015, **10**, 2716-2724; c) Y. Gong, S. Somersan Karakaya, X. Guo, P. Zheng, B. Gold, Y. Ma, D. Little, J. Roberts, T. Warriar, X. Jiang, M. Pingle, C. F. Nathan, G. Liu, *Eur. J. Med. Chem.*, 2014, **75**, 336-353; d) M. V. Gammons, O. Fedorov, D. Ivison, C. Du, T. Clark, C. Hopkins, M. Hagiwara, A. D. Dick, R. Cox, S. J. Harper, J. C. Hancox, S. Knapp, D. O. Bates, *Invest. Ophthalmol. Visual Sci.*, 2013, **54**, 6052-6062; e) Y.-Y. Cheung, H. Yu, K. Xu, B. Zou, M. Wu, O. B. McManus, M. Li, C. W. Lindsley, C. R. Hopkins, *J. Med. Chem.*, 2012, **55**, 6975-6979.
2. a) B. Seifinoferest, A. Tanbakouchian, B. Larijani, M. Mahdavi, *Asian J. Org. Chem.*, 2021, **10**, 1319-1344; b) J. Bariwal, E. Van der Eycken, *Chem. Soc. Rev.*, 2013, **42**, 9283-9303; c) M. J. West, J. W. B. Fyfe, J. C. Vantourout, A. J. B. Watson, *Chem. Rev.*, 2019, **119**, 12491-12523; d) J.-Q. Chen, J.-H. Li, Z.-B. Dong, *Adv. Synth. Catal.*, 2020, **362**, 3311-3331.
3. Y. Park, Y. Kim, S. Chang, *Chem. Rev.*, 2017, **117**, 9247-9301.
4. a) X. Dong, Q. Liu, Y. Dong, H. Liu, *Chem. Eur. J.*, 2017, **23**, 2481-2511; b) X. Yan, X. Yang, C. Xi, *Catal. Sci. Technol.*, 2014, **4**, 4169-4177; c) M.-L. Louillat, F. W. Patureau, *Chem. Soc. Rev.*, 2014, **43**, 901-910; d) J.-S. Yu, M. Espinosa, H. Noda, M. Shibasaki, *J. Am. Chem. Soc.*, 2019, **141**, 10530-10537.
5. a) J. E. Zweig, D. E. Kim, T. R. Newhouse, *Chem. Rev.*, 2017, **117**, 11680-11752; b) L. Alig, M. Fritz, S. Schneider, *Chem. Rev.*, 2019, **119**, 2681-2751; c) S. R. Tamang, M. Findlater, *Molecules*, 2019, **24**.
6. a) A. Trowbridge, S. M. Walton, M. J. Gaunt, *Chem. Rev.*, 2020, **120**, 2613-2692; b) K. A. Margrey, A. Levens, D. A. Nicewicz, *Angew. Chem. Int. Ed.*, 2017, **56**, 15644-15648.
7. S. H. Cho, J. Y. Kim, S. Y. Lee, S. Chang, *Angew. Chem. Int. Ed.*, 2009, **48**, 9127-9130.
8. J. Y. Kim, S. H. Cho, J. Joseph, S. Chang, *Angew. Chem. Int. Ed.*, 2010, **49**, 9899-9903.
9. D. Monguchi, T. Fujiwara, H. Furukawa, A. Mori, *Org. Lett.*, 2009, **11**, 1607-1610.

10. Y. Li, J. Liu, Y. Xie, R. Zhang, K. Jin, X. Wang, C. Duan, *Org. Biomol. Chem.*, 2012, **10**, 3715-3720.
11. C. Zhu, M. Yi, D. Wei, X. Chen, Y. Wu, X. Cui, *Org. Lett.*, 2014, **16**, 1840-1843.
12. L. D. Tran, J. Roane, O. Daugulis, *Angew. Chem. Int. Ed.*, 2013, **52**, 6043-6046.
13. Q. Yan, Z. Chen, W. Yu, H. Yin, Z. Liu, Y. Zhang, *Org. Lett.*, 2015, **17**, 2482-2485.
14. J. Roane, O. Daugulis, *J. Am. Chem. Soc.*, 2016, **138**, 4601-4607.
15. Q. Yan, T. Xiao, Z. Liu, Y. Zhang, *Adv. Synth. Catal.*, 2016, **358**, 2707-2711.
16. X. Gao, P. Wang, L. Zeng, S. Tang, A. Lei, *J. Am. Chem. Soc.*, 2018, **140**, 4195-4199.
17. S.-K. Zhang, R. C. Samanta, N. Sauermann, L. Ackermann, *Chem. Eur. J.*, 2018, **24**, 19166-19170.
18. L.-B. Zhang, S.-K. Zhang, D. Wei, X. Zhu, X.-Q. Hao, J.-H. Su, J.-L. Niu, M.-P. Song, *Org. Lett.*, 2016, **18**, 1318-1321.
19. N. Sauermann, R. Mei, L. Ackermann, *Angew. Chem. Int. Ed.*, 2018, **57**, 5090-5094.
20. Á. M. Martínez, N. Rodríguez, R. G. Arrayás, J. C. Carretero, *Chem. Commun.*, 2014, **50**, 2801-2803.
21. Q. Li, S.-Y. Zhang, G. He, Z. Ai, W. A. Nack, G. Chen, *Org. Lett.*, 2014, **16**, 1764-1767.
22. Q.-L. Yang, X.-Y. Wang, J.-Y. Lu, L.-P. Zhang, P. Fang, T.-S. Mei, *J. Am. Chem. Soc.*, 2018, **140**, 11487-11494.
23. T. Kawano, K. Hirano, T. Satoh, M. Miura, *J. Am. Chem. Soc.*, 2010, **132**, 6900-6901.
24. T. Matsubara, S. Asako, L. Ilies, E. Nakamura, *J. Am. Chem. Soc.*, 2014, **136**, 646-649.
25. G. Li, C. Jia, K. Sun, Y. Lv, F. Zhao, K. Zhou, H. Wu, *Org. Biomol. Chem.*, 2015, **13**, 3207-3210.
26. L.-L. Xu, X. Wang, B. Ma, M.-X. Yin, H.-X. Lin, H.-X. Dai, J.-Q. Yu, *Chem. Sci.*, 2018, **9**, 5160-5164.
27. a) M. A. Ali, X. Yao, H. Sun, H. Lu, *Org. Lett.*, 2015, **17**, 1513-1516; b) M. A. Ali, X. Yao, G. Li, H. Lu, *Org. Lett.*, 2016, **18**, 1386-1389; c) L. Yang, H. Li, H. Zhang, H. Lu, *Eur. J. Org. Chem.*, 2016, **2016**, 5611-5615.
28. a) X. Ribas, C. Calle, A. Poater, A. Casitas, L. Gómez, R. Xifra, T. Parella, J. Benet-Buchholz, A. Schweiger, G. Mitrikas, M. Solà, A. Llobet, T. D. P. Stack, *J. Am. Chem. Soc.*, 2010, **132**, 12299-12306; b) A. E. King, L. M. Huffman, A. Casitas, M. Costas, X. Ribas, S. S. Stahl, *J. Am. Chem. Soc.*, 2010, **132**, 12068-12073; c) L. M. Huffman, S. S. Stahl, *J. Am. Chem. Soc.*, 2008, **130**, 9196-9197.
29. J. Weng, C. Wang, H. Li, Y. Wang, *Green Chem.*, 2006, **8**, 96-99.

Chapter III

A directing group switch in copper-catalyzed electrophilic C–H amination/migratory annulation cascade: divergent access to benzimidazolone/benzimidazole



Abstract: We present here, a copper-catalyzed electrophilic *ortho*-C–H amination of protected naphthylamines with *N*-(benzoyloxy)amines, cyclization with the pendant amide and carbon to nitrogen 1,2-directing group migration cascade to access *N,N*-disubstituted 2-benzimidazolinones. Remarkably, this highly atom-economic tandem reaction proceeds through a C–H, and C–C bond cleavage and three new C–N bond formations in a single operation. Intriguingly, the reaction cascade was altered by subtle tuning of the directing group from picolinamide to thiopicolinamide furnishing 2-heteroaryl-imidazoles via the extrusion of hydrogen sulfide. This strategy provided a series of benzimidazolones and benzimidazoles in moderate to high yields with low catalyst loading (66 substrates with yield upto 99%). From the control experiments, it was observed that after the C–H amination an incipient tetrahedral oxyanion or thiolate intermediate is formed via intramolecular attack of the primary amine to the amide carbonyl/thiocarbonyl. It undergoes either 1,2-pyridyl shift with the retention of carbonyl moiety or H₂S elimination for scaffold diversification. Remarkably, inspite of a positive influence of copper in the reaction outcome, from our preliminary investigation the benzimidazolone product was also obtained in good to moderate yields in two steps under the metal-free condition. The *N*-pyridyl moiety of the benzimidazolone was removed for further manipulations of the free NH group.

H. M. Begam, S. Nandi, R. Jana, *Chem. Sci.*, 2022, **13**, 5726-5733.

A directing group switch in copper-catalyzed electrophilic C–H amination/migratory annulation cascade: divergent access to benzimidazolone/benzimidazole

III.1. Introduction

Benzimidazolones are important structural motif of many bioactive molecules exhibiting wide range of biological activities and hence, they are used to treat various diseases including cancer, type II diabetes, central nervous system disorders, pain management, and infectious disease.¹ On the other hand, benzimidazole derivatives have also emerged as important heterocyclic systems in medicinal chemistry and drugs and pharmaceuticals discovery program because of their antiparasitic, anticonvulsant, analgesic, antihistaminic, antiulcer, antihypertensive, antiviral, anticancer, antifungal and anti-inflammatory activity. Some benzimidazolone/benzimidazole containing bio-active molecules are shown below (**Figure 1**).²

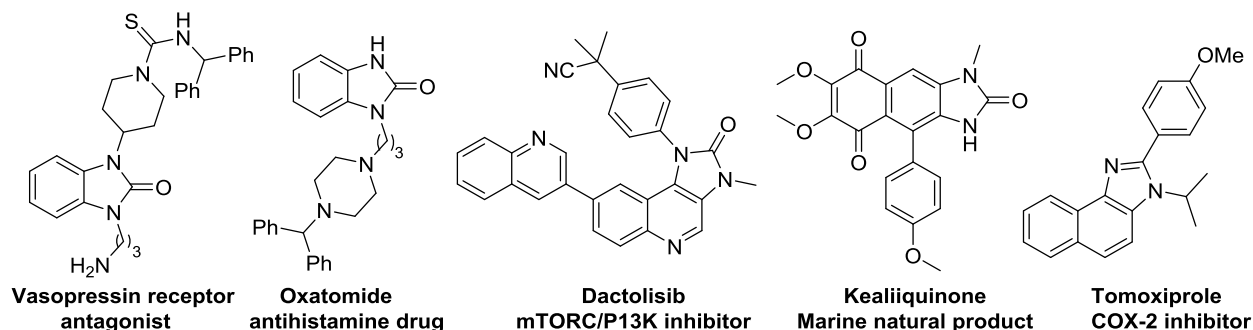
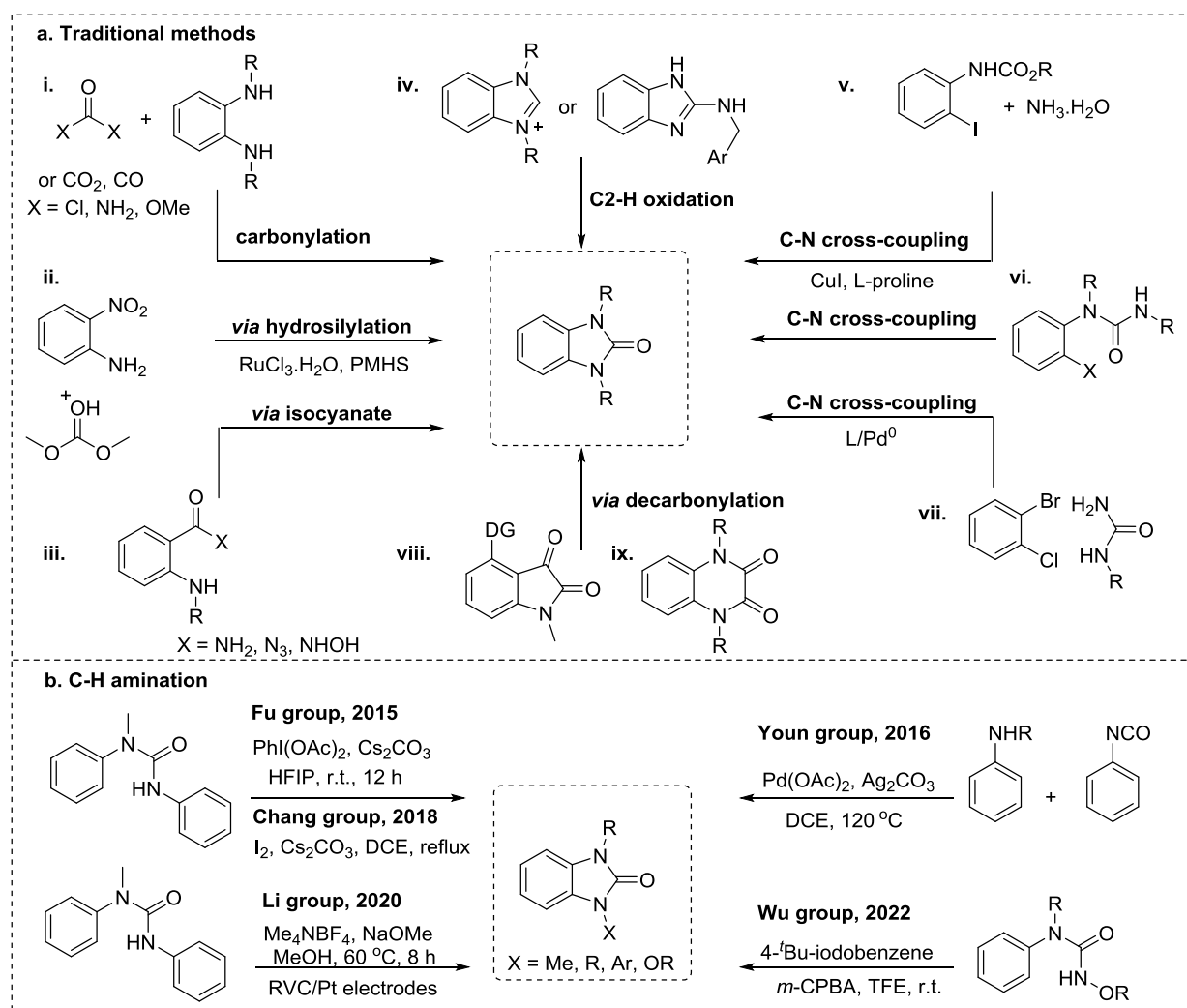


Figure 1. Some selected examples of benzimidazolone/benzimidazole containing bio-active molecules

Conventional approach for the synthesis of benzimidazolones is the carbonylation of substituted benzene-1,2-diamines with various carbonyl sources such as phosgene, triphosgene, and carbonyldiimidazole (CDI), CO₂ and CO.³ To avoid those hazardous carbonyl sources urea and carbonates have also been employed as greener carbonyl source to achieve such reactions (**Scheme 1ai**). In this context, the Bhanage group disclosed a one-pot synthesis of benzimidazolones from 2-nitro anilines with dimethylcarbonate under ruthenium or copper catalysis (**Scheme 1aii**).⁴ However, benzene-1,2-diamines or 2-nitroaniline derivatives are not readily available. Apart from these, *N*-substituted benzimidazolones can also be made directly

from anthranilic acid derivatives *via* rearrangement to isocyanate followed by cyclization (**Scheme 1a**).⁵ On the other hand, C-N cross-coupling reactions have been developed as alternative protocols where the carbon-halogen bonds are converted into C-N bonds by transition-metal catalysis or base promotion. For example, the Ma group in 2009, reported the synthesis of benzimidazolone by CuI/L-proline catalyzed C-N coupling of 2-iodo carbamates with ammonia followed by cyclisation (**Scheme 1av**).⁶ Similar kind of transformations *via* intramolecular C-N coupling has also been developed using 2-halo ureas under Pd and Cu-catalysis or metal-free condition (**Scheme 1avi**).⁷ Formation of benzimidazolones were also reported by Pd(0) catalyzed

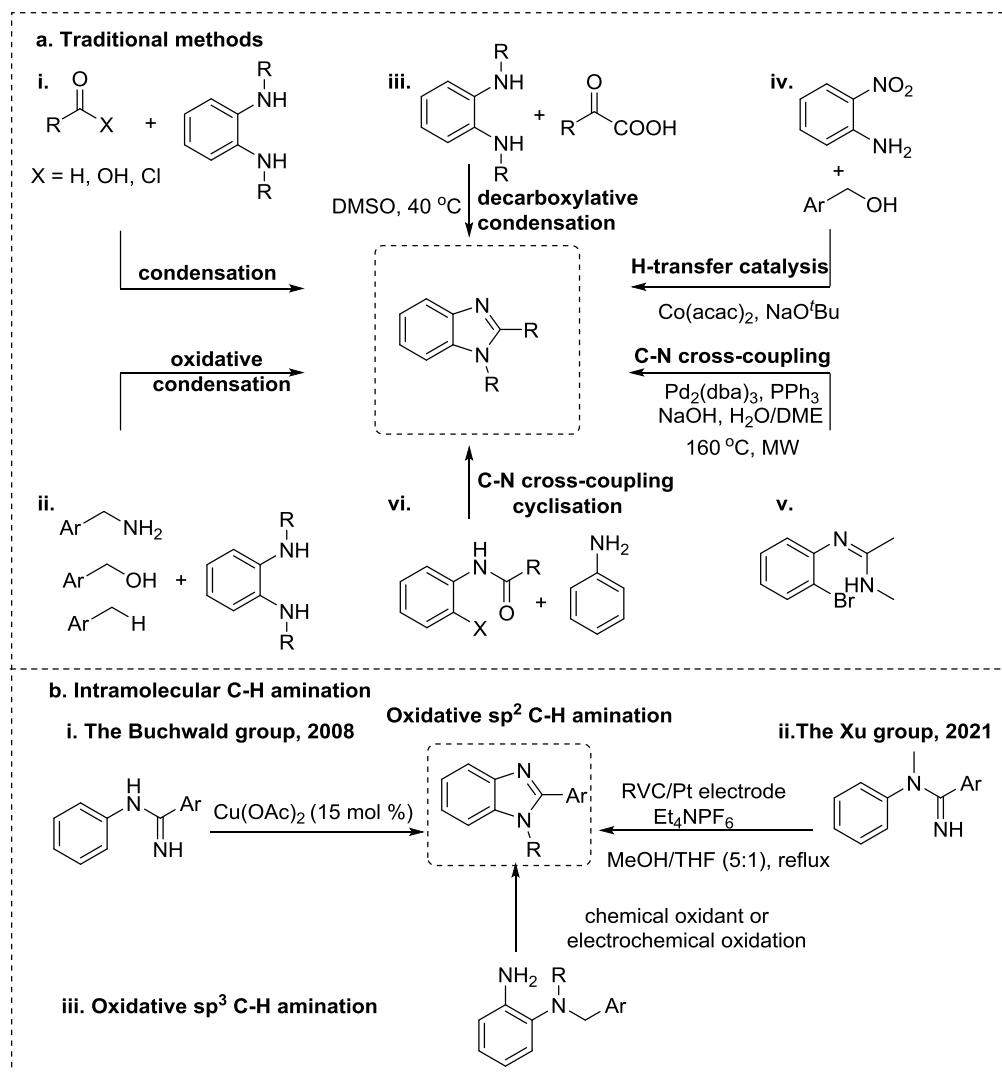


Scheme 1. Traditional methods *vs.* C-H amination for the synthesis of benzimidazolones

intermolecular C-N cross-couplings of 1,2-dihalo benzenes with urea (**Scheme 1avii**).⁸ Synthesis of benzimidazolones has also been achieved by C-2 oxidation of various benzimidazoles either in

metal promoted or metal-free conditions (**Scheme 1aiv**). In this regard the Dong group reported regioselective decarbonylative cycloaddition of isatins with isocyanates to afford benzimidazolones under Rh-catalysis (**Scheme 1aviii**).⁹ In 2017, the Reddy group unveiled a metal free decarbonylative ring-contraction protocol for the synthesis of benzimidazol-2-ones from corresponding quinoxalinediones (**Scheme 1aix**).¹⁰ The highly substituted benzimidazolones were also obtained by metal-catalysed or metal-free intramolecular C-H amination from the corresponding aryl ureas or *in situ* generated aryl ureas (**Scheme 1b**).¹¹

On the other hand, benzimidazoles are generally prepared from benzene 1,2-diamine by condensation with variety of carboxylic acid derivatives. These methods work under harsh



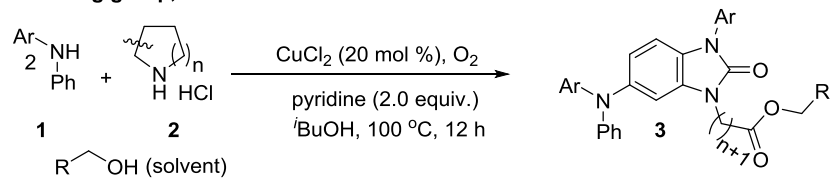
Scheme 2. Traditional methods vs. C-H amination for the synthesis of benzimidazoles

dehydrating reaction conditions, high temperatures and require strong acids in many cases (**Scheme 1ai**).¹² However, coupling with aldehydes occurs at milder conditions but they are two-step process which needs stoichiometric oxidants.¹³ There are many novel methods for the synthesis of benzimidazoles through the coupling of *ortho*-diamines with readily available benzylamines, benzyl alcohols or even alkyl benzenes (**Scheme 1aii**).¹⁴ The Laha group reported the synthesis of benzimidazoles *via* the decarboxylative condensation of *ortho*-diamines with aryl keto carboxylic acids under metal free conditions (**Scheme 1aiii**).¹⁵ In 2019, the Sarkar group reported a cobalt catalyzed synthesis of benzimidazoles by the reaction of *ortho*-nitro anilines with benzyl alcohols *via* H-transfer catalysis (**Scheme 1aiv**).¹⁶ Many protocols for the synthesis of benzimidazoles *via* inter or intramolecular C-N cross-coupling of *ortho*-halo anilides or amidines have also been achieved (**Scheme 1av-vi**).¹⁷ On the other hand, intramolecular oxidative sp² C-H amination reactions have also been emerged for the synthesis of C-2 substituted benzimidazoles (**Scheme 1bi-ii**).¹⁸ Beside these reactions benzimidazoles can also obtained *via* intramolecular oxidative Csp³-H imination reactions using either chemical oxidants or electrochemical oxidation (**Scheme 1biii**).¹⁹

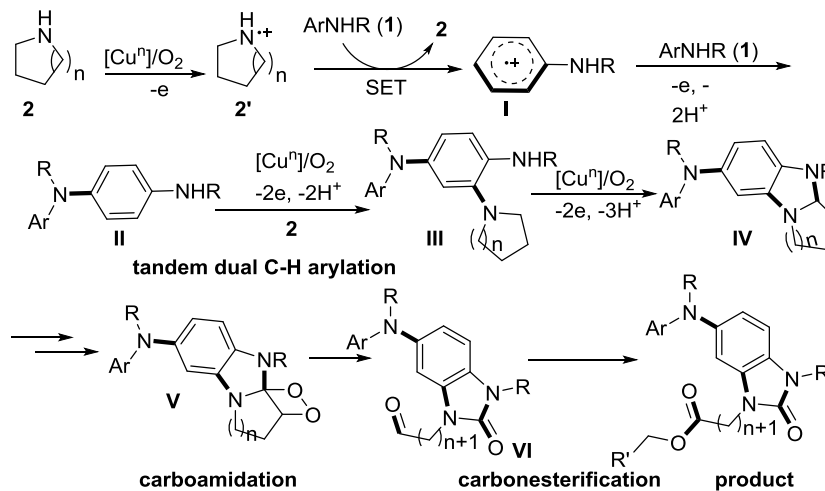
III. 2. Review

Development of cascade reactions having undeniable benefits including atom economy, and also economies of time, labour, resource management and waste generation is upcoming field of research area. This is why cascade reactions are now considered to fall under the banner of “green chemistry”.²⁰ In this direction the Zhang group in 2019, disclosed a useful protocol for the synthesis of functional benzimidazolones from arylamines, dialkylamines, and alcohols (**Scheme 3**).²¹ The reaction proceeds *via* copper-catalyzed dual oxidative C–H aminations followed by alkyl deconstructive carbo-functionalization cascade. Though this method is able to functionalise inert C-H bonds without the installation of directing group, the reaction is very substrate specific and took place in diarylamines only. Anilines, cyclic amines such as tetrahydroquinoline or indolines were ineffective substrates to this protocol.

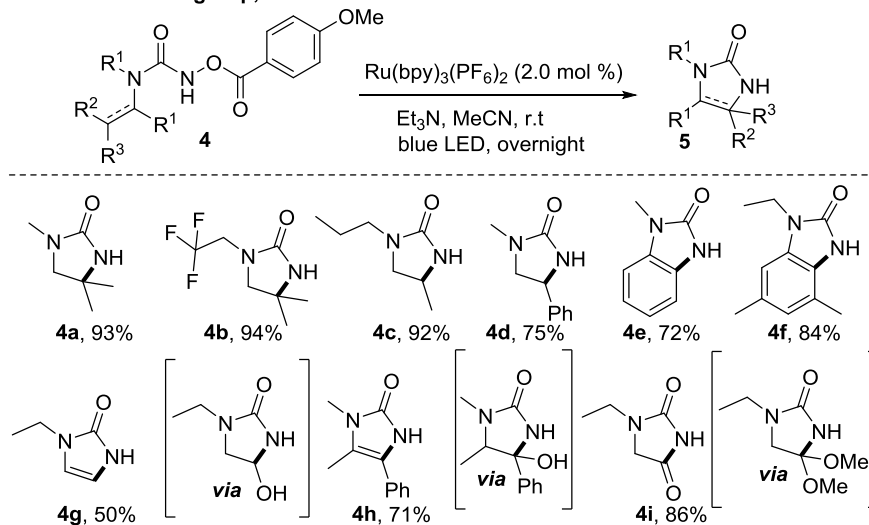
The Zhang group, 2019



Proposed mechanism

Scheme 3. Synthesis of benzimidazolones *via* Cu-catalyzed oxidative dual C-H aminations

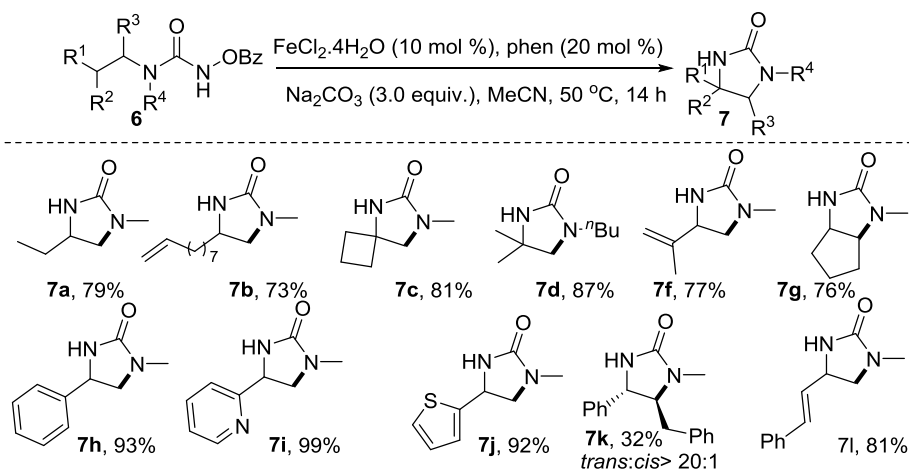
The Beauchemin group, 2020

Scheme 4. Synthesis of imidazolones through C(sp³)-H aminations under photo-redox condition

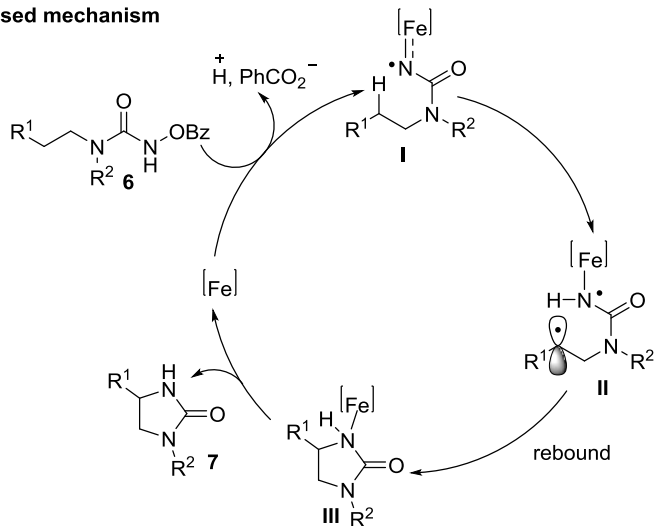
C-H amination with electrophilic amines are found to be a better alternative for the synthesis of benzimidazolones. The Beauchemin group in 2020, reported the synthesis of imidazolones using engineered *O*-benzoyloxy hydroxylamines *via* sp³ C-H amination through the

formation of nitrene intermediate under photo-redox catalysis (**Scheme 4**).²² They designed *O*-acyl hydroxylamine precursors in such a way that they enabled a new photocatalytic C–H amination affording a broad range of imidazolidinones and related heterocycles.

The Meggers group, 2021



Proposed mechanism

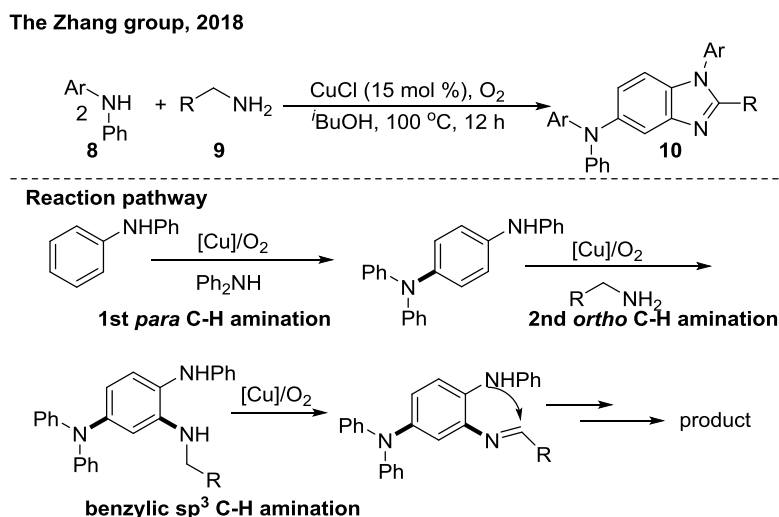


Scheme 5. Synthesis of imidazolidin-2-ones *via* Fe-catalyzed C(sp³)-H aminations

In 2021, the Meggers group also reported similar sp³ C–H amination for the synthesis of imidazolones under iron-catalysis from similar kind of substrates (**Scheme 5**).²³ The amination of C(sp³)-H in their condition was obtained by the insertion of metal-nitrene intermediate into the C–H bond. A broad range of imidazolidin-2-ones were gained with very good functional group tolerance. Mechanistically, the active Fe(II) catalyst binds to phen ligand, then coordinates to the substrate (*N*-benzoyloxyurea). After deprotonation of the N–H group followed by release of the

benzoate leaving group iron nitrenoid intermediate **I** is formed. This metal-nitrenoid species in its triplet state undergoes a 1,5-hydrogen atom transfer (HAT) generating a radical intermediate **II**. The intermediate undergoes a rapid radical rebound process to form intermediate **III**. From this product is released with the regeneration of the iron catalyst for a new catalytic cycle.

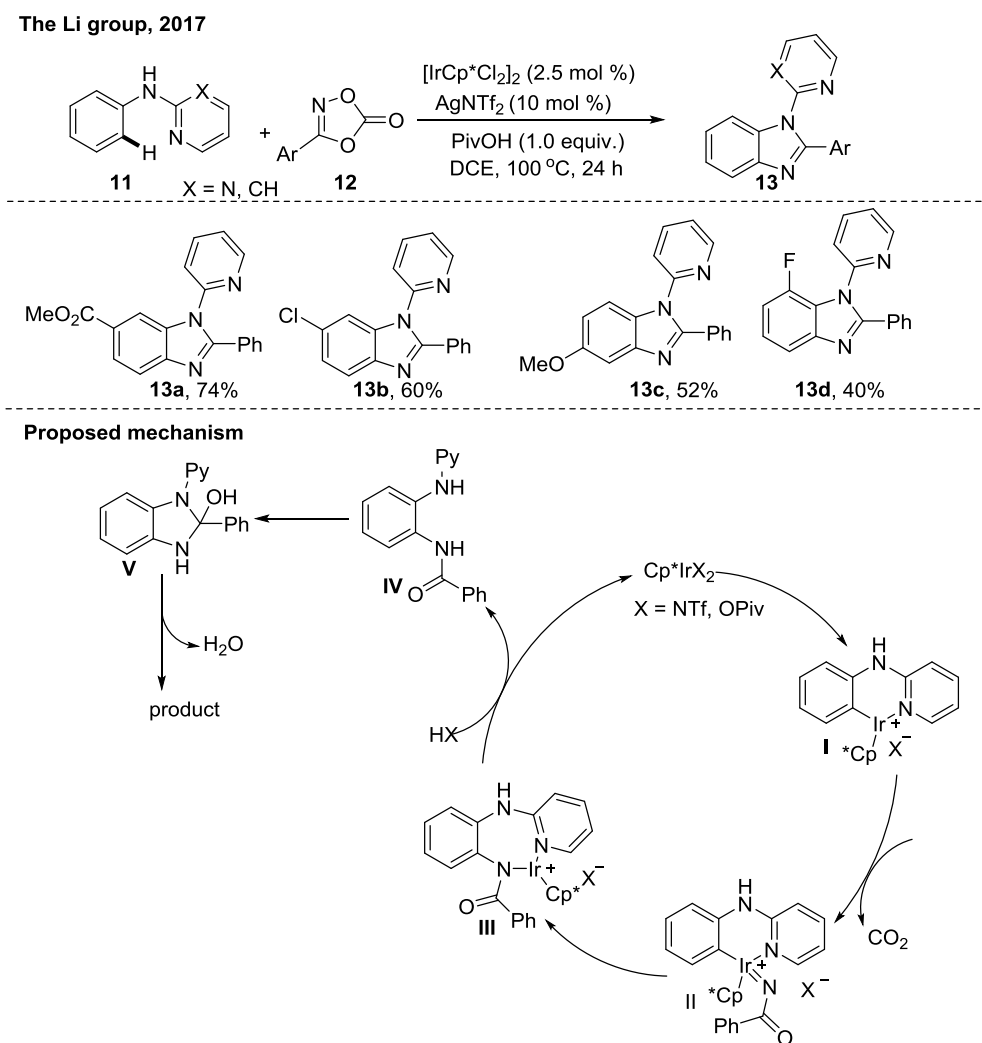
Besides the oxidative C-H amination reactions as mentioned in the previous section benzimidazoles can also be made by intermolecular C-H amination cascade processes. For example, the Zhang group reported the synthesis of 5-diarylamino benzimidazoles *via* radical-induced triple C-H amination cascade under aerobic copper catalysis (**Scheme 6**).²⁴ This cascade reaction involved the combination of two diarylamine and an alkylamine molecules in one-pot. As the reaction is solely controlled by electronics, this reaction works only in diarylamine system only. Although having this limitation this step and atom economic protocol also offered a broad substrate scope with respect to diarylamines with good functional group tolerance.



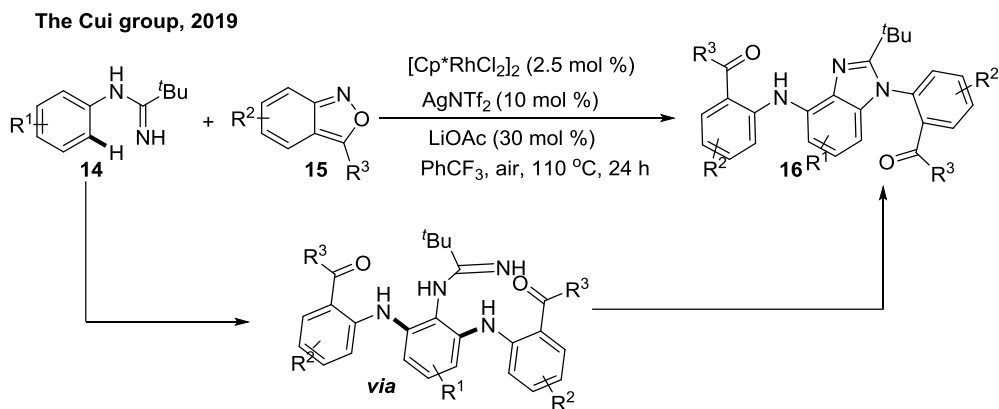
Scheme 6. Synthesis of benzimidazoles *via* triple C-H aminations cascade using nucleophilic amines

Electrophilic amidation or amination/ cyclisation cascade reactions have also been developed for the synthesis of this important scaffold. In this context, the Li group in 2017, disclosed Ir-catalyzed directed *ortho*-C-H amidation/cyclisation cascade for the synthesis of benzimidazoles using dioxazolone as amidating agent (**Scheme 7**).²⁵ Under their optimized condition *meta*-substituted substrates with various electron-withdrawing and halide groups afforded the desired product in good yields and the C-H amidation occurred at the less hindered

ortho-position. In contrast, electron-donating group (-OMe) at *meta* position didn't afford any product limiting this methodology. Other *para*- and *ortho*-substitutions worked well in their condition. Mechanistically, active Ir-catalyst generated *in situ* which forms iridacycle **I** through C-H activation. This iridacycle then coordinates with dioxazolone (**12**) through CO₂ extrusion forming metal-nitrenoid species **II**. After that a migratory insertion followed by protonolysis gives the *ortho*-amidation product **IV**. Intramolecular nucleophilic attack of the aniline *N*-atom to the acyl carbon followed by dehydration affords the product with catalyst regeneration. In 2020, the Chatani group also developed similar strategy using less expensive Rh-catalyst.



Scheme 7. Synthesis of benzimidazoles *via* C-H amidation/cyclisation cascade using electrophilic dioxazolone

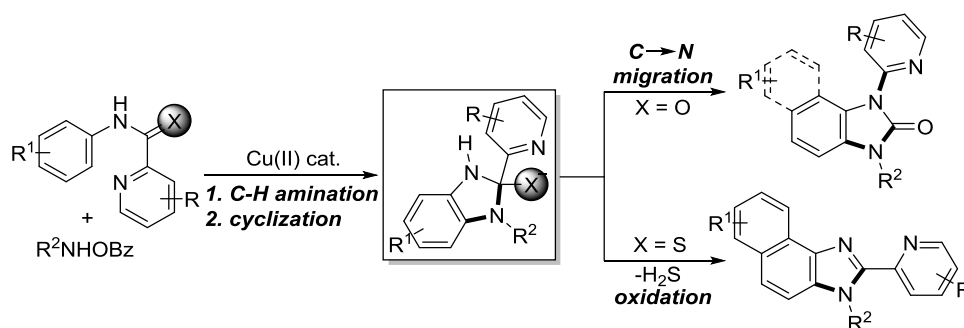


Scheme 8. Synthesis of benzimidazoles *via* C-H amination/cyclisation cascade using electrophilic aminating agent anthranil

A strategy for the synthesis of sophisticated benzimidazoles was reported by the Cui group in 2019, by a Rh-catalysed C-H amination with anthranil followed by cyclisation cascade (**Scheme 8**).²⁶

III. 3. Present work

C-H amination/cyclisation cascade reactions for the synthesis of various valuable *N*-heterocycles are now becoming a growing field of research area. However, most of the C-H amination methods require pre-installation of directing groups in the substrates to control regioselectivity and their subsequent removal. So, the introduction and removal of directing groups is one of the major drawbacks in chelation-assisted C-H functionalization. To by-pass this problem, transient, traceless and inherent directing group strategies were unveiled.²⁷ Very recently, migration and incorporation of a DG into the target molecule has arisen as a practical approach in transition metal-catalyzed C-H functionalization.²⁸ This strategy can provide quick access to complex molecules by maximizing the atom-economy. The Miaura group reported divergent synthesis of indoles and oxazoles controlled by directing-group.²⁹ However, there is no report of a single atom of directing group (O vs. S) switch for scaffold diversification exploiting their innate reactivity in the C-H functionalization/annulation cascade. So, we took an initiative to explore this.



Scheme 9. Directing group switch in copper-catalyzed electrophilic C–H amination/migratory annulation cascade: divergent access to benzimidazolone/benzimidazole

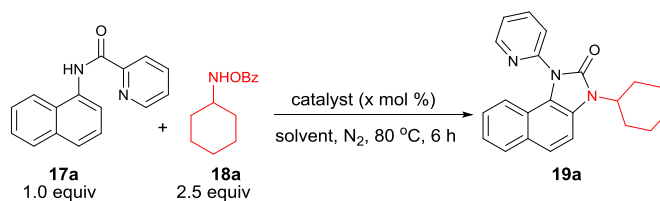
In our previous work we observed an excellent reactivity of bicyclic system towards electrophilic *ortho* C–H amination with *O*-benzoyloxy protected secondary amines.³⁰ We hypothesized that C–H amination with primary amine may initiate an annulation cascade *via* subsequent addition to picolinamide directing group. The incipient oxyanion may trigger 1,2-migration of directing group to provide benzimidazolone. Instead, thiophilic copper may endorse the extrusion of hydrogen sulfide to provide benzimidazole from the corresponding thioamide directing group. C–H amination with aliphatic primary amines are challenging and less explored. However, copper-catalyzed C–H amination with free primary amine is a daunting challenge because of the catalyst inhibition.³¹ Another problem is the competitive intramolecular oxidative cyclization of the corresponding DG which can hamper the intermolecular cascade process.³² The electrophilic C–H amination has arisen as a benevolent alternate for constructing *N*-heterocycles under mild conditions.³³ We hypothesized that C–H amination with electrophilic primary amine surrogate may overcome the catalyst inhibition problem.

III. 4. Result and discussions

To test our hypothesis, picolinamide-protected 1-naphthylamine **17a** and aniline were subjected separately with 1.0 equiv. of *O*-benzoylhydroxylamine **18a** in presence of Cu(OAc)₂·H₂O in DMSO at 80 °C for 6 hrs. Successfully, **17a** provided the expected imidazolone product **19a** in 44% yield but aniline substrate remained unsuccessful (**Table 1**). Further optimization study revealed that out of other solvents DMSO found to be best. This cascade reaction provided excellent yields 93% and 87% with just 5.0 and 1.0 mol % catalyst loading respectively. Even 5 mol % metallic copper also furnished the product in very good yield. Free primary amines (instead

of **18a**) along with different external oxidants such as PIDA, $K_2S_2O_8$ or Bz_2O_2 were able to give the desired product in <5%, 12% and 32% yields respectively suggesting the poor ability of free amines over the protected *O*-benzoylhydroxylamine. 1.2 equiv of **18a** along with 1.0 equiv Bz_2O_2 afforded the product in lesser yield 58%. Other transition metal catalysts such as $Pd(OAc)_2$, $Co(OAc)_2$, $Ni(OAc)_2$, $Mn(OAc)_2$, $FeCl_2$, $FeBr_2$ etc. were found to be less effective or ineffective to undergo this cascade process

Table 1 Optimization of the reaction conditions for benzimidazolone^{a,b}



| Entry | Catalyst | X | Oxidant | Solvent | Yield ^b (19a) |
|-----------------|------------------------|-----|---------|---------|--------------------------------------|
| 1 ^c | $Cu(OAc)_2 \cdot H_2O$ | 10 | - | DMSO | 44 |
| 2 | $Cu(OAc)_2 \cdot H_2O$ | 10 | - | H_2O | 0 |
| 3 | $Cu(OAc)_2 \cdot H_2O$ | 10 | - | MeCN | 39 |
| 4 | $Cu(OAc)_2 \cdot H_2O$ | 10 | - | dioxane | 62 |
| 5 | $Cu(OAc)_2 \cdot H_2O$ | 10 | - | DMSO | 90 |
| 6 | $Cu(OAc)_2 \cdot H_2O$ | 5 | - | DMSO | 93 |
| 7 | $Cu(OAc)_2 \cdot H_2O$ | 2.5 | - | DMSO | 90 |
| 8 | $Cu(OAc)_2 \cdot H_2O$ | 1.0 | - | DMSO | 87 |
| 9 | $Cu(OAc)_2 \cdot H_2O$ | 0.5 | - | DMSO | 72 |
| 10 ^d | $Cu(OAc)_2 \cdot H_2O$ | 0 | - | DMSO | 0 |
| 11 ^e | $Cu(OAc)_2 \cdot H_2O$ | 2.5 | - | DMSO | 56 |
| 12 | Cu powder | 5 | - | DMSO | 83 |

| | | | | | |
|-----------------|--|----|--------------------------------|------|----|
| 13 ^f | Cu(OAc) ₂ .H ₂ O | 10 | PIDA | DMSO | >5 |
| 14 ^g | Cu(OAc) ₂ .H ₂ O | 10 | Bz ₂ O ₂ | DMSO | 58 |
| 15 | Pd(OAc) ₂ | 10 | - | DMSO | >5 |
| 16 | Co(OAc) ₂ | 10 | - | DMSO | 20 |

^aAll reactions were carried out in 0.2 mmol scale. ^bYields refer to here are overall isolated yields. ^c1.0 equiv. **18a** was used. ^d25% *ortho* aminated product was obtained. ^eReaction was performed at room temperature. ^fFree amine was used as amine source and oxidant 2.5 equiv. ^g1.0 equiv. Bz₂O₂ and 1.2 equiv. of **18a** were used.

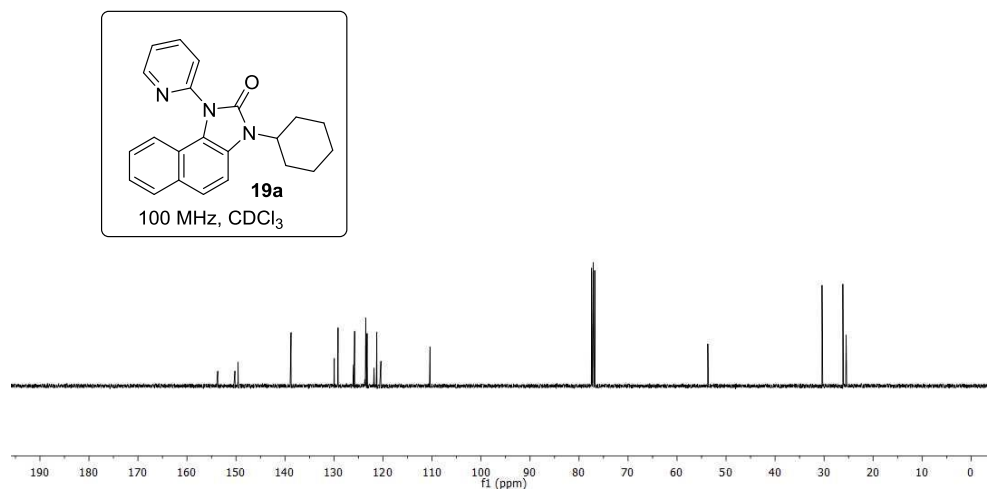
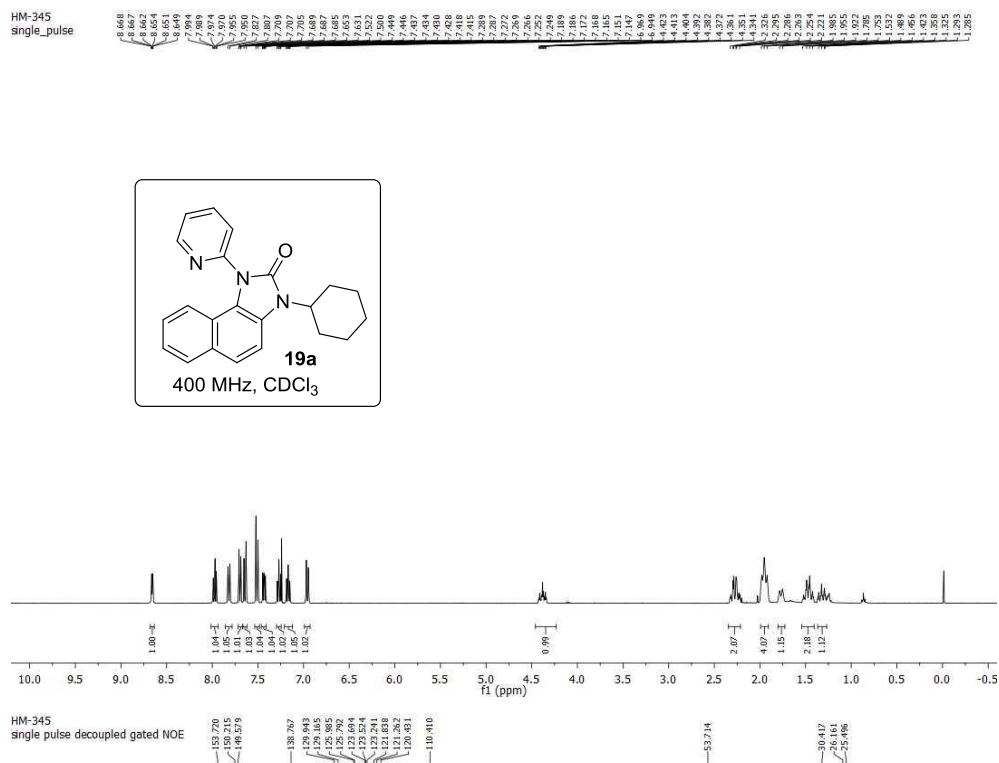
Characteristics peaks in ¹HNMR spectrum of compound 16a

1. Firstly, the amide proton in the range of δ value 10.0-11.0 ppm was disappeared in the product.
2. Appearance of one multiplet in the region δ 4.42-4.34 ppm corresponding to 1 proton and another five multiplets ranging from δ 2.33 to 1.29 ppm corresponding to total 10 protons indicated the incorporation of cyclohexyl moiety from the amine source.

Characteristics peaks in ¹³C NMR spectrum of compound 16a

1. In ¹³C NMR four new peaks in the aliphatic region δ 53.7-25.5 ppm were appeared. The peak at δ 53.7 ppm is for the carbon atom attached to the N-atom.

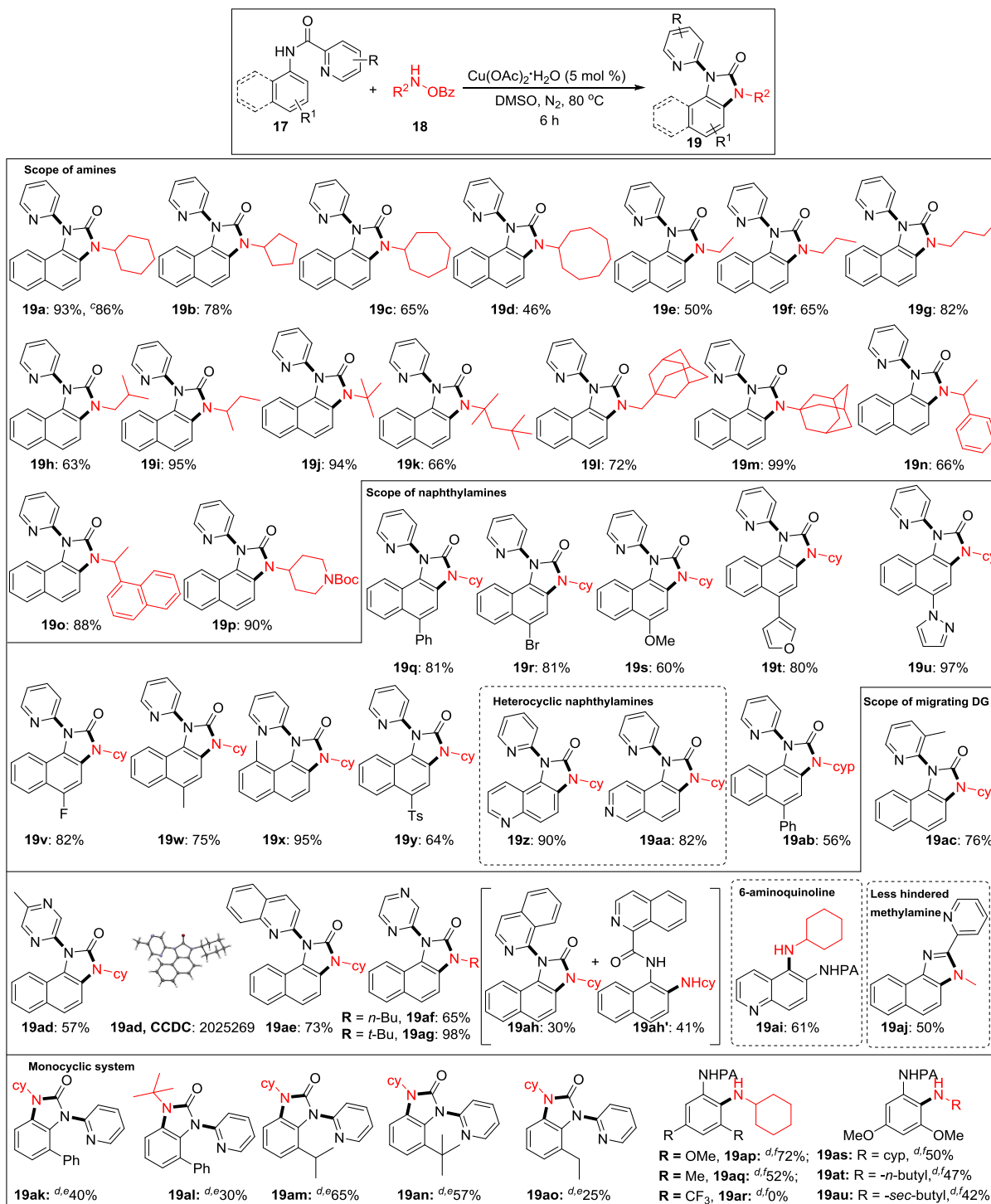
Mass of the compound was 2 units less than *ortho* amination product indicating the missing of two protons. Finally, X-ray crystallography data confirmed the exact structure.



Under the optimized reaction condition, a large variety of cyclic and acyclic primary amines supplied a library desired products in good to high yields (**Table 2**). Cyclohexylamine delivered an excellent 93% yield of the desired product (**19a**), whereas cyclopentyl, cycloheptyl and cyclooctylamines gave slightly lower 78%, 65% and 46% yields respectively (**19b-19d**). With

acyclic amines, yields improved with the increase in chain length (**19e-19g**) and steric bulk. Sterically hindered *sec*-butyl (**19i**), *tert*-butyl (**19j**), adamantylamine (**19m**) gave excellent to almost quantitative yields revealing a positive influence of steric factor of amines on the rearrangement cascade. A competitive experiment of **17a** with two different amines, **18m** and **18n** provided **19m** and **19n** in 70% and 28% yields respectively. Many substituted 1-naphthylamines including methyl substitution at the C-8 position delivered high to excellent yields of the desired products (**19q-19y**). Picolinamide protected amino-quinoline and isoquinoline afforded the rearranged products in admirable yields (**19z**, **19aa**). Successfully, various (2-*N*-heteroaryl) anilides worked as outstanding directing groups and incorporated into the benzimidazolones (**19ac-19ah**). Remarkably, 3-methyl picolinamide delivered the corresponding *N*-pyridyl product (**3ac**) *via ipso*-substitution. Likewise, amides of 5-methyl pyrazinoic (**19ad**, CCDC 2025269), quinaldic (**19ae**) and pyrazinoic acid (**19af**, **19ag**) also supplied the products in comparable yields. Isoquinoline-1-carbamide gave a mixture of benzimidazolone **19ah** and C–H amination product **19ah'**. This may be the result of unfavourable formation of the tetrahedral intermediate for steric cause. In case of 6-aminoquinoline, the reaction stopped at the C–H amination step (**19ai**). Moreover, less hindered methyl amine delivered the corresponding 2-pyridylbenzimidazole (**19aj**, CCDC 2025266) conveying the role of steric and trajectory of the amine after C-H amination on the consequent rearrangement reaction.

Table 2 Substrate scope of benzimidazolones^{a,b}

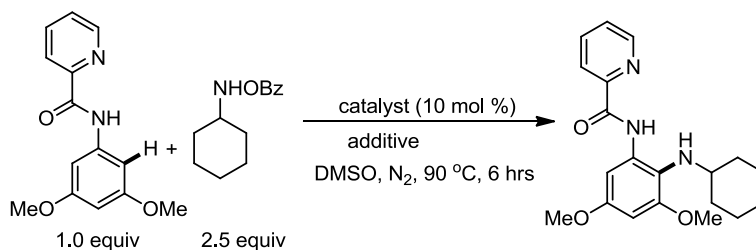


Reaction conditions: **17** (0.20 mmol), **18** (0.50 mmol), Cu(OAc)₂.H₂O (0.01 mmol), Dry DMSO (2.0 mL), N₂, 80 °C, and 6 h. ^aAll reactions were carried out in 0.2 mmol scale. ^bYields refer to the overall isolated yields with respect to **17**. ^c0.2 mmol scale reaction. ^d10 mol % Cu(OAc)₂.H₂O is used. ^eReaction temperature was 100 °C. ^fAdditional 2.0 equiv. LiO^tBu is used and reaction

temperature was 90 °C. In the competition experiment: **17a** (0.20 mmol), **18m** (0.50 mmol), **18n** (0.50 mmol), Cu(OAc)₂.H₂O (0.01 mmol), Dry DMSO (2.0 mL), N₂, 80 °C, and 6 h.

After that various picolinamide protected *ortho*, *meta*, *para* substituted anilines were subjected under the same condition. Successfully, picolinamide protected 2-phenyl aniline gave 30% rearranged product and 3,5-dimethoxy aniline afforded *ortho* amination product (35%). After the attainment of these results next we turned our consideration to optimize these reactions. After numerous screening of various solvents, base or acid additives, ligands there was no noteworthy progress in rearrangement reaction of 2-phenyl aniline picolinamide. Increasing temperature to 100 °C the product yield was slightly increased to 40%. Then different *ortho* substituted anilines were subjected to this condition but *ortho* substituted anilines only (with electron donating bulky groups) afforded the rearranged benzimidazolones in moderate to good (**19ak-19ao**) yields. After several screenings use of additional 2.0 equiv LiO^tBu gave the *ortho* C–H amination product in 3,5-dimethoxy aniline with 72% yield at 90 °C (**19ap**). While 3,5-dimethyl substituted picolinamide provided the C–H amination product in 52% yield, the corresponding 3,5-bis(trifluoromethyl)aniline substrate stayed unreactive showing an intense role of electronic nature (**19aq, 19ar**). Besides cyclohexylamine, other amines also gave the *ortho* C–H amination products in moderate yields (**19as-19au**). However, no benzimidazolones were obtained even at low catalyst loading suggests that an *ortho* substitution w.r.t picolinamide has a decisive role for the preceding rearrangement reaction.

Table 3 Optimisation of C-H amination in monocyclic system^{a,b}



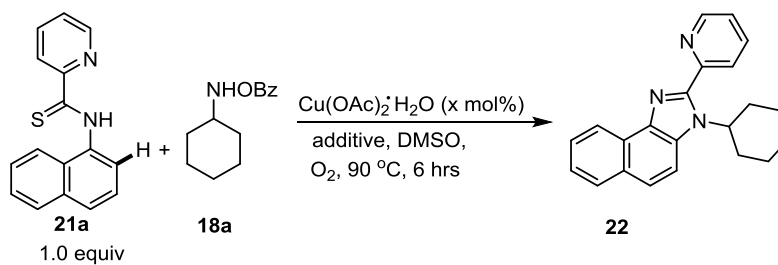
| Entry | Catalyst | Additive | Yield (%) |
|----------------|--|----------|-----------|
| 1 | Cu(OAc) ₂ .H ₂ O | - | 35 |
| 2 ^c | Cu(OAc) ₂ .H ₂ O | - | 25 |

| | | | |
|----------------|---|---------------------------------|-----------|
| 3 | Cu(OTf) ₂ | - | 10< |
| 4 | Pd(OAc) ₂ | - | nr |
| 5 | Cu(OAc) ₂ .H ₂ O | 1,10-phen | 15 |
| 6 | Cu(OAc) ₂ .H ₂ O | K ₂ CO ₃ | 58 |
| 7 ^d | Cu(OAc) ₂ .H ₂ O | K ₂ CO ₃ | 50 |
| 8 ^e | Cu(OAc) ₂ .H ₂ O | K ₂ CO ₃ | 54 |
| 9 | Cu(OAc) ₂ .H ₂ O | Na ₂ CO ₃ | 45 |
| 10 | Cu(OAc) ₂ .H ₂ O | Cs ₂ CO ₃ | 43 |
| 11 | Cu(OAc) ₂ .H ₂ O | KOAc | 30 |
| 12 | Cu(OAc)₂.H₂O | LiO^tBu | 72 |

^aAll reactions were carried out in 0.2 mmol scale. ^bYields refer to here are overall isolated yields.

^cTemperature 100 °C and time 12 hrs. ^dAir. ^eO₂ atm.

2-pyridylbenzimidazoles are an important class of compounds usually used as excellent ligands for metal complexation and glukokinase activator, etc. This is why we turned our attention towards the optimization of the reaction for benzimidazole.³⁴ Primarily, we started the optimization of benzimidazole with **17a** and **18a**. All our efforts using different acidic solvents such as AcOH or TFE, use of acid additives such as BzOH, TsOH, and high temperature (120 °C) to assist the dehydration after cyclization were unsuccessful. Satisfyingly, the corresponding picolinimidamide afforded the imidazole product in 30% yield in 12 hrs. As thioamides have been evidenced as excellent directing groups in Pd- or Co-catalyzed C–H functionalizations,³⁵ we assumed that thiophilic copper may trigger the extrusion of hydrogen sulfide from thioamide instead of 1,2-pyridyl migration to give the desired benzimidazole product. Successfully, the thiopicolinamide **21a** under the above reaction condition, afforded the desired 2-pyridylbenzimidazole solely albeit in low yield. After a number of screenings, use of 3.0 equiv. of **18a**, 20 mol % Cu(OAc)₂.H₂O and 1.2 equiv. of K₂CO₃ in DMSO at 90 °C under O₂ atmosphere furnished the desired product in 88% yield. During the optimization we observed that both K₂CO₃ and O₂ are crucial otherwise yield diminished significantly.

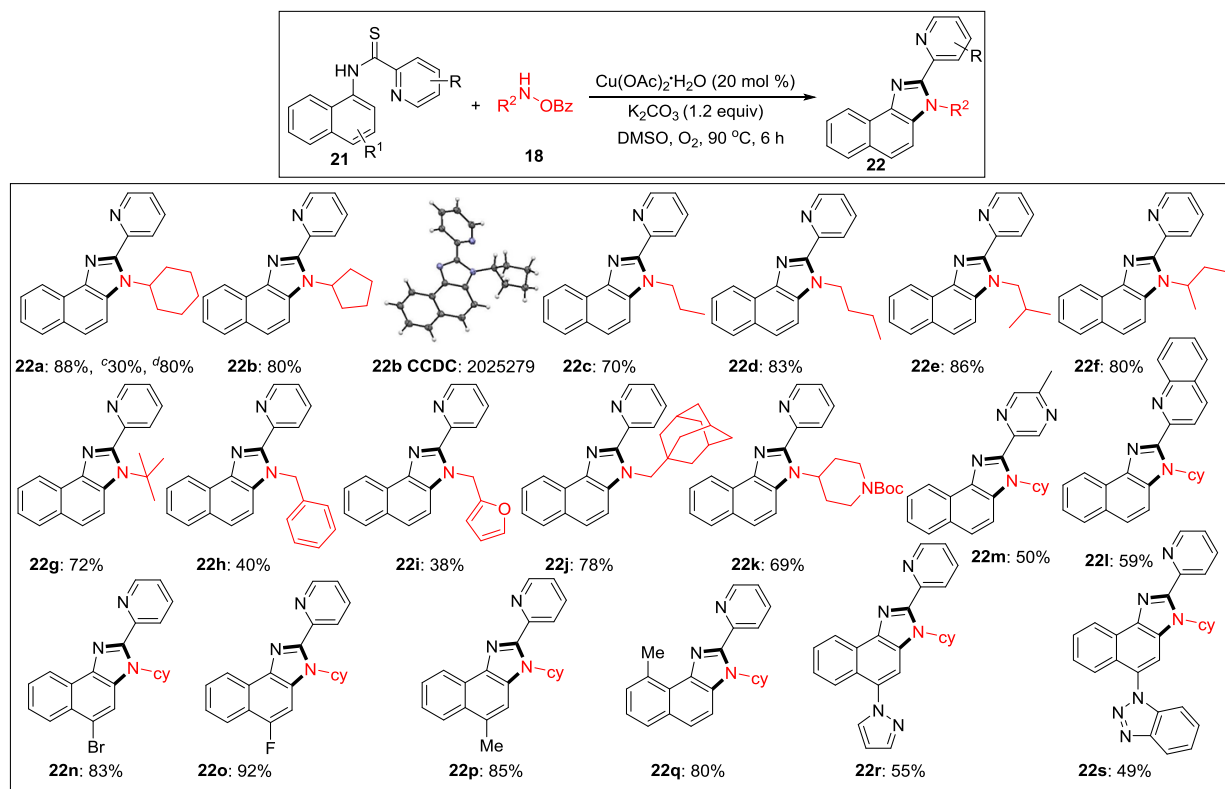
Table 4 Optimization of the reaction conditions for benzimidazole^{a,b}

| Entry | Amine source (equiv.) | Cu(OAc) ₂ .H ₂ O (mol %) | Additive | Yield (%) |
|-----------------------|-----------------------|--|---|-----------|
| 1 ^c | 2.5 | 10 | - | 38 |
| 2 ^d | 2.5 | 10 | - | 40 |
| 3 | 2.5 | 10 | - | 46 |
| 4 | 2.5 | 20 | - | 48 |
| 5 | 3.0 | 10 | - | 50 |
| 6 | 3.0 | 20 | - | 53 |
| 7 ^e | 3.0 | 20 | - | 34 |
| 8 ^f | 3.0 | 20 | - | 40 |
| 9 ^g | 3.0 | 20 | - | 40 |
| 10 | 3.0 | 20 | 1.2 equiv. K ₂ CO ₃ | 58 |
| 11 ^h | 3.0 | 20 | 1.2 equiv. K ₂ CO ₃ | 64 |
| 12ⁱ | 3.0 | 20 | 1.2 equiv. K₂CO₃ | 88 |
| 13 ⁱ | 3.0 | 20 | - | 64 |
| 14 ⁱ | 3.0 | 10 | 1.2 equiv. K ₂ CO ₃ | 70 |
| 15 ^{i,j} | 3.0 | 10 | 1.2 equiv. K ₂ CO ₃ | 0 |

^aAll reactions were carried out in 0.2 mmol scale. ^bYields refer to here are overall isolated yields. ^cReaction was continued for 3 hrs. ^dReaction was carried out at 100 °C. ^eReaction was carried out in dry toluene. ^fReaction was carried out in dry 1,4-dioxane. ^gReaction was carried out in dry THF. ^hReaction was carried out in air. ⁱReaction was carried under O₂ atm. ^jReaction was performed with substrate **17a** instead of **21a**.

During the substrate scope studies, we observed a positive influence of the increasing chain length of the linear amines (**22c-22d**, **Table 5**). But with isomeric acyclic amines, unlikely to imidazolones, yield decreases with increasing α -substitution (**22d-22g**). Benzylamine, furylamine, adamantanemethylamine and 4-amino-1-boc piperidine afforded the products in moderate yields (**22h-22k**). Thioamides of 5-methyl pyrazine-2-carboxylic acid and 2-quinaldic acids also provided the imidazole product in moderate yields (**22l**, **22m**). Various substituted 1-naphthylamines at different positions also underwent the reaction providing the desired product in medium to good yields (**22n-22s**). The reaction is also reproducible in 2.0 mmol scale demonstrating practicability of this methodology. Thio-picolinamide of monocyclic anilines under the same condition mostly oxidized to picolinamide.

Table 5 Substrate scope of benzimidazoles^{a,b}

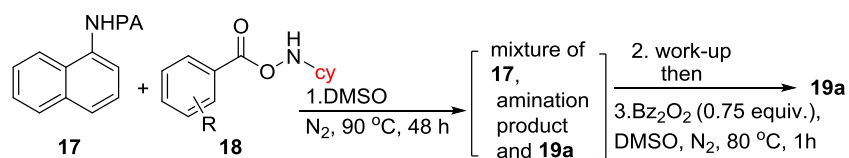


Reaction conditions: **21** (0.20 mmol), **22** (0.60 mmol), $\text{Cu}(\text{OAc})_2 \cdot \text{H}_2\text{O}$ (0.04 mmol), K_2CO_3 (0.24 mmol), Dry DMSO (2.0 mL), O_2 , 90 °C, and 6 h. ^aAll reactions were carried out in 0.2 mmol scale. ^bYields refer to overall isolated yields with respect to **21**. ^cPicolinimidamide **21a'** used as substrate. ^dReaction in 2.0 mmol scale.

III. 5. Metal-free conditions for benzimidazolones

Fascinated by the initial C–H amination product formation under the metal-free conditions (entry 10, **table 1**), we speculated whether it can be re-optimized to get the desired benzimidazolones. Primarily, a mixture of C–H amination product **17a'**, imidazolone **19a** and unreacted starting material was got which was subjected to the succeeding cyclization reaction.

Table 6 Optimization of the metal-free condition^{a,b}



| Entry | Amine source | Equiv. of 18 | Yield ^b (19) |
|-----------------|---|---------------------|----------------------------------|
| 1 | 18a : R = H | 2.5 | 25 |
| 2 | 18a : R = H | 4.0 | 25 |
| 4 | 18a₂ : R = 4-NMe ₂ | 4.0 | 65 |
| 5 | 18a₃ : R = 4-CF ₃ | 4.0 | 10 |
| 6 | 18a₄ : R = 4- ^t Bu | 4.0 | 20 |
| 7 | 18a₅ : R = 4-OMe | 4.0 | 41 |
| 8 | 18a₆ : R = 3,5-di Cl | 4.0 | 0 |
| 9 | 18a₇ : R = pentafluoro | 4.0 | 25 |
| 10 ^c | 18b₂ : R = 4-NMe ₂ | 4.0 | 44 |
| 11 ^d | 18a₂ : R = 4-NMe ₂ | 4.0 | 70 |

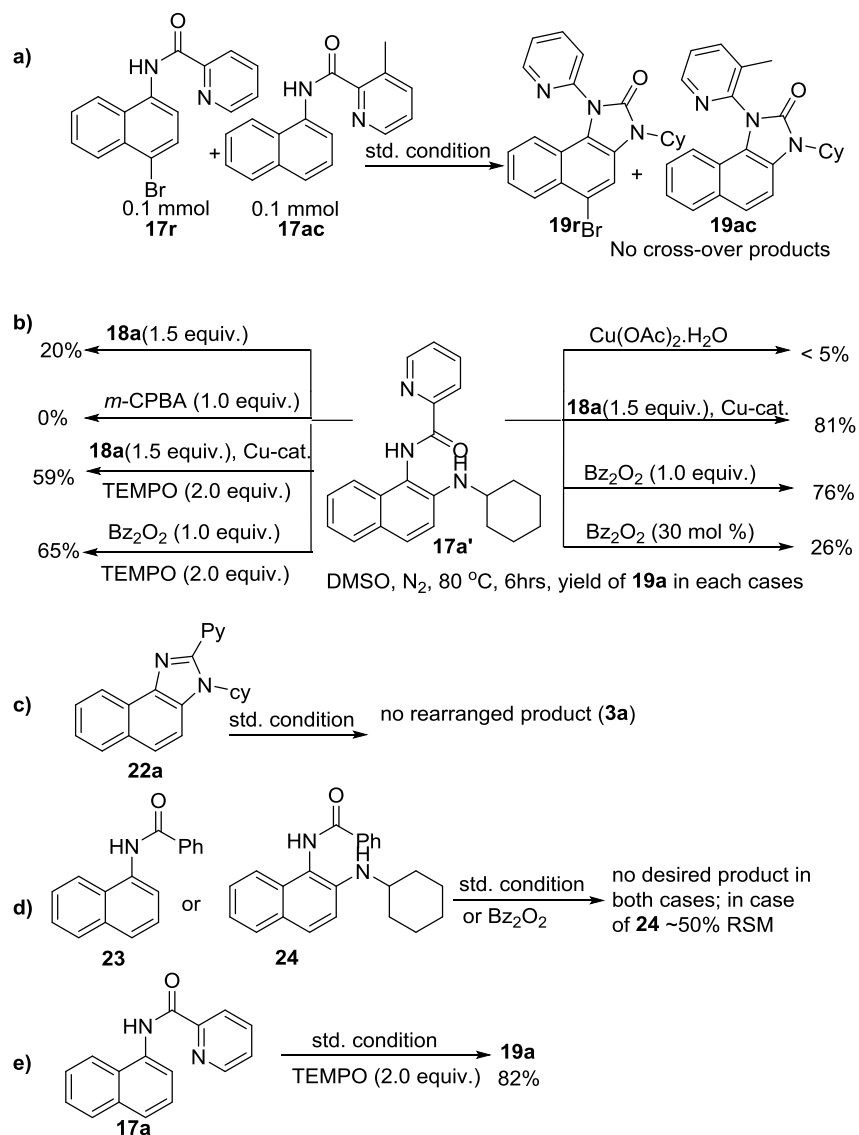
Reaction conditions: **1st step**: **17** (0.10 mmol), **18** (0.40 mmol), Dry DMSO (1.0 mL), N₂, 90 °C, and 48 h. **2nd step**: Bz₂O₂ (0.75 equiv.), DMSO, N₂, 80 °C, and 1h. ^aAll reactions were carried out in 0.1 mmol scale. ^bYields refer to here are isolated yields after two steps with respect to **17**. ^cProtected cyclopentylamine was used and reaction time was 12 h. ^dSubstrate **17r** was used.

However, work up of the reaction mixture followed by addition of benzoyl peroxide transformed the C–H amination product to the desired annulation product at 80 °C. Increasing the amount of amine source **18a** to 4.0 equiv. or temperature to 90 °C the yield wasn't enhanced. Delightfully, varying many different substitutions in the phenyl ring of **18**, we found that 4-NMe₂ substitution provided the product in 65% yield. Protected cyclopentylamine gave the desired product in 44% yield in 12 hrs. Monocyclic substrates remained unreactive under this metal-free condition. To note, the probability of metal contamination was omitted using all new glass-wares, freshly distilled solvents and repeating the reaction at least four times. Although, this metal-free, two-step method has inherent restrictions, we expect that it has intense mechanistic implications.

III. 6. Investigation of reaction mechanism

To gain understanding of the reaction mechanism we performed numerous control experiments. When an equimolar mixture of **17r** and **17ac** was treated in the optimized condition **19r** and **19ac** were obtained and formation of no cross-over product suggests that 1,2-pyridyl migration is intramolecular in nature (**Scheme 10a**). Unsymmetrical substitution in the migrating group as in case of 5-methyl pyrazine anilide **17ad** delivered the imidazolone product **19ad** only through *ipso* C–N bond formation (**Table 2**). Either carrying out the reaction at low temperature for smaller time or quenching the reaction after 1.5 h, we were able to isolate C–H amination product **17a'**. Heating this preformed C–H amination product **17a'** in absence of **18a** 5% product was obtained. But, a combination of copper catalyst and *O*-benzoylhydroxylamine **18a** (1.5 equiv.) or even benzoylperoxide alone provided the desired **19a** in high yields (**Scheme 10b**). Therefore, **18a** acts not only as amine source but also as an oxidant for catalytic turnover. Moreover, the imidazole product **22a** was not transformed into the corresponding imidazolone **19a** under the reaction condition signifying a plausible concerted cyclization/1-2 pyridyl migration path (**Scheme 10c**). Instead of picolinamide **17a**, the corresponding benzanilides **23** or **24** do not provide any desired product (**Scheme 10d**). **24** doesn't undergo rearrangement even in presence of Bz₂O₂ which is suggestive of that the pyridyl-nitrogen is not only needed in the directed C–H amination but also in the succeeding steps. To inspect the association of radical in this C–H amination/migratory annulation cascade, we did the reaction in presence of 2.0 equiv. of TEMPO. The yield was slightly reduced from 93% to 82% (**Scheme 10e**). Further, cyclization from a preformed amination product **17a'** provided in almost similar yield in presence of TEMPO. Hence, single electron transfer (SET) route may be excluded in the migratory cyclization step. Then we accomplished time dependent ¹H NMR experiment to get an idea about any intermediate forming during the course of the rearrangement reaction. We took **17a'** in a NMR tube in DMSO-d₆ and 1.0 equiv. of Bz₂O₂ was added to it for recording the time-dependent ¹H NMR spectra at room temperature (**Fig. 2**). After 5-7 min, a new peak probably corresponding to H_b or H_{b'} appeared at 8.71 which was slowly reduced and finally diminished while the desired product was formed. In this experiment, the chemical shift of *ortho* proton of pyridine (H_a) in **17a'** is suggestive for the development of intermediate **VII** or **VIIa'** which progressively shifted to more upfield in the intermediates and then in the product. It indicates that the electron withdrawing effect of the amide-carbonyl is no longer persists in the intermediate directing towards either of the intermediates **VII** or **VIIa'** (H_b or H_{b'}). As the chemical shift value in the intermediate is nearer to the product than the starting

material, we assume that the new C–N bond may already have been made which is in favor of the intermediate **VIIa'**.



Scheme 10 Control experiments.

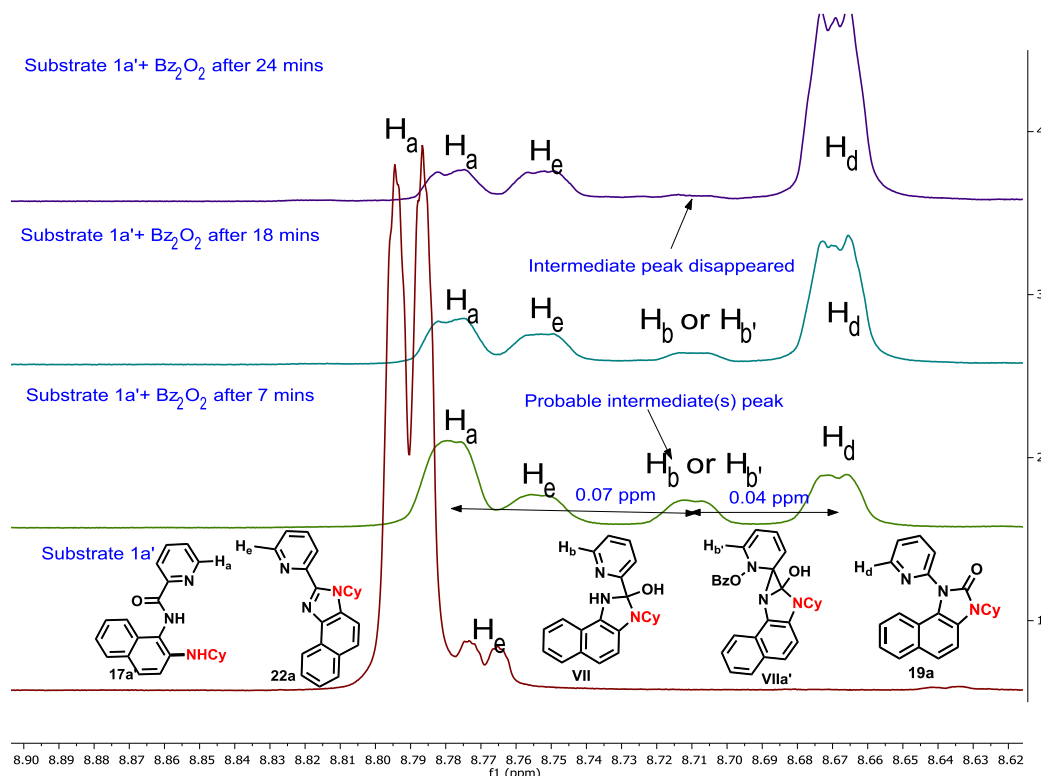
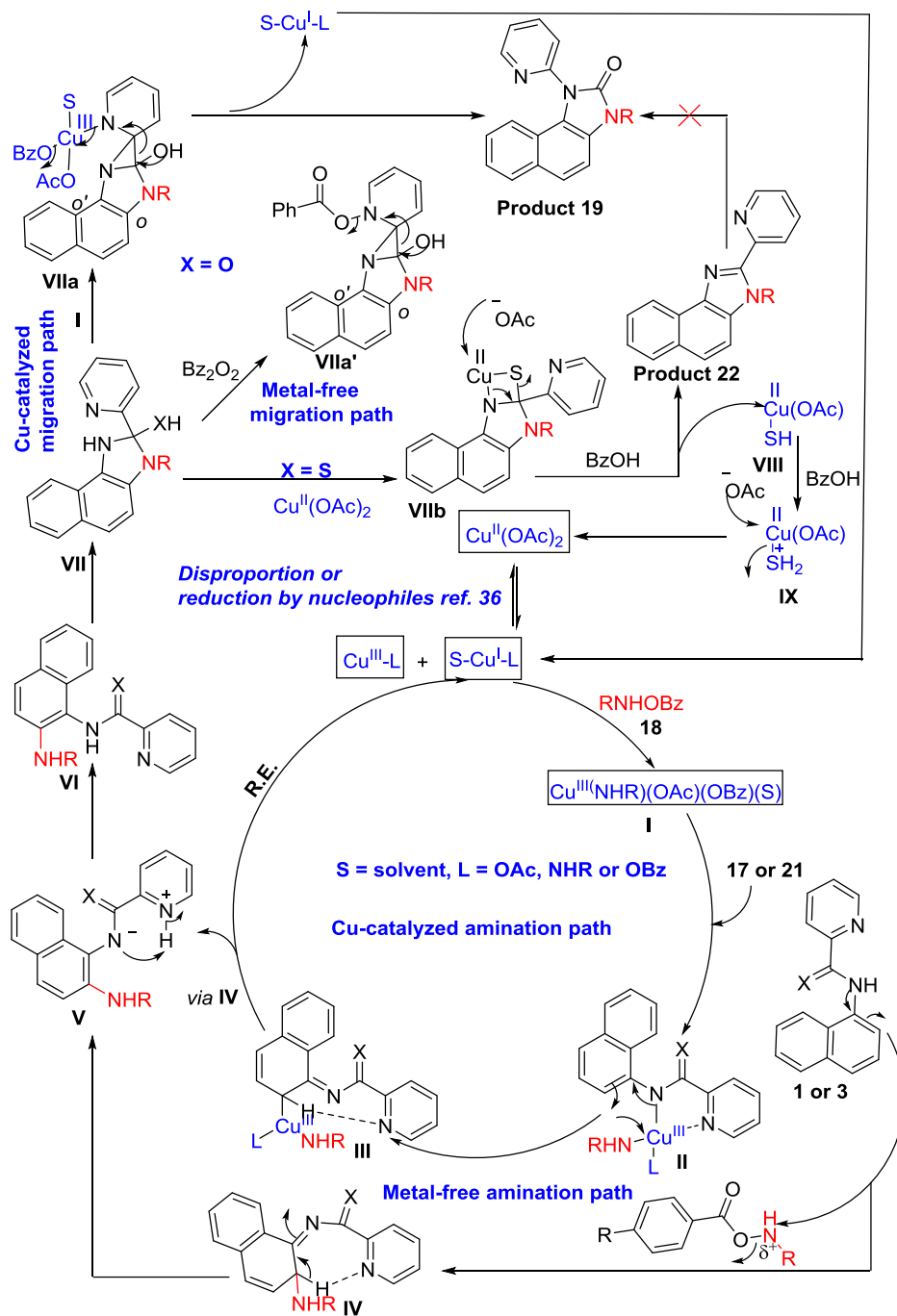


Fig. 2 Time dependent ^1H NMR experiment.

A $\text{Cu}^{\text{I}}/\text{Cu}^{\text{III}}$ cycle is probably involved in this cascade process as reported by the Li, Gaunt, Stahl and other groups.³⁶ Based on our control experiments and the above literature reports $\text{Cu}(\text{II})$ salt first generates an active Cu^{I} species on disproportionation which undergoes oxidative addition with the hydroxyl amine **18** to form a Cu^{III} complex, **I** (Scheme 11). This complex then undergoes chelation with the substrates **17** or **21** forming **II** which on electrophilic aromatic substitution type reaction forms intermediate **III**. Likewise, intermediate **IV** may also be formed under the metal-free condition. Pyridine of the picolinamide may act as a proton shuttle that abstracts *ortho* proton and supplies to the amide nitrogen in the course of rearomatisation through intermediate **V** giving the *ortho* amination products **VI**. Then, a tetrahedral intermediate **VII** is formed by the intramolecular attack of the amine moiety to the amide/thioamide carbonyl group. The nucleophilic nitrogen may attack at the *ipso* position of the pyridine moiety in presence of second molecule of the Cu^{III} -complex **I**, making **VIIa** which elucidates the need of an excess (2.5 equiv.) amount of *O*-benzoylhydroxylamine.³⁷ Similar type of intermediate, **VIIa'** may be generated in presence of Bz_2O_2 in the metal-free pathway. This type of three-membered cyclic intermediate is

claimed by the Feng group for aryl migration.³⁸ A similar O→C pyridyl migration through de-aromatization of pyridine ring was also described.³⁹ Then a 1,2-pyridyl migration from C→N may



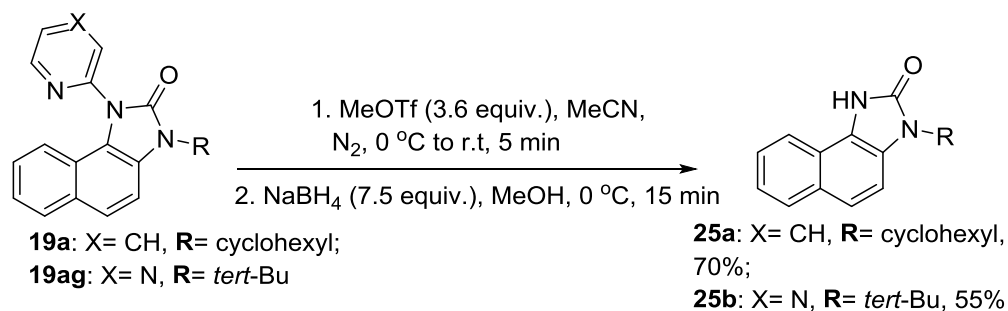
Scheme 11 Proposed reaction mechanism.

occur to afford the corresponding benzimidazolone product **19** with regeneration of the active Cu^I species. **VIIa'** may also give the product in similar way. It is additionally supported by the

information that electron donating substitution (e.g., ethyl, isopropyl in case of monocyclic anilines) at the *o*'-position has a positive impact in the reaction outcome. However, *tert*-Bu group may be hindering the reaction to an extent because of steric inhibition. Owing to the discrete reactivity of thiol compared to the corresponding oxygen analogue,⁴⁰ a putative 4-membered cyclic intermediate **VIIIb** may be formed with thiophilic copper from the tetrahedral thiolate intermediate (**Scheme 11**). Next, exclusion of hydrogen sulphide delivers the thermodynamically favourable benzimidazoles (**22**) by regenerating Cu(II).

III. 7. Deprotection of *N*-heteroaryls of the benzimidazolone product

For expanding the synthetic efficacy of this migratory annulation cascade, the pyridine and pyrazine moieties were successfully deprotected from the representative benzimidazolones (**19a**, **19ag**) under a reducing condition giving **25a** and **25b** in 70% and 55% yield respectively (**Scheme 12**).⁴¹ The free –NH moiety may be further employed to accomplish further molecular diversity.



Scheme 12. Deprotection of *N*- heteroaryls of the benzimidazolone product.

III. 8. Conclusion

In conclusion, we have established a directing group dependent complete switch of the product selectivity in copper-catalyzed electrophilic C–H amination using *O*-benzoyloxy protected primary amines. The benzimidazolones are obtained *via* an unique electrophilic *ortho* C–H amination with primary amines, intramolecular cyclization and 1,2-directing group migration from carbon to nitrogen center cascade process. Extraordinarily, cleavage of one C–H and C–C bonds and formation of three new C–N bonds take place in a single set-up in this migratory annulation cascade. Amazingly, shifting the picolinamide directing group to the corresponding thiopicolinamide the chemoselectivity is completely switched forming 2-pyridylbenzimidazoles *via* the extrusion of H₂S. Low-cost copper catalyst, scale-up synthesis, low catalyst loading,

controlled scaffold diversification are some of the practical features of this tandem reaction. The benzimidazolone product is also obtained in good to moderate yields in two steps under metal-free conditions but the metal-free condition is not generalised.

III. 9. Experimental section

Preparation of the starting materials

General procedure for the preparation of thioamides from corresponding picolinamides

To a mixture of picolinamide (2.50 mmol) and Lawesson's reagent (0.52 g, 1.28 mmol) was added toluene (10 mL) and the solution refluxed for 12-48 hrs. The mixture was then filtered and solvent was removed under reduced pressure to afford a yellow solid material which was purified by column chromatography using solvent mixtures of petroleum ether and ethyl acetate to give the desired product (yellow solid). Using this method, thioamide of other amides were also prepared.

General procedure for the preparation of picolinimidamide

In an oven dried two-necked RB charged with 2-cyano pyridine (520 mg, 5.0 mmol) and 1-naphthylamine (715 mg, 5.0 mmol) under nitrogen atmosphere 10 ml dry DCE was added and cooled to 0 °C. Then AlCl₃ (665 mg, 5.0 mmol from glove box), was added portion wise to avoid overheating. The reaction mixture was stirred at this temperature for 10 minutes then at rt for 5 minutes. Then this mixture was heated to 80 °C for several hours under N₂ atmosphere. After consumption of the starting materials. The reaction mixture was diluted with 20 mL dichloromethane and washed with 15 mL of 6N NaOH. The resulting organic layer was separated and dried over Na₂SO₄ and solvent was removed under reduced pressure. Then this crude product was washed with distilled hexane three times and dried under high vacuum to give the desired product which can be used without further purification.

Representative Procedure 1 for imidazolone

In an oven dried 15 mL sealed tube containing a stir bar was added corresponding picolinamide (0.2 mmol, 1.0 equiv), *O*-benzoylhydroxylamine (0.5 mmol, 2.5 equiv.) and Cu(OAc)₂·H₂O (0.01 mmol). Dry DMSO (2mL) was then added and N₂ gas was purged for 2 minutes. The mixture was stirred at 80 °C for 6 hrs. After allotted time the reaction mixture was cooled to room temperature. The mixture was diluted with EtOAc (15 mL) and washed with saturated aq. NaHCO₃ solution

(25mL), followed by brine solution (25 mL) and dried over Na₂SO₄, and evaporated in *vacuo*. The crude mixture was loaded on a silica gel column chromatography and purified using (Hexane/EtOAc) to give the desired imidazolone product.

Representative Procedure for imidazole

In an oven dried 15 mL sealed tube containing a stir bar was added corresponding thiopicolinamide (0.2 mmol, 1.0 equiv), *O*-benzoylhydroxylamine (0.5 mmol, 3.0 equiv.), Cu(OAc)₂·H₂O (0.04 mmol) and K₂CO₃ (0.24 mmol). Dry DMSO (2mL) was then added and O₂ gas was purged for 2 minutes. [Note: amount of O₂ should be sufficient for better reaction and so large amount of empty space is required. For scale up reaction (2.0 mmol) 100 mL pressure tube was used]. The mixture was stirred at 90 °C for 6 hrs. After allotted time the reaction mixture was cooled to room temperature. The mixture was diluted with EtOAc (15 mL) and washed with saturated aq. NaHCO₃ solution (25mL), followed by brine solution (25 mL) and dried over Na₂SO₄, and evaporated in *vacuo*. The crude mixture was loaded on a silica gel column chromatography and purified using (Hexane/EtOAc) to give the desired imidazole product.

Representative Procedure 2 for imidazolone in 2-substituted aniline system

In an oven dried 15 mL sealed tube containing a stir bar was added corresponding picolinamide (0.2 mmol, 1.0 equiv), *O*-benzoylhydroxylamine (0.5 mmol, 2.5 equiv.) and Cu(OAc)₂·H₂O (0.02 mmol). Dry DMSO (2mL) was then added and N₂ gas was purged for 2 minutes. The mixture was stirred at 100 °C for 6 hrs. After allotted time the reaction mixture was cooled to room temperature. The mixture was diluted with EtOAc (15 mL) and washed with saturated aq. NaHCO₃ solution (25mL), followed by brine solution (25 mL) and dried over Na₂SO₄, and evaporated in *vacuo*. The crude mixture was loaded on a silica gel column chromatography and purified using (Hexane/EtOAc) to give the desired imidazolone product.

Representative Procedure for amination in aniline system

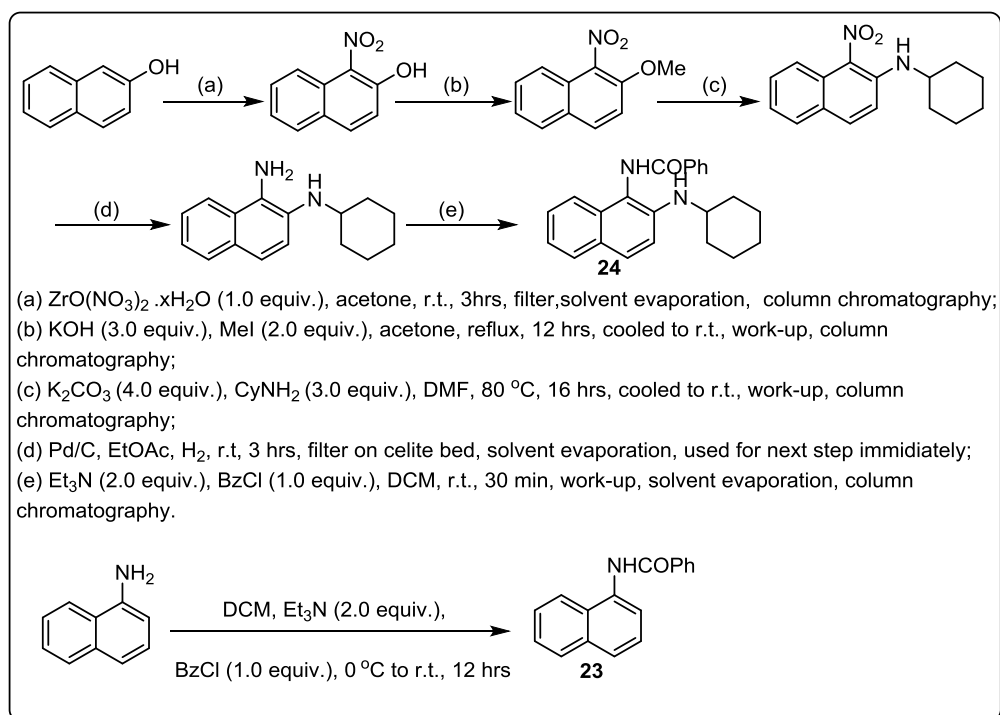
In an oven dried 15 mL sealed tube containing a stir bar was added corresponding picolinamide (0.2 mmol, 1.0 equiv), *O*-benzoylhydroxylamine (0.5 mmol, 2.5 equiv.), LiO^tBu (0.4 mmol, 2.0 equiv.) and Cu(OAc)₂·H₂O (0.02 mmol). Dry DMSO (2mL) was then added and N₂ gas was purged for 2 minutes. The mixture was stirred at 90 °C for 6 hrs. After allotted time the reaction mixture was cooled to room temperature. The mixture was diluted with EtOAc (15 mL) and washed with

saturated aq. NaHCO_3 solution (25mL), followed by brine solution (25 mL) and dried over Na_2SO_4 , and evaporated in *vacuo*. The crude mixture was loaded on a silica gel column chromatography and purified using (Hexane/EtOAc) to give the desired amination product.

Procedure for synthesis of compound 17a'

In an oven dried RB containing a stir bar was added picolinamide **17a** (2 mmol, 1.0 equiv), *O*-benzoylhydroxylamine (2 mmol, 1.0 equiv.) and $\text{Cu}(\text{OAc})_2 \cdot \text{H}_2\text{O}$ (0.2 mmol). Dry DMSO (15 mL) was then added and N_2 gas was purged for 2 minutes. The mixture was stirred at room temperature for 6 hrs. The mixture was diluted with EtOAc (100 mL) and washed with saturated aq. NaHCO_3 solution (50 mL), followed by brine solution (50 mL) and dried over Na_2SO_4 , and evaporated in *vacuo*. The crude mixture was loaded on a silica gel column chromatography and purified using (Hexane/EtOAc) to give the amination product.

Procedure for the preparation of 23 and 24



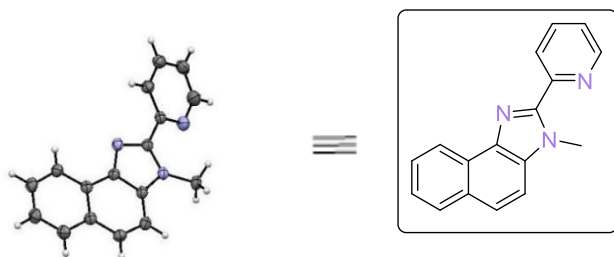
Procedure for deprotection of pyridyl group of Benzimidazolone product

This deprotection was done according to a condition for the deprotection of N-pyridyl group.⁶ In an oven dried RB containing a stir bar was added the benzimidazolone and dry MeCN and it was

cooled to 0 °C in an ice-bath under N₂ atmosphere. Ice-cooled MeOTf (3.6 equiv.) was added dropwise to this solution. After addition the mixture was stirred at r.t. for 10 minutes. Then to this mixture MeOH (4 mL) was added and further cooled to 0 °C in an ice-bath. NaBH₄ (7.0 equiv.) was added portion-wise and stirred at this temperature for 15 minutes. After that the solvent was evaporated and diluted with EtOAc, washed with water and dried over Na₂SO₄. This was concentrated under vacuum followed by column chromatography gave the desired product.

III.10. X-ray crystallography data

The crystals were grown in dichloromethane solvent. The pure compound was dissolved in dichloromethane slow evaporation led to the crystal **19aj**. The crystal data was collected in X-ray spectroscopy (Bruker Kappa Apex-2, CCD Area Detector), and the data was analyzed using OLEX2 software. The structure is given below.



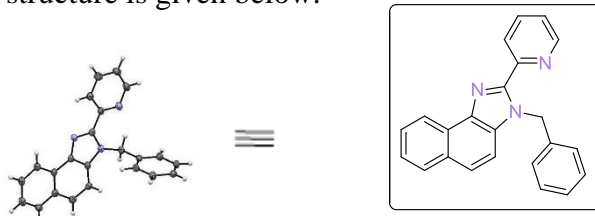
Thermal ellipsoid plot of **19aj**. Ellipsoids are represented with 50% probability.

X-ray determined molecular structure of **19aj**, CCDC: 2025266

| | |
|---------------------|--|
| Identification code | HM_430A_0m_a |
| Empirical formula | C ₁₈ H ₁₅ N ₂ |
| Formula weight | 259.32 |
| Temperature/K | 100.0 |
| Crystal system | monoclinic |
| Space group | P2 ₁ /n |
| a/Å | 10.9333(3) |

| | |
|---|---|
| b/Å | 7.3400(2) |
| c/Å | 16.2518(5) |
| α /° | 90 |
| β /° | 98.6550(10) |
| γ /° | 90 |
| Volume/Å ³ | 1289.36(6) |
| Z | 4 |
| $\rho_{\text{calc}}/\text{cm}^3$ | 1.336 |
| μ/mm^{-1} | 0.612 |
| F(000) | 548.0 |
| Crystal size/mm ³ | 0.2 × 0.2 × 0.2 |
| Radiation | CuK α ($\lambda = 1.54178$) |
| 2 Θ range for data collection/° | 13.262 to 132.918 |
| Index ranges | -12 ≤ h ≤ 12, -8 ≤ k ≤ 8, -19 ≤ l ≤ 17 |
| Reflections collected | 18364 |
| Independent reflections | 2259 [R _{int} = 0.0807, R _{sigma} = 0.0459] |
| Data/restraints/parameters | 2259/0/183 |
| Goodness-of-fit on F ² | 1.056 |
| Final R indexes [I ≥ 2 σ (I)] | R ₁ = 0.0733, wR ₂ = 0.2003 |
| Final R indexes [all data] | R ₁ = 0.0760, wR ₂ = 0.2033 |
| Largest diff. peak/hole / e Å ⁻³ | 0.55/-0.66 |

The crystals were grown in dichloromethane solvent. The pure compound was dissolved in dichloromethane slow evaporation led to the crystal **22h**. The crystal data was collected in X-ray spectroscopy (Bruker Kappa Apex-2, CCD Area Detector), and the data was analyzed using OLEX2 software. The structure is given below.



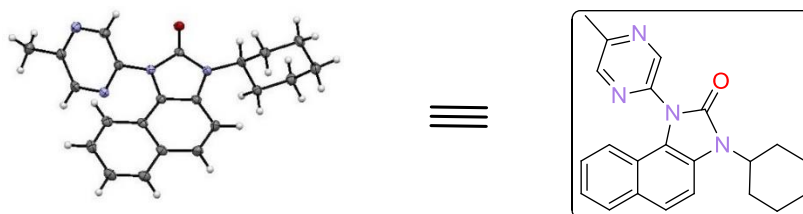
Thermal ellipsoid plot of **22h**. Ellipsoids are represented with 50% probability.

X-ray determined molecular structure of **22h**, CCDC: 2025275

| | |
|-----------------------|--|
| Identification code | K_101_0m_a |
| Empirical formula | C ₂₃ H ₁₈ N ₃ |
| Formula weight | 336.40 |
| Temperature/K | 100.0 |
| Crystal system | monoclinic |
| Space group | P2 ₁ /n |
| a/Å | 11.8246(5) |
| b/Å | 8.7668(4) |
| c/Å | 16.2183(7) |
| α/° | 90 |
| β/° | 90.457(2) |
| γ/° | 90 |
| Volume/Å ³ | 1681.20(13) |
| Z | 4 |

| | |
|--|---|
| $\rho_{\text{calc}}/\text{cm}^3$ | 1.329 |
| μ/mm^{-1} | 0.618 |
| F(000) | 708.0 |
| Crystal size/ mm^3 | $0.35 \times 0.29 \times 0.28$ |
| Radiation | $\text{CuK}\alpha$ ($\lambda = 1.54178$) |
| 2Θ range for data collection/ $^\circ$ | 10.91 to 133.22 |
| Index ranges | $-14 \leq h \leq 13, -10 \leq k \leq 10, -18 \leq l \leq 19$ |
| Reflections collected | 16494 |
| Independent reflections | 2930 [$R_{\text{int}} = 0.0772, R_{\text{sigma}} = 0.0536$] |
| Data/restraints/parameters | 2930/0/235 |
| Goodness-of-fit on F^2 | 1.105 |
| Final R indexes [$I \geq 2\sigma(I)$] | $R_1 = 0.0624, wR_2 = 0.1540$ |
| Final R indexes [all data] | $R_1 = 0.0667, wR_2 = 0.1575$ |
| Largest diff. peak/hole / $e \text{ \AA}^{-3}$ | 0.25/-0.66 |

The crystals were grown in dichloromethane solvent. The pure compound was dissolved in dichloromethane slow evaporation led to the crystal **19ad**. The crystal data was collected in X-ray spectroscopy (Bruker Kappa Apex-2, CCD Area Detector), and the data was analyzed using OLEX2 software. The structure is given below. **19ad**, CCDC: 2025269

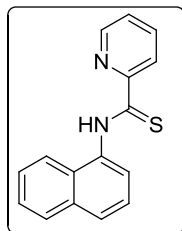


| | |
|--|---|
| Identification code | HM_583_0m_a |
| Empirical formula | C _{2.44} H _{2.44} N _{0.44} O _{0.11} |
| Formula weight | 39.83 |
| Temperature/K | 100.0 |
| Crystal system | triclinic |
| Space group | P-1 |
| a/Å | 7.9957(2) |
| b/Å | 10.4307(2) |
| c/Å | 12.5078(3) |
| α /° | 67.7270(10) |
| β /° | 89.0730(10) |
| γ /° | 71.4000(10) |
| Volume/Å ³ | 908.36(4) |
| Z | 18 |
| $\rho_{\text{calc}}/\text{cm}^3$ | 1.310 |
| μ/mm^{-1} | 0.658 |
| F(000) | 380.0 |
| Crystal size/mm ³ | 0.80 × 0.28 × 0.27 |
| Radiation | CuK α ($\lambda = 1.54178$) |
| 2 Θ range for data collection/° | 7.692 to 133.402 |

| | |
|--|---|
| Index ranges | $-9 \leq h \leq 8, -12 \leq k \leq 12, -14 \leq l \leq 14$ |
| Reflections collected | 28821 |
| Independent reflections | 3182 [$R_{\text{int}} = 0.0634, R_{\text{sigma}} = 0.0334$] |
| Data/restraints/parameters | 3182/0/245 |
| Goodness-of-fit on F^2 | 1.088 |
| Final R indexes [$I \geq 2\sigma(I)$] | $R_1 = 0.0424, wR_2 = 0.0985$ |
| Final R indexes [all data] | $R_1 = 0.0438, wR_2 = 0.0994$ |
| Largest diff. peak/hole / $e \text{ \AA}^{-3}$ | 0.21/-0.25 |

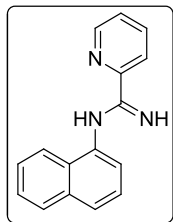
III.11. Spectral data

N-(naphthalen-1-yl)pyridine-2-carbothioamide (21a)



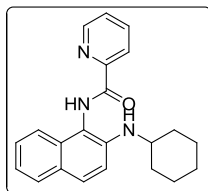
Column chromatography (SiO₂, eluting with 95:5 hexane/ethyl acetate) afforded the desired product as a yellow solid, mp 124-126 °C. ¹H NMR (400 MHz, CDCl₃): δ 12.36 (s, 1H), 8.84 (dt, $J_1 = 8.0$ Hz, $J_2 = 0.8$ Hz, 1H), 8.63-8.61 (m, 1H), 8.33 (d, $J = 7.2$ Hz, 1H), 8.03-7.99 (m, 1H), 7.95-7.89 (m, 2H), 7.85 (d, $J = 8.4$ Hz, 1H), 7.60-7.49 (m, 4H); ¹³C NMR (100 MHz, CDCl₃): δ 190.2, 151.5, 146.8, 137.7, 134.4, 134.3, 128.9, 128.4, 127.7, 126.8, 126.5, 126.3, 125.5, 125.3, 122.9, 121.6; HRMS (ESI, m/z) calcd. For C₁₆H₁₃N₂S [$M+H$]⁺: 265.0799; found: 265.0802.

N-(naphthalen-1-yl)picolinimidamide (21a')



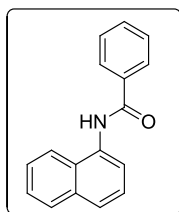
Washing with distilled hexane afforded the desired product as a violet solid, mp 118-120 °C. ^1H NMR (400 MHz, CDCl_3): δ 8.63 (d, $J = 8.0$ Hz, 1H), 8.61-8.59 (m, 1H), 8.10 (d, $J = 8.0$ Hz, 1H), 7.89-7.83 (m, 2H), 7.59 (d, $J = 8.4$ Hz, 1H), 7.49-7.38 (m, 4H), 7.09 (d, $J = 7.6$ Hz, 1H), 6.29-5.17 (br. s); ^{13}C NMR (100 MHz, CDCl_3): δ 152.9, 151.3, 148.1, 137.0, 134.8, 128.1, 127.4, 126.4, 126.2, 125.4, 123.9, 123.4, 122.0, 116.3; HRMS (ESI, m/z) calcd. For $\text{C}_{16}\text{H}_{14}\text{N}_3$ $[\text{M}+\text{H}]^+$: 248.1188; found: 248.1185.

***N*-(2-(cyclohexylamino)naphthalen-1-yl)picolinamide (17a')**



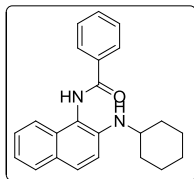
Column chromatography (SiO_2 , eluting with 85:15 hexane/ethyl acetate) afforded the desired product as a brown gummy liquid. ^1H NMR (400 MHz, CDCl_3): δ 9.76 (s, 1H), 8.68-8.67 (m, 1H), 8.34 (dt, $J_1 = 7.6$ Hz, $J_2 = 1.2$ Hz, 1H), 7.91 (td, $J_1 = 7.6$ Hz, $J_2 = 1.6$ Hz, 1H), 7.73-7.68 (m, 3H), 7.51-7.48 (m, 1H), 7.41-7.37 (m, 1H), 7.23-7.19 (m, 2H), 3.51-3.44 (m, 1H), 2.12-2.08 (m, 2H), 1.79-1.74 (m, 2H), 1.65-1.61 (m, 1H), 1.43-1.21 (m, 5H); ^{13}C NMR (100 MHz, CDCl_3): δ 163.4, 149.8, 148.4, 141.5, 137.7, 131.5, 128.7, 128.3, 127.3, 127.0, 126.6, 122.8, 122.1, 120.5, 115.4, 113.0, 51.9, 33.8, 25.9, 25.1; HRMS (ESI, m/z) calcd. For $\text{C}_{22}\text{H}_{24}\text{N}_3\text{O}$ $[\text{M}+\text{H}]^+$: 346.1919; found: 346.1922.

***N*-(naphthalen-1-yl)benzamide (23)**



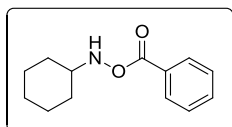
Column chromatography (SiO₂, eluting with 90:10 hexane/ethyl acetate) afforded the desired product as white fluffy solid. ¹H NMR (400 MHz, CDCl₃): δ 8.27 (s, 1H), 7.98-7.95 (m, 3H), 7.90-7.87 (m, 2H), 7.73 (d, *J* = 8.4 Hz, 1H), 7.58-7.55 (m, 1H), 7.51-7.46 (m, 5H); ¹³C NMR (100 MHz, CDCl₃): δ 166.4, 134.9, 134.3, 132.5, 132.0, 128.94, 128.90, 127.6, 127.3, 126.5, 126.2, 126.1, 125.9, 121.5, 120.9.

***N*-(2-(cyclohexylamino)naphthalen-1-yl)benzamide (24)**



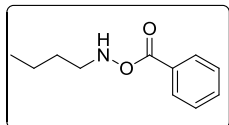
Column chromatography (SiO₂, eluting with 90:10 hexane/ethyl acetate) afforded the desired product as white fluffy solid. ¹H NMR (400 MHz, CDCl₃ + CD₃OD): δ 8.01-7.98 (m, 2H), 7.68-7.64 (m, 2H), 7.58-7.51 (m, 2H), 7.49-7.45 (m, 2H), 7.33-7.28 (m, 1H), 7.17-7.01 (m, 2H), 3.39-3.30 (m, 1H), 1.98 (d, *J* = 12.8 Hz, 2H), 1.69-1.61 (m, 2H), 1.58-1.54 (m, 1H), 1.35-1.12 (m, 5H); ¹³C NMR (100 MHz, CDCl₃ + CD₃OD): δ 171.8, 137.7, 136.1, 135.6, 133.0, 132.8, 132.1, 132.0, 131.6, 131.0, 126.5, 124.8, 119.8, 56.8, 37.3, 33.6, 29.6, 28.9; HRMS (ESI, *m/z*) calcd. For C₂₃H₂₅N₂O [M+H]⁺: 345.1967; found: 345.1964.

***O*-benzoyl-*N*-cyclohexylhydroxylamine (18a)**



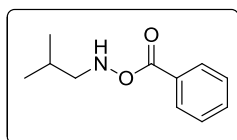
Column chromatography (SiO₂, eluting with 98:2 hexane/ethyl acetate) afforded the desired product as colourless liquid. ¹H NMR (400 MHz, CDCl₃): δ 8.02-7.99 (m, 2H), 7.58-7.53 (m, 1H), 7.45-7.41 (m, 2H), 3.07-2.99 (m, 1H), 1.98-1.94 (m, 2H), 1.81-1.74 (m, 2H), 1.64-1.59 (m, 1H), 1.31-1.17 (m, 5H); ¹³C NMR (100 MHz, CDCl₃): δ 167.0, 133.3, 129.4, 128.6, 59.9, 30.4, 25.9, 24.1.

***O*-benzoyl-*N*-butylhydroxylamine (18g)**



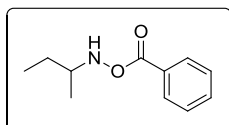
Column chromatography (SiO₂, eluting with 98:2 hexane/ethyl acetate) afforded the desired product as colourless liquid. ¹H NMR (400 MHz, CDCl₃): δ 8.03-7.99 (m, 2H), 7.86 (br. s, 1H), 7.58-7.54 (m, 1H), 7.46-7.42 (m, 2H), 3.13 (t, *J* = 7.2 Hz, 2H), 1.63-1.56 (m, 2H), 1.47-1.38 (m, 2H), 0.94 (t, *J* = 7.6 Hz, 3H); ¹³C NMR (100 MHz, CDCl₃): δ 167.0, 133.4, 129.4, 128.6, 52.4, 29.3, 20.3, 13.9.

***O*-benzoyl-*N*-isobutylhydroxylamine (18h)**



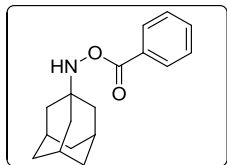
Column chromatography (SiO₂, eluting with 98:2 hexane/ethyl acetate) afforded the desired product as colourless liquid. ¹H NMR (400 MHz, CDCl₃): δ 8.02-7.99 (m, 2H), 7.96 (br. s, 1H), 7.58-7.54 (m, 1H), 7.46-7.41 (m, 2H), 2.95 (d, *J* = 6.8 Hz, 2H), 1.99-1.89 (m, 1H), 1.00 (d, *J* = 6.8 Hz, 6H); ¹³C NMR (100 MHz, CDCl₃): δ 166.9, 133.4, 129.4, 128.6, 60.2, 26.5, 20.6.

***O*-benzoyl-*N*-(*sec*-butyl)hydroxylamine (18i)**



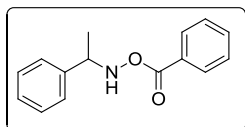
Column chromatography (SiO₂, eluting with 98:2 hexane/ethyl acetate) afforded the desired product as colourless liquid. ¹H NMR (400 MHz, CDCl₃): δ 8.03-7.99 (m, 2H), 7.58-7.54 (m, 1H), 7.46-7.42 (m, 2H), 3.11 (sextet, *J* = 6.4 Hz, 1H), 1.71-1.61 (m, 1H), 1.50-1.39 (m, 1H), 1.17 (d, *J* = 6.4 Hz, 3H), 0.98 (t, *J* = 7.2 Hz, 3H); ¹³C NMR (100 MHz, CDCl₃): δ 167.0, 133.3, 129.4, 128.6, 58.2, 26.8, 17.6, 10.3.

***N*-((3*s*,5*s*,7*s*)-adamantan-1-yl)-*O*-benzoylhydroxylamine (18m)**



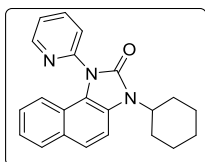
Column chromatography (SiO₂, eluting with 98:2 hexane/ethyl acetate) afforded the desired product as crystalline solid. ¹H NMR (400 MHz, CDCl₃): δ 8.03-8.01 (m, 2H), 7.59-7.55 (m, 1H), 7.47-7.43 (m, 2H), 2.11 (s, 3H), 1.76 (d, *J* = 2.8 Hz, 6H), 1.71-1.62 (m, 6H); ¹³C NMR (100 MHz, CDCl₃): δ 167.0, 133.3, 129.4, 128.6, 56.4, 40.1, 36.5, 29.2.

***O*-benzoyl-*N*-(1-phenylethyl)hydroxylamine (18n)**

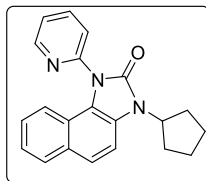


Column chromatography (SiO₂, eluting with 98:2 hexane/ethyl acetate) afforded the desired product as colourless liquid. ¹H NMR (400 MHz, CDCl₃): δ 7.97-7.94 (m, 2H), 7.56-7.51 (m, 1H), 7.45-7.35 (m, 6H), 7.32-7.28 (m, 1H), 4.34 (q, *J* = 6.8 Hz, 2H), 1.55 (d, *J* = 6.8 Hz, 3H); ¹³C NMR (100 MHz, CDCl₃): δ 166.9, 141.3, 133.4, 129.4, 128.7, 128.6, 128.5, 127.9, 127.2, 61.0, 19.8.

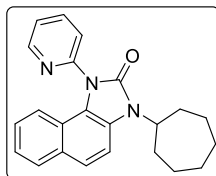
3-cyclohexyl-1-(pyridin-2-yl)-1,3-dihydro-2*H*-naphtho[1,2-*d*]imidazol-2-one (19a)



The general procedure 1 for imidazolone was followed. Column chromatography (SiO₂, eluting with 75:25 hexane/ethyl acetate) afforded the desired product as a light brown solid (63.8 mg, 93% yield), mp 142-144 °C. ¹H NMR (400 MHz, CDCl₃): δ 8.67-8.65 (m, 1H), 7.97 (td, *J*₁ = 8.0 Hz, *J*₂ = 2.0 Hz, 1H), 7.82 (d, *J* = 8.0 Hz, 1H), 7.70 (dt, *J*₁ = 8.0 Hz, *J*₂ = 0.8 Hz, 1H), 7.64 (d, *J* = 8.8 Hz, 1H), 7.51 (d, *J* = 8.8 Hz, 1H), 7.45-7.41 (m, 1H), 7.29-7.25 (m, 1H), 7.19-7.15 (m, 1H), 6.96 (d, *J* = 8.0 Hz, 1H), 4.42-4.34 (m, 1H), 2.33-2.22 (m, 2H), 1.99-1.92 (m, 4H), 1.77 (d, *J* = 12.8 Hz, 1H), 1.53-1.42 (m, 2H), 1.36-1.29 (m, 1H); ¹³C NMR (100 MHz, CDCl₃): δ 153.7, 150.2, 149.6, 138.8, 129.9, 129.2, 126.0, 125.8, 123.7, 123.5, 123.2, 121.8, 121.3, 120.4, 110.4, 53.7, 30.4, 26.2, 25.5; HRMS (ESI, *m/z*) calcd. For C₂₂H₂₂N₃O [*M*+*H*]⁺: 344.1763; found: 344.1760.

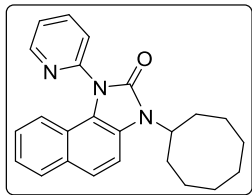
3-cyclopentyl-1-(pyridin-2-yl)-1,3-dihydro-2H-naphtho[1,2-d]imidazol-2-one (19b)

The general procedure 1 for imidazolone was followed. Column chromatography (SiO₂, eluting with 75:25 hexane/ethyl acetate) afforded the desired product as a light brown solid (51 mg, 78% yield), mp 138-140 °C. ¹H NMR (400 MHz, CDCl₃): δ 8.67-8.65 (m, 1H), 7.97 (td, *J*₁ = 8.0 Hz, *J*₂ = 2.0 Hz, 1H), 7.82 (dd, *J*₁ = 8.4 Hz, *J*₂ = 0.4 Hz, 1H), 7.69 (dt, *J*₁ = 8.0 Hz, *J*₂ = 0.8 Hz, 1H), 7.65 (d, *J* = 8.8 Hz, 1H), 7.45-7.40 (m, 2H), 7.29-7.24 (m, 1H), 7.19-7.15 (m, 1H), 6.97 (d, *J* = 8.8 Hz, 1H), 4.97 (quintet, *J* = 8.8 Hz, 1H), 2.29-2.20 (m, 2H), 2.14-1.97 (m, 4H), 1.80-1.73 (m, 2H); ¹³C NMR(100 MHz, CDCl₃):δ 153.9, 150.2, 149.6, 138.8, 130.0, 129.2, 125.8, 125.6, 123.8, 123.6, 123.5, 123.3, 121.9, 121.2, 120.5, 110.1, 54.0, 29.3, 25.3; HRMS (ESI, *m/z*) calcd. For C₂₁H₂₀N₃O [M+H]⁺: 330.1606; found: 330.1644.

3-cycloheptyl-1-(pyridin-2-yl)-1,3-dihydro-2H-naphtho[1,2-d]imidazol-2-one (19c)

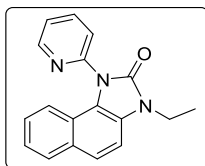
The general procedure 1 for imidazolone was followed. Column chromatography (SiO₂, eluting with 75:25 hexane/ethyl acetate) afforded the desired product as a light brown solid (46.4 mg, 65% yield), mp 154-156 °C. ¹H NMR (400 MHz, CDCl₃): δ 8.67-8.65 (m, 1H), 7.98 (td, *J*₁ = 8.0 Hz, *J*₂ = 2.0 Hz, 1H), 7.82 (d, *J* = 8.4 Hz, 1H), 7.70 (dt, *J*₁ = 8.0 Hz, *J*₂ = 0.8 Hz, 1H), 7.64 (d, *J* = 8.8 Hz, 1H), 7.47-7.42 (m, 2H), 7.29-7.25 (m, 1H), 7.19-7.15 (m, 1H), 6.97 (d, *J* = 8.8 Hz, 1H), 4.62-4.55 (m, 1H), 2.37-2.29 (m, 2H), 2.07-2.03 (m, 2H), 1.88-1.85 (m, 2H), 1.73-1.64 (m, 6H); ¹³C NMR (100 MHz, CDCl₃): δ 153.5, 150.2, 149.5, 138.8, 130.0, 129.2, 125.8, 125.7, 123.7, 123.49, 123.47, 123.3, 121.8, 121.3, 120.5, 110.5, 55.6, 32.9, 27.7, 25.9; HRMS (ESI, *m/z*) calcd. For C₂₃H₂₄N₃O [M+H]⁺: 358.1919; found: 358.1921.

3-cyclooctyl-1-(pyridin-2-yl)-1,3-dihydro-2H-naphtho[1,2-d]imidazol-2-one (19d)



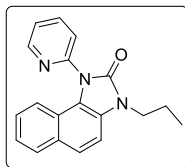
The general procedure 1 for imidazolone was followed. Column chromatography (SiO₂, eluting with 75:25 hexane/ethyl acetate) afforded the desired product as a light brown solid (34 mg, 46% yield), mp 156-158 °C. ¹H NMR (400 MHz, CDCl₃): δ 8.66-8.64 (m, 1H), 7.97 (td, *J*₁ = 8.0 Hz, *J*₂ = 2.0 Hz, 1H), 7.82 (d, *J* = 8.0 Hz, 1H), 7.71 (dt, *J*₁ = 8.0 Hz, *J*₂ = 0.8 Hz, 1H), 7.64 (d, *J* = 8.8 Hz, 1H), 7.45-7.41 (m, 2H), 7.29-7.25 (m, 1H), 7.19-7.15 (m, 1H), 6.99 (d, *J* = 8.8 Hz, 1H), 4.75-4.69 (m, 1H), 2.39-2.31 (m, 2H), 2.02-1.97 (m, 2H), 1.89-1.84 (m, 2H), 1.79-1.60 (m, 8H); ¹³C NMR (100 MHz, CDCl₃): δ 153.5, 150.2, 149.5, 138.7, 130.0, 129.2, 125.8, 125.5, 123.6, 123.5, 123.4, 123.3, 121.9, 121.3, 120.5, 110.6, 54.1, 32.6, 26.4, 26.2, 25.5; HRMS (ESI, *m/z*) calcd. For C₂₄H₂₆N₃O [M+H]⁺: 372.2076; found: 372.2076.

3-ethyl-1-(pyridin-2-yl)-1,3-dihydro-2*H*-naphtho[1,2-*d*]imidazol-2-one (19e)



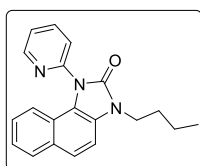
The general procedure 1 for imidazolone was followed. Column chromatography (SiO₂, eluting with 75:25 hexane/ethyl acetate) afforded the desired product as a light brown solid (29 mg, 50% yield), mp 96-98 °C. ¹H NMR (400 MHz, CDCl₃): δ 8.68-8.66 (m, 1H), 7.98 (td, *J*₁ = 8.0 Hz, *J*₂ = 2.0 Hz, 1H), 7.84 (d, *J* = 8.0 Hz, 1H), 7.72-7.68 (m, 2H), 7.46-7.42 (m, 1H), 7.34 (d, *J* = 8.4 Hz, 1H), 7.31-7.27 (m, 1H), 7.22-7.18 (m, 1H), 7.02 (d, *J* = 9.2 Hz, 1H), 4.09 (q, *J* = 7.2 Hz, 2H), 1.43 (t, *J* = 7.2 Hz, 3H); ¹³C NMR (100 MHz, CDCl₃): δ 153.9, 150.1, 149.6, 138.9, 130.4, 129.3, 126.2, 125.9, 123.8, 123.7, 123.5, 123.4, 121.8, 121.2, 120.5, 108.9, 36.3, 13.9; HRMS (ESI, *m/z*) calcd. For C₁₈H₁₆N₃O [M+H]⁺: 290.1293; found: 290.1296.

3-propyl-1-(pyridin-2-yl)-1,3-dihydro-2*H*-naphtho[1,2-*d*]imidazol-2-one (19f)



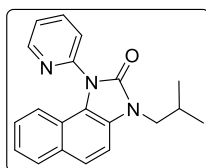
The general procedure 1 for imidazolone was followed. Column chromatography (SiO₂, eluting with 75:25 hexane/ethyl acetate) afforded the desired product as a light brown solid (39.4 mg, 65% yield), mp 134-136 °C. ¹H NMR (400 MHz, CDCl₃): δ 8.66 (d, *J* = 3.6 Hz, 1H), 7.97 (t, *J* = 7.6 Hz, 1H), 7.82 (d, *J* = 8.4 Hz, 1H), 7.71-7.66 (m, 2H), 7.45-7.41 (m, 1H), 7.33 (d, *J* = 8.4 Hz, 1H), 7.27 (t, *J* = 7.2 Hz, 1H), 7.19 (t, *J* = 8.0 Hz, 1H), 7.01 (d, *J* = 8.8 Hz, 1H), 3.98 (t, *J* = 7.2 Hz, 2H), 1.87 (sextet, *J* = 7.2 Hz, 2H), 1.02 (t, *J* = 7.2 Hz, 3H); ¹³C NMR (100 MHz, CDCl₃): δ 154.2, 150.1, 149.6, 138.8, 130.4, 129.3, 126.6, 125.9, 123.8, 123.7, 123.5, 123.4, 121.7, 121.3, 120.5, 109.1, 43.1, 22.1, 11.5; HRMS (ESI, *m/z*) calcd. For C₁₉H₁₈N₃O [M+H]⁺: 304.1450; found: 304.1451.

3-butyl-1-(pyridin-2-yl)-1,3-dihydro-2H-naphtho[1,2-d]imidazol-2-one (19g)



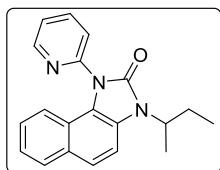
The general procedure 1 for imidazolone was followed. Column chromatography (SiO₂, eluting with 75:25 hexane/ethyl acetate) afforded the desired product as a creamy white solid (52 mg, 82% yield), mp 104-106 °C. ¹H NMR (400 MHz, CDCl₃): δ 8.68-8.67 (m, 1H), 7.99 (td, *J*₁ = 8.0 Hz, *J*₂ = 2.0 Hz, 1H), 7.85-7.83 (m, 1H), 7.72 (dt, *J*₁ = 8.0 Hz, *J*₂ = 0.8 Hz, 1H), 7.69 (d, *J* = 8.8 Hz, 1H), 7.47-7.43 (m, 1H), 7.34 (d, *J* = 8.8 Hz, 1H), 7.31-7.27 (m, 1H), 7.22-7.18 (m, 1H), 7.04-7.02 (m, 1H), 4.03 (t, *J* = 7.2 Hz, 2H), 1.86-1.79 (m, 2H), 1.51-1.41 (m, 2H), 0.97 (t, *J* = 7.6 Hz, 3H); ¹³C NMR (100 MHz, CDCl₃): δ 154.2, 150.1, 149.5, 138.9, 130.4, 129.3, 126.6, 125.9, 123.8, 123.7, 123.5, 123.4, 121.7, 121.3, 120.5, 109.1, 41.3, 30.8, 20.2, 13.8; HRMS (ESI, *m/z*) calcd. For C₂₀H₂₀N₃O [M+H]⁺: 318.1606; found: 318.1657.

3-isobutyl-1-(pyridin-2-yl)-1,3-dihydro-2H-naphtho[1,2-d]imidazol-2-one (19h)



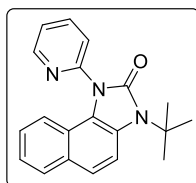
The general procedure 1 for imidazolone was followed. Column chromatography (SiO₂, eluting with 75:25 hexane/ethyl acetate) afforded the desired product as a light brown solid (40 mg, 63% yield). mp 112-114 °C. ¹H NMR (400 MHz, CDCl₃): δ 8.67 (s, 1H), 7.98 (td, *J*₁ = 7.6 Hz, *J*₂ = 1.6 Hz, 1H), 7.83 (d, *J* = 7.6 Hz, 1H), 7.72 (d, *J* = 8.0 Hz, 1H), 7.67 (d, *J* = 8.8 Hz, 1H), 7.46-7.43 (m, 1H), 7.34-7.26 (m, 2H), 7.22-7.18 (m, 1H), 7.03 (d, *J* = 8.4 Hz, 1H), 3.82 (d, *J* = 7.6 Hz, 2H), 2.34-2.24 (m, 1H), 1.02 (d, *J* = 6.8 Hz, 6H); ¹³C NMR (100 MHz, CDCl₃): δ 154.5, 150.1, 149.4, 138.8, 130.4, 129.3, 126.9, 125.9, 123.7, 123.5, 123.4, 121.6, 121.3, 120.5, 109.4, 48.9, 28.3, 20.3; HRMS (ESI, *m/z*) calcd. For C₂₀H₂₀N₃O [M+H]⁺: 318.1606; found: 318.1608.

3-(*sec*-butyl)-1-(pyridin-2-yl)-1,3-dihydro-2*H*-naphtho[1,2-*d*]imidazol-2-one (19i)



The general procedure 1 for imidazolone was followed. Column chromatography (SiO₂, eluting with 75:25 hexane/ethyl acetate) afforded the desired product as light brown solid (60 mg, 95% yield), mp 112-114 °C. ¹H NMR (400 MHz, CDCl₃): δ 8.68-8.66 (m, 1H), 7.98 (td, *J*₁ = 7.6 Hz, *J*₂ = 2.0 Hz, 1H), 7.82 (d, *J* = 8.0 Hz, 1H), 7.71 (dt, *J*₁ = 8.0 Hz, *J*₂ = 0.8 Hz, 1H), 7.65 (d, *J* = 8.4 Hz, 1H), 7.46-7.42 (m, 2H), 7.30-7.26 (m, 1H), 7.20-7.16 (m, 1H), 6.99 (dd, *J*₁ = 8.8 Hz, *J*₂ = 0.8 Hz, 1H), 4.61-4.51 (m, 1H), 2.24-2.13 (m, 1H), 1.98-1.87 (m, 1H), 1.61 (d, *J* = 6.8 Hz, 3H), 0.93 (t, *J* = 7.6 Hz, 3H); ¹³C NMR (100 MHz, CDCl₃): δ 153.9, 150.1, 149.5, 138.8, 130.0, 129.2, 126.0, 125.8, 123.7, 123.6, 123.5, 123.4, 121.8, 121.3, 120.5, 110.2, 51.8, 27.6, 18.8, 11.5; HRMS (ESI, *m/z*) calcd. For C₂₀H₂₀N₃O [M+H]⁺: 318.1606; found: 318.1610.

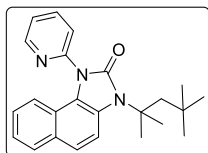
3-(*tert*-butyl)-1-(pyridin-2-yl)-1,3-dihydro-2*H*-naphtho[1,2-*d*]imidazol-2-one (19j)



The general procedure 1 for imidazolone was followed. Column chromatography (SiO₂, eluting with 75:25 hexane/ethyl acetate) afforded the desired product as a creamy white powder (59.6 mg, 94% yield), mp 154-156 °C. ¹H NMR (400 MHz, CDCl₃): δ 8.67 (dd, *J*₁ = 4.8 Hz, *J*₂ = 1.2 Hz,

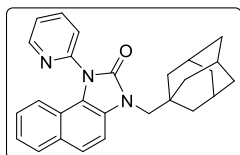
1H), 7.96 (td, $J_1 = 8.0$ Hz, $J_2 = 2.0$ Hz, 1H), 7.79 (d, $J = 8.0$ Hz, 1H), 7.75 (d, $J = 9.2$ Hz, 1H), 7.66 (d, $J = 8.0$ Hz, 1H), 7.58 (d, $J = 9.2$ Hz, 1H), 7.45-7.42 (m, 1H), 7.28-7.24 (m, 1H), 7.15-7.11 (m, 1H), 6.85 (d, $J = 8.8$ Hz, 1H), 1.88 (s, 9H); ^{13}C NMR (100 MHz, CDCl_3): δ 154.1, 150.4, 149.7, 138.8, 129.7, 128.9, 126.6, 125.7, 124.0, 123.8, 123.7, 122.6, 122.4, 121.3, 120.0, 113.1, 58.8, 29.8; HRMS (ESI, m/z) calcd. For $\text{C}_{20}\text{H}_{20}\text{N}_3\text{O}$ $[\text{M}+\text{H}]^+$: 318.1606; found: 318.1606.

1-(pyridin-2-yl)-3-(2,4,4-trimethylpentan-2-yl)-1,3-dihydro-2H-naphtho[1,2-*d*]imidazol-2-one (19k)



The general procedure 1 for imidazolone was followed. Column chromatography (SiO_2 , eluting with 75:25 hexane/ethyl acetate) afforded the desired product as a creamy white solid (49 mg, 66% yield), mp 120–122 °C. ^1H NMR (400 MHz, CDCl_3): δ 8.68-8.66 (m, 1H), 7.95 (td, $J_1 = 8.0$ Hz, $J_2 = 2.0$ Hz, 1H), 7.81-7.78 (m, 2H), 7.62 (dt, $J_1 = 8.0$ Hz, $J_2 = 0.4$ Hz, 1H), 7.59 (d, $J = 8.8$ Hz, 1H), 7.45-7.41 (m, 1H), 7.29-7.25 (m, 1H), 7.16-7.12 (m, 1H), 6.86 (d, $J = 8.8$ Hz, 1H), 2.18 (s, 2H), 1.98 (s, 6H), 0.92 (s, 9H); ^{13}C NMR (100 MHz, CDCl_3): δ 154.4, 150.5, 149.8, 138.8, 129.6, 128.8, 127.1, 125.6, 124.0, 123.8, 123.7, 122.51, 122.49, 121.4, 120.0, 113.5, 62.4, 51.1, 31.9, 31.2, 31.0; HRMS (ESI, m/z) calcd. For $\text{C}_{24}\text{H}_{28}\text{N}_3\text{O}$ $[\text{M}+\text{H}]^+$: 374.2232; found: 374.2235.

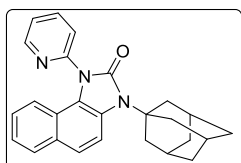
3-(((3s)-adamantan-1-yl)methyl)-1-(pyridin-2-yl)-1,3-dihydro-2H-naphtho[1,2-*d*]imidazol-2-one (19l)



The general procedure 1 for imidazolone was followed. Column chromatography (SiO_2 , eluting with 80:20 hexane/ethyl acetate) afforded the desired product as a light brown solid (59 mg, 72% yield), mp 198–200 °C. ^1H NMR (400 MHz, CDCl_3): δ 8.68 (d, $J = 3.6$ Hz, 1H), 7.98 (td, $J_1 = 8.0$ Hz, $J_2 = 2.0$ Hz, 1H), 7.84-7.82 (m, 1H), 7.73 (d, $J = 8.0$ Hz, 1H), 7.66 (d, $J = 8.4$ Hz, 1H), 7.46-7.43 (m, 1H), 7.38 (d, $J = 8.8$ Hz, 1H), 7.31-7.26 (m, 1H), 7.22-7.18 (m, 1H), 7.05-7.02 (m, 1H),

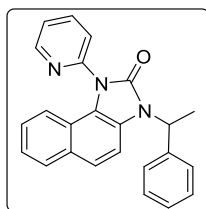
3.69 (s, 2H), 1.98 (s, 3H), 1.71-1.60 (m, 12H); ^{13}C NMR (100 MHz, CDCl_3): δ 155.2, 150.1, 149.4, 138.9, 130.3, 129.3, 128.2, 125.9, 123.67, 123.66, 123.4, 121.6, 121.3, 120.3, 110.3, 53.9, 41.2, 36.8, 36.4, 28.3; HRMS (ESI, m/z) calcd. For $\text{C}_{27}\text{H}_{28}\text{N}_3\text{O}$ $[\text{M}+\text{H}]^+$: 410.2232; found: 410.2231.

3-((3s,5s,7s)-adamantan-1-yl)-1-(pyridin-2-yl)-1,3-dihydro-2H-naphtho[1,2-*d*]imidazol-2-one (19m)



The general procedure 1 for imidazolone was followed. Column chromatography (SiO_2 , eluting with 80:20 hexane/ethyl acetate) afforded the desired product as a light brown solid (77 mg, 98% yield), mp 164-166 °C. ^1H NMR (400 MHz, CDCl_3): δ 8.67-8.65 (m, 1H), 7.98-7.93 (m, 1H), 7.85 (dd, $J_1 = 8.8$ Hz, $J_2 = 1.2$ Hz, 1H), 7.78 (d, $J = 8.0$ Hz, 1H), 7.66-7.63 (m, 1H), 7.54 (d, $J = 9.2$ Hz, 1H), 7.44-7.41 (m, 1H), 7.28-7.23 (m, 1H), 7.14-7.10 (m, 1H), 6.85 (d, $J = 9.2$ Hz, 1H), 2.68 (s, 6H), 2.25 (s, 3H), 1.80 (dd, $J_1 = 32.4$ Hz, $J_2 = 12.0$ Hz, 6H); ^{13}C NMR (100 MHz, CDCl_3): δ 154.0, 150.5, 149.7, 138.7, 129.5, 128.8, 126.4, 125.6, 124.0, 123.72, 123.67, 122.6, 122.2, 121.3, 120.0, 113.6, 61.1, 40.9, 36.3, 30.1; HRMS (ESI, m/z) calcd. For $\text{C}_{26}\text{H}_{26}\text{N}_3\text{O}$ $[\text{M}+\text{H}]^+$: 396.2076; found: 396.2076

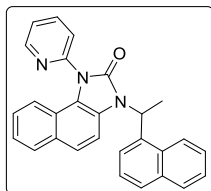
3-(1-phenylethyl)-1-(pyridin-2-yl)-1,3-dihydro-2H-naphtho[1,2-*d*]imidazol-2-one (19n)



The general procedure 1 for imidazolone was followed. Column chromatography (SiO_2 , eluting with 75:25 hexane/ethyl acetate) afforded the desired product as a pale yellow solid (48.2 mg, 66% yield), mp 136-138 °C. ^1H NMR (400 MHz, CDCl_3): δ 8.70-8.69 (m, 1H), 8.01 (td, $J_1 = 8.0$ Hz, $J_2 = 2.0$ Hz, 1H), 7.78-7.75 (m, 2H), 7.49-7.44 (m, 4H), 7.36-7.32 (m, 2H), 7.29-7.24 (m, 2H), 7.19-7.16 (m, 1H), 7.02-6.98 (m, 2H), 6.01 (q, $J = 7.2$ Hz, 1H), 1.99 (d, $J = 7.2$ Hz, 3H); ^{13}C NMR (100 MHz, CDCl_3): δ 154.2, 150.1, 149.6, 139.8, 138.9, 130.1, 129.2, 128.8, 127.7, 126.9, 125.8, 125.4,

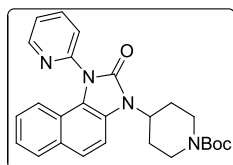
123.8, 123.7, 123.5, 123.4, 121.9, 121.2, 120.4, 110.8, 51.2, 17.7; HRMS (ESI, m/z) calcd. For $C_{24}H_{20}N_3O$ $[M+H]^+$: 366.1606; found: 366.1606.

3-(1-(naphthalen-1-yl)ethyl)-1-(pyridin-2-yl)-1,3-dihydro-2H-naphtho[1,2-d]imidazol-2-one (19o)



The general procedure 1 for imidazolone was followed. Column chromatography (SiO_2 , eluting with 75:25 hexane/ethyl acetate) afforded the desired product as a light brown solid (73 mg, 88% yield), mp 222-224 °C. 1H NMR (400 MHz, $CDCl_3$): δ 8.69 (d, $J = 4.8$ Hz, 1H), 8.25 (d, $J = 8.4$ Hz, 1H), 8.01 (td, $J_1 = 7.6$ Hz, $J_2 = 1.6$ Hz, 1H), 7.96 (d, $J = 7.2$ Hz, 1H), 7.86 (d, $J = 8.4$ Hz, 1H), 7.81 (d, $J = 8.0$ Hz, 1H), 7.77 (d, $J = 8.0$ Hz, 1H), 7.68 (d, $J = 8.4$ Hz, 1H), 7.58 (t, $J = 8.0$ Hz, 1H), 7.51- 7.40 (m, 3H), 7.36 (d, $J = 8.8$ Hz, 1H), 7.22-7.18 (m, 1H), 7.14-7.10 (m, 2H), 6.93 (d, $J = 8.8$ Hz, 1H), 6.63 (q, $J = 6.8$ Hz, 1H), 2.11 (d, $J = 6.8$ Hz, 3H); ^{13}C NMR (100 MHz, $CDCl_3$): δ 153.9, 150.1, 149.7, 138.9, 134.9, 134.0, 131.8, 129.9, 129.4, 129.1, 128.9, 127.1, 126.1, 125.7, 125.6, 125.0, 124.8, 123.8, 123.59, 123.57, 123.51, 123.3, 122.0, 121.2, 120.3, 110.6, 48.9, 18.1; HRMS (ESI, m/z) calcd. For $C_{28}H_{22}N_3O$ $[M+H]^+$: 416.1763; found: 416.1766.

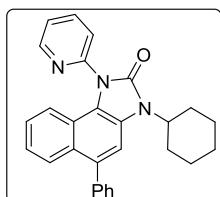
tert-butyl 4-(2-oxo-1-(pyridin-2-yl)-1H-naphtho[1,2-d]imidazol-3(2H)-yl)piperidine carboxylate (19p)



The general procedure 1 for imidazolone was followed. Column chromatography (SiO_2 , eluting with 70:30 hexane/ethyl acetate) afforded the desired product as a creamy white solid (80 mg, 90% yield), mp 174-176 °C. 1H NMR (400 MHz, $CDCl_3$): δ 8.68-8.66 (m, 1H), 7.99 (td, $J_1 = 8.0$ Hz, $J_2 = 2.0$ Hz, 1H), 7.83 (d, $J = 8.0$ Hz, 1H), 7.69 (dt, $J_1 = 8.0$ Hz, $J_2 = 0.8$ Hz, 1H), 7.65 (d, $J = 8.8$ Hz, 1H), 7.48-7.45 (m, 2H), 7.31-7.27 (m, 1H), 7.20-7.16 (m, 1H), 6.94 (d, $J = 8.8$ Hz, 1H), 4.62-4.54

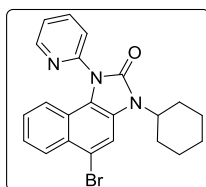
(m, 1H), 4.35-4.33 (br. s, 2H), 2.90 (t, $J = 12.4$ Hz, 2H), 2.50-2.40 (m, 2H), 1.92 (d, $J = 12.4$ Hz, 2H), 1.50 (s, 9H); ^{13}C NMR (100 MHz, CDCl_3): δ 154.8, 153.6, 150.0, 149.7, 138.9, 130.1, 129.2, 125.9, 125.4, 123.9, 123.8, 123.52, 123.50, 121.9, 121.2, 120.4, 110.2, 80.0, 51.8, 29.5, 28.6; HRMS (ESI, m/z) calcd. For $\text{C}_{26}\text{H}_{29}\text{N}_4\text{O}_3$ $[\text{M}+\text{H}]^+$: 445.2240; found: 445.2237.

3-cyclohexyl-5-phenyl-1-(pyridin-2-yl)-1,3-dihydro-2H-naphtho[1,2-*d*]imidazol-2-one (19q)



The general procedure 1 for imidazolone was followed. Column chromatography (SiO_2 , eluting with 75:25 hexane/ethyl acetate) afforded the desired product as a creamy white solid (67.8 mg, 81% yield), mp 186-188 °C. ^1H NMR (400 MHz, CDCl_3): δ 8.68-8.66 (m, 1H), 7.99 (td, $J_1 = 7.6$ Hz, $J_2 = 2.0$ Hz, 1H), 7.83-7.80 (m, 1H), 7.74 (dt, $J_1 = 8.0$ Hz, $J_2 = 0.8$ Hz, 1H), 7.53-7.48 (m, 4H), 7.47-7.42 (m, 3H), 7.23-7.16 (m, 2H), 7.05-7.03 (m, 1H), 4.41-4.33 (m, 1H), 2.33-2.23 (m, 2H), 1.99-1.90 (m, 4H), 1.73 (d, $J = 13.2$ Hz, 1H), 1.50-1.40 (m, 2H), 1.32-1.26 (m, 1H); ^{13}C NMR (100 MHz, CDCl_3): δ 153.9, 150.3, 149.6, 141.1, 138.8, 136.0, 130.5, 128.4, 128.2, 127.46, 127.44, 125.71, 125.67, 123.63, 123.61, 123.4, 121.51, 121.46, 120.6, 111.4, 53.8, 30.4, 26.1, 25.4; HRMS (ESI, m/z) calcd. For $\text{C}_{28}\text{H}_{26}\text{N}_3\text{O}$ $[\text{M}+\text{H}]^+$: 420.2076; found: 420.2075.

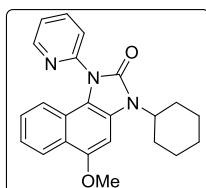
5-bromo-3-cyclohexyl-1-(pyridin-2-yl)-1,3-dihydro-2H-naphtho[1,2-*d*]imidazol-2-one (19r)



The general procedure 1 for imidazolone was followed. Column chromatography (SiO_2 , eluting with 75:25 hexane/ethyl acetate) afforded the desired product as a creamy white solid (68 mg, 81% yield), mp 168-170 °C. ^1H NMR (400 MHz, CDCl_3): δ 8.65-8.63 (m, 1H), 8.25-8.22 (m, 1H), 7.98 (td, $J_1 = 7.6$ Hz, $J_2 = 2.0$ Hz, 1H), 7.83 (s, 1H), 7.69 (dt, $J_1 = 8.0$ Hz, $J_2 = 0.8$ Hz, 1H), 7.46-7.43 (m, 1H), 7.40-7.35 (m, 1H), 7.40-7.35 (m, 1H), 7.22-7.18 (m, 1H), 6.99-6.96 (m, 1H), 4.36-4.28 (m, 1H), 2.29-2.19 (m, 2H), 1.95 (d, $J = 11.2$ Hz, 4H), 1.77 (d, $J = 12.8$ Hz, 1H), 1.52-1.42 (m,

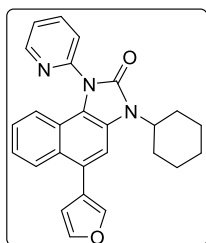
2H), 1.38-1.30 (m, 1H); ^{13}C NMR (100 MHz, CDCl_3): δ 153.6, 150.0, 149.7, 138.9, 128.5, 127.8, 126.5, 126.2, 124.9, 123.9, 123.5, 121.9, 121.7, 121.2, 116.7, 114.4, 53.9, 30.4, 26.1, 25.4; HRMS (ESI, m/z) calcd. For $\text{C}_{22}\text{H}_{21}\text{BrN}_3\text{O}$ $[\text{M}+\text{H}]^+$: 422.0868; found: 422.0886.

3-cyclohexyl-5-methoxy-1-(pyridin-2-yl)-1,3-dihydro-2H-naphtho[1,2-*d*]imidazol-2-one (19s)



The general procedure 1 for imidazolone was followed. Column chromatography (SiO_2 , eluting with 70:30 hexane/ethyl acetate) afforded the desired product as a brown solid (44.7 mg, 60% yield), mp 166-168 °C. ^1H NMR (400 MHz, CDCl_3): δ 8.64-8.62 (m, 1H), 8.27-8.25 (m, 1H), 7.95 (td, $J_1 = 8.0$ Hz, $J_2 = 2.0$ Hz, 1H), 7.70 (dt, $J_1 = 8.0$ Hz, $J_2 = 0.8$ Hz, 1H), 7.41-7.37 (m, 1H), 7.29-7.25 (m, 1H), 7.22-7.18 (m, 1H), 6.98-6.96 (m, 1H), 6.87 (s, 1H), 4.35-4.27 (m, 1H), 4.05 (s, 3H), 2.34-2.24 (m, 2H), 1.99-1.93 (m, 4H), 1.78 (d, $J = 12.8$ Hz, 1H), 1.54-1.43 (m, 2H), 1.37-1.28 (m, 1H); ^{13}C NMR (100 MHz, CDCl_3): δ 153.9, 152.6, 150.3, 149.4, 138.6, 126.5, 126.1, 123.3, 123.21, 123.18, 122.8, 121.8, 121.3, 121.0, 115.4, 90.8, 56.3, 53.8, 30.4, 26.2, 25.6; HRMS (ESI, m/z) calcd. For $\text{C}_{23}\text{H}_{24}\text{N}_3\text{O}_2$ $[\text{M}+\text{H}]^+$: 374.1869; found: 374.1874.

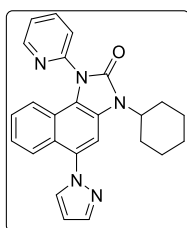
3-cyclohexyl-5-(furan-3-yl)-1-(pyridin-2-yl)-1,3-dihydro-2H-naphtho[1,2-*d*]imidazol-2-one (19t)



The general procedure 1 for imidazolone was followed. Column chromatography (SiO_2 , eluting with 75:25 hexane/ethyl acetate) afforded the desired product as a light brown solid (65.4 mg, 80% yield), mp 190-192 °C. ^1H NMR (400 MHz, CDCl_3): δ 8.67-8.66 (m, 1H), 8.07-8.05 (m, 1H), 7.99 (td, $J_1 = 8.0$ Hz, $J_2 = 2.0$ Hz, 1H), 7.72 (dt, $J_1 = 8.0$ Hz, $J_2 = 0.8$ Hz, 1H), 7.65 (dd, $J_1 = 1.6$ Hz, J_2

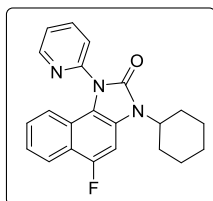
= 0.8 Hz, 1H), 7.59 (t, $J = 1.6$ Hz, 1H), 7.47-7.43 (m, 2H), 7.29-7.25 (m, 1H), 7.21-7.17 (m, 1H), 7.04-7.01 (m, 1H), 6.68 (dd, $J_1 = 2.0$ Hz, $J_2 = 0.8$ Hz, 1H), 4.40-4.32 (m, 1H), 2.33-2.22 (m, 2H), 1.99-1.91 (m, 4H), 1.76 (d, $J = 12.8$ Hz, 1H), 1.53-1.42 (m, 2H), 1.36-1.28 (m, 1H); ^{13}C NMR (100 MHz, CDCl_3): δ 153.8, 150.2, 149.5, 143.0, 140.6, 138.9, 128.5, 127.0, 126.3, 125.8, 125.7, 123.8, 123.7, 123.4, 121.7, 121.6, 120.7, 113.0, 111.4, 53.8, 30.4, 26.1, 25.4; HRMS (ESI, m/z) calcd. For $\text{C}_{26}\text{H}_{24}\text{N}_3\text{O}$ $[\text{M}+\text{H}]^+$: 410.1869; found: 410.1870.

3-cyclohexyl-5-(1H-pyrazol-1-yl)-1-(pyridin-2-yl)-1,3-dihydro-2H-naphtho[1,2-*d*]imidazol-2-one (19u)



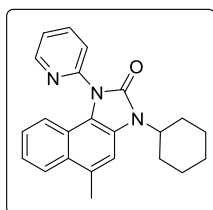
The general procedure 1 for imidazolone was followed. Column chromatography (SiO_2 , eluting with 70:30 hexane/ethyl acetate) afforded the desired product as a creamy white solid (79.3 mg, 97% yield), mp 192-194 °C. ^1H NMR (400 MHz, CDCl_3): δ 8.68-8.66 (m, 1H), 8.01 (td, $J_1 = 7.6$ Hz, $J_2 = 2.0$ Hz, 1H), 7.85-7.84 (m, 1H), 7.76 (dd, $J_1 = 2.4$ Hz, $J_2 = 0.8$ Hz, 1H), 7.73 (dt, $J_1 = 8.0$ Hz, $J_2 = 0.8$ Hz, 1H), 7.62 (s, 1H), 7.54-7.51 (m, 1H), 7.48-7.45 (m, 1H), 7.30-7.25 (m, 1H), 7.23-7.19 (m, 1H), 7.05-7.02 (m, 1H), 6.56 (t, $J = 2.0$ Hz, 1H), 4.37-4.29 (m, 1H), 2.31-2.21 (m, 2H), 1.97-1.89 (m, 4H), 1.73 (d, $J = 12.8$ Hz, 1H), 1.49-1.39 (m, 2H), 1.33-1.25 (m, 1H); ^{13}C NMR (100 MHz, CDCl_3): δ 153.8, 149.9, 149.7, 140.9, 139.0, 133.0, 132.6, 126.4, 126.1, 125.2, 124.9, 124.0, 123.96, 123.5, 122.5, 121.6, 120.5, 108.95, 106.7, 54.1, 30.3, 26.1, 25.3; HRMS (EI, m/z) calcd. For $\text{C}_{25}\text{H}_{24}\text{N}_5\text{O}$ $[\text{M}+\text{H}]^+$: 410.1981; found: 410.1985.

3-cyclohexyl-5-fluoro-1-(pyridin-2-yl)-1,3-dihydro-2H-naphtho[1,2-*d*]imidazol-2-one (19v)



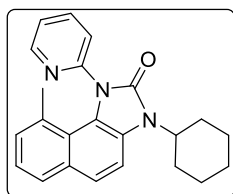
The general procedure 1 for imidazolone was followed. Column chromatography (SiO₂, eluting with 75:25 hexane/ethyl acetate) afforded the desired product as a light brown crystalline solid (47 mg, 65% yield), mp 142-144 °C. ¹H NMR (400 MHz, CDCl₃): 8.65-8.64 (m, 1H), 8.08 (d, *J* = 8.0 Hz, 1H), 7.98 (td, *J*₁ = 7.6 Hz, *J*₂ = 1.6 Hz, 1H), 7.71 (dt, *J*₁ = 8.0 Hz, *J*₂ = 0.8 Hz, 1H), 7.45-7.42 (m, 1H), 7.35- 7.21 (m, 3H), 7.00-6.98 (m, 1H), 4.38-4.29 (m, 1H), 2.27-2.17 (m, 2H), 1.97-1.93 (m, 4H), 1.78 (d, *J* = 12.8 Hz, 1H), 1.53-1.41 (m, 2H), 1.36-1.29 (m, 1H); ¹³C NMR (100 MHz, CDCl₃): δ 155.5 (d, *J* = 244.7 Hz), 153.9, 150.0, 149.5, 138.9, 126.8, 125.2 (d, *J* = 12.5 Hz), 123.7, 123.69, 123.3, 121.7 (d, *J* = 6.3 Hz), 121.2 (d, *J* = 2.7 Hz), 120.8 (d, *J* = 4.8 Hz), 119.5 (d, *J* = 16.8 Hz), 117.9, 96.1 (d, *J* = 27.7 Hz), 53.9, 30.3, 26.1, 25.4; ¹⁹F NMR (376 MHz, CDCl₃): δ -127.04 (s, 1F); HRMS (ESI, *m/z*) calcd. For C₂₂H₂₁FN₃O₃ [M+H]⁺: 362.1669; found: 362.1667.

3-cyclohexyl-5-methyl-1-(pyridin-2-yl)-1,3-dihydro-2*H*-naphtho[1,2-*d*]imidazol-2-one (19w)



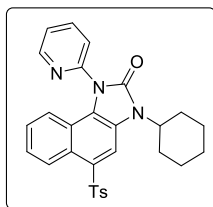
The general procedure 1 for imidazolone was followed. Column chromatography (SiO₂, eluting with 75:25 hexane/ethyl acetate) afforded the desired product as a light brown solid (53.5 mg, 75% yield), mp 134-136 °C. ¹H NMR (400 MHz, CDCl₃): δ 8.66-8.64 (m, 1H), 7.99-7.94 (m, 2H), 7.69 (dt, *J*₁ = 8.0 Hz, *J*₂ = 0.4 Hz, 1H), 7.43-7.40 (m, 1H), 7.37 (s, 1H), 7.34-7.30 (m, 1H), 7.21-7.16 (m, 1H), 7.02 (d, *J* = 8.4 Hz, 1H), 4.40-4.32 (m, 1H), 2.76 (s, 3H), 2.34-2.24 (m, 2H), 1.98-1.92 (m, 4H), 1.78 (d, *J* = 12.4 Hz, 1H), 1.53-1.43 (m, 2H), 1.39-1.31 (m, 1H), 1.25 (grease); ¹³C NMR (100 MHz, CDCl₃): δ 153.8, 150.4, 149.5, 138.8, 129.6, 128.8, 125.7, 125.5, 125.3, 123.5, 123.39, 123.36, 121.8, 120.7, 120.5, 111.3, 53.7, 30.4, 26.2, 25.5, 20.3; HRMS (ESI, *m/z*) calcd. For C₂₃H₂₄N₃O [M+H]⁺: 358.1919; found: 358.1920.

3-cyclohexyl-9-methyl-1-(pyridin-2-yl)-1,3-dihydro-2*H*-naphtho[1,2-*d*]imidazol-2-one (19x)



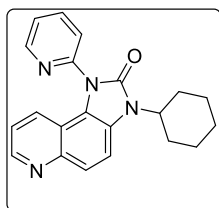
The general procedure 1 for imidazolone was followed. Column chromatography (SiO₂, eluting with 75:25 hexane/ethyl acetate) afforded the desired product as a light brown solid (67.8 mg, 95 % yield), mp 164-166 °C. ¹H NMR (400 MHz, CDCl₃): δ 8.33-8.31 (m, 1H), 7.87 (td, *J*₁ = 8.0 Hz, *J*₂ = 2.0 Hz, 1H), 7.78 (d, *J* = 8.0 Hz, 1H), 7.69-7.66 (m, 2H), 7.45 (d, *J* = 8.8 Hz, 1H), 7.25-7.20 (m, 2H), 7.08 (d, *J* = 7.2 Hz, 1H), 4.38-4.30 (m, 1H), 2.34-2.23 (m, 2H), 1.94 (d, *J* = 11.2 Hz, 4H), 1.77-1.74 (m, 4H), 1.51-1.41 (m, 2H), 1.36-1.28 (m, 1H); ¹³C NMR (100 MHz, CDCl₃): δ 155.1, 153.3, 148.3, 138.2, 131.1, 131.0, 129.0, 128.5, 127.1, 125.3, 123.5, 123.2, 122.2, 122.1, 121.6, 109.7, 53.9, 30.2, 26.2, 25.5, 21.7; HRMS (ESI, *m/z*) calcd. For C₂₃H₂₄N₃O [M+H]⁺: 358.1919; found: 358.1925.

3-cyclohexyl-1-(pyridin-2-yl)-5-tosyl-1,3-dihydro-2*H*-naphtho[1,2-*d*]imidazol-2-one (19y)



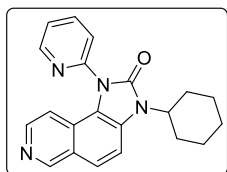
The general procedure 1 for imidazolone was followed. Column chromatography (SiO₂, eluting with 70:30 hexane/ethyl acetate) afforded the desired product as a light brown powder (63.6 mg, 64% yield), mp 172-174 °C. ¹H NMR (400 MHz, CDCl₃): 8.63-8.62 (m, 1H), 8.60 (s, 1H), 8.58 (dt, *J*₁ = 8.8 Hz, *J*₂ = 0.8 Hz, 1H), 8.01 (td, *J*₁ = 7.6 Hz, *J*₂ = 1.6 Hz, 1H), 7.81-7.78 (m, 2H), 7.69 (dt, *J*₁ = 8.0 Hz, *J*₂ = 0.8 Hz, 1H), 7.49-7.46 (m, 1H), 7.35- 7.31 (m, 1H), 7.25-7.23 (m, 2H), 7.19-7.14 (m, 1H), 7.00-6.97 (m, 1H), 4.45-4.37 (m, 1H), 2.39-2.28 (m, 5H), 2.00-1.96 (m, 4H), 1.79 (d, *J* = 12.4 Hz, 1H), 1.57-1.46 (m, 2H), 1.42-1.34 (m, 1H); ¹³C NMR (100 MHz, CDCl₃): δ 153.6, 149.8, 149.4, 144.0, 139.2, 130.1, 129.8, 127.3, 127.1, 126.3, 125.8, 125.7, 125.4, 124.4, 123.7, 122.2, 120.6, 114.2, 54.4, 30.4, 25.2, 21.6; HRMS (ESI, *m/z*) calcd. For C₂₉H₂₈N₃O₃S [M+H]⁺: 498.1851; found: 498.1853.

3-cyclohexyl-1-(pyridin-2-yl)-1,3-dihydro-2*H*-imidazo[4,5-*f*]quinolin-2-one (19z)



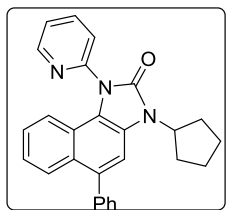
The general procedure 1 for imidazolone was followed. Column chromatography (SiO₂, eluting with 65:35 hexane/ethyl acetate) afforded the desired product as a creamy white powder (62 mg, 90% yield), mp 144-146 °C. ¹H NMR (400 MHz, CDCl₃): δ 8.73 (d, *J* = 3.6 Hz, 1H), 8.64-8.62 (m, 1H), 8.01-7.93 (m, 2H), 7.74-7.72 (m, 2H), 7.45-7.41 (m, 2H), 7.11-7.08 (m, 1H), 4.42-4.34 (m, 1H), 2.32-2.21 (m, 2H), 1.97-1.92 (m, 4H), 1.77 (d, *J* = 12.8 Hz, 1H), 1.52-1.41 (m, 2H), 1.36-1.28 (m, 1H); ¹³C NMR (100 MHz, CDCl₃): δ 153.7, 149.7, 149.5, 148.8, 144.6, 139.0, 129.7, 126.2, 124.6, 123.9, 123.2, 121.1, 120.2, 115.9, 113.5, 53.9, 36.4, 26.1, 25.4; HRMS (ESI, *m/z*) calcd. For C₂₁H₂₀N₄ONa [M+Na]⁺: 367.1535; found: 367.1551.

3-cyclohexyl-1-(pyridin-2-yl)-1,3-dihydro-2*H*-imidazo[4,5-*f*]isoquinolin-2-one (19aa)



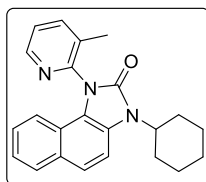
The general procedure 1 for imidazolone was followed. Column chromatography (SiO₂, eluting with 65:35 hexane/ethyl acetate) afforded the desired product as a creamy white powder (56.4 mg, 82% yield), mp 160-162 °C. ¹H NMR (400 MHz, CDCl₃): δ 9.20 (s, 1H), 8.68-8.66 (m, 1H), 8.20 (d, *J* = 5.6 Hz, 1H), 8.01 (td, *J*₁ = 8.0 Hz, *J*₂ = 2.0 Hz, 1H), 7.82 (d, *J* = 8.8 Hz, 1H), 7.74 (d, *J* = 7.6 Hz, 1H), 7.65 (d, *J* = 8.8 Hz, 1H), 7.49-7.46 (m, 1H), 6.84 (d, *J* = 6.0 Hz, 1H), 4.44-4.36 (m, 1H), 2.32-2.23 (m, 2H), 1.96 (d, *J* = 11.6 Hz, 4H), 1.79 (d, *J* = 12.8 Hz, 1H), 1.53-1.43 (m, 2H), 1.37-1.29 (m, 1H); ¹³C NMR (100 MHz, CDCl₃): δ 153.5, 152.8, 149.5, 149.3, 141.6, 139.0, 129.8, 124.0, 123.8, 123.2, 122.8, 120.5, 114.8, 111.8, 54.1, 30.4, 26.1, 25.4; HRMS (ESI, *m/z*) calcd. For C₂₁H₂₁N₄O [M+H]⁺: 345.1715; found: 345.1721.

3-cyclopentyl-5-phenyl-1-(pyridin-2-yl)-1,3-dihydro-2*H*-naphtho[1,2-*d*]imidazol-2-one (19ab)



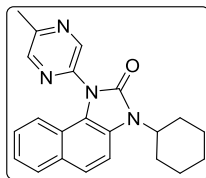
The general procedure 1 for imidazolone was followed. Column chromatography (SiO₂, eluting with 75:25 hexane/ethyl acetate) afforded the desired product as a creamy white powder (45.4 mg, 56% yield), mp 142-144 °C. ¹H NMR (400 MHz, CDCl₃): δ 8.68-8.67 (m, 1H), 8.01 (td, *J*₁ = 8.0 Hz, *J*₂ = 2.0 Hz, 1H), 7.85-7.83 (m, 1H), 7.75 (dt, *J*₁ = 8.0 Hz, *J*₂ = 0.8 Hz, 1H), 7.53-7.42 (m, 6H), 7.36 (s, 1H), 7.24-7.16 (m, 2H), 7.07-7.03 (m, 1H), 4.94 (quintet, *J* = 8.8 Hz, 1H), 2.31-2.22 (m, 2H), 2.13-2.06 (m, 2H), 2.01-1.92 (m, 2H), 1.76-1.70 (m, 2H); ¹³C NMR: (100 MHz, CDCl₃): δ 154.0, 150.2, 149.6, 141.1, 138.9, 136.1, 130.4, 128.4, 128.3, 127.5, 127.4, 125.7, 125.5, 123.7, 123.6, 123.4, 121.5, 120.7, 111.1, 54.1, 29.3, 25.1; HRMS (ESI, *m/z*) calcd. For C₂₇H₂₄N₃O [M+H]⁺: 406.1919; found: 406.1917.

3-cyclohexyl-1-(3-methylpyridin-2-yl)-1,3-dihydro-2*H*-naphtho[1,2-*d*]imidazol-2-one (19ac)



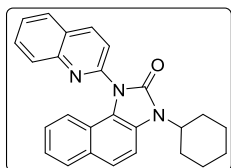
The general procedure 1 for imidazolone was followed. Column chromatography (SiO₂, eluting with 75:25 hexane/ethyl acetate) afforded the desired product as a light brown crystalline solid (54.3 mg, 76% yield), mp 192-194 °C. ¹H NMR (400 MHz, CDCl₃): δ 8.52 (s, 1H), 7.83-7.80 (m, 2H), 7.62 (d, *J* = 8.8 Hz, 1H), 7.54 (d, *J* = 8.4 Hz, 1H), 7.42 (dd, *J*₁ = 7.6 Hz, *J*₂ = 4.8 Hz, 1H), 7.26-7.22 (m, 1H), 7.13-7.09 (m, 1H), 6.63 (d, *J* = 8.8 Hz, 1H), 4.45-4.37 (m, 1H), 2.30-2.23 (m, 5H), 1.99-1.92 (m, 4H), 1.77 (d, *J* = 12.8 Hz, 1H), 1.53-1.44 (m, 2H), 1.37-1.29 (m, 1H); ¹³C NMR (100 MHz, CDCl₃): δ 153.0, 149.3, 147.6, 140.4, 133.4, 129.7, 129.1, 126.1, 125.8, 124.8, 123.5, 122.6, 122.1, 120.3, 119.9, 110.6, 53.6, 30.6, 30.5, 26.1, 25.5, 17.5; HRMS (ESI, *m/z*) calcd. For C₂₃H₂₄N₃O [M+H]⁺: 358.1919; found: 358.1921.

3-cyclohexyl-1-(5-methylpyrazin-2-yl)-1,3-dihydro-2*H*-naphtho[1,2-*d*]imidazol-2-one (19ad)



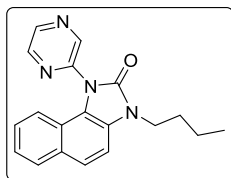
The general procedure 1 for imidazolone was followed. Column chromatography (SiO₂, eluting with 70:30 hexane/ethyl acetate) afforded the desired product as a light brown solid (40.8 mg, 57% yield), mp 134-136 °C. ¹H NMR (400 MHz, CDCl₃): 8.89 (d, *J* = 0.8 Hz, 1H), 8.50 (s, 1H), 7.84 (d, *J* = 8.0 Hz, 1H), 7.67 (d, *J* = 8.8 Hz, 1H), 7.52 (d, *J* = 8.8 Hz, 1H), 7.32-7.28 (m, 1H), 7.24-7.19 (m, 1H), 6.98 (dd, *J*₁ = 8.8 Hz, *J*₂ = 0.8 Hz, 1H), 4.43-4.34 (m, 1H), 2.72 (s, 3H), 2.32-2.21 (m, 2H), 1.98-1.93 (m, 4H), 1.78 (d, *J* = 12.4 Hz, 1H), 1.54-1.42 (m, 2H), 1.36-1.29 (m, 1H); ¹³C NMR (100 MHz, CDCl₃): δ 153.6, 153.5, 144.4, 143.4, 143.3, 129.9, 129.4, 126.4, 126.1, 123.72, 123.69, 121.5, 121.1, 120.3, 110.5, 53.9, 30.4, 26.1, 25.5, 21.4; HRMS (ESI, *m/z*) calcd. For C₂₂H₂₃N₃O [M+H]⁺: 359.1872; found: 359.1887.

3-cyclohexyl-1-(quinolin-2-yl)-1,3-dihydro-2*H*-naphtho[1,2-*d*]imidazol-2-one (19ae)



The general procedure 1 for imidazolone was followed. Column chromatography (SiO₂, eluting with 75:25 hexane/ethyl acetate) afforded the desired product as a creamy white powder (57.4 mg, 73% yield), mp 188-190 °C. ¹H NMR (400 MHz, CDCl₃): δ 8.42 (d, *J* = 8.4 Hz, 1H), 8.05-8.02 (m, 1H), 7.97 (dd, *J*₁ = 8.0 Hz, *J*₂ = 0.8 Hz, 1H), 7.84-7.82 (m, 2H), 7.77-7.73 (m, 1H), 7.64-7.62 (m, 2H), 7.54 (d, *J* = 8.8 Hz, 1H), 7.28-7.24 (m, 1H), 7.08-7.07 (m, 2H), 4.46-4.38 (m, 1H), 2.35-2.25 (m, 2H), 2.01-1.93 (m, 4H), 1.78 (d, *J* = 13.2 Hz, 1H), 1.54-1.44 (m, 2H), 1.38-1.30 (m, 1H); ¹³C NMR (100 MHz, CDCl₃): δ 153.8, 149.6, 147.3, 138.9, 130.3, 130.0, 129.3, 129.1, 127.8, 127.6, 127.4, 126.3, 125.7, 123.5, 121.73, 121.68, 121.2, 120.7, 110.4, 53.7, 30.4, 26.2, 25.5; HRMS (ESI, *m/z*) calcd. For C₂₆H₂₄N₃O [M+H]⁺: 394.1919; found: 394.1920.

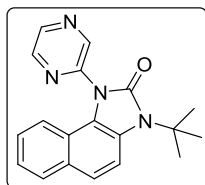
3-butyl-1-(pyrazin-2-yl)-1,3-dihydro-2*H*-naphtho[1,2-*d*]imidazol-2-one (19af)



The general procedure 1 for imidazolone was followed. Column chromatography (SiO₂, eluting with 70:30 hexane/ethyl acetate) afforded the desired product as a light brown crystalline solid

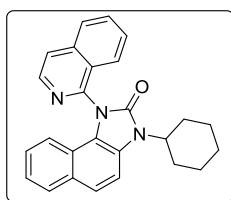
(41.3 mg, 65% yield), mp 140-142 °C. ^1H NMR (400 MHz, CDCl_3): δ 9.07 (s, 1H), 8.69-8.63 (m, 2H), 7.86 (d, $J = 8.0$ Hz, 1H), 7.73 (d, $J = 8.8$ Hz, 1H), 7.36-7.30 (m, 2H), 7.27-7.23 (m, 1H), 7.04 (d, $J = 8.4$ Hz, 1H), 4.03 (t, $J = 7.2$ Hz, 2H), 1.86-1.79 (m, 2H), 1.50-1.41 (m, 2H), 0.97 (t, $J = 7.6$ Hz, 3H); ^{13}C NMR (100 MHz, CDCl_3): δ 153.9, 146.9, 144.4, 143.7, 143.4, 130.4, 129.6, 127.2, 126.2, 124.6, 123.8, 121.3, 121.0, 120.4, 109.2, 41.5, 30.7, 20.2, 13.8; HRMS (ESI, m/z) calcd. For $\text{C}_{19}\text{H}_{18}\text{N}_4\text{O}$ $[\text{M}+\text{H}]^+$: 319.1559; found: 319.1558.

3-(*tert*-butyl)-1-(pyrazin-2-yl)-1,3-dihydro-2*H*-naphtho[1,2-*d*]imidazol-2-one (19ag)



The general procedure 1 for imidazolone was followed. Column chromatography (SiO_2 , eluting with 70:30 hexane/ethyl acetate) afforded the desired product as a creamy white powder (62.3 mg, 98% yield), mp 148-150 °C. ^1H NMR (400 MHz, CDCl_3): δ 9.00 (d, $J = 1.6$ Hz, 1H), 8.68 (d, $J = 2.4$ Hz, 1H), 8.63 (dd, $J_1 = 2.4$ Hz, $J_2 = 1.2$ Hz, 1H), 7.82 (d, $J = 8.4$ Hz, 1H), 7.76 (d, $J = 9.2$ Hz, 1H), 7.63 (d, $J = 9.2$ Hz, 1H), 7.32-7.28 (m, 1H), 7.21-7.16 (m, 1H), 6.85 (d, $J = 8.4$ Hz, 1H), 1.88 (s, 9H); ^{13}C NMR (100 MHz, CDCl_3): δ 153.8, 147.2, 145.1, 143.8, 143.6, 129.7, 129.1, 127.2, 126.0, 123.9, 123.2, 121.9, 121.3, 119.9, 113.1, 59.1, 29.8; HRMS (ESI, m/z) calcd. For $\text{C}_{19}\text{H}_{19}\text{N}_4\text{O}$ $[\text{M}+\text{H}]^+$: 319.1559; found: 319.1563.

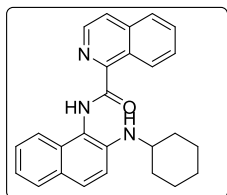
3-cyclohexyl-1-(isoquinolin-1-yl)-1,3-dihydro-2*H*-naphtho[1,2-*d*]imidazol-2-one (19ah)



The general procedure 1 for imidazolone was followed. Column chromatography (SiO_2 , eluting with 70:30 hexane/ethyl acetate) afforded the desired product as a white powder (23.6 mg, 30% yield), mp 184-186 °C. ^1H NMR (400 MHz, CDCl_3): δ 8.60 (d, $J = 5.6$ Hz, 1H), 8.00 (d, $J = 8.4$ Hz, 1H), 7.94 (d, $J = 8.8$ Hz, 1H), 7.91 (d, $J = 6.0$ Hz, 1H), 7.82-7.56 (m, 2H), 7.67 (d, $J = 8.8$ Hz, 1H), 7.61-7.57 (m, 2H), 7.22-7.18 (m, 1H), 6.99-6.95 (m, 1H), 6.44 (d, $J = 8.4$ Hz, 1H), 4.99-4.41

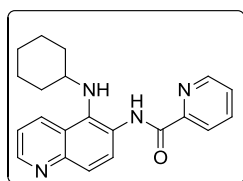
(m, 1H), 2.37-2.27 (m, 2H), 2.07-1.95 (m, 4H), 1.79 (d, $J = 11.6$ Hz, 1H), 1.56-1.44 (m, 2H), 1.39-1.31 (m, 1H); ^{13}C NMR (100 MHz, CDCl_3): δ 153.8, 141.7, 138.5, 131.5, 129.8, 129.1, 128.9, 127.1, 126.7, 126.1, 125.6, 123.5, 123.1, 122.8, 120.4, 120.1, 110.6, 53.7, 30.7, 26.2, 25.5; HRMS (ESI, m/z) calcd. For $\text{C}_{26}\text{H}_{24}\text{N}_3\text{O}$ $[\text{M}+\text{H}]^+$: 394.1919; found: 394.1920.

***N*-(2-(cyclohexylamino)naphthalen-1-yl)isoquinoline-1-carboxamide (19ah')**



The general procedure 1 for imidazolone was followed. Column chromatography (SiO_2 , eluting with 85:15 hexane/ethyl acetate) afforded the desired product as a yellow fluffy solid (32.4 mg, 41% yield), mp 134-136 °C. ^1H NMR (400 MHz, CDCl_3): δ 9.96 (s, 1H), 9.67-9.64 (m, 1H), 8.62 (d, $J = 5.6$ Hz, 1H), 7.92-7.90 (m, 2H), 7.81 (d, $J = 8.4$ Hz, 1H), 7.78-7.69 (m, 4H), 7.43-7.39 (m, 1H), 7.28-7.21 (m, 2H), 3.52-3.46 (m, 1H), 2.12-2.09 (m, 2H), 1.79-1.74 (m, 2H), 1.64-1.60 (m, 1H), 1.42-1.19 (m, 5H); ^{13}C NMR (100 MHz, CDCl_3): δ 165.2, 160.5, 154.8, 147.9, 140.5, 131.6, 130.8, 129.1, 128.3, 128.0, 127.4, 127.1, 127.0, 125.0, 122.3, 120.8, 110.9, 33.6, 25.9, 25.0; HRMS (ESI, m/z) calcd. For $\text{C}_{26}\text{H}_{26}\text{N}_3\text{O}$ $[\text{M}+\text{H}]^+$: 396.2076; found: 396.2078.

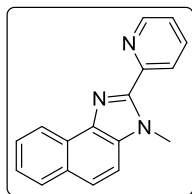
***N*-(5-(cyclohexylamino)quinolin-6-yl)picolinamide (19ai)**



The general procedure 1 for imidazolone was followed. Column chromatography (SiO_2 , eluting with 80:20 hexane/ethyl acetate) afforded the desired product as a pale yellow solid (42.2 mg, 61% yield), mp 146-148 °C. ^1H NMR (400 MHz, CDCl_3): δ 10.98 (s, 1H), 8.87 (d, $J = 9.2$ Hz, 1H), 8.81 (dd, $J_1 = 4.0$ Hz, $J_2 = 1.6$ Hz, 1H), 8.67-8.65 (m, 1H), 8.33 (dt, $J_1 = 7.6$ Hz, $J_2 = 1.2$ Hz, 1H), 8.29-8.27 (m, 1H), 7.94-7.89 (m, 2H), 7.49-7.46 (m, 1H), 7.37 (dd, $J_1 = 8.4$ Hz, $J_2 = 4.0$ Hz, 1H), 3.35 (s, 1H), 3.02-2.95 (m, 1H), 2.06-2.02 (m, 2H), 1.73-1.68 (m, 2H), 1.59-1.55 (m, 1H), 1.39-1.30 (m, 2H), 1.67-1.08 (m, 3H); ^{13}C NMR (100 MHz, CDCl_3): δ 162.3, 150.4, 148.9, 148.2, 146.2,

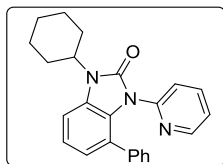
137.7, 131.6, 131.0, 130.6, 126.5, 125.9, 125.5, 123.6, 122.6, 120.8, 58.6, 34.8, 25.9, 25.4; HRMS (ESI, m/z) calcd. For C₂₁H₂₃N₄O₃ [M+H]⁺: 347.1872; found: 347.1889.

3-methyl-2-(pyridin-2-yl)-3H-naphtho[1,2-d]imidazole (19aj)



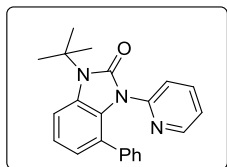
The general procedure 1 for imidazolone was followed. Column chromatography (SiO₂, eluting with 90:10 hexane/ethyl acetate) afforded the desired product as a colorless crystalline solid (26 mg, 50% yield), mp 108-110 °C. ¹H NMR (400 MHz, CDCl₃): δ 8.74 (d, *J* = 8.0 Hz, 1H), 8.70-8.68 (m, 1H), 8.51 (d, *J* = 8.0 Hz, 1H), 7.93 (d, *J* = 8.0 Hz, 1H), 7.85 (td, *J*₁ = 7.6 Hz, *J*₂ = 1.2 Hz, 1H), 7.74 (d, *J* = 8.8 Hz, 1H), 7.66-7.62 (m, 1H), 7.56-7.48 (m, 2H), 7.33-7.30 (m, 1H), 4.36 (s, 3H); ¹³C NMR (100 MHz, CDCl₃): δ 150.9, 148.7, 148.3, 138.2, 136.9, 133.6, 130.6, 128.6, 127.2, 126.7, 124.8, 124.73, 124.67, 123.4, 122.1, 110.5, 33.1; HRMS (ESI, m/z) calcd. For C₁₇H₁₄N₃ [M+H]⁺: 260.1188; found: 260.1196.

1-cyclohexyl-4-phenyl-3-(pyridin-2-yl)-1,3-dihydro-2H-benzo[d]imidazol-2-one (19ak)



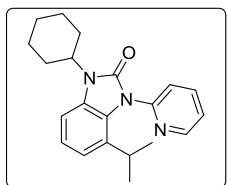
The general procedure 2 for imidazolone was followed. Column chromatography (SiO₂, eluting with 80:20 hexane/ethyl acetate) afforded the desired product as a white solid (29.5 mg, 40% yield), mp 196-198 °C. ¹H NMR (400 MHz, CDCl₃): δ 7.87-7.85 (m, 1H), 7.54 (td, *J*₁ = 8.0 Hz, *J*₂ = 2.0 Hz, 1H), 7.32 (d, *J* = 8.0 Hz, 1H), 7.25-7.17 (m, 2H), 7.06-6.89 (m, 7H), 4.38-4.29 (m, 1H), 2.32-2.22 (m, 2H), 1.94 (d, *J* = 10.8 Hz, 4H), 1.76 (d, *J* = 12.8 Hz, 1H), 1.51-1.42 (m, 2H), 1.35-1.25 (m, 1H); ¹³C NMR (100 MHz, CDCl₃): δ 153.5, 148.5, 148.1, 138.7, 137.3, 130.2, 128.3, 127.6, 126.4, 126.1, 125.7, 123.8, 122.2, 122.0, 121.9, 108.3, 53.6, 29.9, 26.1, 25.5; HRMS (ESI, m/z) calcd. For C₂₄H₂₄N₃O [M+H]⁺: 370.1919; found: 370.1913.

1-(tert-butyl)-4-phenyl-3-(pyridin-2-yl)-1,3-dihydro-2H-benzo[d]imidazol-2-one (19al)



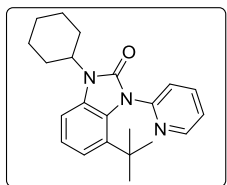
The general procedure 2 for imidazolone was followed was followed. Column chromatography (SiO₂, eluting with 80:20 hexane/ethyl acetate) afforded the desired product as a white solid (20.5 mg, 30% yield), mp 228-230 °C. ¹H NMR (400 MHz, CDCl₃): δ 7.93 (d, *J* = 3.6 Hz, 1H), 7.51-7.46 (m, 2H), 7.23 (d, *J* = 7.6 Hz, 1H), 7.14 (t, *J* = 8.0 Hz, 1H), 7.03-6.89 (m, 7H), 1.86 (s, 9H); ¹³C NMR (100 MHz, CDCl₃): δ 153.8, 148.6, 148.1, 138.8, 137.2, 130.9, 128.4, 127.6, 126.3, 126.2, 125.6, 123.8, 122.8, 121.9, 121.5, 111.2, 58.7, 29.6; HRMS (ESI, *m/z*) calcd. For C₂₂H₂₂N₃O [M+H]⁺: 344.1763; found: 344.1752.

1-cyclohexyl-4-isopropyl-3-(pyridin-2-yl)-1,3-dihydro-2H-benzo[d]imidazol-2-one (19am)



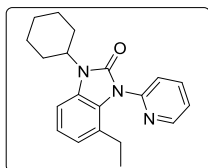
The general procedure 2 for imidazolone was followed was followed. Column chromatography (SiO₂, eluting with 80:20 hexane/ethyl acetate) afforded the desired product as a creamy white solid (43.5 mg, 65% yield), mp 164-166 °C. ¹H NMR (400 MHz, CDCl₃): δ 8.58 (dd, *J*₁ = 4.8 Hz, *J*₂ = 2.0 Hz, 1H), 7.89 (td, *J*₁ = 7.6 Hz, *J*₂ = 2.0 Hz, 1H), 7.57 (d, *J* = 8.0 Hz, 1H), 7.37-7.34 (m, 1H), 7.12-7.04 (m, 2H), 7.00-6.98 (m, 1H), 4.29-4.21 (m, 1H), 2.46-2.36 (m, 1H), 2.27-2.16 (m, 2H), 1.89 (d, *J* = 11.2 Hz, 4H), 1.73 (d, *J* = 12.8 Hz, 1H), 1.48-1.38 (m, 2H), 1.32-1.24 (m, 1H), 1.02 (d, *J* = 6.8 Hz, 6H); ¹³C NMR (100 MHz, CDCl₃): δ 153.9, 150.6, 149.0, 138.4, 132.4, 129.8, 126.1, 123.5, 123.4, 122.3, 119.0, 106.9, 53.5, 29.9, 27.7, 26.1, 25.5, 23.2; HRMS (ESI, *m/z*) calcd. For C₂₁H₂₆N₃O [M+H]⁺: 336.2076; found: 336.2067.

4-(tert-butyl)-1-cyclohexyl-3-(pyridin-2-yl)-1,3-dihydro-2H-benzo[d]imidazol-2-one (19an)



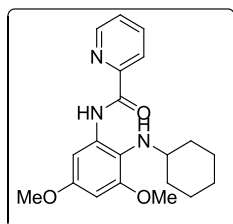
The general procedure 2 for imidazolone was followed was followed. Column chromatography (SiO₂, eluting with 80:20 hexane/ethyl acetate) afforded the desired product as a creamy white solid (40 mg, 57% yield), mp 160-162 °C. ¹H NMR (400 MHz, CDCl₃): δ 8.49 (dd, *J*₁ = 4.8 Hz, *J*₂ = 1.6 Hz, 1H), 7.86 (td, *J*₁ = 7.6 Hz, *J*₂ = 2.0 Hz, 1H), 7.60 (d, *J* = 8.0 Hz, 1H), 7.31-7.28 (m, 1H), 7.17 (dd, *J*₁ = 8.0 Hz, *J*₂ = 1.6 Hz, 1H), 7.12-7.04 (m, 2H), 4.22-4.14 (m, 1H), 2.29-2.18 (m, 2H), 1.91-1.85 (m, 4H), 1.72 (d, *J* = 12.8 Hz, 1H), 1.46-1.35 (m, 2H), 1.30-1.22 (m, 1H), 1.07 (s, 9H); ¹³C NMR (100 MHz, CDCl₃): δ 155.6, 153.8, 148.7, 138.1, 136.5, 132.2, 127.3, 124.5, 123.2, 122.6, 121.7, 107.1, 53.8, 34.9, 31.4, 29.7, 26.2, 25.5; HRMS (ESI, *m/z*) calcd. For C₂₂H₂₈N₃O [M+H]⁺: 350.2232; found: 350.2225.

1-cyclohexyl-4-ethyl-3-(pyridin-2-yl)-1,3-dihydro-2*H*-benzo[*d*]imidazol-2-one (19ao)



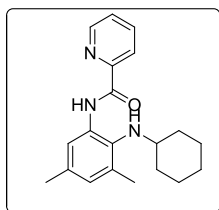
The general procedure 2 for imidazolone was followed was followed. Column chromatography (SiO₂, eluting with 90:10 hexane/ethyl acetate) afforded the desired product as a creamy white solid (16 mg, 25% yield). ¹H NMR (400 MHz, CDCl₃): δ 8.60-8.58 (m, 1H), 7.89 (td, *J*₁ = 7.6 Hz, *J*₂ = 1.6 Hz, 1H), 7.58 (dt, *J*₁ = 8.0 Hz, *J*₂ = 0.8 Hz, 1H), 7.37-7.34 (m, 1H), 7.09-7.04 (m, 2H), 6.89-6.88 (m, 1H), 4.30-4.22 (m, 1H), 2.26-2.19 (m, 4H), 1.89 (d, *J* = 9.6 Hz, 4H), 1.73 (d, *J* = 12.8 Hz, 1H), 1.48-1.38 (m, 2H), 1.32-1.24 (m, 1H), 0.89 (t, *J* = 7.2 Hz, 3H); ¹³C NMR (100 MHz, CDCl₃): δ 153.8, 150.0, 148.9, 138.3, 129.7, 127.4, 126.6, 123.6, 123.4, 122.4, 122.1, 107.2, 53.5, 29.9, 26.1, 25.5, 25.1, 14.2; HRMS (ESI, *m/z*) calcd. For C₂₀H₂₄N₃O [M+H]⁺: 322.1919; found: 322.1913.

N-(2-(cyclohexylamino)-3,5-dimethoxyphenyl)picolinamide (19ap)



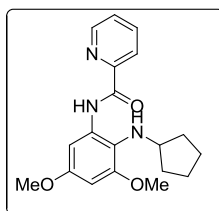
The general procedure for amination in aniline system was followed. Column chromatography (SiO₂, eluting with 90:10 hexane/ethyl acetate) afforded the desired product as a gummy liquid (51 mg, 72% yield). ¹H NMR (400 MHz, CDCl₃): δ 11.04 (s, 1H), 8.62-8.60 (m, 1H), 8.25 (dt, *J*₁ = 8.0 Hz, *J*₂ = 0.8 Hz, 1H), 7.89 (d, *J* = 2.8 Hz, 1H), 7.85 (td, *J*₁ = 8.0 Hz, *J*₂ = 2.0 Hz, 1H), 7.43-7.39 (m, 1H), 6.25 (d, *J* = 2.8 Hz, 1H), 3.82 (s, 3H), 3.77 (s, 3H), 2.74-2.68 (m, 1H), 1.93 (d, *J* = 12.8 Hz, 2H), 1.69-1.65 (m, 2H), 1.50 (s, 1H), 1.27-1.19 (m, 3H), 1.15-1.09 (m, 2H); ¹³C NMR (100 MHz, CDCl₃): δ 162.0, 156.8, 154.9, 150.6, 148.3, 137.5, 134.8, 126.2, 122.3, 119.5, 95.9, 94.9, 57.8, 55.7, 55.6, 34.2, 26.1, 25.3; HRMS (ESI, *m/z*) calcd. For C₂₀H₂₆N₃O₃ [M+H]⁺: 356.1974; found: 356.1973.

***N*-(2-(cyclohexylamino)-3,5-dimethylphenyl)picolinamide (19aq)**



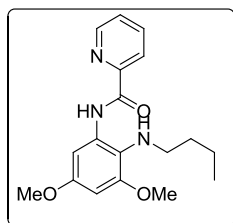
The general procedure for amination in aniline system was followed. Column chromatography (SiO₂, eluting with 95:5 hexane/ethyl acetate) afforded the desired product as a gummy liquid (33.5 mg, 52% yield). ¹H NMR (400 MHz, CDCl₃): δ 10.87 (s, 1H), 8.63-8.61 (m, 1H), 8.29 (dt, *J*₁ = 7.6 Hz, *J*₂ = 1.2 Hz, 1H), 8.23 (s, 1H), 7.88 (td, *J*₁ = 7.6 Hz, *J*₂ = 1.6 Hz, 1H), 7.45-7.42 (m, 1H), 6.75 (m, 1H), 2.84-2.77 (m, 1H), 2.31 (s, 3H), 2.26 (s, 3H), 2.06-2.03 (m, 2H), 1.71-1.68 (m, 2H), 1.55-1.54 (m, 1H), 1.32-1.25 (m, 2H), 1.13-1.08 (m, 3H); ¹³C NMR (100 MHz, CDCl₃): δ 161.9, 150.8, 148.1, 137.5, 133.5, 133.2, 131.5, 126.6, 126.1, 122.4, 118.6, 58.0, 34.7, 25.9, 25.5, 21.3, 18.3; HRMS (ESI, *m/z*) calcd. For C₂₀H₂₆N₃O [M+H]⁺: 324.2076; found: 324.2066.

***N*-(2-(cyclopentylamino)-3,5-dimethoxyphenyl)picolinamide (19as)**



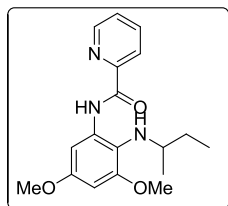
The general procedure for amination in aniline system was followed was followed. Column chromatography (SiO₂, eluting with 90:10 hexane/ethyl acetate) afforded the desired product as a gummy liquid (34 mg, 50% yield). ¹H NMR (400 MHz, CDCl₃): δ 11.13 (s, 1H), 8.64-8.62 (m, 1H), 8.26 (dt, *J*₁ = 8.0 Hz, *J*₂ = 0.8 Hz, 1H), 7.92 (d, *J* = 2.4 Hz, 1H), 7.86 (td, *J*₁ = 7.6 Hz, *J*₂ = 1.6 Hz, 1H), 7.45-7.41 (m, 1H), 6.26 (d, *J* = 2.8 Hz, 1H), 3.84 (s, 3H), 3.79 (s, 3H), 3.47 (quintet, *J* = 5.6 Hz, 1H), 1.80-1.70 (m, 4H), 1.56-1.46 (m, 4H); ¹³C NMR (100 MHz, CDCl₃): δ 162.1, 157.1, 155.2, 150.6, 148.3, 137.5, 135.3, 126.2, 122.3, 119.9, 95.8, 95.0, 60.8, 55.6, 33.2, 23.6; HRMS (ESI, *m/z*) calcd. For C₁₉H₂₄N₃O₃ [M+H]⁺: 342.1818; found: 342.1819.

***N*-(2-(butylamino)-3,5-dimethoxyphenyl)picolinamide (19at)**



The general procedure for amination in aniline system was followed was followed. Column chromatography (SiO₂, eluting with 90:10 hexane/ethyl acetate) afforded the desired product as a gummy liquid (31 mg, 47% yield). ¹H NMR (400 MHz, CDCl₃): δ 11.03 (s, 1H), 8.65-8.63 (m, 1H), 8.28-8.25 (m, 1H), 7.90-7.86 (m, 2H), 7.46-7.43 (m, 1H), 6.28 (d, *J* = 2.4 Hz, 1H), 3.84 (s, 3H), 3.81 (s, 3H), 2.85 (t, *J* = 7.2 Hz, 2H), 1.61 (quintet, *J* = 7.2 Hz, 2H), 1.49-1.39 (m, 2H), 0.89 (t, *J* = 7.2 Hz, 3H); ¹³C NMR (100 MHz, CDCl₃): δ 162.3, 157.1, 154.6, 150.5, 148.3, 137.5, 134.5, 126.3, 122.3, 96.2, 95.2, 55.8, 55.7, 49.8, 32.8, 20.3, 14.1; HRMS (ESI, *m/z*) calcd. For C₁₈H₂₄N₃O₃ [M+H]⁺: 330.1818; found: 330.1822.

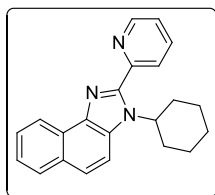
***N*-(2-(*sec*-butylamino)-3,5-dimethoxyphenyl)picolinamide (19au)**



The general procedure for amination in aniline system was followed was followed. Column chromatography (SiO₂, eluting with 90:10 hexane/ethyl acetate) afforded the desired product as a

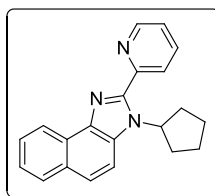
gummy liquid (27.6 mg, 42% yield). ^1H NMR (400 MHz, CDCl_3): δ 11.03 (s, 1H), 8.63-8.62 (m, 1H), 8.26 (dt, $J_1 = 7.6$ Hz, $J_2 = 1.2$ Hz, 1H), 7.89-7.85 (m, 2H), 7.45-7.42 (m, 1H), 6.27 (d, $J = 2.4$ Hz, 1H), 3.84 (s, 3H), 3.79 (s, 3H), 2.98-2.90 (m, 1H), 1.68-1.57 (m, 1H), 1.47-1.39 (m, 1H), 1.04 (d, $J = 6.4$ Hz, 3H), 0.95 (t, $J = 12.8$ Hz, 3H); ^{13}C NMR (100 MHz, CDCl_3): δ 162.1, 156.9, 154.9, 150.6, 148.3, 137.5, 134.9, 126.2, 122.3, 96.1, 95.1, 55.7, 30.2, 19.9, 10.5; HRMS (ESI, m/z) calcd. For $\text{C}_{18}\text{H}_{24}\text{N}_3\text{O}_3$ $[\text{M}+\text{H}]^+$: 330.1818; found: 330.1826.

3-cyclohexyl-2-(pyridin-2-yl)-3H-naphtho[1,2-d]imidazole (22a)



The general procedure for imidazole was followed. Column chromatography (SiO_2 , eluting with 90:10 hexane/ethyl acetate) afforded the desired product as a white solid (58 mg, 88% yield), mp 88-90°C. ^1H NMR (400 MHz, CDCl_3): δ 8.77 (d, $J = 8.0$ Hz, 1H), 8.72-8.70 (m, 1H), 8.36 (d, $J = 8.0$ Hz, 1H), 7.92 (d, $J = 8.0$ Hz, 1H), 7.89-7.83 (m, 2H), 7.68 (d, $J = 8.8$ Hz, 1H), 7.64-7.60 (m, 1H), 7.51-7.47 (m, 1H), 7.36-7.33 (m, 1H), 5.59-5.52 (m, 1H), 2.39-2.29 (m, 2H), 2.16-2.12 (m, 2H), 1.99-1.94 (m, 2H), 1.81 (d, $J = 12.4$ Hz, 1H), 1.52-1.34 (m, 3H); ^{13}C NMR (100 MHz, CDCl_3): δ 148.9, 137.0, 131.3, 130.1, 128.6, 128.2, 126.6, 125.83, 125.8, 124.9, 123.81, 123.79, 123.55, 123.53, 122.2, 113.7, 57.2, 31.8, 26.3, 25.6; HRMS (ESI, m/z) calcd. For $\text{C}_{22}\text{H}_{22}\text{N}_3$ $[\text{M}+\text{H}]^+$: 328.1814; found: 328.1822.

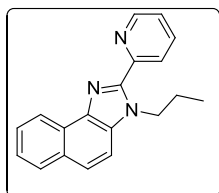
3-cyclopentyl-2-(pyridin-2-yl)-3H-naphtho[1,2-d]imidazole (22b)



The general procedure for imidazole was followed. Column chromatography (SiO_2 , eluting with 90:10 hexane/ethyl acetate) afforded the desired product as a light brown solid (50 mg, 80% yield), mp 146-148 °C. ^1H NMR (400 MHz, CDCl_3): δ 8.73-8.72 (m, 1H), 8.51-8.48 (m, 1H), 8.25 (dt, $J_1 = 8.0$ Hz, $J_2 = 1.2$ Hz, 1H), 8.02-7.98 (m, 2H), 7.81 (d, $J = 9.2$ Hz, 1H), 7.75 (d, $J = 9.2$ Hz, 1H),

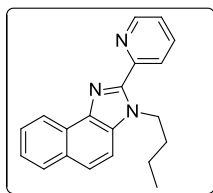
7.62-7.58 (m, 1H), 7.50-7.46 (m, 2H), 6.09 (quintet, $J = 9.2$ Hz, 1H), 2.25-2.14 (m, 4H), 2.05-1.98 (m, 2H), 1.75-1.68 (m, 2H); ^{13}C NMR (100 MHz, CDCl_3): δ 151.1, 149.4, 149.3, 138.9, 137.9, 130.9, 130.2, 128.9, 127.4, 126.9, 125.7, 125.3, 124.5, 124.1, 121.8, 113.7, 57.7, 31.0, 25.3; HRMS (ESI, m/z) calcd. For $\text{C}_{21}\text{H}_{20}\text{N}_3$ $[\text{M}+\text{H}]^+$: 314.1657; found: 314.1653.

3-propyl-2-(pyridin-2-yl)-3H-naphtho[1,2-*d*]imidazole (22c)



The general procedure for imidazole was followed. Column chromatography (SiO_2 , eluting with 90:10 hexane/ethyl acetate) afforded the desired product as a light brown solid (40 mg, 70% yield), mp 58-60 °C. ^1H NMR (400 MHz, CDCl_3): δ 8.75 (d, $J = 8.0$ Hz, 1H), 8.68-8.66 (m, 1H), 8.52 (dt, $J_1 = 8.0$ Hz, $J_2 = 0.8$ Hz, 1H), 7.93 (d, $J = 8.4$ Hz, 1H), 7.84 (td, $J_1 = 8.0$ Hz, $J_2 = 1.6$ Hz, 1H), 7.72 (d, $J = 8.8$ Hz, 1H), 7.66-7.62 (m, 1H), 7.55 (d, $J = 8.8$ Hz, 1H), 7.52-7.48 (m, 1H), 7.31-7.28 (m, 1H), 4.89 (t, $J = 7.2$ Hz, 2H), 1.98-1.89 (m, 2H), 0.93 (t, $J = 7.2$ Hz, 3H), ^{13}C NMR (100 MHz, CDCl_3): δ 151.0, 148.7, 148.0, 138.2, 136.8, 133.1, 130.6, 128.5, 127.3, 126.6, 124.74, 124.66, 124.5, 123.3, 122.0, 110.9, 47.2, 24.0, 11.4; HRMS (ESI, m/z) calcd. For $\text{C}_{19}\text{H}_{18}\text{N}_3$ $[\text{M}+\text{H}]^+$: 288.1501; found: 288.1497.

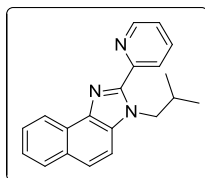
3-butyl-2-(pyridin-2-yl)-3H-naphtho[1,2-*d*]imidazole (22d)



The general procedure for imidazole was followed. Column chromatography (SiO_2 , eluting with 90:10 hexane/ethyl acetate) afforded the desired product as a light brown solid (50 mg, 83% yield), mp 158-160 °C. ^1H NMR (400 MHz, CDCl_3): δ 9.69 (d, $J = 8.4$ Hz, 1H), 9.41 (d, $J = 8.0$ Hz, 1H), 8.78 (d, $J = 4.4$ Hz, 1H), 8.12 (td, $J_1 = 7.6$ Hz, $J_2 = 1.2$ Hz, 1H), 7.97 (d, $J = 2.0$ Hz, 1H), 7.95 (d, $J = 3.2$ Hz, 1H), 7.86-7.82 (m, 1H), 7.68-7.61 (m, 2H), 7.54 (dd, $J_1 = 7.6$ Hz, $J_2 = 4.8$ Hz, 1H), 5.04 (t, $J = 7.6$ Hz, 2H), 1.98-1.94 (m, 2H), 1.44 (sextet, $J = 7.6$ Hz, 2H), 0.97 (t, $J = 7.2$ Hz, 3H);

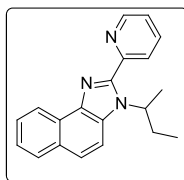
^{13}C NMR (100 MHz, CDCl_3): δ 149.6, 143.7, 143.2, 138.4, 131.7, 130.1, 129.2, 129.0, 128.6, 128.2, 127.8, 126.5, 125.3, 109.6, 46.9, 32.0, 20.0, 13.6; HRMS (ESI, m/z) calcd. For $\text{C}_{20}\text{H}_{20}\text{N}$ $[\text{M}+\text{H}]^+$: 302.1657; found: 302.1663.

3-isobutyl-2-(pyridin-2-yl)-3*H*-naphtho[1,2-*d*]imidazole (22e)



The general procedure for imidazole was followed. Column chromatography (SiO_2 , eluting with 90:10 hexane/ethyl acetate) afforded the desired product as a brown solid (52 mg, 86% yield), mp 74-76 °C. ^1H NMR (400 MHz, CDCl_3): δ 8.76-8.73 (m, 1H), 8.67-8.66 (m, 1H), 8.52 (dt, $J_1 = 8.0$ Hz, $J_2 = 1.2$ Hz, 1H), 7.93 (d, $J = 7.6$ Hz, 1H), 7.84 (td, $J_1 = 8.0$ Hz, $J_2 = 2.0$ Hz, 1H), 7.72 (d, $J = 8.8$ Hz, 1H), 7.66-7.62 (m, 1H), 7.55 (d, $J = 9.2$ Hz, 1H), 7.52-7.47 (m, 1H), 7.32-7.28 (m, 1H), 4.79 (d, $J = 7.2$ Hz, 2H), 2.31-2.20 (m, 1H), 0.88 (d, $J = 6.4$ Hz, 6H); ^{13}C NMR (100 MHz, CDCl_3): δ 151.2, 148.5, 148.2, 138.2, 136.8, 133.5, 130.5, 128.5, 127.3, 126.6, 124.8, 124.7, 124.4, 123.3, 122.0, 111.3, 52.6, 30.1, 20.2; HRMS (ESI, m/z) calcd. For $\text{C}_{20}\text{H}_{20}\text{N}_3$ $[\text{M}+\text{H}]^+$: 302.1579; found: 302.1658.

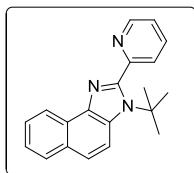
3-(sec-butyl)-2-(pyridin-2-yl)-3*H*-naphtho[1,2-*d*]imidazole (22f)



The general procedure for imidazole was followed. Column chromatography (SiO_2 , eluting with 90:10 hexane/ethyl acetate) afforded the desired product as a light brown solid (48 mg, 80% yield), mp 88-90 °C. ^1H NMR (400 MHz, CDCl_3): δ 8.76 (d, $J = 8.0$ Hz, 1H), 8.70-8.68 (m, 1H), 8.37 (dt, $J_1 = 8.0$ Hz, $J_2 = 0.8$ Hz, 1H), 7.92 (d, $J = 8.0$ Hz, 1H), 7.85 (td, $J_1 = 7.6$ Hz, $J_2 = 2.0$ Hz, 1H), 7.77 (d, $J = 8.8$ Hz, 1H), 7.67 (d, $J = 8.8$ Hz, 1H), 7.65-7.61 (m, 1H), 7.52-7.47 (m, 1H), 7.33-7.30 (m, 1H), 5.89-5.81 (m, 1H), 2.33-2.21 (m, 1H), 2.03-1.92 (m, 1H), 1.76 (d, $J = 7.2$ Hz, 3H), 0.74 (d, $J = 7.2$ Hz, 3H); ^{13}C NMR (100 MHz, CDCl_3): δ 151.3, 149.2, 148.7, 139.1, 136.9, 131.1,

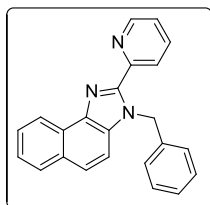
130.1, 128.3, 127.4, 126.5, 125.7, 124.8, 123.8, 123.4, 122.1, 113.3, 54.9, 28.8, 20.2, 11.2; HRMS (ESI, m/z) calcd. For $C_{20}H_{20}N_3$ $[M+H]^+$: 302.1579; found: 302.1660.

3-(tert-butyl)-2-(pyridin-2-yl)-3H-naphtho[1,2-d]imidazole (22g)



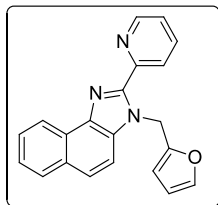
The general procedure for imidazole was followed. Column chromatography (SiO_2 , eluting with 80:20 hexane/ethyl acetate) afforded the desired product as light brown solid (43 mg, 72 % yield), mp 146-148 °C. 1H NMR (400 MHz, $CDCl_3$): δ 8.75 (d, $J = 8.0$ Hz, 1H), 8.71-8.69 (m, 1H), 7.92-7.88 (m, 2H), 7.84 (td, $J_1 = 7.6$ Hz, $J_2 = 2.0$ Hz, 1H), 7.77 (d, $J = 7.6$ Hz, 1H), 7.70 (d, $J = 9.2$ Hz, 1H), 7.61-7.57 (m, 1H), 7.51-7.47 (m, 1H), 7.40-7.37 (m, 1H), 1.70 (m, 9H); ^{13}C NMR (100 MHz, $CDCl_3$): δ 148.9, 136.6, 130.0, 128.0, 126.6, 125.9, 125.1, 124.0, 123.6, 122.5, 122.4, 114.9, 31.5; HRMS (ESI, m/z) calcd. For $C_{20}H_{20}N_3$ $[M+H]^+$: 302.1579; found: 302.1660.

3-benzyl-2-(pyridin-2-yl)-3H-naphtho[1,2-d]imidazole (22h)



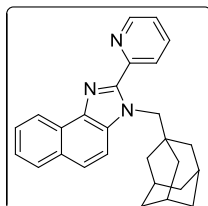
The general procedure 1 for imidazolone was followed. Column chromatography (SiO_2 , eluting with 90:10 hexane/ethyl acetate) afforded the desired product as a pale yellow solid (26.8 mg, 40% yield), mp 144-142 °C. 1H NMR (400 MHz, $CDCl_3$): δ 8.78 (d, $J = 8.4$ Hz, 1H), 8.62-8.60 (m, 1H), 8.57 (d, $J = 8.0$ Hz, 1H), 7.91 (d, $J = 8.0$ Hz, 1H), 7.84 (td, $J_1 = 8.0$ Hz, $J_2 = 2.0$ Hz, 1H), 7.67-7.63 (m, 2H), 7.52-7.48 (m, 1H), 7.44 (d, $J = 8.8$ Hz, 1H), 7.30-7.27 (m, 1H), 7.22-7.13 (m, 5H), 6.30 (s, 2H); ^{13}C NMR (100 MHz, $CDCl_3$): δ 150.6, 148.7, 147.9, 137.6, 136.9, 133.2, 130.7, 128.7, 128.5, 127.5, 127.1, 126.8, 124.9, 124.7, 123.6, 122.1, 111.1, 49.2; HRMS (ESI, m/z) calcd. For $C_{24}H_{18}N_3$ $[M+H]^+$: 336.1501; found: 336.1502.

3-(furan-2-ylmethyl)-2-(pyridin-2-yl)-3H-naphtho[1,2-d]imidazole (22i)



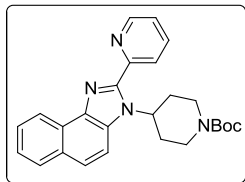
The general procedure 1 for imidazolone was followed. Column chromatography (SiO₂, eluting with 90:10 hexane/ethyl acetate) afforded the desired product as a yellow solid (24.7 mg, 38% yield), mp 122-124 °C. ¹H NMR (400 MHz, CDCl₃): δ 8.75 (d, *J* = 8.4 Hz, 1H), 8.71-8.69 (m, 1H), 8.56 (d, *J* = 8.0 Hz, 1H), 7.93 (d, *J* = 8.4 Hz, 1H), 7.86 (td, *J*₁ = 8.0 Hz, *J*₂ = 2.0 Hz, 1H), 7.76-7.70 (m, 2H), 7.66-7.62 (m, 1H), 7.52-7.48 (m, 1H), 7.35-7.31 (m, 1H), 7.26 (dd, *J*₁ = 1.6 Hz, *J*₂ = 0.8 Hz, 1H), 6.29 (s, 2H), 6.22-6.19 (m, 2H); ¹³C NMR (100 MHz, CDCl₃): δ 150.8, 148.5, 147.4, 142.3, 137.0, 133.1, 130.7, 128.5, 127.0, 126.7, 124.9, 124.8, 123.6, 122.1, 111.1, 110.5, 108.3, 42.3; HRMS (ESI, *m/z*) calcd. For C₂₁H₁₆N₃O [M+H]⁺: 326.1293; found: 326.1294.

3-((3r,5r,7r)-adamantan-1-ylmethyl)-2-(pyridin-2-yl)-3H-naphtho[1,2-d]imidazole (22j)



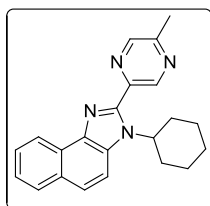
The general procedure for imidazole was followed. Column chromatography (SiO₂, eluting with 90:10 hexane/ethyl acetate) afforded the desired product as a creamy white solid (61 mg, 78% yield), mp 176–178 °C. ¹H NMR (400 MHz, CDCl₃): δ 8.75 (d, *J* = 8.0 Hz, 1H), 8.67-8.65 (m, 1H), 8.41 (dt, *J*₁ = 8.0 Hz, *J*₂ = 0.8 Hz, 1H), 7.93 (d, *J* = 8.0 Hz, 1H), 7.86 (td, *J*₁ = 7.6 Hz, *J*₂ = 2.0 Hz, 1H), 7.70 (d, *J* = 8.8 Hz, 1H), 7.66-7.62 (m, 1H), 7.59 (d, *J* = 8.8 Hz, 1H), 7.51-7.47 (m, 1H), 7.33-7.30 (m, 1H), 1.79 (s, 3H), 1.57-1.36 (m, 14H); ¹³C NMR (100 MHz, CDCl₃): δ 152.0, 149.1, 148.4, 137.1, 134.2, 130.4, 128.7, 128.4, 127.1, 126.7, 125.2, 124.8, 124.1, 123.5, 122.0, 112.4, 55.8, 41.0, 36.8, 36.6, 28.3; HRMS (ESI, *m/z*) calcd. For C₂₇H₂₈N₃ [M+H]⁺: 394.2283; found: 394.2304.

tert-butyl 4-(2-(pyridin-2-yl)-3H-naphtho[1,2-d]imidazol-3-yl)piperidine-1-carboxylate (22k)



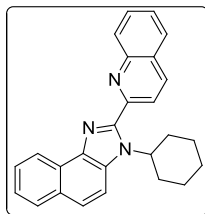
The general procedure for imidazole was followed. Column chromatography (SiO₂, eluting with 85:15 hexane/ethyl acetate) afforded the desired product as a creamy white solid (59 mg, 69 % yield), mp 112-114 °C. ¹H NMR (400 MHz, CDCl₃): δ 8.76 (d, *J* = 8.0 Hz, 1H), 8.69-8.67 (m, 1H), 8.44 (d, *J* = 8.0 Hz, 1H), 7.93-7.87 (m, 2H), 7.74 (d, *J* = 9.2 Hz, 1H), 7.68 (d, *J* = 9.2 Hz, 1H), 7.65-7.61 (m, 1H), 7.52-7.48 (m, 1H), 7.37-7.34 (m, 1H), 5.94-5.85 (m, 1H), 4.35 (s, 2H), 2.88 (t, *J* = 9.6 Hz, 2H), 2.59-2.49 (m, 2H), 2.10 (dd, *J*₁ = 12.0 Hz, *J*₂ = 2.0 Hz, 2H), 1.53 (s, 9H); ¹³C NMR (100 MHz, CDCl₃): δ 154.9, 148.8, 148.3, 137.2, 131.1, 130.1, 128.3, 126.8, 125.8, 125.1, 124.3, 123.7, 122.1, 113.2, 80.0, 55.4, 30.8, 28.6; HRMS (ESI, *m/z*) calcd. For C₂₆H₂₉N₄O₂ [M+H]⁺: 429.2291; found: 429.2285.

3-cyclohexyl-2-(5-methylpyrazin-2-yl)-3H-naphtho[1,2-*d*]imidazole (22l)



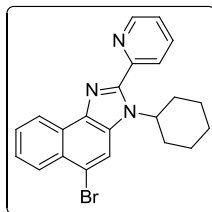
The general procedure for imidazole was followed. Column chromatography (SiO₂, eluting with 85:15 hexane/ethyl acetate) afforded the desired product as a pale yellow powder (40.3 mg, 59% yield), mp 188-190 °C. ¹H NMR (400 MHz, CDCl₃): δ 9.46 (s, 1H), 8.74 (d, *J* = 8.0 Hz, 1H), 8.51 (s, 1H), 7.91 (d, *J* = 8.0 Hz, 1H), 7.82 (d, *J* = 9.2 Hz, 1H), 7.68 (d, *J* = 9.2 Hz, 1H), 7.65-7.61 (m, 1H), 7.52-7.48 (m, 1H), 5.45-5.37 (m, 1H), 2.65 (s, 3H), 2.38-2.29 (m, 2H), 2.11 (d, *J* = 11.2 Hz, 2H), 1.96 (d, *J* = 12.8 Hz, 2H), 1.81 (d, *J* = 11.6 Hz, 1H), 1.50-1.34 (m, 3H); ¹³C NMR (100 MHz, CDCl₃): δ 153.1, 146.17, 146.16, 145.7, 142.7, 131.5, 130.1, 128.3, 127.3, 126.7, 125.0, 124.1, 122.1, 113.5, 57.3, 31.9, 26.2, 25.6, 21.7; HRMS (ESI, *m/z*) calcd. For C₂₂H₂₃N₄ [M+H]⁺: 343.1923; found: 343.1926.

3-cyclohexyl-2-(quinolin-2-yl)-3H-naphtho[1,2-*d*]imidazole (22m)



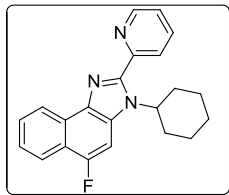
The general procedure for imidazole was followed. Column chromatography (SiO₂, eluting with 90:10 hexane/ethyl acetate) afforded the desired product as a creamy white solid (38 mg, 50% yield), mp 180-182 °C. ¹H NMR (400 MHz, CDCl₃): δ 8.80 (d, *J* = 8.0 Hz, 1H), 8.61 (d, *J* = 8.8 Hz, 1H), 8.31 (d, *J* = 8.4 Hz, 1H), 8.11 (d, *J* = 8.8 Hz, 1H), 7.93 (d, *J* = 8.0 Hz, 1H), 7.89-7.86 (m, 2H), 7.78-7.73 (m, 1H), 7.70 (d, *J* = 9.2 Hz, 1H), 7.67-7.63 (m, 1H), 7.60-7.56 (m, 1H), 7.53-7.49 (m, 1H), 6.14-6.06 (m, 1H), 2.47-2.37 (m, 2H), 2.27-2.24 (m, 2H), 2.02 (d, *J* = 13.6 Hz, 2H), 1.85 (d, *J* = 12.8 Hz, 1H), 1.61-1.50 (m, 2H), 1.47-1.39 (m, 1H); ¹³C NMR (100 MHz, CDCl₃): δ 151.0, 148.3, 147.4, 136.6, 132.0, 130.1, 129.83, 129.79, 128.3, 127.8, 127.6, 127.5, 127.2, 126.6, 124.9, 124.1, 122.9, 122.2, 113.8, 57.5, 32.0, 26.5, 25.8; HRMS (ESI, *m/z*) calcd. For C₂₆H₂₄N₃ [M+H]⁺: 378.1970; found: 378.1974.

5-bromo-3-cyclohexyl-2-(pyridin-2-yl)-3H-naphtho[1,2-*d*]imidazole (22n)



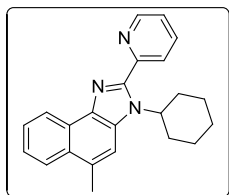
The general procedure for imidazole was followed. Column chromatography (SiO₂, eluting with 90:10 hexane/ethyl acetate) afforded the desired product as a creamy white powder (67 mg, 83% yield), mp 154-156 °C. ¹H NMR (400 MHz, CDCl₃): δ 8.79 (d, *J* = 8.0 Hz, 1H), 8.72-8.70 (m, 1H), 8.35 (dt, *J*₁ = 8.0 Hz, *J*₂ = 0.8 Hz, 1H), 8.31-8.29 (m, 1H), 8.19 (s, 1H), 7.88 (td, *J*₁ = 7.6 Hz, *J*₂ = 2.0 Hz, 1H), 7.69-7.65 (m, 1H), 7.62-7.57 (m, 1H), 7.38-7.34 (m, 1H), 5.59-5.52 (m, 1H), 2.33-2.23 (m, 2H), 2.16-2.12 (m, 2H), 2.00-1.96 (m, 2H), 1.82-1.79 (m, 1H), 1.52-1.37 (m, 3H); ¹³C NMR (100 MHz, CDCl₃): δ 148.9, 137.0, 131.2, 128.6, 128.2, 127.8, 127.3, 126.8, 126.1, 125.8, 123.7, 122.5, 117.6, 57.4, 31.9, 26.2, 25.5; HRMS (ESI, *m/z*) calcd. For C₂₂H₂₁BrN₃ [M+H]⁺: 406.0919; found: 406.0926.

3-cyclohexyl-5-fluoro-2-(pyridin-2-yl)-3H-naphtho[1,2-*d*]imidazole (22o)



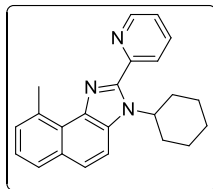
The general procedure for imidazole was followed. Column chromatography (SiO₂, eluting with 90:10 hexane/ethyl acetate) afforded the desired product as a white solid (63.5 mg, 92% yield), mp 128-130 °C. ¹H NMR (400 MHz, CDCl₃): δ 8.77 (d, *J* = 8.0 Hz, 1H), 8.71-8.69 (m, 1H), 8.34 (d, *J* = 8.0 Hz, 1H), 8.14 (d, *J* = 8.0 Hz, 1H), 7.87 (td, *J*₁ = 7.6 Hz, *J*₂ = 1.6 Hz, 1H), 7.69-7.66 (m, 1H), 7.57-7.53 (m, 2H), 7.36-7.33 (m, 1H), 5.61-5.23 (m, 1H), 2.31-2.21 (m, 2H), 2.15-2.11 (m, 2H), 1.99-1.95 (m, 2H), 1.82-1.78 (m, 1H), 1.52-1.33 (m, 3H); ¹³C NMR (100 MHz, CDCl₃): δ 155.7 (d, *J* = 245.4 Hz), 151.0, 148.9, 136.9, 129.9 (d, *J* = 13.4 Hz), 128.6, 127.6, 127.4 (d, *J* = 5.3 Hz), 125.5, 125.0, 123.5, 122.1, 121.3 (d, *J* = 5.7 Hz), 120.8 (d, *J* = 18.2 Hz), 98.2 (d, *J* = 27.3 Hz), 57.2, 31.7, 26.2, 25.6; ¹⁹F NMR (376 MHz, CDCl₃): δ -126.54 (s, 1F); HRMS (ESI, *m/z*) calcd. For C₂₂H₂₁FN₃ [M+H]⁺: 346.1720; found: 346.1719.

3-cyclohexyl-5-methyl-2-(pyridin-2-yl)-3H-naphtho[1,2-d]imidazole (22p)



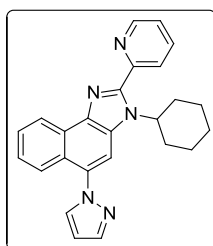
The general procedure for imidazole was followed. Column chromatography (SiO₂, eluting with 90:10 hexane/ethyl acetate) afforded the desired product as creamy white solid (58 mg, 85% yield), mp 132-134 °C. ¹H NMR (400 MHz, CDCl₃): δ 8.95 (s, 1H), 8.73-8.71 (m, 1H), 8.48 (s, 1H), 8.04 (d, *J* = 8.4 Hz, 1H), 7.93-7.89 (m, 1H), 7.69-7.65 (m, 2H), 7.58-7.55 (m, 1H), 7.38-7.35 (m, 1H), 5.59-5.50 (m, 1H), 2.81 (s, 3H), 2.40-2.31 (m, 2H), 2.16-2.12 (m, 2H), 1.99-1.96 (m, 2H), 1.83-1.79 (m, 1H), 1.52-1.37 (m, 3H); ¹³C NMR (100 MHz, CDCl₃): δ 151.2, 148.8, 148.0, 137.9, 136.9, 131.1, 130.1, 129.4, 127.3, 126.3, 125.6, 124.7, 123.3, 122.6, 113.9, 57.1, 31.9, 26.3, 25.6, 20.7; HRMS (ESI, *m/z*) calcd. For C₂₃H₂₄N₃ [M+H]⁺: 342.1970; found: 342.1971.

3-cyclohexyl-9-methyl-2-(pyridin-2-yl)-3H-naphtho[1,2-d]imidazole (22q)



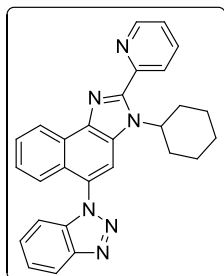
The general procedure for imidazole was followed. Column chromatography (SiO₂, eluting with 90:10 hexane/ethyl acetate) afforded the desired product as a creamy white solid (54.5 mg, 80% yield), mp 140-142 °C. ¹H NMR (400 MHz, CDCl₃): δ 8.70-8.68 (m, 1H), 8.42 (dt, *J*₁ = 8.0 Hz, *J*₂ = 0.8 Hz, 1H), 7.87-7.82 (m, 2H), 7.79-7.76 (m, 1H), 7.67 (d, *J* = 8.8 Hz, 1H), 7.43-7.36 (m, 2H), 7.32- 7.29 (m, 1H), 5.86-5.78 (m, 1H), 3.29 (s, 3H), 2.43-2.33 (m, 2H), 2.16-2.11 (m, 2H), 1.99-1.95 (m, 2H), 1.81 (d, *J* = 11.2 Hz, 1H), 1.55-1.35 (m, 3H); ¹³C NMR (100 MHz, CDCl₃): δ 148.6, 147.3, 136.8, 135.0, 132.53, 132.48, 131.0, 128.5, 126.5, 126.4, 125.7, 124.6, 124.2, 123.2, 113.5, 56.9, 31.7, 26.3, 25.7, 23.8; HRMS (ESI, *m/z*) calcd. For C₂₃H₂₄N₃ [M+H]⁺: 342.1970; found: 342.1973.

3-cyclohexyl-5-(1H-pyrazol-1-yl)-2-(pyridin-2-yl)-3H-naphtho[1,2-d]imidazole (22r)



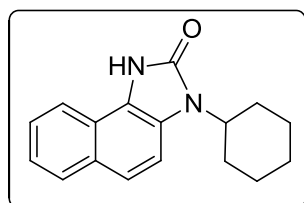
The general procedure for imidazole was followed. Column chromatography (SiO₂, eluting with 80:20 hexane/ethyl acetate) afforded the desired product as a creamy white solid (43 mg, 55% yield), mp 174-176 °C. ¹H NMR (400 MHz, CDCl₃): δ 8.85 (d, *J* = 8.0 Hz, 1H), 8.73-8.71 (m, 1H), 8.38 (d, *J* = 8.0 Hz, 1H), 7.95 (s, 1H), 7.92-7.84 (m, 3H), 7.68-7.64 (m, 1H), 7.60 (d, *J* = 8.0 Hz, 1H), 7.50-7.46 (m, 1H), 7.39-7.35 (m, 1H), 6.58 (t, *J* = 2.0 Hz, 1H), 5.62-5.54 (m, 1H), 2.34-2.23 (m, 2H), 2.17-2.13 (m, 2H), 1.96-1.91 (m, 2H), 1.76 (d, *J* = 12.4 Hz, 1H), 1.50-1.40 (m, 2H), 1.37-1.29 (m, 1H); ¹³C NMR (100 MHz, CDCl₃): δ 149.9, 149.0, 140.8, 137.1, 133.5, 132.5, 129.9, 127.3, 127.2, 126.6, 126.0, 125.9, 123.8, 123.6, 122.5, 112.1, 106.5, 57.5, 32.0, 26.2, 25.4; HRMS (ESI, *m/z*) calcd. For C₂₅H₂₄N₅ [M+H]⁺: 394.2032; found: 394.2036.

5-(1H-benzo[d][1,2,3]triazol-1-yl)-3-cyclohexyl-2-(pyridin-2-yl)-3H-naphtho[1,2-d]imidazole (22s)

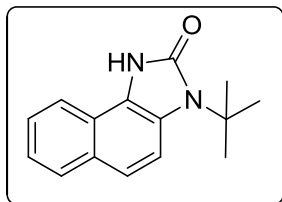


The general procedure for imidazole was followed. Column chromatography (SiO₂, eluting with 80:20 hexane/ethyl acetate) afforded the desired product as a creamy white solid (43.5 mg, 49% yield), mp 214-216 °C. ¹H NMR (400 MHz, CDCl₃): δ 8.90 (d, *J* = 8.0 Hz, 1H), 8.74-8.73 (m, 1H), 8.40 (d, *J* = 7.6 Hz, 1H), 8.26-8.21 (m, 1H), 8.07 (s, 1H), 7.91 (td, *J*₁ = 8.0 Hz, *J*₂ = 2.0 Hz, 1H), 7.71-7.67 (m, 1H), 7.51-7.46 (m, 2H), 7.45-7.37 (m, 2H), 7.30-7.27 (m, 2H), 5.67-5.59 (m, 1H), 2.29-2.16 (m, 4H), 1.91 (d, *J* = 13.2 Hz, 2H), 1.72 (d, *J* = 12.8 Hz, 1H), 1.49-1.38 (m, 2H), 1.31-1.20 (m, 1H); ¹³C NMR (100 MHz, CDCl₃): δ 150.6, 150.5, 149.0, 145.8, 140.3, 137.1, 135.4, 130.0, 128.3, 128.1, 127.6, 127.5, 126.2, 125.96, 125.92, 124.4, 123.9, 123.2, 122.8, 120.3, 113.6, 110.7, 57.6, 32.1, 26.1, 25.3; HRMS (ESI, *m/z*) calcd. For C₂₈H₂₅N₆ [M+H]⁺: 445.2141; found: 445.2140.

3-cyclohexyl-1H-naphtho[1,2-d]imidazol-2(3H)-one (25a)

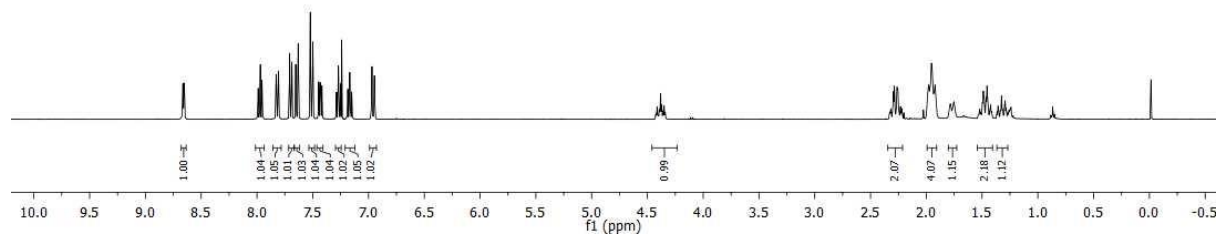
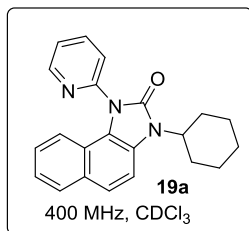
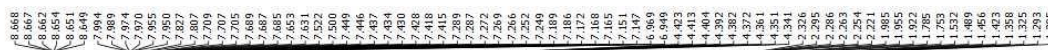
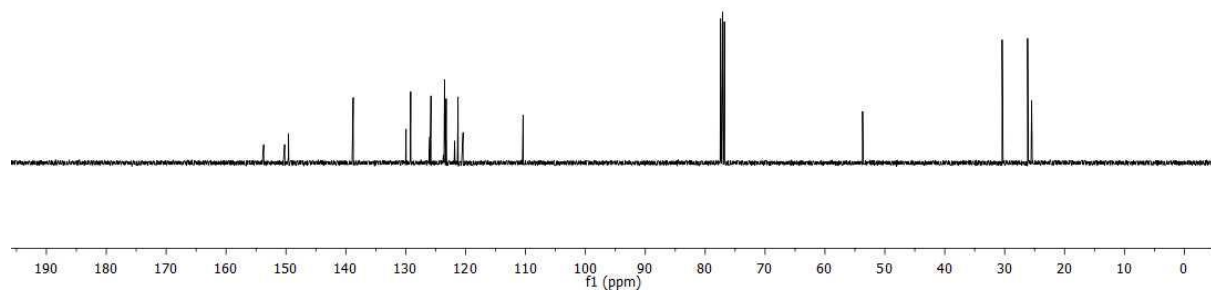
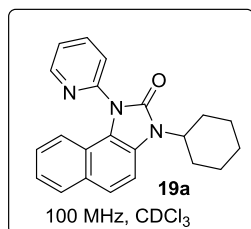


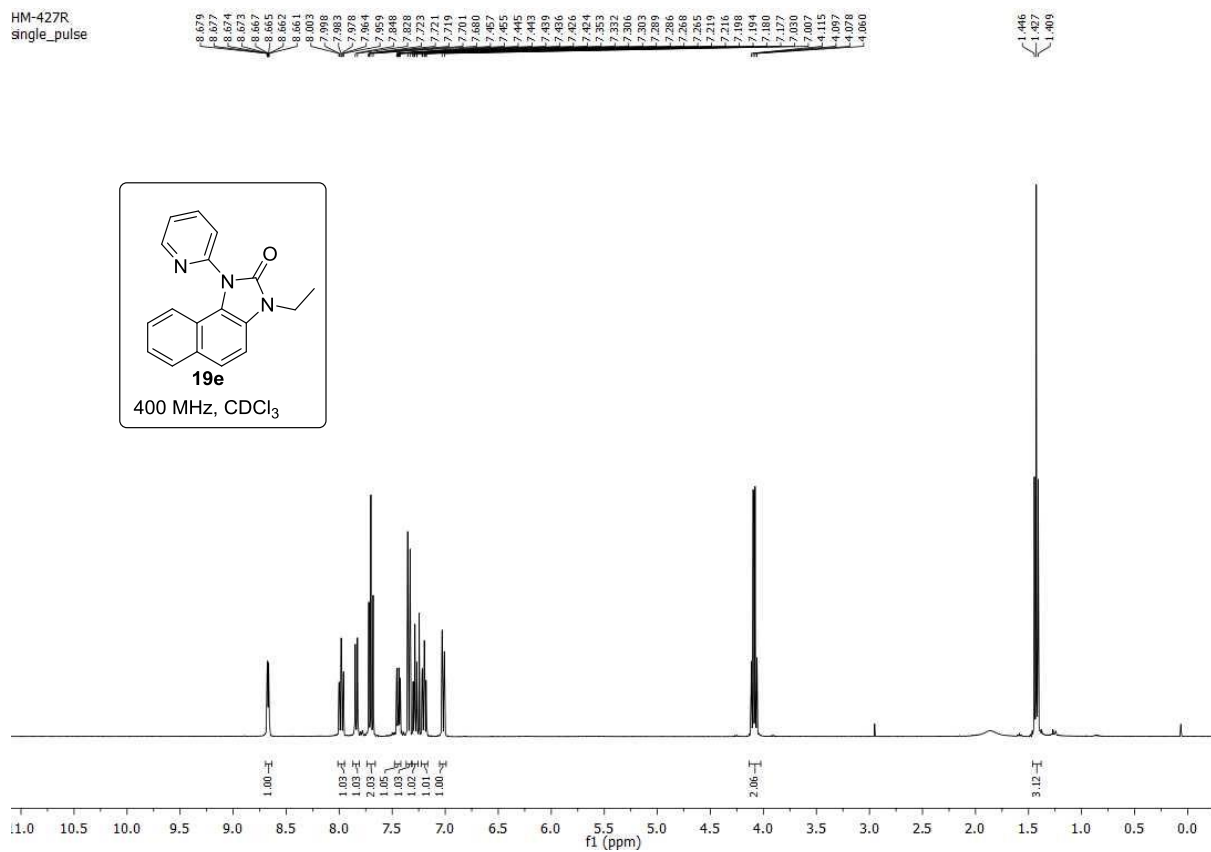
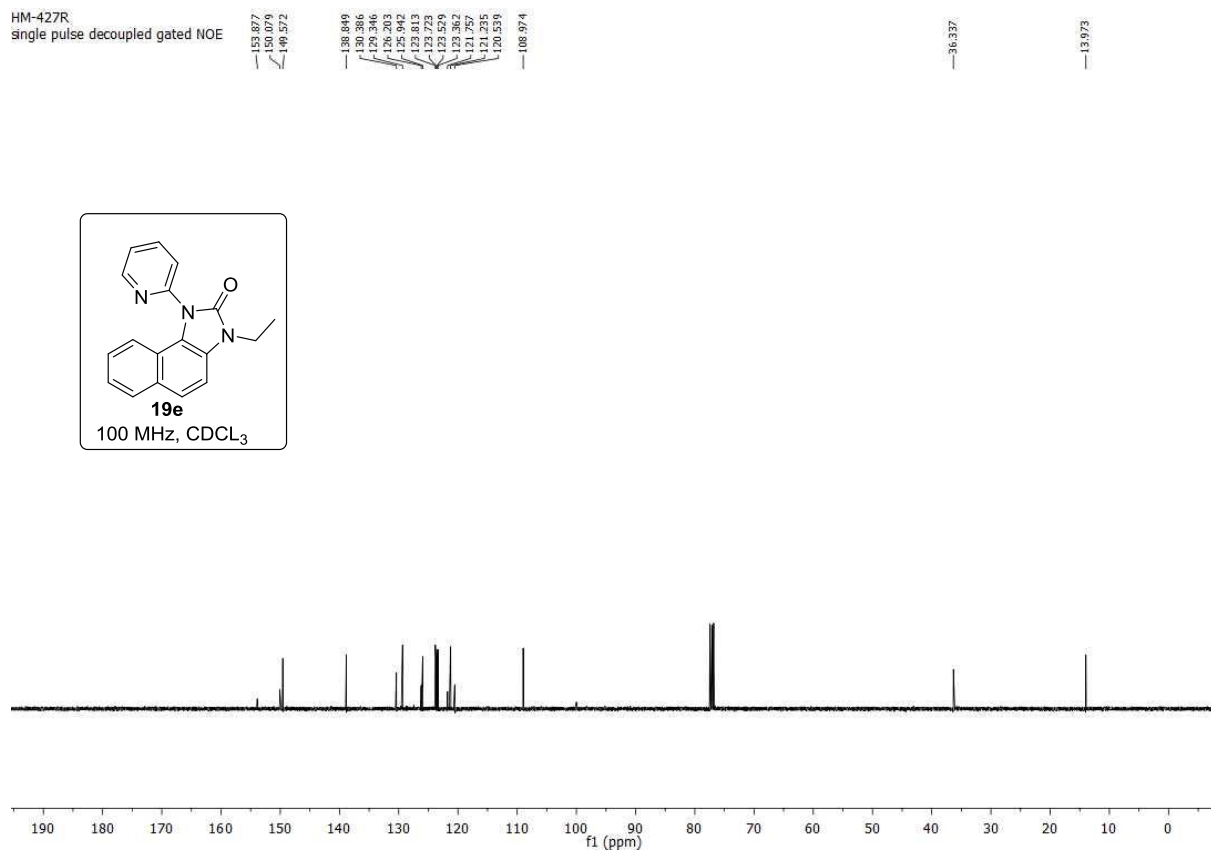
Column chromatography (SiO₂, eluting with 75:25 hexane/ethyl acetate) afforded the desired product as a light pink solid. ¹H NMR (400 MHz, CDCl₃): δ 11.40 (s, 1H), 8.04 (d, *J* = 8.0 Hz, 1H), 7.85 (d, *J* = 8.4 Hz, 1H), 7.58-7.53 (m, 2H), 7.50 (d, *J* = 8.8 Hz, 1H), 7.41-7.37 (m, 1H), 4.51-4.24 (m, 1H), 2.28-2.18 (m, 2H), 1.99-1.94 (m, 4H), 1.81 (d, *J* = 12.8 Hz, 1H), 1.59-1.48 (m, 2H), 1.39-1.32 (m, 1H); ¹³C NMR (100 MHz, CDCl₃): δ 155.4, 129.1, 128.6, 126.5, 124.9, 124.2, 122.5, 121.4, 120.6, 119.9, 110.9, 53.1, 30.8, 26.1, 25.5; HRMS (ESI, *m/z*) calcd. For C₁₇H₁₉N₂O [M+H]⁺: 267.1497; found: 267.1506.

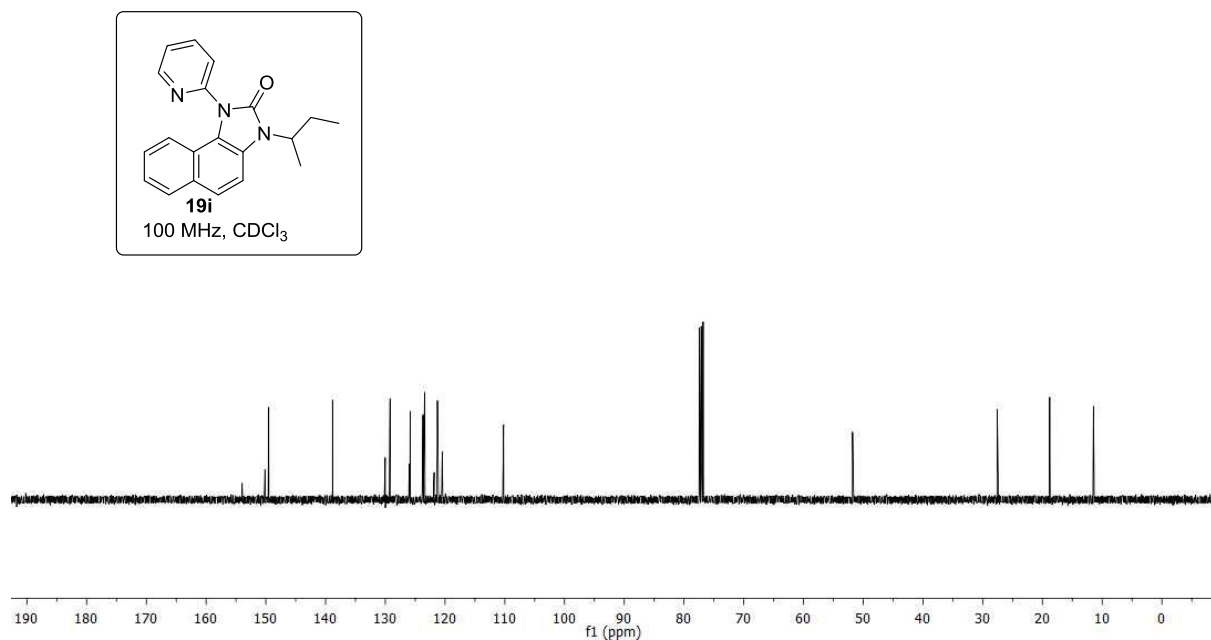
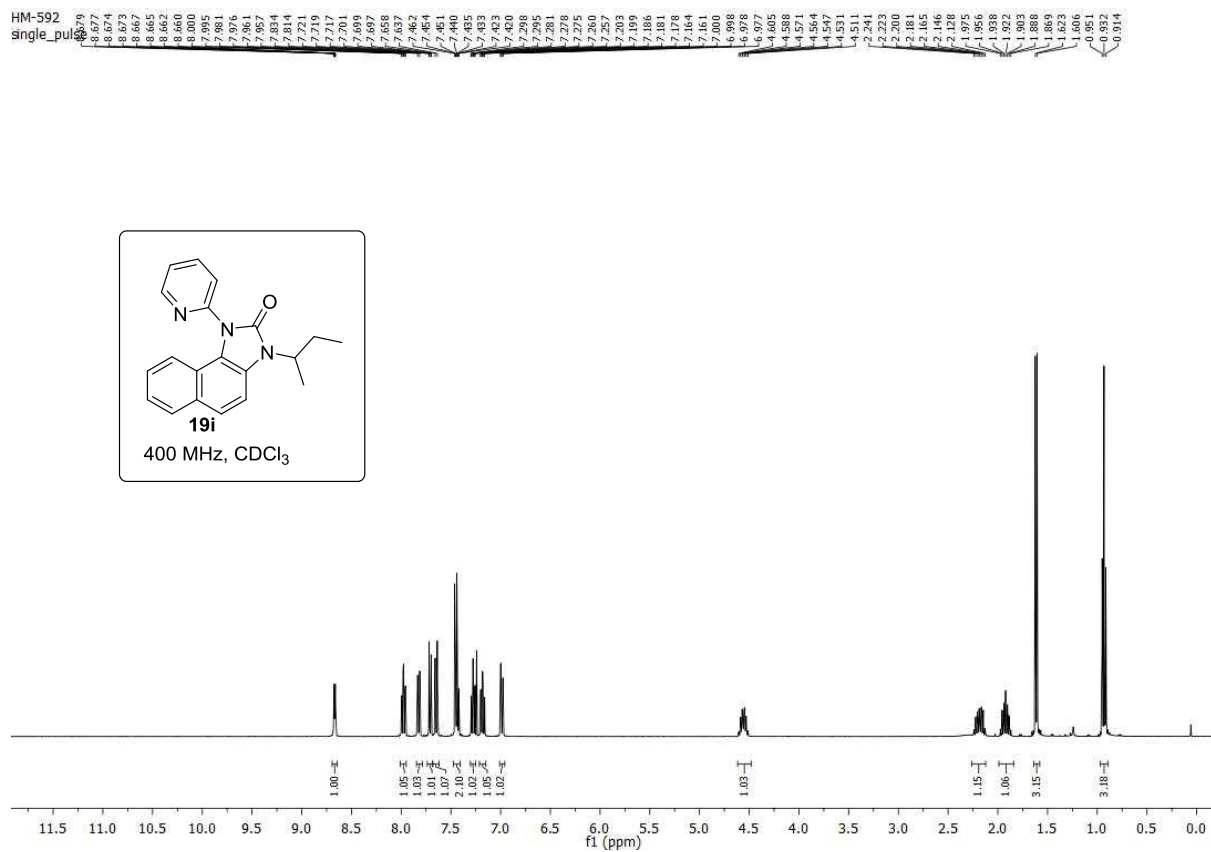
3-(*tert*-butyl)-1H-naphtho[1,2-d]imidazol-2(3H)-one (25b)

Column chromatography (SiO₂, eluting with 75:25 hexane/ethyl acetate) afforded the desired product as a white solid. ¹H NMR (400 MHz, CDCl₃): δ 11.71 (s, 1H), 8.05 (d, *J* = 8.4 Hz, 1H) 7.83 (d, *J* = 8.4 Hz, 1H), 7.69 (d, *J* = 8.8 Hz, 1H), 7.54-7.49 (m, 2H), 7.41-7.39 (m, 1H), 1.91 (s, 9H); ¹³C NMR (100 MHz, CDCl₃): δ 156.3, 128.8, 128.3, 126.2, 125.7, 124.3, 123.2, 120.7, 120.6, 119.7, 113.3, 58.6, 29.8; HRMS (ESI, *m/z*) calcd. For C₁₅H₁₇N₂O [M+H]⁺: 241.1341; found: 241.1344.

III.12. ¹H and ¹³C NMR spectra

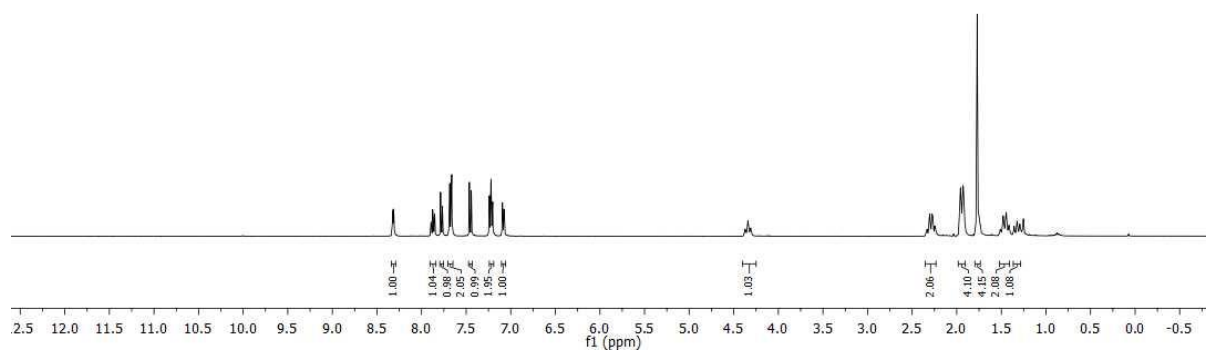
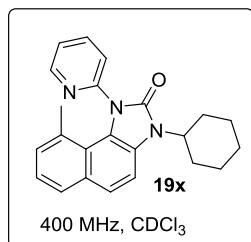
HM-345
single_pulseHM-345
single_pulse decoupled gated NOE

HM-427R
single_pulseHM-427R
single_pulse decoupled gated NOE



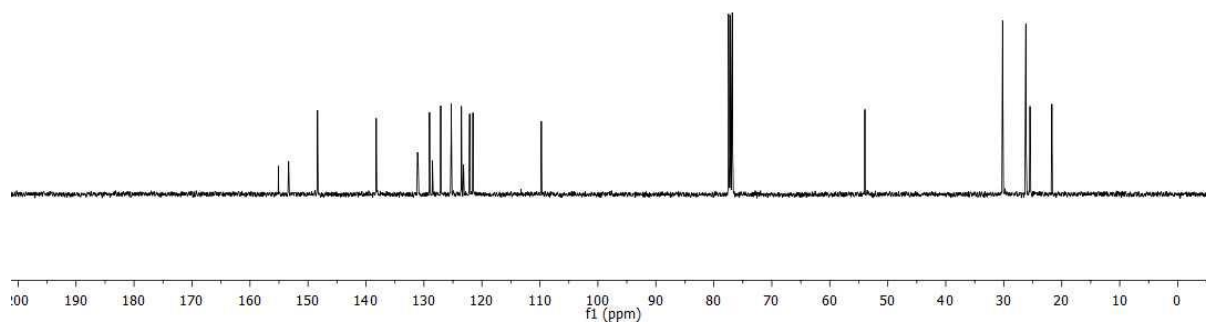
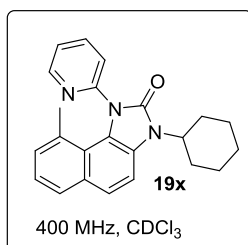
HM-810
single_pulse

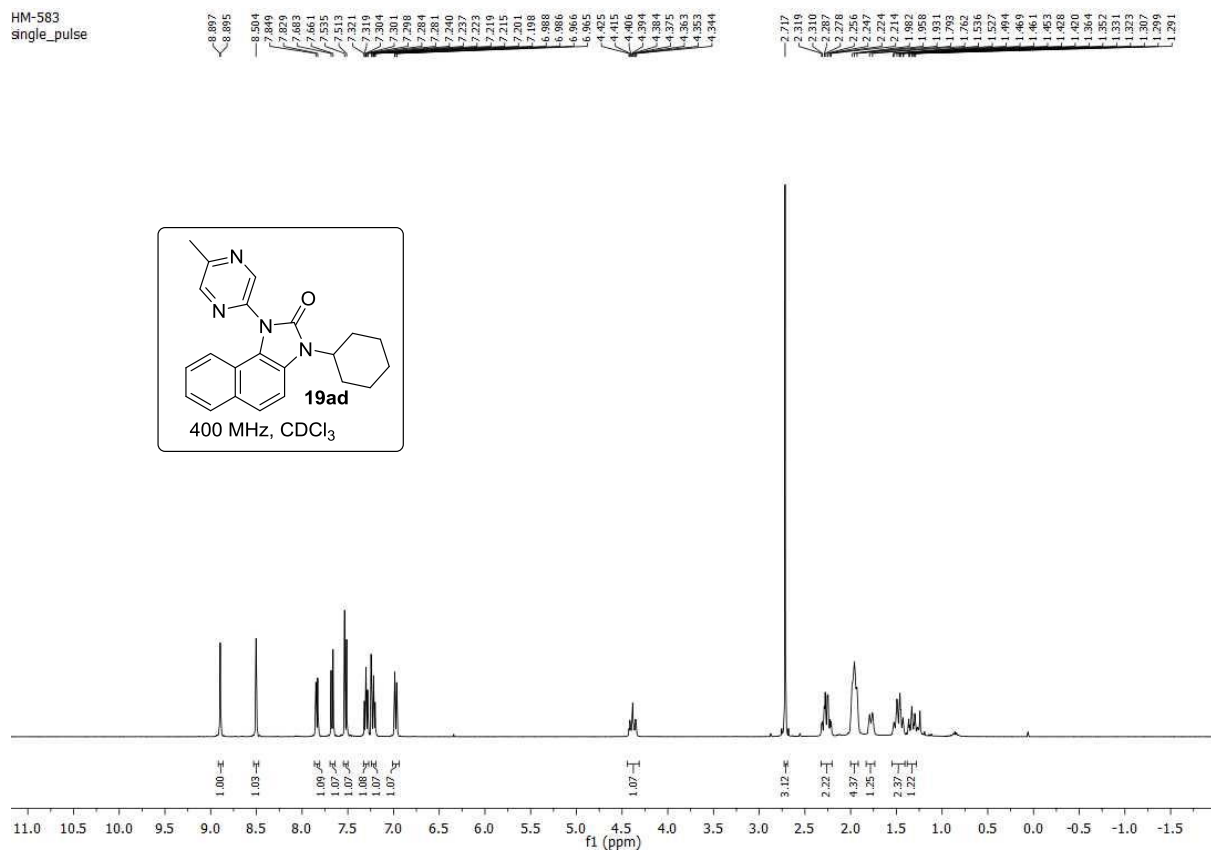
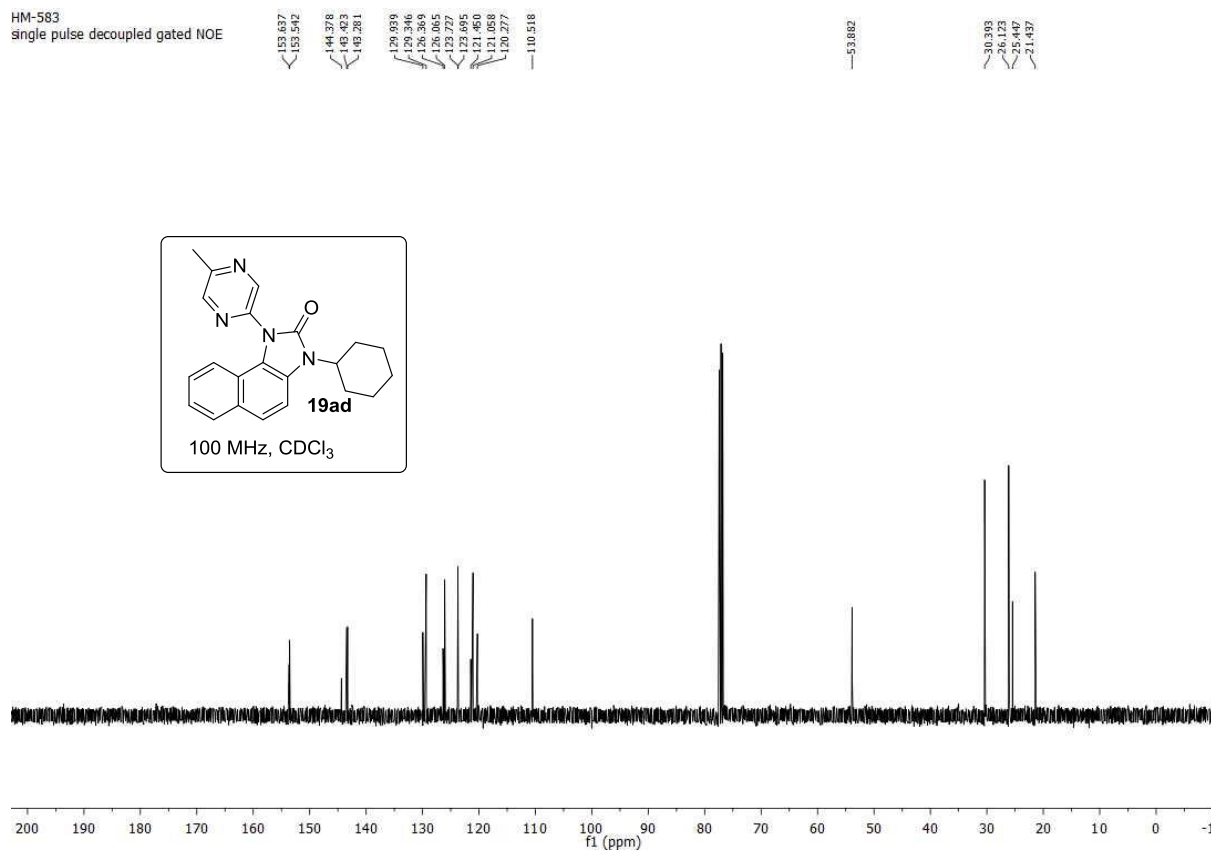
8.325
8.322
8.313
8.310
7.895
7.890
7.875
7.866
7.857
7.852
7.786
7.766
7.688
7.684
7.668
7.664
7.464
7.442
7.240
7.221
7.208
7.203
7.193
7.075
4.381
4.373
4.364
4.350
4.341
4.335
4.330
4.310
4.303
4.303
2.339
2.332
2.309
2.301
2.299
2.290
2.286
1.957
1.929
1.771
1.760
1.750
1.740
1.577
1.479
1.446
1.465
1.386
1.356
1.351
1.324
1.292
1.284



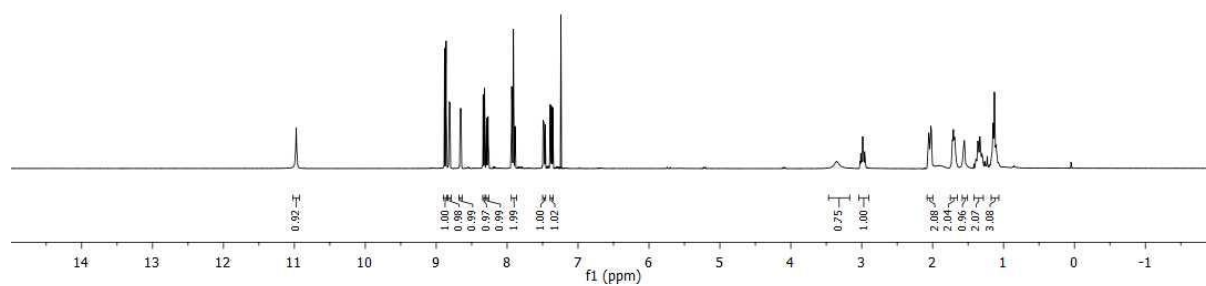
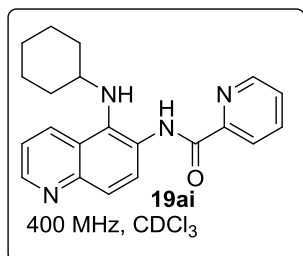
HM-810
single pulse decoupled gated NOE

155.099
153.339
148.354
138.729
131.110
131.022
129.832
129.816
127.108
125.305
123.534
123.168
122.164
122.113
121.354
109.749
53.946
30.192
26.478
21.691



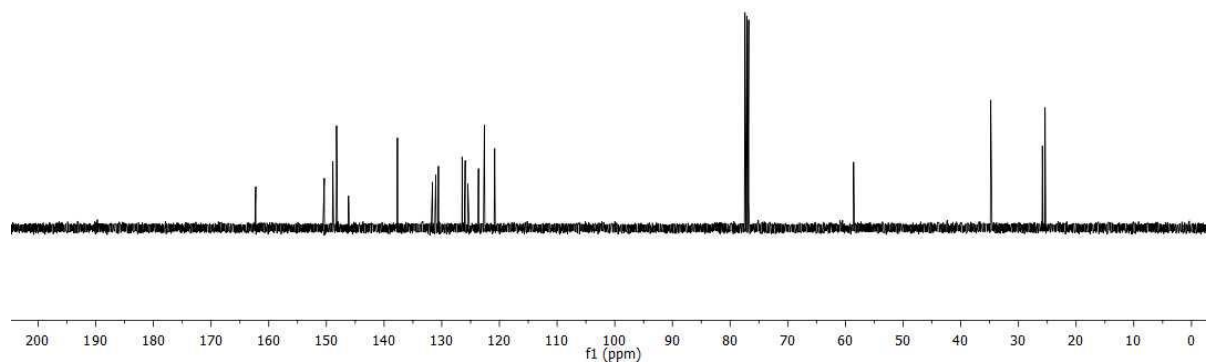
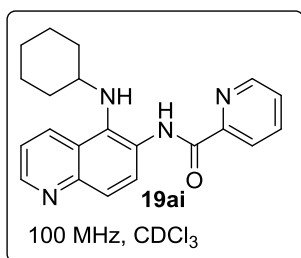
HM-583
single_pulseHM-583
single_pulse decoupled gated NOE

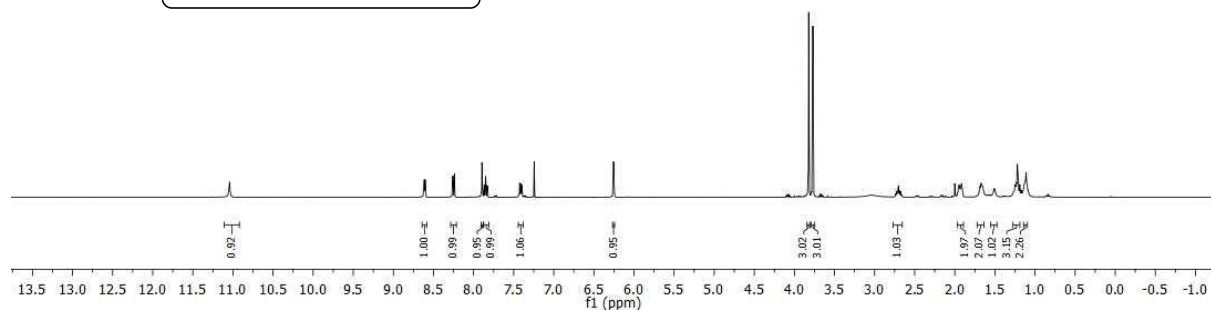
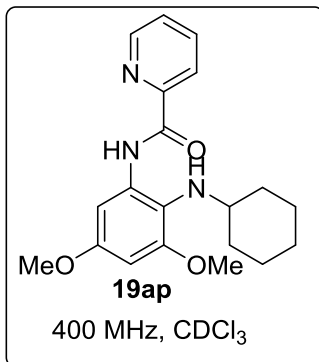
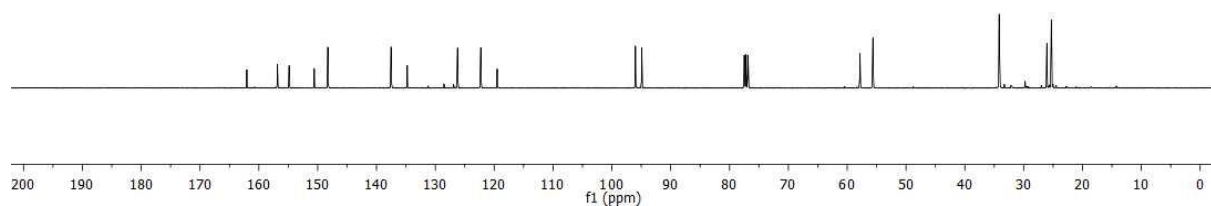
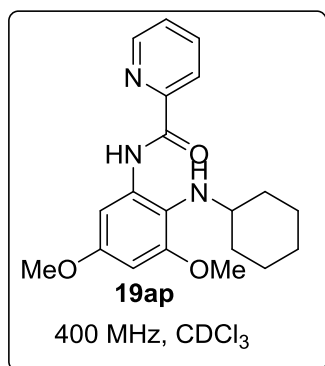
HM-421 1
single pulse decoupled gated NOE



HM-421 1
single pulse decoupled gated NOE

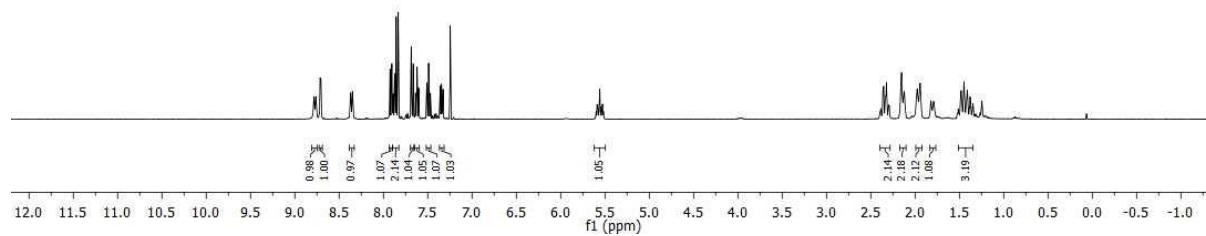
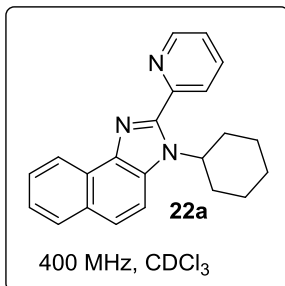
102.253, 150.760, 148.881, 148.243, 146.159, 137.684, 131.892, 131.033, 130.578, 126.470, 125.936, 125.473, 123.837, 123.613, 120.822, 58.584, 34.800, 25.855, 25.387.



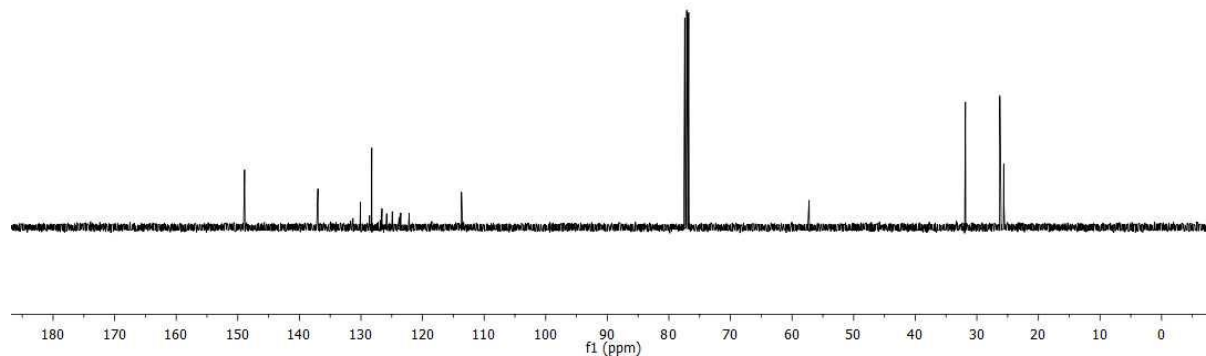
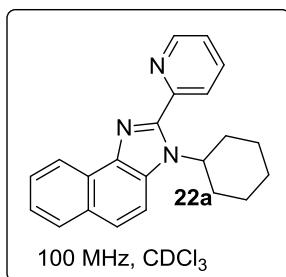
HM-1130
single_pulseHM-1130
single pulse decoupled gated NOE

HM-766
single_pulse

8.784
8.774
8.719
8.717
8.715
8.713
8.707
8.705
8.701
8.701
8.370
8.350
7.925
7.905
7.894
7.890
7.871
7.856
7.856
7.833
7.886
7.664
7.640
7.630
7.620
7.602
7.599
7.511
7.507
7.483
7.480
7.477
7.473
7.470
7.360
7.357
7.348
7.345
7.345
7.338
7.338
7.326
7.326
5.589
5.588
5.577
5.517
2.384
2.363
2.354
2.323
2.292
2.163
2.153
2.126
2.121
2.121
1.989
1.976
1.970
1.965
1.960
1.790
1.521
1.512
1.504
1.480
1.447
1.429
1.397
1.397

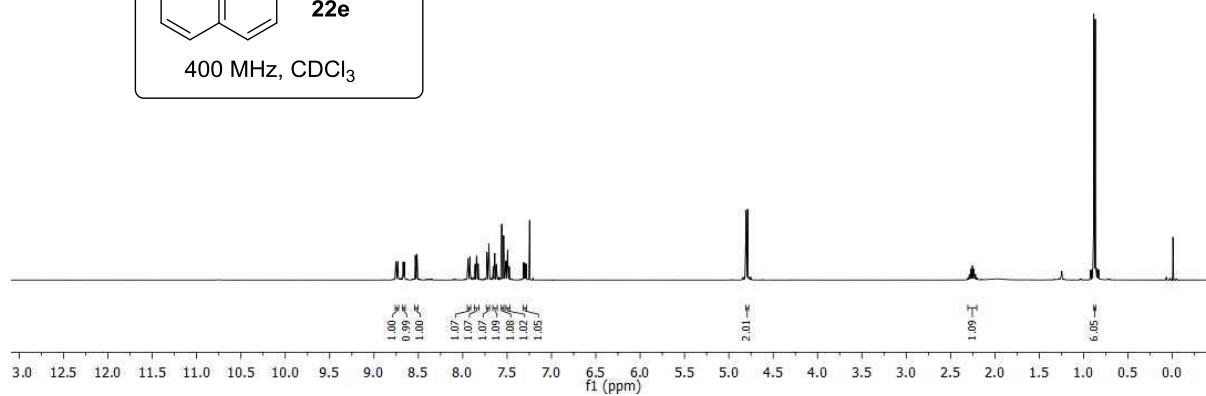
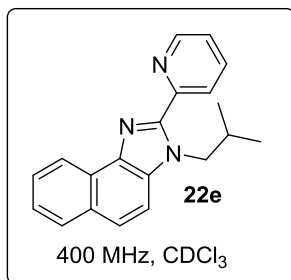
HM-766
single pulse decoupled gated NOE

148.894
136.040
131.729
130.079
128.594
128.239
126.582
125.829
125.482
125.402
123.806
123.791
123.545
123.534
122.198
113.879
-57.228
-31.854
-26.267
-25.630

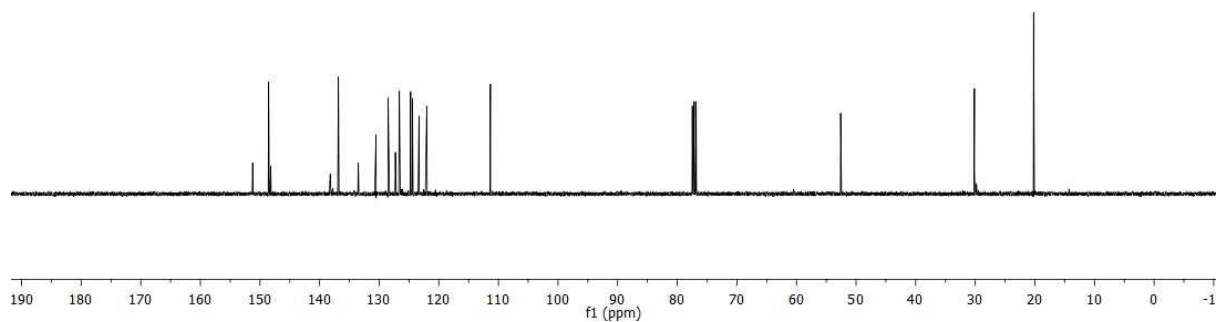
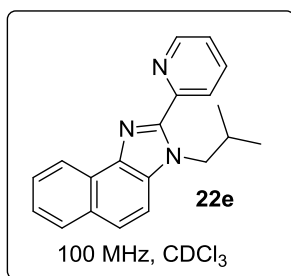


HM-815
single_pulse

8.765
8.756
8.752
8.734
8.729
8.674
8.672
8.668
8.662
8.660
8.658
8.656
8.537
8.532
8.517
8.514
8.512
7.939
7.930
7.885
7.882
7.845
7.841
7.826
7.821
7.727
7.705
7.685
7.666
7.641
7.638
7.635
7.621
7.618
7.614
7.598
7.581
7.558
7.512
7.512
7.497
7.494
7.491
7.484
7.474
7.316
7.313
7.304
7.297
7.284
7.285
7.275
4.887
4.887
4.789
2.306
2.289
2.271
2.254
2.254
2.218
2.202
0.885
0.885

HM-815
single_pulse decoupled gated NOE

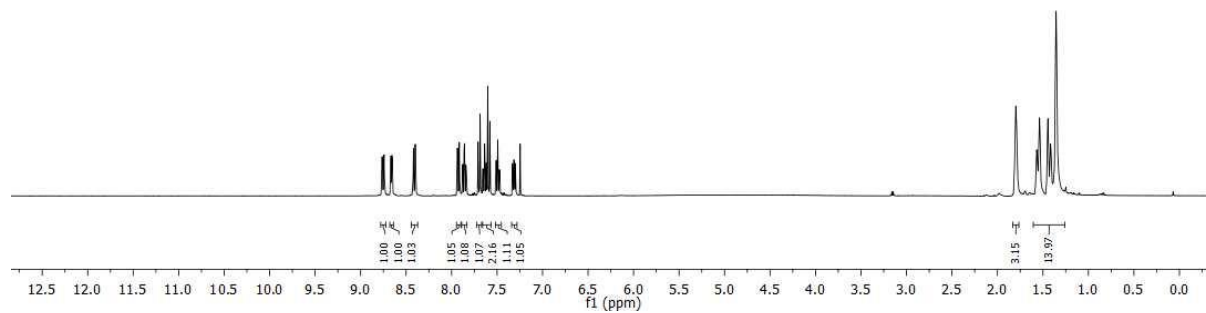
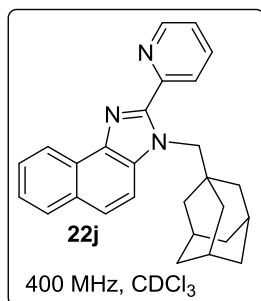
151.227
148.545
148.197
138.210
137.507
133.607
130.574
128.502
127.286
126.620
124.747
124.606
124.450
123.316
122.015
111.341
52.580
30.140
20.212



HM-783
single_pulse

8.763
8.762
8.670
8.668
8.666
8.664
8.658
8.656
8.654
8.652
8.651
8.419
8.417
8.402
8.399
8.398
8.396
7.916
7.882
7.877
7.863
7.861
7.858
7.856
7.708
7.686
7.657
7.655
7.640
7.637
7.635
7.630
7.617
7.602
7.580
7.513
7.510
7.492
7.492
7.489
7.475
7.472
7.331
7.328
7.319
7.318
7.312
7.300
7.300
7.297

1.798
1.568
1.537
1.445
1.416
1.355



HM-783

single_pulse decoupled gated NOE

151.966
149.114
148.374
137.118
134.233
130.407
128.655
128.655
127.888
126.648
126.648
124.784
124.667
123.519
122.015
112.279

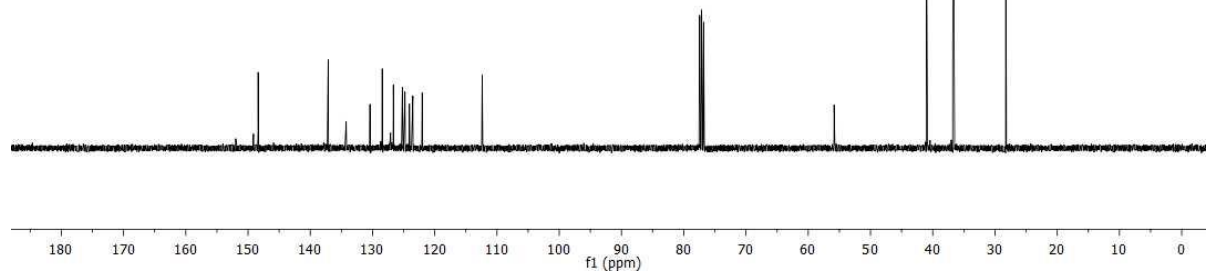
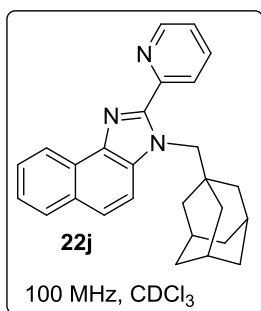
-55.842

-40.986

36.724

36.629

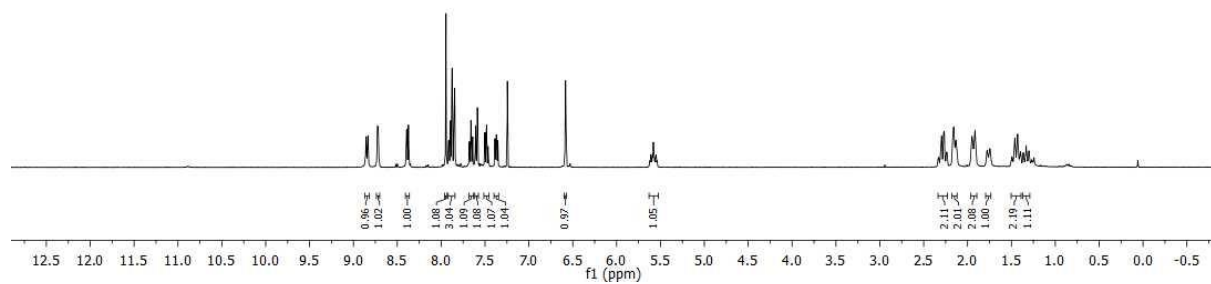
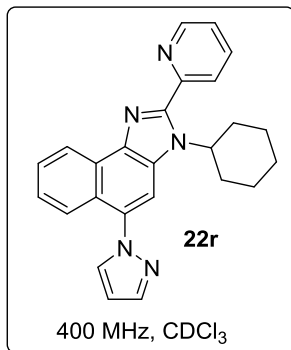
-28.289



HM-793
single_pulse

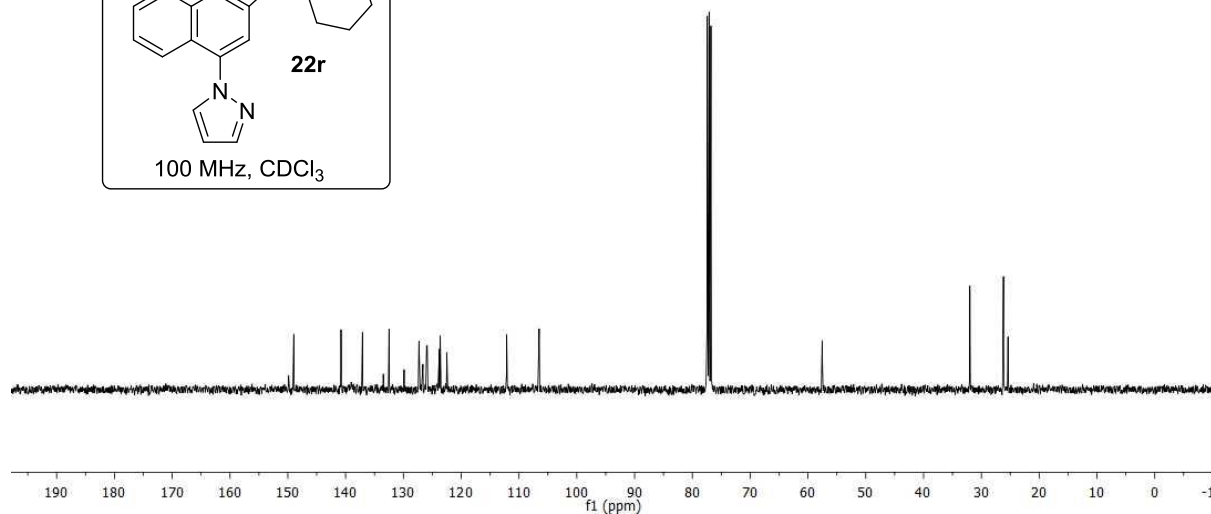
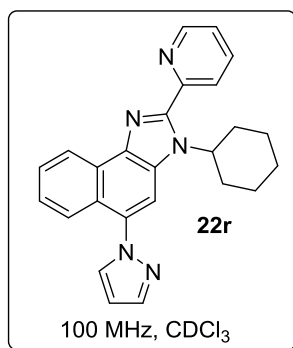
8.855
8.835
8.731
8.729
8.722
8.719
8.715
8.713
8.393
8.373
7.945
7.912
7.897
7.893
7.877
7.873
7.850
6.987
6.577

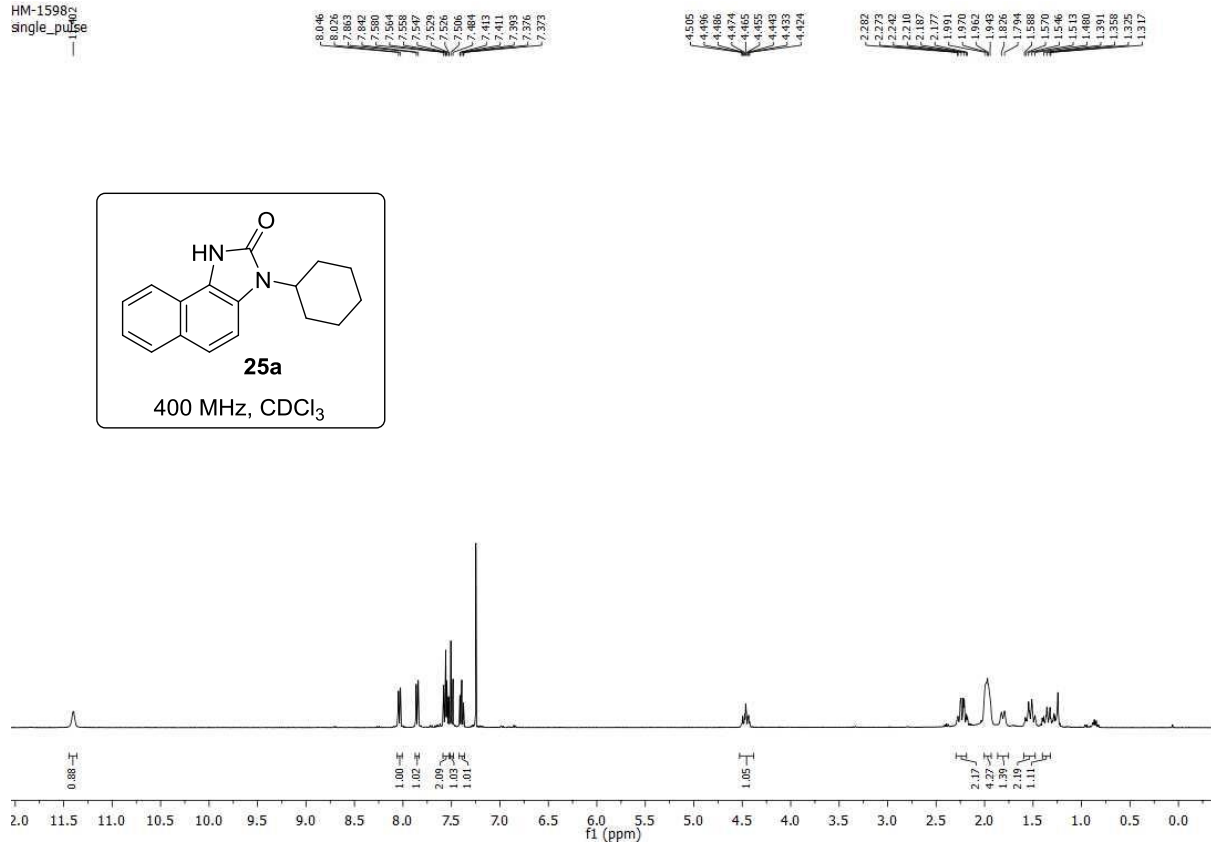
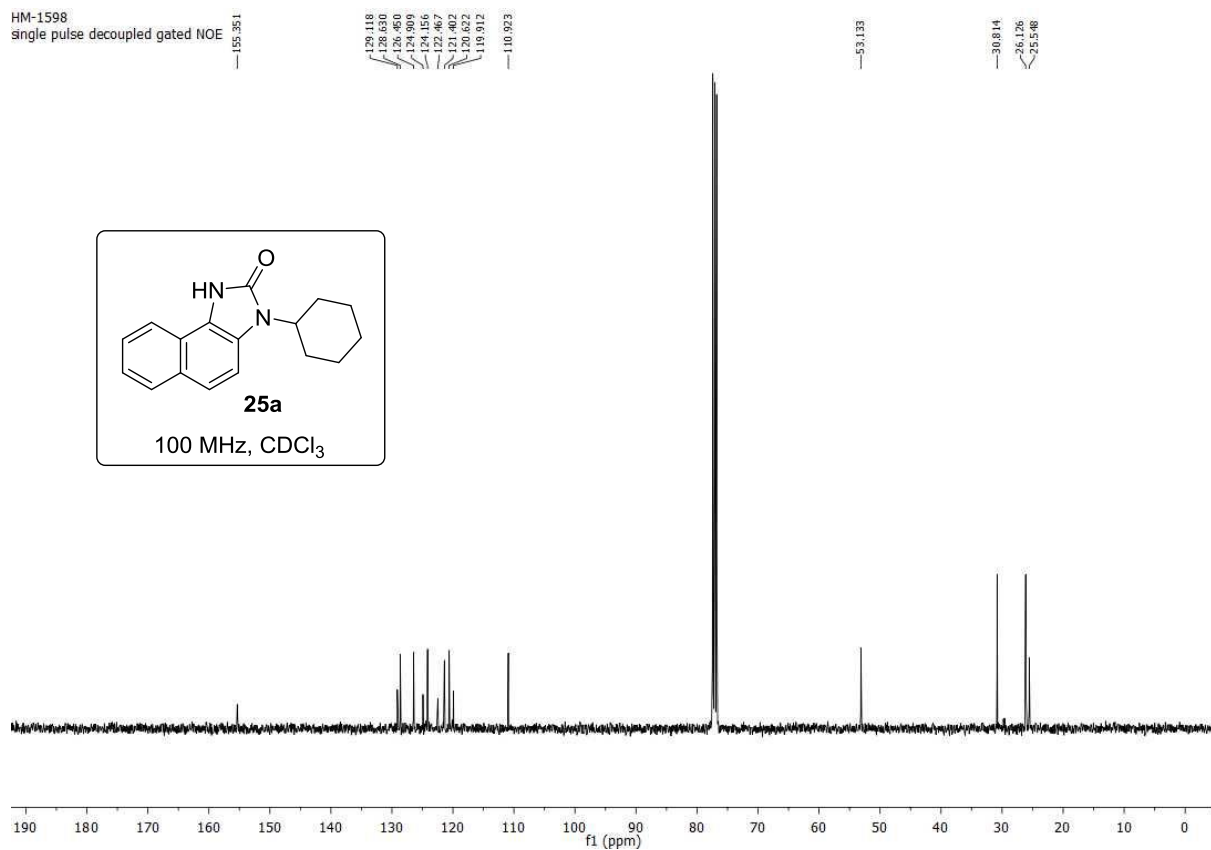
2.335
2.337
2.296
2.273
2.265
2.234
2.233
2.159
2.133
2.128
1.949
1.915
1.776
1.469
1.464
1.462
1.459
1.397
1.384
1.369
1.301
1.292

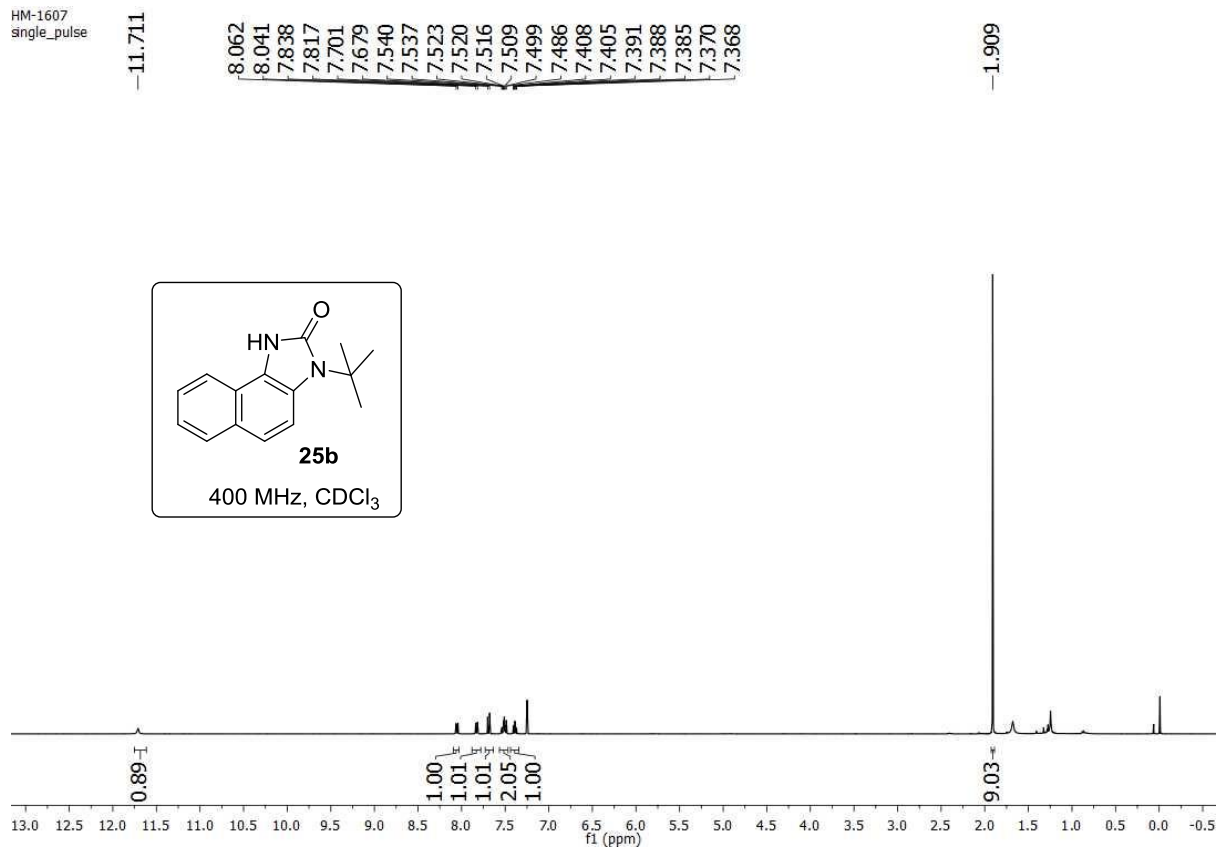
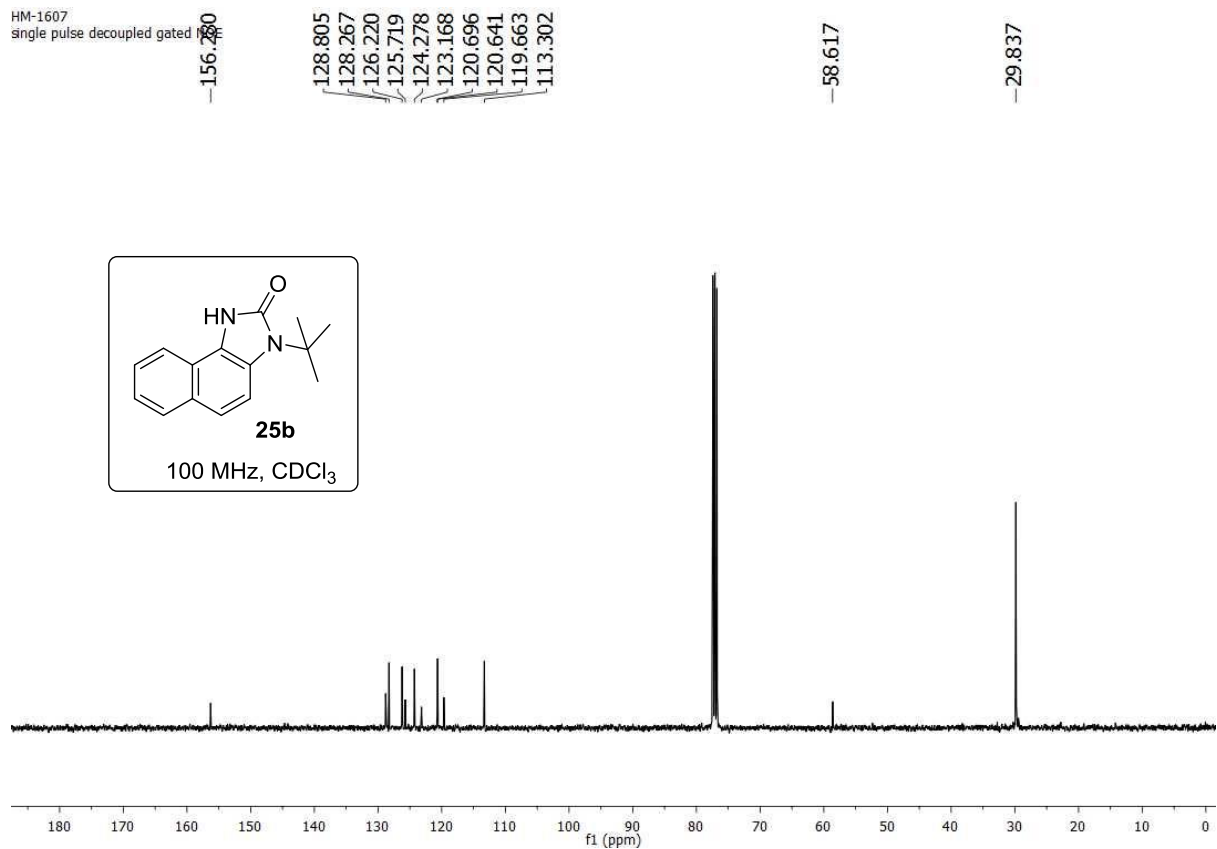
HM-793
single pulse decoupled gated NOE

149.850
148.866
140.794
137.084
133.478
132.484
129.874
129.711
127.715
126.623
125.979
125.883
123.829
123.634
122.486
112.132
106.307

57.542
31.998
26.179
25.388



HM-1598
single pulseHM-1598
single pulse decoupled gated NOE

HM-1607
single_pulseHM-1607
single_pulse decoupled gated

III.13. References

1. a) H. Omura, M. Kawai, A. Shima, Y. Iwata, F. Ito, T. Masuda, A. Ohta, N. Makita, K. Omoto, H. Sugimoto, A. Kikuchi, H. Iwata, K. Ando, *Bioorg. Med. Chem. Lett.*, 2008, **18**, 3310-3314; b) W. S. Palmer, G. Poncet-Montange, G. Liu, A. Petrocchi, N. Reyna, G. Subramanian, J. Theroff, A. Yau, M. Kost-Alimova, J. P. Bardenhagen, E. Leo, H. E. Shepard, T. N. Tieu, X. Shi, Y. Zhan, S. Zhao, M. C. Barton, G. Draetta, C. Toniatti, P. Jones, M. Geck Do, J. N. Andersen, *J. Med. Chem.*, 2016, **59**, 1440-1454; c) W. Liu, F. Lau, K. Liu, H. B. Wood, G. Zhou, Y. Chen, Y. Li, T. E. Akiyama, G. Castriota, M. Einstein, C. Wang, M. E. McCann, T. W. Doebber, M. Wu, C. H. Chang, L. McNamara, B. McKeever, R. T. Mosley, J. P. Berger, P. T. Meinke, *J. Med. Chem.*, 2011, **54**, 8541-8554; d) M. L. Barreca, A. Rao, L. De Luca, M. Zappalà, A.-M. Monforte, G. Maga, C. Pannecouque, J. Balzarini, E. De Clercq, A. Chimirri, P. Monforte, *J. Med. Chem.*, 2005, **48**, 3433-3437; e) A. Satoh, T. Sagara, H. Sakoh, M. Hashimoto, H. Nakashima, T. Kato, Y. Goto, S. Mizutani, T. Azuma-Kanoh, T. Tani, S. Okuda, O. Okamoto, S. Ozaki, Y. Iwasawa, H. Ohta, H. Kawamoto, *J. Med. Chem.*, 2009, **52**, 4091-4094; f) Q. Li, T. Li, K. W. Woods, W.-Z. Gu, J. Cohen, V. S. Stoll, T. Galicia, C. Hutchins, D. Frost, S. H. Rosenberg, H. L. Sham, *Bioorg. Med. Chem. Lett.*, 2005, **15**, 2918-2922.
2. a) Y. Bansal, O. Silakari, *Bioorg. Med. Chem.*, 2012, **20**, 6208-6236; b) M. Gaba, S. Singh, C. Mohan, *Eur. J. Med. Chem.*, 2014, **76**, 494-505.
3. a) L. Troisi, C. Granito, S. Perrone, F. Rosato, *Tetrahedron Lett.*, 2011, **52**, 4330-4332; b) B. Yu, H. Zhang, Y. Zhao, S. Chen, J. Xu, L. Hao, Z. Liu, *ACS Catal.*, 2013, **3**, 2076-2082.
4. D. B. Nale, B. M. Bhanage, *Green Chem.*, 2015, **17**, 2480-2486.
5. N. Wiriya, D. Yamano, S. Hongsibsong, M. Pattarawarapan, W. Phakhodee, *Synlett*.
6. X. Diao, Y. Wang, Y. Jiang, D. Ma, *J. Org. Chem.*, 2009, **74**, 7974-7977.
7. a) M. McLaughlin, M. Palucki, I. W. Davies, *Org. Lett.*, 2006, **8**, 3311-3314; b) N. Barbero, M. Carril, R. SanMartin, E. Domínguez, *Tetrahedron*, 2008, **64**, 7283-7288; c) A. Beyer, C. M. M. Reucher, C. Bolm, *Org. Lett.*, 2011, **13**, 2876-2879; d) Z. Li, H. Sun, H. Jiang, H. Liu, *Org. Lett.*, 2008, **10**, 3263-3266.
8. J. B. Ernst, N. E. S. Tay, N. T. Jui, S. L. Buchwald, *Org. Lett.*, 2014, **16**, 3844-3846.
9. R. Zeng, P.-h. Chen, G. Dong, *ACS Catal.*, 2016, **6**, 969-973.
10. R. D. Shingare, A. S. Kulkarni, R. L. Sutar, D. S. Reddy, *ACS Omega*, 2017, **2**, 5137-5141.

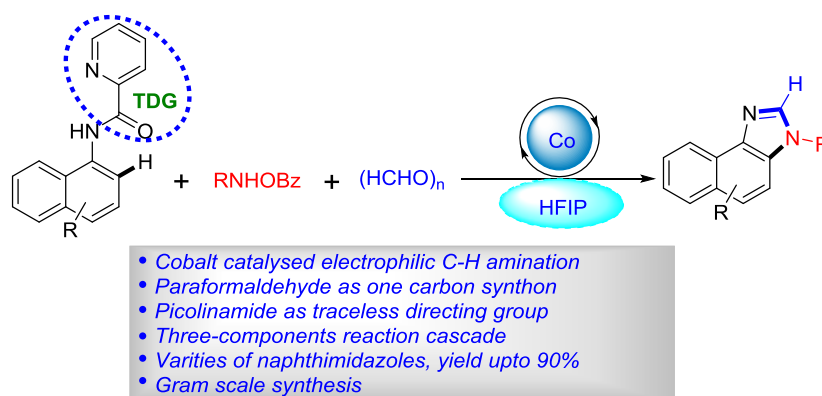
11. a) J. Yu, C. Gao, Z. Song, H. Yang, H. Fu, *Eur. J. Org. Chem.*, 2015, **2015**, 5869-5875; b) S. W. Youn, Y. H. Kim, *Org. Lett.*, 2016, **18**, 6140-6143; c) Y. Meng, B. Wang, L. Ren, Q. Zhao, W. Yu, J. Chang, *New J. Chem.*, 2018, **42**, 13790-13796; d) J.-S. Li, P.-P. Yang, X.-Y. Xie, S. Jiang, L. Tao, Z.-W. Li, C.-H. Lu, W.-D. Liu, *Adv. Synth. Catal.*, 2020, **362**, 1977-1981; e) Y. Wang, Y.-Y. Sun, Y.-M. Cui, Y.-X. Yu, Z.-G. Wu, *J. Org. Chem.*, 2022, **87**, 3234-3241.
12. a) R. W. Middleton, D. G. Wibberley, *J. Heterocycl. Chem.*, 1980, **17**, 1757-1760; b) G. V. Reddy, V. V. V. N. S. Rama Rao, B. Narsaiah, P. Shanthan Rao, *Synth. Commun.*, 2002, **32**, 2467-2476; c) S. S. Panda, R. Malik, S. C. Jain, *Curr. Org. Chem.*, 2012, **16**, 1905-1919.
13. a) M. Curini, F. Epifano, F. Montanari, O. Rosati, S. Taccone, *Synlett*, 2004, **2004**, 1832-1834; b) L.-H. Du, Y.-G. Wang, *Synthesis*, 2007, **2007**, 675-678; c) B. Das, H. Holla, Y. Srinivas, *Tetrahedron Lett.*, 2007, **48**, 61-64; d) R. Varala, A. Nasreen, R. Enugala, S. R. Adapa, *Tetrahedron Lett.*, 2007, **48**, 69-72.
14. a) E. Skolia, M. K. Apostolopoulou, N. F. Nikitas, C. G. Kokotos, *Eur. J. Org. Chem.*, 2021, **2021**, 422-428; b) A. J. Blacker, M. M. Farah, M. I. Hall, S. P. Marsden, O. Saidi, J. M. J. Williams, *Org. Lett.*, 2009, **11**, 2039-2042.
15. J. K. Laha, M. K. Hunjan, *J. Org. Chem.*, 2022, **87**, 2315-2323.
16. S. Das, S. Mallick, S. De Sarkar, *J. Org. Chem.*, 2019, **84**, 12111-12119.
17. a) C. T. Brain, J. T. Steer, *J. Org. Chem.*, 2003, **68**, 6814-6816; b) E. P. Arnold, P. K. Mondal, D. C. Schmitt, *ACS Comb. Sci.*, 2020, **22**, 1-5; c) N. Zheng, K. W. Anderson, X. Huang, H. N. Nguyen, S. L. Buchwald, *Angew. Chem. Int. Ed.*, 2007, **46**, 7509-7512.
18. a) G. Brasche, S. L. Buchwald, *Angew. Chem. Int. Ed.*, 2008, **47**, 1932-1934; b) H.-B. Zhao, J.-L. Zhuang, H.-C. Xu, *ChemSusChem*, 2021, **14**, 1692-1695.
19. A. Bose, S. Sau, P. Mal, *Eur. J. Org. Chem.*, 2019, **2019**, 4105-4109.
20. a) P. T. W. J. C. Anastas, *Green chemistry : theory and practice*, Oxford University Press, Oxford 1998; b) A. S. Matlack, *Introduction to green chemistry*, Marcel Dekker, New York, 2001.
21. T. Liang, H. Zhao, L. Gong, H. Jiang, M. Zhang, *iScience*, 2019, **15**, 127-135.
22. R. A. Ivanovich, D. E. Polat, A. M. Beauchemin, *Org. Lett.*, 2020, **22**, 6360-6364.

23. L. Jarrige, Z. Zhou, M. Hemming, E. Meggers, *Angew. Chem. Int. Ed.*, 2021, **60**, 6314-6319.
24. T. Liang, Z. Tan, H. Zhao, X. Chen, H. Jiang, M. Zhang, *ACS Catal.*, 2018, **8**, 2242-2246.
25. J. Xia, X. Yang, Y. Li, X. Li, *Org. Lett.*, 2017, **19**, 3243-3246.
26. S. Huang, H. Li, X. Sun, L. Xu, L. Wang, X. Cui, *Org. Lett.*, 2019, **21**, 5570-5574.
27. a) G. Rani, V. Luxami, K. Paul, *Chem. Commun.*, 2020, **56**, 12479-12521; b) M. Font, J. M. Quibell, G. J. P. Perry, I. Larrosa, *Chem. Commun.*, 2017, **53**, 5584-5597; c) P. Gandeepan, L. Ackermann, *Chem*, 2018, **4**, 199-222.
28. a) R. Manoharan, M. Jeganmohan, *Org. Biomol. Chem.*, 2018, **16**, 8384-8389; b) D. Kalsi, N. Barsu, B. Sundararaju, *Chem. Eur. J.*, 2018, **24**, 2360-2364; c) H. Ikemoto, R. Tanaka, K. Sakata, M. Kanai, T. Yoshino, S. Matsunaga, *Angew. Chem. Int. Ed.*, 2017, **56**, 7156-7160; d) X. Wu, Y. Lu, J. Qiao, W. Dai, X. Jia, H. Ni, X. Zhang, H. Liu, F. Zhao, *Org. Lett.*, 2020, **22**, 9163-9168; e) G. Liu, Y. Shen, Z. Zhou, X. Lu, *Angew. Chem. Int. Ed.*, 2013, **52**, 6033-6037; f) C. Zhu, R. Kuniyil, B. B. Jei, L. Ackermann, *ACS Catal.*, 2020, **10**, 4444-4450; g) X. Zhou, Z. Li, Z. Zhang, P. Lu, Y. Wang, *Org. Lett.*, 2018, **20**, 1426-1429; h) Y. Chen, D. Wang, P. Duan, R. Ben, L. Dai, X. Shao, M. Hong, J. Zhao, Y. Huang, *Nat. Commun.*, 2014, **5**, 4610; i) Y. Cheng, S. Yu, Y. He, G. An, G. Li, Z. Yang, *Chem. Sci.*, 2021, **12**, 3216-3225.
29. C. Yamamoto, K. Takamatsu, K. Hirano, M. Miura, *J. Org. Chem.*, 2017, **82**, 9112-9118.
30. H. M. Begam, R. Choudhury, A. Behera, R. Jana, *Org. Lett.*, 2019, **21**, 4651-4656.
31. B. K. Singh, A. Polley, R. Jana, *J. Org. Chem.*, 2016, **81**, 4295-4303.
32. a) G. Brasche, S. L. Buchwald, *Angew. Chem. Int. Ed.*, 2008, **47**, 1932-1934; b) S. Ueda, H. Nagasawa, *Angew. Chem. Int. Ed.*, 2008, **47**, 6411-6413.
33. a) X. Dong, Q. Liu, Y. Dong, H. Liu, *Chem. Eur. J.*, 2017, **23**, 2481-2511; b) X. Yan, X. Yang, C. Xi, *Catal. Sci. Technol.*, 2014, **4**, 4169-4177; c) M.-L. Louillat, F. W. Patureau, *Chem. Soc. Rev.*, 2014, **43**, 901-910; d) J.-S. Yu, M. Espinosa, H. Noda, M. Shibasaki, *J. Am. Chem. Soc.*, 2019, **141**, 10530-10537.
34. a) D. Mondal, S. Biswas, A. Paul, S. Baitalik, *Inorg. Chem.*, 2017, **56**, 7624-7641; b) A. Klapars, K. R. Campos, J. H. Waldman, D. Zewge, P. G. Dormer, C.-y. Chen, *J. Org. Chem.*, 2008, **73**, 4986-4993.

35. a) P. W. Tan, A. M. Mak, M. B. Sullivan, D. J. Dixon, J. Seayad, *Angew. Chem. Int. Ed.*, 2017, **56**, 16550-16554; b) T. Yamauchi, F. Shibahara, T. Murai, *Org. Lett.*, 2015, **17**, 5392-5395; c) K.-X. Tang, C.-M. Wang, T.-H. Gao, C. Pan, L.-P. Sun, *Org. Chem. Front.*, 2017, **4**, 2167-2169; d) Y.-H. Liu, P.-X. Li, Q.-J. Yao, Z.-Z. Zhang, D.-Y. Huang, M. D. Le, H. Song, L. Liu, B.-F. Shi, *Org. Lett.*, 2019, **21**, 1895-1899; e) R.-H. Liu, Q.-C. Shan, X.-H. Hu, T.-P. Loh, *Chem. Commun.*, 2019, **55**, 5519-5522; f) Z.-Z. Zhang, G. Liao, H.-M. Chen, B.-F. Shi, *Org. Lett.*, 2021, **23**, 2626-2631; g) Z.-J. Cai, C.-X. Liu, Q. Wang, Q. Gu, S.-L. You, *Nat. Commun.*, 2019, **10**, 4168; h) A. T. Tran, J.-Q. Yu, *Angew. Chem. Int. Ed.*, 2017, **56**, 10530-10534; i) A. Modi, P. Sau, N. Chakraborty, B. K. Patel, *Adv. Synth. Catal.*, 2019, **361**, 1368-1375.
36. a) B. Chen, X.-L. Hou, Y.-X. Li, Y.-D. Wu, *J. Am. Chem. Soc.*, 2011, **133**, 7668-7671; b) J. Phipps Robert, J. Gaunt Matthew, *Science*, 2009, **323**, 1593-1597; c) X. Ribas, C. Calle, A. Poater, A. Casitas, L. Gómez, R. Xifra, T. Parella, J. Benet-Buchholz, A. Schweiger, G. Mitrikas, M. Solà, A. Llobet, T. D. P. Stack, *J. Am. Chem. Soc.*, 2010, **132**, 12299-12306; d) A. E. King, L. M. Huffman, A. Casitas, M. Costas, X. Ribas, S. S. Stahl, *J. Am. Chem. Soc.*, 2010, **132**, 12068-12073.
37. X.-G. Liu, H. Gao, S.-S. Zhang, Q. Li, H. Wang, *ACS Catal.*, 2017, **7**, 5078-5086.
38. C.-Q. Wang, Y. Zhang, C. Feng, *Angew. Chem. Int. Ed.*, 2017, **56**, 14918-14922.
39. J. Yang, G. B. Dudley, *J. Org. Chem.*, 2009, **74**, 7998-8000.
40. K. C. Nicolaou, D. G. McGarry, P. K. Somers, C. A. Veale, G. T. Furst, *J. Am. Chem. Soc.*, 1987, **109**, 2504-2506.
41. V. Smout, A. Pesciulli, S. Verbeeck, E. A. Mitchell, W. Herrebout, P. Bultinck, C. M. L. Vande Velde, D. Berthelot, L. Meerpoel, B. U. W. Maes, *J. Org. Chem.*, 2013, **78**, 9803-9814.

Chapter IV

Cobalt catalysed electrophilic C-H amination/cyclisation cascade with *O*-benzoyloxy primary amines using paraformaldehyde as C1 synthon: direct access to naphthimidazoles using picolinamide as traceless directing group



Abstract: A concise and efficient method has been developed herein for the synthesis of valuable naphthimidazole derivatives. It involves earth-abundant cobalt catalysed electrophilic *ortho* C-H amination/cyclisation cascade with *O*-benzoyloxy primary amines using paraformaldehyde as one carbon synthon. Picolinamide DG has been utilised as a trace-less directing group. The reaction conditions are very simple and easy handling making this methodology valuable and appealing.

Manuscript is under preparation.

Cobalt catalysed electrophilic C-H amination/cyclisation cascade with *O*-benzoyloxy primary amines using paraformaldehyde as C1 synthon: direct access to naphthimidazoles using picolinamide as traceless directing group

IV.1. Introduction

2-Unsubstituted imidazoles/benzimidazoles are core structures of many bioactive molecules exhibiting important biological properties such as FabI, Nek2 and lymphocyte specific kinase (Lck) inhibition (**Figure 1**).¹ These moieties are also present in many marketed anti-cytomegalovirus drugs such as ganciclovir, valacyclovir and valganciclovir (**Figure 1**).² In addition, they also serve as precursors for the preparation of an important class of *N*-heterocyclic carbenes (NHCs) that have been effectively employed as ligands in organocatalysis and also in transition metal catalysis.³ 2-Substituted benzimidazoles are being valuable *N*-heterocycle with wide range of biological properties can be synthesized from the 2-unsubstituted benzimidazoles via C2-H functionalization or by many other methods. So, therefore, development of efficient protocols for the synthesis of 2-unsubstituted benzimidazoles is highly demanding.

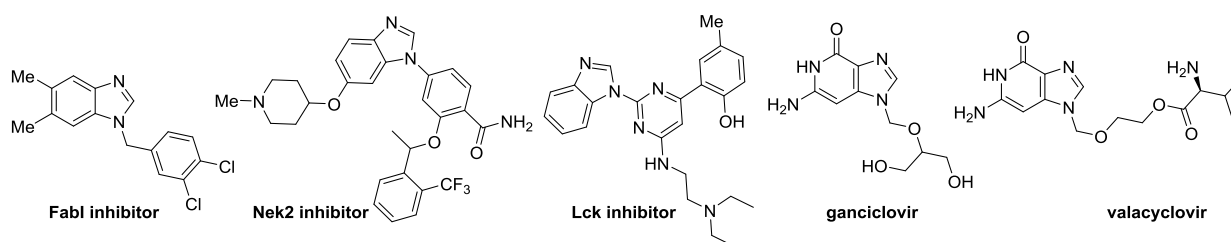
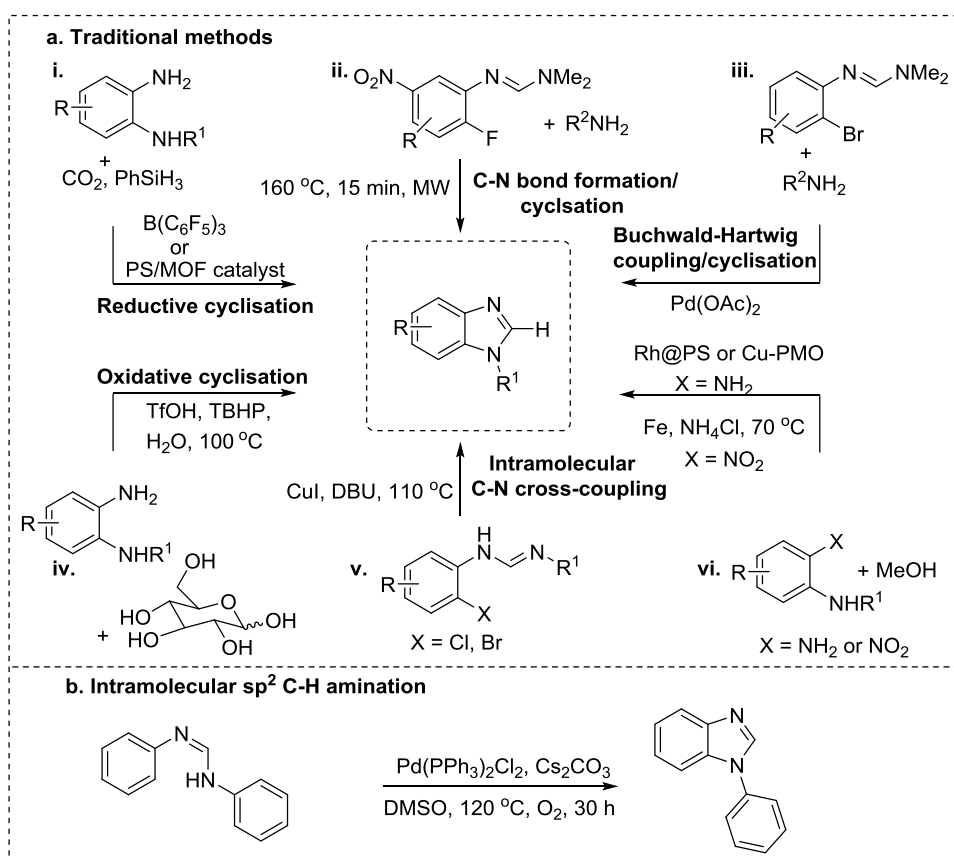


Figure 1. Some examples of 2-unsubstituted imidazole/benzimidazole containing bio-active molecules

Traditionally, they are prepared by coupling benzene-1,2-diamines with various C-1 synthons. For example, CO₂ has been utilized as C-1 synthon for the synthesis of 2-unsubstituted benzimidazoles under many reducing conditions (**Scheme 2ai**).⁴ MeOH also served as C-1 synthon to synthesize 2-unsubstituted benzimidazoles from benzene-1,2-diamines or 2-nitroanilines (**Scheme 2avii**).⁵ In this context, the Senadi group in 2020, disclosed D-glucose as C-1 synthon for the same purpose via an oxidative cyclization mechanism (**Scheme 2aiv**).⁶ DMSO has also been utilized as C-1 synthon for the same purpose.⁷ These benzimidazoles can also be made by reacting *ortho*-fluoro aryl formamides with primary amine under microwave condition (**Scheme**

2a).⁸ The reaction takes place through substitution of fluoro groups with the amine followed by intramolecular cyclisation. A copper catalyzed intramolecular C-N cross-coupling method was also reported by the Glorius group in 2009, for the synthesis of these 2-unsubstituted benzimidazoles from the corresponding aryl formamidines (**Scheme 2av**).⁹ In 2021, the Liu group reported the synthesis of *N*-1-alkyl-2-unsubstituted benzimidazoles *via* Pd-catalyzed Buchwald-Hartwig coupling followed by intramolecular cyclisation starting from *ortho*-bromo formimidamides (**Scheme 2a**).¹⁰ Synthesis of these 2-unsubstituted benzimidazoles has also been achieved by intramolecular aerobic oxidative C-H amination under Pd-catalysis (**Scheme 2b**).¹¹



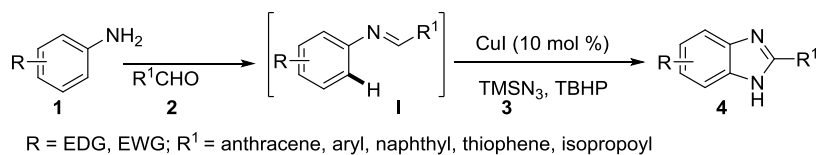
Scheme 2. Traditional methods vs. C-H amination for the synthesis of 2-unsubstituted benzimidazole

IV.2. Review

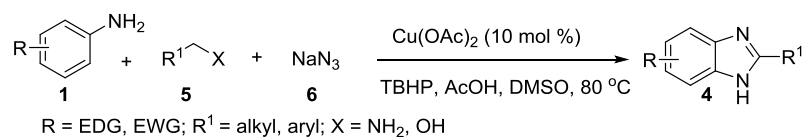
A detailed discussion on the synthesis of benzimidazoles *via* nucleophilic or electrophilic C-H amination involving two-component cascade reactions has been mentioned in the previous chapter. On the other hand, multicomponent cascade reactions would be very promising as they are

considered as an ideal route for the total synthesis of natural products and also for efficient construction of complex molecules from simple precursors in one-pot.¹² These reactions are generally more atom-economic as well as step-economic than the stepwise synthesis.

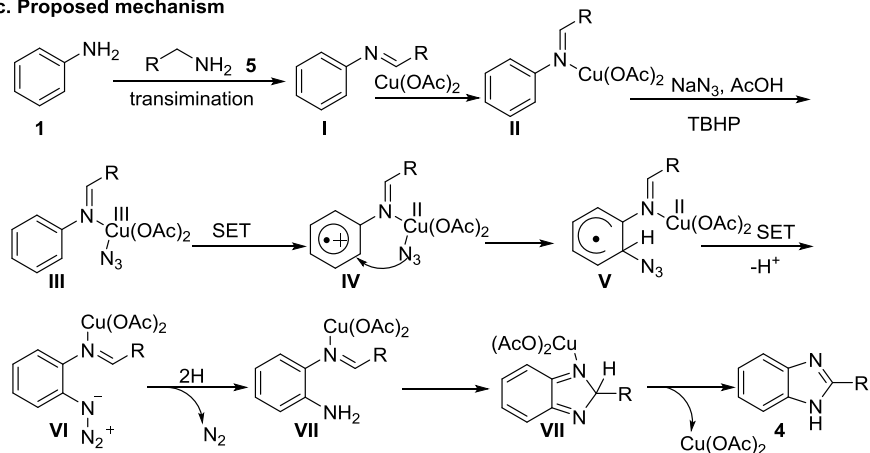
a. The Punniamurthy group, 2014



b. The Punniamurthy group, 2016



c. Proposed mechanism

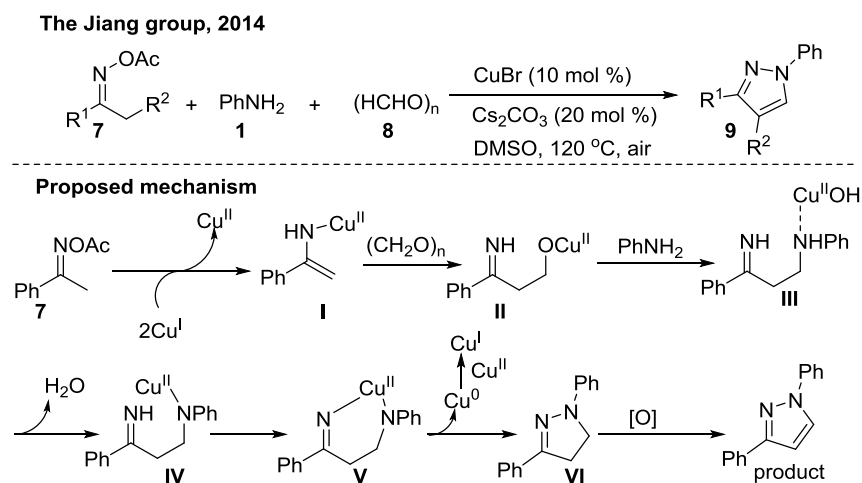


Scheme 3. Copper catalyzed three-component reaction cascade for the synthesis of benzimidazoles

Cascade reactions involving C-N bond formation for the synthesis of various valuable *N*-heterocycles are very promising research field.¹³ Multi-component Mannich alkylation and click reactions have explored for the synthesis of *N*-heterocycles.¹⁴ Synthesis of benzimidazoles has also been achieved by C-N bond forming multi-component cascade mostly using three-component reactions. In this direction the Punniamurthy group in 2014, unveiled an efficient protocol for the synthesis of benzimidazoles *via* copper catalyzed three-component reaction cascade (**Scheme 3a**).¹⁵ The reaction proceeds through formation of an imine by condensation of anilines with aldehydes followed by *ortho*-C-H amination with azides using this imine as directing group and then oxidative cyclisation.

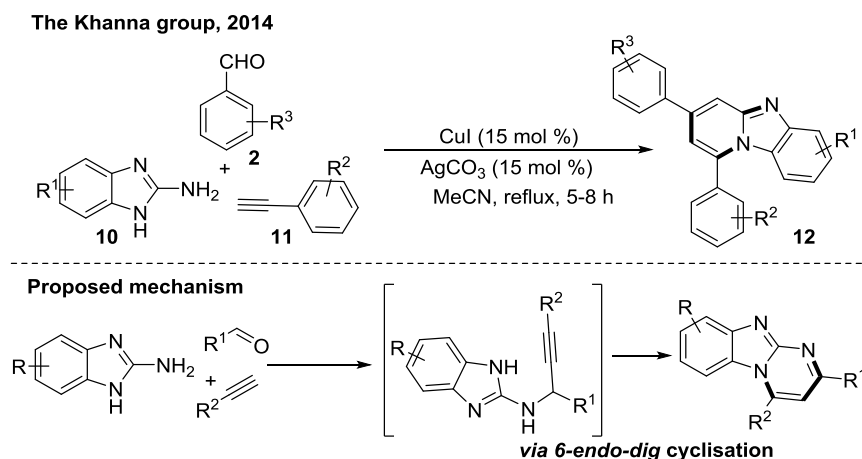
In 2016, the same group reported another three-component reaction strategy for the synthesis of benzimidazoles using benzyl alcohols/amines instead of aldehydes under copper catalysis (**Scheme 3b**).¹⁶ This reaction proceeds through almost similar mechanism (**Scheme 3c**). Under this oxidizing condition the benzyl alcohol/amine forms the imine. Then this imine undergoes *ortho*-C-H amination with azides *via* a SET mechanism. The *ortho*-azido imine then converts to *ortho*-amino imine by N₂ extrusion. This *ortho*-amino aryl imine then on oxidative cyclisation affords the product with regeneration of copper catalyst. Both the reactions were able to give the products in moderate to good yields with wide range of substrate scope.

In their seminal work, the Jiang group in 2014 reported the synthesis of variety of 1,3- as well as 1,3,4-substituted pyrazoles *via* a copper-catalyzed three-component cascade reactions involving oxime esters, amines and aldehydes (**Scheme 4**).¹⁷ Mechanistically, this reaction proceeds through N-O bond cleavage of the oxime acetate promoted by copper followed by C-C/C-N/N-N bond formations giving pyrazolines **VI**. This pyrazolines on oxidative dehydrogenation by Cu/O₂ system provided the corresponding pyrazoles.



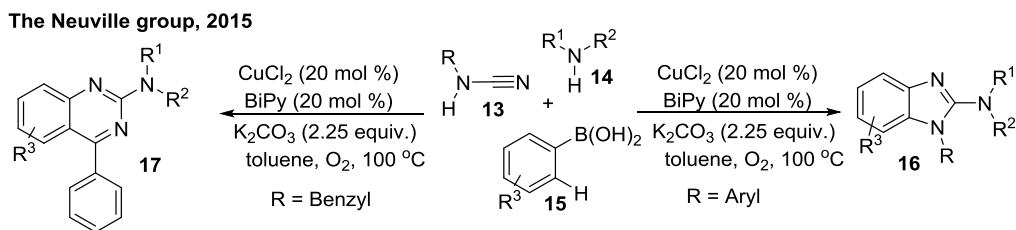
Scheme 4. Copper catalyzed synthesis of pyrazoles *via* a three-component coupling reaction

In the same year, the Khanna group developed a copper catalysed three-component cascade protocol for making *N*-fused imidazo heterocycles (**Scheme 5**).¹⁸ This reaction involves the coupling between 2-amino benzimidazole, aldehyde and a terminal alkyne. The reaction proceeds *via* a *6-endo-dig* cyclisation step. Starting from the substrates to the product the reaction involves two new C-N bonds and one C-C bond formations.



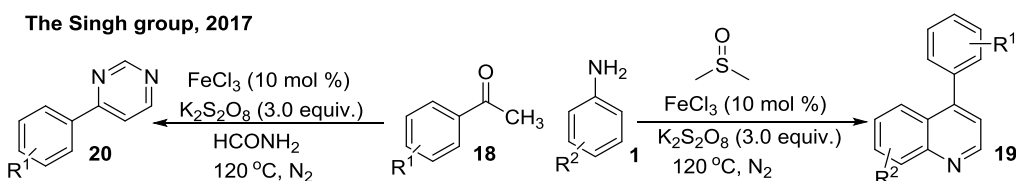
Scheme 5. Copper catalyzed synthesis of imidazo[1,2- a]pyrimidines *via* a three-component coupling reaction

Then in 2015, the Neuville group disclosed efficient methodology for the synthesis of 2-aminobenzimidazoles and 2-aminoquinazolines *via* a three-component reaction between aryl boronic acids, amines and cyanamides under a copper catalyzed condition (**Scheme 6**).¹⁹



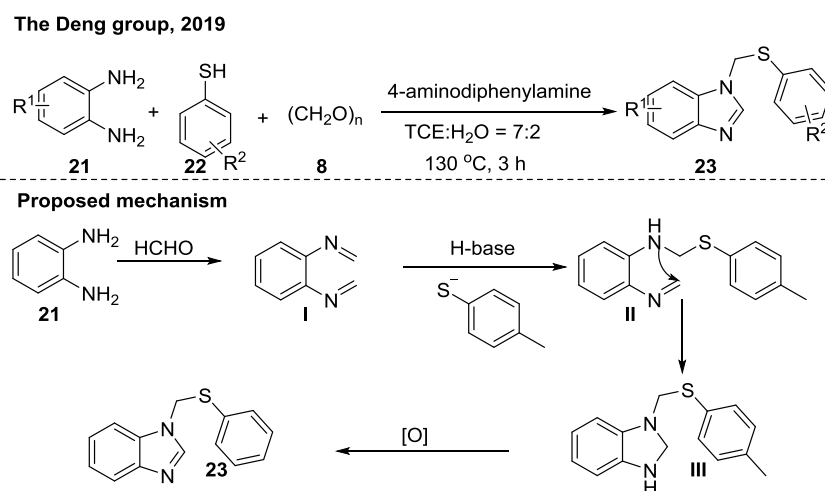
Scheme 6. Copper catalyzed synthesis of 2-aminobenzimidazoles and 2-aminoquinazolines

In the year 2017 Singh and his co-workers unveiled a Fe-catalysed three-component coupling reaction to synthesize 4-arylquinolines and 4-arylpyrimidines using DMSO and formamides as methine ($=\text{CH}-$) source respectively (**Scheme 7**).²⁰

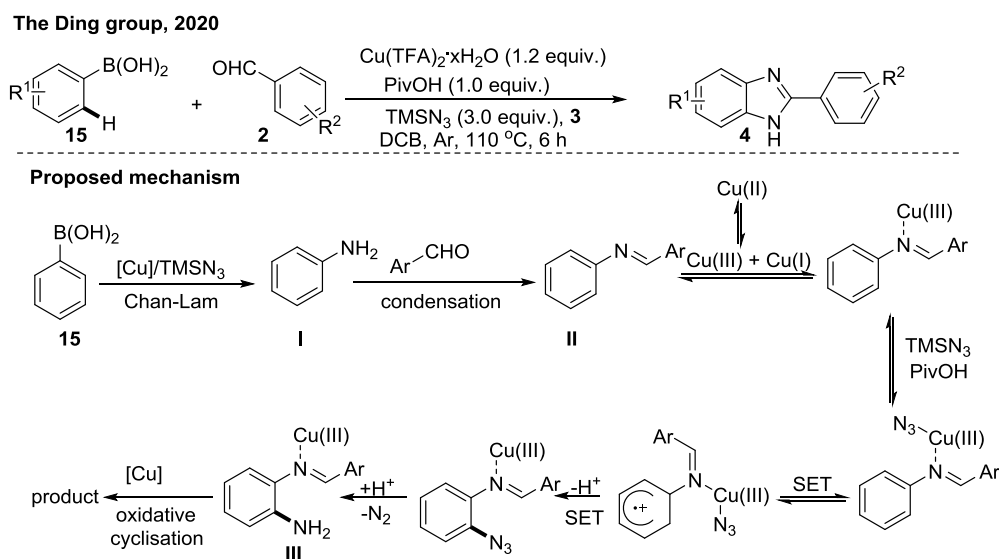


Scheme 7. Iron catalyzed synthesis of 4-arylquinolines and 4-arylpyrimidines

The Deng group in 2019, reported the synthesis of 2-unsubstituted benzimidazoles *via* a three component reaction between *ortho*-phenylenediamine, thiol and paraformaldehyde under a metal free condition (**Scheme 8**).²¹ 4-aminodiphenylamine was used as base for this transformation in 1,1,1,2-tetrachloro ethane/water medium. Mechanistically, *ortho*-diamine first forms diimine with paraformaldehyde. Then thiolate anion formed from the thiol by proton abstraction reacts with one of the α -carbon of the imine. The nucleophilic attack by NH group to the other α -carbon of the imine followed by oxidation gives the product.



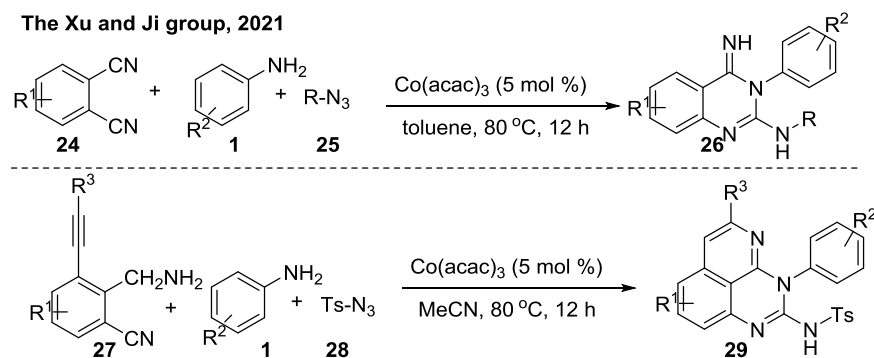
Scheme 8. Metal-free three-component reaction cascade for the synthesis of benzimidazoles



Scheme 9. Synthesis of benzimidazoles *via* Chan-lam coupling/condensation/C-H amination/cyclisation cascade

In 2020, the Ding group unveiled the synthesis of benzimidazoles through a three-component coupling using aryl boronic acids (**10**), azide (**3**) and aldehydes (**2**) which proceeded in a cascade manner under copper mediated condition (**Scheme 9**).²² In this strategy a copper boronic acids first undergoes copper catalyzed Chan-Lam coupling with TMS-azide to generate aniline *in situ*, which on condensation with aldehyde forms an imine **II**. Then a copper catalyzed *ortho* C-H amination with the azide using that imine as transient directing group gives **III**. The *ortho*-amino group then attacks imine α -carbon atom followed by oxidation to afford the product.

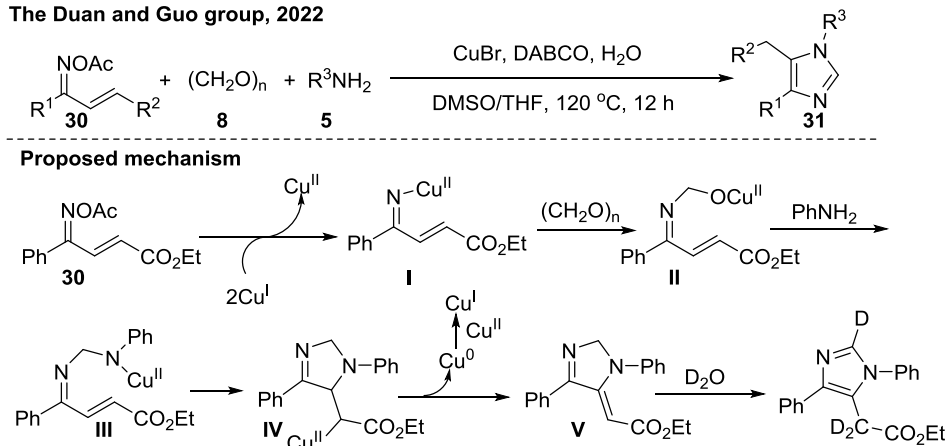
In 2021, the Xu and Ji group developed a cobalt catalyzed three-component coupling strategy for the synthesis of quinazoline derivatives (**Scheme 10**).²³ This protocol involves the reaction between amines isocyanides and azides.



Scheme 10. Cobalt catalyzed three-component coupling for the synthesis of quinazoline derivatives

Very recently, the Duan and Guo group disclosed an efficient synthesis of 2-unsubstituted imidazoles through a copper catalyzed three-component reaction of oxime ester of α,β -unsaturated ketones, amine and paraformaldehyde (**Scheme 11**).²⁴ The method afforded a broad range of substrates scope with good functional group tolerance. Mechanistically, the Cu(I) on reacting with oxime ester **30** generates iminylcopper(II) intermediate **I**. Then nucleophilic attack of this intermediate on paraformaldehyde, **8** followed by coupling with anilines forms intermediate **III**. Intramolecular Michael addition followed by β -hydride elimination gives intermediate **V** which on tautomerization with the help of water affords the product.

The Duan and Guo group, 2022



Scheme 11. Copper-catalyzed three-component reaction cascade using paraformaldehyde for the synthesis of imidazoles

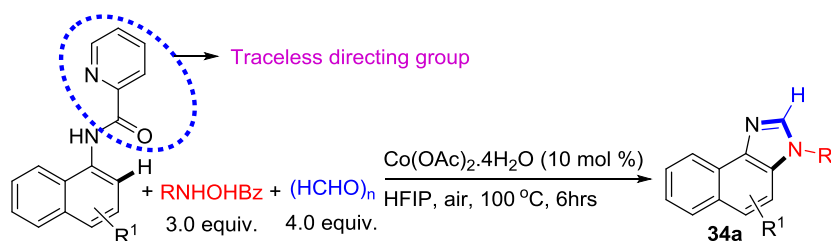
IV.3. Present work

Although having some examples of transition metal catalyzed multicomponent reactions involving C-H amination as discussed in the previous section, this field is under developed. To the best of our knowledge there is no report for the synthesis of 2-unsubstituted benzimidazoles through multicomponent coupling *via* C-H amination using electrophilic amine surrogates. However, most of the C-H amination methods require pre-installation of directing groups in the substrates to control regioselectivity and their subsequent removal.²⁵ So, the introduction and removal of directing groups is one of the major drawbacks in chelation-assisted C-H functionalization. To bypass this problem, transient, traceless and inherent directing group strategies were unveiled.²⁶ Traceless directing group strategy that has been employed to increase step economy in a methodology where the DG is removed in the same pot after the desired directed C-H functionalisation reaction is being achieved. Picolinamide directing group has been utilized as traceless directing group for carbonylative/alkenylative cyclisation under cobalt catalysis.²⁷ Paraformaldehyde has been incorporated into more complex molecules as carbonyl, acetyl, hydroxymethyl or carbon source through Rh, Pd, Co-catalyzed cross-coupling as well as direct C-H functionalization.²⁸ Paraformaldehyde has also been used as a C1 source for the synthesis of azacycles through multicomponent cascade reactions involving C-N bond formation as shown in **Scheme 4, 8 and 11**.

Out of many earth abundant cost-efficient 3d transition metal complexes, environmentally benign cobalt catalysts have very good potential for applications in C-H functionalisations.²⁹

Cobalt having lower electronegativity as compared to Pd, Ru and other group 9 elements generates more nucleophilic organometallic cobalt complexes resulting unprecedented reaction pathways in transition-metal catalysed C–H functionalisation reactions. Till now several works have reported for the synthesis of various important heterocycles through cobalt catalysed annulation reactions *via* C-H activation.³⁰ Besides these a significant advancement has also been achieved in cobalt catalysed C-N bond formation through C-H amination as well as C-H amidation reactions.³¹ The Paul Knochel group has made a significant success in cobalt catalysed electrophilic amination reactions with various zinc reagents using anthranil or *O*-benzoyl protected hydroxylamines as aminating reagents.³² But limited number of works on cobalt catalysed electrophilic C-H amination have been succeeded.³³

So we hypothesized that picolinamides may undergo directed *ortho*-C-H amination with primary *O*-benzoyloxyamines followed by formation of iminium with paraformaldehyde. The NH group of the picolinamide may attack the carbon of the iminium and subsequent hydrolysis of the amide lead to the 2-unsubstituted benzimidazoles. Though the picolinamide protected monocyclic anilines were unsuccessful the naphthalene system afforded the desired product as per our hypothesis.



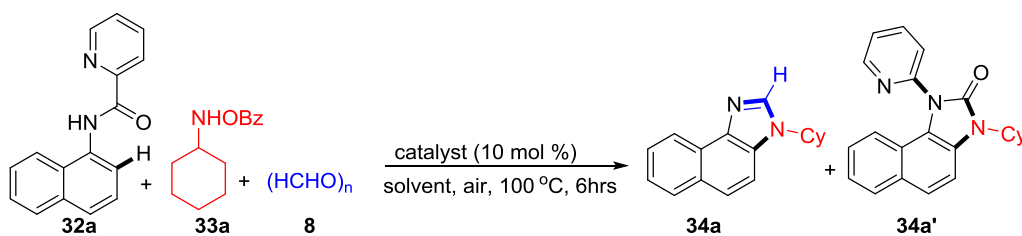
Scheme 12. Cobalt-catalyzed three-component reaction cascade *via* electrophilic C-H amination using paraformaldehyde for the synthesis of naphthimidazoles

IV. 4. Result and discussions

We started our optimization using picolinamide of 1-naphthylamine (**32a**), *O*-benzoyl-*N*-cyclohexylhydroxylamine (**33a**), paraformaldehyde (**8**) as model substrates. Initially we got our desired product **34a** in 15% yield along with 55% of the rearrangement product **34a'** when a mixture of **32a**, 1 equiv. **33a** and 6 equiv. paraformaldehyde in DMSO was heated in 100°C under air atm. using 10 mol % of CuI in DMSO. When the reaction was performed with free

cyclohexylamine instead of **33a** no reaction took place. Using 35% HCHO solution the product was obtained in 20% yield and the yield of **34a'** was lowered to 38%. Addition of 1.5 equiv. K_2CO_3 hampered the formation of desired product. Using 1.5 equiv. AcOH the product didn't improve the yield. Replacing DMSO solvent with TFE 22% of the desired product was obtained. 10 mol % $Co(OAc)_2 \cdot 4H_2O$ was able to improve the yield in 40% and also the yield of undesired **34a'** was diminished significantly. Increment in the amount of **33a** to 2.5 equiv. furnished the desired product in 72% yield. When the reaction was performed in N_2 atmosphere the yield was slightly decreased to 70%. Lowering the amount of paraformaldehyde to 4.0 equiv. afforded lower yield 66%. Higher temperature (110 °C) also decreased the product formation. Use of 0.5 equiv. PivOH also lowered the product yield. Changing the solvent to DCE decreased the yield significantly. HFIP was found to be the best solvent where desired product was obtained in 80% yield and most interestingly the formation of undesired **34a'** was stopped completely. Using 3.0 equiv. of **33a** we got the product yield in 88%. Under this condition 35% HCHO solution instead of paraformaldehyde also furnished the product in comparable yield. CuI was found to be ineffective to provide the product in HFIP solvent. In order to observe the efficiency of other pyridine based amide DGs we performed the reaction using substrates **32A-32D** but all of them found to give inferior results than picolinamide.

Table 1. Optimization of the Reaction Conditions^{a,b}



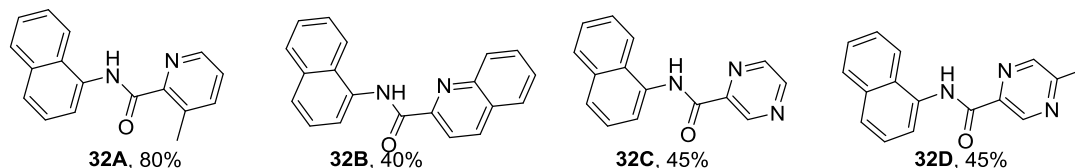
| entry | catalyst | Ratio of 33a / 8 (equiv) | solvent | yield (%) 34a / 34a' |
|----------------|-------------------------|---|---------|---------------------------------------|
| 1 | CuI | 1/6 | DMSO | 15/55 |
| 2 ^c | CuI | 1/6 | DMSO | 0/0 |
| 3 ^d | CuI | 1/5 | DMSO | 20/38 |
| 4 ^e | CuI | 1/6 | DMSO | 0/42 |
| 5 ^f | CuI | 1/6 | DMSO | 15/45 |
| 6 | CuI | 1/6 | TFE | 22/45 |
| 7 | $Co(OAc)_2 \cdot 4H_2O$ | 1/6 | TFE | 40/10 |
| 8 | $Co(OAc)_2 \cdot 4H_2O$ | 2.5/6 | TFE | 72/15 |

| | | | | |
|-----------------|--|------------|-------------|-------------|
| 9 ^g | Co(OAc) ₂ .4H ₂ O | 2.5/6 | TFE | 70/15 |
| 10 | Co(OAc) ₂ .4H ₂ O | 2.5/4 | TFE | 66/15 |
| 11 ^h | Co(OAc) ₂ .4H ₂ O | 2.5/4 | TFE | 60/20 |
| 12 ⁱ | Co(OAc) ₂ .4H ₂ O | 2.5/4 | TFE | 60/12 |
| 13 | Co(OAc) ₂ .4H ₂ O | 2.5/4 | DCE | 24/35 |
| 14 | Co(OAc) ₂ .4H ₂ O | 2.5/4 | HFIP | 80/0 |
| 15 | Co(OAc)₂.4H₂O | 3/4 | HFIP | 88/0 |
| 16 ^d | Co(OAc) ₂ .4H ₂ O | 3/5 | HFIP | 84/0 |
| 18 | CuI | 3/4 | HFIP | n.r. |

^aAll reactions were carried out in 0.2 mmol scale. ^bYields refer to here are overall isolated yields.

^cFree amine was used. ^d5.0 equiv. 35% HCHO solution was used. ^e1.5 equiv. K₂CO₃ was used. ^f1.5 equiv. AcOH was used. ^gReaction was performed under N₂ atm. ^hReaction temperature was 110 °C. ⁱ0.5 equiv. PivOH was used.

Scheme 8. Exploration of other directing groups



Characteristics peaks in ¹HNMR spectrum of compound 34a

1. Firstly, the amide proton in the range of δ value 10.0-11.0 ppm was disappeared in the product.
2. Appearance of one multiplet in the region δ 4.30-4.23 ppm corresponding to 1 proton and another five multiplets ranging from δ 2.27 to 1.27 ppm corresponding to total 10 protons indicated the incorporation of cyclohexyl moiety from the amine source.
3. Four aromatic protons were vanished. This indicated that pyridine moiety is no longer attached to the product.
4. And a characteristic singlet was found in δ 8.04 ppm corresponding to 1 proton.

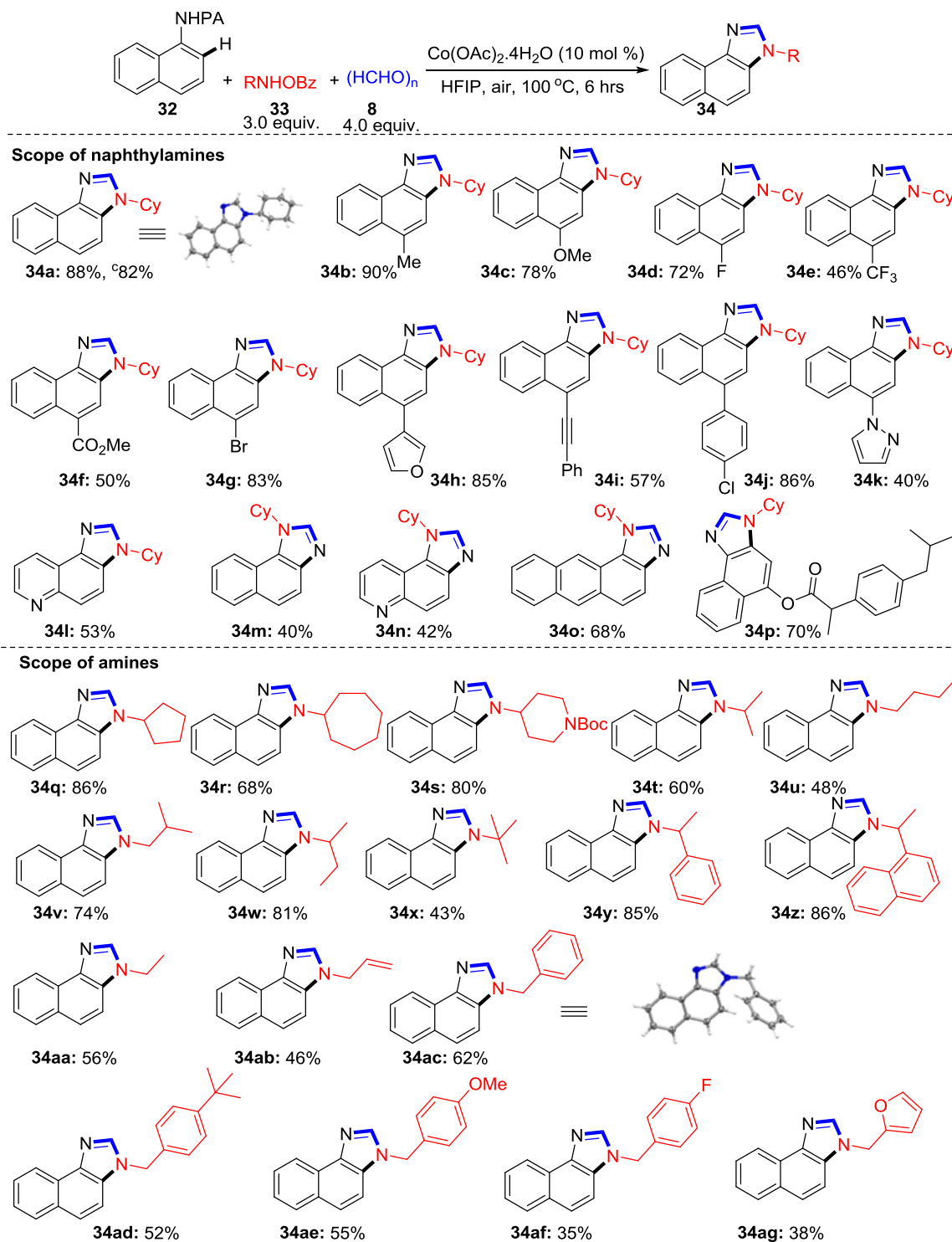
Characteristics peaks in ¹HNMR spectrum of compound 34a

1. In ¹³C NMR four new peaks in the aliphatic region δ 55.7-25.5 ppm were appeared. The peak at δ 55.7 ppm is for the carbon atom attached to the N-atom.
2. Five peaks in the aromatic region was missing.

Under the optimized condition we surveyed the generality of the reaction with respect to naphthylamines (**Table 2**). Unsubstituted naphthylamine gave the product (**34a**) in 88% and 82% yield respectively in 0.2 and 4.0 mmol scale. Electron donating groups such as methoxy, methyl and aryl groups were proceeded well affording the desired product 78-90% yield (**34b**, **34c**, **34h-34j**). Electron withdrawing groups such as fluoro, trifluoromethyl and ester groups provided lesser yield (**34d-34f**). Bromo, alkyne and pyrazole groups were well tolerated under this condition (**34g**, **34j-34k**). Notably, heterocyclic 5-amino quinoline substrate also participated this reaction furnishing the product albeit in moderate yield (**34l**). 2-naphthylamine, 6-amino quinoline and 2-amino anthracene substrates also produced the product in low to moderate yields (**34m-34o**). Moreover, ibuprofen ester containing substrate was also well tolerated under this condition (**15p**).

Subsequently, a variety of aliphatic primary *O*-benzoyloxy amines were tested under the optimized condition. Cyclopentylamine furnished the product in very good yield (**34q**). Increasing the ring size to cycloheptylamine product yield was decreased slightly (**34r**). Reaction with isomeric butylamines indicated that secondary alkyl group containing amines were the best followed by primary and then tertiary with 81%, 74%, 48% and 43% respectively (**34u-34x**). Isopropylamine gave slightly lesser yield 60% (**34t**). Other secondary alkyl group based amines such as α -methyl benzylamine and α -methyl naphthylamines afforded the products in very good yields (**34y-34z**). Ethylamine furnished the product in moderate yield (**34aa**). Allylamine, benzylamine and furfurylamines were also proved to be feasible to this reaction although yields

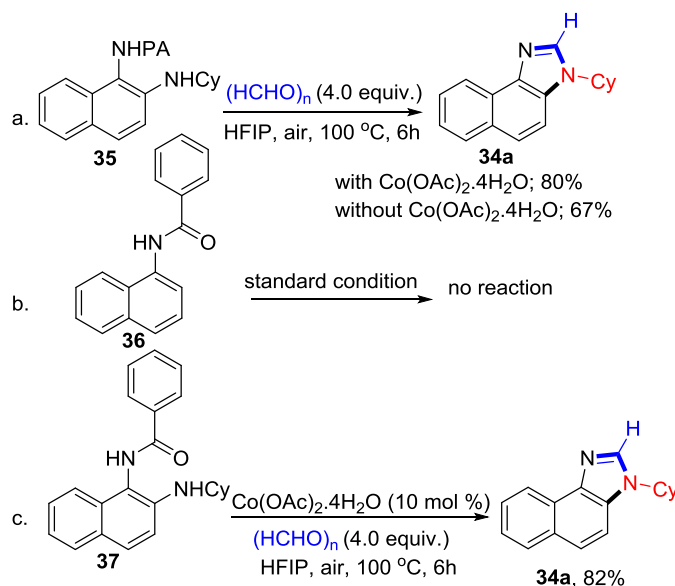
Table 2. Substrate Scope of naphthyamines^{a,b}



^aAll reactions were carried out in 0.3 mmol scale. ^bYields refer to the overall isolated yields. ^c4.0 mmol scale reaction.

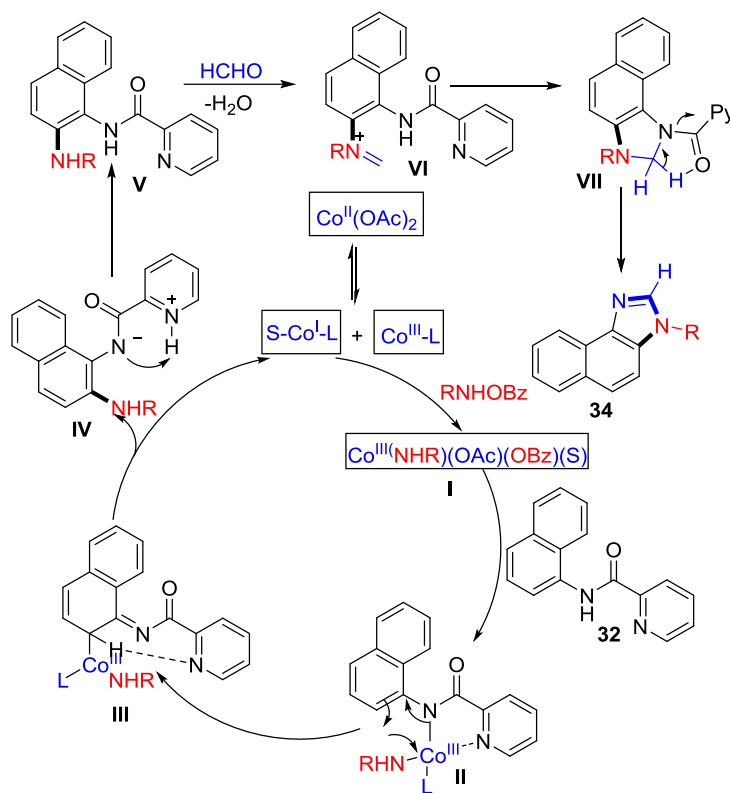
were not satisfactory (**34ab**, **34ac**, **34ah**). Various substitution on the benzylamine part such as *tert*-butyl, methoxy, chloro and fluoro groups were underwent the reaction in low to moderate yield (**34ad-34ag**).

IV. 5. Reaction mechanism



Scheme 13. Control experiments

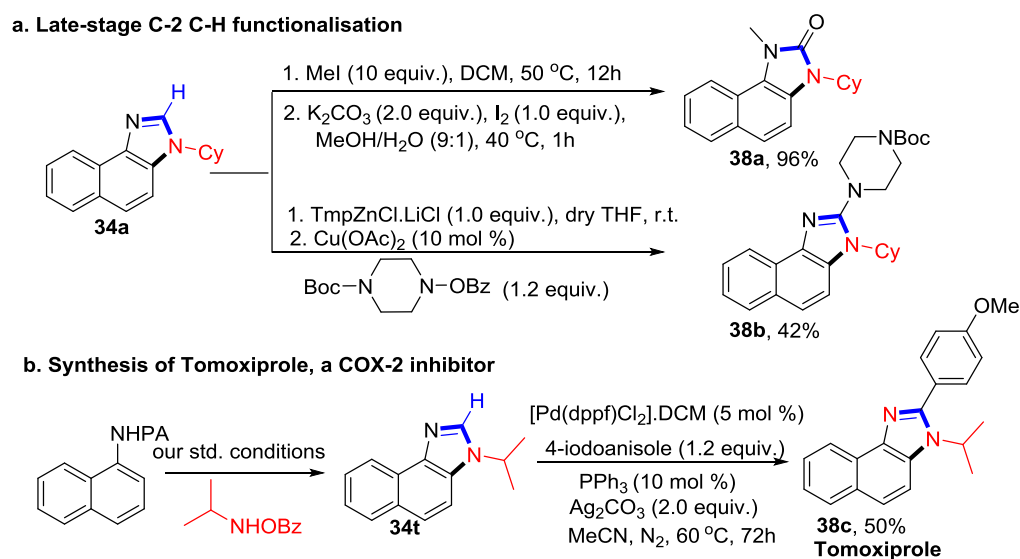
To gain insight into the mechanism some control experiments were performed. When the pre-formed *ortho*-amino picolinamide was subjected to react with paraformaldehyde in absence or presence of cobalt catalyst, the product was obtained in 80% and 67% yield respectively in 6 hrs (**Scheme 13a**). This indicates that Co-catalyst slightly assist the subsequent reaction after amination. Benzamide of naphthylamine didn't afford the desired product under the standard condition (**Scheme 13b**). But *ortho*-amino benzamide of naphthylamine successfully furnished the product in 82% yield (**Scheme 13c**). These experiments suggest that the pyridine N-atom is necessary for C-H amination step but for the subsequent reactions it is not required.



Scheme 14. Proposed catalytic cycle

Based on the control experiments and our previous work the Co(II) first undergoes disproportionation to generate a Co(I) species which on oxidative addition to the N-O bond of the aminating reagent forms a Co(III) complex **I** (Scheme 14). This complex then undergoes chelation with the substrate forming **II**. This is converted to complex **III** after electrophilic metalation and subsequent reductive elimination forms **IV** with the regeneration of Co(I). **IV** after proton exchange eliminates the *ortho* amination product **V**. This then reacts with formaldehyde to form the iminium salt **VI** and nucleophilic attack of the amide NH group to the α -carbon of the iminium generates **VII**. Finally, hydrolysis gives the product.

IV. 6. Product derivatisation



Scheme 15. Product derivatizations and utility of the method for the synthesis of COX-2 inhibitor

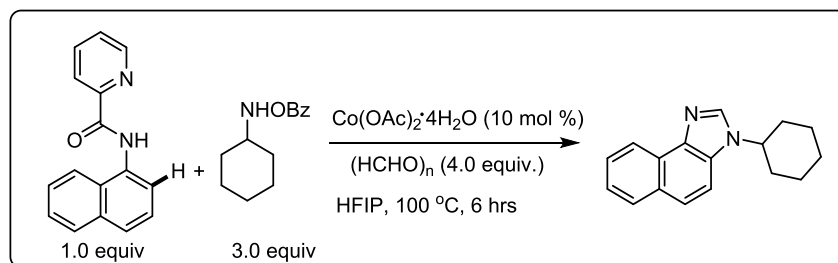
The naphthimidazole product, **34a** formed by our method is further utilized for the synthesis of naphthimidazolone (**38a**) and 2-amino naphthimidazole (**38b**) by C2-H oxidation and amination reactions respectively (**Scheme 15a**). A COX-2 inhibitor Tomoxiprole (**38c**) has also been synthesized by C2-H arylation of compound prepared by our method (**Scheme 15b**).

IV. 7. Conclusion

In conclusion, we have developed an efficient one-pot three-component protocol for the synthesis of varieties of 2-unsubstituted naphthimidazoles through earth-abundant cobalt-catalysed electrophilic *ortho* C-H amination followed by cyclisation cascade with paraformaldehyde as one carbon synthon. Naphthimidazole derivatives were obtained in good yields through the efficient intermolecular C–N and C–C bond formations. Use of air stable cobalt catalyst simple operations, broad substrate scopes, functional group tolerance and scalability, product derivatisation, synthetic applications for COX-2 inhibitor enhance the attractiveness of the transformations.

IV. 8. Experimental section

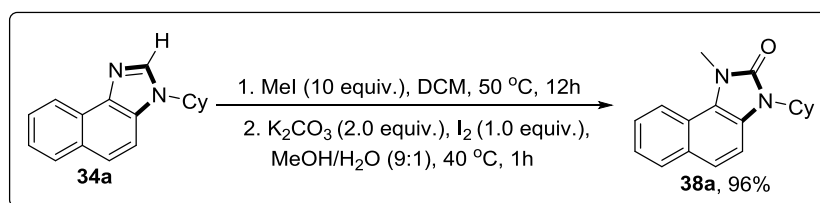
Representative Procedure for imidazole



In an oven dried 15 mL sealed tube containing a stir bar was added corresponding picolinamide (0.3 mmol, 1.0 equiv.), *O*-benzoylhydroxylamine (0.9 mmol, 3.0 equiv.), $(\text{HCHO})_n$ (36 mg, 1.2 mmol, 4.0 equiv.) and $\text{Co}(\text{OAc})_2 \cdot 4\text{H}_2\text{O}$ (0.03 mmol). HFIP (3 mL) was then added. The mixture was stirred at 100 °C for 6 hrs. After allotted time the reaction mixture was cooled to room temperature. The mixture was diluted with DCM (50 mL) and washed with saturated aq. NaHCO_3 solution (25 mL), followed by brine solution (25 mL) and dried over anhydrous Na_2SO_4 , and evaporated in *vacuo*. The crude mixture was loaded on a silica gel column chromatography and purified using (Hexane/Acetone) to give the desired imidazole product.

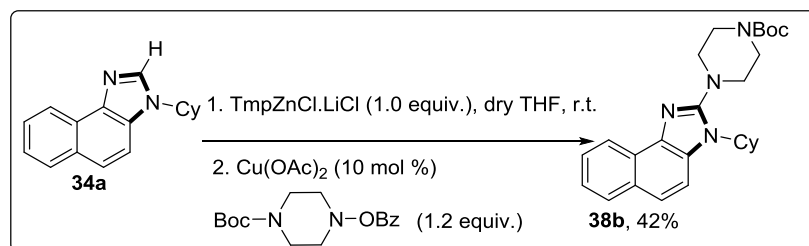
Note: Work-up or column chromatography using EtOAc can't be performed. Because EtOAc is hydrolysed through nucleophilic ester hydrolysis mechanism by these naphthimidazoles to produce high-boiling AcOH which can't be removed by rotary evaporation.

Procedure for C2-H oxidation



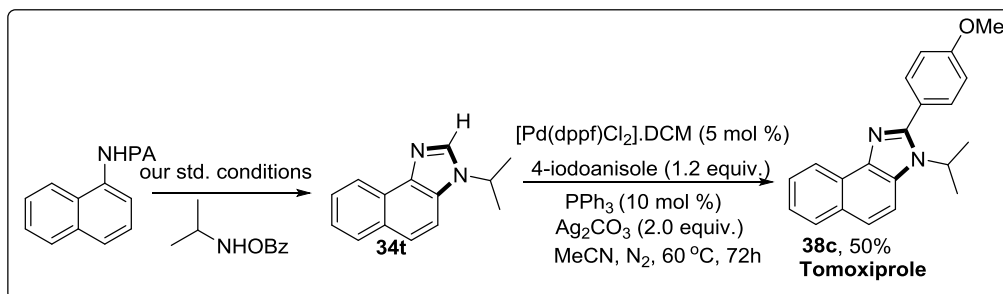
In an oven dried R.B. containing a stir bar charged with **34a** (0.5 mmol) in DCM was added MeI (10 equiv.). Then the mixture fitted with reflux condenser was heated at 50 °C for 12 hrs. After cooling to room temperature the solvent was evaporated under rotary evaporation. To this K_2CO_3 (2.0 equiv.), I_2 (1.0 equiv.) and MeOH/ H_2O (9:1) 3 mL were added and heated to 40 °C for 1 h). After cooling to room temperature the solvent was evaporated. 50 mL EtOAc was added to it and washed with water and dried over anhydrous Na_2SO_4 , and evaporated in *vacuo*. The crude mixture was loaded on a silica gel column chromatography and purified using (Hexane/EtOAc) to give the desired imidazolone product.

Procedure for C2-H amination



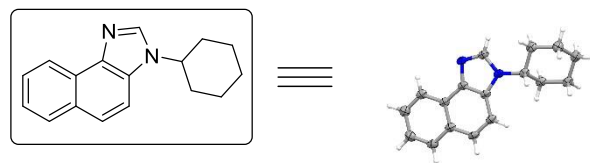
In an oven dried R.B. containing a stir bar and charged with **34a** (0.5 mmol) in dry THF under Ar atmosphere was added TmpZnCl.LiCl in THF solution (1.0 equiv.) dropwise and stirred at room temperature for 30 minutes. After that a mixture of Cu(OAc)₂ (10 mol%), the amine-OBz (1.2 equiv.) in dry THF under Ar atmosphere was added dropwise to the previous mixture at room temperature and stirred at r.t. for 12 hrs. After this time the reaction was quenched with saturated NH₄Cl solution. Then after solvent evaporation EtOAc was added and washed with water dried over anhydrous Na₂SO₄, and evaporated in *vacuo*. The crude mixture was loaded on a silica gel column chromatography and purified using (Hexane/EtOAc) to give the desired product.

Procedure for the synthesis of Tomoxiprole



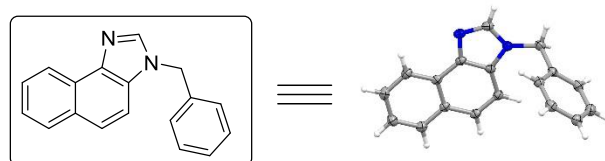
4t was prepared following our method. An oven dried reaction vial containing a stir bar and charged with **4t** (0.5 mmol) was added [Pd(dppf)Cl₂].DCM (5 mol %), PPh₃ (10 mol %), 4-iodoanisole (1.2 equiv.), Ag₂CO₃ (2.0 equiv.) and then MeCN (4 mL) was added. Then the mixture was heated to 60 °C for 72 hrs. After the allotted time the mixture was cooled to room temperature and filtered through celite pad. Then crude obtained after the solvent evaporation was purified by silica gel column chromatography using (Hexane/EtOAc) to give the desired product.

IV.9. X-ray crystallography data



| | |
|------------------------------------|--|
| Identification code | HM1418 |
| Empirical formula | C ₁₇ H ₁₈ N ₂ |
| Formula weight | 250.33 |
| Temperature/K | 100.0 |
| Crystal system | monoclinic |
| Space group | P2 ₁ /c |
| a/Å | 13.2417(9) |
| b/Å | 12.7619(9) |
| c/Å | 7.8090(5) |
| α/° | 90 |
| β/° | 99.428(3) |
| γ/° | 90 |
| Volume/Å ³ | 1301.81(15) |
| Z | 4 |
| ρ _{calc} /cm ³ | 1.277 |
| μ/mm ⁻¹ | 0.580 |
| F(000) | 536.0 |
| Crystal size/mm ³ | 0.15 × 0.12 × 0.02 |
| Radiation | Cu Kα (λ = 1.54178) |
| 2θ range for data collection/° | 9.688 to 144.96 |
| Index ranges | -16 ≤ h ≤ 15, -15 ≤ k ≤ 15, -8 ≤ l ≤ 9 |

| | |
|--|--|
| Reflections collected | 25331 |
| Independent reflections | 2532 [$R_{\text{int}} = 0.0811$, $R_{\text{sigma}} = 0.0436$] |
| Data/restraints/parameters | 2532/0/173 |
| Goodness-of-fit on F^2 | 1.071 |
| Final R indexes [$I \geq 2\sigma(I)$] | $R_1 = 0.0672$, $wR_2 = 0.1766$ |
| Final R indexes [all data] | $R_1 = 0.0699$, $wR_2 = 0.1801$ |
| Largest diff. peak/hole / $e \text{ \AA}^{-3}$ | 0.46/-0.37 |

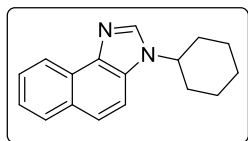


| | |
|------------------------|-------------------|
| Identification code | HM1804_2_0m |
| Empirical formula | $C_{18}H_{14}N_2$ |
| Formula weight | 258.31 |
| Temperature/K | 100.00 |
| Crystal system | monoclinic |
| Space group | $P2_1/n$ |
| $a/\text{\AA}$ | 6.5843(3) |
| $b/\text{\AA}$ | 9.6121(4) |
| $c/\text{\AA}$ | 20.5866(8) |
| $\alpha/^\circ$ | 90 |
| $\beta/^\circ$ | 93.7440(10) |
| $\gamma/^\circ$ | 90 |
| Volume/ \AA^3 | 1300.12(9) |
| Z | 4 |

| | |
|--|---|
| $\rho_{\text{calc}}/\text{cm}^3$ | 1.320 |
| μ/mm^{-1} | 0.607 |
| F(000) | 544.0 |
| Crystal size/ mm^3 | $0.15 \times 0.12 \times 0.02$ |
| Radiation | $\text{CuK}\alpha$ ($\lambda = 1.54178$) |
| 2Θ range for data collection/ $^\circ$ | 8.608 to 144.446 |
| Index ranges | $-7 \leq h \leq 8, -11 \leq k \leq 11, -25 \leq l \leq 24$ |
| Reflections collected | 23131 |
| Independent reflections | 2472 [$R_{\text{int}} = 0.0487, R_{\text{sigma}} = 0.0328$] |
| Data/restraints/parameters | 2472/0/181 |
| Goodness-of-fit on F^2 | 1.064 |
| Final R indexes [$I \geq 2\sigma(I)$] | $R_1 = 0.0422, wR_2 = 0.1115$ |
| Final R indexes [all data] | $R_1 = 0.0432, wR_2 = 0.1125$ |
| Largest diff. peak/hole / $e \text{ \AA}^{-3}$ | 0.20/-0.17 |

IV.10. Spectral data

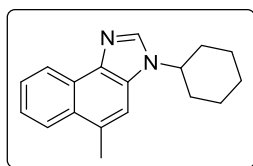
3-cyclohexyl-3*H*-naphtho[1,2-*d*]imidazole (34a)



The general procedure for imidazole was followed. Column chromatography (SiO_2 , eluting with 90:10 hexane/acetone) afforded the desired product as a white solid (66 mg, 88% yield); mp: 148-150 $^\circ\text{C}$. ^1H NMR (400 MHz, CDCl_3): δ 8.65-8.63 (m, 1H), 8.03 (s, 1H), 7.92 (d, $J = 8.0$ Hz, 1H), 7.69 (d, $J = 8.0$ Hz, 1H), 7.64-7.60 (m, 1H), 7.54 (d, $J = 8.0$ Hz, 1H), 7.49-7.45 (m, 1H), 4.31-4.23 (m, 1H), 2.27-2.23 (m, 2H), 2.01-1.96 (m, 2H), 1.89-1.78 (m, 3H), 1.58-1.46 (m, 2H), 1.39-1.27 (m, 1H); ^{13}C NMR (100 MHz, CDCl_3): δ 139.3, 138.1, 130.2, 129.7, 128.4, 127.5, 126.6, 124.5,

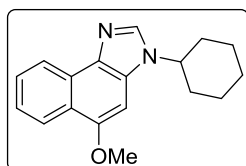
123.7, 121.8, 110.8, 55.7, 33.7, 25.8, 25.5; HRMS (ESI, m/z) calcd. For C₁₇H₁₉N₂ [M+H]⁺: 251.1548; found: 251.1571.

3-cyclohexyl-5-methyl-3*H*-naphtho[1,2-*d*]imidazole (34b)



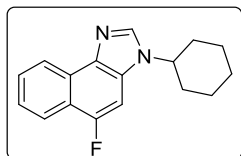
The general procedure for imidazole was followed. Column chromatography (SiO₂, eluting with 90:10 hexane/acetone) afforded the desired product as a light brown gummy solid (71 mg, 90% yield). ¹H NMR (400 MHz, DMSO-*d*₆): δ 8.47-8.44 (m, 1H), 8.23 (s, 1H), 8.01 (d, *J* = 8.0 Hz, 1H), 7.68 (d, *J* = 0.8 Hz, 1H), 7.59-7.55 (m, 1H), 7.49-7.45 (m, 1H), 4.43-4.35 (m, 1H), 2.69 (s, 3H), 2.06-2.02 (m, 2H), 1.89-1.88 (m, 4H), 1.69 (d, *J* = 12.8 Hz, 1H), 1.53-1.43 (m, 2H), 1.33 - 1.25 (m, 1H); ¹³C NMR (100 MHz, DMSO-*d*₆): δ 139.2, 137.8, 129.6, 129.4, 129.3, 127.5, 126.4, 125.4, 124.6, 122.1, 112.5, 54.9, 33.5, 25.7, 25.4, 20.3; HRMS (ESI, m/z) calcd. For C₁₈H₂₁N₂ [M+H]⁺: 265.1705; found: 265.1713.

3-cyclohexyl-5-methoxy-3*H*-naphtho[1,2-*d*]imidazole (34c)



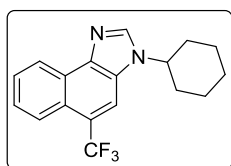
The general procedure for imidazole was followed. Column chromatography (SiO₂, eluting with 90:10 hexane/acetone) afforded the desired product as a light orange solid (66 mg, 78% yield); mp: 98-100 °C. ¹H NMR (400 MHz, DMSO-*d*₆): δ 8.39-8.36 (m, 1H), 8.18-8.16 (m, 2H), 7.59-7.55 (m, 1H), 7.43-7.39 (m, 1H), 7.24 (s, 1H), 4.46-4.39 (m, 1H), 2.69 (s, 3H), 2.06-2.03 (m, 2H), 1.85-1.67 (m, 4H), 1.69 (d, *J* = 12.8 Hz, 1H), 1.55-1.44 (m, 2H), 1.31-1.21 (m, 1H); ¹³C NMR (100 MHz, DMSO-*d*₆): δ 152.4, 138.3, 132.8, 130.0, 127.6, 127.3, 124.1, 123.1, 122.9, 121.5, 91.3, 56.6, 54.5, 33.6, 25.8, 25.4; HRMS (ESI, m/z) calcd. For C₁₈H₂₁N₂O [M+H]⁺: 281.1654; found: 281.1643.

3-cyclohexyl-5-fluoro-3*H*-naphtho[1,2-*d*]imidazole (34d)



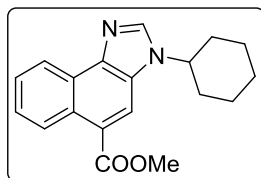
The general procedure for imidazole was followed. Column chromatography (SiO₂, eluting with 90:10 hexane/acetone) afforded the desired product as a creamy white solid (58 mg, 72% yield); mp: 114-116 °C. ¹H NMR (400 MHz, DMSO-d₆): δ 8.47-8.44 (m, 1H), 8.34 (s, 1H), 8.05 (d, *J* = 8.4 Hz, 1H), 7.82 (d, *J* = 11.2 Hz, 1H), 7.68-7.64 (m, 1H), 7.56-7.52 (m, 1H), 4.45-4.37 (m, 1H), 2.05-2.01 (m, 2H), 1.87-1.77 (m, 4H), 1.68 (d, *J* = 12.8 Hz, 1H), 1.52-1.41 (m, 2H), 1.32-1.21 (m, 1H); ¹³C NMR (100 MHz, DMSO-d₆): δ 155.2 (d, *J* = 242.0 Hz), 140.3, 135.2, 128.7 (d, *J* = 13.8 Hz), 127.9, 127.3 (d, *J* = 6.2 Hz), 125.2 (d, *J* = 1.3 Hz), 121.9 (d, *J* = 2.7 Hz), 121.4 (d, *J* = 5.6 Hz), 120.3 (d, *J* = 18.5, Hz), 97.2 (d, *J* = 26.7 Hz), 55.1, 33.4, 25.7, 25.3; HRMS (ESI, *m/z*) calcd. For C₁₇H₁₈FN₂ [M+H]⁺: 269.1454; found: 269.1442.

3-cyclohexyl-5-(trifluoromethyl)-3H-naphtho[1,2-*d*]imidazole (34e)



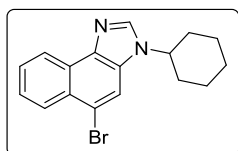
The general procedure for imidazole was followed. Column chromatography (SiO₂, eluting with 90:10 hexane/acetone) afforded the desired product as a light orange solid (49 mg, 46% yield); mp: 98-100 °C. ¹H NMR (400 MHz, DMSO-d₆): δ 8.62-8.58 (m, 2H), 8.39 (s, 1H), 8.11 (d, *J* = 9.6 Hz, 1H), 7.72-7.68 (m, 1H), 7.64-7.60 (m, 1H), 4.68-4.60 (m, 1H), 2.06-2.03 (m, 2H), 1.88-1.81 (m, 4H), 1.69 (d, *J* = 12.4 Hz, 1H), 1.56-1.46 (m, 2H), 1.31-1.20 (m, 1H); ¹³C NMR (100 MHz, DMSO-d₆): δ 169.8, 142.8, 141.7, 127.9, 127.7, 127.6, 126.5, 125.3, 124.64 (q, *J* = 2.6 Hz), 122.7, 119.5 (q, *J* = 29.6 Hz), 112.7 (q, *J* = 6.5 Hz), 54.8, 33.7, 25.6, 25.5; HRMS (ESI, *m/z*) calcd. For C₁₈H₁₈F₃N₂ [M+H]⁺: 319.1422; found: 319.1412.

methyl 3-cyclohexyl-3H-naphtho[1,2-*d*]imidazole-5-carboxylate (34f)



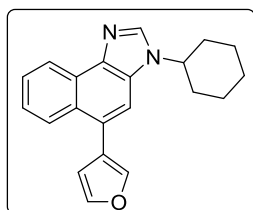
The general procedure for imidazole was followed. Column chromatography (SiO₂, eluting with 90:10 hexane/acetone) afforded the desired product as a light brown gummy solid (46 mg, 50% yield). ¹H NMR (400 MHz, DMSO-d₆): δ 8.82 (d, *J* = 8.8 Hz, 1H), 8.57-8.54 (m, 2H), 8.48 (s, 1H), 7.66-7.62 (m, 1H), 7.58-7.54 (m, 1H), 4.59-4.52 (m, 1H), 3.94 (s, 3H), 2.08-2.03 (m, 2H), 1.89-1.79 (m, 4H), 1.69 (d, *J* = 12.4 Hz, 1H), 1.56-1.46 (m, 2H), 1.30-1.20 (m, 1H); ¹³C NMR (100 MHz, DMSO-d₆): δ 168.1, 142.9, 142.2, 128.4, 127.9, 127.4, 127.0, 126.6, 126.2, 122.2, 121.9, 116.8, 54.9, 52.7, 33.7, 25.6, 25.4; HRMS (ESI, *m/z*) calcd. For C₁₉H₂₁N₂O₂ [M+H]⁺: 309.1603; found: 309.1605.

5-bromo-3-cyclohexyl-3*H*-naphtho[1,2-*d*]imidazole (34g)



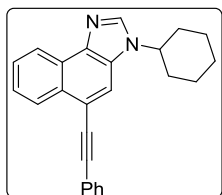
The general procedure for imidazole was followed. Column chromatography (SiO₂, eluting with 90:10 hexane/acetone) afforded the desired product as a creamy white solid (82 mg, 83% yield); mp: 118-120 °C. ¹H NMR (400 MHz, CDCl₃): δ 8.67-8.64 (m, 1H), 8.31-8.28 (m, 1H), 8.03 (s, 1H), 7.89 (s, 1H), 7.67-7.63 (m, 1H), 7.59-7.57 (m, 1H), 4.24-4.17 (m, 1H), 2.25-2.21 (m, 2H), 2.00-1.95 (m, 2H), 1.84-1.75 (m, 3H), 1.57-1.45 (m, 2H), 1.37-1.29 (m, 1H); ¹³C NMR (100 MHz, CDCl₃): δ 139.0, 138.5, 129.6, 128.3, 128.0, 127.9, 127.4, 125.8, 122.2, 117.7, 114.9, 55.9, 33.7, 25.7, 25.4; HRMS (ESI, *m/z*) calcd. For C₁₇H₁₈BrN₂ [M+H]⁺: 329.0653; found: 329.0663.

3-cyclohexyl-5-(furan-3-yl)-3*H*-naphtho[1,2-*d*]imidazole (34h)



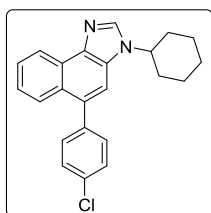
The general procedure for imidazole was followed. Column chromatography (SiO₂, eluting with 90:10 hexane/acetone) afforded the desired product as a light yellow solid (81 mg, 85% yield); mp: 156-158 °C. ¹H NMR (400 MHz, DMSO-d₆): δ 8.72-8.69 (m, 1H), 8.12 (dt, *J*₁ = 8.4 Hz, *J*₂ = 1.2 Hz, 1H), 8.05 (s, 1H), 7.67 (dd, *J*₁ = 1.6 Hz, *J*₂ = 0.8 Hz, 1H), 7.66-7.62 (m, 1H), 7.60 (t, *J* = 1.6 Hz, 1H), 7.52 (s, 1H), 7.49-7.45 (m, 1H), 6.72 (dd, *J*₁ = 1.6 Hz, *J*₂ = 0.8 Hz, 1H), 4.32-4.24 (m, 1H), 2.29-2.25 (m, 2H), 2.01-1.96 (m, 2H), 1.90-1.80 (m, 3H), 1.58-1.46 (m, 2H), 1.39-1.31 (m, 1H); ¹³C NMR (100 MHz, DMSO-d₆): δ 142.9, 140.5, 139.1, 138.3, 129.2, 129.0, 127.6, 126.6, 126.5, 125.5, 124.8, 122.1, 113.0, 111.7, 55.7, 33.8, 25.8, 25.5; HRMS (ESI, *m/z*) calcd. For C₂₁H₂₁N₂O [M+H]⁺: 317.1654; found: 317.1664.

3-cyclohexyl-5-(phenylethynyl)-3*H*-naphtho[1,2-*d*]imidazole (34i)



The general procedure for imidazole was followed. Column chromatography (SiO₂, eluting with 90:10 hexane/acetone) afforded the desired product as a yellow fluffy solid (60 mg, 57% yield); mp: 68-70 °C. ¹H NMR (400 MHz, DMSO-d₆): δ 8.51-8.42 (m, 3H), 8.24 (s, 1H), 7.69-7.59 (m, 4H), 7.47-7.40 (m, 3H), 4.54 (t, *J* = 11.2 Hz, 1H), 2.07 (d, *J* = 9.2 Hz, 2H), 1.90-1.84 (m, 4H), 1.70 (d, *J* = 12.4 Hz, 1H), 1.56-1.47 (m, 2H), 1.33-1.23 (m, 1H); ¹³C NMR (100 MHz, DMSO-d₆): δ 141.6, 139.8, 131.9, 129.7, 129.43, 129.39, 129.3, 127.5, 127.2, 126.8, 125.9, 123.2, 122.2, 117.0, 114.6, 93.7, 88.9, 55.0, 33.6, 25.7, 25.4; HRMS (ESI, *m/z*) calcd. For C₂₅H₂₃N₂ [M+H]⁺: 351.1861; found: 351.1846.

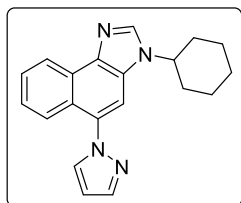
5-(4-chlorophenyl)-3-cyclohexyl-3*H*-naphtho[1,2-*d*]imidazole (34j)



The general procedure for imidazole was followed. Column chromatography (SiO₂, eluting with 90:10 hexane/acetone) afforded the desired product as a yellow powder (93 mg, 86% yield); mp:

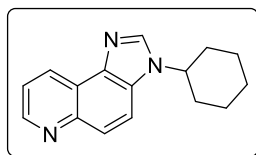
124-126 °C. ^1H NMR (400 MHz, DMSO- d_6): δ 8.54 (d, $J = 8.0$ Hz, 1H), 8.38 (s, 1H), 7.76-7.72 (m, 2H), 7.61-7.39 (m, 6H), 4.49 (t, $J = 10.4$ Hz, 1H), 2.07-2.04 (m, 2H), 1.88-1.79 (m, 4H), 1.66 (d, $J = 11.2$ Hz, 1H), 1.51-1.41 (m, 2H), 1.29-1.23 (m, 1H); ^{13}C NMR (100 MHz, DMSO- d_6): δ 140.4, 140.1, 138.7, 133.9, 132.6, 132.5, 129.5, 128.9, 128.2, 127.5, 126.7, 126.5, 125.0, 122.1, 113.2, 54.9, 33.6, 25.7, 25.4; HRMS (ESI, m/z) calcd. For $\text{C}_{23}\text{H}_{22}\text{ClN}_2$ $[\text{M}+\text{H}]^+$: 361.1472; found: 361.1471.

3-cyclohexyl-5-(1H-pyrazol-1-yl)-3H-naphtho[1,2-*d*]imidazole (34k)



The general procedure for imidazole was followed. Column chromatography (SiO_2 , eluting with 90:10 hexane/acetone) afforded the desired product as a light brown gummy solid (38 mg, 40% yield). ^1H NMR (400 MHz, DMSO- d_6): δ 8.55-8.54 (m, 1H), 8.49 (s, 1H), 8.15 (dd, $J_1 = 2.4$ Hz, $J_2 = 0.8$ Hz, 1H), 8.05 (s, 1H), 7.81 (dd, $J_1 = 2.0$ Hz, $J_2 = 0.8$ Hz, 1H), 7.66-7.62 (m, 1H), 7.53-7.52 (m, 1H), 7.48-7.43 (m, 1H), 6.58 (t, $J = 2.0$ Hz, 1H), 4.57-4.50 (m, 1H), 2.08-2.04 (m, 2H), 1.91-1.81 (m, 4H), 1.68 (d, $J = 12.4$ Hz, 1H), 1.54-1.43 (m, 2H), 1.33-1.25 (m, 1H); ^{13}C NMR (100 MHz, DMSO- d_6): δ 141.4, 140.8, 138.8, 133.6, 133.1, 128.7, 127.5, 127.2, 126.5, 125.6, 124.3, 121.9, 110.9, 106.8, 55.0, 33.6, 25.6, 25.3; HRMS (ESI, m/z) calcd. For $\text{C}_{20}\text{H}_{21}\text{N}_4$ $[\text{M}+\text{H}]^+$: 317.1766; found: 317.1755.

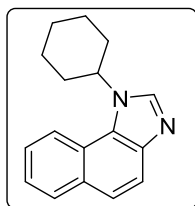
3-cyclohexyl-3H-imidazo[4,5-*f*]quinoline (34l)



The general procedure for imidazole was followed. Column chromatography (SiO_2 , eluting with 90:10 hexane/acetone) afforded the desired product as a pale yellow solid (40 mg, 53% yield); mp: 144-146 °C. ^1H NMR (400 MHz, DMSO- d_6): δ 8.82 (dd, $J_1 = 4.4$ Hz, $J_2 = 2.0$ Hz, 1H), 8.79-8.77 (m, 1H), 8.43 (s, 1H), 8.06 (d, $J = 9.2$ Hz, 1H), 7.81 (d, $J = 9.2$ Hz, 1H), 7.56 (dd, $J_1 = 8.0$ Hz, $J_2 = 4.0$ Hz, 1H), 4.50-4.42 (m, 1H), 2.05-2.02 (m, 2H), 1.89-1.79 (m, 4H), 1.67 (d, $J = 13.2$ Hz, 1H),

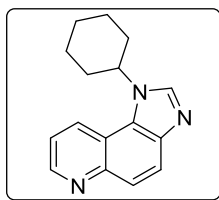
1.52-1.42 (m, 2H), 1.30-1.22 (m, 1H); ^{13}C NMR (100 MHz, DMSO- d_6): δ 148.7, 145.9, 141.1, 138.4, 129.9, 129.8, 124.2, 122.3, 121.8, 115.5, 55.2, 33.2, 25.7, 25.3; HRMS (ESI, m/z) calcd. For $\text{C}_{16}\text{H}_{18}\text{N}_3$ $[\text{M}+\text{H}]^+$: 252.1501; found: 252.1502.

1-cyclohexyl-1*H*-naphtho[1,2-*d*]imidazole (34m)

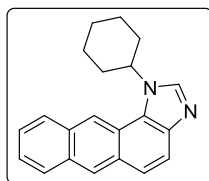


The general procedure for imidazole was followed. Column chromatography (SiO_2 , eluting with 90:10 hexane/acetone) afforded the desired product as a white powder (30 mg, 40% yield); mp: 140-142 $^\circ\text{C}$. ^1H NMR (400 MHz, DMSO- d_6): δ 8.36 (s, 1H), 8.28 (d, $J = 8.4$ Hz, 1H), 8.02 (dd, $J_1 = 8.4$ Hz, $J_2 = 1.2$ Hz, 1H), 7.75 (d, $J = 8.4$ Hz, 1H), 7.67 (d, $J = 8.8$ Hz, 1H), 7.65-7.60 (m, 1H), 7.50-7.46 (m, 1H), 4.91-4.84 (m, 1H), 2.26 (d, $J = 12.0$ Hz, 2H), 1.89-1.58 (m, 7H), 1.34-1.26 (m, 1H); ^{13}C NMR (100 MHz, DMSO- d_6): δ 141.6, 140.4, 131.4, 129.9, 127.3, 126.8, 124.5, 123.8, 122.2, 120.9, 120.6, 56.9, 33.8, 25.8, 25.6; HRMS (ESI, m/z) calcd. For $\text{C}_{17}\text{H}_{19}\text{N}_2$ $[\text{M}+\text{H}]^+$: 251.1548; found: 251.1545.

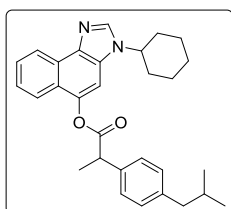
1-cyclohexyl-1*H*-imidazo[4,5-*f*]quinoline (34n)



The general procedure for imidazole was followed. Column chromatography (SiO_2 , eluting with 90:10 hexane/acetone) afforded the desired product as a light brown solid (32 mg, 42% yield); mp: 148-150 $^\circ\text{C}$. ^1H NMR (400 MHz, DMSO- d_6): δ 8.84 (dd, $J_1 = 4.4$ Hz, $J_2 = 1.6$ Hz, 1H), 8.68 (d, $J = 8.4$ Hz, 1H), 8.45 (s, 1H), 7.99 (d, $J = 8.8$ Hz, 1H), 7.80 (d, $J = 8.8$ Hz, 1H), 7.62 (dd, $J_1 = 8.8$ Hz, $J_2 = 4.4$ Hz, 1H), 4.91-4.84 (m, 1H), 2.34 (d, $J = 11.2$ Hz, 2H), 1.88-1.60 (m, 7H), 1.33-1.25 (m, 1H); ^{13}C NMR (100 MHz, DMSO- d_6): δ 148.1, 146.5, 141.4, 141.3, 129.4, 126.6, 124.9, 123.9, 121.5, 117.5, 56.8, 33.6, 25.6, 25.5; HRMS (ESI, m/z) calcd. For $\text{C}_{16}\text{H}_{18}\text{N}_3$ $[\text{M}+\text{H}]^+$: 252.1501; found: 252.1497.

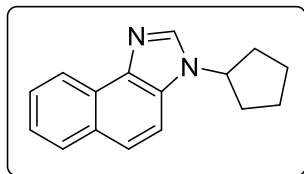
1-cyclohexyl-1H-anthra[1,2-d]imidazole (34o)

The general procedure for imidazole was followed. Column chromatography (SiO₂, eluting with 90:10 hexane/acetone) afforded the desired product as a creamy white solid (61 mg, 68% yield); mp: 154-156 °C. ¹H NMR (400 MHz, DMSO-d₆): δ 8.79 (s, 1H), 8.65 (s, 1H), 8.36 (s, 1H), 8.19 (d, *J* = 8.0 Hz, 1H), 8.07 (d, *J* = 8.8 Hz, 1H), 7.81 (d, *J* = 8.8 Hz, 1H), 7.73 (d, *J* = 9.2 Hz, 1H), 7.57-7.49 (m, 2H), 5.14-5.07 (m, 1H), 2.35 (d, *J* = 12.0 Hz, 2H), 1.93-1.77 (m, 7H), 1.37-1.28 (m, 1H); ¹³C NMR (100 MHz, DMSO-d₆): δ 141.0, 139.6, 131.6, 130.5, 130.1, 128.9, 128.3, 128.2, 126.4, 126.3, 125.8, 124.5, 121.8, 121.5, 118.9, 57.0, 33.8, 25.7, 25.5; HRMS (ESI, *m/z*) calcd. For C₂₁H₂₁N₂ [M+H]⁺: 301.1705; found: 301.1703.

3-cyclohexyl-3H-naphtho[1,2-d]imidazol-5-yl 2-(4-isobutylphenyl)propanoate (34p)

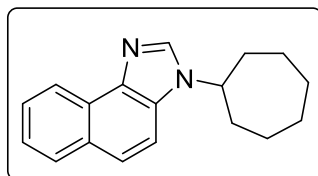
The general procedure for imidazole was followed. Column chromatography (SiO₂, eluting with 90:10 hexane/acetone) afforded the desired product as a light brown gummy liquid (95 mg, 70% yield). ¹H NMR (400 MHz, DMSO-d₆): δ 8.40 (dt, *J*₁ = 8.0 Hz, *J*₂ = 0.8 Hz, 1H), 8.35 (s, 1H), 7.69 (s, 1H), 7.57-7.53 (m, 1H), 7.40 (d, *J* = 8.4 Hz, 2H), 7.25-7.18 (m, 4H), 4.44-4.36 (m, 1H), 4.24 (q, *J* = 7.2 Hz, 1H), 2.44 (d, *J* = 6.8 Hz, 2H), 2.02-1.99 (m, 2H), 1.86-1.78 (m, 5H), 1.67 (d, *J* = 13.2 Hz, 1H), 1.58 (d, *J* = 7.2 Hz, 3H), 1.50-1.40 (m, 2H), 1.28-1.21 (m, 1H), 0.85 (d, *J* = 6.4 Hz, 6H); ¹³C NMR (100 MHz, DMSO-d₆): δ 173.7, 142.6, 140.9, 140.5, 137.9, 136.8, 129.91, 129.88, 128.2, 127.33, 127.27, 124.8, 123.7, 121.9, 105.4, 55.0, 44.87, 44.76, 33.5, 33.4, 33.2, 25.7, 25.3, 22.7, 22.6, 18.6; HRMS (ESI, *m/z*) calcd. For C₃₀H₃₅N₂O₂ [M+H]⁺: 455.2699; found: 455.2697.

3-cyclopentyl-3H-naphtho[1,2-d]imidazole (34q)



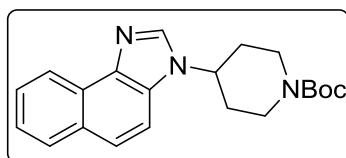
The general procedure for imidazole was followed. Column chromatography (SiO₂, eluting with 90:10 hexane/acetone) afforded the desired product as a creamy white solid (61 mg, 86% yield); mp: 114-116 °C. ¹H NMR (400 MHz, DMSO-d₆): δ 8.47-8.44 (m, 1H), 8.31 (s, 1H), 7.95 (d, *J* = 8.4 Hz, 1H), 7.74 (d, *J* = 8.8 Hz, 1H), 7.69 (d, *J* = 8.8 Hz, 1H), 7.59-7.55 (m, 1H), 7.46-7.41 (m, 1H), 4.93-4.86 (m, 1H), 2.23-2.14 (m, 2H), 1.97-1.89 (m, 2H), 1.86-1.77 (m, 2H), 1.72-1.67 (m, 2H); ¹³C NMR (100 MHz, DMSO-d₆): δ 140.2, 139.2, 130.5, 130.2, 128.9, 127.4, 126.7, 124.7, 123.4, 121.7, 112.4, 56.9, 32.7, 24.1; HRMS (ESI, *m/z*) calcd. For C₁₆H₁₇N₂ [M+H]⁺: 237.1392; found: 237.1394.

3-cycloheptyl-3H-naphtho[1,2-*d*]imidazole (34r)



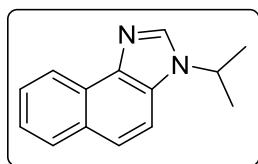
The general procedure for imidazole was followed. Column chromatography (SiO₂, eluting with 90:10 hexane/acetone) afforded the desired product as a creamy white solid (54 mg, 68% yield); mp: 98-100 °C. ¹H NMR (400 MHz, DMSO-d₆): δ 8.42 (d, *J* = 8.0 Hz, 1H), 8.33 (s, 1H), 7.95 (d, *J* = 8.0 Hz, 1H), 7.78 (d, *J* = 9.2 Hz, 1H), 7.69 (d, *J* = 8.8 Hz, 1H), 7.58-7.54 (m, 1H), 7.45-7.41 (m, 1H), 4.66-4.59 (m, 1H), 2.08-2.03 (m, 4H), 1.79-1.58 (m, 8H); ¹³C NMR (100 MHz, DMSO-d₆): δ 140.2, 138.9, 130.1, 129.7, 128.9, 127.4, 126.7, 124.6, 123.3, 121.6, 112.4, 57.5, 35.5, 27.5, 24.7; HRMS (ESI, *m/z*) calcd. For C₁₈H₂₁N₂ [M+H]⁺: 265.1705; found: 265.1714.

tert-butyl 4-(3H-naphtho[1,2-*d*]imidazol-3-yl)piperidine-1-carboxylate (34s)



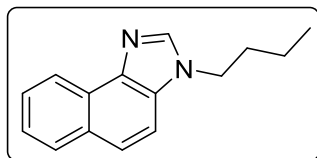
The general procedure for imidazole was followed. Column chromatography (SiO₂, eluting with 90:10 hexane/acetone) afforded the desired product as a creamy white solid (84 mg, 80% yield); mp: 182-184 °C. ¹H NMR (400 MHz, DMSO-d₆): δ 8.42 (d, *J* = 8.0 Hz, 1H), 8.39 (s, 1H), 7.96 (d, *J* = 8.0 Hz, 1H), 7.83 (d, *J* = 8.0 Hz, 1H), 7.72 (d, *J* = 8.8 Hz, 1H), 7.59-7.54 (m, 1H), 7.46-7.40 (m, 1H), 4.72-4.64 (m, 1H), 4.13 (d, *J* = 11.6 Hz, 2H), 2.95 (br.s, 2H), 2.07-1.89 (m, 4H), 1.41 (s, 9H); ¹³C NMR (100 MHz, DMSO-d₆): δ 154.3, 140.0, 138.8, 130.2, 130.0, 128.9, 127.3, 126.8, 124.7, 123.4, 121.6, 112.1, 79.5, 53.1, 32.6, 28.6; HRMS (ESI, *m/z*) calcd. For C₂₁H₂₆N₃O₂ [M+H]⁺: 352.2025; found: 352.2029.

3-isopropyl-3*H*-naphtho[1,2-*d*]imidazole (34t)



The general procedure for imidazole was followed. Column chromatography (SiO₂, eluting with 90:10 hexane/acetone) afforded the desired product as a creamy white solid (38 mg, 60% yield); mp: 108-110 °C. ¹H NMR (400 MHz, DMSO-d₆): δ 8.44-8.43 (m, 1H), 8.35 (s, 1H), 7.96 (d, *J* = 7.6 Hz, 1H), 7.79 (d, *J* = 8.8 Hz, 1H), 7.70 (d, *J* = 8.8 Hz, 1H), 7.58-7.54 (m, 1H), 7.46-7.41 (m, 1H), 4.88-4.78 (m, 1H), 1.55 (d, *J* = 6.8 Hz, 6H); ¹³C NMR (100 MHz, DMSO-d₆): δ 139.9, 139.1, 130.1, 129.9, 128.9, 127.4, 126.7, 124.6, 123.3, 121.6, 112.3, 47.8, 23.1; HRMS (ESI, *m/z*) calcd. For C₁₄H₁₅N₂ [M+H]⁺: 211.1235; found: 211.1240.

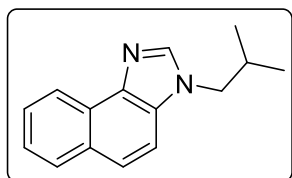
3-butyl-3*H*-naphtho[1,2-*d*]imidazole (34u)



The general procedure for imidazole was followed. Column chromatography (SiO₂, eluting with 90:10 hexane/acetone) afforded the desired product as a light brown gummy solid (33 mg, 48% yield). ¹H NMR (400 MHz, DMSO-d₆): δ 8.44-8.41 (m, 1H), 8.24 (s, 1H), 7.95 (d, *J* = 8.0 Hz, 1H), 7.75 (d, *J* = 8.8 Hz, 1H), 7.70 (d, *J* = 8.8 Hz, 1H), 7.58-7.54 (m, 1H), 7.45-7.41 (m, 1H), 4.30 (t, *J* = 7.2 Hz, 1H), 1.77 (qu, *J* = 7.2 Hz, 2H), 1.27-1.18 (m, 2H), 0.85 (t, *J* = 7.2 Hz, 3H); ¹³C

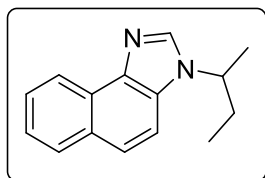
NMR (100 MHz, DMSO-d₆): δ 142.4, 138.9, 130.6, 130.1, 128.9, 127.3, 126.7, 124.6, 123.5, 121.6, 112.0, 44.6, 32.5, 19.9, 13.9; HRMS (ESI, m/z) calcd. For C₁₅H₁₇N₂ [M+H]⁺: 225.1392; found: 225.1402.

3-isobutyl-3H-naphtho[1,2-d]imidazole (34v)



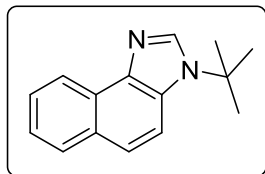
The general procedure for imidazole was followed. Column chromatography (SiO₂, eluting with 90:10 hexane/acetone) afforded the desired product as a light brown solid (50 mg, 74% yield); mp: 74-76 °C. ¹H NMR (400 MHz, DMSO-d₆): δ 8.44-8.42 (m, 1H), 8.22 (s, 1H), 7.95 (d, *J* = 8.0 Hz, 1H), 7.76 (d, *J* = 8.8 Hz, 1H), 7.69 (d, *J* = 8.8 Hz, 1H), 7.59-7.55 (m, 1H), 7.46-7.41 (m, 1H), 4.12 (d, *J* = 7.2 Hz, 2H), 2.16-2.08 (m, 1H), 0.83 (d, *J* = 6.8 Hz, 6H); ¹³C NMR (100 MHz, DMSO-d₆): δ 142.8, 138.8, 130.9, 130.1, 128.9, 127.3, 126.7, 124.6, 123.5, 121.5, 112.3, 51.9, 29.6, 20.2; HRMS (ESI, m/z) calcd. For C₁₅H₁₇N₂ [M+H]⁺: 225.1392; found: 225.1402.

3-(sec-butyl)-3H-naphtho[1,2-d]imidazole (34w)



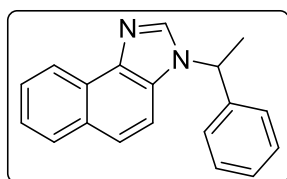
The general procedure for imidazole was followed. Column chromatography (SiO₂, eluting with 90:10 hexane/acetone) afforded the desired product as a light brown gummy solid (54 mg, 81% yield). ¹H NMR (400 MHz, DMSO-d₆): δ 8.45-8.43 (m, 1H), 8.33 (s, 1H), 7.95 (d, *J* = 8.4 Hz, 1H), 7.78 (d, *J* = 8.8 Hz, 1H), 7.68 (d, *J* = 8.8 Hz, 1H), 7.58-7.54 (m, 1H), 7.45-7.41 (m, 1H), 4.62-4.53 (m, 1H), 1.97-1.82 (m, 2H), 1.53 (d, *J* = 6.8 Hz, 3H), 0.71 (t, *J* = 7.6 Hz, 3H); ¹³C NMR (100 MHz, DMSO-d₆): δ 140.5, 139.0, 130.2, 130.1, 128.9, 127.4, 126.7, 124.6, 123.3, 121.6, 112.4, 53.6, 29.8, 21.2, 11.0; HRMS (ESI, m/z) calcd. For C₁₅H₁₇N₂ [M+H]⁺: 225.1392; found: 225.1401.

3-(tert-butyl)-3H-naphtho[1,2-d]imidazole (34x)



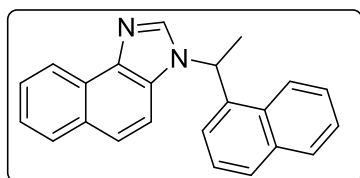
The general procedure for imidazole was followed. Column chromatography (SiO₂, eluting with 90:10 hexane/acetone) afforded the desired product as a light brown gummy solid (29 mg, 43% yield). ¹H NMR (400 MHz, DMSO-d₆): δ 8.46-8.44 (m, 1H), 8.23 (s, 1H), 7.98-7.94 (m, 2H), 7.67 (d, *J* = 9.2 Hz, 1H), 7.58-7.54 (m, 1H), 7.46-7.42 (m, 1H), 1.72 (s, 9H); ¹³C NMR (100 MHz, DMSO-d₆): δ 140.5, 140.0, 129.6, 129.5, 128.6, 127.4, 126.6, 124.8, 122.9, 121.7, 114.7, 56.8, 29.8; HRMS (ESI, *m/z*) calcd. For C₁₅H₁₇N₂ [M+H]⁺: 225.1392; found: 225.1388.

3-(1-phenylethyl)-3H-naphtho[1,2-d]imidazole (34y)



The general procedure for imidazole was followed. Column chromatography (SiO₂, eluting with 90:10 hexane/acetone) afforded the desired product as a yellow solid (69 mg, 85% yield); mp: 114-116 °C. ¹H NMR (400 MHz, DMSO-d₆): δ 8.58 (s, 1H), 8.46-8.43 (m, 1H), 7.91 (d, *J* = 8.4 Hz, 1H), 7.62 (d, *J* = 8.8 Hz, 1H), 7.58-7.55 (m, 2H), 7.43-7.41 (m, 1H), 7.30-7.28 (m, 4H), 7.24-7.21 (m, 1H), 5.94 (q, *J* = 6.8 Hz, 1H), 1.97 (d, *J* = 7.2 Hz, 3H); ¹³C NMR (100 MHz, DMSO-d₆): δ 142.4, 140.5, 139.2, 130.3, 130.2, 129.3, 128.9, 128.2, 127.3, 126.8, 126.6, 124.8, 123.5, 121.6, 112.5, 55.0, 21.7; HRMS (ESI, *m/z*) calcd. For C₁₉H₁₇N₂ [M+H]⁺: 273.1392; found: 273.1382.

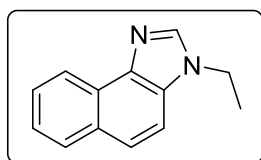
3-(1-(naphthalen-1-yl)ethyl)-3H-naphtho[1,2-d]imidazole (34z)



The general procedure for imidazole was followed. Column chromatography (SiO₂, eluting with 90:10 hexane/acetone) afforded the desired product as a creamy white solid (83 mg, 86% yield);

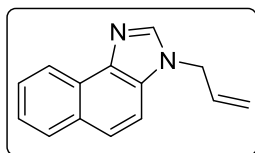
mp: 178-180 °C. ^1H NMR (400 MHz, DMSO- d_6): δ 8.66 (dd, $J_1 = 8.0$ Hz, $J_2 = 0.4$ Hz, 1H), 8.11 (s, 1H), 7.97-7.87 (m, 3H), 7.82 (d, $J = 8.4$ Hz, 1H), 7.66-7.62 (m, 1H), 7.57 (d, $J = 8.8$ Hz, 1H), 7.53-7.46 (m, 3H), 7.37 (t, $J = 8.0$ Hz, 1H), 7.27 (dd, $J_1 = 8.8$ Hz, $J_2 = 1.6$ Hz, 1H), 7.15 (d, $J = 7.2$ Hz, 1H), 6.46 (q, $J = 6.4$ Hz, 1H), 2.15 (d, $J = 7.2$ Hz, 3H); ^{13}C NMR (100 MHz, DMSO- d_6): δ 139.3, 139.0, 136.0, 134.0, 130.4, 130.0, 129.4, 129.2, 128.4, 127.3, 127.2, 126.8, 126.2, 125.6, 124.8, 124.3, 123.3, 122.0, 121.9, 110.9, 51.9, 21.4; HRMS (ESI, m/z) calcd. For $\text{C}_{23}\text{H}_{19}\text{N}_2$ $[\text{M}+\text{H}]^+$: 323.1548; found: 323.1550.

3-ethyl-3*H*-naphtho[1,2-*d*]imidazole (34aa)



The general procedure for imidazole was followed. Column chromatography (SiO_2 , eluting with 90:10 hexane/acetone) afforded the desired product as a light brown solid (33 mg, 56% yield); mp: 120-122 °C. ^1H NMR (400 MHz, DMSO- d_6): δ 8.45-8.42 (m, 1H), 8.27 (s, 1H), 7.97-7.95 (m, 1H), 7.76 (d, $J = 8.8$ Hz, 1H), 7.70 (d, $J = 8.8$ Hz, 1H), 7.59-7.55 (m, 1H), 7.46-7.42 (m, 1H), 4.34 (q, $J = 7.2$ Hz, 2H), 1.42 (t, $J = 7.6$ Hz, 3H); ^{13}C NMR (100 MHz, DMSO- d_6): δ 141.9, 139.1, 130.3, 130.1, 128.9, 127.3, 126.7, 124.6, 123.4, 121.6, 111.9, 39.9, 16.3; HRMS (ESI, m/z) calcd. For $\text{C}_{13}\text{H}_{13}\text{N}_2$ $[\text{M}+\text{H}]^+$: 197.1079; found: 197.1080.

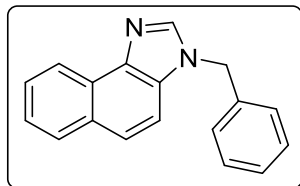
3-allyl-3*H*-naphtho[1,2-*d*]imidazole (34ab)



The general procedure for imidazole was followed. Column chromatography (SiO_2 , eluting with 90:10 hexane/acetone) afforded the desired product as a light brown gummy liquid (29 mg, 46% yield). ^1H NMR (400 MHz, DMSO- d_6): δ 8.46-8.43 (m, 1H), 8.24 (s, 1H), 7.96 (d, $J = 8.0$ Hz, 1H), 7.72-7.66 (m, 2H), 7.60-7.56 (m, 1H), 7.46-7.42 (m, 1H), 6.10-6.01 (m, 1H), 5.09-5.04 (m, 1H), 5.20-5.16 (m, 1H), 5.00-4.98 (m, 2H); ^{13}C NMR (100 MHz, DMSO- d_6): δ 142.4, 139.0,

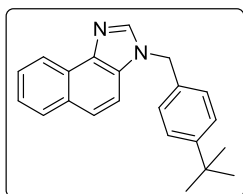
134.3, 130.6, 130.2, 129.0, 127.3, 126.8, 124.7, 123.6, 121.6, 117.9, 112.1, 47.3; HRMS (ESI, m/z) calcd. For $C_{14}H_{13}N_2$ $[M+H]^+$: 209.1079; found: 209.1087.

3-benzyl-3*H*-naphtho[1,2-*d*]imidazole (34ac)



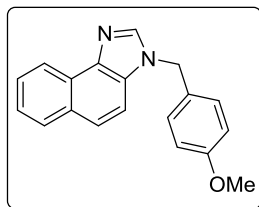
The general procedure for imidazole was followed. Column chromatography (SiO_2 , eluting with 90:10 hexane/acetone) afforded the desired product as a light brown solid (48 mg, 62% yield); mp: 96-98 °C. 1H NMR (400 MHz, $DMSO-d_6$): δ 8.45-8.43 (m, 2H), 7.95-7.92 (m, 1H), 7.69-7.65 (m, 2H), 7.60-7.55 (m, 1H), 7.46-7.42 (m, 1H), 7.30-7.27 (m, 4H), 7.25-7.22 (m, 1H), 5.59 (s, 2H); ^{13}C NMR (100 MHz, $DMSO-d_6$): δ 142.7, 139.2, 137.7, 130.5, 130.2, 129.3, 128.9, 128.3, 127.8, 127.3, 126.8, 124.8, 123.7, 121.6, 112.2, 48.4; HRMS (ESI, m/z) calcd. For $C_{18}H_{15}N_2$ $[M+H]^+$: 259.1235; found: 259.1239.

3-(4-(*tert*-butyl)benzyl)-3*H*-naphtho[1,2-*d*]imidazole (34ad)



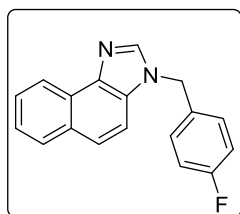
The general procedure for imidazole was followed. Column chromatography (SiO_2 , eluting with 90:10 hexane/acetone) afforded the desired product as a pale yellow solid (49 mg, 52% yield); mp: 88-90 °C. 1H NMR (400 MHz, $DMSO-d_6$): δ 8.45-8.42 (m, 2H), 7.93 (d, $J = 8.0$ Hz, 1H), 7.71 (d, $J = 8.8$ Hz, 1H), 7.66 (d, $J = 9.2$ Hz, 1H), 7.57-7.55 (m, 1H), 7.45-7.41 (m, 1H), 7.31-7.28 (m, 2H), 7.23-7.19 (m, 2H), 5.53 (s, 2H), 1.17 (s, 9H); ^{13}C NMR (100 MHz, $DMSO-d_6$): δ 150.7, 142.6, 139.2, 134.8, 130.5, 130.1, 128.9, 127.6, 127.3, 126.8, 125.9, 124.7, 123.7, 121.6, 112.2, 48.0, 34.7, 31.6; HRMS (ESI, m/z) calcd. For $C_{22}H_{23}N_3O$ $[M+H]^+$: 315.1861; found: 315.1860.

3-(4-methoxybenzyl)-3*H*-naphtho[1,2-*d*]imidazole (34ae)



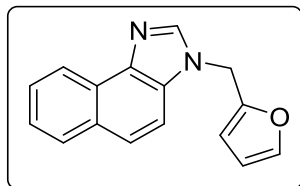
The general procedure for imidazole was followed. Column chromatography (SiO₂, eluting with 90:10 hexane/acetone) afforded the desired product as a light brown solid (48 mg, 55% yield); mp: 106-108 °C. ¹H NMR (400 MHz, DMSO-d₆): δ 8.47-8.42 (m, 1H), 8.42 (s, 1H), 7.93 (d, *J* = 8.0 Hz, 1H), 7.70-7.65 (m, 2H), 7.59-7.55 (m, 1H), 7.45-7.41 (m, 1H), 7.29-7.25 (m, 2H), 6.87-6.83 (m, 2H), 5.49 (s, 2H), 3.65 (s, 3H); ¹³C NMR (100 MHz, DMSO-d₆): δ 159.4, 142.5, 139.2, 130.4, 130.1, 129.5, 129.4, 128.9, 127.3, 126.8, 124.7, 123.6, 121.6, 114.6, 112.2, 55.6, 47.9; HRMS (ESI, *m/z*) calcd. For C₁₉H₁₇N₂O [M+H]⁺: 289.1341; found: 289.1340.

3-(4-fluorobenzyl)-3H-naphtho[1,2-*d*]imidazole (34af)



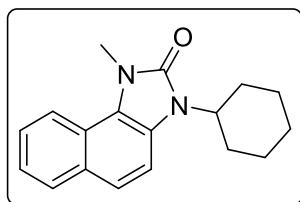
The general procedure for imidazole was followed. Column chromatography (SiO₂, eluting with 90:10 hexane/acetone) afforded the desired product as a light brown gummy solid (29 mg, 35% yield). ¹H NMR (400 MHz, DMSO-d₆): δ 8.43-8.41 (m, 2H), 7.94 (d, *J* = 8.4 Hz, 1H), 7.71-7.66 (m, 2H), 7.59-7.55 (m, 1H), 7.46-7.42 (m, 1H), 7.38-7.34 (m, 2H), 7.16-7.11 (m, 2H), 5.58 (s, 2H); ¹³C NMR (100 MHz, DMSO-d₆): δ 162.2 (d, *J* = 242.5 Hz), 142.6, 139.2, 133.9, 130.2, 131.1 (d, *J* = 56.3 Hz), 130.1 (d, *J* = 8.2 Hz), 129.1, 128.9, 127.3, 126.9, 124.8 (d, *J* = 104.0 Hz), 121.6, 116.1 (d, *J* = 21.3 Hz), 112.1, 47.6; HRMS (ESI, *m/z*) calcd. For C₁₈H₁₄FN₂ [M+H]⁺: 277.1141; found: 277.1137.

3-(furan-2-ylmethyl)-3H-naphtho[1,2-*d*]imidazole (34ag)



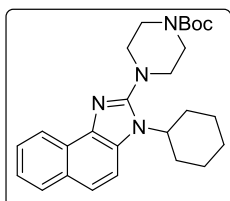
The general procedure for imidazole was followed. Column chromatography (SiO₂, eluting with 90:10 hexane/acetone) afforded the desired product as a light brown gummy liquid (28 mg, 38% yield). ¹H NMR (400 MHz, DMSO-d₆): δ 8.44-8.42 (m, 1H), 8.34 (s, 1H), 7.95 (d, *J* = 8.0 Hz, 1H), 7.80 (d, *J* = 8.8 Hz, 1H), 7.71 (d, *J* = 8.8 Hz, 1H), 7.59-7.55 (m, 2H), 7.46-7.43 (m, 1H), 6.55 (dd, *J*₁ = 3.2 Hz, *J*₂ = 0.8 Hz, 1H), 6.39 (dd, *J*₁ = 3.2 Hz, *J*₂ = 2.0 Hz, 1H), 5.62 (s, 2H); ¹³C NMR (100 MHz, DMSO-d₆): δ 150.4, 143.8, 142.4, 139.0, 130.4, 130.2, 128.9, 127.2, 126.8, 124.8, 123.8, 121.6, 112.1, 111.2, 109.5, 41.5; HRMS (ESI, *m/z*) calcd. For C₁₆H₁₃N₂ [M+H]⁺: 249.1028; found: 249.1020.

3-cyclohexyl-1-methyl-1,3-dihydro-2H-naphtho[1,2-*d*]imidazol-2-one (38a)



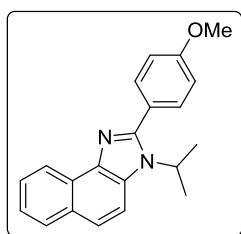
Column chromatography (SiO₂, eluting with 80:20 hexane/EtOAc) afforded the desired product as a creamy white powder (134 mg, 96% yield); mp: 122-124 °C. ¹H NMR (400 MHz, DMSO-d₆): δ 8.33 (d, *J* = 8.4 Hz, 1H), 7.87 (d, *J* = 8.4 Hz, 1H), 7.57 (d, *J* = 8.8 Hz, 1H), 7.50-7.46 (m, 2H), 7.38-7.34 (m, 1H), 4.42-4.35 (m, 1H), 3.94 (s, 3H), 2.29-2.18 (m, 2H), 1.95-1.89 (m, 4H), 1.77 (d, *J* = 12.4 Hz, 1H), 1.54-1.42 (m, 2H), 1.37-1.30 (m, 1H); ¹³C NMR (100 MHz, DMSO-d₆): δ 154.2, 129.6, 129.4, 126.1, 124.7, 123.4, 122.9, 121.7, 120.9, 120.2, 110.5, 53.6, 31.0, 30.6, 26.2, 25.5; HRMS (ESI, *m/z*) calcd. For C₁₈H₂₁N₂O [M+H]⁺: 281.1654; found: 281.1649.

tert-butyl 4-(3-cyclohexyl-3H-naphtho[1,2-*d*]imidazol-2-yl)piperazine-1-carboxylate (38b)



Column chromatography (SiO₂, eluting with 85:15 hexane/EtOAc) afforded the desired product as a white solid (91 mg, 42% yield); mp: 172-174 °C. ¹H NMR (400 MHz, DMSO-d₆): δ 8.54-8.52 (m, 1H), 7.86 (d, *J* = 8.0 Hz, 1H), 7.64 (d, *J* = 8.8 Hz, 1H), 7.58-7.52 (m, 2H), 7.43-7.39 (m, 1H), 4.36-4.28 (m, 1H), 3.66 (t, *J* = 4.8 Hz, 4H), 3.23 (t, *J* = 5.2 Hz, 4H), 2.31-2.21 (m, 2H), 2.01-1.91 (m, 4H), 1.49 (s, 9H), 1.48-1.37 (m, 3H); ¹³C NMR (100 MHz, DMSO-d₆): δ 155.5, 154.9, 137.1, 129.6, 128.8, 128.2, 126.7, 125.9, 124.1, 121.8, 121.7, 112.5, 80.1, 55.8, 31.9, 28.5, 26.4, 25.6; HRMS (ESI, *m/z*) calcd. For C₂₆H₃₅N₄O₂ [M+H]⁺: 435.2760; found: 435.2750.

3-isopropyl-2-(4-methoxyphenyl)-3*H*-naphtho[1,2-*d*]imidazole (38c)



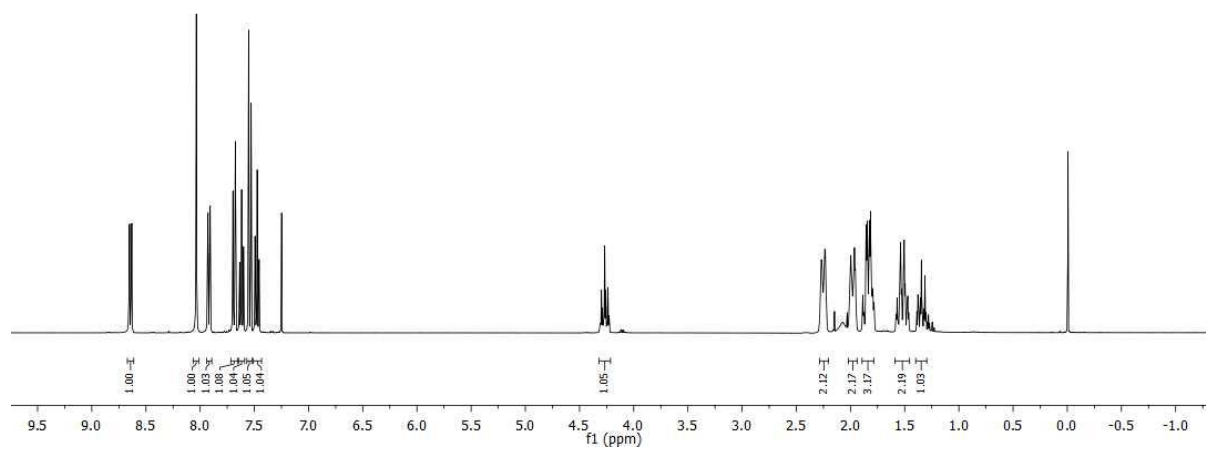
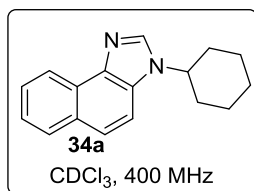
Column chromatography (SiO₂, eluting with 80:20 hexane/EtOAc) afforded the desired product as a creamy white solid (79 mg, 50% yield). ¹H NMR (400 MHz, DMSO-d₆): δ 8.72-8.69 (m, 1H), 7.92 (d, *J* = 8.4 Hz, 1H), 7.75 (d, *J* = 9.2 Hz, 1H), 7.76-7.57 (m, 4H), 7.49-7.45 (m, 1H), 7.07-7.03 (m, 2H), 4.90-4.83 (m, 1H), 3.88 (s, 3H), 1.68 (d, *J* = 6.8 Hz, 6H); ¹³C NMR (100 MHz, DMSO-d₆): δ 160.7, 151.6, 139.4, 131.2, 129.9, 129.8, 128.2, 127.3, 126.3, 124.6, 123.7, 122.9, 122.0, 114.3, 112.7, 55.5, 48.9, 22.0; HRMS (ESI, *m/z*) calcd. For C₂₁H₂₁N₂O [M+H]⁺: 317.1654; found: 317.1646.

IV.11. ¹H and ¹³C NMR spectra

HM-1522
single pulse

8.653
8.652
8.651
8.633
8.631
8.626
8.625
7.928
7.908
7.697
7.675
7.638
7.635
7.614
7.614
7.600
7.597
7.552
7.550
7.496
7.491
7.477
7.474
7.470
7.466
7.463

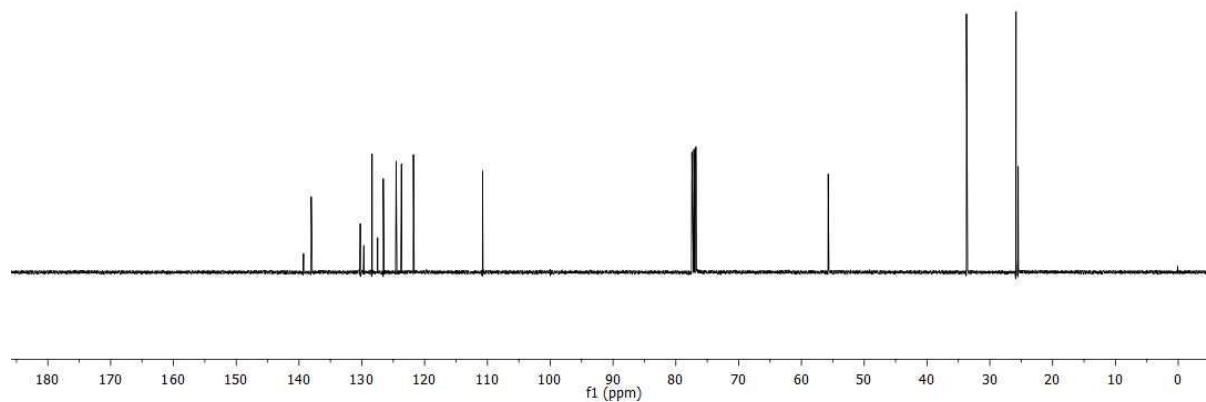
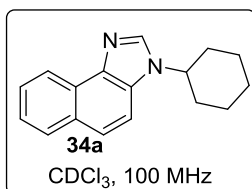
4.307
4.288
4.288
4.277
4.277
4.269
4.269
4.247
4.238
4.229
4.220
2.270
2.265
2.261
2.261
2.237
2.232
2.065
1.997
1.989
1.963
1.963
1.886
1.878
1.855
1.846
1.824
1.816
1.794
1.784
1.578
1.570
1.561
1.546
1.537
1.512
1.494
1.491
1.463
1.387
1.378
1.369
1.346
1.333
1.313
1.304
1.281
1.271

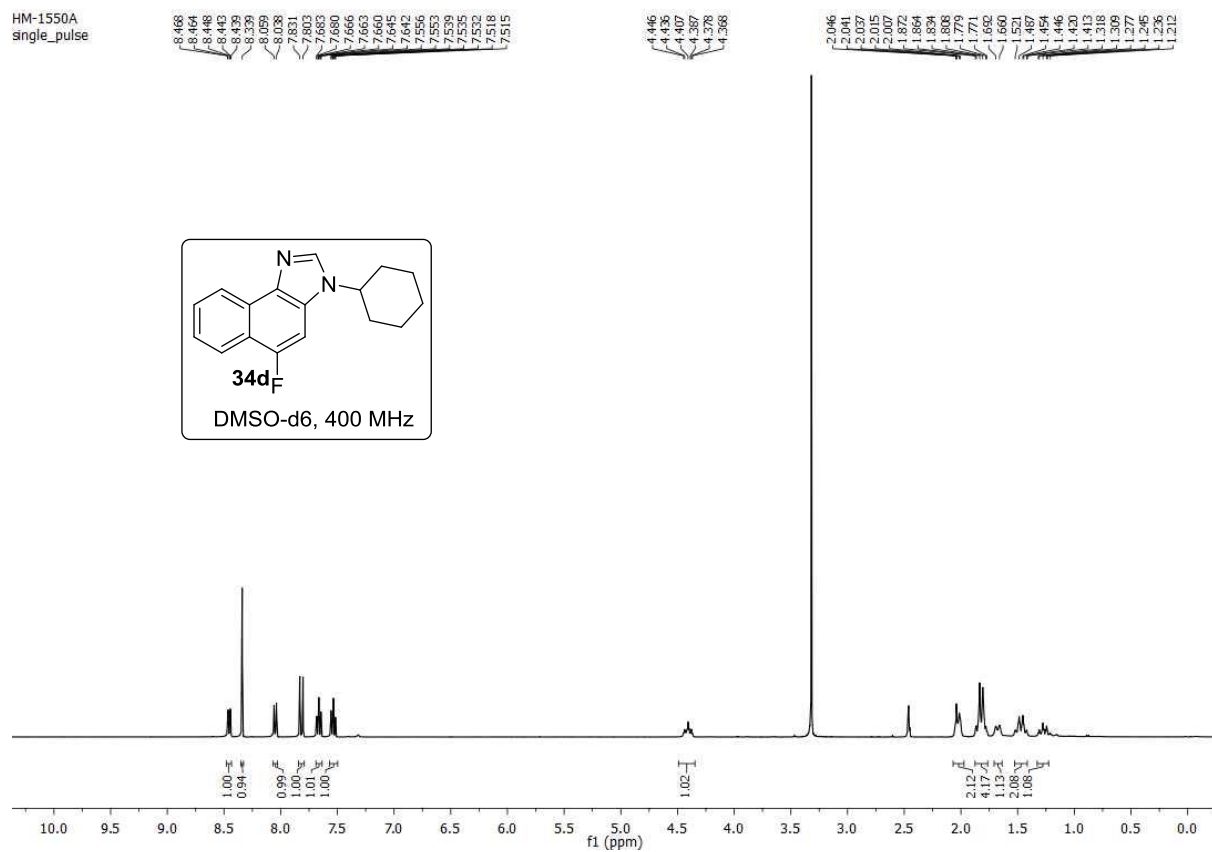
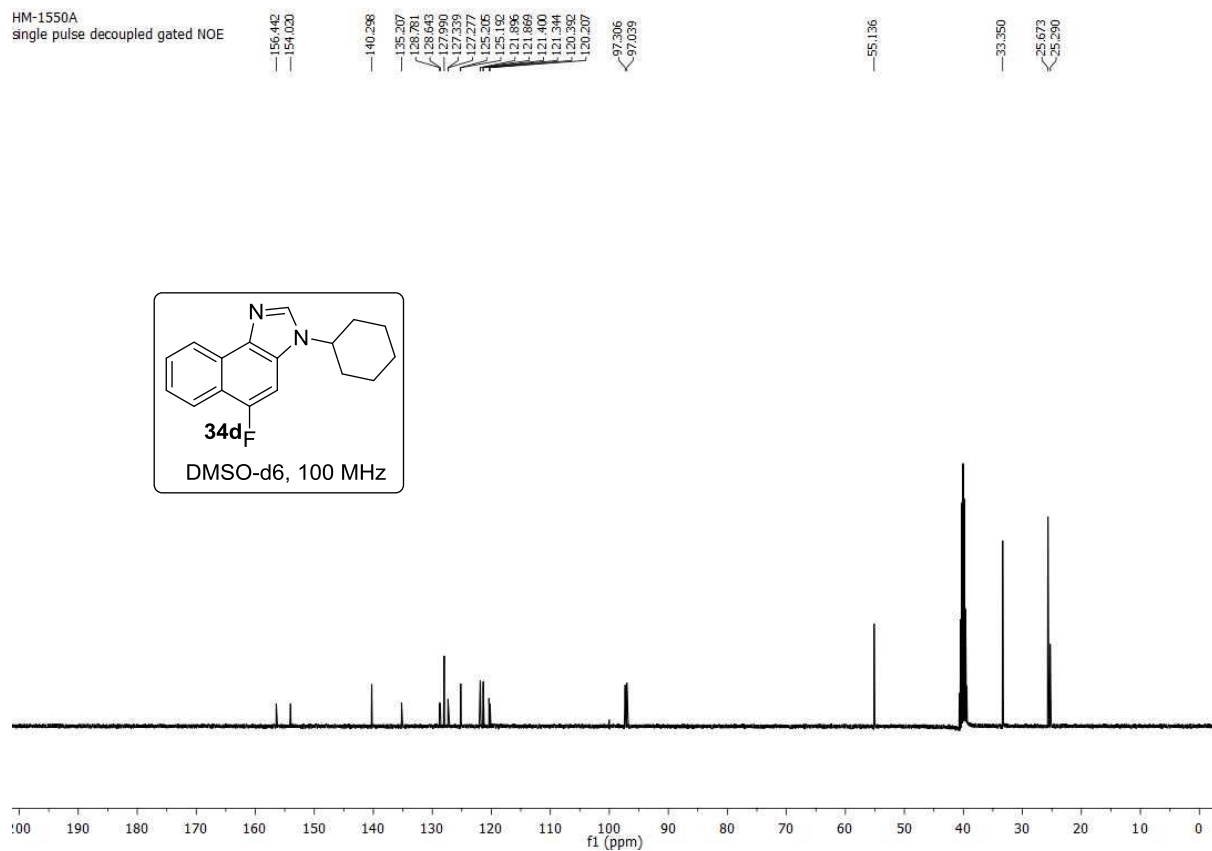


HM-1522
single pulse decoupled gated NOE

130.270
130.053
130.248
129.686
129.353
129.686
126.580
124.541
123.693
121.786
110.774

55.745
33.717
25.821
25.480



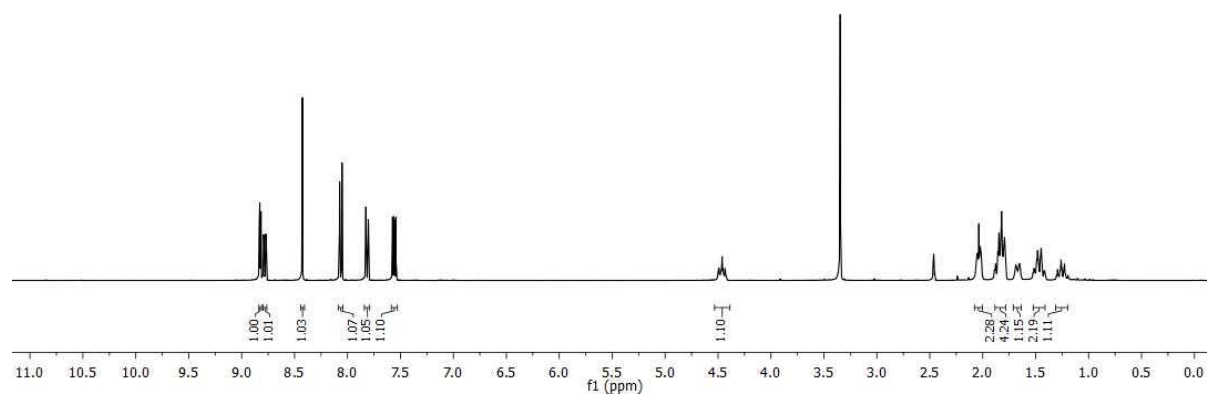
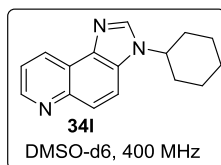
HM-1550A
single_pulseHM-1550A
single_pulse decoupled gated NOE

HM-1778
single_pulse

8.833
8.828
8.822
8.818
8.794
8.792
8.789
8.788
8.773
8.769
8.767
8.436
8.052
7.826
7.803
7.574
7.564
7.554
7.543

4.501
4.492
4.482
4.472
4.462
4.453
4.443
4.433

2.048
2.041
2.019
1.887
1.878
1.856
1.847
1.822
1.794
1.686
1.665
1.524
1.515
1.481
1.449
1.415
1.301
1.289
1.260
1.251
1.219

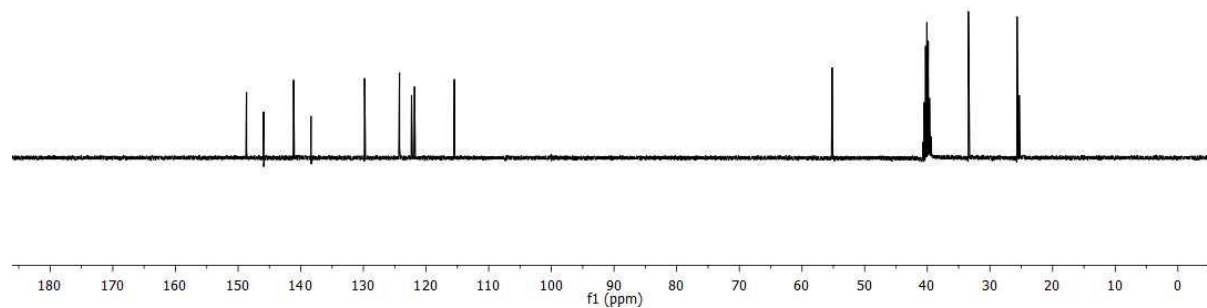
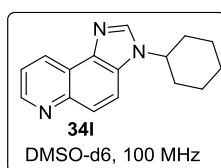


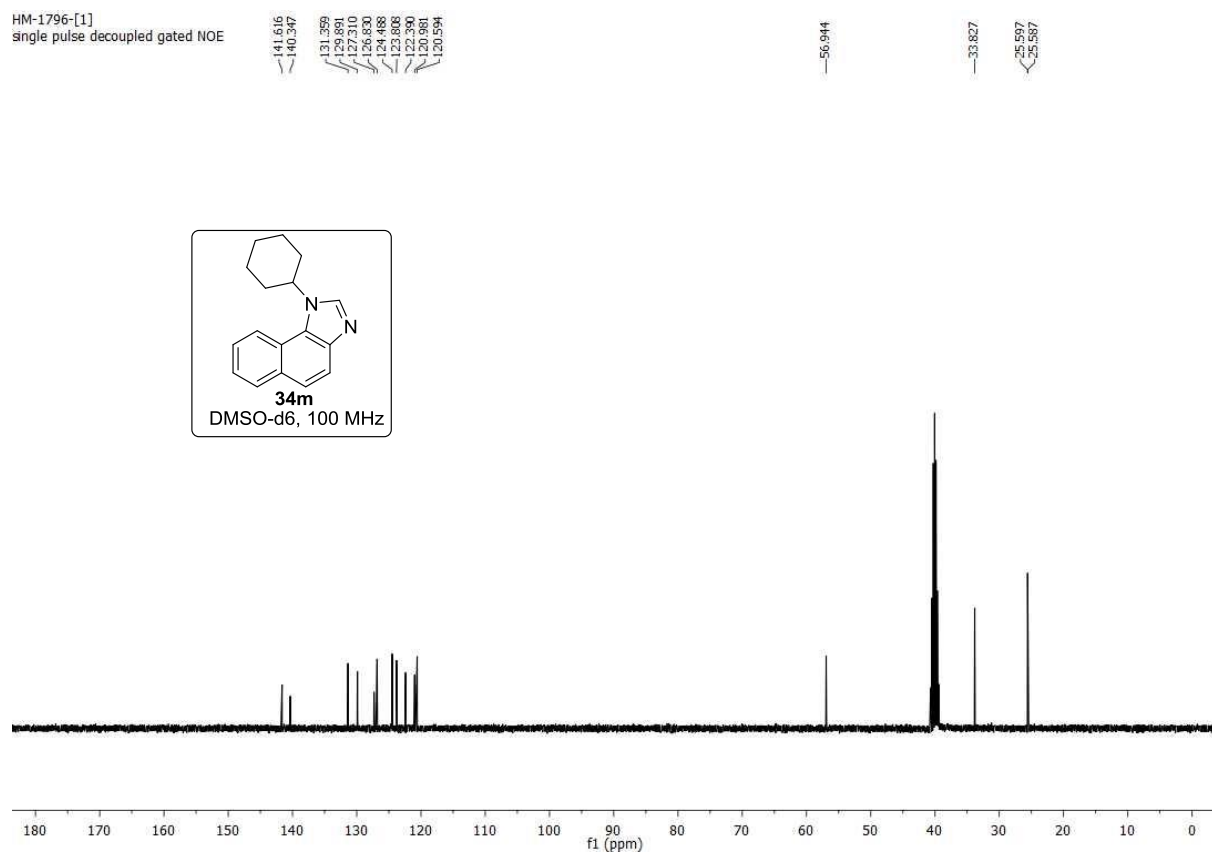
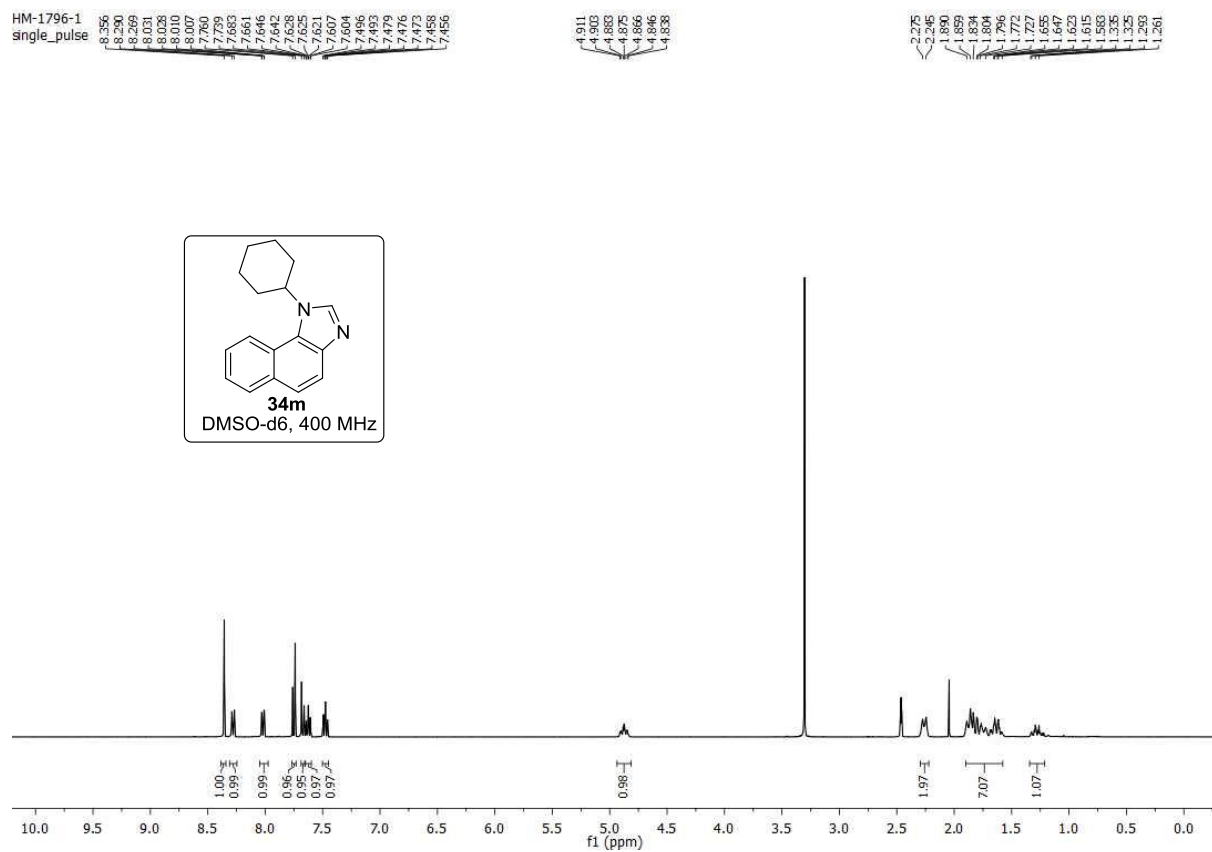
HM-1778
single_pulse decoupled gated NOE

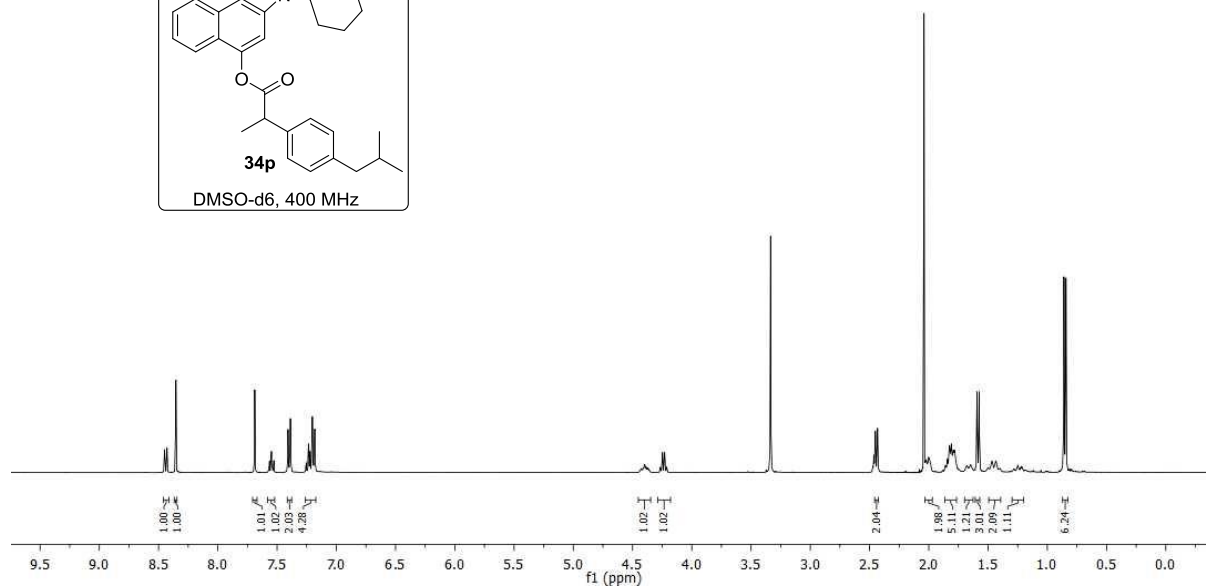
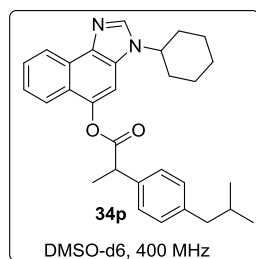
148.656
145.917
141.134
138.362
129.871
129.807
124.238
122.313
121.843
115.482

55.192

33.443
25.671
25.324



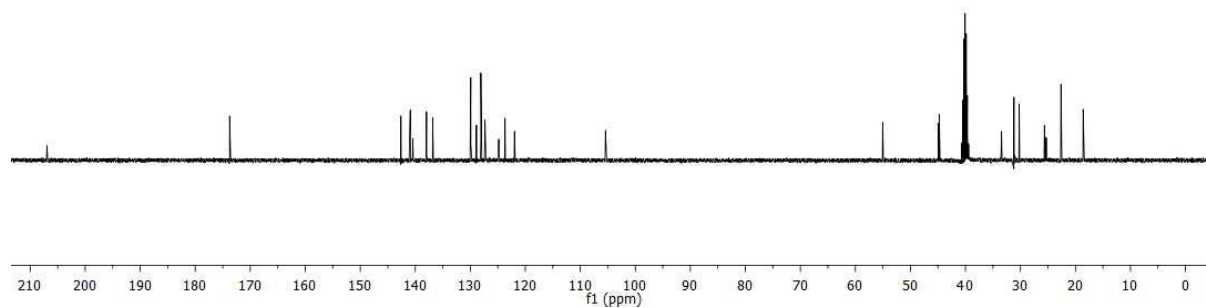
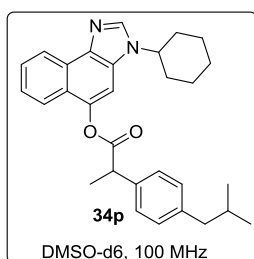


HM-1822
single_pulse8.451
8.449
8.448
8.431
8.429
8.427
8.354
7.688
7.687
7.553
7.551
7.547
7.543
7.530
7.526
7.481
7.387
7.253
7.224
7.221
7.208
7.202
7.185
7.1824.435
4.434
4.378
4.379
4.368
4.358
4.359
4.265
4.247
4.230
4.2142.450
2.433
2.019
2.002
1.992
1.992
1.860
1.843
1.826
1.782
1.782
1.684
1.646
1.593
1.575
1.501
1.467
1.454
1.400
1.392
1.249
1.228
1.216
1.055
1.045HM-1822
single_pulse decoupled gated NOE

173.738

142.612
140.908
140.449
137.957
136.825
128.906
128.884
128.076
127.330
127.270
124.826
123.867
121.961

105.428

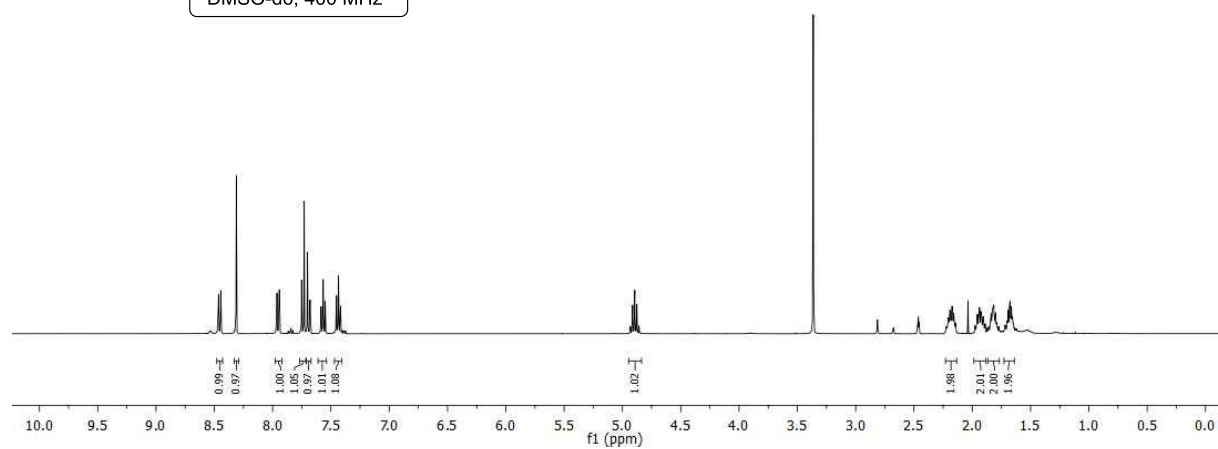
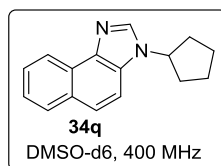
55.023
44.870
44.767
33.508
33.428
31.659
26.522
25.323
22.655
22.631
18.597

HM-1741
single_pulse

8.465 8.463 8.462 8.445 8.443 8.441 8.311 7.963 7.942 7.751 7.729 7.720 7.630 7.587 7.587 7.584 7.569 7.566 7.549 7.548 7.466 7.465 7.462 7.438 7.435 7.431 7.417 7.414

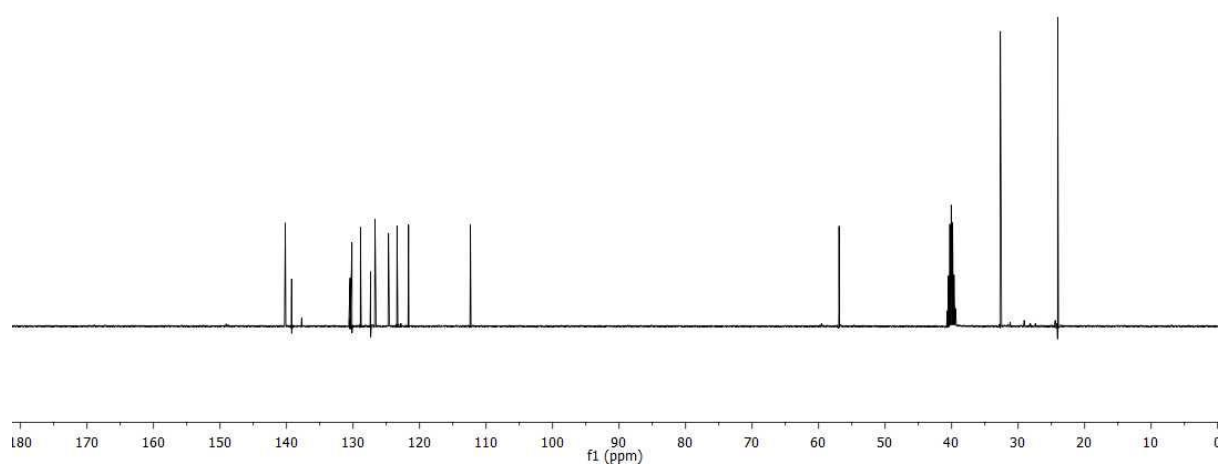
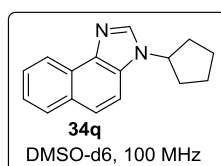
4.931 4.895 4.876 4.858

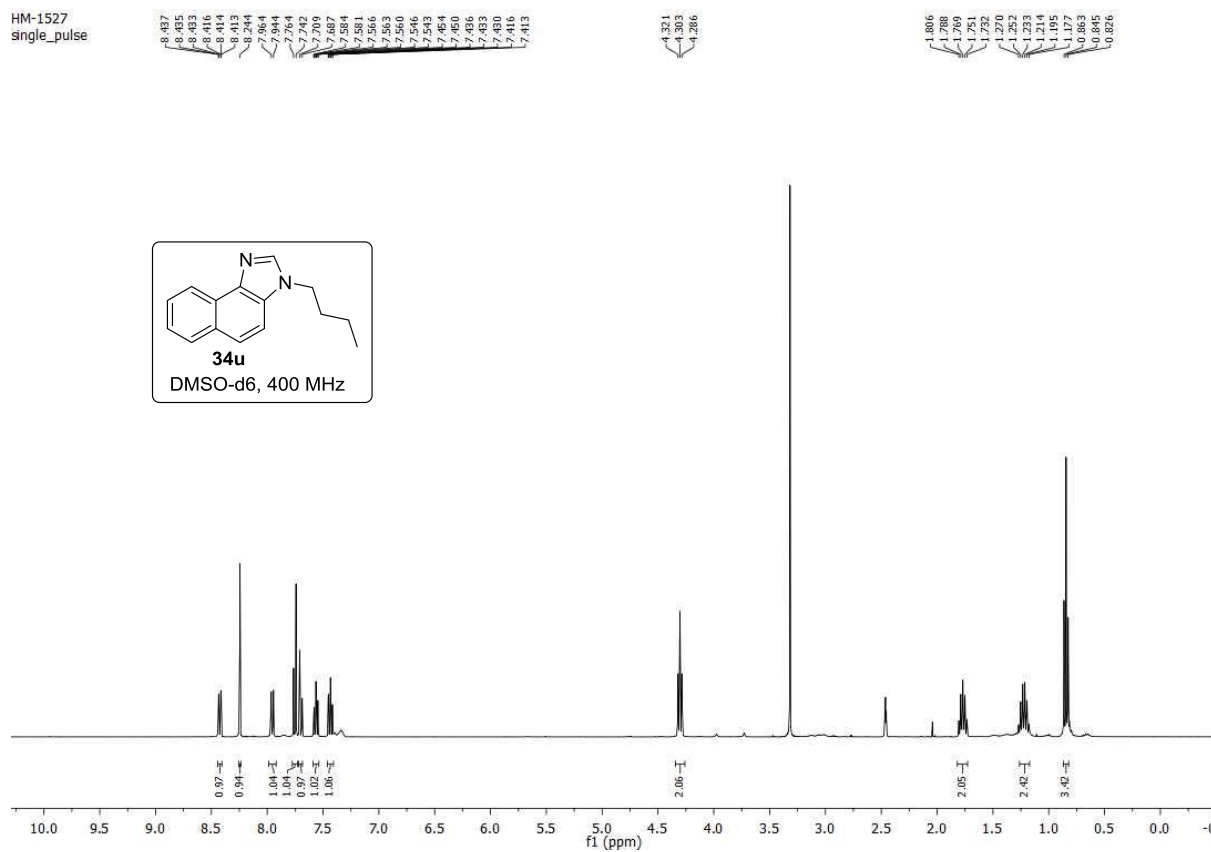
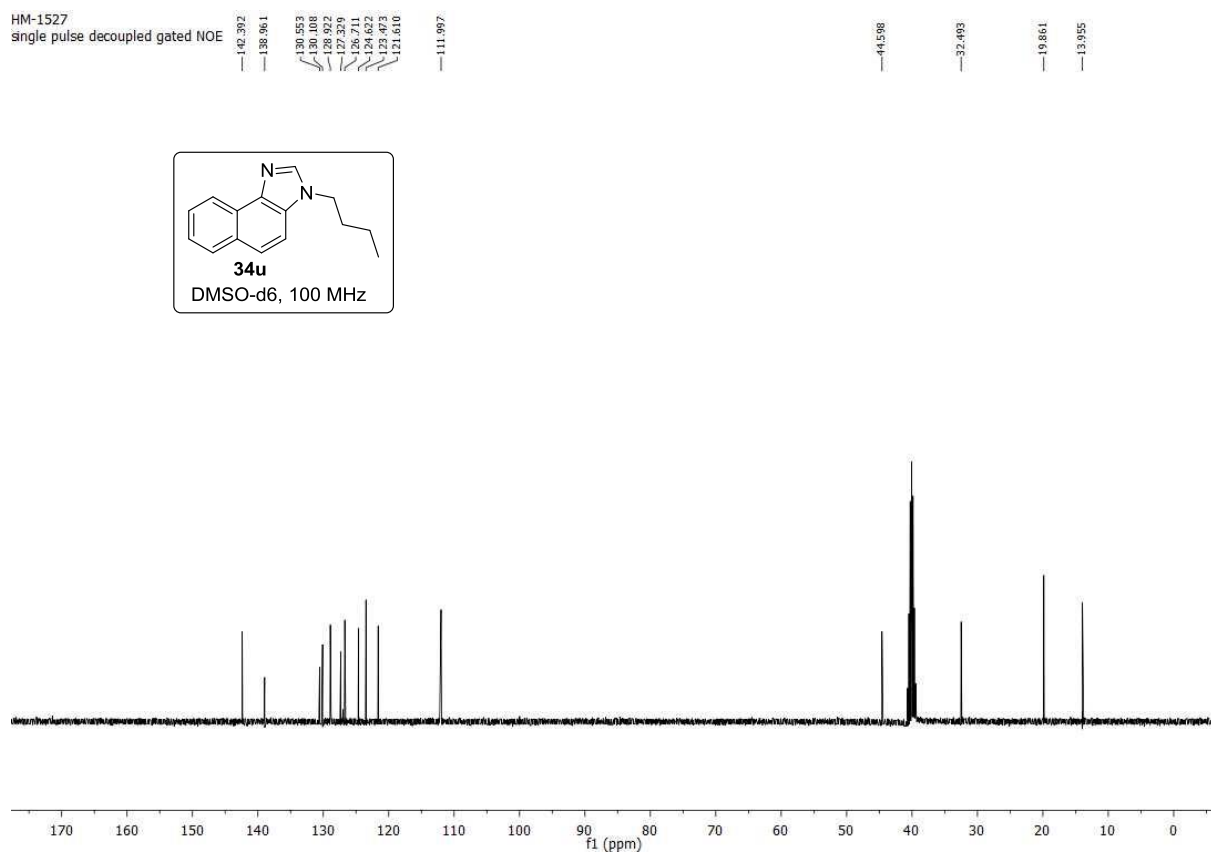
2.225 2.206 2.192 2.173 2.159 2.141 2.122 1.968 1.958 1.938 1.920 1.907 1.889 1.887 1.832 1.822 1.800 1.772 1.722 1.701 1.692 1.676 1.657 1.655

HM-1741
single_pulse decoupled gated NOE

140.194 139.247 130.447 130.165 128.889 127.355 126.707 124.675 123.354 121.855 112.355

56.034 32.678 24.055



HM-1527
single_pulseHM-1527
single pulse decoupled gated NOE

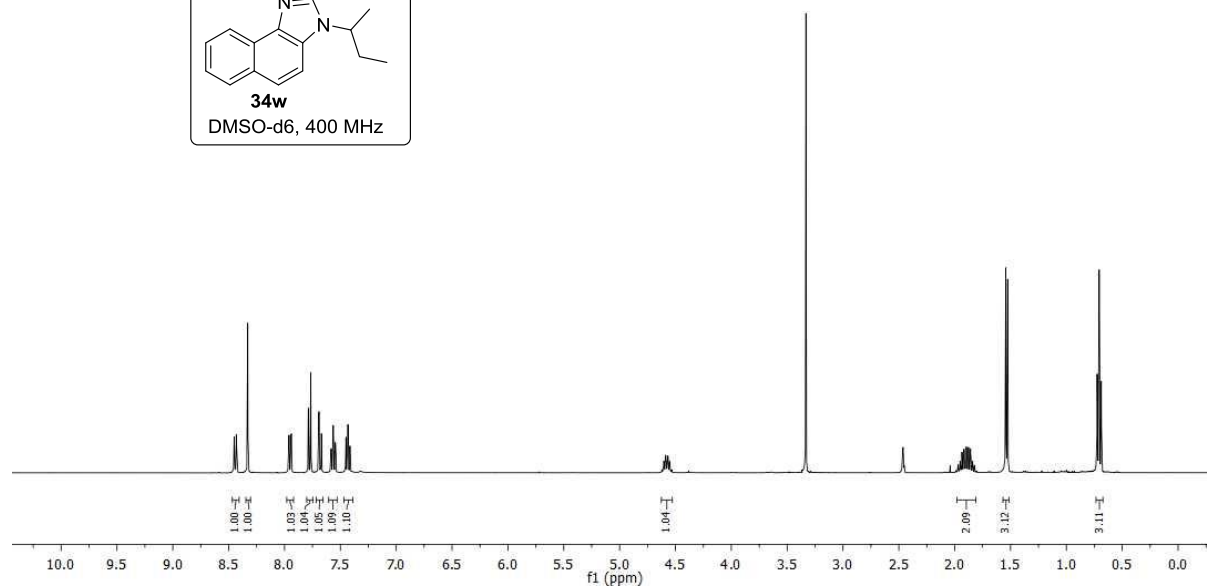
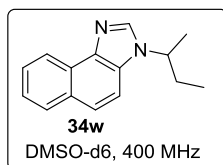
HM-1749
single_pulse

8.454
8.452
8.450
8.449
8.448
8.436
8.438
8.437
8.329
7.960
7.959
7.787
7.787
7.692
7.692
7.584
7.581
7.580
7.580
7.546
7.543
7.453
7.450
7.436
7.432
7.429
7.415
7.412

4.620
4.604
4.588
4.567
4.551
4.534

1.970
1.949
1.935
1.896
1.890
1.823
1.543
1.526

0.735
0.706
0.688

HM-1749
single pulse decoupled gated NOE

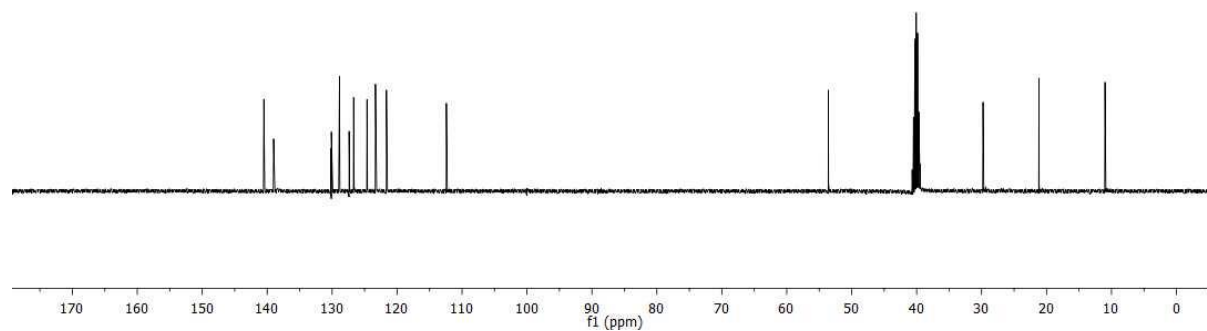
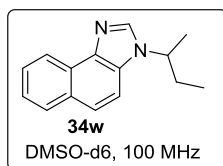
140.511
139.010
130.211
130.125
128.867
127.386
126.681
124.631
123.323
121.638
-112.407

-53.586

-29.780

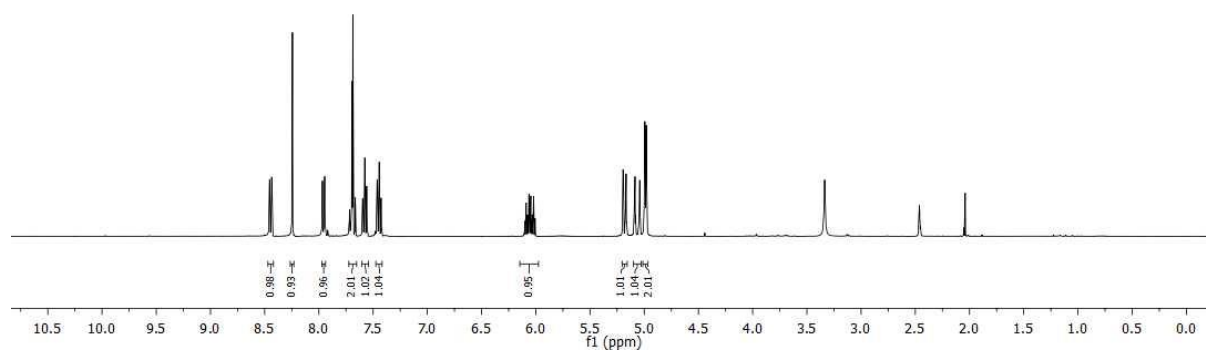
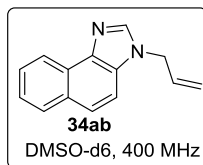
-21.164

-11.002



HM-1805
single_pulse

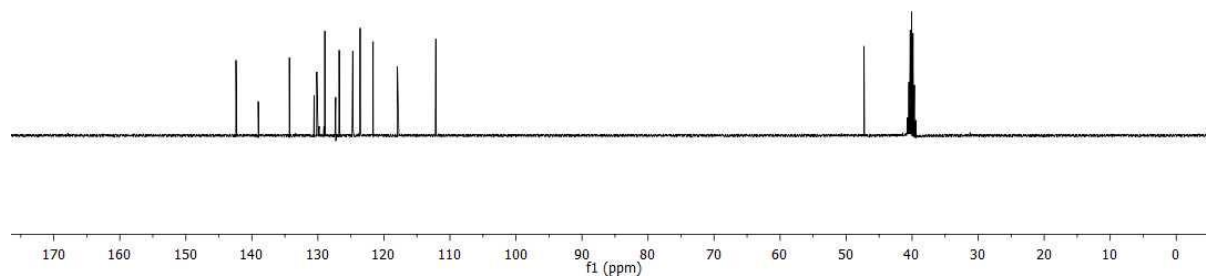
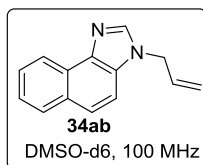
8.456
8.454
8.453
8.451
8.432
8.244
7.967
7.947
7.717
7.697
7.687
7.664
7.597
7.594
7.580
7.577
7.573
7.568
7.556
7.464
7.461
7.447
7.444
7.440
7.436
7.433
6.102
6.088
6.075
6.062
6.046
6.030
6.014
5.199
5.196
5.192
5.189
5.184
5.174
5.170
5.167
5.163
5.092
5.088
5.084
5.080
5.049
5.045
5.042
5.038
4.998
4.994
4.990
4.984
4.980
4.976

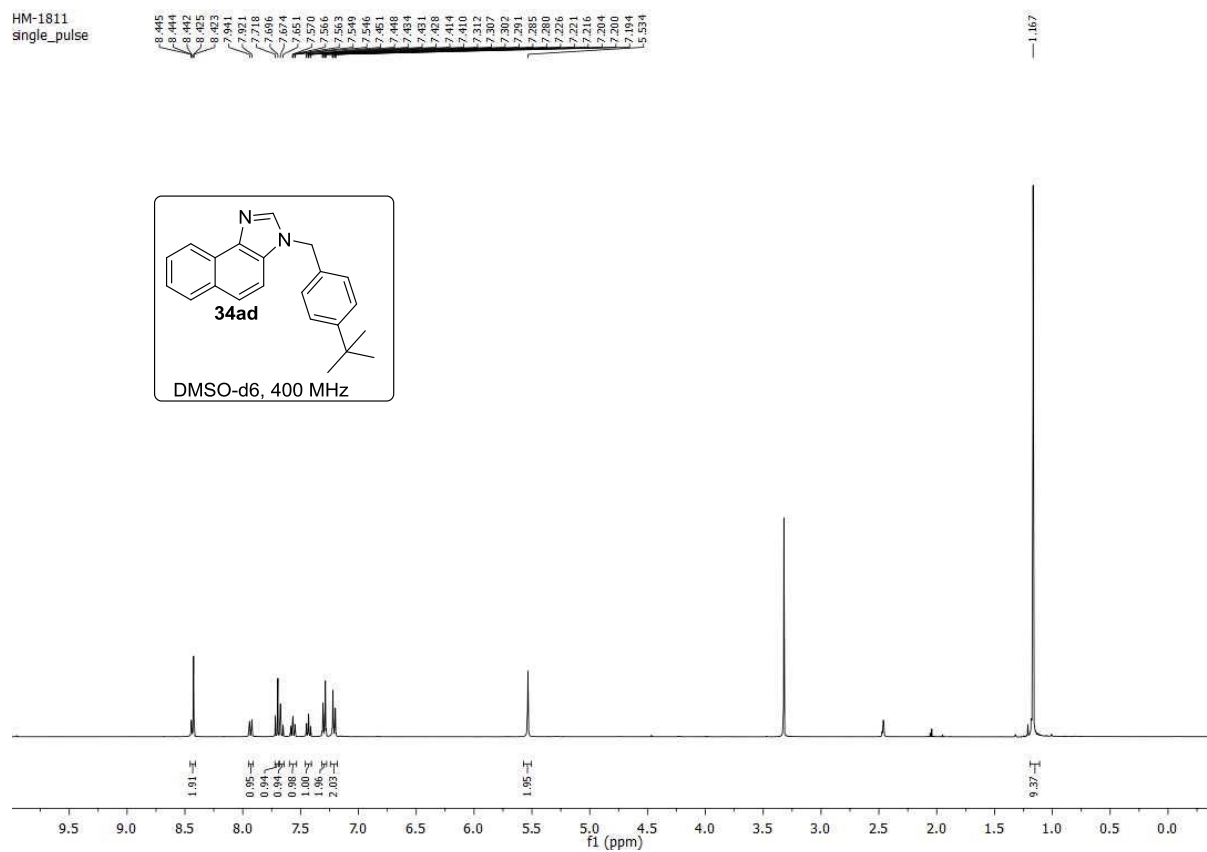
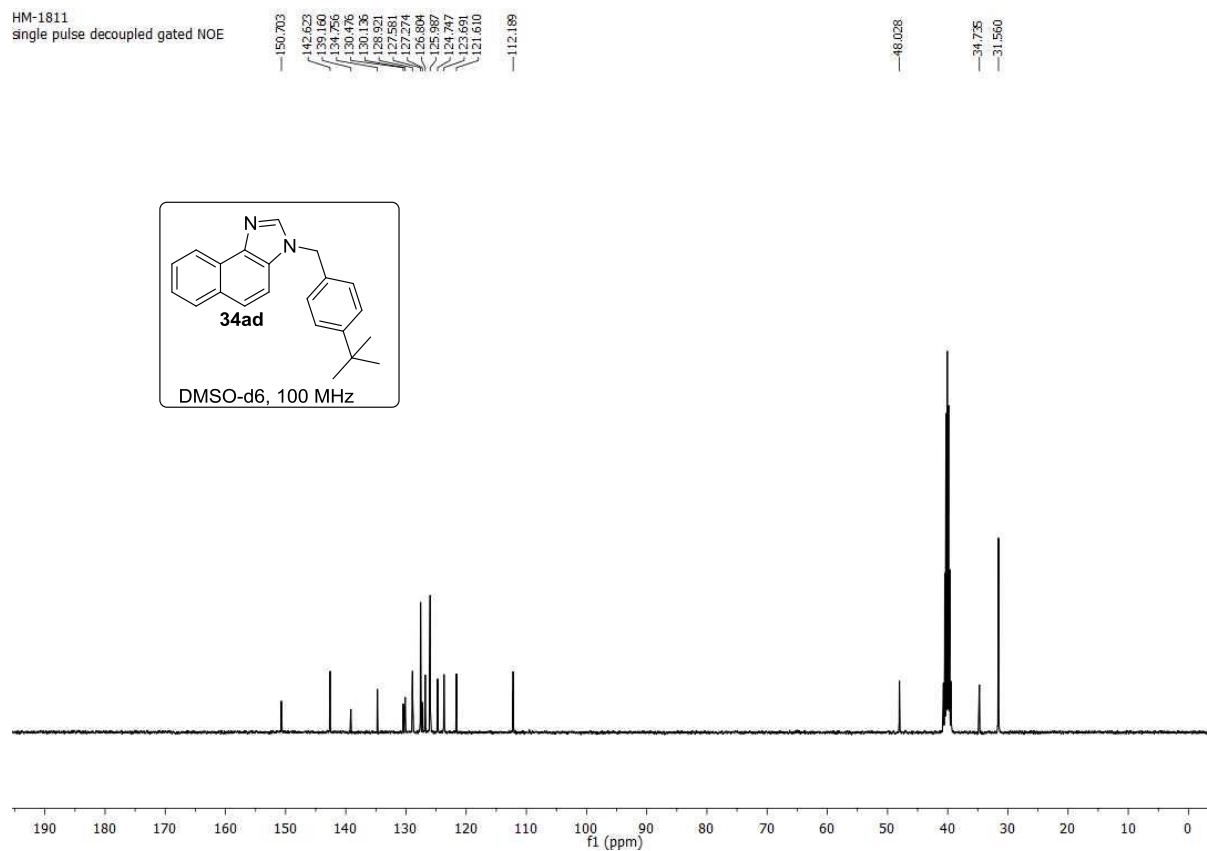


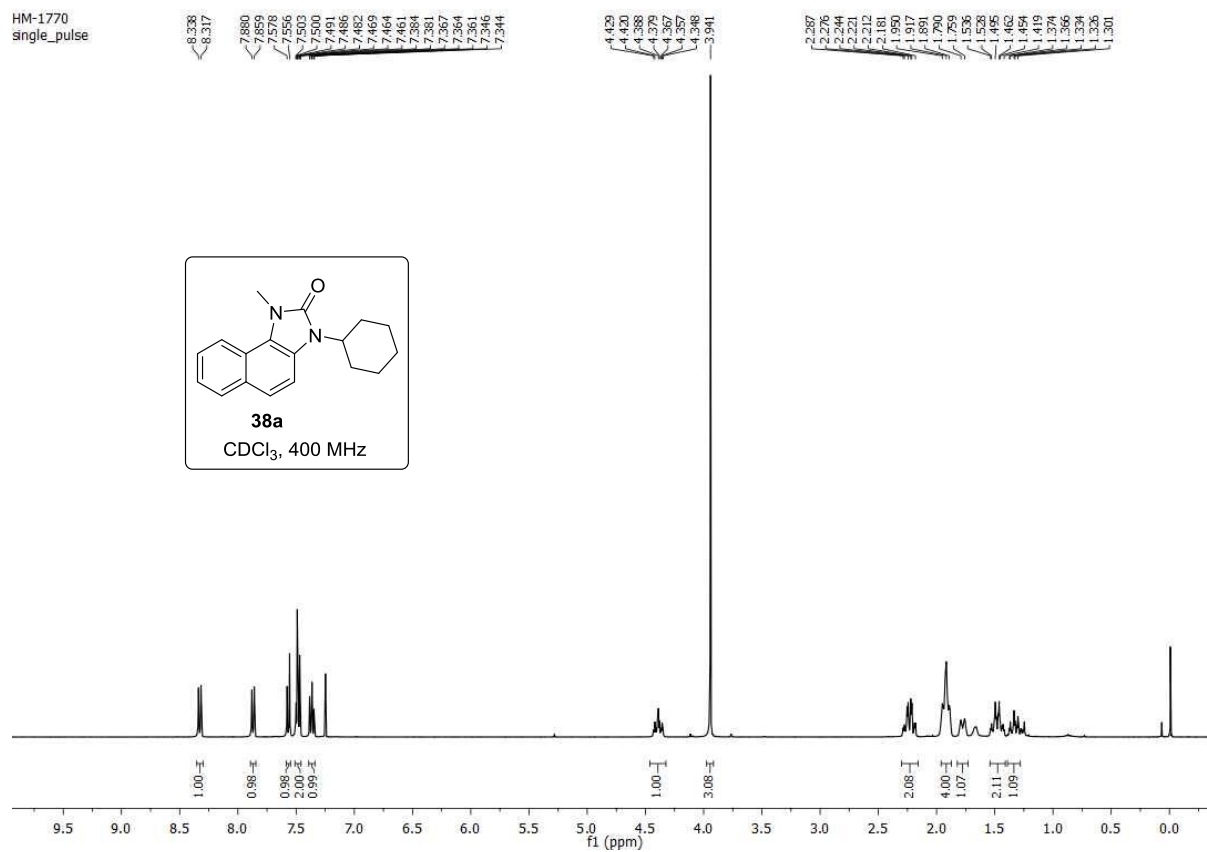
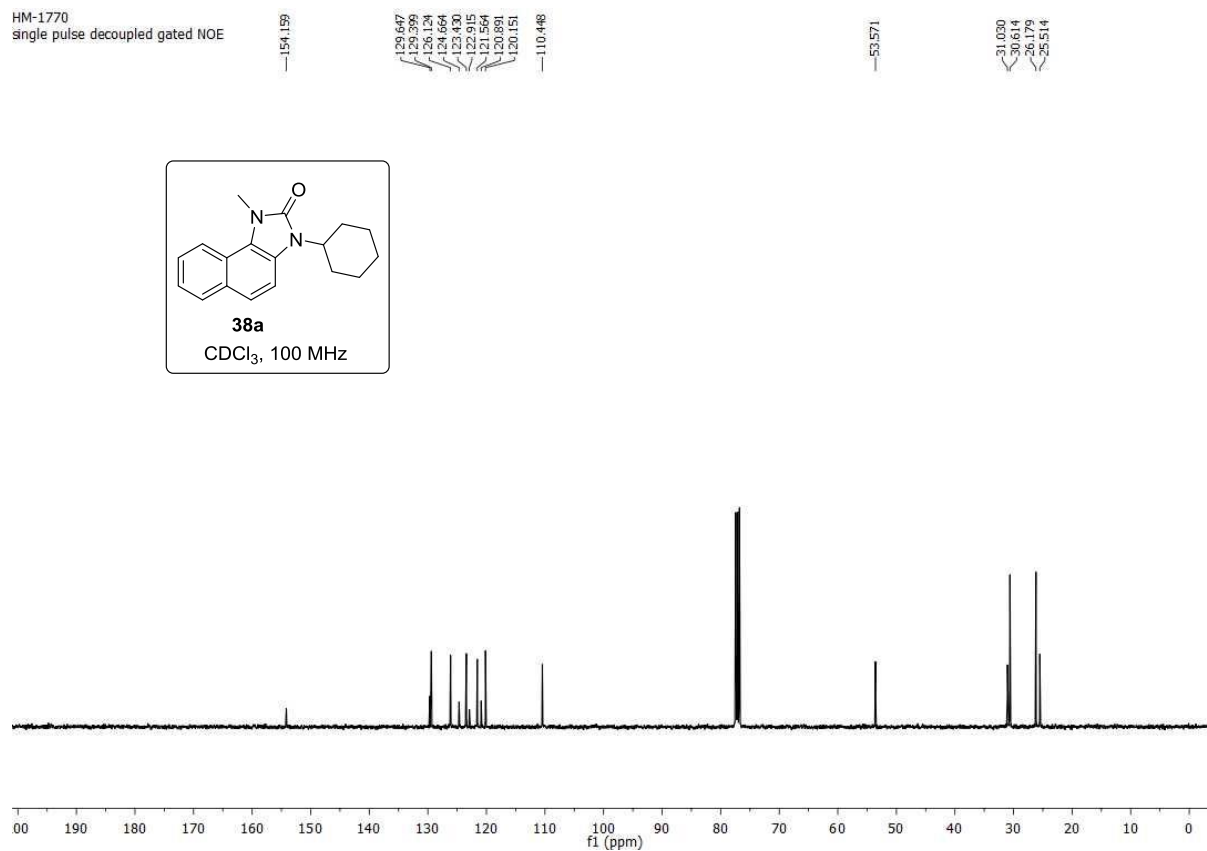
HM-1805
single_pulse decoupled gated NOE

142.404
139.034
134.319
130.583
130.170
128.953
127.303
126.777
125.426
121.637
117.960
112.141

47.278



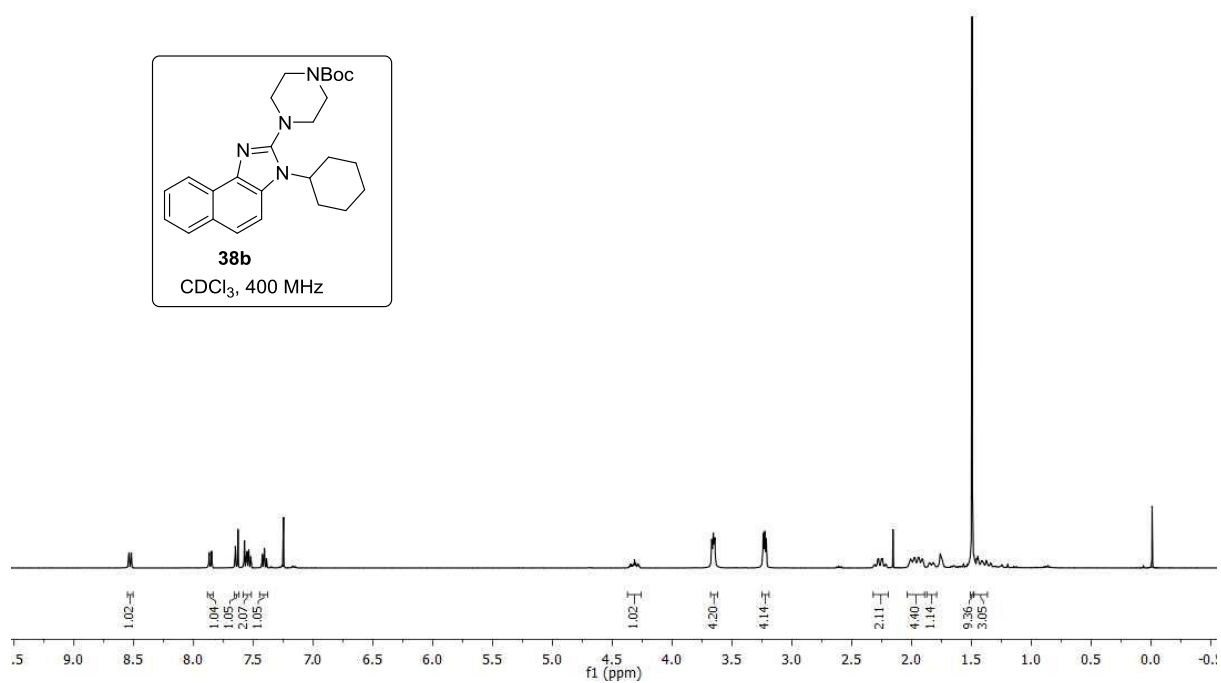
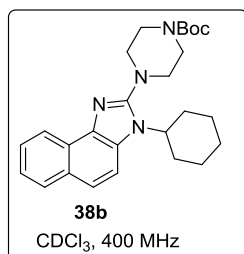
HM-1811
single_pulseHM-1811
single pulse decoupled gated NOE

HM-1770
single_pulseHM-1770
single_pulse decoupled gated NOE

HM-1768
single pulse

8.41
8.539
8.538
8.530
8.519
8.517
8.870
7.850
7.841
7.659
7.575
7.559
7.556
7.553
7.542
7.539
7.535
7.521
7.518
7.438
7.435
7.411
7.408
7.391
7.387

4.356
4.359
4.315
4.284
4.275
3.669
3.657
3.644
3.240
3.227
3.214
2.309
2.283
2.276
2.252
2.241
2.038
1.975
1.940
1.907
1.849
1.819
1.494
1.477
1.456
1.446
1.441
1.397
1.377



HM-1768
single pulse decoupled gated NOE

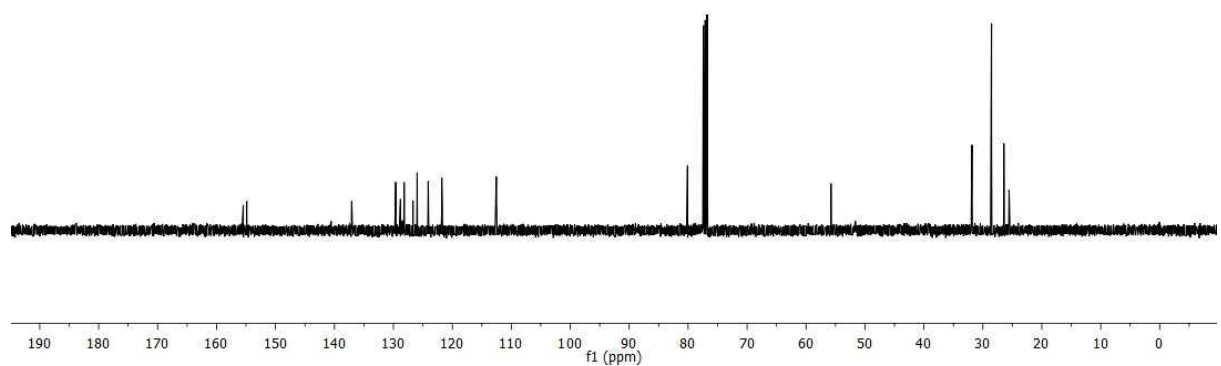
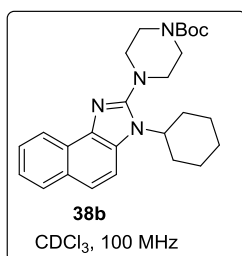
155.136
154.895

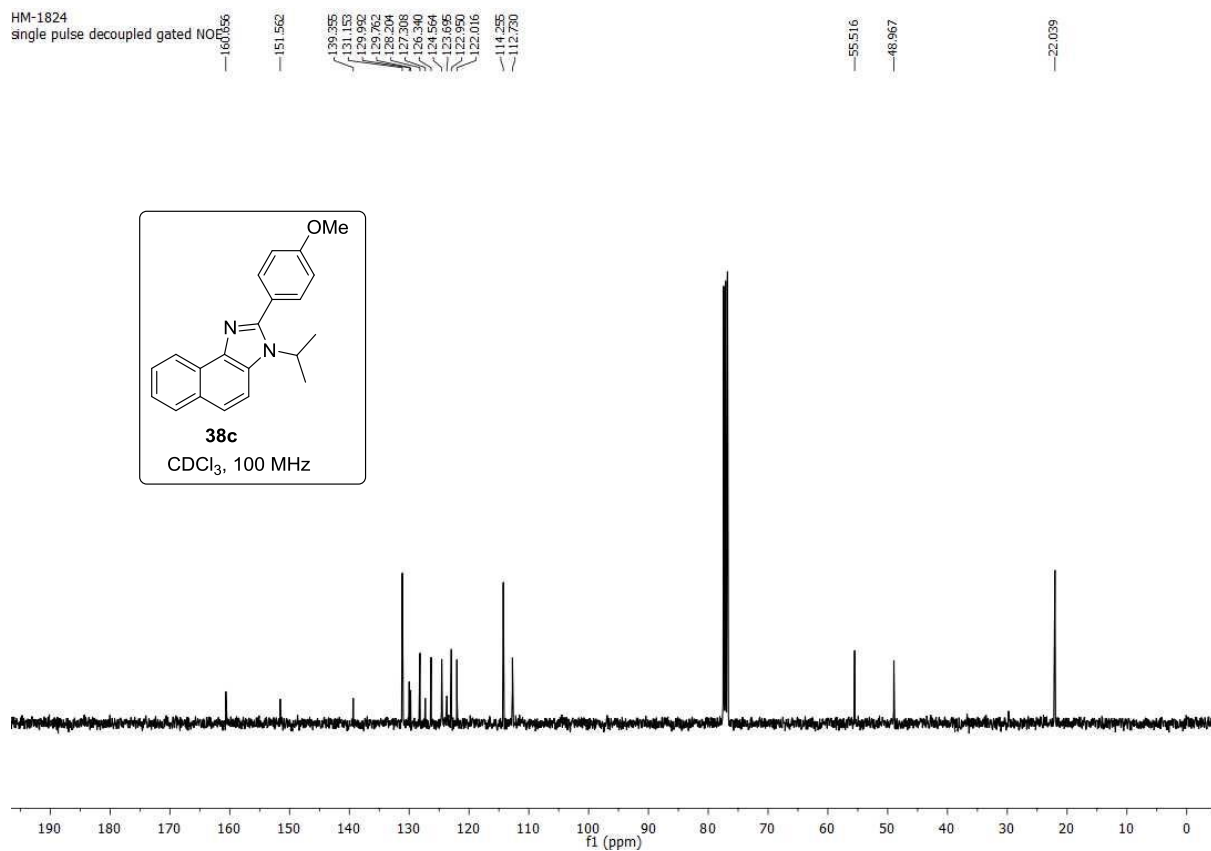
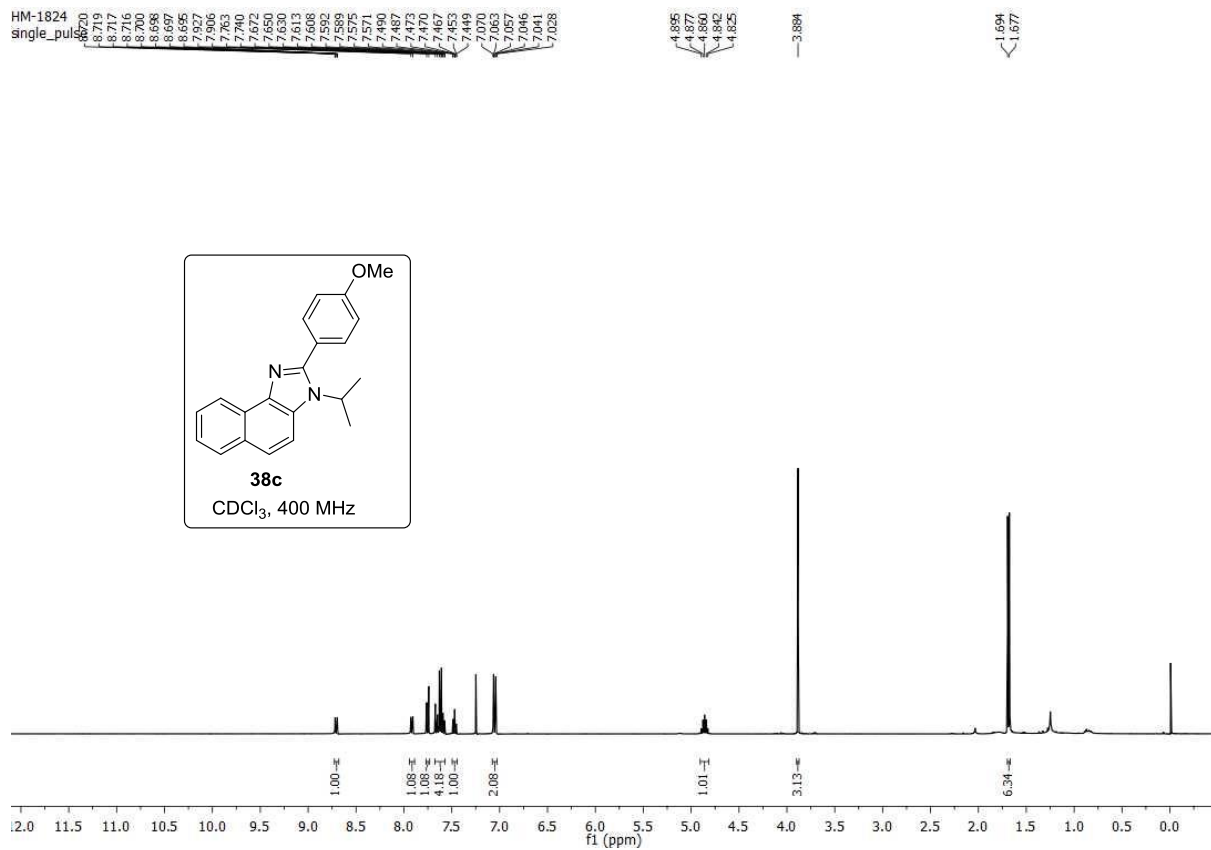
137.075
128.591
128.795
128.129
125.984
124.050
121.800
121.715
112.539

80.097

55.767

31.850
28.533
26.441
25.555





IV.12. References

1. a) S. Solanki, P. Innocenti, C. Mas-Droux, K. Boxall, C. Barillari, R. L. M. van Montfort, G. W. Aherne, R. Bayliss, S. Hoelder, *J. Med. Chem.*, 2011, **54**, 1626-1639; b) M. Sabat, J. C. VanRens, M. J. Laufersweiler, T. A. Brugel, J. Maier, A. Golebiowski, B. De, V. Easwaran, L. C. Hsieh, R. L. Walter, M. J. Meikel, A. Evdokimov, M. J. Janusz, *Bioorg. Med. Chem. Lett.*, 2006, **16**, 5973-5977; c) T. L. Mistry, L. Truong, A. K. Ghosh, M. E. Johnson, S. Mehboob, *ACS Infect. Dis.*, 2017, **3**, 54-61.
2. K. K. Biron, *Antiviral Res.*, 2006, **71**, 154-163.
3. a) A. Chan, K. A. Scheidt, *J. Am. Chem. Soc.*, 2007, **129**, 5334-5335; b) K.-i. Iwamoto, M. Hamaya, N. Hashimoto, H. Kimura, Y. Suzuki, M. Sato, *Tetrahedron Lett.*, 2006, **47**, 7175-7177; c) A. Miyashita, Y. Suzuki, Y. Okumura, T. Higashino, *Chem. Pharm. Bull.*, 1996, **44**, 252-254.
4. Z. Ye, J. Chen, *ACS Catal.*, 2021, **11**, 13983-13999.
5. a) A. J. Blacker, M. M. Farah, M. I. Hall, S. P. Marsden, O. Saidi, J. M. J. Williams, *Org. Lett.*, 2009, **11**, 2039-2042; b) Z. Sun, G. Bottari, K. Barta, *Green Chem.*, 2015, **17**, 5172-5181; c) H. Li, Y. Zhang, Z. Yan, Z. Lai, R. Yang, M. Peng, Y. Sun, J. An, *Green Chem.*, 2022, **24**, 748-753; d) S. Sharma, A. Sharma, Yamini, P. Das, *Adv. Synth. Catal.*, 2019, **361**, 67-72.
6. D. Raja, A. Philips, P. Palani, W.-Y. Lin, S. Devikala, G. C. Senadi, *J. Org. Chem.*, 2020, **85**, 11531-11540.
7. X. Zhu, F. Zhang, D. Kuang, G. Deng, Y. Yang, J. Yu, Y. Liang, *Org. Lett.*, 2020, **22**, 3789-3793.
8. X. Liu, H. Cao, F. Bie, P. Yan, Y. Han, *Tetrahedron Lett.*, 2019, **60**, 1057-1059.
9. K. Hirano, A. T. Biju, F. Glorius, *J. Org. Chem.*, 2009, **74**, 9570-9572.
10. F. Bie, Y. Yao, H. Cao, Y. Shi, P. Yan, J. Ma, Y. Han, X. Liu, *Synth. Commun.*, 2021, **51**, 2387-2396.
11. R. K. Kumar, T. Punniyamurthy, *RSC Adv.*, 2012, **2**, 4616-4619.
12. a) Y. Wang, A. A. Cobo, A. K. Franz, *Org. Chem. Front.*, 2021, **8**, 4315-4348; b) L. Song, E. V. Van der Eycken, *Chem. Eur. J.*, 2021, **27**, 121-144; c) K. Kanti Das, S. Manna, S.

- Panda, *Chem. Commun.*, 2021, **57**, 441-459; d) Z. Zhang, Y. You, C. Hong, *Macromol. Rapid Commun.*, 2018, **39**, 1800362.
13. a) H. Shen, Z. Xie, *J. Am. Chem. Soc.*, 2010, **132**, 11473-11480; b) R. C. Simon, N. Richter, E. Busto, W. Kroutil, *ACS Catal.*, 2014, **4**, 129-143; c) T. Matsuda, H. Ito, *Org. Biomol. Chem.*, 2018, **16**, 6703-6707; d) F. Ye, Y. Ge, A. Spannenberg, H. Neumann, M. Beller, *Nat. Commun.*, 2020, **11**, 5383; e) X. Chen, J. Lin, B. Wang, X. Tian, *Org. Lett.*, 2020, **22**, 7704-7708; f) Y. Kim, M. R. Kumar, N. Park, Y. Heo, S. Lee, *J. Org. Chem.*, 2011, **76**, 9577-9583; g) Z. Hou, S. Oishi, Y. Suzuki, T. Kure, I. Nakanishi, A. Hirasawa, G. Tsujimoto, H. Ohno, N. Fujii, *Org. Biomol. Chem.*, 2013, **11**, 3288-3296.
14. a) Z. Lai, R. Wu, J. Li, X. Chen, L. Zeng, X. Wang, J. Guo, Z. Zhao, H. Sajiki, S. Cui, *Nat. Commun.*, 2022, **13**, 435; b) M. M. Heravi, V. Zadsirjan, M. Dehghani, T. Ahmadi, *Tetrahedron*, 2018, **74**, 3391-3457; c) P. V. Chavan, U. V. Desai, P. P. Wadgaonkar, S. R. Tapase, K. M. Kodam, A. Choudhari, D. Sarkar, *Bioorg. Chem.*, 2019, **85**, 475-486.
15. D. Mahesh, P. Sadhu, T. Punniyamurthy, *J. Org. Chem.*, 2015, **80**, 1644-1650.
16. D. Mahesh, P. Sadhu, T. Punniyamurthy, *J. Org. Chem.*, 2016, **81**, 3227-3234.
17. X. Tang, L. Huang, J. Yang, Y. Xu, W. Wu, H. Jiang, *Chem. Commun.*, 2014, **50**, 14793-14796.
18. A. Kumar, M. Kumar, S. Maurya, R. S. Khanna, *J. Org. Chem.*, 2014, **79**, 6905-6912.
19. L. Q. Tran, J. Li, L. Neuville, *J. Org. Chem.*, 2015, **80**, 6102-6108.
20. S. D. Jadhav, A. Singh, *Org. Lett.*, 2017, **19**, 5673-5676.
21. J. Tian, S. Yuan, F. Xiao, H. Huang, G.-J. Deng, *RSC Adv.*, 2019, **9**, 30570-30574.
22. Z. Xie, F. Zhou, K. Ding, *Adv. Synth. Catal.*, 2020, **362**, 3442-3446.
23. S. Jiang, W.-B. Cao, X.-P. Xu, S.-J. Ji, *Org. Lett.*, 2021, **23**, 6740-6744.
24. G. Xu, C. Jia, X. Wang, H. Yan, S. Zhang, Q. Wu, N. Zhu, J. Duan, K. Guo, *Org. Lett.*, 2022, **24**, 1060-1065.
25. a) R. L. Carvalho, R. G. Almeida, K. Murali, L. A. Machado, L. F. Pedrosa, P. Dolui, D. Maiti, E. N. da Silva Júnior, *Org. Biomol. Chem.*, 2021, **19**, 525-547; b) C. Sambiagio, D. Schönbauer, R. Blicck, T. Dao-Huy, G. Pototschnig, P. Schaaf, T. Wiesinger, M. F. Zia, J. Wencel-Delord, T. Besset, B. U. W. Maes, M. Schnürch, *Chem. Soc. Rev.*, 2018, **47**, 6603-6743.

26. a) G. Rani, V. Luxami, K. Paul, *Chem. Commun.*, 2020, **56**, 12479-12521; b) J. I. Higham, J. A. Bull, *Org. Biomol. Chem.*, 2020, **18**, 7291-7315; c) M. Font, J. M. Quibell, G. J. P. Perry, I. Larrosa, *Chem. Commun.*, 2017, **53**, 5584-5597; d) P. Gandeepan, L. Ackermann, *Chem*, 2018, **4**, 199-222.
27. a) F. Ling, C. Ai, Y. Lv, W. Zhong, *Adv. Synth. Catal.*, 2017, **359**, 3707-3712; b) F. Ling, C. Zhang, C. Ai, Y. Lv, W. Zhong, *J. Org. Chem.*, 2018, **83**, 5698-5706; c) J. Ying, L.-Y. Fu, G. Zhong, X.-F. Wu, *Org. Lett.*, 2019, **21**, 5694-5698; d) L. Lukasevics, A. Cizikovs, L. Grigorjeva, *Org. Lett.*, 2020, **22**, 2720-2723; e) Q. Gao, J.-M. Lu, L. Yao, S. Wang, J. Ying, X.-F. Wu, *Org. Lett.*, 2021, **23**, 178-182; f) L. Lukasevics, A. Cizikovs, L. Grigorjeva, *Org. Lett.*, 2021, **23**, 2748-2753; g) C. Kuai, L. Wang, B. Li, Z. Yang, X. Cui, *Org. Lett.*, 2017, **19**, 2102-2105; h) A. Cizikovs, L. Lukasevics, L. Grigorjeva, *Tetrahedron*, 2021, **93**, 132307.
28. a) H. Wang, J. Cai, H. Huang, G.-J. Deng, *Org. Lett.*, 2014, **16**, 5324-5327; b) W. Li, X.-F. Wu, *J. Org. Chem.*, 2014, **79**, 10410-10416; c) T. Furusawa, T. Morimoto, N. Oka, H. Tanimoto, Y. Nishiyama, K. Kakiuchi, *Chem. Lett.*, 2016, **45**, 406-408; d) X. Cheng, Y. Peng, J. Wu, G.-J. Deng, *Org. Biomol. Chem.*, 2016, **14**, 2819-2823; e) X. Xu, Y. Yang, X. Chen, X. Zhang, W. Yi, *Org. Biomol. Chem.*, 2017, **15**, 9061-9065; f) R. Chun, S. Kim, S. H. Han, S. Han, S. H. Lee, N. K. Mishra, Y. H. Jung, H. S. Kim, I. S. Kim, *Adv. Synth. Catal.*, 2019, **361**, 1617-1626; g) C. Zhou, J. Zhao, W. Chen, M. Imerhasan, J. Wang, *Eur. J. Org. Chem.*, 2020, **2020**, 6485-6488.
29. a) M. Moselage, J. Li, L. Ackermann, *ACS Catal.*, 2016, **6**, 498-525; b) A. Baccalini, S. Vergura, P. Dolui, G. Zanoni, D. Maiti, *Org. Biomol. Chem.*, 2019, **17**, 10119-10141.
30. S. Prakash, R. Kuppusamy, C.-H. Cheng, *ChemCatChem*, 2018, **10**, 683-705.
31. a) J. Y. Kim, S. H. Cho, J. Joseph, S. Chang, *Angew. Chem. Int. Ed.*, 2010, **49**, 9899-9903; b) L.-B. Zhang, S.-K. Zhang, D. Wei, X. Zhu, X.-Q. Hao, J.-H. Su, J.-L. Niu, M.-P. Song, *Org. Lett.*, 2016, **18**, 1318-1321; c) Q. Yan, T. Xiao, Z. Liu, Y. Zhang, *Adv. Synth. Catal.*, 2016, **358**, 2707-2711; d) N. Sauermann, R. Mei, L. Ackermann, *Angew. Chem. Int. Ed.*, 2018, **57**, 5090-5094; e) X. Wu, K. Yang, Y. Zhao, H. Sun, G. Li, H. Ge, *Nat. Commun.*, 2015, **6**, 6462; f) S. Sunny, R. Karvembu, *Adv. Synth. Catal.*, 2021, **363**, 4309-4331; g) J. Lee, S. Jin, D. Kim, S. H. Hong, S. Chang, *J. Am. Chem. Soc.*, 2021, **143**, 5191-5200.

32. a) Y.-H. Chen, S. Graßl, P. Knochel, *Angew. Chem. Int. Ed.*, 2018, **57**, 1108-1111; b) J. Li, E. Tan, N. Keller, Y.-H. Chen, P. M. Zehetmaier, A. C. Jakowetz, T. Bein, P. Knochel, *J. Am. Chem. Soc.*, 2019, **141**, 98-103.
33. L. Liu, Z. Zhang, Y. Wang, Y. Zhang, J. Li, *Synthesis*, 2020, **52**, 3881-3890.

List of Publications

1. Bairy, G.; Das, S.; **Begam, H. M.**; Jana, R., Exceedingly Fast, Direct Access to Dihydroisoquinolino[1,2-b]quinazolinones through a Ruthenium(II)-Catalyzed Redox-Neutral C–H Alkylation/Hydroamination Cascade. *Org. Lett.* **2018**, *20*, 7107-7112.
2. **Begam, H. M.**; Choudhury, R.; Behera, A.; Jana, R., Copper-Catalyzed Electrophilic *Ortho* C(sp²)–H Amination of Aryl Amines: Dramatic Reactivity of Bicyclic System. *Org. Lett.* **2019**, *21*, 4651-4656.
3. Das, P.; **Begam, H. M.**; Bhunia, S. K.; Jana, R., Photoredox-Catalyzed Tandem Demethylation of N,N-Dimethyl Anilines Followed by Amidation with α -Keto or Alkynyl Carboxylic Acids. *Adv. Synth. Catal.* **2019**, *361*, 4048-4054.
4. Manna, K.; **Begam, H. M.**; Samanta, K.; Jana, R., Overcoming the Deallylation Problem: Palladium(II)-Catalyzed Chemo-, Regio-, and Stereoselective Allylic Oxidation of Aryl Allyl Ether, Amine, and Amino Acids. *Org. Lett.* **2020**, *22*, 7443-7449.
5. Jana, R.; **Begam, H. M.**; Dinda, E., The emergence of the C–H functionalization strategy in medicinal chemistry and drug discovery. *Chem. Commun.* **2021**, *57*, 10842-10866.
6. **Begam, H. M.**; Nandi, S.; Jana, R., A directing group switch in copper-catalyzed electrophilic C–H amination/migratory annulation cascade: divergent access to benzimidazolone/benzimidazole. *Chem. Sci.* **2022**, *13*, 5726-5733.
7. **Begam, H. M.**; Pradhan, K.; Kasarla, V.; Jana, R., Cobalt Catalysed Electrophilic C-H amination/Cyclisation cascade with *O*-benzoyloxy primary amines using paraformaldehyde as C1 synthon: Direct Access to Naphthimidazoles Using Picolinamide as Traceless Directing Group. *Manuscript is under preparation.*

List of Attended conferences

1. Begam, H. M., Indo-Australian Workshop on RATIONAL DRUG DESIGN, (CSIR-IICB, Salt-Lake campus, 2018).
2. Begam, H. M., International Conference on Chemistry for Human Development (ICCHD, Kolkata-2018).
3. Begam, H. M.; Jana, R., International Conference on Chemistry for Human Development (ICCHD, Kolkata-2020). Poster presentation (Title of the poster: Copper-Catalyzed Electrophilic *Ortho* C(sp²)–H Amination of Aryl Amines: Dramatic Reactivity of Bicyclic System).

REPRINTS

Copper-Catalyzed Electrophilic Ortho C(sp²)–H Amination of Aryl Amines: Dramatic Reactivity of Bicyclic System

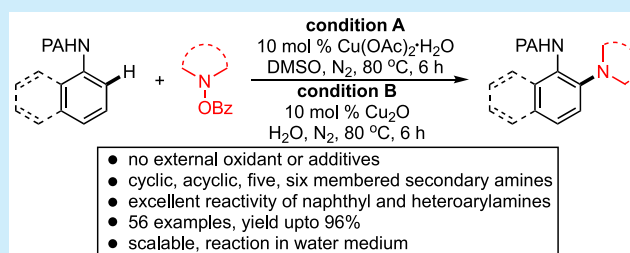
Hasina Mamataj Begam,[†] Rajarshee Choudhury,^{†,‡} Ashok Behera,[†] and Ranjan Jana^{*,†,‡}

[†]Organic and Medicinal Chemistry Division, CSIR-Indian Institute of Chemical Biology, 4 Raja S. C. Mullick Road, Jadavpur, Kolkata-700032, West Bengal, India

[‡]National Institute of Pharmaceutical Education and Research (NIPER), Kolkata-700054, West Bengal, India

S Supporting Information

ABSTRACT: A practical copper-catalyzed, 2-picolinamide-directed *ortho* C–H amination of anilines with benzoyl-protected hydroxylamines has been disclosed that proceeds smoothly without any external stoichiometric oxidant or additives. Remarkably, besides anilines, bicyclic naphthyl or heterocyclic amines furnished amination products with five- and six-membered cyclic and acyclic amines at the *ortho* position selectively. This electrophilic C–H amination also proceeds smoothly in water under slightly modified reaction conditions.



Efficient construction of C–N bonds represents one of the mainstays of research in organic synthesis over the last decades, because of the exponential use of nitrogen-containing molecules in pharmaceutical, medicinal, and materials science.¹ Following the pioneer works of Buchwald and Hartwig regarding palladium-catalyzed C–N bond formation from aryl halides and amines,² an impressive array of Earth-abundant, inexpensive copper-catalyzed C–N coupling reactions have been explored.³ A mechanistically distinct copper-catalyzed/mediated oxidative C–N coupling using organometallic reagents has also been developed under mild conditions.⁴ A paradigm shift from transition-metal-catalyzed cross-coupling with organometallic reagents to direct C–H amination strategy has been observed in the last decades. In this vein, the research groups of Yu and Chatani independently reported copper-mediated C–H amination of 2-arylpyridines.⁵ Remarkably, the Daugulis group expanded the scope of C–H amination using removable, bidentate directing groups.⁶ Recently, the Chang group also reported copper-mediated C–H amination with aqueous ammonia.⁷

2-Aminoanilide moiety is ubiquitously found in drug candidates for the treatment of cancer, Alzheimer's disease, wet age-related macular degeneration (wet AMD), and infectious diseases.⁸ In 2014, the research groups of Rodríguez and Chen independently reported copper-catalyzed, 2-picolinamide-directed *ortho* C–H amination of aniline.⁹ However, stoichiometric amount of expensive PhI(OAc)₂ was used as an oxidant, which generates PhI as a byproduct. More recently, an electrochemical synthesis of C–H amination of the same substrate was reported by the Mei group, using tetrabutylammonium iodide (TBAI) as a redox mediator.¹⁰ However, all these protocols are limited to the six-membered cyclic amines only. Acyclic amines, pyrrolidine (<5% yield),

etc. were ineffective and bicyclic 1-naphthylamine was a moderately effective (~50% yield) substrate under these protocols.

As an alternative to oxidative C–H/N–H coupling, an umpolung strategy employing R₂N⁺ species is emerging for electrophilic amination under mild conditions.¹¹ In this direction, palladium,¹² rhodium,¹³ ruthenium,¹⁴ and iron¹⁵ catalysis has been explored where a high-valent metal center is believed to be involved in the catalytic cycle. Although copper-catalyzed electrophilic amination using organometallic reagents has been well-explored,¹⁶ electrophilic C–H amination by a copper catalyst is limited to the electron-deficient systems in nondirected fashion.¹⁷ A copper-mediated electrophilic C–H amination with oximes to primary amines was reported by the Yu group.¹⁸ To the best of our knowledge, copper-catalyzed directed electrophilic C–H amination has not been reported.

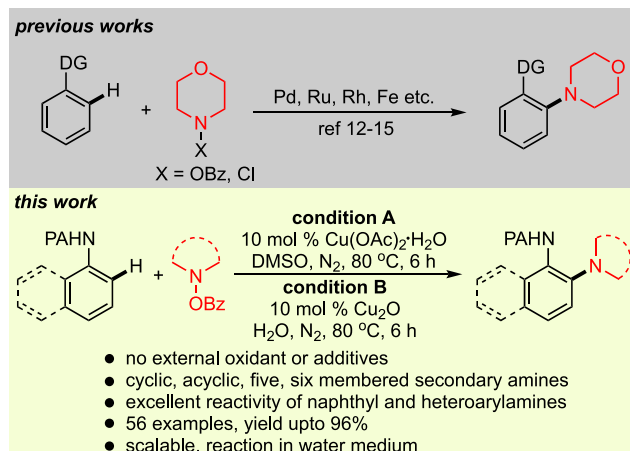
We report here, a practically useful and general methodology for the *ortho* C–H amination of aryl amines using *O*-benzoylhydroxylamines without any stoichiometric external oxidant (Scheme 1). Surprisingly, we observed the superior reactivity of the naphthylamines, which were inferior substrates in previous methods.

To optimize the reaction condition, we chose 2-picolinamide protected aniline **1a** and *O*-benzoyl hydroxylmorpholine **2a** as model substrates, which is summarized in Table 1. After several screenings, we found that, when **1a** was heated at 80 °C for 6 h under a nitrogen atmosphere with 2.5 equiv of **2a** in the presence of 10 mol % of Cu(OAc)₂·H₂O in dimethylsulfoxide (DMSO), the desired *ortho* aminated product was isolated in 94% yield. No product was formed

Received: May 2, 2019

Published: June 3, 2019

Scheme 1. Copper-Catalyzed C–H Amination of Anilines

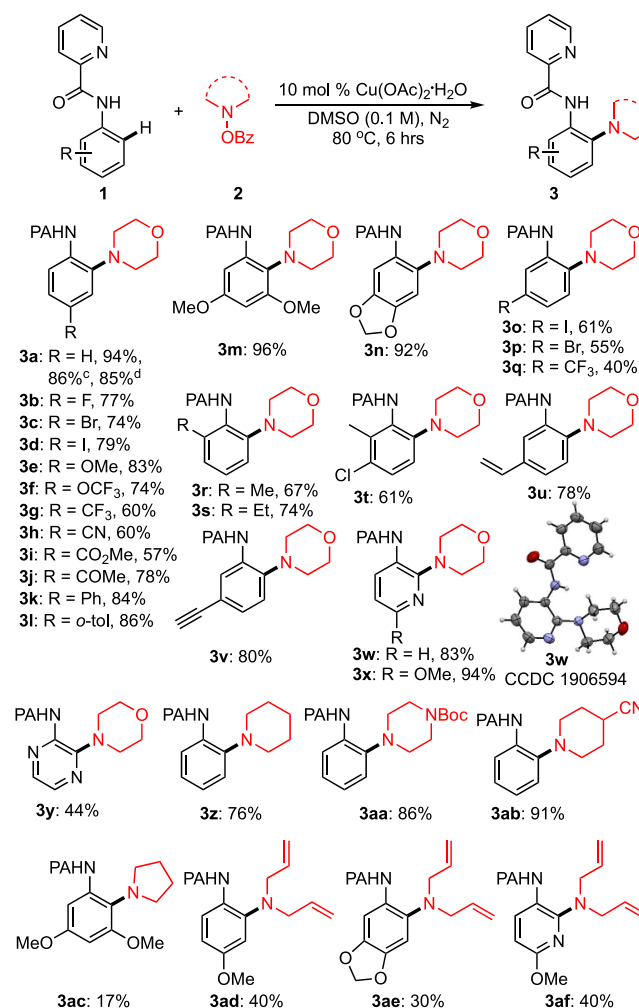
Table 1. Optimization of the Reaction Conditions^{a,b}

| entry | deviation from optimized condition | yield ^b (%) |
|-------|--|------------------------|
| 1 | none | 94 |
| 2 | no Cu(OAc) ₂ ·H ₂ O | nr |
| 3 | Cu(OTf) ₂ instead of Cu(OAc) ₂ ·H ₂ O | 76 |
| 4 | CuOAc instead of Cu(OAc) ₂ ·H ₂ O | 84 |
| 5 | Cu ₂ O instead of Cu(OAc) ₂ ·H ₂ O | 78 |
| 6 | Cu powder instead of Cu(OAc) ₂ ·H ₂ O | 85 |
| 7 | O ₂ atm instead of N ₂ | 72 |
| 8 | air instead of N ₂ | 65 |
| 9 | 25 °C instead of 80 °C | 51 |
| 10 | 1.0 equiv of 2 | 40 |
| 11 | 3.5 equiv of 2 | 95 |
| 12 | morpholine/Bz ₂ O ₂ instead of 2 | 50 |

^aAll reactions were performed in 0.2 mmol scale. ^bYields referenced here are overall isolated yields.

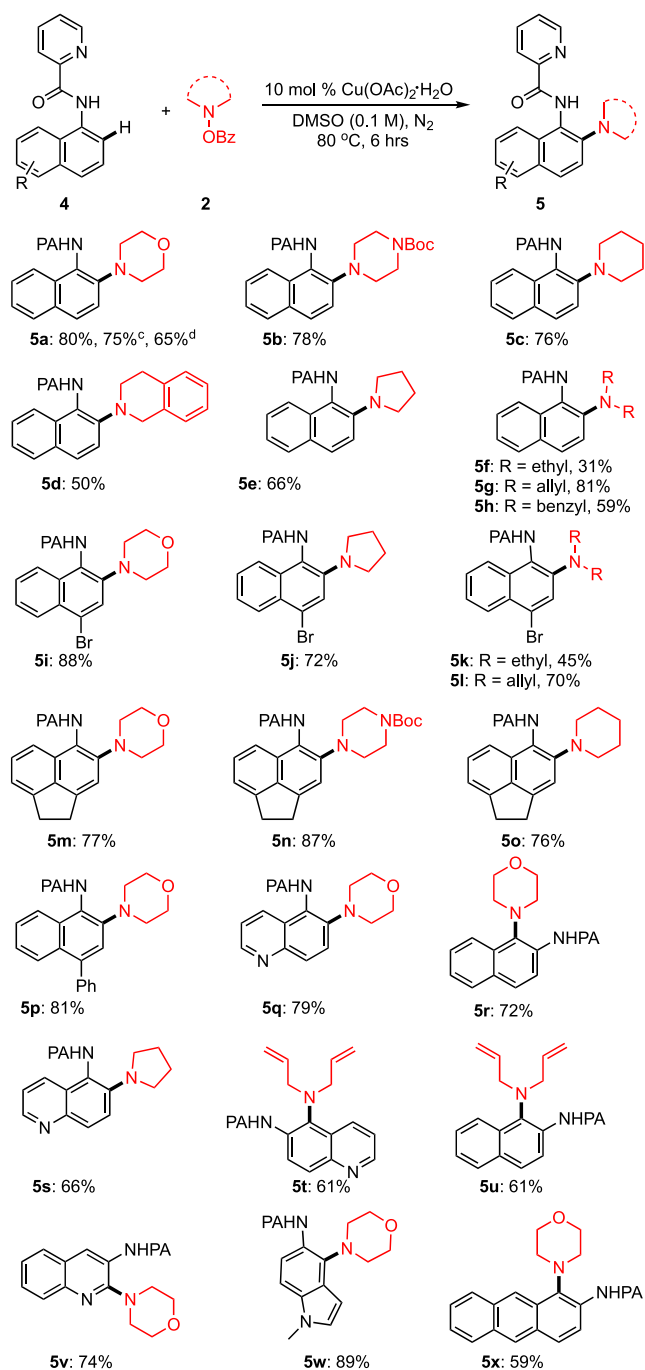
in the absence of a copper catalyst. Cu(OTf)₂, Cu₂O provided amination product in lower yields. Interestingly, inexpensive copper powder that had been dissolved in the course of reaction was also able to provide amination product in 85% yield, demonstrating the superior reactivity of the electrophilic amine surrogate. When the reaction was performed under an air or oxygen atmosphere, the yield was decreased, presumably because of decomposition via overoxidation of the amination product. The reaction at room temperature provided 51% of the desired product. The reaction with copper nanoparticle (~50 nm) and lower catalyst loading (i.e., 5 mol %) Cu powder provided yields of 65%–70%.

Under the optimized reaction conditions, we examined the substrate scope (Scheme 2). Aniline moieties containing fluoro, bromo, iodo at the *para* position (3b–3d, see Scheme 2) gave moderate yields under the optimized reaction conditions. As expected, electron-rich substrates furnished better yields than electron-deficient anilines. Electron-donating methoxy, phenyl, *O*-tolylxy substitution at the *para* position (3e, 3k, 3l; see Scheme 2) provided good yields. On the other hand, electron-withdrawing trifluoromethoxy, trifluoromethyl,

Scheme 2. Substrate Scope with Monocyclic (Het)aromatic Anilides^{a,b}

^aReactions were performed in 0.2 mmol scale. ^bYields refer to isolated pure compounds. ^cReaction performed in gram scale. ^d10 mol % Cu powder was used.

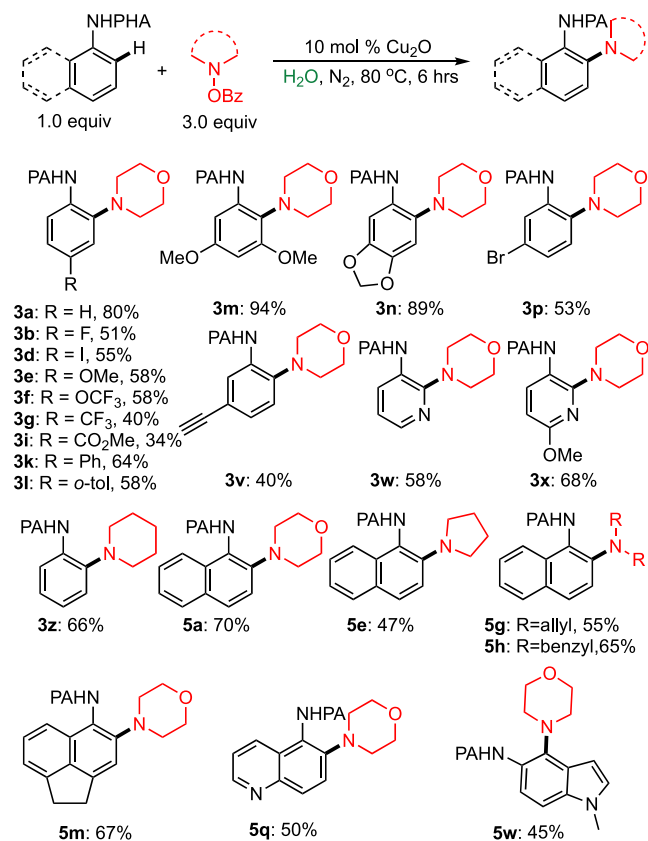
cyno substitution at the same position gave moderate yields (3f–3h, see Scheme 2). Ester and keto groups are found to be tolerable under this condition, providing moderate yields of the desired product (3i–3j, see Scheme 2). *meta*-Dimethoxy-, methylene dioxy-substituted anilines gave excellent yields (3m, 3n; see Scheme 2). Iodo, bromo substitution at the *meta* position afforded lower yields than their corresponding *para* substitution (3o, 3p; see Scheme 2). Vinylic group and terminal alkyne group also survived under the optimized condition providing very good yields (3u, 3v; see Scheme 2). Remarkably, sterically congested *ortho* methyl-, ethyl-substituted anilines also furnished moderate yields, which were poor substrates in the previous reports (3r–3t, see Scheme 2). This method was also applicable to the heterocyclic amines. For example, 3-amino pyridine derivatives yielded desired product in excellent yields (3w, 3x; see Scheme 2) and the amination at the 2-position was confirmed by X-ray crystallography (3w, CCDC 1906594), whereas 2-amino pyridine was ineffective. Picolinamide of 2-aminopyrazine also provided amination product, albeit in moderate yield (3y, see Scheme 2). Other six-membered amines such as piperidine, N-Boc-protected piperazine, 4-cyano-piperidine also provided the amination

Scheme 3. Substrate Scope with Polycyclic (Het)aromatic Anilides^{a,b}

^aReactions were performed in 0.20 mmol scale. ^bYields refer to isolated pure compounds. ^cReaction performed in gram scale. ^d10 mol % Cu powder was used.

products in good to excellent yields (3z–3ab, Scheme 2). Besides six-membered cyclic amines, this method is also applicable for five-membered cyclic amines 3ac and acyclic amines, although the yields are not satisfactory (3ad–3af).

Next, we turn our attention to examine the scope of conjugated naphthylamines which were inferior substrates in the previous reports (yields of ~50%). Gratifyingly, 1-naphthylamine furnished 80% yield of the *ortho* amination product under the optimized condition (5a, see Scheme 3).

Scheme 4. Electrophilic C–H Amination in Water^{a,b}

^aReactions were performed in 0.2 mmol scale. ^bYields refer to isolated pure compounds.

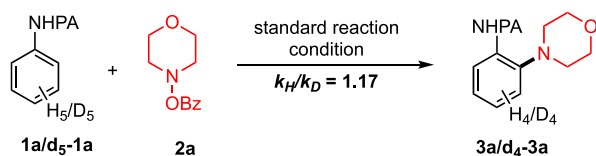
Other six-membered amines were also effective to furnish moderate to high yields (5b–5d, see Scheme 3). Remarkably, this bicyclic system also exhibits superior reactivity to five-membered pyrrolidine (5e, 5j, 5s; see Scheme 3) and acyclic amines (5f, 5g, 5h, 5k, 5l, 5t, 5u; see Scheme 3) providing good to high yields. Substituted naphthylamines (5i–5p, Scheme 3) were also effective furnishing comparable yields of the amination product. Heterocycles such as quinoline (5s, 5v) and indole (5w) were also proven to be excellent substrates. Tricyclic 2-amino anthracene was less reactive to some extent, yielding 59% amination product (5x).

To demonstrate practicability of this present method further, we performed the amination reaction in water as an environmentally benign and green solvent (Scheme 4).¹⁹ Gratifyingly, carboxamide-protected anilines and naphthalenes provided the corresponding *ortho* amination product using copper(I) oxide in lieu of copper(II) acetate (for detail optimization, see the Supporting Information). While electron-rich substrates (3m, 3n; see Scheme 4) furnished comparable yields to DMSO, the electron-deficient substrates (3g, 3i; see Scheme 4) afforded moderate yields. Other bicycles (5a, 5e, 5g, 5h, 5m) and heterocycles (3w, 3x, 5q, 5w) also underwent amination reaction in water, providing moderate to good yields. To note, nucleophilic-free amines were ineffective under this condition to provide the corresponding amination product.

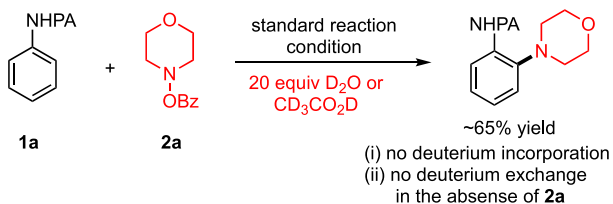
To understand the mechanism of this copper-catalyzed electrophilic amination, we performed several control experiments (Scheme 5). From a competitive experiment between 1a

Scheme 5. Control Experiments

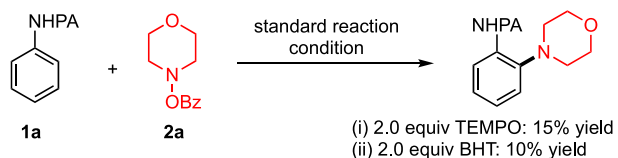
a) primary kinetic isotope experiment



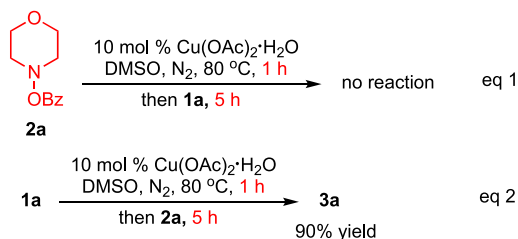
b) deuterium exchange experiment



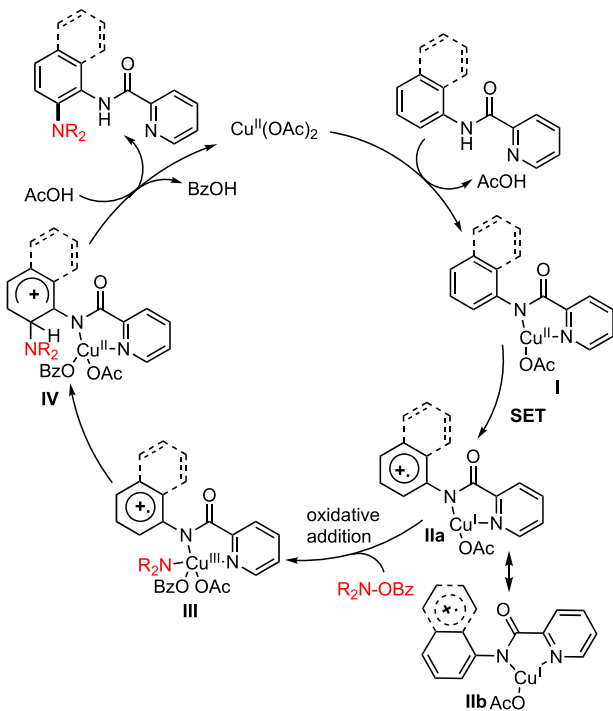
c) radical scavenger experiment



d) Sequence of addition experiment

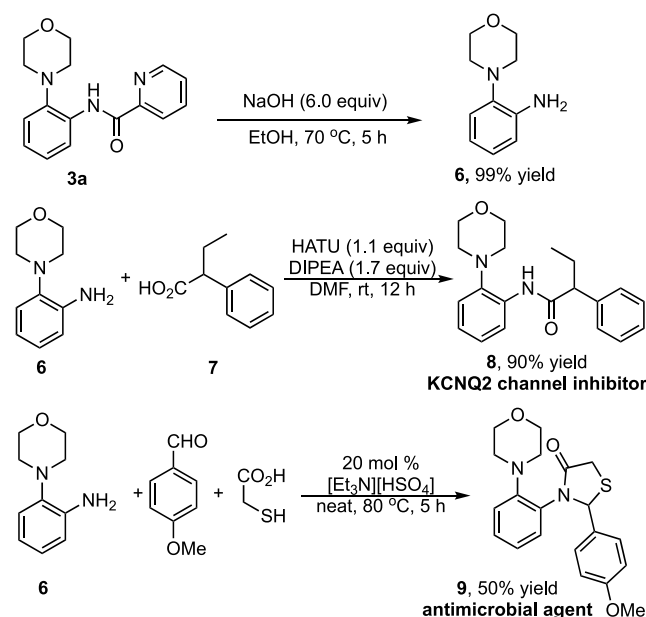


Scheme 6. Plausible Catalytic Cycle



and *d*₅-1a, the primary kinetic isotope effect k_H/k_D was determined to be 1.17, which indicates that C–H bond

Scheme 7. Directing Group Deprotection and Product Derivatization



cleavage may not be involved in the rate-limiting step (Scheme 5a). When substrate 1a was subjected to the reaction conditions in the presence of 20.0 equiv D₂O or CD₃COOD with or without an amine source, no *ortho* H–D exchange occurred, suggesting that no reversible *ortho* C–H insertion happened (Scheme 5b). The addition of radical scavengers such as 2.0 equiv of TEMPO and BHT in the reaction medium suppressed the reaction significantly, indicating a probable radical pathway (Scheme 5c). Furthermore, when 1a was heated for 1 h in the presence of a copper catalyst in DMSO, followed by the addition of an amine source, and stirring was continued for 5 h; the corresponding amination product was obtained in comparable yields. However, the reverse addition sequence yielded no product. It indicates that, initially, chelation of substrate with copper in bidentate fashion occurs to generate complex-I, followed by one electron transfer to generate the Cu(I) complex (IIa). This single electron transfer mechanism is further supported by the fact that naphthyls are susceptible for diverse amines than the corresponding anilines, presumably because of better resonance stabilization. Inversely, oxidative addition followed by chelation may not be operative.

From these control experiments and previous literature reports,²⁰ a plausible mechanistic cycle is proposed (Scheme 6). Initial coordination of copper with bidentate 2-picolinamide may generate complex I. Subsequently, one-electron reduction of complex I lead to the formation of copper(I) complex II, which might be better resonance-stabilized in the case of naphthalenes. This Cu(I) complex may undergo oxidative addition to *O*-benzoylhydroxylamines to generate a high-valent Cu(III) species (III). Amine transfer to the arenes, followed by deprotonation, may provide the desired C–H amination product and copper(II) for the subsequent runs.

The electrophilic amination was also performed in gram-scale and the 2-picolinamide directing group was removed by excess NaOH–ethanol under reflux condition (Scheme 7). Amide coupling with the free diamine, 6 with 7 furnished a

KCNQ2 channel inhibitor.²¹ Furthermore, a three-component coupling in neat condition provided an antimicrobial agent.²²

In conclusion, we have developed a mild copper-catalyzed 2-picolinamide directed electrophilic *ortho*-amination of anilines and naphthylamines with *O*-benzoylhydroxylamines. The reaction proceeds smoothly without any external oxidants or additives. Notably, bicyclic anilines were also effective substrates to a broad scope of dialkylamines under this electrophilic amination strategy, which is a remarkable discovery, compared to the existing methods. The amination has also been demonstrated in water, providing an environmentally benign methodology. Thus, we anticipate that this practical electrophilic amination will be highly applicable in academia and industrial research.

■ ASSOCIATED CONTENT

Supporting Information

The Supporting Information is available free of charge on the ACS Publications website at DOI: [10.1021/acs.orglett.9b01546](https://doi.org/10.1021/acs.orglett.9b01546).

Experimental procedures, spectroscopic data, X-ray crystallography data, ¹H and ¹³C NMR spectra for all synthesized compounds (PDF)

■ Accession Codes

CCDC 1906594 contains the supplementary crystallographic data for this paper. These data can be obtained free of charge via www.ccdc.cam.ac.uk/data_request/cif, or by emailing data_request@ccdc.cam.ac.uk, or by contacting The Cambridge Crystallographic Data Centre, 12 Union Road, Cambridge CB2 1EZ, UK; fax: +44 1223 336033.

■ AUTHOR INFORMATION

Corresponding Author

*E-mail: rjana@iicb.res.in.

ORCID

Ranjan Jana: [0000-0002-5473-0258](https://orcid.org/0000-0002-5473-0258)

Notes

The authors declare no competing financial interest.

■ ACKNOWLEDGMENTS

This work was supported by DST, SERB, Government of India for the Ramanujan fellowship; Award No. SR/S2/RJN-97/2012 and Extra Mural Research Grant No. EMR/2014/000469 for financial support. H.M.B. and A.B. thank CSIR for their fellowships.

■ REFERENCES

- (1) For selected reviews, see: (a) Park, Y.; Kim, Y.; Chang, S. Transition Metal-Catalyzed C–H Amination: Scope, Mechanism, and Applications. *Chem. Rev.* **2017**, *117*, 9247–9301. (b) Ruiz-Castillo, P.; Buchwald, S. L. Applications of Palladium-Catalyzed C–N Cross-Coupling Reactions. *Chem. Rev.* **2016**, *116*, 12564–12649. (c) Bariwal, J.; Van der Eycken, E. C–N bond forming cross-coupling reactions: an overview. *Chem. Soc. Rev.* **2013**, *42*, 9283–9303. (d) Collet, F.; Dodd, R. H.; Dauban, P. Catalytic C–H amination: recent progress and future directions. *Chem. Commun.* **2009**, 5061–5074. (e) Yang, B. H.; Buchwald, S. L. Palladium-catalyzed amination of aryl halides and sulfonates. *J. Organomet. Chem.* **1999**, *576*, 125–146.
- (2) (a) Louie, J.; Hartwig, J. F. Palladium-catalyzed synthesis of arylamines from aryl halides. Mechanistic studies lead to coupling in the absence of tin reagents. *Tetrahedron Lett.* **1995**, *36*, 3609–3612.

- (b) Guram, A. S.; Buchwald, S. L. Palladium-Catalyzed Aromatic Aminations with in situ Generated Aminostannanes. *J. Am. Chem. Soc.* **1994**, *116*, 7901–7902. (c) Paul, F.; Patt, J.; Hartwig, J. F. Palladium-catalyzed formation of carbon-nitrogen bonds. Reaction intermediates and catalyst improvements in the hetero cross-coupling of aryl halides and tin amides. *J. Am. Chem. Soc.* **1994**, *116*, 5969–5970.

- (3) For Cu-catalyzed cross-coupling reactions for C–N formation, see: (a) Gao, J.; Bhunia, S.; Wang, K.; Gan, L.; Xia, S.; Ma, D. Discovery of N-(Naphthalen-1-yl)-N'-alkyl Oxalamide Ligands Enables Cu-Catalyzed Aryl Amination with High Turnovers. *Org. Lett.* **2017**, *19*, 2809–2812. (b) Zhou, W.; Fan, M.; Yin, J.; Jiang, Y.; Ma, D. CuI/Oxalic Diamide Catalyzed Coupling Reaction of (Hetero)Aryl Chlorides and Amines. *J. Am. Chem. Soc.* **2015**, *137*, 11942–11945. (c) Zhang, Y.; Yang, X.; Yao, Q.; Ma, D. CuI/DMPAO-Catalyzed N-Arylation of Acyclic Secondary Amines. *Org. Lett.* **2012**, *14*, 3056–3059.

- (4) (a) Hardouin Duparc, V.; Bano, G. L.; Schaper, F. Chan–Evans–Lam Couplings with Copper Iminoarylsulfonate Complexes: Scope and Mechanism. *ACS Catal.* **2018**, *8*, 7308–7325. (b) Sueki, S.; Kuninobu, Y. Copper-Catalyzed N- and O-Alkylation of Amines and Phenols using Alkylborane Reagents. *Org. Lett.* **2013**, *15*, 1544–1547. (c) Quach, T. D.; Batey, R. A. Ligand- and Base-Free Copper(II)-Catalyzed C–N Bond Formation: Cross-Coupling Reactions of Organoboron Compounds with Aliphatic Amines and Anilines. *Org. Lett.* **2003**, *5*, 4397–4400.

- (5) (a) Chen, X.; Hao, X.-S.; Goodhue, C. E.; Yu, J.-Q. *J. Am. Chem. Soc.* **2006**, *128*, 6790–6791. (b) Uemura, T.; Imoto, S.; Chatani, N. *Chem. Lett.* **2006**, *35*, 842–843.

- (6) (a) Roane, J.; Daugulis, O. A General Method for Aminoquinoline-Directed, Copper-Catalyzed sp² C–H Bond Amination. *J. Am. Chem. Soc.* **2016**, *138*, 4601–4607. (b) Tran, L. D.; Roane, J.; Daugulis, O. Directed Amination of Non-Acidic Arene C–H Bonds by a Copper–Silver Catalytic System. *Angew. Chem., Int. Ed.* **2013**, *52*, 6043–6046.

- (7) (a) Kim, H.; Heo, J.; Kim, J.; Baik, M.-H.; Chang, S. Copper-Mediated Amination of Aryl C–H Bonds with the Direct Use of Aqueous Ammonia via a Disproportionation Pathway. *J. Am. Chem. Soc.* **2018**, *140*, 14350–14356. (b) Kim, H.; Chang, S. The Use of Ammonia as an Ultimate Amino Source in the Transition Metal-Catalyzed C–H Amination. *Acc. Chem. Res.* **2017**, *50*, 482–486.

- (8) (a) Doran, T. M.; Gao, Y.; Simanski, S.; McEnaney, P.; Kodadek, T. High affinity binding of conformationally constrained synthetic oligomers to an antigen-specific antibody: Discovery of a diagnostically useful synthetic ligand for murine Type 1 diabetes autoantibodies. *Bioorg. Med. Chem. Lett.* **2015**, *25*, 4910–4917. (b) Abdul-Hay, S. O.; Bannister, T. D.; Wang, H.; Cameron, M. D.; Caulfield, T. R.; Masson, A.; Bertrand, J.; Howard, E. A.; McGuire, M. P.; Crisafulli, U.; Rosenberry, T. R.; Topper, C. L.; Thompson, C. R.; Schürer, S. C.; Madoux, F.; Hodder, P.; Leissring, M. A. Selective Targeting of Extracellular Insulin-Degrading Enzyme by Quasi-Irreversible Thiol-Modifying Inhibitors. *ACS Chem. Biol.* **2015**, *10*, 2716–2724. (c) Gong, Y.; Somersan Karakaya, S.; Guo, X.; Zheng, P.; Gold, B.; Ma, Y.; Little, D.; Roberts, J.; Warriar, T.; Jiang, X.; Pingle, M.; Nathan, C. F.; Liu, G. Benzimidazole-based compounds kill Mycobacterium tuberculosis. *Eur. J. Med. Chem.* **2014**, *75*, 336–353. (d) Gammons, M. V.; Fedorov, O.; Ivson, D.; Du, C.; Clark, T.; Hopkins, C.; Hagiwara, M.; Dick, A. D.; Cox, R.; Harper, S. J.; Hancox, J. C.; Knapp, S.; Bates, D. O. Topical Antiangiogenic SRPK1 Inhibitors Reduce Choroidal Neovascularization in Rodent Models of Exudative AMD. *Invest. Ophthalmol. Visual Sci.* **2013**, *54*, 6052–6062. (e) Cheung, Y.-Y.; Yu, H.; Xu, K.; Zou, B.; Wu, M.; McManus, O. B.; Li, M.; Lindsley, C. W.; Hopkins, C. R. Discovery of a Series of 2-Phenyl-N-(2-(pyrrolidin-1-yl)phenyl)acetamides as Novel Molecular Switches that Modulate Modes of Kv7.2 (KCNQ2) Channel Pharmacology: Identification of (S)-2-Phenyl-N-(2-(pyrrolidin-1-yl)phenyl)butanamide (ML252) as a Potent, Brain Penetrant Kv7.2 Channel Inhibitor. *J. Med. Chem.* **2012**, *55*, 6975–6979.

- (9) (a) Martínez, Á. M.; Rodríguez, N.; Arrayás, R. G.; Carretero, J. C. Copper-catalyzed ortho-C–H amination of protected anilines with secondary amines. *Chem. Commun.* **2014**, *50*, 2801–2803. (b) Li, Q.; Zhang, S.-Y.; He, G.; Ai, Z.; Nack, W. A.; Chen, G. Copper-Catalyzed Carboxamide-Directed Ortho Amination of Anilines with Alkylamines at Room Temperature. *Org. Lett.* **2014**, *16*, 1764–1767.
- (10) Yang, Q.-L.; Wang, X.-Y.; Lu, J.-Y.; Zhang, L.-P.; Fang, P.; Mei, T.-S. Copper-Catalyzed Electrochemical C–H Amination of Arenes with Secondary Amines. *J. Am. Chem. Soc.* **2018**, *140*, 11487–11494.
- (11) (a) Dong, X.; Liu, Q.; Dong, Y.; Liu, H. Transition-Metal-Catalyzed Electrophilic Amination: Application of O-Benzoylhydroxylamines in the Construction of the C–N Bond. *Chem. - Eur. J.* **2017**, *23*, 2481–2511. (b) Yan, X.; Yang, X.; Xi, C. Recent progress in copper-catalyzed electrophilic amination. *Catal. Sci. Technol.* **2014**, *4*, 4169–4177. (c) Louillat, M.-L.; Patureau, F. W. Oxidative C–H amination reactions. *Chem. Soc. Rev.* **2014**, *43*, 901–910.
- (12) Yoo, E. J.; Ma, S.; Mei, T.-S.; Chan, K. S. L.; Yu, J.-Q. Pd-Catalyzed Intermolecular C–H Amination with Alkylamines. *J. Am. Chem. Soc.* **2011**, *133*, 7652–7655.
- (13) (a) Wu, K.; Fan, Z.; Xue, Y.; Yao, Q.; Zhang, A. Rh(III)-Catalyzed Intermolecular C–H Amination of 1-Aryl-1H-pyrazol-5(4H)-ones with Alkylamines. *Org. Lett.* **2014**, *16*, 42–45. (b) Ng, K.-H.; Zhou, Z.; Yu, W.-Y. Rhodium(III)-Catalyzed Intermolecular Direct Amination of Aromatic C–H Bonds with N-Chloroamines. *Org. Lett.* **2012**, *14*, 272–275. (c) Grohmann, C.; Wang, H.; Glorius, F. Rh[III]-Catalyzed Direct C–H Amination Using N-Chloroamines at Room Temperature. *Org. Lett.* **2012**, *14*, 656–659.
- (14) Shang, M.; Zeng, S.-H.; Sun, S.-Z.; Dai, H.-X.; Yu, J.-Q. Ru(II)-Catalyzed ortho-C–H Amination of Arenes and Heteroarenes at Room Temperature. *Org. Lett.* **2013**, *15*, 5286–5289.
- (15) Matsubara, T.; Asako, S.; Ilies, L.; Nakamura, E. Synthesis of Anthranilic Acid Derivatives through Iron-Catalyzed Ortho Amination of Aromatic Carboxamides with N-Chloroamines. *J. Am. Chem. Soc.* **2014**, *136*, 646–649.
- (16) (a) McDonald, S. L.; Wang, Q. Copper-Catalyzed α -Amination of Phosphonates and Phosphine Oxides: A Direct Approach to α -Amino Phosphonic Acids and Derivatives. *Angew. Chem., Int. Ed.* **2014**, *53*, 1867–1871. (b) Nguyen, M. H.; Smith, A. B. Copper-Catalyzed Electrophilic Amination of Organolithiums Mediated by Recoverable Siloxane Transfer Agents. *Org. Lett.* **2013**, *15*, 4872–4875. (c) Yan, X.; Chen, C.; Zhou, Y.; Xi, C. Copper-Catalyzed Electrophilic Amination of Alkenylzirconocenes with O-Benzoylhydroxylamines: An Efficient Method for Synthesis of Enamines. *Org. Lett.* **2012**, *14*, 4750–4753. (d) Rucker, R. P.; Whittaker, A. M.; Dang, H.; Lalic, G. Synthesis of Hindered Anilines: Copper-Catalyzed Electrophilic Amination of Aryl Boronic Esters. *Angew. Chem.* **2012**, *124*, 4019–4022. (e) Matsuda, N.; Hirano, K.; Satoh, T.; Miura, M. Copper-Catalyzed Amination of Ketene Silyl Acetals with Hydroxylamines: Electrophilic Amination Approach to α -Amino Acids. *Angew. Chem., Int. Ed.* **2012**, *51*, 11827–11831. (f) Berman, A. M.; Johnson, J. S. Copper-Catalyzed Electrophilic Amination of Diorganozinc Reagents. *J. Am. Chem. Soc.* **2004**, *126*, 5680–5681.
- (17) (a) Li, G.; Jia, C.; Sun, K.; Lv, Y.; Zhao, F.; Zhou, K.; Wu, H. Copper(ii)-catalyzed electrophilic amination of quinoline N-oxides with O-benzoyl hydroxylamines. *Org. Biomol. Chem.* **2015**, *13*, 3207–3210. (b) Yotphan, S.; Beukeaw, D.; Reutrakul, V. Synthesis of 2-aminobenzoxazoles via copper-catalyzed electrophilic amination of benzoxazoles with O-benzoyl hydroxylamines. *Tetrahedron* **2013**, *69*, 6627–6633. (c) Matsuda, N.; Hirano, K.; Satoh, T.; Miura, M. Copper-Catalyzed Direct Amination of Electron-Deficient Arenes with Hydroxylamines. *Org. Lett.* **2011**, *13*, 2860–2863.
- (18) Xu, L.-L.; Wang, X.; Ma, B.; Yin, M.-X.; Lin, H.-X.; Dai, H.-X.; Yu, J.-Q. *Chem. Sci.* **2018**, *9*, 5160–5164.
- (19) (a) Kitanosono, T.; Masuda, K.; Xu, P.; Kobayashi, S. Catalytic Organic Reactions in Water toward Sustainable Society. *Chem. Rev.* **2018**, *118*, 679–746. (b) Yang, L.; Li, H.; Zhang, H.; Lu, H. Palladium-Catalyzed Intramolecular C–H Amination in Water. *Eur. J. Org. Chem.* **2016**, *2016*, 5611–5615. (c) Lipshutz, B. H.; Chung, D. W.; Rich, B. Aminations of Aryl Bromides in Water at Room Temperature. *Adv. Synth. Catal.* **2009**, *351*, 1717–1721.
- (20) (a) Ribas, X.; Calle, C.; Poater, A.; Casitas, A.; Gómez, L.; Xifra, R.; Parella, T.; Benet-Buchholz, J.; Schweiger, A.; Mitrikas, G.; Solà, M.; Llobet, A.; Stack, T. D. P. Facile C–H Bond Cleavage via a Proton-Coupled Electron Transfer Involving a C–H...CuII Interaction. *J. Am. Chem. Soc.* **2010**, *132*, 12299–12306. (b) King, A. E.; Huffman, L. M.; Casitas, A.; Costas, M.; Ribas, X.; Stahl, S. S. Copper-Catalyzed Aerobic Oxidative Functionalization of an Arene C–H Bond: Evidence for an Aryl-Copper(III) Intermediate. *J. Am. Chem. Soc.* **2010**, *132*, 12068–12073. (c) Huffman, L. M.; Stahl, S. S. Carbon–Nitrogen Bond Formation Involving Well-Defined Aryl-Copper(III) Complexes. *J. Am. Chem. Soc.* **2008**, *130*, 9196–9197.
- (21) Cheung, Y.-Y.; Yu, H.; Xu, K.; Zou, B.; Wu, M.; McManus, O. B.; Li, M.; Lindsley, C. W.; Hopkins, C. R. Discovery of a Series of 2-Phenyl-N-(2-(pyrrolidin-1-yl)phenyl)acetamides as Novel Molecular Switches that Modulate Modes of Kv7.2 (KCNQ2) Channel Pharmacology: Identification of (S)-2-Phenyl-N-(2-(pyrrolidin-1-yl)phenyl)butanamide (ML252) as a Potent, Brain Penetrant Kv7.2 Channel Inhibitor. *J. Med. Chem.* **2012**, *55*, 6975–6979.
- (22) (a) Subhedar, D. D.; Shaikh, M. H.; Arkile, M. A.; Yeware, A.; Sarkar, D.; Shingate, B. B. Facile synthesis of 1,3-thiazolidin-4-ones as antitubercular agents. *Bioorg. Med. Chem. Lett.* **2016**, *26*, 1704–1708. (b) Weng, J.; Wang, C.; Li, H.; Wang, Y. Novel quaternary ammonium ionic liquids and their use as dual solvent-catalysts in the hydrolytic reaction. *Green Chem.* **2006**, *8*, 96–99.

Cite this: *Chem. Sci.*, 2022, 13, 5726

All publication charges for this article have been paid for by the Royal Society of Chemistry

A directing group switch in copper-catalyzed electrophilic C–H amination/migratory annulation cascade: divergent access to benzimidazolone/benzimidazole†

Hasina Mamataj Begam, Shantanu Nandi and Ranjan Jana *

We present here a copper-catalyzed electrophilic *ortho* C–H amination of protected naphthylamines with *N*-(benzoxy)amines, cyclization with the pendant amide, and carbon to nitrogen 1,2-directing group migration cascade to access *N,N*-disubstituted 2-benzimidazolones. Remarkably, this highly atom-economic tandem reaction proceeds through a C–H and C–C bond cleavage and three new C–N bond formations in a single operation. Intriguingly, the reaction cascade was altered by the subtle tuning of the directing group from picolinamide to thiopicolinamide furnishing 2-heteroaryl-imidazoles *via* the extrusion of hydrogen sulfide. This strategy provided a series of benzimidazolones and benzimidazoles in moderate to high yields with low catalyst loading (66 substrates with yields up to 99%). From the control experiments, it was observed that after the C–H amination an incipient tetrahedral oxyanion or thiolate intermediate is formed *via* an intramolecular attack of the primary amine to the amide/thioamide carbonyl. It undergoes either a 1,2-pyridyl shift with the retention of the carbonyl moiety or H₂S elimination for scaffold diversification. Remarkably, in spite of a positive influence of copper in the reaction outcome, from our preliminary investigations, the benzimidazolone product was obtained in good to moderate yields in two steps under metal-free conditions. The *N*-pyridyl moiety of the benzimidazolone was removed for further manipulation of the free NH group.

Received 10th March 2022
Accepted 13th April 2022

DOI: 10.1039/d2sc01420c

rsc.li/chemical-science

Introduction

At the threshold of an era of automated organic synthesis, the cascade reaction encompassing C–H activation is emerging as a powerful tool for the rapid construction and late-stage diversification of functional molecules in a step- and atom-economic manner.¹ In this cascade process, a command to control chemoselectivity using an inherent chemical reporter enables to achieve rapid molecular diversity.² However, the introduction and removal of directing groups is one of the major drawbacks in chelation-assisted C–H functionalization.³ To circumvent, transient, traceless, and inherent directing group strategies were unveiled.⁴ Very recently, the migration and incorporation of a directing group into the target molecule has emerged as a practical strategy in transition metal-catalyzed C–H functionalization to access rapid molecular complexity maximizing atom-economy.⁵ In this direction, cobalt and rhodium-catalyzed

stereoselective syntheses of tetra-substituted alkenes were reported through the migration of the directing group.⁶ The Ackermann group reported a cobalt-catalyzed pyridine-directing group migration/annulation cascade in C–H activation.⁷ The Wang group reported manganese-catalyzed C–H activation/enaminylation/DG migration cascade in an *N*-pyridyl protected indole system.⁸ The Huang group demonstrated a multitasking directing group strategy for structural diversification in C–H activation cascade.⁹ Very recently, the Li group reported a Pd-catalyzed domino C4-arylation/3,2-carbonyl directing group migration in indoles.¹⁰ To the best of our knowledge, there is no report of a single atom of a directing group (O vs. S) switch for scaffold diversification exploiting their innate reactivity in the C–H functionalization/annulation cascade. Benzimidazolone and benzimidazole are prevalent in pharmaceuticals, agrochemicals, pigments, herbicides, and fine chemicals (Fig. 1).¹¹ The synthesis of these privileged scaffolds primarily relies on *ortho*-phenylenediamine or *ortho*-haloanilines.¹² Recently, the oxidative annulation of anilides/aniline is emerging as an attractive strategy for expanding the substrate scope.¹³ The Zhang group reported the copper-catalyzed synthesis of benzimidazolones and benzimidazoles exploiting the SOMO-stabilized radical cation of diarylamines (Scheme 1a).¹⁴ The electrophilic C–H amination has emerged as

Organic and Medicinal Chemistry Division, CSIR-Indian Institute of Chemical Biology, 4 Raja S. C. Mullick Road, Jadavpur, Kolkata-700032, West Bengal, India. E-mail: rjana@iicb.res.in

† Electronic supplementary information (ESI) available: Optimization details, general procedures, spectral data, crystal data, NMR experiments. CCDC 2025266, 2025269, 2025275, 2025279 and 2025280. For ESI and crystallographic data in CIF or other electronic format see <https://doi.org/10.1039/d2sc01420c>



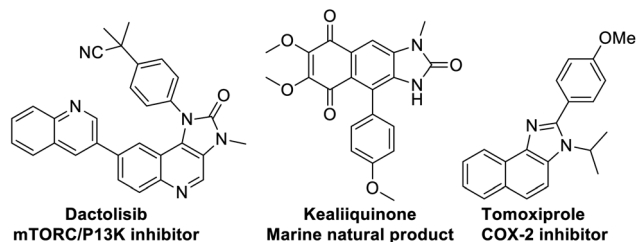
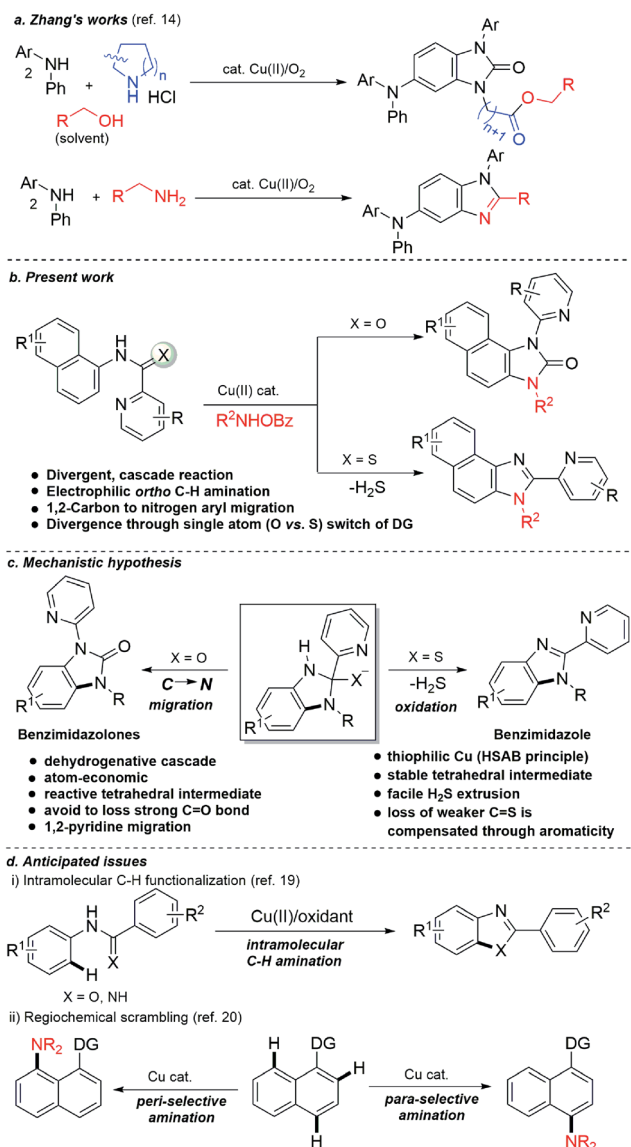


Fig. 1 Biologically important imidazolone/imidazole core.



Scheme 1 Cascade synthesis of benzimidazole and benzimidazolones.

a benign alternative to construct *N*-heterocycles under mild conditions.¹⁵ Although a Ru(II)-catalyzed O → N migration during benzimidazole to benzimidazolone conversion is reported,¹⁶ direct C-2 aryl migration is not reported. We disclose here a novel single atom of a directing group switch strategy for

the chemoselective synthesis of 1,3-dihydro-2*H*-naphtho[1,2-*d*]imidazole-2-one *via* electrophilic *ortho* C-H amination, intramolecular cyclization, C → N 1,2-pyridyl shift or 2-(pyridin-2-yl)-3*H*-naphtho[1,2-*d*]imidazole derivatives through an electrophilic C-H amination/annulation cascade (Scheme 1b).

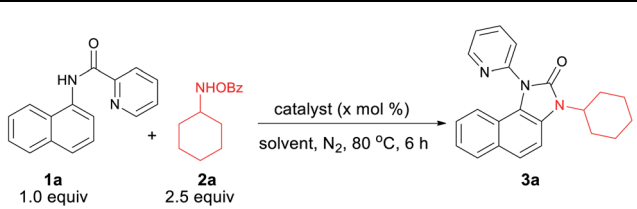
Contrary to the previous procedures, we observed an excellent reactivity of the bicyclic system towards electrophilic *ortho* C-H amination with secondary amines under our optimized reaction condition.¹⁷ We hypothesized that C-H amination with primary amine may initiate an annulation cascade *via* subsequent addition to the picolinamide directing group. The incipient oxyanion may trigger the 1,2-migration of the directing group to provide benzimidazolone. Instead, thiophilic copper may endorse the extrusion of hydrogen sulfide to provide benzimidazole from the corresponding thioamide directing group (Scheme 1c). However, (1) copper-catalyzed C-H amination with a primary amine is a formidable challenge due to the catalyst inhibition;¹⁸ (2) a deleterious intramolecular oxidative cyclization of the corresponding directing group may impede the cascade process¹⁹ (Scheme 1d(i)); (3) competing *peri*- and *para*-C-H amination of naphthalene should be suppressed²⁰ (Scheme 1d(ii)). Furthermore, C-H amination with aliphatic primary amines is challenging and less explored.²¹

Results and discussion

We hypothesized that C-H amination with electrophilic primary amine surrogates may overcome the catalyst inhibition problem. To test our hypothesis, picolinamide-protected 1-naphthylamine **1a**, and 1.0 equiv. of *O*-benzoylhydroxylamine **2a** was subjected to our previous reaction condition to afford the expected imidazolone product **3a** in 44% yield. In the course of further optimization, DMSO was found to be the optimal solvent and excellent yields of this tandem reaction, *e.g.*, 93% and 87% were obtained with just 5.0 and 1.0 mol% catalyst loading, respectively (Table 1). Other copper catalysts, lower reaction temperature, and 1.2 equiv. of **2a** provided inferior results. Free primary amines along with external oxidants such as PIDA, K₂S₂O₈ or Bz₂O₂ were able to furnish the desired product in <5%, 12% and 32% yields, respectively. Using 1.2 equiv. of **2a** along with 1.0 equiv. Bz₂O₂ the yield was dropped to 58%. Other metal catalysts such as Pd(OAc)₂, Co(OAc)₂, Ni(OAc)₂, Mn(OAc)₂, FeCl₂, and FeBr₂ were less or ineffective for this transformation (for detailed optimization, see the ESI†). Other aminating reagents such as anthranil, benzisoxazole, or oxime esters under the same condition could not afford any desired product.

Under the optimized reaction condition, cyclic as well as acyclic primary amines furnished the desired products in good to high yields (Table 2). Cyclohexylamine provided an excellent 93% yield of the desired product (**3a**), whereas cyclopentyl, cycloheptyl, and cyclooctylamines afforded slightly lower 78%, 65%, and 46% yields, respectively (**3b–3d**). In the case of acyclic amines, yields increased with the increase in chain length (**3e–3g**) and steric bulk. Surprisingly, sterically hindered *sec*-butyl (**3i**), *tert*-butyl (**3j**), adamantylamine (**3m**) provided almost quantitative yields exhibiting a positive influence of steric bulk



Table 1 Optimization of the reaction conditions^{a,b}


| Entry | Catalyst | X | Oxidant | Solvent | Yield ^b (3a) |
|-----------------|--|-----|--------------------------------|------------------|-------------------------|
| 1 ^c | Cu(OAc) ₂ ·H ₂ O | 10 | — | DMSO | 44 |
| 2 | Cu(OAc) ₂ ·H ₂ O | 10 | — | H ₂ O | 0 |
| 3 | Cu(OAc) ₂ ·H ₂ O | 10 | — | MeCN | 39 |
| 4 | Cu(OAc) ₂ ·H ₂ O | 10 | — | Dioxane | 62 |
| 5 | Cu(OAc) ₂ ·H ₂ O | 10 | — | DMSO | 90 |
| 6 | Cu(OAc) ₂ ·H ₂ O | 5 | — | DMSO | 93 |
| 7 | Cu(OAc) ₂ ·H ₂ O | 2.5 | — | DMSO | 90 |
| 8 | Cu(OAc) ₂ ·H ₂ O | 1.0 | — | DMSO | 87 |
| 9 | Cu(OAc) ₂ ·H ₂ O | 0.5 | — | DMSO | 72 |
| 10 ^d | Cu(OAc) ₂ ·H ₂ O | 0 | — | DMSO | 0 |
| 11 ^e | Cu(OAc) ₂ ·H ₂ O | 2.5 | — | DMSO | 56 |
| 12 | Cu powder | 5 | — | DMSO | 83 |
| 13 ^f | Cu(OAc) ₂ ·H ₂ O | 10 | PIDA | DMSO | >5 |
| 14 ^g | Cu(OAc) ₂ ·H ₂ O | 10 | Bz ₂ O ₂ | DMSO | 58 |
| 15 | Pd(OAc) ₂ | 10 | — | DMSO | >5 |
| 16 | Co(OAc) ₂ | 10 | — | DMSO | 20 |

^a All reactions were carried out on a 0.2 mmol scale. ^b Yields refer to here are overall isolated yields. ^c 1.0 equiv. **2a** was used. ^d 25% *ortho* aminated product was obtained. ^e Reaction was performed at room temperature. ^f Free amine was used as amine source and 2.5 equiv. PIDA as oxidant. ^g 1.0 equiv. Bz₂O₂ and 1.2 equiv. of **2a** were used.

of amines on the rearrangement cascade. Competition experiment of **1a** with **2m** and **2n** afforded **3m** and **3n** in 70% and 28%, respectively. Several substituted 1-naphthylamines including methyl substitution at the C8 position provided high to excellent yields of the desired products (**3q–3y**). Heterocyclic amino quinoline and isoquinoline provided the rearranged product in excellent yields (**3z**, **3aa**). Delightedly, diverse (2-*N*-heteroaryl) anilides serve as excellent directing groups and are incorporated into the benzimidazolones (**3ac–3ah**). Interestingly, 3-methyl picolinamide provided the corresponding *N*-pyridyl product (**3ac**) *via ipso*-substitution. Similarly, the amides of 5-methyl pyrazinoic (**3ad**, CCDC 2025269), quinaldic (**3ae**), and pyrazinoic acid (**3af**, **3ag**) also furnished in comparable yields. Isoquinoline-1-carbamide provided a mixture of benzimidazolone **3ah** and C–H amination product **3ah'**. This may be the result of an unfavourable tetrahedral intermediate due to steric reasons. 6-Aminoquinoline provided the C–H amination at the C5 position. Furthermore, sterically less hindered methyl amine provided a corresponding 2-pyridylbenzimidazole (**3aj**, CCDC 2025266), imparting the role of steric and trajectory of the C–H amination on the subsequent rearrangement reaction.

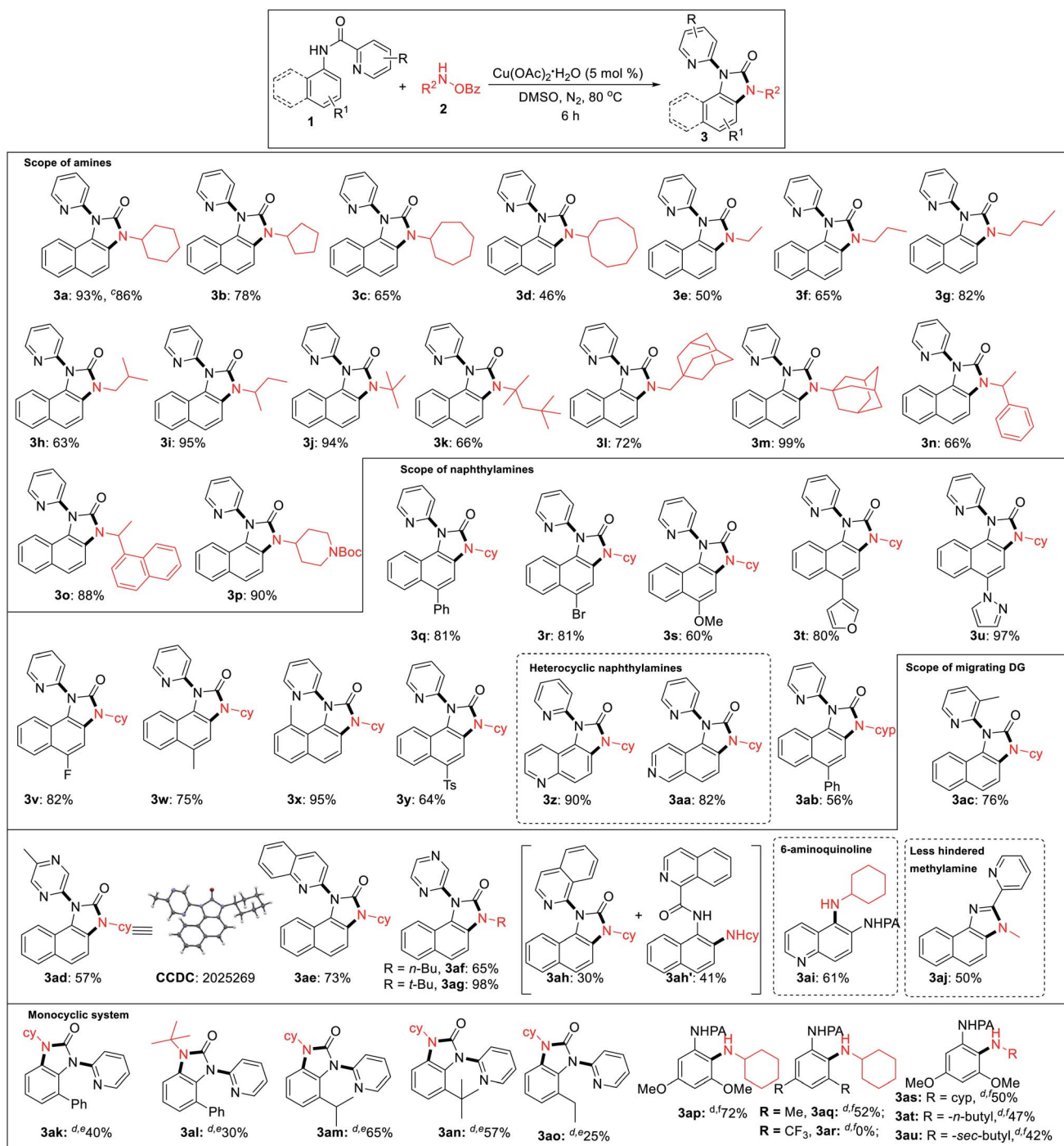
We performed the reaction with various *ortho*, *meta*, *para*-substituted anilines under the same condition and successfully we got 30% rearranged product in 2-phenyl aniline and *ortho* amination product (35%) in a 3,5-dimethoxy aniline system. After getting these results, we turned our attention to optimize

these reactions (for detailed optimization; see the ESI†). After several screenings of solvents, base or acid additives, ligands there was no significant improvement in the rearrangement reaction of 2-phenyl aniline picolinamide. Increasing temperature to 100 °C product yield increased to 40%. Then, we performed the reaction in different *ortho*-substituted anilines (electron-donating bulky groups) to obtain rearranged benzimidazolones in moderate to good yields (**3ak–3ao**). Finally, we were able to get an *ortho* C–H amination product in 3,5-dimethoxy aniline with 72% yield at 90 °C using 2.0 equiv. LiO^tBu (**3ap**). While 3,5-dimethyl substituted picolinamide furnished the C–H amination product in 52% yield, the corresponding 3,5-bis(trifluoromethyl)aniline substrate remained unreactive indicating a profound role of electronic nature (**3aq**, **3ar**). Besides cyclohexylamine, other amines also afforded the *ortho* C–H amination products in moderate yields (**3as–3au**). However, no benzimidazolones were formed even at a low catalyst loading or additives, suggesting that an *ortho* substitution w.r.t. picolinamide is crucial for the subsequent rearrangement reaction.

2-Pyridylbenzimidazoles are an important class of compounds generally used as excellent ligands for metal complexation and glukokinase activator.²² We turned our attention to optimize the reaction for benzimidazole. Initially, we started the optimization of benzimidazole with **1a** and **2a**. All our efforts using different acidic solvents such as AcOH or TFE, acid additives such as BzOH, TsOH, and high temperature (120 °C) to facilitate dehydration after cyclization were in vain. Gratifyingly, the corresponding picolinimidamide afforded the imidazole product in 30% yield in 12 h. Since thioamides have been proved as excellent directing groups in Pd- or Co-catalyzed C–H functionalizations,²³ we hypothesized that thiophilic copper²⁴ may trigger the liberation of hydrogen sulfide from thioamide instead of 1,2-pyridyl migration to furnish the desired benzimidazole product. Hence, examining thio-picolinamide **4a** under the reaction condition resulted in the desired 2-pyridylbenzimidazole exclusively albeit in a low yield. After several screenings (for detailed optimization, see the ESI†), using 3.0 equiv. of **2a**, 20 mol% Cu(OAc)₂·H₂O and 1.2 equiv. of K₂CO₃ in DMSO at 90 °C under O₂ atmosphere the desired product was obtained in 88% yield. During the optimization, we found K₂CO₃ and O₂ to be crucial otherwise yield dropped significantly.

During the substrate scope studies, we observed a positive influence of the increasing chain length of the linear amines (**5c–5d**, Table 3). Unlike imidazolones, the yields of isomeric acyclic amines decreased with the increase in α -substitution (**5d–5g**). Benzylamine, furylamine, adamantanemethylamine and 4-amino-1-boc piperidine afforded the products in moderate yields (**5h–5k**). Thioamides of 5-methyl pyrazine-2-carboxylic acid and 2-quinaldic acids also provided the imidazole product in moderate yields (**5l**, **5m**). Various substituted 1-naphthylamines at different positions also underwent the reaction providing the desired product in medium to good yields (**5n–5s**). The reaction is also reproducible on a 2.0 mmol scale demonstrating the practicability of this methodology. The



Table 2 Substrate scope of benzimidazolones^{a,b,g}

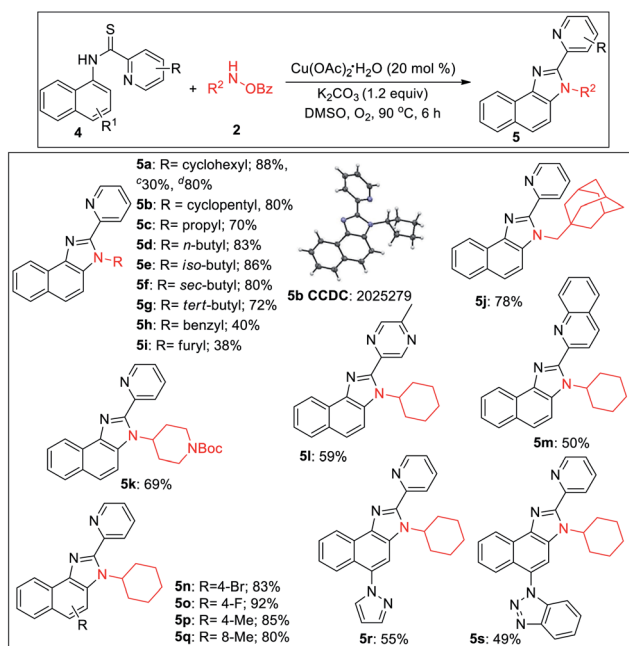
^a All reactions were carried out in 0.2 mmol scale. ^b Yields refer to the overall isolated yields with respect to **1**. ^c 2.0 mmol scale reaction. ^d 10 mol% Cu(OAc)₂·H₂O is used. ^e Reaction temperature was 100 °C. ^f Additional 2.0 equiv. LiO^tBu is used and reaction temperature was 90 °C. In the competition experiment: **1a** (0.20 mmol), **2m** (0.50 mmol), **2n** (0.50 mmol), Cu(OAc)₂·H₂O (0.01 mmol), dry DMSO (2.0 mL), N₂, 80 °C, and 6 h. ^g Reaction conditions: **1** (0.20 mmol), **2** (0.50 mmol), Cu(OAc)₂·H₂O (0.01 mmol), Dry DMSO (2.0 mL), N₂, 80 °C, and 6 h.

thio-picolinamide of monocyclic anilines under the same condition mostly oxidized to picolinamide.

Intrigued by the initial C–H amination product formation under the metal-free conditions (entry 10, Table 1), we

wondered whether it can be re-optimized to achieve the desired benzimidazolones. Initially, a mixture of C–H amination product **1a'**, imidazolone **3a** and unreacted starting material was obtained, which was subjected to the subsequent



Table 3 Substrate scope of benzimidazoles^{a,b,e}

^a All reactions were carried out in 0.2 mmol scale. ^b Yields refer to overall isolated yields with respect to **4**. ^c Picolinimidamide **4a'** used as substrate. ^d Reaction in 2.0 mmol scale. ^e Reaction conditions: **4** (0.20 mmol), **2** (0.60 mmol), $\text{Cu}(\text{OAc})_2 \cdot \text{H}_2\text{O}$ (0.04 mmol), K_2CO_3 (0.24 mmol), dry DMSO (2.0 mL), O_2 , 90 °C, and 6 h.

cyclization reaction (Table 4). However, the work-up of the reaction mixture and the subsequent addition of benzoyl peroxide converted the C–H amination product to the desired

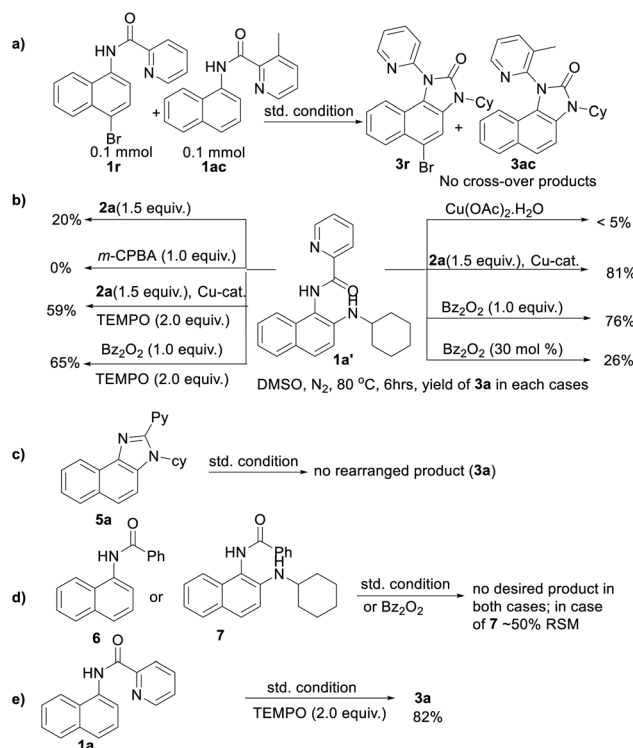
Table 4 Optimization of the metal-free condition^{a,b,e}

| Entry | Amine source | Equiv. of 2 | Yield ^b (%) |
|-----------------|--|-------------|------------------------|
| 1 | 2a : R = H | 2.5 | 25 |
| 2 | 2a : R = H | 4.0 | 25 |
| 4 | 2a₂ : R = 4-NMe ₂ | 4.0 | 65 |
| 5 | 2a₃ : R = 4-CF ₃ | 4.0 | 10 |
| 6 | 2a₄ : R = 4- <i>t</i> Bu | 4.0 | 20 |
| 7 | 2a₅ : R = 4-OMe | 4.0 | 41 |
| 8 | 2a₆ : R = 3,5-di Cl | 4.0 | 0 |
| 9 | 2a₇ : R = pentafluoro | 4.0 | 25 |
| 10 ^c | 2b₂ : R = 4-NMe ₂ | 4.0 | 44 |
| 11 ^d | 2a₂ : R = 4-NMe ₂ | 4.0 | 70 |

^a All reactions were carried out on a 0.1 mmol scale. ^b Yields refer to here are isolated yields after two steps with respect to **1**. ^c Protected cyclopentylamine was used and reaction time was 12 h. ^d Substrate **1r** was used. ^e Reaction conditions: 1st step: **1** (0.10 mmol), **2** (0.40 mmol), dry DMSO (1.0 mL), N_2 , 90 °C, and 48 h. 2nd step: Bz_2O_2 (0.75 equiv.), DMSO, N_2 , 80 °C, and 1 h.

annulation product. Increasing the amine source **2a** to 4.0 equiv. or temperature to 90 °C did not improve the yield. Gratifyingly, varying different substituents in the phenyl ring of **2**, we observed that 4-NMe₂ substitution furnished the product in 65% yield. Protected cyclopentylamine afforded the desired product in 44% yield in 12 h. Monocyclic substrates were unreactive under metal-free conditions. Notably, the possibility of metal contamination was excluded by using all new glass-ware, freshly distilled solvents, and repeating the reaction at least four times. Although, this metal-free, two-step process has inherent limitations, we anticipate that it has profound mechanistic implications.

To gain insight into the reaction mechanism, when an equimolar mixture of **1r** and **1ac** was treated in our reaction condition, **3r** and **3ac** were formed and no cross-over product was isolated suggesting an intramolecular 1,2-pyridyl migration (Scheme 2a). Unsymmetrically-substituted 5-methyl pyrazine anilide **1ad** afforded the imidazolone product **3ad** exclusively through *ipso* C–N bond formation (Table 2). Either performing the reaction at room temperature for a shorter time or quenching the reaction after 1.5 h, a mixture of the starting material, C–H amination product **1a'**, and rearranged product were observed. Heating a preformed C–H amination product **1a'** in absence of **2a** <5% product was formed. However, a combination of copper catalyst and *O*-benzoylhydroxylamine **2a** (1.5 equiv.) or even benzoylperoxide alone furnished the desired **3a** in high yields (Scheme 2b). Therefore, besides an aminating agent, **2a** also acts as an oxidant for catalytic turnover. Furthermore, the imidazole product **5a** was not converted into the corresponding imidazolone **3a** under the



Scheme 2 Control experiments.



reaction condition, suggesting a plausible concerted cyclization/1,2-pyridyl migration pathway (Scheme 2c). In place of picolinamide **1a**, the corresponding benzanilide **6** or **7** did not furnish any desired product (Scheme 2d). **7** does not undergo any rearrangement even in the presence of Bz_2O_2 , suggesting that the pyridyl-nitrogen is not only involved in the directed C–H amination but also in the subsequent steps. In both conditions, **7** underwent decomposition with 50% starting material recovery. To examine the involvement of radicals in this C–H amination/migratory annulation cascade, we performed the reaction in the presence of 2.0 equiv. of TEMPO. The yield was slightly decreased from 93% to 82% (Scheme 2e). Further, cyclization from a pre-formed amination product **1a'** furnished an almost similar yield in the presence of TEMPO. Hence, the single electron transfer (SET) process may not be involved in the migratory cyclization step. Then, we performed the time-dependent ^1H NMR experiment to get a clue about the intermediate of the rearrangement reaction. We took **1a'** in a NMR tube in DMSO-d_6 and 1.0 equiv. of Bz_2O_2 was added to it for recording the time-dependent ^1H NMR spectra at room temperature (Fig. 2). After 5–7 min, a new peak corresponding to H_b or $\text{H}_{b'}$ appeared at 8.71, which was slowly decreased and finally diminished while the desired product was formed. In this study, the chemical shift of the *ortho* proton of pyridine (H_a) in **1a'** is indicative of the formation of intermediate **VII** or **VIIa'**, which gradually shifted to more upfield in the intermediates and then in the product (H_d). It indicates that the electron-withdrawing effect of the amide-carbonyl is no longer persists in the intermediate pointing either of the intermediates **VII** or **VIIa'** (H_b or $\text{H}_{b'}$). Since the chemical shift value in the intermediate is closer to the product than the starting material, we assume that the new C–N bond may already have been formed, which is in favor of the intermediate **VIIa'** (for full spectrum, see the ESI †).

A $\text{Cu}^{\text{I}}/\text{Cu}^{\text{III}}$ cycle may be involved in this cascade reaction as reported by the Li, Gaunt, Stahl, and other groups. 25 Based on control experiments and the above literature reports, $\text{Cu}(\text{II})$ salt first undergoes disproportionation to form an active Cu^{I} species, which undergoes oxidative addition to *O*-benzoylhydroxylamine **2**

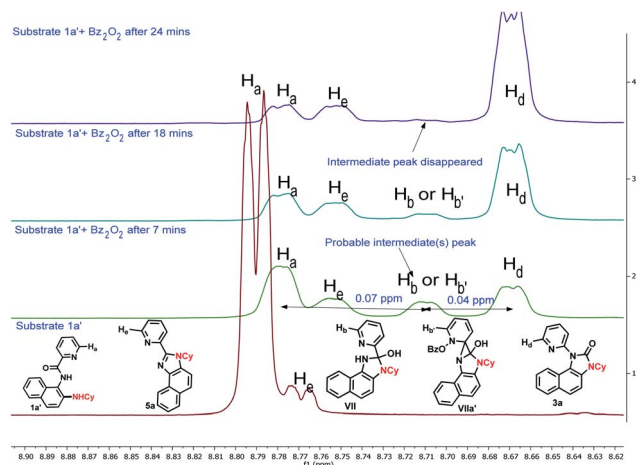
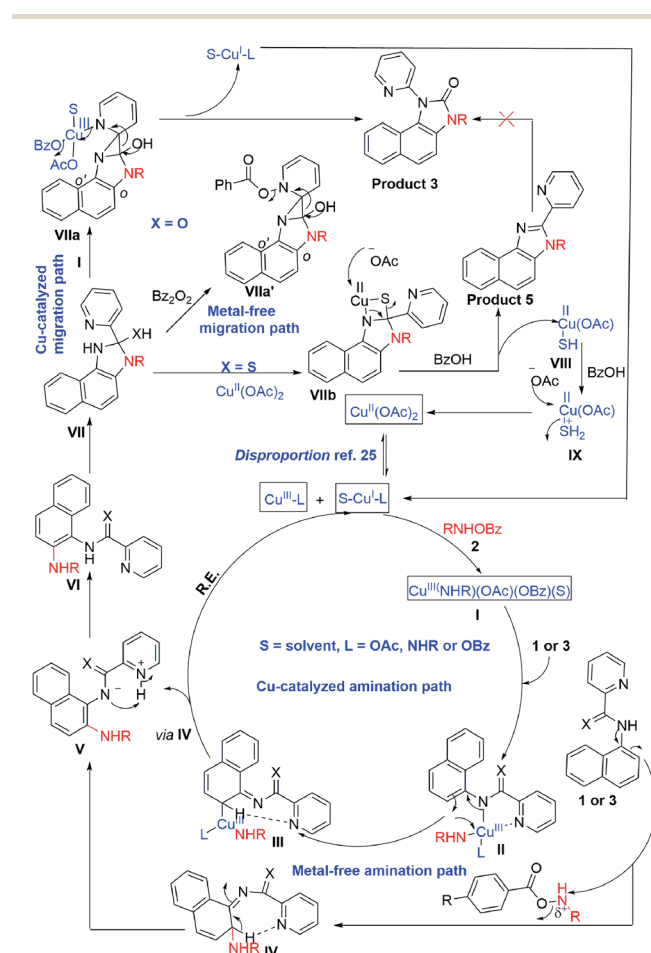


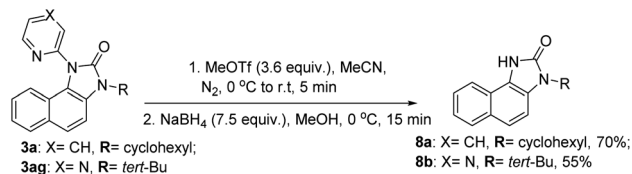
Fig. 2 Time-dependent ^1H NMR experiment.

forming a Cu^{III} complex, **I** (Scheme 3). This complex chelates with the substrate **1** or **3** forming **II**, which then undergoes electrophilic aromatic substitution type reaction generating **III**. Similarly, intermediate **IV** may also form under metal-free conditions. The pyridine of the picolinamide may work as a proton shuttle that abstracts *ortho* proton and delivers to the amide nitrogen during rearomatization through **V** providing *ortho* amination products **VI**. Next, a tetrahedral intermediate **VII** may form through the intramolecular attack of the amine moiety to the amide/thioamide carbonyl group. The nucleophilic nitrogen may attack at the *ipso* position of the pyridine moiety in the presence of the second molecule of the Cu^{III} -complex **I**, forming **VIIa** that explains the need for an excess (2.5 equiv.) amount of *O*-benzoylhydroxylamine. 26 A similar kind of an intermediate, **VIIa'** may generate in the presence of Bz_2O_2 in the metal-free pathway. This kind of a three-membered cyclic intermediate is claimed by the Feng group for aryl migration. 27 A similar $\text{O} \rightarrow \text{C}$ pyridyl migration through the de-aromatization of the pyridine ring was reported. 28 Then, a 1,2-pyridyl migration from $\text{C} \rightarrow \text{N}$ may take place to furnish the corresponding benzimidazolone product **3** and regenerates the active Cu^{I} species. **VIIa'** also furnishes the product in a similar fashion. It is further supported by the fact that electron-donating substitution (*e.g.* ethyl, isopropyl in case of



Scheme 3 Proposed reaction mechanism.





Scheme 4 Deprotection of the *N*-heteroaryls of the benzimidazolone product.

monocyclic anilines) at the *o'*-position has a positive influence in the reaction outcome. However, the *tert*-Bu group may hinder the reaction slightly due to steric inhibition. Owing to the distinct reactivity of thiol than the corresponding oxygen analogue,²⁹ a putative 4-membered cyclic intermediate **VIIb** may form with thiophilic copper from the tetrahedral thiolate intermediate (Scheme 3). Subsequently, the elimination of hydrogen sulphide provides the thermodynamically favourable benzimidazoles (**5**) regenerating Cu(II). However, the exact mechanism is not clear at this moment and warrants further studies.

Our efforts to utilize the pendant pyridine moiety for further C–H functionalization (thioarylation, alkynylation) at the *peri*-position remained unsuccessful at this moment. However, to expand the synthetic utility of this migratory annulation cascade, the pyridine and pyrazine moieties were deprotected from the representative benzimidazolones (**3a**, **3ag**) using a reported condition providing **8a** and **8b** in 70% and 55% yield, respectively (Scheme 4).³⁰ The free –NH moiety can be further manipulated to achieve further molecular diversity.

Conclusions

In conclusion, we have demonstrated a directing group-dependent complete switch of product selectivity in copper-catalyzed electrophilic C–H amination with protected primary amines. The benzimidazolones are formed *via* an unprecedented electrophilic *ortho* C–H amination with primary amines, intramolecular cyclization, and 1,2-directing group migration from carbon to the nitrogen center. Remarkably, one C–H and C–C bond cleavage and three new C–N bond formations take place in a single operation in this migratory annulation cascade. Strikingly, by changing the picolinamide directing group to the corresponding thiopicolinamide, the chemoselectivity is switched to form 2-pyridylbenzimidazoles *via* the extrusion of H₂S. Inexpensive copper catalyst, scale-up synthesis, low catalyst loading, and controlled scaffold diversification are some of the practical aspects of this tandem reaction. From the preliminary studies, the benzimidazolone product was also obtained in good to moderate yields in two steps under metal-free conditions. The in-depth mechanistic studies and investigation of metal-free conditions of this divergent tandem reaction is undergoing in our laboratory.

Data availability

All experimental data is available in the ESI.† No computation component is present in this manuscript.

Author contributions

R. J. conceptualized and supervised the project and wrote the manuscript. H. M. B. performed the experiments and wrote the manuscript. S. N. analyzed the crystal structure.

Conflicts of interest

There are no conflicts to declare.

Acknowledgements

This work was supported by DST, SERB, Govt. of India, Core Research Grant No. CRG/2021/006717. HMB and SN thank CSIR and DST-Inspire respectively for their fellowships.

Notes and references

- (a) J. Wencel-Delord and F. Glorius, *Nat. Chem.*, 2013, **5**, 369–375; (b) A. Baccalini, G. Faita, G. Zanoni and D. Maiti, *Chem.–Eur. J.*, 2020, **26**, 9749–9783; (c) L. Song and E. V. Van der Eycken, *Chem.–Eur. J.*, 2021, **27**, 121–144.
- (a) T. A. Davis, T. K. Hyster and T. Rovis, *Angew. Chem., Int. Ed.*, 2013, **52**, 14181–14185; (b) J. Kim, S.-W. Park, M.-H. Baik and S. Chang, *J. Am. Chem. Soc.*, 2015, **137**, 13448–13451; (c) C. Yamamoto, K. Takamatsu, K. Hirano and M. Miura, *J. Org. Chem.*, 2017, **82**, 9112–9118.
- (a) X. Chen, K. M. Engle, D.-H. Wang and J.-Q. Yu, *Angew. Chem., Int. Ed.*, 2009, **48**, 5094–5115; (b) C. Sambigiato, D. Schönbauer, R. Blicke, T. Dao-Huy, G. Pototschnig, P. Schaaf, T. Wiesinger, M. F. Zia, J. Wencel-Delord, T. Besset, B. U. W. Maes and M. Schnürch, *Chem. Soc. Rev.*, 2018, **47**, 6603–6743; (c) R. L. Carvalho, R. G. Almeida, K. Murali, L. A. Machado, L. F. Pedrosa, P. Dolui, D. Maiti and E. N. da Silva Júnior, *Org. Biomol. Chem.*, 2021, **19**, 525–547.
- (a) G. Rani, V. Luxami and K. Paul, *Chem. Commun.*, 2020, **56**, 12479–12521; (b) J. I. Higham and J. A. Bull, *Org. Biomol. Chem.*, 2020, **18**, 7291–7315; (c) M. Font, J. M. Quibell, G. J. P. Perry and I. Larrosa, *Chem. Commun.*, 2017, **53**, 5584–5597; (d) P. Gandeepan and L. Ackermann, *Chem*, 2018, **4**, 199–222.
- (a) J. Zhang, H. Xie, H. Zhu, S. Zhang, M. Reddy Lonka and H. Zou, *ACS Catal.*, 2019, **9**, 10233–10244; (b) Z. He and Y. Huang, *ACS Catal.*, 2016, **6**, 7814–7823; (c) R. Manoharan and M. Jeganmohan, *Org. Biomol. Chem.*, 2018, **16**, 8384–8389; (d) X. Zhou, H. Xu, Q. Yang, H. Chen, S. Wang and H. Zhao, *Chem. Commun.*, 2019, **55**, 8603–8606; (e) J. Sun, G. Wang, L. Hao, J. Han, H. Li, G. Duan, G. You, F. Li and C. Xia, *ChemCatChem*, 2019, **11**, 2799–2802; (f) D. Kalsi, N. Barsu and B. Sundararaju, *Chem.–Eur. J.*, 2018, **24**, 2360–2364; (g) S. Qiu, S. Zhai, H. Wang, C. Tao, H. Zhao and H. Zhai, *Adv. Synth. Catal.*, 2018, **360**, 3271–3276; (h) Y. Wu, C. Pi, Y. Wu and X. Cui, *Chem. Soc. Rev.*, 2021, **50**, 3677–3689.
- (a) H. Ikemoto, R. Tanaka, K. Sakata, M. Kanai, T. Yoshino and S. Matsunaga, *Angew. Chem., Int. Ed.*, 2017, **56**, 7156–



- 7160; (b) X. Wu, Y. Lu, J. Qiao, W. Dai, X. Jia, H. Ni, X. Zhang, H. Liu and F. Zhao, *Org. Lett.*, 2020, **22**, 9163–9168; (c) G. Liu, Y. Shen, Z. Zhou and X. Lu, *Angew. Chem., Int. Ed.*, 2013, **52**, 6033–6037.
- 7 C. Zhu, R. Kuniyil, B. B. Jei and L. Ackermann, *ACS Catal.*, 2020, **10**, 4444–4450.
- 8 X. Zhou, Z. Li, Z. Zhang, P. Lu and Y. Wang, *Org. Lett.*, 2018, **20**, 1426–1429.
- 9 Y. Chen, D. Wang, P. Duan, R. Ben, L. Dai, X. Shao, M. Hong, J. Zhao and Y. Huang, *Nat. Commun.*, 2014, **5**, 4610.
- 10 Y. Cheng, S. Yu, Y. He, G. An, G. Li and Z. Yang, *Chem. Sci.*, 2021, **12**, 3216–3225.
- 11 (a) M. Beesu, S. S. Malladi, L. M. Fox, C. D. Jones, A. Dixit and S. A. David, *J. Med. Chem.*, 2014, **57**, 7325–7341; (b) D. B. Nale and B. M. Bhanage, *Green Chem.*, 2015, **17**, 2480–2486.
- 12 (a) S. W. Youn and Y. H. Kim, *Org. Lett.*, 2016, **18**, 6140–6143; (b) R. Zeng, P.-h. Chen and G. Dong, *ACS Catal.*, 2016, **6**, 969–973; (c) D. Li and T. Ollevier, *Org. Lett.*, 2019, **21**, 3572–3575; (d) A. J. Blacker, M. M. Farah, M. I. Hall, S. P. Marsden, O. Saidi and J. M. J. Williams, *Org. Lett.*, 2009, **11**, 2039–2042; (e) J.-P. Wan, S.-F. Gan, J.-M. Wu and Y. Pan, *Green Chem.*, 2009, **11**, 1633–1637; (f) E. Skolia, M. K. Apostolopoulou, N. F. Nikitas and C. G. Kokotos, *Eur. J. Org. Chem.*, 2021, **2021**, 422–428.
- 13 (a) Y. Park, Y. Kim and S. Chang, *Chem. Rev.*, 2017, **117**, 9247–9301; (b) J. Xia, X. Yang, Y. Li and X. Li, *Org. Lett.*, 2017, **19**, 3243–3246; (c) S. M. Khake and N. Chatani, *Org. Lett.*, 2020, **22**, 3655–3660.
- 14 (a) T. Liang, H. Zhao, L. Gong, H. Jiang and M. Zhang, *iScience*, 2019, **15**, 127–135; (b) T. Liang, Z. Tan, H. Zhao, X. Chen, H. Jiang and M. Zhang, *ACS Catal.*, 2018, **8**, 2242–2246.
- 15 (a) X. Dong, Q. Liu, Y. Dong and H. Liu, *Chem.–Eur. J.*, 2017, **23**, 2481–2511; (b) X. Yan, X. Yang and C. Xi, *Catal. Sci. Technol.*, 2014, **4**, 4169–4177; (c) M.-L. Louillat and F. W. Patureau, *Chem. Soc. Rev.*, 2014, **43**, 901–910; (d) J.-S. Yu, M. Espinosa, H. Noda and M. Shibasaki, *J. Am. Chem. Soc.*, 2019, **141**, 10530–10537.
- 16 (a) C. S. Yeung, T. H. H. Hsieh and V. M. Dong, *Chem. Sci.*, 2011, **2**, 544–551; (b) M. Seki and Y. Takahashi, *Synthesis*, 2021, **53**, 2689–2692.
- 17 H. M. Begam, R. Choudhury, A. Behera and R. Jana, *Org. Lett.*, 2019, **21**, 4651–4656.
- 18 B. K. Singh, A. Polley and R. Jana, *J. Org. Chem.*, 2016, **81**, 4295–4303.
- 19 (a) G. Brasche and S. L. Buchwald, *Angew. Chem., Int. Ed.*, 2008, **47**, 1932–1934; (b) S. Ueda and H. Nagasawa, *Angew. Chem., Int. Ed.*, 2008, **47**, 6411–6413.
- 20 (a) C. Zu, T. Zhang, F. Yang, Y. Wu and Y. Wu, *J. Org. Chem.*, 2020, **85**, 12777–12784; (b) S. Pradhan, P. B. De and T. Punniyamurthy, *J. Org. Chem.*, 2017, **82**, 4883–4890; (c) J. Xu, K. Du, J. Shen, C. Shen, K. Chai and P. Zhang, *ChemCatChem*, 2018, **10**, 3675–3679.
- 21 (a) J. Roane and O. Daugulis, *J. Am. Chem. Soc.*, 2016, **138**, 4601–4607; (b) H. Kim and S. Chang, *ACS Catal.*, 2015, **5**, 6665–6669; (c) P. Patel and S. Chang, *Org. Lett.*, 2014, **16**, 3328–3331; (d) K.-H. Ng, Z. Zhou and W.-Y. Yu, *Chem. Commun.*, 2013, **49**, 7031–7033; (e) Y. Xue, Z. Fan, X. Jiang, K. Wu, M. Wang, C. Ding, Q. Yao and A. Zhang, *Eur. J. Org. Chem.*, 2014, **2014**, 7481–7488; (f) K. Wu, Z. Fan, Y. Xue, Q. Yao and A. Zhang, *Org. Lett.*, 2014, **16**, 42–45.
- 22 (a) D. Mondal, S. Biswas, A. Paul and S. Baitalik, *Inorg. Chem.*, 2017, **56**, 7624–7641; (b) A. Klapars, K. R. Campos, J. H. Waldman, D. Zewge, P. G. Dormer and C.-y. Chen, *J. Org. Chem.*, 2008, **73**, 4986–4993.
- 23 (a) P. W. Tan, A. M. Mak, M. B. Sullivan, D. J. Dixon and J. Seayad, *Angew. Chem., Int. Ed.*, 2017, **56**, 16550–16554; (b) T. Yamauchi, F. Shibahara and T. Murai, *Org. Lett.*, 2015, **17**, 5392–5395; (c) K.-X. Tang, C.-M. Wang, T.-H. Gao, C. Pan and L.-P. Sun, *Org. Chem. Front.*, 2017, **4**, 2167–2169; (d) Y.-H. Liu, P.-X. Li, Q.-J. Yao, Z.-Z. Zhang, D.-Y. Huang, M. D. Le, H. Song, L. Liu and B.-F. Shi, *Org. Lett.*, 2019, **21**, 1895–1899; (e) R.-H. Liu, Q.-C. Shan, X.-H. Hu and T.-P. Loh, *Chem. Commun.*, 2019, **55**, 5519–5522; (f) Z.-Z. Zhang, G. Liao, H.-M. Chen and B.-F. Shi, *Org. Lett.*, 2021, **23**, 2626–2631; (g) Z.-J. Cai, C.-X. Liu, Q. Wang, Q. Gu and S.-L. You, *Nat. Commun.*, 2019, **10**, 4168; (h) A. T. Tran and J.-Q. Yu, *Angew. Chem., Int. Ed.*, 2017, **56**, 10530–10534; (i) A. Modi, P. Sau, N. Chakraborty and B. K. Patel, *Adv. Synth. Catal.*, 2019, **361**, 1368–1375; (j) F. Shibahara, Y. Asai and T. Murai, *Asian J. Org. Chem.*, 2018, **7**, 1323–1326; (k) S. R. Yetra, Z. Shen, H. Wang and L. Ackermann, *Beilstein J. Org. Chem.*, 2018, **14**, 1546–1553.
- 24 (a) K. P. Kepp, *Inorg. Chem.*, 2016, **55**, 9461–9470; (b) K. Sandeep, A. Siva Reddy and K. C. Kumara Swamy, *Org. Biomol. Chem.*, 2019, **17**, 6880–6894; (c) S. N. M. Boddapati, R. Tamminana, R. K. Gollapudi, S. Nurbasha, M. E. Assal, O. Alduhaish, M. R. H. Siddiqui, H. B. Bollikolla and S. F. Adil, *Molecules*, 2020, **25**, 1788.
- 25 (a) B. Chen, X.-L. Hou, Y.-X. Li and Y.-D. Wu, *J. Am. Chem. Soc.*, 2011, **133**, 7668–7671; (b) R. J. Phipps and M. J. Gaunt, *Science*, 2009, **323**, 1593–1597; (c) X. Ribas, C. Calle, A. Poater, A. Casitas, L. Gómez, R. Xifra, T. Parella, J. Benet-Buchholz, A. Schweiger, G. Mitrikas, M. Solà, A. Llobet and T. D. P. Stack, *J. Am. Chem. Soc.*, 2010, **132**, 12299–12306; (d) A. E. King, L. M. Huffman, A. Casitas, M. Costas, X. Ribas and S. S. Stahl, *J. Am. Chem. Soc.*, 2010, **132**, 12068–12073.
- 26 X.-G. Liu, H. Gao, S.-S. Zhang, Q. Li and H. Wang, *ACS Catal.*, 2017, **7**, 5078–5086.
- 27 C.-Q. Wang, Y. Zhang and C. Feng, *Angew. Chem., Int. Ed.*, 2017, **56**, 14918–14922.
- 28 J. Yang and G. B. Dudley, *J. Org. Chem.*, 2009, **74**, 7998–8000.
- 29 K. C. Nicolaou, D. G. McGarry, P. K. Somers, C. A. Veale and G. T. Furst, *J. Am. Chem. Soc.*, 1987, **109**, 2504–2506.
- 30 V. Smout, A. Peschiulli, S. Verbeeck, E. A. Mitchell, W. Herrebout, P. Bultinck, C. M. L. Vande Velde, D. Berthelot, L. Meerpoel and B. U. W. Maes, *J. Org. Chem.*, 2013, **78**, 9803–9814.



Overcoming the Deallylation Problem: Palladium(II)-Catalyzed Chemo-, Regio-, and Stereoselective Allylic Oxidation of Aryl Allyl Ether, Amine, and Amino Acids

Kartic Manna, Hasina Mamataj Begam, Krishanu Samanta, and Ranjan Jana*



Cite This: *Org. Lett.* 2020, 22, 7443–7449



Read Online

ACCESS |



Metrics & More

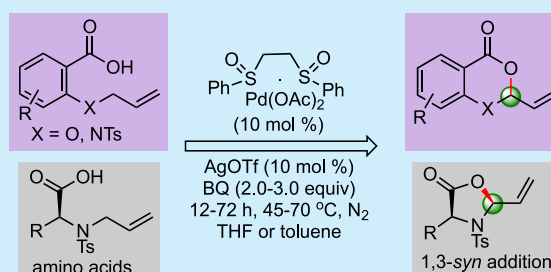


Article Recommendations



Supporting Information

ABSTRACT: We report herein a Pd(II)/bis-sulfoxide-catalyzed intramolecular allylic C–H acetoxylation of aryl allyl ether, amine, and amino acids with the retention of a labile allyl moiety. Mechanistically, the reaction proceeds through a distinct double-bond isomerization from the allylic to the vinylic position followed by intramolecular carboxypalladation and the β -hydride elimination pathway. For the first time, C–H oxidation of *N*-allyl-protected amino acids to furnish five-membered heterocycles through 1,3-syn-addition is established with excellent diastereoselectivity.



- circumvented the deallylation problem
- highly chemo-, regio- and stereoselective
- olefin isomerization/carboxypalladation pathway

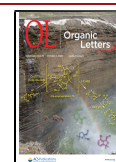
The palladium-catalyzed Tsuji–Trost reaction with activated precursors such as allyl acetate, carbonate, hydroxyl, and halides has been extensively explored for allylic alkylation.¹ In the last decades, the direct allylic C–H functionalization of simple alkenes with the retention of a double bond for further synthetic manipulations has streamlined this transformation.² Mechanistically, the crucial π -allyl Pd complex is formed through concerted metalation deprotonation (CMD) or concerted proton and two-electron transfer for a subsequent cross-coupling reaction.³ Because of their intriguing mechanistic aspects, other metals such as iridium,⁴ rhodium,⁵ and copper⁶ and transition-metal-free approaches such as the catalytic heteroene reaction using a chalcogen oxidant⁷ and the sodium amide-catalyzed generation of nucleophilic allyl species⁸ have been explored. Still, the development of a highly chemo-, regio-, and stereoselective allylic C–H bond functionalization is a formidable challenge. In this vein, the White group has made a significant contribution to inter- and intramolecular allylic C–H functionalization by employing a Pd(II)/sulfoxide-benzoquinone serial ligand catalyst.⁹ Subsequently, sulfoxide-oxazoline,¹⁰ phosphoric acid,¹¹ phosphoramidite,¹² 4,5-diazfluoren-9-one,¹³ and even dimethyl sulfoxide¹⁴ were proved to be effective ligands for allylic C–H functionalization.

Conventionally, an allyl moiety attached to a heteroatom such as oxygen or nitrogen undergoes deallylation under palladium catalysis due to facile oxidative addition to the C–O or C–N bond or hydrolytic cleavage (Scheme 1a).¹⁵ Hence, it has been explored for the chemoselective deprotection of complex molecules,¹⁶ fluorogenic probes,¹⁷ prodrug activation,¹⁸ and allyl transfer.¹⁹ Therefore, allylic functionalization

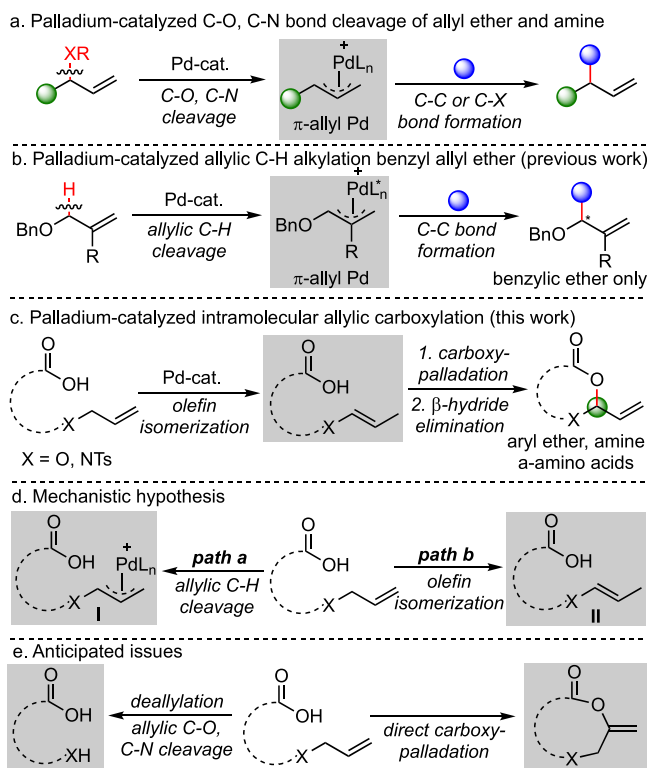
with the retention of this leaving group is extremely rare.²⁰ Recently, the Gong group reported an intermolecular asymmetric allylic C–H functionalization of benzyl allyl ether only (Scheme 1b).²¹ However, the palladium-catalyzed extremely labile allylic C–H functionalization of phenolic, aniline, or aliphatic amines is unknown. Furthermore, the underlying mechanism of allylic C–H functionalization is highly ambiguous due to the competitive allylic C–H bond cleavage/ π -allyl Pd complex formation versus olefin isomerization/nucleopalladation/ β -hydride elimination pathways (Scheme 2d).²² However, the latter olefin isomerization relay is extremely fascinating for the site-selective remote functionalization.²³ For the first time, we have disclosed a Pd(II)/bis-sulfoxide-catalyzed intramolecular allylic C–H acetoxylation of salicylic and anthranilic acid derivatives with the retention of an extremely labile allyl group, which proceeds through the allylic to vinylic olefin isomerization/carboxypalladation/ β -hydride elimination pathway (Scheme 1c). Remarkably, a highly diastereoselective intramolecular cyclization of *N*-allyl-protected amino acids through 1,3-syn-addition is also unveiled. The oxidation takes place chemo-, regio-, and stereoselectively at the allylic α -proton to furnish six- or five-

Received: July 24, 2020

Published: September 21, 2020

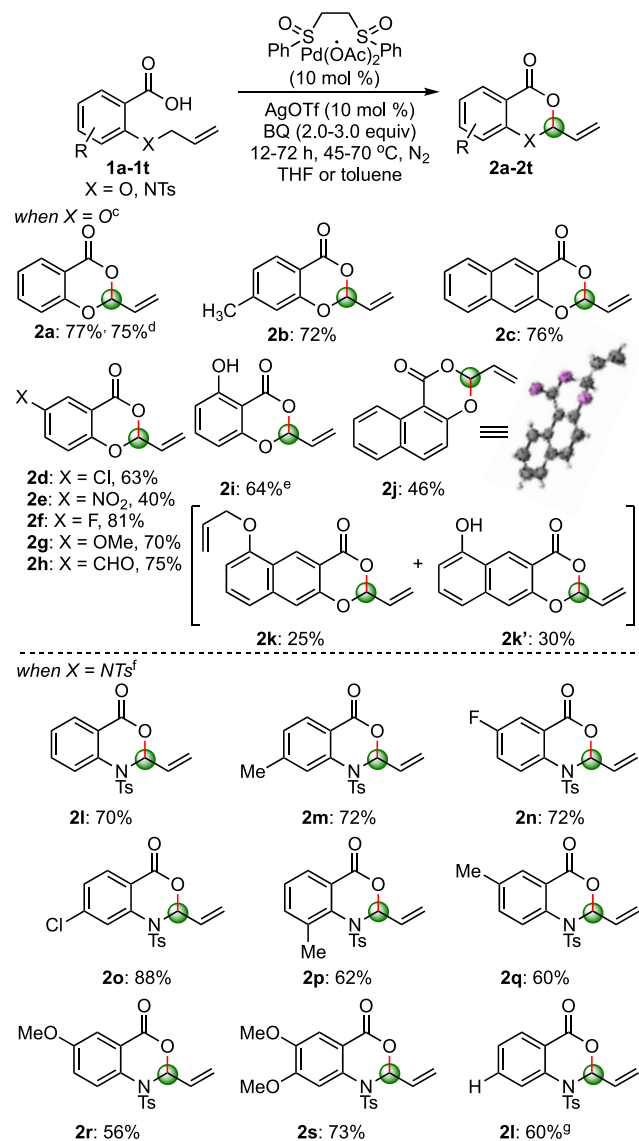


Scheme 1. Palladium-Catalyzed Functionalization of Allylic Ether and Amines



member rings obviating deallylation or direct carboxypalladation pathways (Scheme 1e).

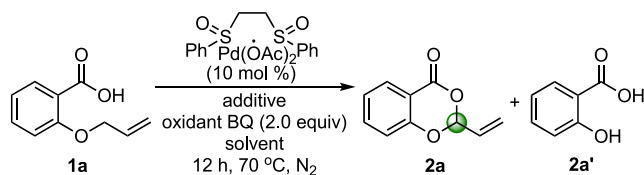
To optimize the reaction conditions, a mixture of 2-(allyloxy)benzoic acid **1a**, Pd(OAc)₂ (10 mol %) as the catalyst, and Ag₂CO₃ (2 equiv) as the oxidant was heated in 1,4-dioxane solvent at 120 °C under a N₂ atmosphere. Gratifyingly, we isolated the desired oxinone product, **2a**, in 20% yield after 24 h (entry 1, Table 1). Next, we examined various Pd catalysts such as PdCl₂, Pd(TFA)₂, Pd-(CH₃CN)₂Cl₂, Pd(PPh₃)₄, Pd₂(dba)₃, and so on. However, the yield of the desired product was not improved, and the deallylation product via the C–O bond cleavage was formed. Subsequently, using various oxidizing agents, for example, Ag₂O, K₂S₂O₈, PIDA, BQ, and so on, did not improve the yield of the desired product. (For details, see the Supporting Information.) Interestingly, we observed that in the presence of Pd(OAc)₂, using AgOTf as a Lewis acid and BQ as an oxidant, the yield of the desired product was increased to 29% at 70 °C along with the deallylation product (35%) (entry 2, Table 1). Other additives such as NaOTf, DIPEA, B(C₆F₅)₃, (BuO)₂PO₂H, TsOH, and TfOH were proved to be inferior to AgOTf, predominantly providing the deallylation product. Among various solvents such as DCM, toluene, DCE, and so on, THF provided the best results in 30% yield of desired product along with deallylation (entry 3, Table 1). Commonly used ligands in allylic C–H activation, such as 2,2'-bipyridine, diazafluorenone (entry 5, Table 1), 1,10-phenanthroline (entry 6, Table 1), and so on were ineffective in this case. The White group has shown that bis-sulfoxide/benzoquinone (BQ) serial ligands on palladium efficiently render allylic C–H oxidation.^{9c,f} Gratifyingly, the formation of the deallylation product was completely suppressed using the catalytic Pd(II)acetate/bis-sulfoxide complex (White catalyst, cat. 1), silver triflate,

Scheme 2. Substrate Scope of Aromatic Acid Derivatives^{a,b}

^aReactions were carried out on a 0.2 mmol scale. ^bYields refer to the average of isolated yields of two experiments. ^cReaction time 12 h. ^d1.0 mmol scale reaction. ^eDiallylated substrate. ^f3.0 equiv of BQ, 45 °C, 72 h. ^gDebromination at the four-position.

and benzoquinone (2 equiv), providing the desired product in 82% yield in THF (entry 8, Table 1).

Subsequently, we explored the substrate scope under the optimized reaction conditions. Electron-donating substituents such as methyl (**2b**, Scheme 2) and methoxy (**2g**, Scheme 2) furnished the oxinone product in high yields. Electron-withdrawing groups such as nitro (**2e**, Scheme 2) also furnished the desired product in moderate yield. Halogens such as chloro (**2d**, Scheme 2) and fluoro (**2f**, Scheme 2) remained intact under the reaction conditions, furnishing excellent yields. Interestingly, aldehyde functionality (**2h**, Scheme 2) was well-tolerated under these mild conditions. We observed a proximity effect on deallylation versus C–H oxidation reaction. When 2,6-diallyloxy-benzoic acid was subjected to the reaction conditions, a monodeallylated product was obtained in good yield (**2i**). Furthermore, 2,8-allyloxy-2-naphthoic acid (**1k**) furnished a mixture of 8-allyloxy

Table 1. Optimization of the Reaction Conditions^a

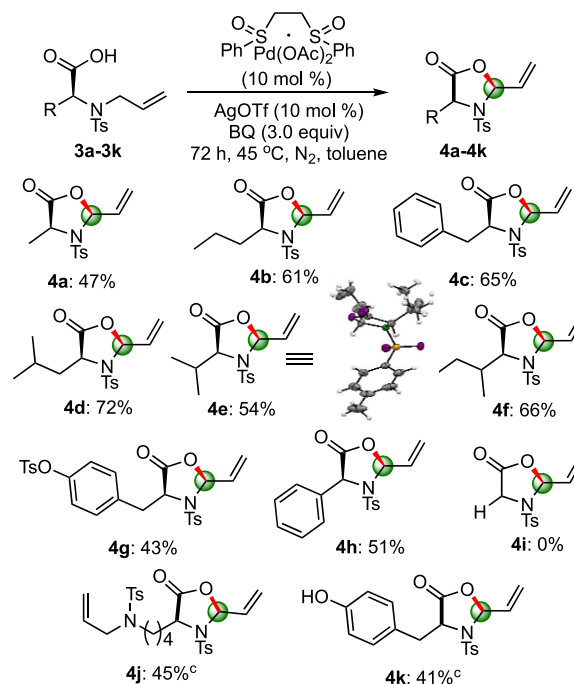
| entry | catalyst | additive | solvent | yield (%) | 2a/2a' |
|------------------|----------------------|--------------|-------------|-----------|--------------|
| 1 ^b | Pd(OAc) ₂ | | 1,4-dioxane | 30 | 20/10 |
| 2 ^c | Pd(OAc) ₂ | AgOTf | 1,4-dioxane | 89 | 29/35 |
| 3 ^c | Pd(OAc) ₂ | AgOTf | THF | 90 | 30/60 |
| 4 ^c | Pd(TFA) ₂ | AgOTf | THF | 81 | 15/44 |
| 5 ^{c,d} | Pd(OAc) ₂ | AgOTf | THF | 68 | 07/42 |
| 6 ^{c,e} | Pd(OAc) ₂ | AgOTf | THF | 63 | 08/39 |
| 7 ^{c,f} | Pd(OAc) ₂ | AgOTf | THF | 66 | 17/35 |
| 8 | 1 | AgOTf | THF | 82 | 82/00 |
| 9 | 1 | AgOTf | toluene | 54 | 54/00 |
| 10 | 1 | AgOTf | DCM | 54 | 47/07 |
| 11 | 1 | NaOTf | THF | 10 | 00/10 |
| 12 | 1 | DIPEA | THF | 12 | 00/12 |

^aAll reactions were carried out on a 0.2 mmol scale. ^b2 equiv of Ag₂CO₃ was used as the oxidant, and the reaction was run at 120 °C for 24 h. ^cRemaining yield was the saturated analogue of **2a** (**2a'**). ^d10 mol % DAF was used. ^e10 mol % 1,10-Phen was used. ^f20 mol % DMSO was used.

(**2k**) and 8-hydroxy (**2k'**) oxinone. However, 3-(allyloxy)-2-naphthoic acid (**1c**) and 2-(allyloxy)-1-naphthoic acid (**1j**) provided the corresponding oxinone in high to moderate yield, and the products were unambiguously characterized by X-ray crystallography (**2j**; CCDC 2009840).

Next, we were motivated to examine the feasibility of the allylic C–H oxidation of *N*-allyl anthranilic acids. We observed the prominent role of the protecting group of the *N*-allyl moiety on the reaction outcome, where free or allyl, methyl, and –Boc groups were unsuccessful. We assumed that the *N*-center should be comparably electronegative to the oxygen atom to effect an α -C–H bond cleavage. As anticipated, the corresponding –NTs (**11**) furnished the desired product in 46% yield under the previously optimized reaction conditions. Furthermore, after stirring the reaction mixture for 72 h at 45 °C in toluene using 3.0 equiv of BQ, the yield was increased to 70%. Under these optimized conditions, a wide range of anthranilic acid derivatives underwent intramolecular allylic C–H oxidation to provide the corresponding oxazinones (**2l**–**2s**). Although fluoro- (**2n**) and chloro- (**2o**) substituents were intact, bromo- was dehalogenated under the reaction conditions, presumably via the oxidative addition of the *in situ*-generated Pd(0).

Finally, we have explored a novel stereoselective allylic C–H oxidation of *N*-allyl amino acids to access 2-vinylloxazolidin-5-one derivatives. Hence, an enantiomerically pure *N*-allyl, *N*-tosyl substrate **3a** was prepared from (*S*)-alanine and subjected to the reaction condition to afford the cyclized product in 47% yield.²⁴ Subsequently, a series of substrates from natural and unnatural amino acids were synthesized and examined under the optimized conditions to provide the corresponding 2-vinylloxazolidin-5-one in moderate to high yields with high (>20:1) diastereoselectivity (Scheme 3). From the X-ray crystal structure analysis (**4e**; CCDC 2009842), it was observed that the newly formed C–O bond is syn to the α -carboxylic acid, exclusively providing *S,S*-isomer. It was also

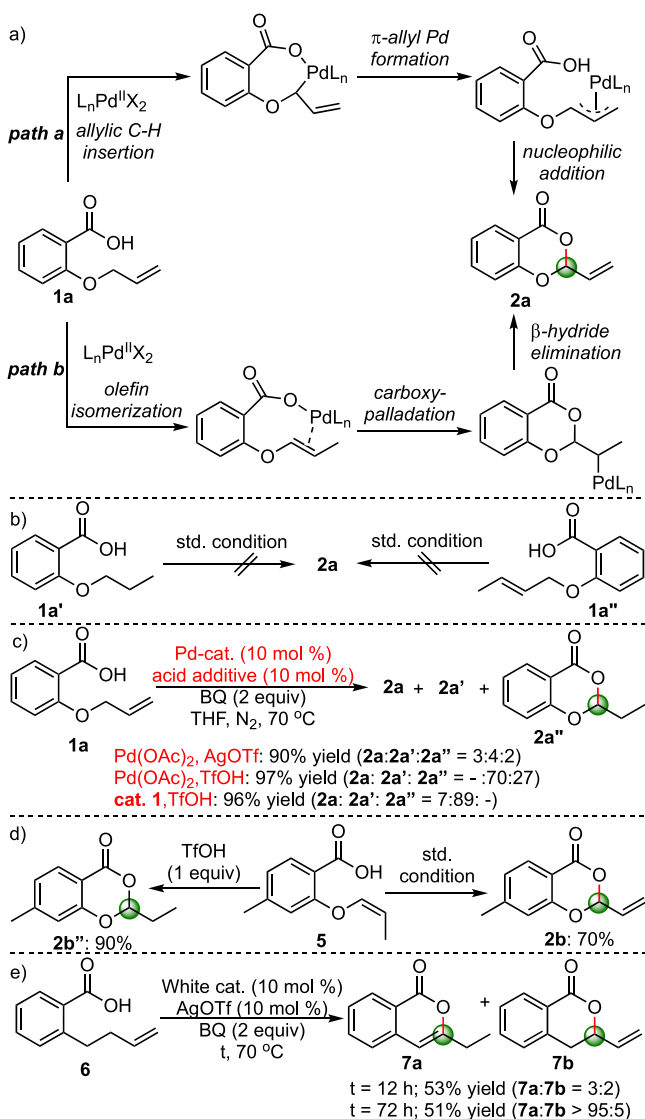
Scheme 3. Substrate Scope of Amino Acids^{a,b}

^aAll reactions were carried out on a 0.2 mmol scale. ^bYields refer to the average of isolated yields of at least two experiments. ^cStarted from a racemic substrate; enantiomer with syn (*S,S* or *R,R*) product formed.

observed that because of steric hindrance, the isopropyl group exhibits an anisotropic effect in the solid state. A 1:1 diastereoisomeric mixture of compound **4f** was obtained from the corresponding 1:1 diastereoisomeric starting material **3f**. Furthermore, racemic **3j** and **3k** provided the corresponding cyclized products in racemic mixtures. However, no product is formed in the absence of any substitution at the α -position (**4i**). Likewise, the yield of the desired product increases with the increase in steric bulk at the α -substitution, for example, methyl, propyl, benzyl, and isobutyl (**4a**, **4b**, **4c**, **4d**, Scheme 3) and valine versus isoleucine (**4e**, **4f**). For the lysine substrate bearing two *N*-allyl groups at α - and ϵ -carbon, C–H cleavage selectively took place at the α -*N*-allyl moiety (**4j**). Whereas *L*-(*S*) amino acid derivatives exclusively provided the (*S,S*) product, the racemic substrates (*R/S*) provided exclusive *R,R* and *S,S* (**4j**, **4k**) stereochemistry, indicating the highly diastereoselective syn addition of the pendant carboxylic acid.

As hypothesized, the reaction may proceed through two distinct mechanistic pathways. In **path a**, a palladium-catalyzed allylic C–H bond cleavage to generate a π -allyl Pd species followed by the intramolecular nucleophilic addition of carboxylic acid to furnish the desired product is plausible. Alternatively, a palladium-catalyzed double-bond isomerization from the allylic to the vinylic position followed by carboxypalladation and β -hydride elimination may also lead to the desired product (Scheme 4a). From control studies, we observed that the reaction with a saturated analogue **1a'** or with an internal olefin **1a''** did not furnish any desired product (Scheme 4b). Interestingly, a mixture of desired product **2a**, deallylation product **2a'**, and saturated analogue **2a''** was obtained under both Lewis acid and Bronsted acid conditions using Pd(OAc)₂ in lieu of **cat. 1** (Scheme 4c). This saturated

Scheme 4. Mechanistic Possibilities and Control Experiments

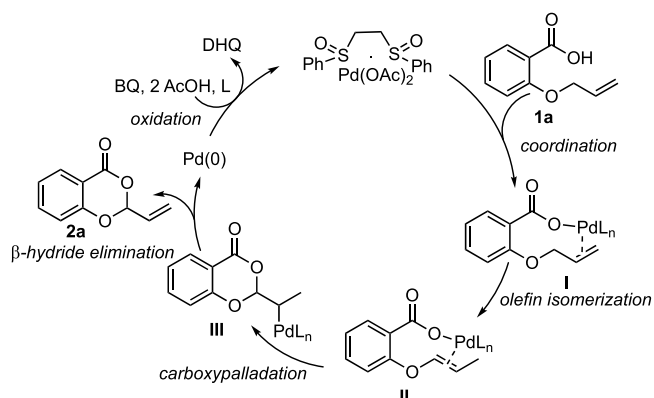


analogue may form either through protodemetalation of the incipient alkyl-palladium species, which is formed through carboxypalladation, or through acid-catalyzed carboxylation of vinylic ether. However, the reaction in the presence of triflic acid predominantly led to the formation of the deallylation product. This could be attributed to the unavailability of the carboxylate anion for nucleophilic addition due to the protonation under a strong acidic medium. Hence, deleterious palladium-catalyzed C–O bond activation may take place. To probe the olefin isomerization pathway, a vinylic ether **5** was separately prepared and subjected to the reaction conditions, furnishing 70% of the desired product (Scheme 4d). From the kinetic studies with allylic (**1b**) and vinylic substrates (**5**), it was observed that the reaction proceeds at a faster rate in the initial stage with **5** compared with **1b** and at a similar rate in the later stage. (For details, see the SI.) Thus palladium-catalyzed olefin isomerization could be the slow step; subsequently, carboxypalladation/ β -hydride elimination provides the desired product. The propensity of olefin isomerization under the reaction conditions was further probed using a homoallylic carbon analogue **6**. When **6** was subjected to the

reaction conditions, a mixture of 3-ethyl-1H-isochroman-1-one, **7a**, and 3-vinylisochroman-1-one, **7b**, was obtained after 12 h. However, stirring the reaction mixture for 72 h led to the formation of the thermodynamically more stable **7a** exclusively through double-bond isomerization (Scheme 4e). In contrast with the previous report, we demonstrate here that Pd(II)/bis-sulfoxide/benzoquinone prefers a double-bond isomerization/nucleopalladation pathway for allylic ether or amine substrates.^{22b}

From our control experiments, we propose that initially, a palladium complex is localized to the carboxylate site, and a palladium-assisted double-bond isomerization from the allylic to the vinylic position takes place to generate intermediate **II** (Scheme 5). Subsequently, intramolecular carboxypalladation

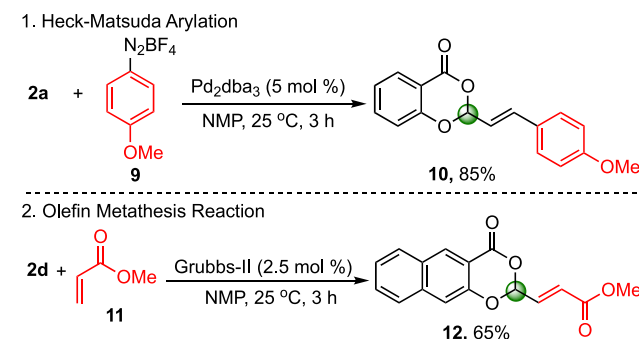
Scheme 5. Plausible Catalytic Cycle for Allylic Oxidation



to form **III** followed by β -hydride elimination furnishes the desired product (Scheme 5). Finally, Pd(0) is oxidized to Pd(II) by benzoquinone to complete the catalytic cycle.

The product was further functionalized to demonstrate the utility of the terminal double bond (Scheme 6). A Heck–

Scheme 6. Product Derivatization



Matsuda reaction of **2a** with diazonium salt **9** afforded the corresponding arylation product in 85% yield. Furthermore, a cross-olefin metathesis reaction with methyl acrylate **11** using Grubb's II catalyst afforded the metathesis product in 65% yield.

In conclusion, we have developed a palladium-catalyzed highly chemo-, regio-, and stereoselective allylic C–H oxidation of allyl ether, amine, and amino acids. A conventional palladium-catalyzed deallylation problem through C–O/C–N bond cleavage is overcome and tuned toward allylic C–H bond oxidation. Moreover, competitive π -allyl Pd formation via allylic C–H bond cleavage versus olefin isomerization/

carboxypalladation has been elucidated to probe whether the latter pathway is operative. Remarkably, a highly stereoselective 1,3-syn-addition is established for the C–H oxidation of *N*-allyl-protected amino acids. We anticipate that the present transformation and mechanistic insight will be helpful for further research.

■ ASSOCIATED CONTENT

SI Supporting Information

The Supporting Information is available free of charge at <https://pubs.acs.org/doi/10.1021/acs.orglett.0c02465>.

Experimental procedures, spectroscopic data, ¹H and ¹³C NMR spectra for all synthesized compounds (PDF)

Accession Codes

CCDC 2009840 and 2009842 contain the supplementary crystallographic data for this paper. These data can be obtained free of charge via www.ccdc.cam.ac.uk/data_request/cif, or by emailing data_request@ccdc.cam.ac.uk, or by contacting The Cambridge Crystallographic Data Centre, 12 Union Road, Cambridge CB2 1EZ, UK; fax: +44 1223 336033.

■ AUTHOR INFORMATION

Corresponding Author

Ranjan Jana – Organic and Medicinal Chemistry Division, CSIR-Indian Institute of Chemical Biology, Kolkata 700032, West Bengal, India; Academy of Scientific and Innovative Research (AcSIR), Ghaziabad 201002, Uttar Pradesh, India; orcid.org/0000-0002-5473-0258; Email: rjana@iicb.res.in

Authors

Kartic Manna – Organic and Medicinal Chemistry Division, CSIR-Indian Institute of Chemical Biology, Kolkata 700032, West Bengal, India; Academy of Scientific and Innovative Research (AcSIR), Ghaziabad 201002, Uttar Pradesh, India
Hasina Mamataj Begam – Organic and Medicinal Chemistry Division, CSIR-Indian Institute of Chemical Biology, Kolkata 700032, West Bengal, India
Krishanu Samanta – Organic and Medicinal Chemistry Division, CSIR-Indian Institute of Chemical Biology, Kolkata 700032, West Bengal, India; Academy of Scientific and Innovative Research (AcSIR), Ghaziabad 201002, Uttar Pradesh, India

Complete contact information is available at: <https://pubs.acs.org/doi/10.1021/acs.orglett.0c02465>

Notes

The authors declare no competing financial interest.

■ ACKNOWLEDGMENTS

This work was supported by DST, SERB, Govt. of India, core research grant no. EMR/2014/000469 and Ramanujan fellowship, award no. SR/S2/RJN-97/2012. K.M., H.M.B., and K.S. thank CSIR and UGC for their fellowships.

■ REFERENCES

(1) For reviews, see: (a) James, J.; Jackson, M.; Guiry, P. J. Palladium-Catalyzed Decarboxylative Asymmetric Allylic Alkylation: Development, Mechanistic Understanding and Recent Advances. *Adv. Synth. Catal.* **2019**, *361*, 3016–3049. (b) Weaver, J. D.; Recio, A.; Grenning, A. J.; Tunge, J. A. Transition Metal-Catalyzed Decarboxylative Allylation and Benzoylation Reactions. *Chem. Rev.* **2011**, *111*,

1846–1913. (c) Trost, B. M.; Machacek, M. R.; Aponick, A. Predicting the Stereochemistry of Diphenylphosphino Benzoic Acid (DPPBA)-Based Palladium-Catalyzed Asymmetric Allylic Alkylation Reactions: A Working Model. *Acc. Chem. Res.* **2006**, *39*, 747–760. (d) Trost, B. M.; Crawley, M. L. Asymmetric Transition-Metal-Catalyzed Allylic Alkylations: Applications in Total Synthesis. *Chem. Rev.* **2003**, *103*, 2921–2944. (e) Trost, B. M.; Van Vranken, D. L. Asymmetric Transition Metal-Catalyzed Allylic Alkylations. *Chem. Rev.* **1996**, *96*, 395–422.

(2) For reviews, see: (a) Fernandes, R. A.; Nallasivam, J. L. Catalytic allylic functionalization via π -allyl palladium chemistry. *Org. Biomol. Chem.* **2019**, *17* (38), 8647–8672. (b) Lorion, M. M.; Obler, J.; Poli, G. Palladium catalyzed oxidative aminations and oxylation: where are we? *Pure Appl. Chem.* **2016**, *88* (4), 381–389. (c) Liron, F.; Obler, J.; Lorion, M. M.; Poli, G. Direct Allylic Functionalization Through Pd-Catalyzed C–H Activation. *Eur. J. Org. Chem.* **2014**, *2014* (27), 5863–5883. (d) Davies, H. M. L.; Nikolai, J. Catalytic and enantioselective allylic C–H activation with donor-acceptor-substituted carbenoids. *Org. Biomol. Chem.* **2005**, *3* (23), 4176–4187. For seminal work, see: (e) Kitching, W.; Rappoport, Z.; Winstein, S.; Young, W. G. Allylic Oxidation of Olefins by Palladium Acetate. *J. Am. Chem. Soc.* **1966**, *88*, 2054–2055. (f) Chen, M. S.; White, M. C. A Sulfoxide-Promoted, Catalytic Method for the Regioselective Synthesis of Allylic Acetates from Monosubstituted Olefins via C–H Oxidation. *J. Am. Chem. Soc.* **2004**, *126*, 1346–1347. (g) Lin, S.; Song, C.-X.; Cai, G.-X.; Wang, W.-H.; Shi, Z.-J. Intra/Intermolecular Direct Allylic Alkylation via Pd(II)-Catalyzed Allylic C–H Activation. *J. Am. Chem. Soc.* **2008**, *130*, 12901–12903.

(3) Engelin, C.; Jensen, T.; Rodriguez-Rodriguez, S.; Fristrup, P. Mechanistic Investigation of Palladium-Catalyzed Allylic C–H Activation. *ACS Catal.* **2013**, *3*, 294–302.

(4) (a) Lei, H.; Rovis, T. Ir-Catalyzed Intermolecular Branch-Selective Allylic C–H Amidation of Unactivated Terminal Olefins. *J. Am. Chem. Soc.* **2019**, *141*, 2268–2273. (b) Knecht, T.; Mondal, S.; Ye, J.-H.; Das, M.; Glorius, F. Intermolecular, Branch-Selective, and Redox-Neutral Cp*Ir(III)-Catalyzed Allylic C–H Amidation. *Angew. Chem., Int. Ed.* **2019**, *58*, 7117–7121. (c) Wang, Z.; He, Z.; Zhang, L.; Huang, Y. Iridium-Catalyzed Aerobic α , β -Dehydrogenation of γ,δ -Unsaturated Amides and Acids: Activation of Both α - and β -C–H bonds through an Allyl-Iridium Intermediate. *J. Am. Chem. Soc.* **2018**, *140*, 735–740. (d) Sharma, A.; Hartwig, J. F. Enantioselective Functionalization of Allylic C–H Bonds Following a Strategy of Functionalization and Diversification. *J. Am. Chem. Soc.* **2013**, *135*, 17983–17989.

(5) (a) Harris, R. J.; Park, J.; Nelson, T. A. F.; Iqbal, N.; Salgueiro, D. C.; Bacsá, J.; MacBeth, C. E.; Baik, M.-H.; Blakey, S. B. The Mechanism of Rhodium-Catalyzed Allylic C–H Amination. *J. Am. Chem. Soc.* **2020**, *142*, 5842–5851. (b) Archambeau, A.; Rovis, T. Rhodium(III)-Catalyzed Allylic C(sp³)-H Activation of Alkenyl Sulfonamides: Unexpected Formation of Azabicycles. *Angew. Chem., Int. Ed.* **2015**, *54*, 13337–13340. (c) Li, Q.; Yu, Z.-X. Conjugated Diene-Assisted Allylic C–H Bond Activation: Cationic Rh(I)-Catalyzed Syntheses of Polysubstituted Tetrahydropyrroles, Tetrahydrofurans, and Cyclopentanes from Ene-2-Dienes. *J. Am. Chem. Soc.* **2010**, *132*, 4542–4543. (d) Li, Q.; Yu, Z.-X. Enantioselective Rhodium-Catalyzed Allylic C–H Activation for the Addition to Conjugated Dienes. *Angew. Chem., Int. Ed.* **2011**, *50*, 2144–2147.

(6) (a) Li, J.; Zhang, Z.; Wu, L.; Zhang, W.; Chen, P.; Lin, Z.; Liu, G. Site-specific allylic C–H bond functionalization with a copper-bound N-centred radical. *Nature* **2019**, *574*, 516–521. (b) Qin, L.; Sharique, M.; Tambar, U. K. Controllable, Sequential, and Stereoselective C–H Allylic Alkylation of Alkenes. *J. Am. Chem. Soc.* **2019**, *141*, 17305–17313. (c) Xu, J.; Fu, Y.; Luo, D.-F.; Jiang, Y.-Y.; Xiao, B.; Liu, Z.-J.; Gong, T.-J.; Liu, L. Copper-Catalyzed Trifluoromethylation of Terminal Alkenes through Allylic C–H Bond Activation. *J. Am. Chem. Soc.* **2011**, *133*, 15300–15303.

(7) (a) Bayeh, L.; Le, P. Q.; Tambar, U. K. Catalytic allylic oxidation of internal alkenes to a multifunctional chiral building block. *Nature* **2017**, *547*, 196–200. (b) Bayeh, L.; Tambar, U. K. Catalytic

Asymmetric Intermolecular Allylic Functionalization of Unactivated Internal Alkenes. *ACS Catal.* **2017**, *7*, 8533–8543.

(8) Bao, W.; Kossen, H.; Schneider, U. Formal Allylic C(sp³)-H Bond Activation of Alkenes Triggered by a Sodium Amide. *J. Am. Chem. Soc.* **2017**, *139*, 4362–4365.

(9) For selected examples, see: (a) Ammann, S. E.; Rice, G. T.; White, M. C. Terminal Olefins to Chromans, Isochromans, and Pyrans via Allylic C–H Oxidation. *J. Am. Chem. Soc.* **2014**, *136*, 10834–10837. (b) Osberger, T. J.; White, M. C. N-Boc Amines to Oxazolidinones via Pd(II)/Bis-sulfoxide/Bronsted Acid Co-Catalyzed Allylic C–H Oxidation. *J. Am. Chem. Soc.* **2014**, *136*, 11176–11181. (c) Young, A. J.; White, M. C. Allylic C–H Alkylation of Unactivated α -Olefins: Serial Ligand Catalysis Resumed. *Angew. Chem., Int. Ed.* **2011**, *50*, 6824–6827. (d) Rice, G. T.; White, M. C. Allylic C–H Amination for the Preparation of syn-1,3-Amino Alcohol Motifs. *J. Am. Chem. Soc.* **2009**, *131*, 11707–11711. (e) Fraunhoffer, K. J.; Prabakaran, N.; Sirois, L. E.; White, M. C. Macrolactonization via Hydrocarbon Oxidation. *J. Am. Chem. Soc.* **2006**, *128*, 9032–9033. (f) Chen, M. S.; Prabakaran, N.; Labenz, N. A.; White, M. C. Serial Ligand Catalysis: A Highly Selective Allylic C–H Oxidation. *J. Am. Chem. Soc.* **2005**, *127*, 6970–6971.

(10) (a) Ma, R.; Young, J.; Promontorio, R.; Dannheim, F. M.; Pattillo, C. C.; White, M. C. Synthesis of anti-1,3 Amino Alcohol Motifs via Pd(II)/SOX Catalysis with the Capacity for Stereodivergence. *J. Am. Chem. Soc.* **2019**, *141*, 9468–9473. (b) Liu, W.; Ali, S. Z.; Ammann, S. E.; White, M. C. Asymmetric Allylic C–H Alkylation via Palladium(II)/cis-ArSOX Catalysis. *J. Am. Chem. Soc.* **2018**, *140*, 10658–10662. (c) Ma, R.; White, M. C. C–H to C–N Cross-Coupling of Sulfonamides with Olefins. *J. Am. Chem. Soc.* **2018**, *140*, 3202–3205. (d) Ammann, S. E.; Liu, W.; White, M. C. Enantioselective Allylic C–H Oxidation of Terminal Olefins to Isochromans by Palladium(II)/Chiral Sulfoxide Catalysis. *Angew. Chem., Int. Ed.* **2016**, *55*, 9571–9575. (e) Kondo, H.; Yu, F.; Yamaguchi, J.; Liu, G.; Itami, K. Branch-Selective Allylic C–H Carboxylation of Terminal Alkenes by Pd/sox Catalyst. *Org. Lett.* **2014**, *16*, 4212–4215.

(11) (a) Ye, L.; Tian, Y.; Meng, X.; Gu, Q.-S.; Liu, X.-Y. Enantioselective Copper(I)/Chiral Phosphoric Acid Catalyzed Intramolecular Amination of Allylic and Benzylic C–H Bonds. *Angew. Chem., Int. Ed.* **2020**, *59*, 1129–1133. (b) Lin, H.-C.; Wang, P.-S.; Tao, Z.-L.; Chen, Y.-G.; Han, Z.-Y.; Gong, L.-Z. Highly Enantioselective Allylic C–H Alkylation of Terminal Olefins with Pyrazol-5-ones Enabled by Cooperative Catalysis of Palladium Complex and Bronsted Acid. *J. Am. Chem. Soc.* **2016**, *138*, 14354–14361. (c) Wang, P.-S.; Lin, H.-C.; Zhai, Y.-J.; Han, Z.-Y.; Gong, L.-Z. Chiral Counteranion Strategy for Asymmetric Oxidative C(sp³)-H/C(sp³)-H Coupling: Enantioselective α -Allylation of Aldehydes with Terminal Alkenes. *Angew. Chem., Int. Ed.* **2014**, *53*, 12218–12221. (d) Chai, Z.; Rainey, T. J. Pd(II)/Bronsted Acid Catalyzed Enantioselective Allylic C–H Activation for the Synthesis of Spirocyclic Rings. *J. Am. Chem. Soc.* **2012**, *134*, 3615–3618.

(12) (a) Lin, H.-C.; Xie, P.-P.; Dai, Z.-Y.; Zhang, S.-Q.; Wang, P.-S.; Chen, Y.-G.; Wang, T.-C.; Hong, X.; Gong, L.-Z. Nucleophile-Dependent Z/E- and Regioselectivity in the Palladium-Catalyzed Asymmetric Allylic C–H Alkylation of 1,4-Dienes. *J. Am. Chem. Soc.* **2019**, *141*, 5824–5834. (b) Wang, P.-S.; Shen, M.-L.; Wang, T.-C.; Lin, H.-C.; Gong, L.-Z. Access to Chiral Hydropyrimidines through Palladium-Catalyzed Asymmetric Allylic C–H Amination. *Angew. Chem., Int. Ed.* **2017**, *56*, 16032–16036. (c) Wang, P.-S.; Liu, P.; Zhai, Y.-J.; Lin, H.-C.; Han, Z.-Y.; Gong, L.-Z. Asymmetric Allylic C–H Oxidation for the Synthesis of Chromans. *J. Am. Chem. Soc.* **2015**, *137*, 12732–12735. (d) Trost, B. M.; Thaisrivongs, D. A.; Donckele, E. J. Palladium-Catalyzed Enantioselective Allylic Alkylations through C–H Activation. *Angew. Chem., Int. Ed.* **2013**, *52*, 1523–1526. (e) Liu, W.-B.; Zheng, C.; Zhuo, C.-X.; Dai, L.-X.; You, S.-L. Iridium-Catalyzed Allylic Alkylation Reaction with N-Aryl Phosphoramidite Ligands: Scope and Mechanistic Studies. *J. Am. Chem. Soc.* **2012**, *134*, 4812–4821.

(13) (a) Jaworski, J. N.; Kozack, C. V.; Tereniak, S. J.; Knapp, S. M. M.; Landis, C. R.; Miller, J. T.; Stahl, S. S. Operando Spectroscopic and Kinetic Characterization of Aerobic Allylic C–H Acetoxylation Catalyzed by Pd(OAc)₂/4,5-Diazafluoren-9-one. *J. Am. Chem. Soc.* **2019**, *141*, 10462–10474. (b) Sharma, A.; Hartwig, J. F. Enantioselective Functionalization of Allylic C–H Bonds Following a Strategy of Functionalization and Diversification. *J. Am. Chem. Soc.* **2013**, *135*, 17983–17989.

(14) For reviews, see: (a) Sipos, G.; Drinkel, E. E.; Dorta, R. The emergence of sulfoxides as efficient ligands in transition metal catalysis. *Chem. Soc. Rev.* **2015**, *44*, 3834–3860. For selected examples, see: (b) Vemula, S. R.; Kumar, D.; Cook, G. R. Palladium-Catalyzed Allylic Amidation with N-Heterocycles via sp³ C–H Oxidation. *ACS Catal.* **2016**, *6*, 5295–5301. (c) Covell, D. J.; Vermeulen, N. A.; Labenz, N. A.; White, M. C. Polyol Synthesis through Hydrocarbon Oxidation: De Novo Synthesis of L-Galactose. *Angew. Chem., Int. Ed.* **2006**, *45*, 8217–8220. (d) Chen, M. S.; White, M. C. A Sulfoxide-Promoted, Catalytic Method for the Regioselective Synthesis of Allylic Acetates from Monosubstituted Olefins via C–H Oxidation. *J. Am. Chem. Soc.* **2004**, *126*, 1346–1347. (e) Chen, M. S.; White, M. C. A Sulfoxide-Promoted, Catalytic Method for the Regioselective Synthesis of Allylic Acetates from Monosubstituted Olefins via C–H Oxidation. *J. Am. Chem. Soc.* **2004**, *126*, 1346–1347.

(15) For Pd-catalyzed deallylation, see: (a) Mao, Y.; Liu, Y.; Hu, Y.; Wang, L.; Zhang, S.; Wang, W. Pd-Catalyzed Debenzylation and Deallylation of Ethers and Esters with Sodium Hydride. *ACS Catal.* **2018**, *8*, 3016–3020. (b) Ohmura, N.; Nakamura, A.; Hamasaki, A.; Tokunaga, M. Hydrolytic Deallylation of N-Allyl Amides Catalyzed by Pd^{II} Complexes. *Eur. J. Org. Chem.* **2008**, *2008*, 5042–5045. (c) Garro-Helion, F.; Merzouk, A.; Guibe, F. Mild and selective palladium(0)-catalyzed deallylation of allylic amines. Allylamine and diallylamine as very convenient ammonia equivalents for the synthesis of primary amines. *J. Org. Chem.* **1993**, *58*, 6109–6113. (d) Yamada, T.; Goto, K.; Mitsuda, Y.; Tsuji, J. O-allyl ether as a new protective group for oximes and its palladium-catalyzed deprotection. *Tetrahedron Lett.* **1987**, *28*, 4557–4560.

(16) (a) Liu, Z.; Meng, Y.; Yuan, P.; Wang, Z.; Gao, J.-M.; Zheng, H. Total Synthesis of Caesalpinnone. *Org. Lett.* **2020**, *22*, 520–522. (b) Leeder, A. J.; Heap, R. J.; Brown, L. J.; Franck, X.; Brown, R. C. D. A Short Diastereoselective Total Synthesis of (\pm)-Vibrallactone. *Org. Lett.* **2016**, *18*, 5971–5973. (c) Huo, H.-H.; Xia, X.-E.; Zhang, H.-K.; Huang, P.-Q. Enantioselective Total Syntheses of (–)-FR901483 and (+)-8-epi-FR901483. *J. Org. Chem.* **2013**, *78*, 455–465. (d) Kalidindi, S.; Jeong, W. B.; Schall, A.; Bandichhor, R.; Nosse, B.; Reiser, O. Enantioselective synthesis of arglabin. *Angew. Chem., Int. Ed.* **2007**, *46*, 6361–6363. (e) Chen, J.; Chen, X.; Willot, M.; Zhu, J. Asymmetric total syntheses of ecteinascidin 597 and ecteinascidin 583. *Angew. Chem., Int. Ed.* **2006**, *45*, 8028–8032. (f) Vutukuri, D. R.; Bharathi, P.; Yu, Z.; Rajasekaran, K.; Tran, M.-H.; Thayumanavan, S. A Mild Deprotection Strategy for Allyl-Protecting Groups and Its Implications in Sequence Specific Dendrimer Synthesis. *J. Org. Chem.* **2003**, *68*, 1146–1149.

(17) (a) Su, W.; Gu, B.; Hu, X.; Duan, X.; Zhang, Y.; Li, H.; Yao, S. A near-infrared and colorimetric fluorescent probe for palladium detection and bioimaging. *Dyes Pigm.* **2017**, *137*, 293–298. (b) Garner, A. L.; Song, F.; Koide, K. Enhancement of a Catalysis-Based Fluorometric Detection Method for Palladium through Rational Fine-Tuning of the Palladium Species. *J. Am. Chem. Soc.* **2009**, *131*, 5163–5171.

(18) (a) Tonga, G. Y.; Jeong, Y.; Duncan, B.; Mizuhara, T.; Mout, R.; Das, R.; Kim, S. T.; Yeh, Y.-C.; Yan, B.; Hou, S.; Rotello, V. M. Supramolecular regulation of bioorthogonal catalysis in cells using nanoparticle-embedded transition metal catalysts. *Nat. Chem.* **2015**, *7*, 597–603. (b) Weiss, J. T.; Dawson, J. C.; MacLeod, K. G.; Rybski, W.; Fraser, C.; Torres-Sanchez, C.; Patton, E. E.; Bradley, M.; Carragher, N. O.; Unciti-Broceta, A. Extracellular palladium-catalyzed dealkylation of 5-fluoro-1-propargyl-uracil as a bioorthogonally activated prodrug approach. *Nat. Commun.* **2014**, *5*, 4277.

(19) (a) Huo, X.; Quan, M.; Yang, G.; Zhao, X.; Liu, D.; Liu, Y.; Zhang, W. Hydrogen-Bond-Activated Palladium-Catalyzed Allylic Alkylation via Allylic Alkyl Ethers: Challenging Leaving Groups. *Org. Lett.* **2014**, *16*, 1570–1573. (b) Zhao, X.; Liu, D.; Guo, H.; Liu, Y.; Zhang, W. C–N Bond Cleavage of Allylic Amines via Hydrogen Bond Activation with Alcohol Solvents in Pd-Catalyzed Allylic Alkylation of Carbonyl Compounds. *J. Am. Chem. Soc.* **2011**, *133*, 19354–19357.

(20) A nonselective and low-yielding method was reported: Carrillo-Arcos, U. A.; Rojas-Ocampo, J.; Porcel, S. Oxidative cyclization of alkenoic acids promoted by AgOAc. *Dalton Trans* **2016**, *45*, 479–483.

(21) Wang, T.-C.; Fan, L.-F.; Shen, Y.; Wang, P.-S.; Gong, L.-Z. Asymmetric Allylic C–H Alkylation of Allyl Ethers with 2-Acylimidazoles. *J. Am. Chem. Soc.* **2019**, *141*, 10616–10620.

(22) Rajabi, J.; Lorion, M. M.; Ly, V. L.; Liron, F.; Oble, J.; Prestat, G.; Poli, G. Dormant versus Evolving Aminopalladated Intermediates: Toward a Unified Mechanistic Scenario in Pd^{II}-Catalyzed Aminations. *Chem. - Eur. J.* **2014**, *20*, 1539–1546. (b) Strambeanu, I. I.; White, M. C. Catalyst-Controlled C–O versus C–N Allylic Functionalization of Terminal Olefins. *J. Am. Chem. Soc.* **2013**, *135*, 12032–12037. (c) McDonald, R. I.; Stahl, S. S. Modular Synthesis of 1,2-Diamine Derivatives by Palladium-Catalyzed Aerobic Oxidative Cyclization of Allylic Sulfamides. *Angew. Chem., Int. Ed.* **2010**, *49*, 5529–5532.

(23) For representative examples, see: Ross, S. P.; Rahman, A. A.; Sigman, M. S. Development and Mechanistic Interrogation of Interrupted Chain-Walking in the Enantioselective Relay Heck Reaction. *J. Am. Chem. Soc.* **2020**, *142*, 10516–10525. (b) Hamasaki, T.; Aoyama, Y.; Kawasaki, J.; Kakiuchi, F.; Kochi, T. Chain Walking as a Strategy for Carbon-Carbon Bond Formation at Unreactive Sites in Organic Synthesis: Catalytic Cycloisomerization of Various 1,*n*-Dienes. *J. Am. Chem. Soc.* **2015**, *137*, 16163–16171. (c) Mei, T.-S.; Patel, H. H.; Sigman, M. S. Enantioselective construction of remote quaternary stereocentres. *Nature* **2014**, *508*, 340–344. (d) Werner, E. W.; Mei, T.-S.; Burckle, A. J.; Sigman, M. S. Enantioselective Heck Arylations of Acyclic Alkenyl Alcohols Using a Redox-Relay Strategy. *Science* **2012**, *338*, 1455–1458.

(24) For the synthesis of an enantiomerically pure substrate overcoming the racemization problem, see the [Supporting Information](#).

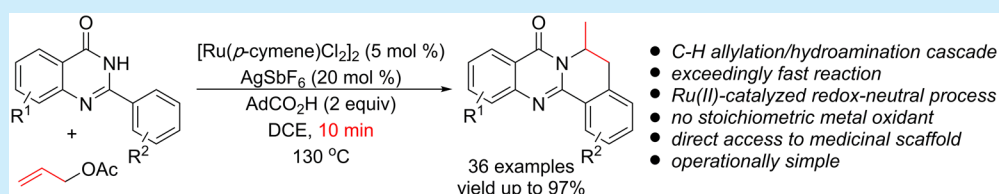
Exceedingly Fast, Direct Access to Dihydroisoquinolino[1,2-*b*]quinazolinones through a Ruthenium(II)-Catalyzed Redox-Neutral C–H Allylation/Hydroamination Cascade

Gurupada Bairy,^{†,‡} Suvankar Das,[†] Hasina Mamataj Begam,[†] and Ranjan Jana^{*,†,‡,§}

[†]Organic and Medicinal Chemistry Division, CSIR-Indian Institute of Chemical Biology, 4 Raja S. C. Mullick Road, Jadavpur, Kolkata 700032, West Bengal, India

[‡]Academy of Scientific and Innovative Research (AcSIR), Kolkata 700032, West Bengal, India

Supporting Information



ABSTRACT: A ruthenium(II)-catalyzed redox-neutral synthesis of dihydroisoquinoline-fused quinazolinone derivatives has been accomplished through the merger of C–H activation and alkene difunctionalization using quinazolinone as an inherent directing group. This intermolecular reaction proceeds rapidly and is complete within 10 min, providing the annulation product in high yields without any stoichiometric metal oxidant. Mechanistically, this tandem reaction proceeds through directed *ortho* C–H allylation followed by hydroamination with the proximal –CONH group, to furnish 6-methyl-5,6-dihydro-8*H*-isoquinolino[1,2-*b*]quinazolin-8-ones in a single operation. The carboxylic acid additive has a dual role in the formation of active catalyst and protodemetalation.

Fused quinazolinone represents an important scaffold ubiquitously found in many natural products, drugs, agrochemicals and other pharmaceutically active ingredients (Figure 1).¹ They are known to exhibit antibiotic, anticancer, antimalarial activities.² Hence the development of efficient methodology for the construction of the quinazolinone moiety has claimed unremitting attention from organic chemists.³ C–H activation is the latest technology added for efficient construction and late-stage modification of functional molecules.⁴ Although an impressive array of C–H activation

strategies have been developed for the π -extension of heterocycles with alkynes,^{5,6} annulation with alkenes is extremely challenging.⁷ This can be attributed to the fact that most C–H activations proceed through high energy pathways at higher temperature where deleterious Fujiwara–Moritani Heck products form predominantly via β -hydride elimination.⁸ However, judicious choice of the catalytic system, e.g., electrophilic metal complexes, may facilitate migratory alkene insertion or reinsertion steps for further functionalization.⁹

Our group is actively engaged in the intermolecular synthesis of heterocycles through the merger of cascade C–H activation and alkene difunctionalization.¹⁰ Based on these strategies, we decided to develop a methodology for the annulation of the 2-arylquinazolinone moiety to achieve analogues of the rutaecarpine alkaloid, a COX-2 inhibitor.¹¹ From the literature, the Xuan group reported a ruthenium-catalyzed synthesis of pyrrolo[2,1-*b*]quinazolin-9(1*H*)-one motifs via a C–H alkylation/aza-Michael addition cascade (Scheme 1).¹²

Although a C–H activation and oxidative cyclization cascade for the construction of five-membered *N*-heterocycles such as indoles, indolines, and 2*H*-isoindoles have been well explored, the synthesis of six-membered rings is less developed.¹³ This can be ascribed to the formation of

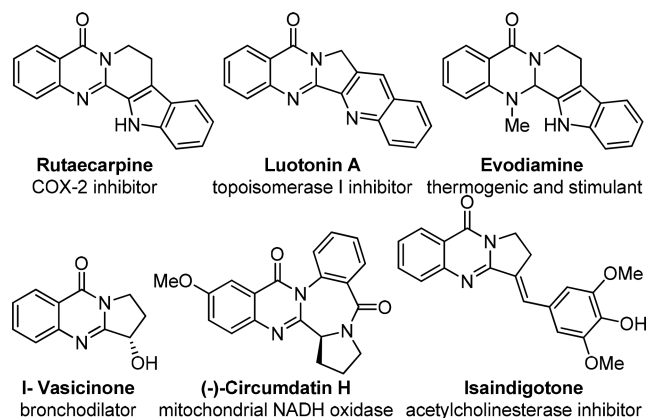
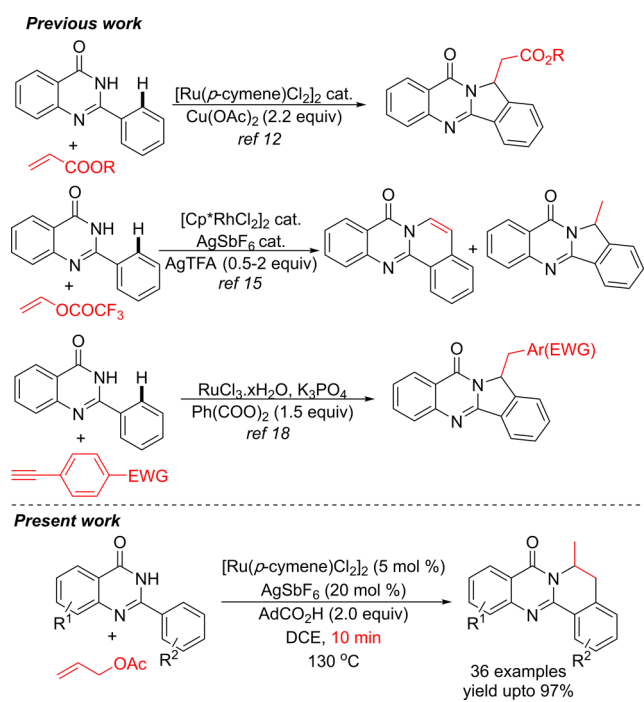


Figure 1. Bioactive fused quinazolinone scaffolds.

Received: September 24, 2018

Published: November 8, 2018

Scheme 1. Ru(II)-Catalyzed C–H Alkylation/Cyclization Cascade



energetically disfavored seven-membered cyclic intermediates and a poor trajectory for cyclization.¹⁴ Recently, Peng and co-workers reported a rhodium-catalyzed C–H alkylation/cyclization of 2-arylquinazolin-4-ones with vinyl trifluoroacetate.¹⁵ However, a mixture of five-membered and six-membered heterocycles was obtained. The Dong group reported a ruthenium(II)-catalyzed synthesis of indolo[2,1-*a*]isoquinolines via C–H alkylation and oxidative cyclization of 2-phenylindoles.¹⁶ However, it was impossible to furnish a selective monoallylation product. Cui and co-workers reported a palladium-catalyzed synthesis of fused polyheterocycles through sequential [4 + 2] and [3 + 2] cycloadditions with alkynes.¹⁷ Furthermore, late-stage diversification of the 2-arylquinazolinone moiety through C–H activation has also been explored.¹⁸ However, the direct synthesis of rutaecarpine analogues via the C–H activation/hydroamination cascade is not known. Here we describe a ruthenium(II)-catalyzed C–H alkylation/cyclization cascade that furnishes 6-methyl-5,6-dihydro-8H-isoquinolino[1,2-*b*]quinazolin-8-ones in intermolecular fashion from inexpensive allyl acetate and 2-arylquinazolinones. The present reaction proceeds through a redox-neutral pathway without any oxidant, is extremely fast, and is highly selective for monoallylation–cyclization.¹⁹

To optimize this cascade protocol, 2-phenylquinazolinone (**1a**) and allyl acetate (**2**) were selected as model substrates. Initially, when 2-phenylquinazolinone and allyl acetate were treated in the presence of catalytic [Cp*RhCl₂]₂, AgSbF₆, and NaOAc at 130 °C in DCE medium for 4 h, the desired product **3a** was obtained in 49% yield along with 16% undesired enamide product (**3a'**) as an inseparable mixture (entry 1, Table 1). In order to improve the yield of **3a** by diminishing the formation of **3a'**, various acid and base additives were examined. Interestingly, instead of sodium acetate, 2 equiv of acetic acid provided **3a** in 77% yield along with a trace amount of **3a'** which is formed through β -hydride elimination of the incipient ruthenium-alkyl species which is formed after alkene

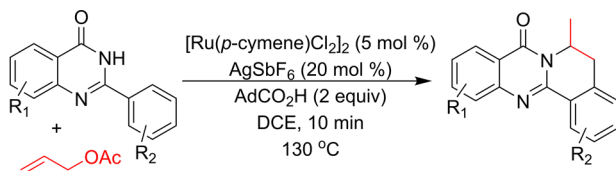
Table 1. Optimization of the Reaction Conditions^a

| entry | catalyst | Ag(I) salts | additive | time (min) | yield ^b 3a/3a' |
|-----------------|--|--------------------|---------------------|------------|---------------------------|
| 1 | [Cp*RhCl ₂] ₂ | AgSbF ₆ | NaOAc | 240 | 49/16 |
| 2 ^c | [Cp*RhCl ₂] ₂ | AgSbF ₆ | NaOAc | 720 | 8/30 |
| 3 | [Cp*RhCl ₂] ₂ | AgSbF ₆ | AcOH | 240 | 77/3 |
| 4 | [Ru(<i>p</i> -cymene)Cl ₂] ₂ | AgSbF ₆ | AcOH | 240 | 61/2 |
| 5 | [Ru(<i>p</i> -cymene)Cl ₂] ₂ | AgSbF ₆ | AcOH | 150 | 69/2 |
| 6 | [Ru(<i>p</i> -cymene)Cl ₂] ₂ | AgSbF ₆ | AcOH | 35 | 72/1 |
| 7 | [Ru(<i>p</i> -cymene)Cl ₂] ₂ | AgSbF ₆ | AcOH | 10 | 61/0 |
| 8 | [Ru(<i>p</i> -cymene)Cl ₂] ₂ | AgSbF ₆ | PhCO ₂ H | 10 | 44/2 |
| 9 | [Ru(<i>p</i> -cymene)Cl ₂] ₂ | AgSbF ₆ | PivOH | 10 | 39/1 |
| 10 | [Ru(<i>p</i> -cymene)Cl ₂] ₂ | AgSbF ₆ | AdCO ₂ H | 10 | 80/0 |
| 11 | [Ru(<i>p</i> -cymene)Cl ₂] ₂ | NaBF ₄ | AdCO ₂ H | 10 | NR |
| 12 | [Ru(<i>p</i> -cymene)Cl ₂] ₂ | NaSbF ₆ | AdCO ₂ H | 10 | NR |
| 13 | [Ru(<i>p</i> -cymene)Cl ₂] ₂ | AgOAc | AdCO ₂ H | 10 | trace |
| 14 | [Ru(<i>p</i> -cymene)Cl ₂] ₂ | AgBF ₄ | AdCO ₂ H | 10 | 6/0 |
| 15 | [Ru(<i>p</i> -cymene)Cl ₂] ₂ | - | AdCO ₂ H | 10 | NR |
| 16 | [Ru(<i>p</i> -cymene)Cl ₂] ₂ | AgSbF ₆ | - | 10 | 10/0 |
| 17 ^d | [Ru(<i>p</i> -cymene)Cl ₂] ₂ | AgSbF ₆ | AdCO ₂ H | 10 | 55/0 |
| 18 ^e | [Ru(<i>p</i> -cymene)Cl ₂] ₂ | AgSbF ₆ | AdCO ₂ H | 10 | 16/0 |

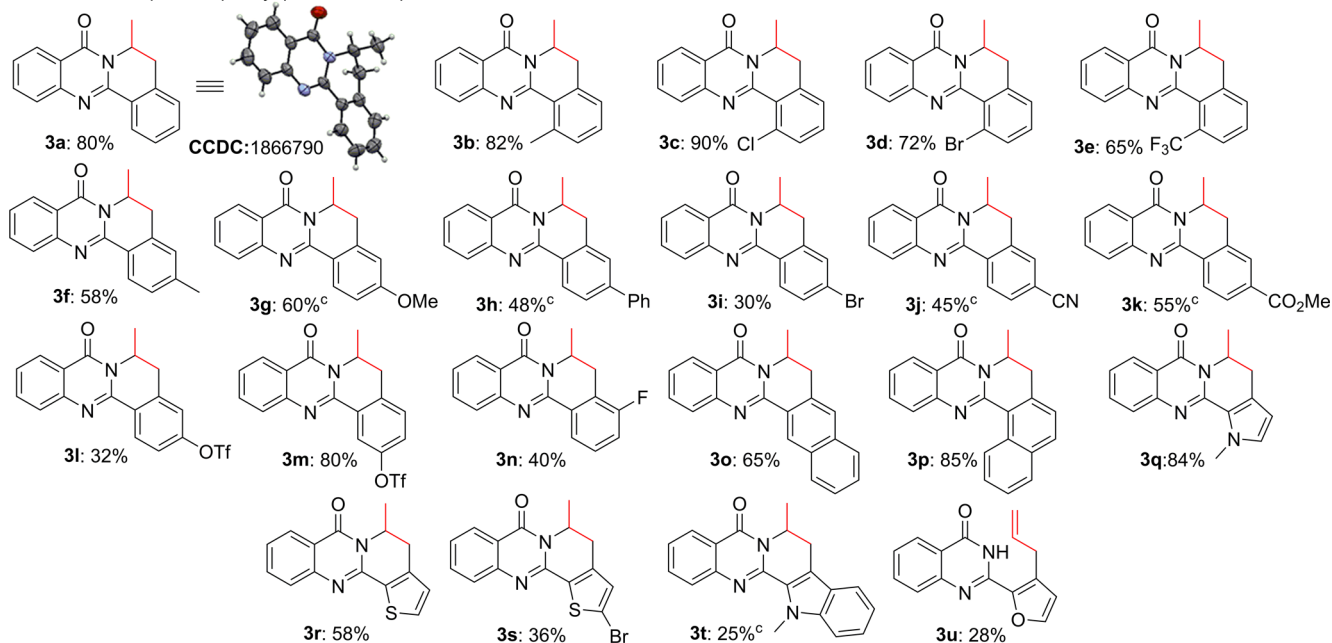
^aAll reactions were carried out in 0.1 mmol scale. ^bYields referred to here are overall isolated yields, and the product distribution was measured from NMR. ^cTemperature 100 °C. ^dAllyl methyl carbonate was used instead of allyl acetate. ^eAllyl alcohol was used instead of allyl acetate.

insertion. Additionally, the ruthenium catalysts are inexpensive compared to rhodium catalysts but exhibit comparable or enhanced reactivity. Keeping these in mind, we decided to optimize further with inexpensive ruthenium catalysts. As hypothesized, when a catalytic amount of (5 mol %) [Ru(*p*-cymene)Cl₂]₂ was employed in the reaction between **1a** and **2** in the presence of AgSbF₆ and acetic acid at 130 °C in DCE, the desired product (**3a**) was isolated in 63% yield, and the formation of **3a'** was suppressed significantly but not diminished completely (entry 4, Table 1). To our delight, **3a** was obtained exclusively in 61% yield when the reaction was carried out for 10 min under the same reaction conditions (entry 7, Table 1). Subsequently, various acid additives were examined to improve the yield further. Among various acids tested, adamantanecarboxylic acid was the most effective due to less nucleophilic and better proton shuttle, while AgSbF₆ was the best additive presumably to generate an active cationic catalyst. Hence the yield of the desired product was increased to 80% without formation of any undesired products. Finally, 5 mol % of [Ru(*p*-cymene)Cl₂]₂, 20 mol % of AgSbF₆, and 2 equiv of AdCO₂H in dichloroethane solvent at 130 °C for 10 min were found to be the optimal conditions for this C–H alkylation/hydroamination cascade reaction.

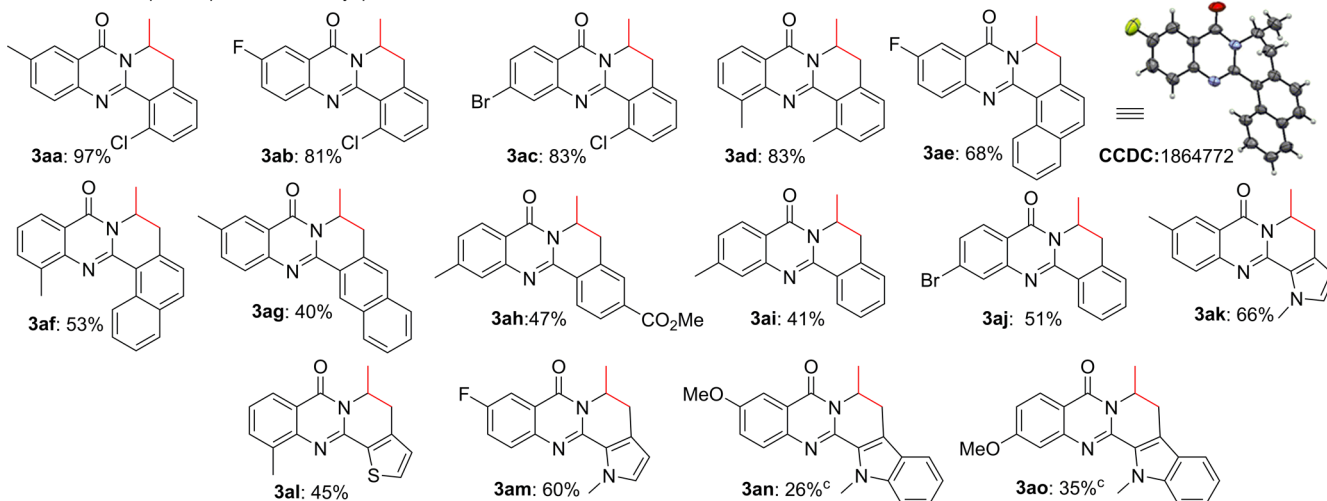
Quinazolinones containing diverse *ortho* substitution at the 2-phenyl moiety such as methyl, chloro, bromo, trifluoromethyl, etc. provided dihydroisoquinolino[1,2-*b*]quinazolinones (**3b**–**3e**, Scheme 2) in excellent yields under the optimized reaction conditions. A range of functional groups at the *para* position such as electron-donating methyl, methoxy, phenyl or electron-withdrawing bromo, cyano, ester,

Scheme 2. Substrate Scope of C–H Allylation/Cyclization Cascade^{a,b}

A. Substrate scope for 2-phenylquinolinone part



B. Substrate scope for quinozolinone aryl part



^aAll reactions were carried out in 0.2 mmol scale. ^bYields refer to the average of isolated yields of at least two experiments. ^cFor 1 h.

etc. were compatible under the reaction conditions providing moderate to high yields (**3f–3l**, Scheme 2). Remarkably, unsubstituted or *para*-substituted phenyls in the quinazolinone afforded monoallylation followed by cyclization products selectively. No diallylation product or their corresponding derivatives were isolated. Although *meta*-methoxy phenyl did not furnish any product, the *meta*-triflate remained intact, furnishing high yield (80%) of the desired product, which also indicates the mild nature of the reaction conditions. 1-Naphthyl derivative **3p** provided a better yield (80%) than the corresponding 2-naphthyl derivative **3o**, further demonstrating

the positive influence of *ortho* substitution. Next, we examined several heteroaromatic quinolinones.

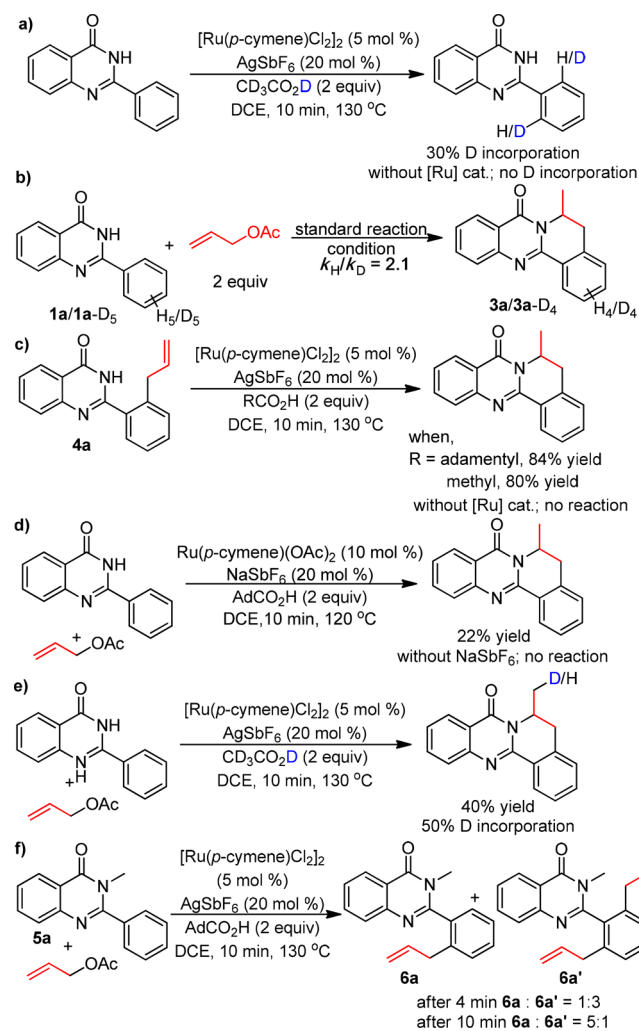
Gratifyingly, methyl-protected 2-pyrrole and 2-thiophene afforded high to good yields of the cyclized product (**3q** and **3r**, Scheme 2). However, 5-bromo-2-thiophene and *N*-methyl-2-indole furnished the corresponding products (**3s** and **3t**, Scheme 2) in low yields, but the corresponding products from indole resemble the structure of rutaecarpine. In the case of 2-furyl derivative **3u**, only the 3-allylation product was isolated, presumably due to the coordination of ruthenium with Lewis basic furan oxygen and amide nitrogen at the opposite side,

prohibiting the subsequent cyclization. It also indicates that the reaction proceeds via a C–H allylation step. However, substituted allyl acetates were ineffective under these annulation reaction conditions.

To examine the substitution effect on the aryl ring of quinazolinones, we prepared several quinolinones with different electron-donating and -withdrawing groups on the aryl ring and subjected them to the standard reaction conditions. Gratifyingly, methyl-, fluoro-, and bromo-substituted quinazolines provided excellent to high yields of the desired product with *ortho*-chloro-2-phenyl substrates (3aa–3ac, Scheme 2). The quinazolinone derived from 3-methylanthralinamide and 2-methylbenzaldehyde afforded the desired cyclization product (3ad, Scheme 2) selectively via sp^2 C–H activation, and no sp^3 C–H activation of the methyl groups was observed. In the case of 1- and 2-naphthyl derivatives at the 2-position, fluoro or methyl substitution on the quinazolinone backbone also afforded the cyclization product (3ae–3ag, Scheme 2) through the C2 and C1 positions, respectively, where the C–H bond at the *peri*-position remained intact. Similarly, 2-heteroaromatics such as *N*-methyl pyrrole, thiophene, and indoles furnished the desired products (3ak–3ao, Scheme 2) albeit in moderate to low yields. Representative compounds (3a and 3ae) have been further characterized by X-ray crystallography (see the SI).

To gain mechanistic insight, when the substrate (1a) was subjected to the standard reaction conditions in the absence of allyl acetate using 2 equiv of CD_3CO_2D , 30% *ortho* H–D exchange was observed (Scheme 3a). No H–D exchange was observed in the absence of the metal catalyst, suggesting the involvement of a reversible directed *ortho* ruthenation. The primary kinetic isotope effect (KIE) from a competitive study between 1a and the corresponding deuterated substrate d_5 -1a was determined as $K_H/K_D = 2.1$ suggesting that the C–H activation may be involved in the rate-determining step (Scheme 3b). When a preformed *ortho*-allyl-2-phenyl quinazolinone (4a) was subjected to the standard reaction conditions, the annulation product was obtained in 84% yield (Scheme 3c), whereas an 80% yield of the annulation product was observed using 2 equiv of AcOH in lieu of adamantyl carboxylic acid. These experiments suggest that the reaction may proceed through sp^2 C–H allylation at the *ortho* position. In the absence of metal catalyst, no cyclization product was formed from the corresponding C–H allylation intermediate, which indicates that although the acid additive has a positive influence on the reaction outcome a ruthenium catalyst was involved in both the C–C and C–N bond formation cascade. To determine the role of acid additive in the active catalyst, $Ru(p\text{-cymene})(OAc)_2$ was prepared separately and subjected to the reaction conditions in combination with $NaSbF_6$ instead of $AgSbF_6$ to afford the desired product in 22% yield (Scheme 3d), whereas no product formation was observed in the absence of $NaSbF_6$, indicating that formation of the electrophilic ruthenium complex facilitates C–H insertion and alkene reinsertion steps. From these experiments it is presumed that $Ru(p\text{-cymene})(\kappa^2\text{-OCOR})_2$ [R = adamantyl] is a more active catalyst precursor than $Ru(p\text{-cymene})(OAc)_2$ which accelerates the C–H allylation step. Cyclization and protodemetalation steps are not dependent on the nature of the acid additive used since almost identical yields are obtained using both catalysts (acetate or adamantyl carboxylate) from the corresponding C–H allylation intermediate. When 1a was subjected to the reaction conditions in the presence of 2 equiv of CD_3CO_2D in

Scheme 3. Control Experiments



lieu of adamantyl carboxylic acid, 50% deuterium incorporation was observed at the 6-methyl group (Scheme 3e) which suggests that the protodemetalation step may be involved in the catalytic cycle. When *N*-methyl-protected quinazolinone 5a was subjected to the standard reaction conditions, mixtures of mono and diallylation at the *ortho* position were formed (Scheme 3f), which indicates that after C–H allylation the subsequent steps proceed spontaneously to provide the annulation product, and further allylation is prohibited by steric encumbrance.

Therefore, based on control experiments and previous reports, a plausible mechanism for this cascade reaction is proposed. $AgSbF_6$ and $AdCO_2H$ are prerequisite additives for the formation of electrophilic active catalyst A where the chloride ion is replaced by the noncoordinating SbF_6^- anion as $AgCl$ precipitation. Then coordination of the nitrogen atom of substrate (1a) into ruthenium of A produces complex B, which undergoes sp^2 *ortho* C–H insertion to form five-membered ruthenacycle C (Scheme 4). This coordinated unsaturated ruthenium complex undergoes migratory alkene insertion to generate intermediate D.^{10c,20} D undergoes a rapid β -acetoxy elimination to generate a C–H allylation product E. Subsequently, the ruthenium complex undergoes migratory alkene insertion to the allyl group to produce the intermediate G through intramolecular C–N bond formation. The

Commun. **2013**, *49*, 481–483. (f) Manikandan, R.; Jeganmohan, M. *Org. Lett.* **2014**, *16*, 912–915. (g) Manikandan, R.; Jeganmohan, M. *Org. Biomol. Chem.* **2015**, *13*, 10420–10436. (h) Kumar, N. Y. P.; Bechtoldt, A.; Raghuvanshi, K.; Ackermann, L. *Angew. Chem., Int. Ed.* **2016**, *55*, 6929–6932.

(7) (a) Thalji, R. K.; Ahrendt, K. A.; Bergman, R. G.; Ellman, J. A. *J. Am. Chem. Soc.* **2001**, *123*, 9692–9693. (b) Scarborough, C. C.; Stahl, S. S. *Org. Lett.* **2006**, *8*, 3251–3254. (c) Wrigglesworth, J. W.; Cox, B.; Lloyd-Jones, G. C.; Booker-Milburn, K. I. *Org. Lett.* **2011**, *13*, 5326–5329. (d) Cajaraville, A.; López, S.; Varela, J. A.; Saá, C. *Org. Lett.* **2013**, *15*, 4576–4579. (e) Mishra, N. K.; Park, J.; Sharma, S.; Han, S.; Kim, M.; Shin, Y.; Jang, J.; Kwak, J. H.; Junga, Y. H.; Kim, In Su *Chem. Commun.* **2014**, *50*, 2350–2352.

(8) For reviews on Fujiwara–Moritani Heck reaction; see: (a) Le Bras, J.; Muzart, J. *Chem. Rev.* **2011**, *111*, 1170–1214. (b) Zhou, L.; Lu, W. *Chem. - Eur. J.* **2014**, *20*, 634–642. For seminal work; see: Moritani, I.; Fujiwara, Y. *Tetrahedron Lett.* **1967**, *8*, 1119–1122.

(9) (a) Chianese, A. R.; Lee, S. J.; Gagne, M. R. *Angew. Chem., Int. Ed.* **2007**, *46*, 4042–4059. (b) McDonald, R. I.; Liu, G.; Stahl, S. S. *Chem. Rev.* **2011**, *111*, 2981–3019. (c) Hanley, P. S.; Hartwig, J. F. *Angew. Chem., Int. Ed.* **2013**, *52*, 8510–8525. (d) Piou, T.; Rovis, T. *J. Am. Chem. Soc.* **2014**, *136*, 11292–11295. (e) Filloux, C. M.; Rovis, T. *J. Am. Chem. Soc.* **2015**, *137*, 508–517. (f) Burton, K. M. E.; Pantazis, D. A.; Belli, R. G.; McDonald, R.; Rosenberg, L. *Organometallics* **2016**, *35*, 3970–3980.

(10) (a) Manna, M. K.; Hossian, A.; Jana, R. *Org. Lett.* **2015**, *17*, 672–675. (b) Manna, M. K.; Bhunia, S. K.; Jana, R. *Chem. Commun.* **2017**, *53*, 6906–6909. (c) Manna, M. K.; Bairy, G.; Jana, R. *J. Org. Chem.* **2018**, *83*, 8390–8400.

(11) (a) Moon, T. C.; Murakami, M.; Kudo, I.; Son, K. H.; Kim, H. P.; Kang, S. S.; Chang, H. W. *Inflammation Res.* **1999**, *48*, 621–625. (b) Lee, E. S.; Kim, S. I.; Lee, S. H.; Jeong, T. C.; Moon, T. C.; Chang, H. W.; Jahng, Y. *Bull. Korean Chem. Soc.* **2005**, *26*, 1975–1980. (c) Lee, S. H.; Son, J.-K.; Jeong, B. S.; Jeong, T.-C.; Chang, H. W.; Lee, E.-S.; Jahng, Y. *Molecules* **2008**, *13*, 272–300.

(12) Zheng, Y.; Song, W.-B.; Zhang, S.-W.; Xuan, L.-J. *Org. Biomol. Chem.* **2015**, *13*, 6474–6478.

(13) (a) Manikandan, R.; Jeganmohan, M. *Org. Lett.* **2014**, *16*, 3568–3571. (b) Wu, J.; Xiang, S.; Zeng, J.; Leow, M.; Liu, X.-W. *Org. Lett.* **2015**, *17*, 222–225. (c) Bian, J.; Qian, X.; Wang, N.; Mu, T.; Li, X.; Sun, H.; Zhang, L.; You, Q.; Zhang, X. *Org. Lett.* **2015**, *17*, 3410–3413.

(14) (a) Cui, S.; Zhang, Y.; Wu, Q. *Chem. Sci.* **2013**, *4*, 3421–3426. (b) Cui, S.; Zhang, Y.; Wang, D.; Wu, Q. *Chem. Sci.* **2013**, *4*, 3912–3916. (c) Wu, S.; Zeng, R.; Fu, C.; Yu, Y.; Zhang, X.; Ma, S. *Chem. Sci.* **2015**, *6*, 2275–2285.

(15) Lou, M.; Deng, Z.; Mao, X.; Fu, Y.; Yang, Q.; Peng, Y. *Org. Biomol. Chem.* **2018**, *16*, 1851–1859.

(16) Xia, Y.-Q.; Dong, L. *Org. Lett.* **2017**, *19*, 2258–2261.

(17) Feng, Y.; Tian, N.; Li, Y.; Jia, C.; Li, X.; Wang, L.; Cui, X. *Org. Lett.* **2017**, *19*, 1658–1661.

(18) Viveki, A. B.; Mhaske, S. B. *J. Org. Chem.* **2018**, *83*, 8906–8913.

(19) (a) Li, B.; Feng, H.; Xu, S.; Wang, B. *Chem. - Eur. J.* **2011**, *17*, 12573–12577. (b) Zhang, Z.; Jiang, H.; Huang, Y. *Org. Lett.* **2014**, *16*, 5976–5979. (c) Manikandan, R.; Jeganmohan, M. *Org. Biomol. Chem.* **2016**, *14*, 7691–7701. (d) Manikandan, R.; Tamizmani, M.; Jeganmohan, M. *Org. Lett.* **2017**, *19*, 6678–6681. (e) Xie, Y.; Wu, X.; Li, C.; Wang, J.; Li, J.; Liu, H. *J. Org. Chem.* **2017**, *82*, 5263–5273. (f) Wang, Z.; Xie, P.; Xia, Y. *Chin. Chem. Lett.* **2018**, *29*, 47–53.

(20) (a) Huang, L.; Wang, Q.; Qi, J.; Wu, X.; Huang, K.; Jiang, H. *Chem. Sci.* **2013**, *4*, 2665–2669. (b) Wang, H.; Schroder, N.; Glorius, F. *Angew. Chem., Int. Ed.* **2013**, *52*, 5386–5389.

(21) (a) Manikandan, R.; Madasamy, P.; Jeganmohan, M. *ACS Catal.* **2016**, *6*, 230–234. (b) Manikandan, R.; Tamizmani, M.; Jeganmohan, M. *Org. Lett.* **2017**, *19*, 6678–6681.

Photoredox-Catalyzed Tandem Demethylation of *N,N*-Dimethyl Anilines Followed by Amidation with α -Keto or Alkynyl Carboxylic Acids

Pritha Das,^a Hasina Mamataj Begam,^a Samir Kumar Bhunia,^{a, b} and Ranjan Jana^{a, b, *}

^a Organic and Medicinal Chemistry Division, CSIR-Indian Institute of Chemical Biology, 4 Raja S. C. Mullick Road, Jadavpur, Kolkata-700032, West Bengal, India

Phone: (+91) 33 2499 5819

fax: (+91) 33 2473 5197

E-mail: rjana@iicb.res.in

^b Academy of Scientific and Innovative Research (AcSIR), Kolkata-700032, India

Manuscript received: April 24, 2019; Revised manuscript received: June 17, 2019;

Version of record online: July 12, 2019



Supporting information for this article is available on the WWW under <https://doi.org/10.1002/adsc.201900525>

Abstract: We report herein, a biomimetic approach for highly selective monodemethylation of *N,N*-dimethyl anilines to generate secondary amines and subsequent coupling with α -ketocarboxylic acids or alkynyl carboxylic acids to form α -ketoamides or alkynamides respectively under visible light photoredox catalyst in a single operation. From the deuterium-labeling experiment, it was probed that demethylation is the slowest step in this tandem process. Whereas, control experiments and spectroscopic studies revealed that photoredox catalyst is also involved in the subsequent amidation step. The reaction proceeds smoothly at room temperature providing moderate to excellent yield of the coupling products. The amides have also been converted to a series of biologically active spiro compounds.

Keywords: photoredox catalysis; demethylation; amidation; α -ketoamides; alkynamides

Introduction

Tandem or domino reaction is comprised of two or more bond cleavage/formation under the identical reaction conditions and the reaction cascade is initiated from the functionalities obtained in the former transformation.^[1] This domino reaction strategy has unique ability to generate molecular complexity reducing numbers of steps and environmental footprints. This process is ubiquitously found in nature for biosynthesis of natural products.^[2] Inspired by nature and owing to the green synthetic aspects, an impressive array of cascade reactions involving anionic, cationic or radical pathways has been well-explored.^[3] In the last decades, visible-light photoredox catalysis has been proved as a powerful strategy with a wide range of applications from small molecule activation to the synthesis of complex natural products mainly through single electron transfer (SET) process.^[4] Owing to close resemblance with the natural processes, there is an increasing demand for the development of environ-

mentally benign tandem reactions under visible-light catalysis.

α -Ketoamides and alkynamides represent two important classes of compounds ubiquitously found in many natural products, pharmaceuticals, macrocycles, molecular probes in chemical biology etc. (Figure 1).^[5] Furthermore, because of the integration of important functional groups such as ketone and amide for α -ketoamides; and alkyne and amide for alkynamides into their backbone they represent a versatile intermediates in organic synthesis.^[6] Hence, a significant effort has been dedicated for the construction of these structural motifs.^[7] The synthesis of α -ketoamides primarily involves amidation of α -ketoacids and α -keto acyl halides,^[8] oxidation of α -hydroxyamides and α -aminoamides,^[9] transition-metal-catalysed double carbonylative amination of aryl halides;^[10] metal catalysed or metal free oxidative coupling from α -ketoaldehyde etc.^[11] The alkynamides are derived through the amide coupling of the propiolic acid derivatives, carbonylative amidation of the corresponding alkyne etc.^[12]

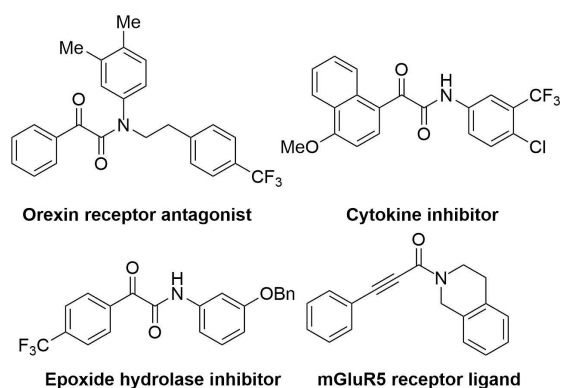
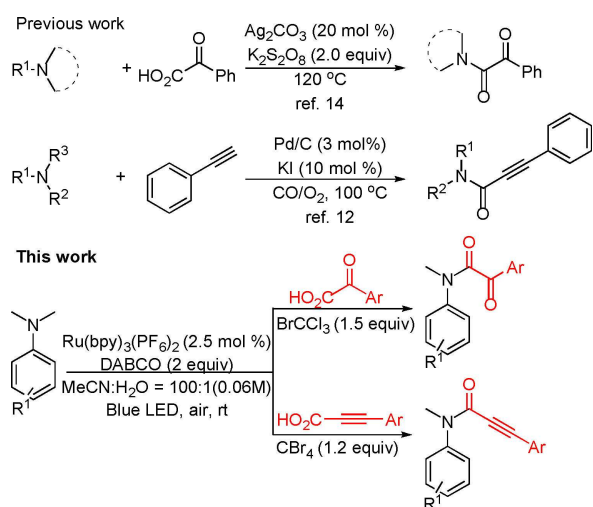


Figure 1. Bioactive α -ketoamides and alkynamides.

Since tertiary amines are readily obtained via over alkylation of amines,^[13] we assumed that *in situ* demethylation of tertiary amines to secondary amines followed by amide formation in a single operation under photoredox catalysis could be an attractive approach. In this vein, the Wang group reported a silver-catalyzed dealkylative-amidation of α -ketoacids with tertiary amines for the synthesis of α -ketoamides.^[14] However, only aliphatic tertiary amines were effective using strong oxidant $K_2S_2O_8$ at high temperature (120 °C). Palladium/charcoal-catalyzed oxidative aminocarbonylation of alkynes with secondary and tertiary amines through *N*-dealkylation was reported for the synthesis of alk-2-ynamides whereas, alkylated anilines were unreactive.^[12] Thus, we were interested to develop a complementary *N*-dealkylative amide coupling reaction under mild conditions with the challenging aniline derivatives. Recently, Rueping and other groups reported Polonovski type *N*-demethylation under photoredox catalysis.^[15] However, to the best of our knowledge there is no report for the



Scheme 1. *N*-Demethylative-amide coupling.

synthesis of α -ketoamides and acetylenic amides from the corresponding α -ketoacids or propiolic acids and tertiary amines under photoredox catalysis (Scheme 1). We report herein, a biomimetic approach for the tandem demethylation of *N,N*-dimethylaniline followed by amidation with α -ketoacids or alkynyl carboxylic acids to furnish α -ketoamides or alkynamides respectively by a single photoredox catalyst. The present reaction initiates through the generation of *N*-centred radical under the irradiation of blue LED at room temperature.

Results and Discussion

N,N-dimethylaniline and phenyl glyoxalic acid were chosen as model substrates to optimize the reaction condition. The results are summarized in the Table 1. When a mixture of *N,N*-dimethylaniline (**1a**) and phenylglyoxalic acid (**2a**) was irradiated under blue LED using 5 mol% of eosin Y as photocatalyst, bromotrichloromethane as oxidant and 10:1 MeCN–H₂O solvent under air, the demethylative amidation product was isolated in 20% yield (Table 1, entry 1). Other oxidants such as TBHP, $K_2S_2O_8$,

Table 1. Optimization of the reaction condition.^[a,b]

| Entry | Photocatalyst | Oxidant | Additive | Yield (%) 3a |
|-------------------|--|--|--------------|---------------------|
| 1 | Eosin Y | BrCCl ₃ | – | 20 |
| 2 | Eosin Y | K ₂ S ₂ O ₈ | – | 15 |
| 3 | Eosin Y | TBHP | – | 0 |
| 4 | Ru(bpy) ₃ (PF ₆) ₂ | BrCCl ₃ | – | 32 |
| 5 ^[c] | Ru(bpy) ₃ (PF ₆) ₂ | BrCCl ₃ | DABCO | 45 |
| 6 | Ru(bpy)₃(PF₆)₂ | BrCCl₃ | DABCO | 80 |
| 7 | Ru(bpy) ₃ (PF ₆) ₂ | – | DABCO | 0 |
| 8 ^[d] | Ru(bpy) ₃ (PF ₆) ₂ | BrCCl ₃ | DABCO | 44 |
| 9 ^[e] | Ru(bpy) ₃ (PF ₆) ₂ | BrCCl ₃ | DABCO | 65 |
| 10 | Mes–Acr–ClO ₄ | BrCCl ₃ | DABCO | 52 |
| 11 ^[f] | Ir(ppy) ₃ | BrCCl ₃ | DABCO | 66 |
| 12 | – | BrCCl ₃ | DABCO | 0 |
| 13 ^[g] | Ru(bpy) ₃ (PF ₆) ₂ | BrCCl ₃ | DABCO | 0 |

^[a] All reactions were carried out in 0.2 mmol scale using **1a** (1.0 equiv.), **2a** (2.0 equiv.), Ru(bpy)₃(PF₆)₂ (2.5 mol%), BrCCl₃ (1.5 equiv.), DABCO (2.0 equiv.) in 100:1 acetonitrile–water (0.06 M) solvent (3 mL) at room temp with blue LED irradiation in aerobic condition.

^[b] Yields refer to here are isolated yields.

^[c] 20% additive was used.

^[d] under nitrogen atmosphere.

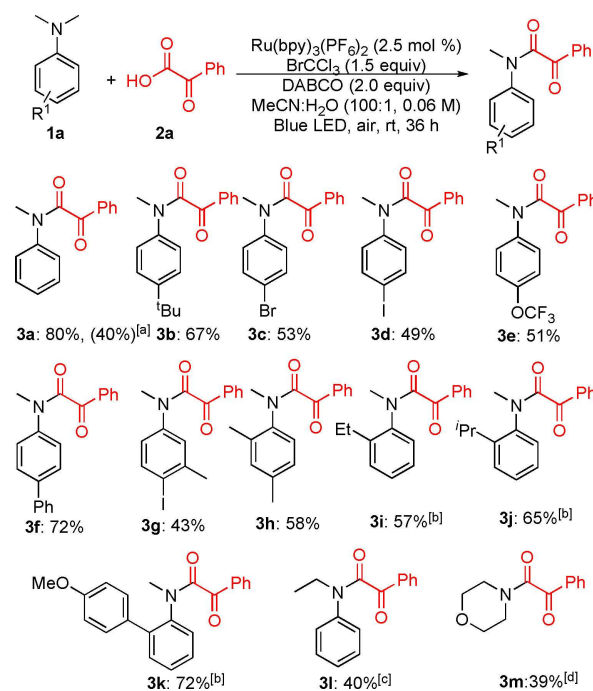
^[e] O₂-balloon.

^[f] white LED.

^[g] without light.

BI-OAc, oxone did not improve the yield of the desired product (entries 4–6, see Table S1 in the Supporting Information, SI). The yield was increased to 32% using 2.5 mol% $\text{Ru}(\text{bpy})_3(\text{PF}_6)_2$ as photocatalyst (entry 4). Gratifyingly, upon addition of 20 mol% DABCO as an additive, the product yield was increased to 45% in 100:1 acetonitrile-water solvent system (entry 5). To our delight, increasing the amount of DABCO to 2.0 equiv., the desired product was isolated in 80% yield in 36 h (entry 6). However, other inorganic (entries 2–3, Table S1 in SI) and organic bases (entries 15–17, Table S1 in SI) such as, K_2CO_3 , Cs_2CO_3 , lutidine, DBU, pyridine were proved to be inferior for this transformation. Organic photoredox catalysts such as Rose Bengal, Mes-Acr-ClO_4 , 9-fluorenone, were unable to increase the yield (entries 18–20, Table S1 in SI). In most of the cases, the starting tertiary amine remained intact in the reaction medium. Whereas, the iridium based photocatalysts such as $(\text{Ir}[\text{dF}(\text{CF}_3)(\text{ppy})]_2(\text{dtbpy}))\text{PF}_6$, $\text{Ir}(\text{ppy})_2(\text{dtbpy})\text{PF}_6$, $\text{Ir}(\text{ppy})_3$ provided better yield to some extent (entries 21–24, Table S1 in SI). However, a portion of *N,N*-dimethylaniline as well as the demethylated *N*-methylaniline were isolated even after 36 hrs of reaction. The yield of amide **3a** was reduced to 58% at 60 °C (entry 33, Table S1 in SI). In this tandem reaction, a photoredox catalyst, light source, BrCCl_3 and DABCO were all necessary, since in the absence of any one component the reaction was suppressed. While an optimum yield (80%) was isolated under the aerial conditions, whereas reaction under inert atmosphere (44% yield) or oxygen atmosphere (65%) provided inferior results (entries 8, 9). Since water is crucial for the demethylation step, we have optimized MeCN-water in 100:1 ratio to obtain optimum yield of **3a**.

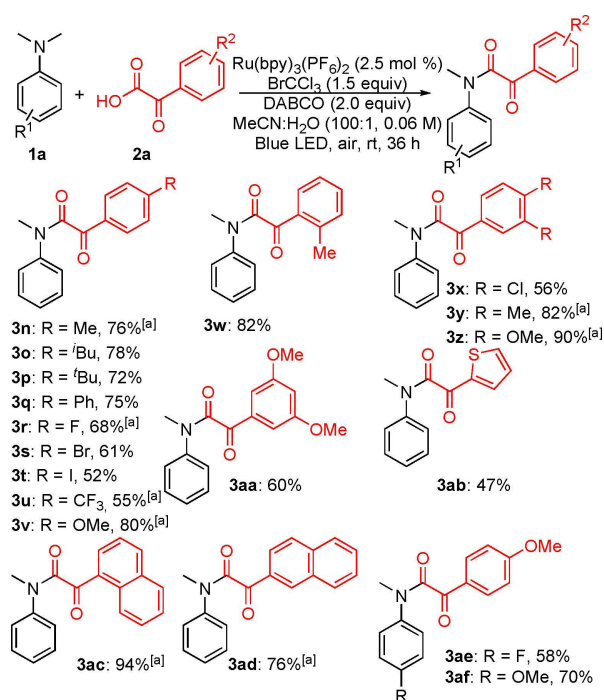
To examine the substrate scope of this tandem reaction, several substituted *N,N*-dimethylanilines were reacted with 2-oxo-2-phenyl acetic acid, **2a** under the optimized reaction conditions (Scheme 2). A variety of functional groups in the phenyl ring of aniline were well-tolerated and furnished the desired product in moderate to good yields. For example, **1a** with bulky *tert*-butyl and halogen (Br, I) substitution at the *para* position yielded 67% (**3b**), 53% (**3c**) and 49% (**3d**) of the desired product respectively. *p*-OCF₃ substituted *N,N*-dimethylaniline furnished 51% of the desired product (**3e**). In presence of *para*-phenyl substitution 72% yield was obtained (**3f**). *Ortho*-substitution also did not hinder the reaction providing the corresponding product in good yield for *ortho* methyl (**3h**), ethyl (**3i**), isopropyl (**3j**) or aryl (**3k**) substituted *N,N*-dimethylaniline. As expected, demethylation/amidation cascade (**3l**) took place predominantly over the corresponding demethylative amidation (10%).^[16] However, the demethylation step generally does not occur with aliphatic tertiary amines. Interestingly, in presence of



Scheme 2. Substrate scope with tertiary aryl amines. Reaction conditions: **1a** (0.2 mmol), **2a** (0.4 mmol), $\text{Ru}(\text{bpy})_3(\text{PF}_6)_2$ (2.5 mol%), DABCO (0.4 mmol), BrCCl_3 (0.3 mmol), MeCN/H₂O=100:1 (0.06 M), blue LED, air, r.t. ^[a]2-oxo-2-phenylacetaldehyde was used instead of **2a**, O₂-ballon. ^[b]Reaction time is 15 h. ^[c]*N*-ethyl-*N*-methyl aniline was used. ^[d]*N*-methylmorpholine was used. 0.5 equiv. TEMPO was added.

0.5 equiv. TEMPO, *N*-methyl morpholine yielded demethylative amidation in 39% (**3m**).^[17] Furthermore, 2-oxo-2-phenylacetaldehyde also provided 40% coupling product in presence of O₂-ballon (**3a**).

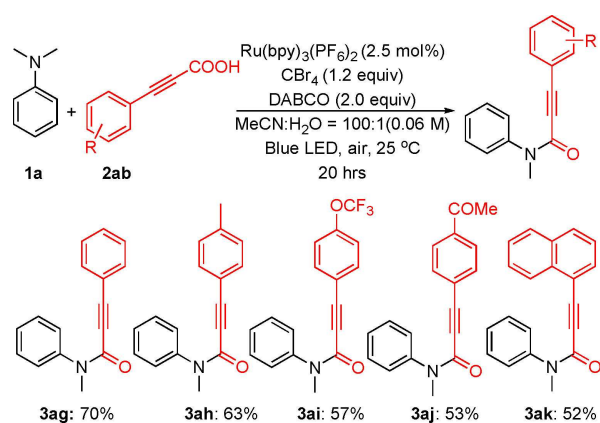
Next, we found that a range of phenyl glyoxylic acid derivatives underwent this cascade reaction smoothly under the optimized reaction condition (Scheme 3). For example, methyl, isobutyl, *tert*-butyl, phenyl substituted acids furnished the desired product in good yields 72–78% (**3n–3q**). Halogens, such as (F, Br, I, **3r–3t**) were also survived under the reaction conditions which is useful for further manipulations through cross-coupling reactions. Electron donating group such as *para*-methoxy (**3v**) has positive influence providing 82% yield, whereas, electron withdrawing group like –CF₃ (**3u**) provided 57% yield. *Ortho* methyl substituted ketoacid also delivered the desired product in 82% yield (**3w**). Dichloro, dimethyl, dimethoxy substituted acids were also compatible providing high to excellent yields (**3x–3z**). Additionally, 2-oxo-2-(thiophen-2-yl)acetic acid, 2-(naphthalen-1-yl)-2-oxoacetic acid, 2-(naphthalen-2-yl)-2-oxoacetic acid reacted efficiently with dimethyl aniline furnishing the desired product in 47%, 94% and 76% respectively (**3ab–3ad**). *para*-Methoxy substituted acid reacted smoothly with *para*-fluoro and *para*-



Scheme 3. Substrate scope with α -keto carboxylic acids. Reaction conditions: **1a** (0.2 mmol), **2a** (0.4 mmol), Ru(bpy)₃(PF₆)₂ (2.5 mol%), DABCO (0.4 mmol), BrCCl₃ (0.3 mmol), MeCN/H₂O = 100:1 (0.06 M), blue LED, air, r.t. ^[a] Reaction time 15 hrs.

methoxy substituted dimethylaniline delivering the desired product in good yields (**3ae**, **3af**).

This demethylation followed by amidation reaction can also be extended to alkynyl carboxylic acids (Scheme 4). The amine **1a** is employed to react with various alkynyl carboxylic acids to furnish the desired products in moderate to good yields. Electron donating



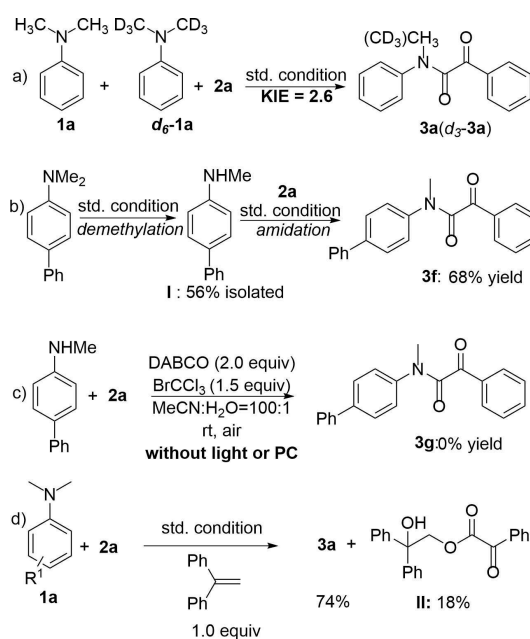
Scheme 4. Substrate scope with phenyl propiolic acid. Reaction conditions: **1a** (0.2 mmol), **2ab** (0.6 mmol), Ru(bpy)₃(PF₆)₂ (2.5 mol%), DABCO (0.4 mmol), CBr₄ (0.24 mmol), MeCN/H₂O = 100:1 (0.06 M), blue LED, air, r.t.

–OCF₃ substituted alkynyl carboxylic acid furnished the amidation product in 57% yield (**3ai**).

Electron-withdrawing –COMe substitution at the acid moiety is well-tolerated delivering moderate yield of the desired product (**3aj**). 3-(Naphthalen-1-yl) propiolic acid also afforded the corresponding product in 52% yield (**3ak**).

Next, we performed a series of control experiments to understand the mechanism of this tandem reaction. From an intermolecular experiment with **1a** and d₆-**1a** the *k_H*/*k_D* was determined as 2.6, which indicates that C–H bond cleavage may be involved in the rate determining step (Scheme 5a). In the absence of **2a**, mono-demethylated product (**I**) was isolated and characterized from 4-phenyl-*N,N*-dimethylaniline (Scheme 5b). Further it was reacted with **2a** to afford the desired amide product (**3f**) in 68% yield. Therefore, initially, photoredox mediated C–N bond cleavage to generate secondary amine intermediate takes place which undergoes subsequent amidation reaction.

When the secondary amine intermediate is allowed to react with **2a** in absence of light or photocatalyst, no desired product was obtained (Scheme 5c). Hence, photoredox catalytic cycle is involved in the amidation step also.^[11] Typically, an activated precursor such as acid bromide or hypobromite may generate through radical pathway from the carboxylic acids for subsequent amide coupling.^[15d] Although, all our efforts to identify this activated precursor were in vain, the corresponding carboxyl radical was trapped by 1,1-diphenylethylene to provide **II** in 18% isolated yield (Scheme 5d). However, we have observed positive influence of 2,2,6,6-tetramethylpiperidinyloxy (TEM-



Scheme 5. Control experiments.

PO) or butylated hydroxytoluene (BHT) in the reaction outcome presumably due to facilitation in the demethylation step.^[17]

In Stern-Volmer quenching experiments of the photocatalyst, it was observed that the emission intensity of excited state of the photocatalyst Ru(bpy)₃(PF₆)₂* was gradually diminished with increasing concentration of both **1a** and **2a** (Figure 2). But such a

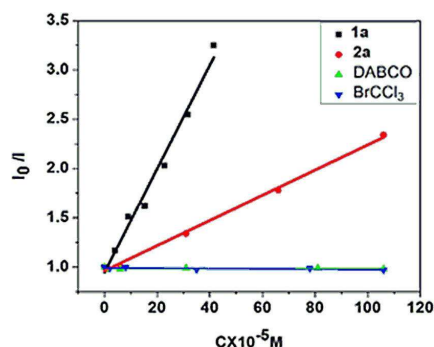
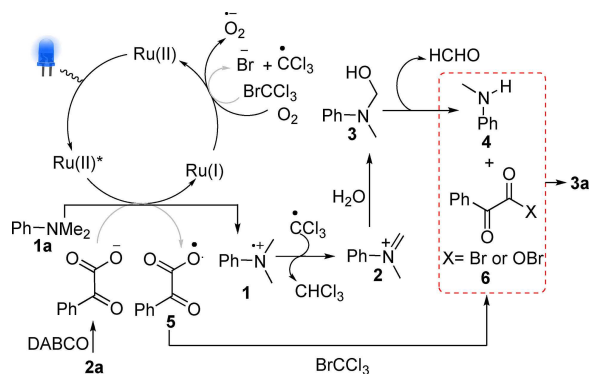


Figure 2. Stern-Volmer plot of Ru(bpy)₃(PF₆)₂ in presence of different components of the reaction. I₀ is the inherent fluorescence intensity of photocatalyst. I is the fluorescence intensity of photocatalyst in the presence of quenchers.

phenomenon was not observed with BrCCl₃ or DABCO. These results suggest that an amine radical cation as well as a carboxyl radical is most likely involved in the reaction.

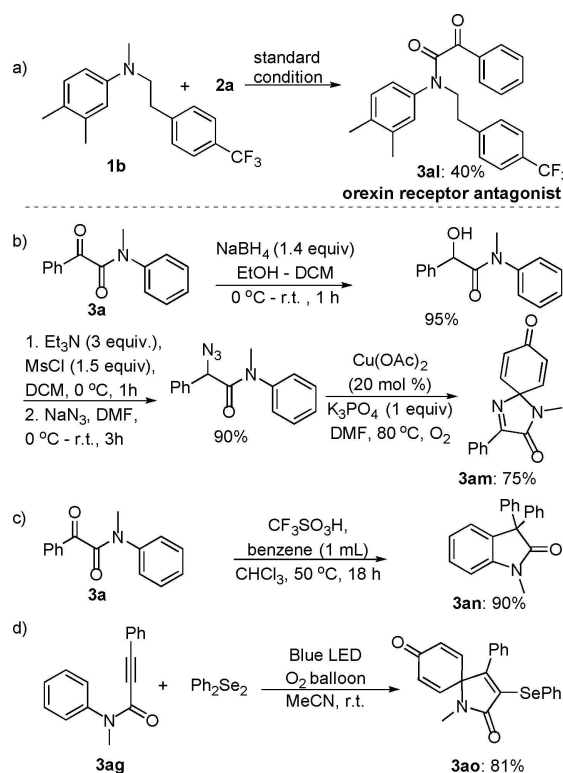
However, the proper mechanistic understanding for the amidation is not clear at this stage and need more detailed study. From these control experiments and previous literatures, a plausible mechanism is depicted in Scheme 6 for this tandem C–N activation/ C–N formation process.^[18] Ru(II)-photocatalyst is first excited upon irradiation of the blue LED to generate the excited state photocatalyst Ru(II)* (E_{1/2}^{red} = 0.77 V vs SCE) which undergoes thermodynamically feasible one electron reduction with *N,N*-dimethylaniline (E_{1/2}^{red} = 0.74 V vs



Scheme 6. Plausible reaction mechanism.

SCE) to form the α -amino radical cation **1**.^[4e] The reduced photocatalyst then returns to its original ground state for the next run by a single electron oxidation with molecular O₂ or BrCCl₃. The generated α -amino radical cation can readily form the iminium cation intermediate **2** by releasing one hydrogen radical, which in the presence of water undergoes demethylation of *N,N*-dimethylaniline by elimination of formaldehyde and secondary amine **4** via the inherently unstable carbinolamine intermediate **3**.^[19] In another catalytic cycle, the excited Ru(II)* can oxidize the carboxylate anion, which is generated from **2a** to carboxylate radical **5**. In presence of BrCCl₃ the carboxylate radical may form the reactive bromide or hypobromite intermediate **6** which upon reacting with **4** furnishes the desired product **3a**.

Next we turned our attention for further utilization of α -ketoamide products to the synthesis of useful molecules. When an ethylaryl substituted aniline **1b** was subjected to the standard reaction condition with **2a**, an orexin receptor antagonist **3aI** was isolated in moderate yield (Scheme 7a).^[20] α -Ketoamide, **3a** is transformed into α -hydroxyamide by chemoselective reduction of the ketone group with NaBH₄. After mesylation of the hydroxyl group followed by S_N² substitution with sodium azide the corresponding azido-amide compound was obtained. It was converted to azaspirocyclohexadieneone **3am** using catalytic Cu (OAc)₂ under oxygen atmosphere (Scheme 7b).^[21]



Scheme 7. Application of demethylative-amide coupling for molecular complexity.

Furthermore, **3a** rearranges to provide 3,3-disubstituted oxyindole **3an** in superacidic condition (Scheme 7c).^[22] The alkynamide product **3ag** undergoes selenylative spirocyclization with diphenyldiselenide to form **3ao** in presence of blue LED under oxygen atmosphere (Scheme 7d).^[23]

Conclusion

In conclusion, we have developed a biomimetic catalytic approach for demethylative-amide bond formation between *N,N*-dimethylaniline and α -ketocarboxylic acid or alkynyl carboxylic acid. These two distinct steps proceed smoothly in a cascade manner under a single visible-light-mediated photoredox catalysis at room temperature. A series of extremely important class of compounds, α -ketoamides and alkynamides have been synthesized through this protocol which ubiquitously found in natural products, peptoids and useful synthetic intermediates. The demethylative-amide coupling products were easily converted to a series of biologically active complex spiro compounds. We anticipate that integration of two or more important reactions in a cascade manner under photoredox catalysis will open a new arena in organic synthesis.

Experimental Section

General Information

Melting points were determined in open end-capillary tubes and are uncorrected. TLC was performed on silica gel plates (Merck silica gel 60, f_{254}), and the spots were visualized with UV light (254 and 365 nm) and KMnO_4 stain. ^1H NMR was recorded at 300 MHz (Bruker-DPX), 400 MHz (JEOL-JNM-ECZ400 S/L1) and 600 MHz (Bruker-Avance) frequency and ^{13}C NMR spectra were recorded at 75 MHz (Bruker-DPX) and 150 MHz (Bruker-Avance) frequency in CDCl_3 solvent using TMS as the internal standard. Chemical shifts were measured in parts per million (ppm) referenced to 0.0 ppm for tetramethylsilane. The following abbreviations were used to explain multiplicities: s = singlet, d = doublet, t = triplet, q = quartet, m = multiplet, br. = broad, Ar = aromatic. Coupling constants, J were reported in Hertz unit (Hz). HRMS (m/z) were measured using ESI (Q-TOF, positive ion) techniques. Infrared (IR) spectra were recorded on Fourier transform infrared spectroscopy; only intense peaks were reported. Fluorescence spectra were recorded on a Perkin Elmer LS 55 Luminescence Spectrometer. Unless otherwise stated, all commercial reagents were used without additional purification. The starting materials α -oxocarboxylic acid,^[24] alkynyl carboxylic acid,^[25] and metal-photocatalysts^[26] were prepared using literature reported method.

General Experimental Procedure for Photoredox Catalyzed α -Ketoamide Synthesis from the Corresponding *N,N*-Dimethylaniline and 2-oxo-2-Phenylacetic Acid. (Scheme 4)

A mixture of *N,N*-dimethyl aniline (0.2 mmol, 1.0 equiv.), Ru(bpy)₃(PF₆)₂ (4.3 mg, 0.005 mmol, 0.025 equiv.), DABCO (44.8 mg, 0.4 mmol, 2.0 equiv.) and 2-oxo-2-phenylacetic acid (60 mg, 0.4 mmol, 2.0 equiv.) was taken in a 25 mL round bottom flask and diluted with 3 mL of acetonitrile solvent. To this mixture, were added bromotrichloromethane (30 μL , 0.3 mmol, 1.5 equiv.) and water (30 μL). The resulting mixture was irradiated under blue LED (48 W) light and stirred at room temperature for 36 h in aerobic condition. After that the acetonitrile solvent was evaporated in reduced pressure and the reaction mixture was poured into ethyl acetate (30.0 mL) and extracted with saturated aqueous NaHCO_3 solution. The organic layer was washed with water (10 mL \times 2) and brine (10 mL), dried over anhydrous Na_2SO_4 and the solvent was evaporated under reduced pressure. The crude product was purified by column chromatography (SiO_2 , eluting with hexane/ethyl acetate) to afford the desired product.

General experimental procedure for photoredox catalyzed alkynamide synthesis from the corresponding *N,N*-dimethylaniline and phenyl propiolic acid. A mixture of *N,N*-dimethyl aniline (0.2 mmol, 1.0 equiv.), Ru(bpy)₃(PF₆)₂ (4.3 mg, 0.005 mmol, 0.025 equiv.), DABCO (44.8 mg, 0.4 mmol, 2.0 equiv.) and phenyl propiolic acid (44 mg, 0.6 mmol, 3.0 equiv.) was taken in a 25 mL round bottom flask and diluted with 3 mL of acetonitrile solvent. To this mixture were added tetrabromomethane (80 mg, 0.24 mmol, 1.2 equiv.) and water (30 μL). The resulting mixture was irradiated under blue LED (48 W) light and stirred at room temperature for 20 h in aerobic condition. After that the acetonitrile solvent was evaporated in reduced pressure and the reaction mixture was poured into ethyl acetate (30.0 mL) and extracted with saturated aqueous NaHCO_3 solution. The organic layer was washed with water (10 mL \times 2) and brine (10 mL), dried over anhydrous Na_2SO_4 and the solvent was evaporated under reduced pressure. The crude product was purified by column chromatography (SiO_2 , eluting with hexane/ethyl acetate) to afford the desired product.

Acknowledgements

This work was supported by DST, SERB, Govt. of India, extra mural research grant no. EMR/2014/000469 and Ramanujan fellowship; award no. SR/S2/RJN-97/2012. PD and HM thank CSIR and SKB thanks UGC for their fellowships.

References

- [1] P. J. Parsons, C. S. Penkett, A. J. Shell, *Chem. Rev.* **1996**, *96*, 195–206.
- [2] C. T. Walsh, B. S. Moore, *Angew. Chem. Int. Ed.* **2019**, *58*, 2–36
- [3] B. T. Ueberbacher, M. Hall, K. Faber, *Nat. Prod. Rep.* **2012**, *29*, 337–350.
- [4] For selected reviews; see: a) L. Marzo, S. K. Pagire, O. Reiser, B. König, *Angew. Chem. Int. Ed.* **2018**, *57*,

- 10034–10072; b) N. A. Romero, D. A. Nicewicz, *Chem. Rev.* **2016**, *116*, 10075–10166; c) M. H. Shaw, J. Twilton, D. W. C. MacMillan, *J. Org. Chem.* **2016**, *81*, 6898–6926; d) J. M. R. Narayanam, C. R. J. Stephenson, *Chem. Soc. Rev.* **2011**, *40*, 102–113. For selected examples; see: e) H. G. Roth, N. A. Romero, D. A. Nicewicz, *Synlett* **2016**, *27*, 714–723.
- [5] a) C. Steuer, C. Gegea, W. Fischl, K. H. Heinonen, R. Bartenschlager, C. D. Klein, *Med. Chem.* **2011**, *19*, 4067–4074; b) S. Venkatraman, F. Velazquez, W. Wu, M. Blackman, K. X. Chen, S. Bogen, L. Nair, X. Tong, R. Chase, A. Hart, S. Agrawal, J. Pichardo, A. Prongay, K. C. Cheng, V. Girijavallabhan, J. Piwinski, N. Y. Shih, F. G. Njoroge, *J. Med. Chem.* **2009**, *52*, 336–346; c) G. Brutona, A. Huxley, P. Hanlon, B. Orlek, D. Eggleston, J. Humphriesa, S. Readshawa, A. West, S. Ashman, M. Brown, K. Moore, A. Pope, K. Dwyer, L. Wang, *Eur. J. Med. Chem.* **2003**, *38*, 351–356.
- [6] A. Muthukumar, S. Sangeetha, G. Sekar, *Org. Biomol. Chem.* **2018**, *16*, 7068–7083.
- [7] For review on the synthesis of α -ketoamides, see: a) C. D. Risi, G. P. Pollini, V. Zanirato, *Chem. Rev.* **2016**, *116*, 3241–3305; b) D. Kumar, S. R. Vemula, G. R. Cook, *ACS Catal.* **2016**, *6*, 4920–4945. For selected examples, see: c) N. C. Mamillapallia, G. Sekar, *RSC Adv.* **2014**, *4*, 61077–61085; d) H. Wang, L. N. Guo, X. H. Duan, *Org. Biomol. Chem.* **2013**, *11*, 4573–4576; e) D. Li, M. Wang, J. Liu, Q. Zhao, L. Wang, *Chem. Commun.* **2013**, *49*, 3640–3642; f) C. Zhang, X. Zong, L. Zhang, N. Jiao, *Org. Lett.* **2012**, *14*, 3280–3283; g) C. Zhang, Z. Xu, L. Zhang, N. Jiao, *Angew. Chem. Int. Ed.* **2011**, *50*, 11088–11092.
- [8] a) F. Ji, H. Peng, X. Zhang, W. Lu, S. Liu, H. Jiang, B. Liu, B. Yin, *J. Org. Chem.* **2015**, *80*, 2092–2102; b) C. Allais, T. Constantieux, J. Rodriguez, *Synthesis* **2009**, *2009* (15), 2523–2530; c) F. Heaney, J. Fenlon, P. McArdle, D. Cunningham, *Org. Biomol. Chem.* **2003**, *1*, 1122–1132.
- [9] a) E. Barbayanni, G. Antonopoulou, G. Kokotos, *Pure Appl. Chem.* **2012**, *84*, 1877–1894; b) L. El Kaïm, R. Gamez-Montaño, L. Grimaud, T. Ibarra-Rivera, *Chem. Commun.* **2008**, 1350–1352; c) A. Papanikos, J. Rademann, M. Meldal, *J. Am. Chem. Soc.* **2001**, *123*, 2176–2181; d) M. S. South, T. A. Dice, J. J. Parlow, *Biotechnol. Bioeng.* **2000**, *71*, 51–57.
- [10] a) E. Müller, G. Péczely, R. Skoda-Földes, E. Takács, G. Kokotos, E. Bellis, L. Kollár, *Tetrahedron* **2005**, *61*, 797–802; b) N. Tsukada, Y. Ohba, Y. J. Inoue, *Organomet. Chem.* **2003**, *687*, 436–443.
- [11] a) A. K. C. Schmidt, C. B. W. Stark, *Org. Lett.* **2011**, *13*, 4164–4167; b) S. Gowrisankar, H. Neumann, M. Beller, *Angew. Chem. Int. Ed.* **2011**, *50*, 5139–5143; c) C. L. Allen, S. Davulcu, J. M. Williams, *J. Org. Lett.* **2010**, *12*, 5096–5099.
- [12] R. S. Mane, B. M. Bhanage, *J. Org. Chem.* **2016**, *81*, 4974–4980.
- [13] a) T. N. Uehara, J. Yamaguchi, K. Itami, *Asian. J. Org. Chem.* **2013**, *2*, 938–942; b) Y. J. Xie, J. H. Hu, Y. Y. Wang, C. G. Xia, H. M. Huang, *J. Am. Chem. Soc.* **2012**, *134*, 20613–20616; c) M. B. Li, Y. Wang, S. K. Tian, *Angew. Chem. Int. Ed.* **2012**, *51*, 2968–2971.
- [14] X. Zhang, W. Yanga, L. Wang, *Org. Biomol. Chem.* **2013**, *11*, 3649–3654.
- [15] a) G. Wu, Y. Li, X. Yu, Y. Gao, H. Chen, *Adv. Synth. Catal.* **2017**, *359*, 687–692; b) F. Liu, Z. Zhang, Z. Bao, H. Xing, Y. Yang, Q. Ren, *Tetrahedron Lett.* **2017**, *58*, 2707–2710; c) M. Rueping, C. Vila, A. Szadkowska, R. M. Koenigs, J. Fronert, *ACS Catal.* **2012**, *2*, 2810–2815. For oxidative *N*-demethylation, see: d) D. A. Leas, Y. Dong, J. L. Vennerstrom, D. E. Stack, *Org. Lett.* **2017**, *19*, 2518–2521; e) Y. Li, L. Ma, F. Jia, Z. Li, *J. Org. Chem.* **2013**, *78*, 5638–5646; f) Z. Dong, P. J. Scammells, *J. Org. Chem.* **2007**, *72*, 9881–9885; g) S. Thavaneswaran, P. J. Scammells, *Nat. Prod. Commun.* **2006**, *1*, 885–897. h) T. Rosenau, A. Hofinger, A. Potthast, P. Kosma, *Org. Lett.* **2004**, *6*, 541–544.
- [16] Y. Miyake, K. Nakajima, Y. Nishibayashi, *J. Am. Chem. Soc.* **2012**, *134*, 3338–3341.
- [17] X. Jia, P. Li, Y. Shao, Y. Yuan, H. Ji, W. Hou, X. Liub, X. Zhang, *Green Chem.* **2017**, *19*, 5568–5574.
- [18] For photomediated amide formation; see: a) V. Srivastava, P. K. Singh, P. P. Singh, *Tetrahedron Lett.* **2018**, *1*, 40–43; b) I. Cohen, A. K. Mishra, G. Parvari, R. Edrei, M. Dantus, Y. Eichena, A. M. Szpilman, *Chem. Commun.* **2017**, *53*, 10128–10131; c) H. Liu, L. Zhao, Y. Yuan, Z. Xu, K. Chen, S. Qiu, H. Tan, *ACS Catal.* **2016**, *6*, 1732–1736; d) T. McCallum, L. Barriault, *J. Org. Chem.* **2015**, *80*, 2874–2878.
- [19] E. Baciocchi, M. Bietti, M. F. Gerini, O. Lanzalunga, *J. Org. Chem.* **2005**, *70*, 5144–5149.
- [20] B. Majumdar, D. Sarma, T. Bhattacharya, T. K. Sarma, *ACS Sustainable Chem. Eng.* **2017**, *5*, 9286–9294.
- [21] S. Chiba, L. Zhang, J. Y. Lee, *J. Am. Chem. Soc.* **2010**, *132*, 7266–7267.
- [22] K. K. S. Sai, P. M. Esteves, E. T. da Penha, D. A. Klumpp, *J. Org. Chem.* **2008**, *73*, 6506–6512.
- [23] H. Sahoo, A. Mandal, S. Dana, M. Baidya, *Adv. Synth. Catal.* **2018**, *360*, 1099–1103.
- [24] A. Hossian, M. K. Manna, K. Manna, R. Jana, *Org. Biomol. Chem.* **2017**, *15*, 6592–6603.
- [25] A. Hossian, K. Manna, P. Das, R. Jana, *ChemistrySelect* **2018**, *3*, 4315–4318.
- [26] A. Singh, K. Teegardin, M. Kelly, K. S. Prasad, S. Krishnan, J. D. Weaver, *J. Organomet. Chem.*, **2015**, *776*, 51–59.



Cite this: *Chem. Commun.*, 2021, 57, 10842

The emergence of the C–H functionalization strategy in medicinal chemistry and drug discovery

Ranjan Jana, *^a Hasina Mamataj Begam^a and Enakshi Dinda^b

Owing to the market competitiveness and urgent societal need, an optimum speed of drug discovery is an important criterion for successful implementation. Despite the rapid ascent of artificial intelligence and computational and bioanalytical techniques to accelerate drug discovery in big pharma, organic synthesis of privileged scaffolds predicted *in silico* for *in vitro* and *in vivo* studies is still considered as the rate-limiting step. C–H activation is the latest technology added into an organic chemist's toolbox for the rapid construction and late-stage modification of functional molecules to achieve the desired chemical and physical properties. Particularly, elimination of prefunctionalization steps, exceptional functional group tolerance, complexity-to-diversity oriented synthesis, and late-stage functionalization of privileged medicinal scaffolds expand the chemical space. It has immense potential for the rapid synthesis of a library of molecules, structural modification to achieve the required pharmacological properties such as absorption, distribution, metabolism, excretion, toxicology (ADMET) and attachment of chemical reporters for proteome profiling, metabolite synthesis, etc. for preclinical studies. Although heterocycle synthesis, late-stage drug modification, ¹⁸F labelling, methylation, etc. *via* C–H functionalization have been reviewed from the synthetic standpoint, a general overview of these protocols from medicinal and drug discovery aspects has not been reviewed. In this feature article, we will discuss the recent trends of C–H activation methodologies such as synthesis of medicinal scaffolds through C–H activation/annulation cascade; C–H arylation for sp²–sp² and sp²–sp³ cross-coupling; C–H borylation/silylation to introduce a functional linchpin for further manipulation; C–H amination for N-heterocycles and hydrogen bond acceptors; C–H fluorination/fluoroalkylation to tune polarity and lipophilicity; C–H methylation: methyl magic in drug discovery; peptide modification and macrocyclization for therapeutics and biologics; fluorescent labelling and radiolabelling for bioimaging; bioconjugation for chemical biology studies; drug-metabolite synthesis for biodistribution and excretion studies; late-stage diversification of drug-molecules to increase efficacy and safety; cutting-edge DNA encoded library synthesis and improved synthesis of drug molecules *via* C–H activation in medicinal chemistry and drug discovery.

Received 28th July 2021,
Accepted 7th September 2021

DOI: 10.1039/d1cc04083a

rsc.li/chemcomm

1. Introduction

In the era of globalization and the emergence of pharmacovigilance, the development of high-quality therapeutics at optimum speed and affordable price is the utmost challenge to meet urgent societal needs.¹ Currently, drug discovery programs are increasingly relying on artificial intelligence and machine learning techniques for decision-making and automation in preclinical studies.² Hence, the integration of several fields such as bioinformatics,

molecular and clinical biology, medicinal chemistry, chemical biology, and pharmacology can accelerate and increase the positive outcome of drug discovery. Despite such developments, organic synthesis is still a key but rate-limiting step in drug discovery.³ Furthermore, studies from big pharma such as AstraZeneca, GlaxoSmithKline, and Pfizer and academic researchers revealed that medicinal chemistry programs are based on a limited number of chemical reactions resulting in overpopulated chemical space with structurally similar scaffolds which increases the risk of off-target toxicity.⁴ Therefore, assimilation of cutting-edge synthetic strategies for the synthesis and diversification of novel medicinal scaffolds is in high demand.

There has been an impressive array of C–H activation methodologies developed in the last decade through which a carbon–hydrogen bond is converted to a functional group for

^aOrganic and Medicinal Chemistry Division, CSIR-Indian Institute of Chemical Biology, 4 Raja S. C. Mullick Road, Kolkata-700032, India.

E-mail: rjana@iicb.res.in

^bDepartment of Chemistry and Environment, Heritage Institute of Technology, Kolkata-700107, India

further manipulation.⁵ Despite several challenges associated with this strategy, the opportunity to synthesize privileged scaffolds through a novel disconnection approach is enormous. Typically, a metal-complex coordinates to a polar group and inserts into the proximal C–H bond to generate an organometallic complex. Subsequently, it undergoes cross-coupling or substitution reactions to furnish a C–C or C–X (X = heteroatom) bond.⁶ The major advantages are as follows: (a) this technology is capable of activating distal *meta*- or *para*-C(sp²)–H and β -, γ - or δ -C(sp³)–H bonds using a suitable directing group;⁷ (b) exceptional compatibility to halogens and other polar functional groups offers a unique opportunity for further diversification which is useful for structure–activity relationship (SAR) studies; (c) mild reaction conditions are suitable for the late-stage functionalization of densely functionalized molecules and natural products; (d) innate

and guided late-stage stapling of molecular probes (fluorescent, radioatom, photoaffinity, *etc.*) with the pharmacophore accelerates mechanism of action studies; (e) the biomimetic catalytic approach for C–H oxidation studies leads to the synthesis of easily inaccessible metabolites and identification of the metabolic hot spot. Still, there are several drawbacks of C–H activation technology such as installation and removal of the directing group, harsh reaction conditions, residual metal contaminants, scale-up issues for process development, *etc.* To circumvent these drawbacks, transient, traceless and inherent directing group or even non-directed C–H activation strategies were unveiled.⁸ Cross dehydrogenative coupling of the heterocycles is an attractive strategy wherein no functional groups except C–H bonds are required in both coupling partners and the reaction takes place through the extrusion of hydrogen gas. Owing to the stringent regulation from the environmental agencies, sustainability is also another dimension in organic synthesis to reduce environmental footprints.⁹ Keeping this in mind, exploration of visible light photoredox-catalysis¹⁰ and synthesis in a flow reactor¹¹ exhibit an impact on C–H activation technology. Furthermore, a feedback-based multidisciplinary approach can translate a therapeutic molecule from bench to bedside at maximum speed and affordable price.

Once a drug discovery program is conceived, the pharmacoinformatics (PI) team plays a critical role in the rapid virtual screening of compound libraries to identify a probable structure of a hit molecule using ligand-based drug design (LBDD),¹² structure-based drug design (SBDD),¹³ and fragment-based drug design (FBDD) strategies.¹⁴ This information is useful to the organic chemist in the next step for the development of new methods and synthesis of a library of molecules. This is one of the most time-consuming steps to synthesize the right molecule with suitable pharmacological properties. Particularly, the integration of multiple data into a single molecule against multi-factorial diseases such as neurodegenerative or autoimmune diseases is extremely challenging. Hence, the adaptation of cutting-edge synthetic technologies such as C–H bond activation is important to accelerate this process. The synthesized molecular libraries are



Ranjan Jana

Ranjan Jana received his PhD from IACS under the supervision of Prof. B. C. Ranu. Then he moved to Bar-Ilan University, Israel for postdoctoral studies with Prof. S. Braverman. Subsequently, He joined the Tunge group at the University of Kansas and the Sigman group at the University of Utah. He started his independent research career at CSIR-Indian Institute of Chemical Biology as a senior scientist in 2012 and was promoted to the role of principal scientist in 2015. His research interest is the divergent synthesis of privileged medicinal scaffolds and active pharmaceutical ingredients (APIs) through tandem C–H activation, alkene difunctionalization and decarboxylative cross-coupling reactions. He has received a Ramanujan fellowship and was elected as a fellow of the West Bengal Academy of Science and Technology.

Ranjan Jana received his PhD from IACS under the supervision of Prof. B. C. Ranu. Then he moved to Bar-Ilan University, Israel for postdoctoral studies with Prof. S. Braverman. Subsequently, He joined the Tunge group at the University of Kansas and the Sigman group at the University of Utah. He started his independent research career at CSIR-Indian Institute of Chemical Biology as a senior scientist in 2012 and was promoted to the role of principal



Hasina Mamataj Begam

development of copper- and cobalt-catalyzed electrophilic C–H amination reactions.

Hasina Mamataj Begam was born in West Bengal, India. In 2014, she received her BSc degree from Malda College affiliated to the University of Gour Banga. In 2016, she received her MSc degree from the University of Gour Banga, where she received a gold medal. Since 2016, she has been continuing her doctoral studies under the supervision of Dr Ranjan Jana at CSIR-Indian Institute of Chemical Biology. Her research project includes the



Enakshi Dinda

she is working as an assistant professor at the Heritage Institute of Technology, Kolkata.

Enakshi Dinda received her BSc degree in chemistry from Haldia Government College in 2003. She completed her post-graduation in Vidyasagar University with specialization in organic chemistry in 2005. She received her PhD degree from IACS in 2011. During her doctoral studies, she worked in the interdisciplinary field of organic chemistry and materials science. She joined Rajabazar Science College as a D. S. Kothari post-doctoral fellow in 2015. Presently,

screened *in vitro* and *in vivo* or in a cell or animal model and feedback is provided to the organic chemist for further modification of the core structure. The identification of a hit molecule to lead optimization requires extensive organic synthesis for structure–activity relationship (SAR) and quantitative structure–activity relationship (QSAR) studies, attachment of molecular probes (fluorescent, radioatom, photoaffinity, *etc.*) for activity- and affinity-based protein profiling (ABPP),¹⁵ target pull-down, non-specific interaction estimation, *etc.* (Fig. 1). Subsequently, the scale-up process is developed under GMP/GLP facilities to generate a sufficient amount of the lead molecule for complete pharmacological profiling, *i.e.* pharmacokinetics (PK) and pharmacodynamics (PD) studies and chronic safety in an animal. At the final step of preclinical studies, the inventors proceed for an Investigational New Drug (IND) application.

In this review, we will discuss the recent developments of some chemical transformations through C–H activation which are relevant to the drug discovery program. It will be conceptual rather than comprehensive describing the recent applications of C–H functionalization in discovery phases with representative examples. These selected chemical transformations are (1) N-heterocycle synthesis through C–H activation/annulation cascade; (2) C–H arylation; (3) C–H borylation/silylation; (4) C–H amination; (5) C–H fluorination/fluoroalkylation; (6) C–H methylation: methyl magic in drug discovery; (7) peptide modification and macrocyclization; (8) fluorescent labelling and radiolabelling for bioimaging; (9) bioconjugation; (10) drug-metabolite synthesis; (11) late-stage diversification of drug-molecules; (12) DNA encoded library

synthesis and (13) improved synthesis of drug molecules *via* C–H activation.

2. N-Heterocycle synthesis through C–H activation/annulation cascade

Chemical methodology and library development (CMLD) for the synthesis of a diversified and complex molecular framework is the foundation of drug discovery programs to identify potent and selective hit molecules by high throughput screening of a large number of compound libraries. Nitrogen heterocycles are among the most significant structural components of pharmaceuticals.¹⁶ Analysis of the database of U.S. FDA-approved drugs reveals that 59% of unique small-molecule drugs contain a nitrogen heterocycle.¹⁷ This could be attributed to the fact that their solubility, lipophilicity, polarity and hydrogen bonding capacity can be modified easily during the optimization of the ADMET properties. Rapid synthesis and diversification of various heterocycles in drugs can be accomplished by applying modern techniques such as metal-catalyzed cross-coupling reactions.¹⁸ Recently, C–H activation has emerged as a powerful tool for the synthesis of heterocyclic molecules.¹⁹ In the last few decades, an aniline and benzoic acid moiety has been widely explored for sp^2 C–H bond functionalization.²⁰ While C–H functionalization of electron-rich anilines predominantly proceeds through electrophilic *ortho* metalation, the benzoic acids proceed through a distinct concerted metalation-deprotonation

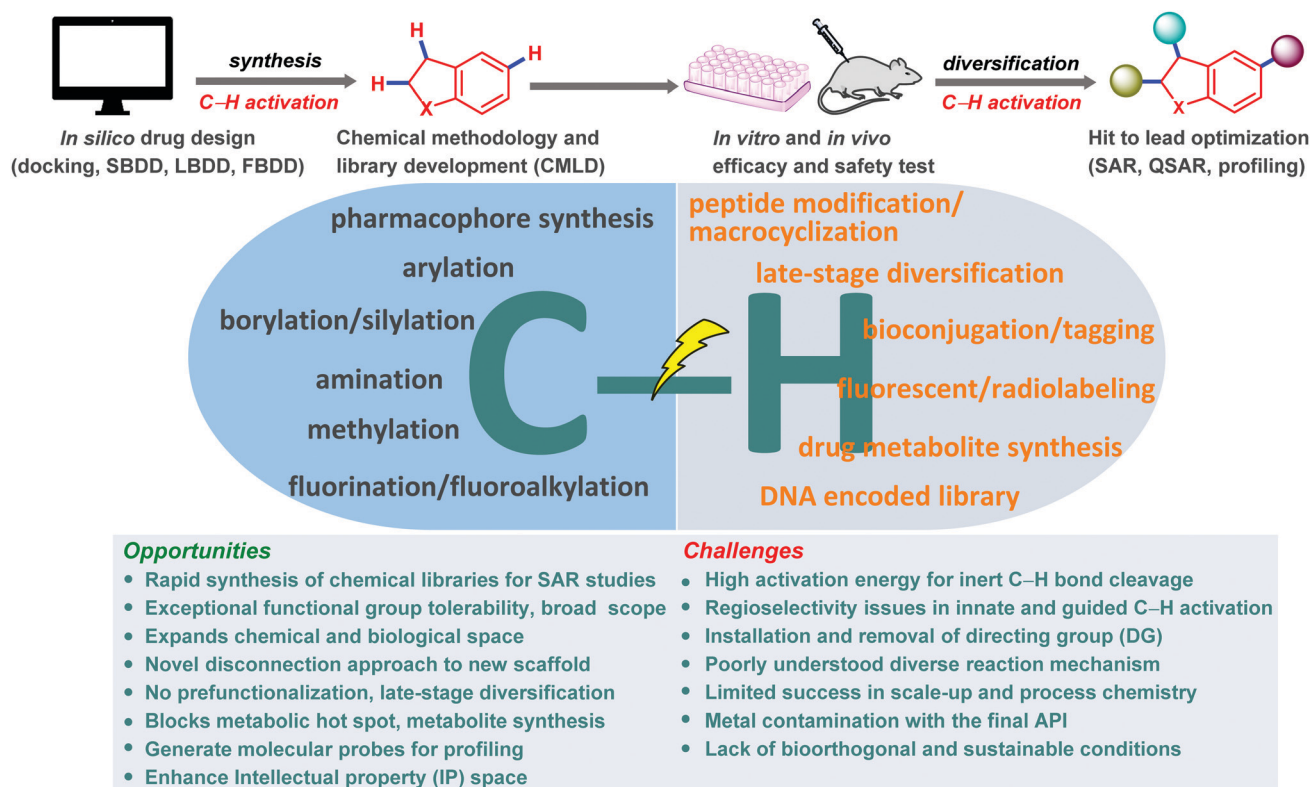


Fig. 1 C–H activation in medicinal chemistry and drug discovery.

(CMD) mechanistic pathway.²¹ Although anilines provide direct access to a plethora of N-heterocycles, we will discuss here the synthesis and late-stage diversification of medicinally relevant indoles²² through C–H bond functionalization as a representative example.²³ Traditionally, the indole core is synthesized *via* Fischer, Larock, Buchwald and Hegedus methods from aryl hydrazines or 2-haloanilines (Scheme 1a).²⁴ Owing to their limited commercial availability and high cost, the transition metal-catalyzed direct synthesis of indole from anilines or protected anilines obviating rigorous prefunctionalization steps has been explored in the last few decades (Scheme 1b and c). In this vein, two distinct strategies have been well explored: (a) intramolecular cyclization of *N*-arylamines or -imines and (b) intermolecular cyclization of anilines and alkynes or alkenes.²⁵ A catalyst-controlled scaffold diversification to indoline,²⁶ annulative π -extension to carbazole²⁷ and late-stage C–H functionalization²⁸ at every carbon beyond C2

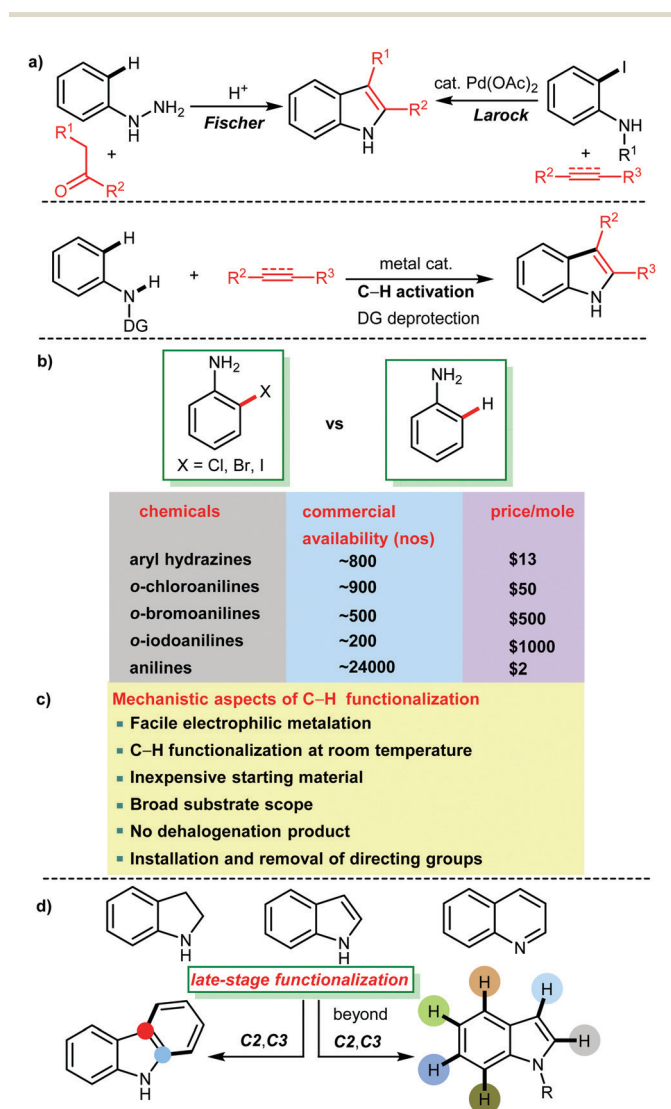
and C3 have been achieved (Scheme 1d). Hence, a vast number of diverse libraries of compounds are generated for comprehensive structure–activity relationship (SAR) studies. This example manifests the power of C–H functionalization in medicinal chemistry and drug discovery.

3. C–H arylation for drug scaffolds

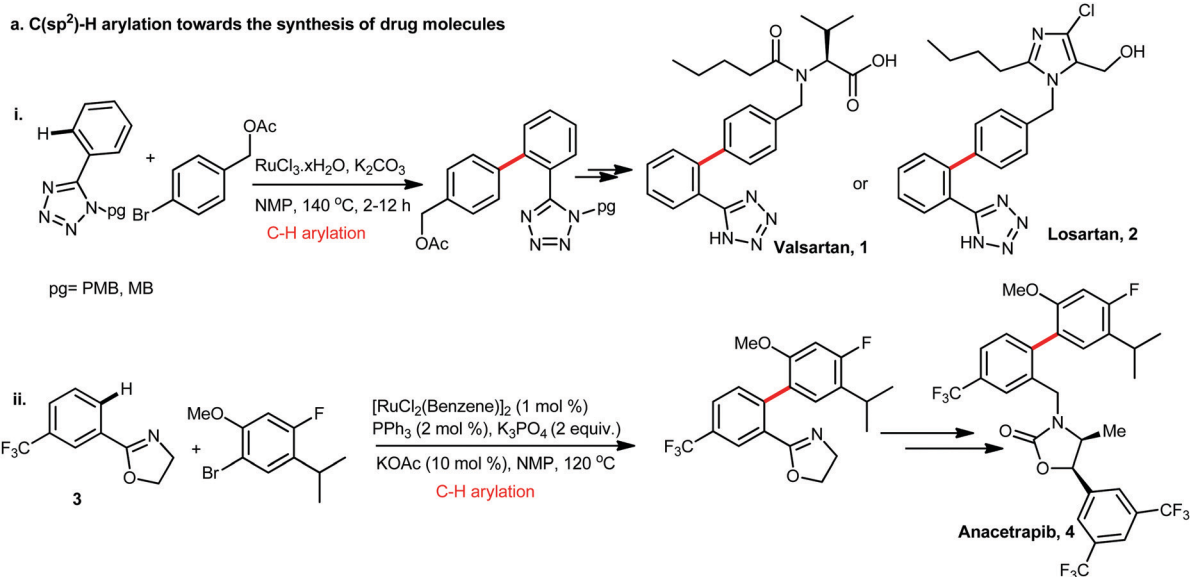
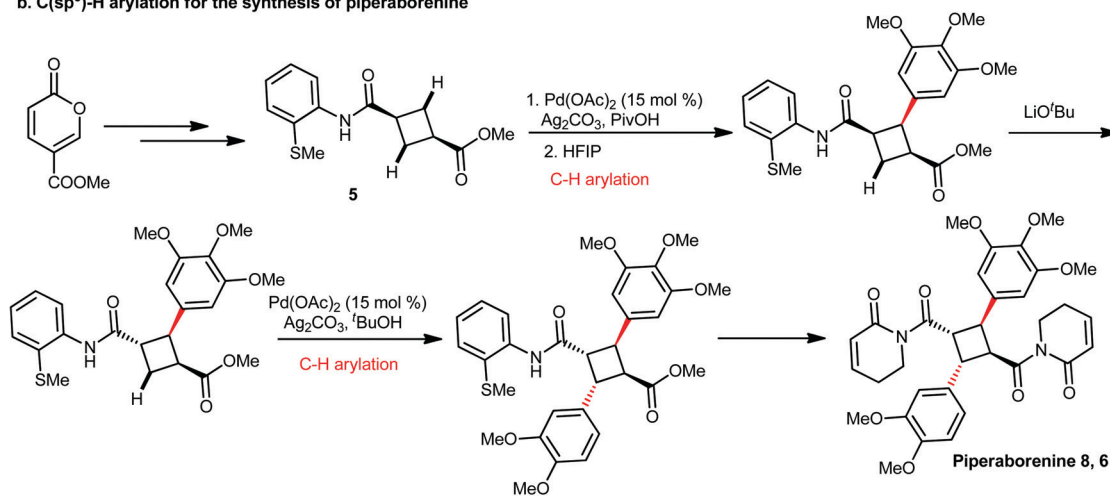
Biaryl moiety is one of the most prevalent structural motifs found in a range of therapeutics including antibiotics, analgesics, and anti-inflammatory, neurological and antihypertensive drugs.²⁹ The prevalence of the biaryl scaffold in pharmaceuticals has been rationalized by its ability to interact with a range of functional groups that are widespread in biological targets.³⁰ Because of its selective binding to proteins and other biological targets, the biaryl scaffold is regarded as a privileged structure. Hence, a sustained effort including palladium-catalyzed Suzuki–Miyaura decarboxylative cross-coupling has been dedicated for the stapling of two aryl moieties together. In the last few decades, C–H arylation using a coordinating/directing group with aryl halides or pseudohalides has been well explored.³¹ In this vein, palladium, ruthenium(II)-catalyzed synthesis of angiotensin-II receptor blockers such as Valsartan (1) and Losartan (2) are noteworthy (Scheme 2ai).³² Similarly, copper(II)/hypervalent iodine combination,³³ nickel-catalyzed arylation,³⁴ and silver-catalyzed Minisci-type arylation of heteroaromatics³⁵ are important developments in this direction. A cyclometalated ruthenium complex has shown remarkable reactivity for the late-stage arylation of drug scaffolds.³⁶ The synthesis of the biaryl core of Anacetrapib (4, Scheme 2aii) (potent activity against hypercholesterolemia found by Merck) was reported by the Ouellet group at Merck *via* Ru-catalyzed C(sp²)-H arylation using the oxazoline (3) directing group.³⁷ Piperarborenines are an important class of natural products exhibiting *in vitro* cytotoxicity against P-388, HT-29 and A549 cancer cell lines.³⁸ The Baran group developed a palladium-catalyzed total synthesis of Piperarborenine 8 (6, Scheme 2b) through two sequential C(sp³)-H arylations of the cyclobutane core (5) with good stereocontrol.³⁹

4. C–H borylation/silylation in medicinal chemistry

Since the ready acceptance of Suzuki–Miyaura cross-coupling in all branches of chemical synthesis, the formation of a carbon–carbon bond has become a major thrust area of research.⁴⁰ Recently, an ample number of synthetic methodologies for borylation of an inert C–H bond have been developed which can be cross-coupled for carbon–carbon and carbon–heteroatom bond formation.⁴¹ Hartwig, Smith III, Chattopadhyay and others have made significant contributions to the research of rhodium- and iridium-catalyzed C–H borylation reactions.⁴² The most important feature of iridium-catalyzed C–H borylation chemistry is that, besides directed *ortho*-borylation,⁴³ a steric-induced C–H borylation takes place at the remote *meta* position with respect to substitution without the need of any directing group.⁴⁴

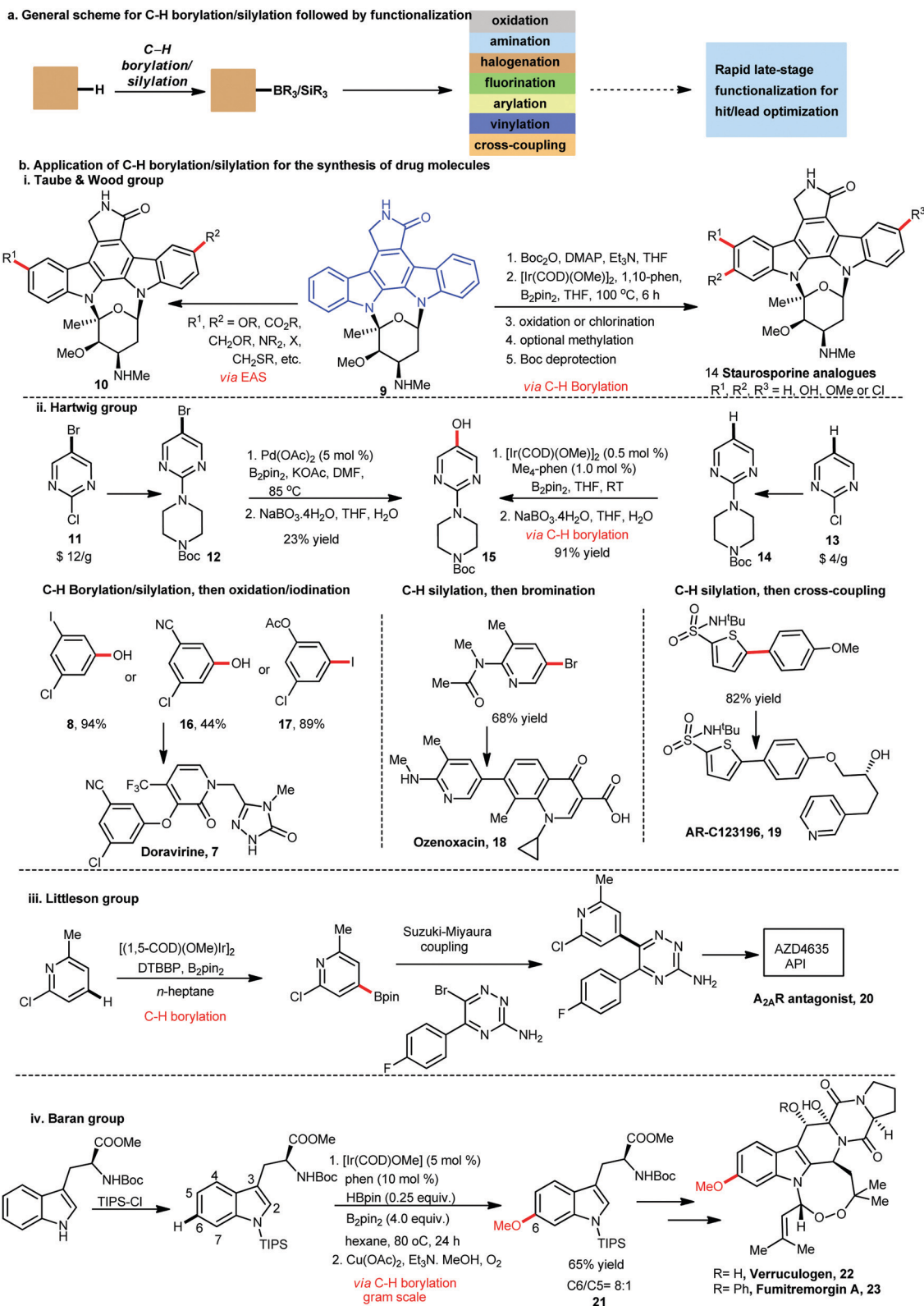


Scheme 1 (a) Chronological development of indole synthesis. (b) Commercial availability (Reaxys) and price (Sigma-Aldrich) of starting materials. (c) Mechanistic considerations. (d) Representative N-heterocycles and late-stage functionalization of indole.

a. C(sp²)-H arylation towards the synthesis of drug moleculesb. C(sp³)-H arylation for the synthesis of piperaborenineScheme 2 C(sp²)-H and C(sp³)-H arylation for the synthesis of drug molecules.

This methodology is particularly useful to expand the chemical space of pharmaceuticals since biaryls with *ortho*- and *para*-substitution are densely populated over a narrow chemical space. Iridium-catalyzed C-H borylation introduces a functional handle into the molecular backbone for further diversification through cross-coupling reactions (Scheme 3a). Gratifyingly, iridium-catalyzed C-H borylation is one of the most successful synthetic methodologies applied for the synthesis of several natural products and large-scale process development. For example, a non-nucleoside reverse transcriptase inhibitor (NNRTI), Doravirin (7), has been synthesized on a kilo-scale through a reliable C-H borylation which is currently under phase III clinical trials for the treatment of HIV infection.⁴⁵ The crucial intermediate 3-chloro-5-iodo-phenol (8) was accessed through a *meta*-selective C-H borylation-oxidation of commercially available 3-iodo-chlorobenzene with 0.8–1.0 mol% iridium(i) catalyst. Staurosporine (9, Scheme 3b) is among the most potent naturally occurring kinase inhibitors and has been proved to be a lead compound for numerous drug

development efforts in several therapeutic areas.⁴⁶ The indole-carbazole (ICZ) moiety of 9 (marked in blue) is crucial for binding to the adenosine triphosphate (ATP) pocket of kinases.⁴⁷ Taube and Wood reported the synthesis of a library of 14 compounds through late-stage modifications of this core for structure-activity relationship (SAR) studies.⁴⁸ They incorporated an Ir-catalyzed C-H borylation in their multistep reaction sequence. Compared to the previously reported electrophilic aromatic substitution (EAS) (which is dependent on the electronic nature and can functionalize at only two positions (10)), this C-H borylation (regioselectivity is dictated by steric factors) provided a larger number of derivatives at a time. For example, this borylation technique afforded mono-borylation at either of the three positions or diborylation at two of the three positions, giving a total of 5 borylated products from which they were able to synthesize a total of 14 staurosporine derivatives by further functionalization. For the synthesis of GPR119 (a potential anti-diabetic), a research group at AstraZeneca prepared a crucial intermediate



Scheme 3 (a) General schemes for C–H borylation/silylation, followed by functionalizations. (b) C(sp²)–H borylation/silylation for the synthesis of drug molecules.

(15, Scheme 3bii), starting from 5-bromo-2-chloropyrimidine **11** (costing around \$ 12 g⁻¹), followed by Pd-catalyzed borylation using the bromo substrate **12** and then oxidation in only 23% yield.

The Hartwig group successfully synthesized the intermediate **15** starting from a cheap starting material, 2-chloropyrimidine, **13** (costing around \$ 4 g⁻¹), followed by Ir-catalyzed C–H borylation

of **14** and then oxidation in 91% yield.⁴⁹ The Hartwig group also developed a catalytic system combining $[\text{Ir}(\text{cod})(\text{OMe})_2]$ and 2,9-Me₂-phenanthroline for the silylation of aryl C–H bonds.⁵⁰ Then they applied this catalyst for the synthesis of intermediates for Doravirin, Ozonoxacin and ARC123196. Doravirin **7**, an anti-HIV drug, can be synthesized from any of the three intermediates (**8**, **16**–**17**). These intermediates are obtained by Ir-catalyzed C–H borylation/silylation, followed by oxidation/iodination, **8**, **16** and **17** (the first one was developed by the Campeau group and the last two were developed by the Hartwig group). The Hartwig group also used this C–H silylation method for the synthesis of intermediates of Ozenoxacin **18** (antibiotic) and ARC123196 **19** (treatment for asthma). AZD4635 (**20**, Scheme 3biii) is an A_{2A}R antagonist currently under clinical trials for the treatment of solid tumors.⁵¹ The Littleton group developed a concise and operationally robust route for the synthesis of a crucial intermediate in 30% overall yield in five steps, from which AZD4635 can be obtained by recrystallization.⁵² Remarkably, they were able to produce 6.5 kg of the active pharmaceutical ingredient (API) using their protocol which involved iridium catalyzed C–H borylation (76% yield) for the subsequent Suzuki–Miyaura biaryl coupling.

Verrucologen **22** and Fumitremorgin A **23** are bioactive alkaloids that contain a unique eight-membered endoperoxide. These polycyclic tryptophan-based alkaloids were first identified for their tremor-inducing activity in mice and they showed activity against multi-drug resistant (MDR) cancer cell lines and also against HIV.⁵³ The Baran group reported the first total synthesis of two important natural products Verrucologen and Fumitremorgin A in 11 and 12 steps, respectively.⁵⁴ These synthetic strategies involved an efficient iridium-catalyzed C–H borylation, followed by Chan–Lam reaction, to get a 6-methoxytryptophan derivative (**21**, Scheme 3biv). This method was very selective to functionalize the C6 position of an *N*,C3-disubstituted indole for the synthesis of indole based natural products and pharmaceuticals.

The Maiti group reported the formal synthesis of the anti-cancer drug TAC101 using a Pd-catalysed *meta* C–H silylation.⁵⁵

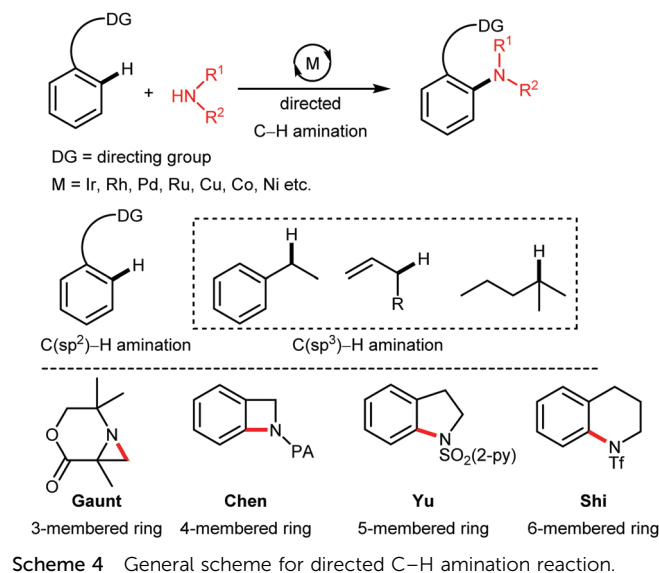
5. C–H amination in drug discovery

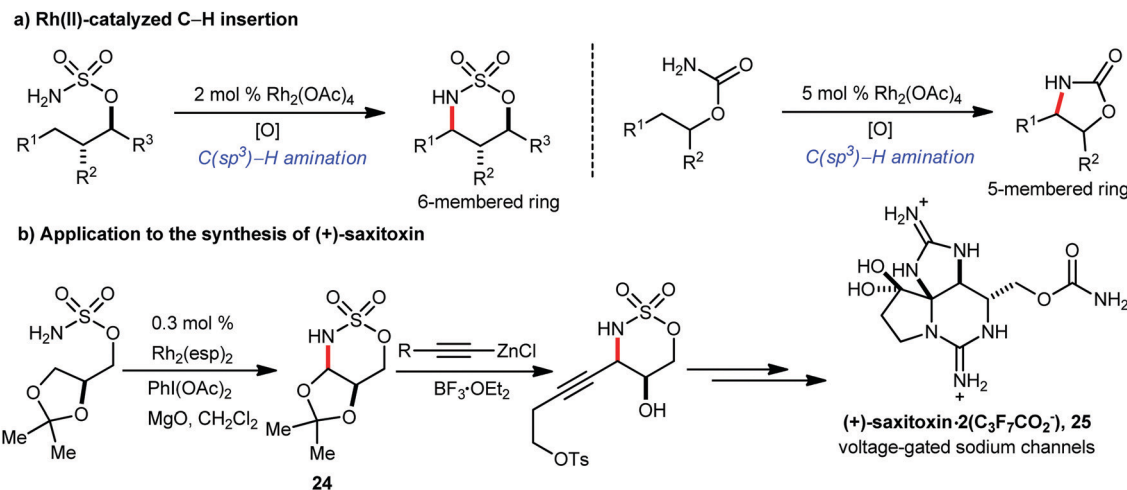
In the biological system, enzymes can oxidize unreactive C–H bonds to alcohols or phenols during biosynthesis and drug metabolism.⁵⁶ However, analogous aminations of C–H bonds are not possible. Owing to the biological activity of nitrogen-containing therapeutic agents and clinically useful natural products, the development of C–N coupling reactions is extremely important in medicinal chemistry.⁵⁷ In fact, parallel to the Suzuki–Miyaura cross-coupling reaction for carbon–carbon bond formation, the C–N coupling reaction has been proved as an indispensable tool in medicinal and process chemistry.⁵⁸ The introduction of an amine moiety into the pharmacophore improves the pharmacokinetics and therapeutic index by increasing polarity, pH-dependent bio-distribution and hydrogen-bonding ability.⁵⁹ One striking illustration is the conversion of Erythromycin to Azithromycin *via* the transformation of the ketone to the corresponding –N(Me)CH₂– group that

can be administered once daily, thus minimizing the treatment time.⁶⁰ Hence, the C–N bond-forming reaction has been continuously evolved through the development of copper-mediated Ullmann type coupling,⁶¹ palladium-catalyzed Buchwald–Hartwig coupling,⁶² copper-mediated/catalyzed oxidative Chan–Evans–Lam coupling⁶³ and the latest direct C–H amination reactions.⁶⁴ Typically, a directing group is used in the substrate for the guided intermolecular C–H amination. Innate C–H amination of benzylic, allylic or even unbiased aliphatic C–H bonds has also been explored.⁶⁵ Furthermore, a wide range of medically relevant cyclic amines starting from three-membered aziridines,⁶⁶ four-membered β-lactams⁶⁷ and benzazetidines,⁶⁸ five-membered indoles,⁶⁹ indolines,⁷⁰ carbazoles, and pyrrolidines, six-membered quinolones and piperidines,⁷¹ *etc.* have been developed (Scheme 4).

A remarkable development in this direction is the rhodium(III)-catalyzed intramolecular nitrene insertion to the proximal inert C–H bonds, furnishing five- or six-membered cyclic amine derivatives.⁷² The Rh₂(esp)₂ catalyst (known as the Du Bois catalyst) is an extremely efficient and general catalyst for C–H amination and nitrene insertion to 3° C–H bonds, which took place with just 0.15 mol% catalyst loading providing quantitative conversion (Scheme 5a). The reliability of this catalytic system was further demonstrated through a concise synthesis of bis-guanidinium toxin (+)-Saxitoxin (STX) **25** which was used for the identification, characterization and study of voltage-gated sodium channels (vg-Na⁺ channels).⁷³ A C–H amination of a glycerol derived enantiomerically pure sulfamate ester (**24**, Scheme 5b) was used as a key step to access the cyclized product which provided (+)-saxitoxin (STX) through subsequent steps.

Another important aspect of C–H amination is the direct introduction of the azide group into the molecule which can be used as a nitrene precursor or for Huisgen ‘click’ cycloadditions and Staudinger ligation reactions. Hence, synthesis of hybrid molecules and bioconjugation of fluorescent or photoreactive probes for affinity-based protein profiling in chemical biology can be performed with minimum perturbation of the lead molecule.



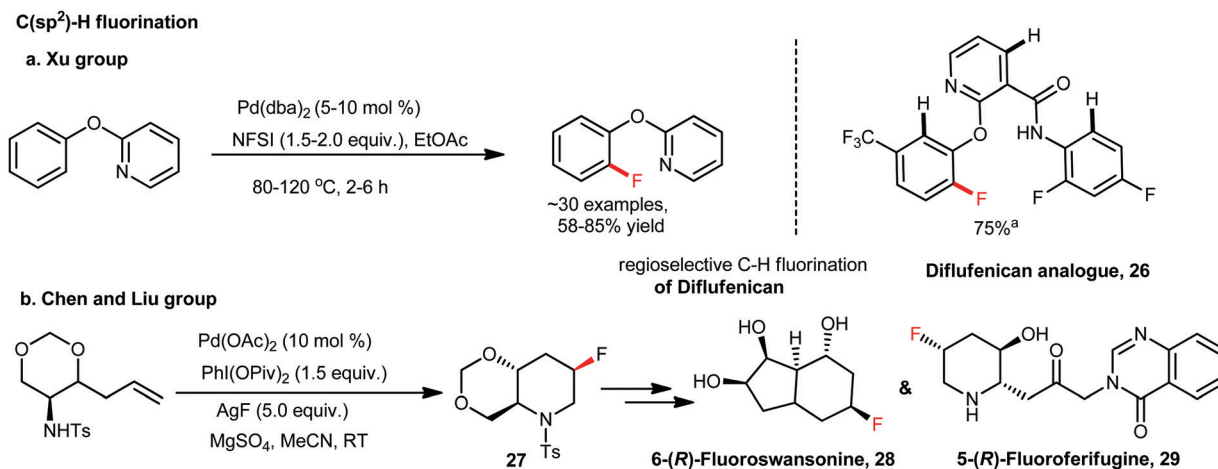


Scheme 5 (a) Rh-Catalysed C–H nitrene insertion. (b) Application to the synthesis of (+)-saxitoxin.

6. C–H fluorination/fluoroalkylation in drug discovery

Fluorine is a magical element frequently used in medicinal chemistry and different phases of drug discovery due to its distinct electronic and physical properties.⁷⁴ Due to the similarity in size, replacement of a hydrogen atom with fluorine results in minimum perturbation of the hit molecule, whereas it influences the potency, conformation, metabolism, membrane permeability, *etc.*⁷⁵ Incorporation of a nonradioactive ¹⁹F atom into the drug molecule offers a unique opportunity for biodistribution, drug metabolism, and excretion property studies *via* high-performance liquid chromatography (HPLC) or liquid chromatography mass spectrometry (LCMS), target protein–drug interaction studies *via* nuclear magnetic resonance (NMR) techniques, magnetic resonance imaging (MRI) contrast agents for clinical diagnosis, *etc.* Furthermore, incorporation of radioactive ¹⁸F into a bioactive molecule or a patient provides an opportunity for positron emission tomography (PET) imaging in medicine, oncology, cardiology, neuroscience and drug development (for further details see Section 9.3). Owing to its

potential as therapeutics and diagnostics, the development of fluorine-containing theranostics is growing.⁷⁶ However, from the mechanistic standpoint, the formation of a carbon–fluorine bond is extremely challenging due to the strong metal–fluorine bond and sluggish reductive elimination. To circumvent this issue, high-valent palladium(IV),⁷⁷ copper(III),⁷⁸ Au(I)/Au(III) redox cycle,⁷⁹ and nickel(III)/(IV)⁸⁰ complexes have been developed which undergo a facile reductive elimination to furnish a carbon–fluorine bond. With the advent of novel catalytic systems, nucleophilic, electrophilic and radical fluorination reactions have been explored. Furthermore, more sustainable Mn(III)/porphyrin,⁸¹ photoredox catalysis,⁸² *etc.* have also been explored. Recently, excellent reviews have been published in the literature.⁸³ The Xu group developed a Pd-catalysed facile and site-selective C–H bond fluorination of phenols using the 2-pyridyloxy group as the auxiliary and NFSI as the fluorinating reagent.⁸⁴ Furthermore, late-stage C–H bond fluorination of bioactive 2-phenoxy nicotinate derivatives such as Diflufenican was also implemented successfully under these conditions to obtain the fluoro-Diflufenican analogue (26, Scheme 6a). Remarkably, a mono-fluorinated product was exclusively obtained



Scheme 6 C(sp²)-H fluorination for the synthesis of drugs or drug analogues.

from the 2-pyridyloxy-directed activation at the sterically less hindered C–H bond under these conditions. The Chen and Liu groups developed an efficient synthesis of the fluoro-piperidine core (27, Scheme 6b) through Pd-catalysed aminofluorination of alkenes with high diastereoselectivity (93:7).⁸⁵ Then they applied this fluoropiperidine core for the first total synthesis of two important fluorinated alkaloids 6-(*R*)-fluoroswansonine 28 and 5-(*R*)-fluorofebrifugine 29. Swainsonine is an anticancer alkaloid having the potential to treat glioma⁸⁶ and gastric carcinoma,⁸⁷ whereas febrifugine⁸⁸ is a quinazolinone alkaloid possessing antimalarial properties.

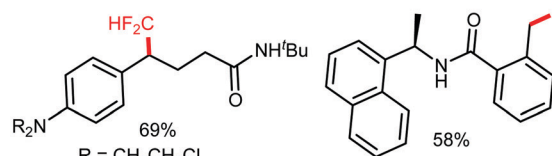
The difluoromethyl (CF₂H) group is important in drug discovery programs because of its isosteric nature to the OH and SH groups and it can act as a lipophilic H-bond donor.⁸⁹ As a result, there are numerous marketed drugs containing the CF₂H group. Roflumilast (for the treatment of inflammatory conditions of the lungs) and Pantoprazole (for the treatment of erosive esophagitis in patients with gastroesophageal reflux) are two frequently prescribed –CF₂H containing marketed drugs. Therefore, methods for the late-stage introduction of the CF₂H motif into complex organic molecules or drug molecules are highly desirable. The Cao and Liu groups reported the first catalytic benzylic C–H difluoromethylation which is simple, selective and scalable.⁹⁰ Their methodology involved copper-catalyzed benzylic C–H difluoromethylation of *N*-chlorocarboxamides and *N*-chloro-carbamates using a zinc reagent as a nucleophilic difluoromethyl source at room temperature (Scheme 7a). This methodology was also applied for the late-stage difluoromethylation of two bioactive molecules such as Chlorambucil and a protease inhibitor to obtain the analogues 30 and 31, respectively. Overcoming the challenges of remote functionalization, the Zhao group developed an efficient ruthenium-catalyzed *para*-selective C–H difluoromethylation of anilides, indolines and tetrahydroquinolines which they applied for the synthesis of a difluoromethylated Carprofen analogue (32, Scheme 7b).⁹¹ The Qing group reported a copper-mediated oxidative C–H difluoromethylation of a variety of heteroarenes using TMSCF₂H as the difluoromethyl source.⁹²

They observed that 9,10-phenanthrenequinone (PQ) plays a crucial role as an oxidant to the success of this difluoromethylation. Their protocol offers an expedient and regioselective synthesis of various difluoromethylated *N*- and/or *O*(*S*)-containing heteroarenes, which cannot be easily accessed by radical difluoromethylation. Under these conditions, the Neosalvianen (the natural product isolated from *Salvia miltiorrhiza*) analogue 33 was difluoromethylated in 85% yield (Scheme 7c). Lou and Xu also developed a novel palladium-catalyzed highly *para*-selective C–H difluoromethylation of various aromatic carbonyls such as aromatic ketones and benzoates using ethyl bromodifluoroacetate as the difluoromethyl source (Scheme 7d).⁹³ They demonstrated that the coordination of Pd with the carbonyls was responsible for the high *para*-selectivity in their method. They also implemented their methodology for the late-stage difluoromethylation of several complex bioactive compounds, *e.g.* Ketoprofen 34, Fenofibrate 35 and Octabenzene 36, analogues.

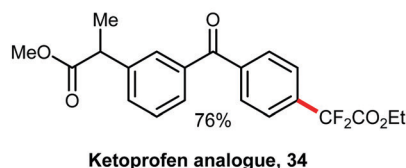
Trifluoroalkylation is also an extremely important transformation frequently used in medicinal chemistry and drug discovery. Installation of the fluoroalkyl group at the metabolic hot-spot increases its pharmacokinetic properties and stability from the metabolic degradation by P450 oxidases *in vivo*. There has been tremendous progress in the installation of trifluoro- and difluoro-methyl groups directly into the organic backbone through a radical pathway.⁹⁴ Baran has developed and commercialized several zinc reagents which spontaneously liberate trifluoromethyl and difluoromethyl radicals for the subsequent reaction.⁹⁵ The Sanford group reported the design and synthesis of a new stable Ni(IV)-complex that mediated C(sp²)-H trifluoromethylation reactions.⁹⁶ Initially, they applied this catalyst in a stoichiometric amount for C–H trifluoromethylation. Subsequently, they successfully developed a catalytic method for the C–H trifluoromethylation of electron-rich arene and heteroarene substrates. This catalytic system was also applied for the C(sp²)-H trifluoromethylation of the bioactive Tadalafil to achieve the trifluoromethylated analogue 37 in reasonable yield (Scheme 8a). The Cook group reported a mild benzylic C–H trifluoromethylation using Grushin's reagent [Cu(bpy)(CF₃)₃]

C(sp²)-H difluoromethylation

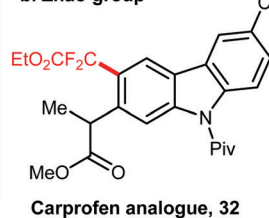
a. Cao and Liu group



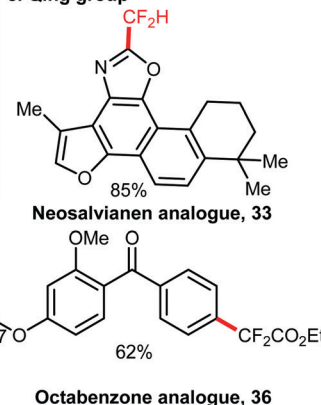
d. Lou and Zhu group



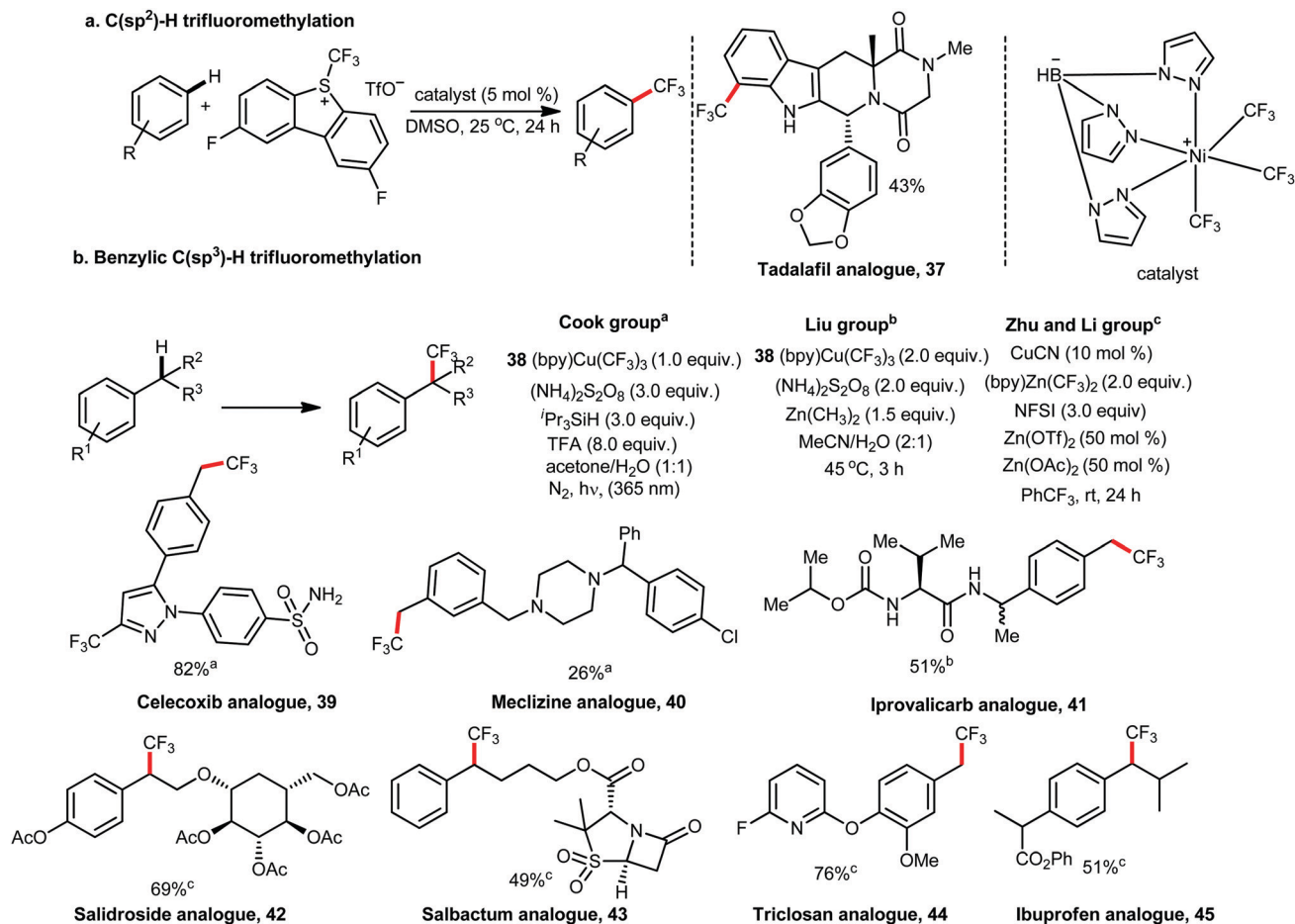
b. Zhao group



c. Qing group



Scheme 7 C(sp²)-H difluoromethylation for the synthesis of drug analogues.

Scheme 8 C(sp²)-H trifluoromethylation for the synthesis of drug analogues.

38 as the 'CF₃' source with high selectivity for the least hindered hydrogen atom.⁹⁷ The reaction furnished mono-trifluoromethylation solely and worked in an environmentally benign acetone/water solvent medium. This method was also applicable for the benzylic C-H trifluoromethylation of some drug molecules such as the Celecoxib analogue **39** and the Meclizine analogue **40** in 82% and 26% yields, respectively (Scheme 8b). The Liu group also independently reported a similar type of work using this Grushin's reagent and its application to the synthesis of the Iprovalicarb analogue **41**.⁹⁸ Zhu and Li have developed a general copper-catalyzed methodology for C-H trifluoromethylation regioselectively at the benzylic position using Zn(CF₃)₂(bpy) as the 'CF₃' source.⁹⁹ This operationally simple method was also found to be very efficient for late-stage C-H trifluoromethylation of many complex organic molecules and known drugs in moderate to good yields. Some of them are Salidroside **42**, Salbactam **43**, Triclosan **44** and Ibuprofen **45** analogues.

7. C-H methylation: the methyl magic presumed in drug discovery

Significant improvements in pharmacological properties are observed by converting a C-H bond to a C-Me bond which is termed by medicinal chemists as "methyl magic".¹⁰⁰

Strategies and techniques for regioselective C-H methylation of C(sp²)-H and C(sp³)-H bonds under mild conditions and their application for the late-stage methylation of complex drugs and natural products is in high demand. The direct C-H methylation approach can deliver drug analogues more easily than the *de novo* synthesis which has a great impact in accelerating the drug development process. Most of the advancements that have been reported for the C-H methylation reactions in the last few years are covered in two reviews by Tim Cernak, Jamie A. Leitch and Darren J. Dixon, and these are represented here as a general scheme (Scheme 9a).¹⁰¹ Some representative late-stage C-H methylation reactions in complex drug or drug-like molecules are worthwhile to include in this review.

In a collaboration between the Yu and Baran groups, a ligand-accelerated *ortho* C(sp²)-H monomethylation of benzoic acids was developed. This C-H methylation and a Pd-catalyzed C(sp²)-H hydroxylation were successfully applied for the synthesis of a sesquiterpenoid antibiotic, (+)-hongoquercin A (**46**, Scheme 9bi).¹⁰² The Johansson and Ackermann group developed a practical methodology for the late-stage C-H methylation of structurally complex drug molecules using a cobalt catalyst.¹⁰³ A stoichiometric amount of cobalt catalyst was required for more complex drug molecules. This method eliminated the pre-functionalization or post-deprotection steps for the C-H methylation of a diverse

a. General scheme for directed C-H methylation

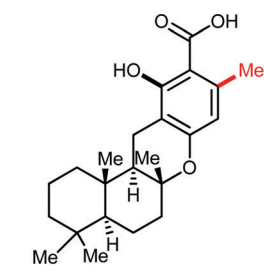


"Me" source = MeOMs, MeBF₃K, MeB(OH)₂, Me-thiophenium salt, DTBP, AcOH, Ac₂O, MeMgBr, MeMgCl, AlMe₃, MeOTs, PhNMe₃

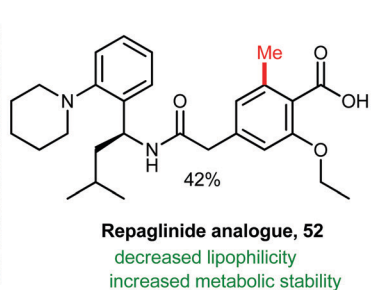
DG = various N-based DGs e.g. pyrimidine, oxime esters, sulfonamides etc. 8-amino quinoline, COOH, CHO and many more

b. C-H methylation for the synthesis of bioactive molecules/ drug analogues

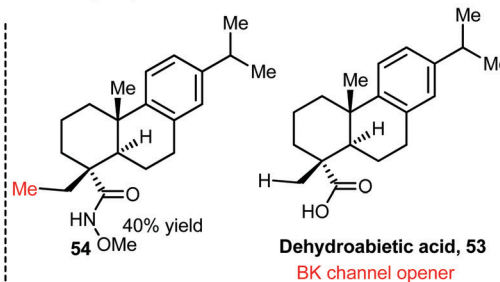
i. Yu and Baran



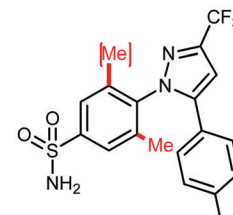
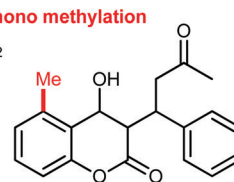
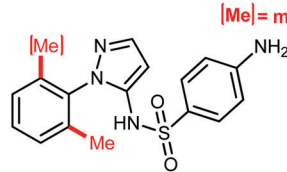
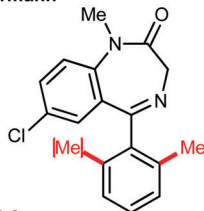
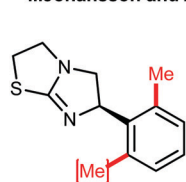
iii. Johansson and Marti'n-Matute



iv. Yu group



ii. Johansson and Ackermann



Levamisole analogue, 47 **Diazepam analogue, 48** **Sulfaphenazole analogue, 49** **Warfarin analogue, 50** **Celecoxib analogue, 51**

Scheme 9 (a) General directed C(sp²)-H methylation and (b) C(sp²)-H methylation for the synthesis of bioactive molecules/drug analogues.

array of marketed drug molecules and natural products (47–51, Scheme 9bii). The physicochemical and biological testing of the mono-methylated and di-methylated analogues in comparison to the corresponding parent compounds indicated that the methylated analogues display better pharmacological properties and modulation *via* C–H methylation often offers further improvements. Johansson and Marti'n-Matute recently reported an iridium-catalyzed carboxylate-directed *ortho* C–H methylation of benzoic acids (Scheme 9biii).¹⁰⁴ The C–H methylation of the marketed drug Repaglinide (blood glucose reduction in type 2 diabetes mellitus) took place efficiently under these conditions to give 52. Biological studies showed increased metabolic stability of Me-Repaglinide compared to the parent drug in both rat hepatocytes and human liver microsomes with desirable reduced lipophilicity. Dehydroabietic acid (diterpene) 53 is identified as an efficient BK channel opener. Compounds with this activity are useful for the treatment of acute stroke, epilepsy and asthma. The Yu group reported a late-stage methylation of the inactive C(sp³)-H bond of the hydroxamic acid version of the natural product to provide 54 (Scheme 9biv) which is quite difficult to functionalize by other methods.¹⁰⁵

8. Amino acid, peptide and protein modification through C–H activation

Peptides and proteins play an important role in governing many biological processes, *e.g.* cell signaling and metabolism.¹⁰⁶ The function of a peptide largely depends on its shape and structure. The primary peptide structure is determined by the order of amino acids. A change in the sequence of amino acids or a bond formation between amino acid side chains (modified peptides) gives rise to changes in the primary peptide structure which in turn causes changes in peptide function. Modified peptides in many cases show extraordinary biological function than a native peptide.¹⁰⁷ For example, the development of radiolabelled or fluorescent peptides through peptide modification can be accomplished through chemical tagging for understanding protein function in a cell.¹⁰⁸ Modified peptides are also found to be better therapeutic agents than small molecule drugs possessing higher target specificity and affinity.¹⁰⁹ Many peptide therapeutics having excellent biological activity show poor pharmacokinetics.¹¹⁰ The potency of such peptides can be increased by creating rigidity through peptide modification (peptide stapling).¹¹¹ Peptide modification reactions fall into three

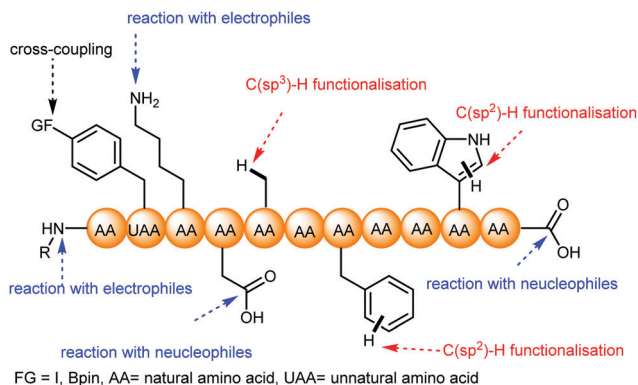


Fig. 2 General strategies for peptide modification.

general categories: (a) reactions with heteroatoms of side chains or terminals of amino acids; (b) cross-coupling with functionalized peptides; and (c) C(sp², sp³)-H functionalization reactions (Fig. 2). The first category cannot be frequently used because these reacting centres are often necessary for peptide function and tedious prefunctionalization steps are required for the cross-coupling reactions. Hence, direct C-H functionalization such as post-synthetic modifications are highly desirable over cross-coupling as they enable modifications of natural peptides in a single step. Recently, late-stage modification of α -amino acids *via* C-H activation keeping the chiral center intact has emerged as a promising technique for the generation of unnatural amino acids.¹¹² In fact, these methodologies have been extended to the modification and stapling of peptides and proteins either through C(sp², sp³)-H functionalization in the aryl/alkyl part of the aromatic/aliphatic amino acid residues or through macrocyclization or stapling reactions *via* C(sp², sp³)-H activation.¹¹³

C-H activation techniques are proved to be extremely efficient over conventional methods such as disulfide linkages, ring-closing metathesis, azide-alkyne click reactions and biaryl linkages involving the borylated phenylalanine derivatives for the synthesis of

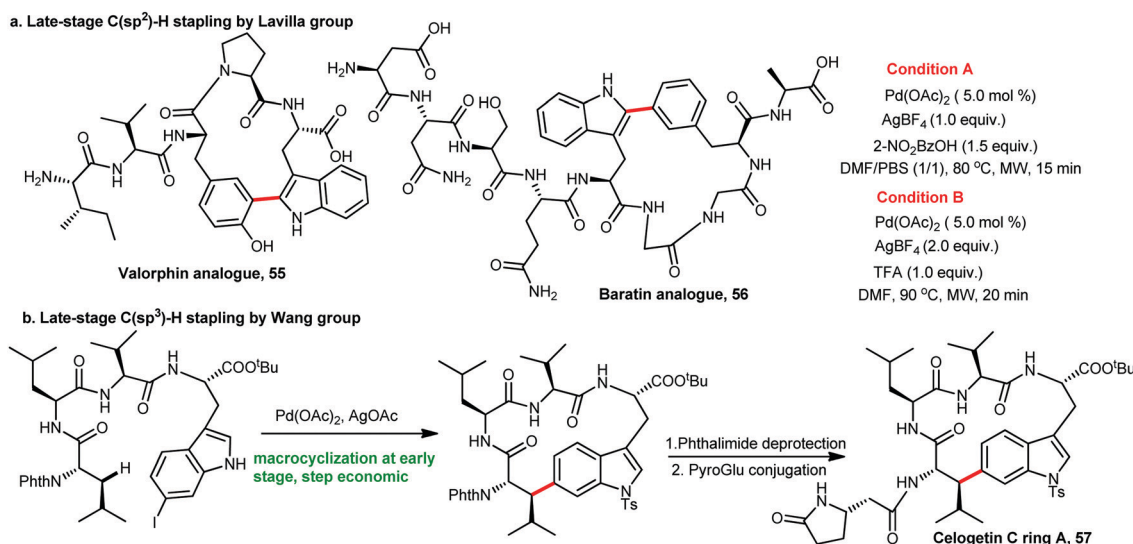
stapled peptides. Albericio, Ackermann, Chen, Lavilla and Wang groups have significant contributions in the field of peptide stapling through C(sp², sp³)-H activation.¹¹⁴ For example, the Lavilla group developed two strategies for the macrocyclization of peptides through C(sp²)-H activation and applied them for the synthesis of the Valorphin analogue **55** (14-membered ring) and the Baratin analogue **56** (17-membered ring) (Scheme 10a).¹¹⁵ The Wang group reported peptide macrocyclization through Pd-catalysed C(sp³)-H arylation (Scheme 10b).¹¹⁶ Using this method, they were able to synthesize one (17-membered ring) of the two rings of Celogetin C ring A **57** in a very step economic manner compared to previous reports which required 6 steps just for macrocyclization.

9. Bioimaging/radiolabelling *via* C-H activation

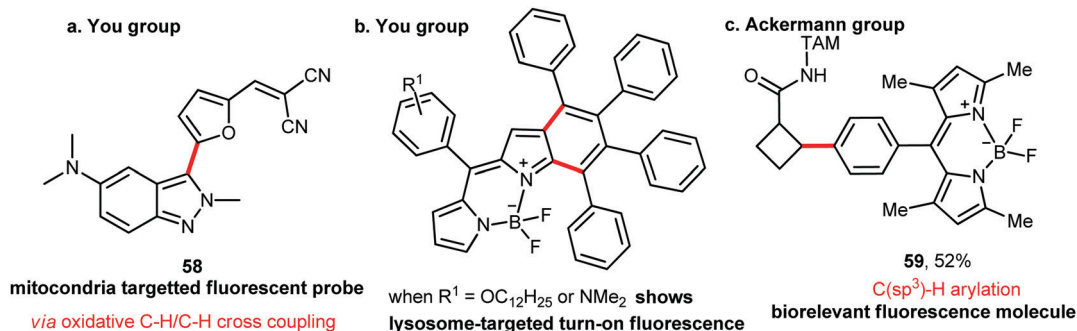
Bioimaging is an important technique frequently used in medicinal chemistry for the localization and biodistribution studies of the lead molecule in the cellular or animal context. It is also an indispensable tool for diagnosis and metabolism studies. Hence, attachment of a tracer element to the lead molecule keeping the biological action intact is extremely challenging. To circumvent this issue, late-stage conjugation of a radiotracer element or a fluorescent dye through C-H activation has received special attention. In this context, we will highlight the synthesis of fluorescent molecules and ¹⁸F labeling *via* C-H activation.

9.1 Fluorescence labeling

Fluorescence imaging is a powerful technique to detect biologically relevant species with the additional ability to visualize morphological details and monitor many physiological processes in living systems.¹¹⁷ Three important features for an organic fluorophore for bioimaging are (1) fluorophores with a low molecular weight as they have exceptional advantages such as



Scheme 10 Peptide modification *via* late-stage C(sp²)-H/C(sp³)-H peptide stapling and its application in natural product synthesis.



Scheme 11 Synthesis of fluorescent probes via C–H activation.

minimal perturbation to living systems and good cell permeability;¹¹⁸ (2) near-infrared (NIR) fluorophores (emission wavelength range of 650–900 nm) are highly desirable for *in vivo* bioanalysis and bioimaging because they undergo minimal photo-damage and low light scattering, and also they can penetrate deep tissues for high-quality imaging;¹¹⁹ and (3) fluorophores should have low cytotoxicity.

The You group developed a methodology to synthesize a library of bi-heteroaryl fluorophores (Indazo-Fluors) *via* an oxidative C–H/C–H cross-coupling reaction between electron-deficient 2H-indazoles with electron-rich heteroarenes using the Pd catalyst.¹²⁰ By fine-tuning of one of the core skeletons, they successfully achieved a low molecular weight near-infrared (NIR) dye (**58**, Scheme 11a) which could light up the mitochondria of living cells specifically with bright red luminescence. The cytotoxicity test in cultured HepG2 cells showed almost no toxicity. The same group developed benzo[*b*]-fused BODIPY based fluorescent probes through a palladium-catalyzed direct C–H functionalization, followed by annulation of BODIPYs with alkynes (Scheme 11b).¹²¹ After cell imaging experiments and cytotoxicity assays, they found that some of the benzo[*b*]-fused BODIPYs had specific lysosome-imaging capacity and turn-on fluorescence emission in cells with low cytotoxicity, suggesting them as potential lysosome-targeted reagents.

The Ackermann group synthesized a library of cyclobutane boron-dipyrrins (BODIPYs) through efficient triazole-assisted secondary C(sp³)-H cyclobutane arylations (Scheme 11c).¹²² They chose the cyclobutane core since cyclobutanes are vital building blocks found in complex natural molecules displaying bio-activities.¹²³ Thus, they successfully generated a library of novel cyclobutane BODIPY molecules, one of which is mentioned here

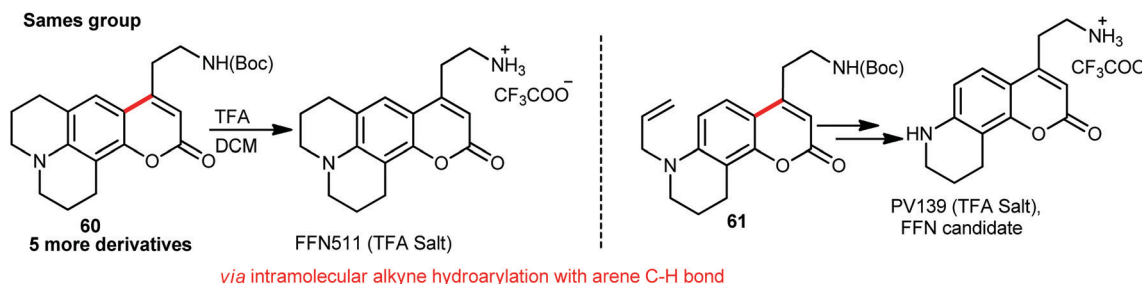
(**59**) as an effective biorelevant molecule for fluorescence-based live-cell imaging.

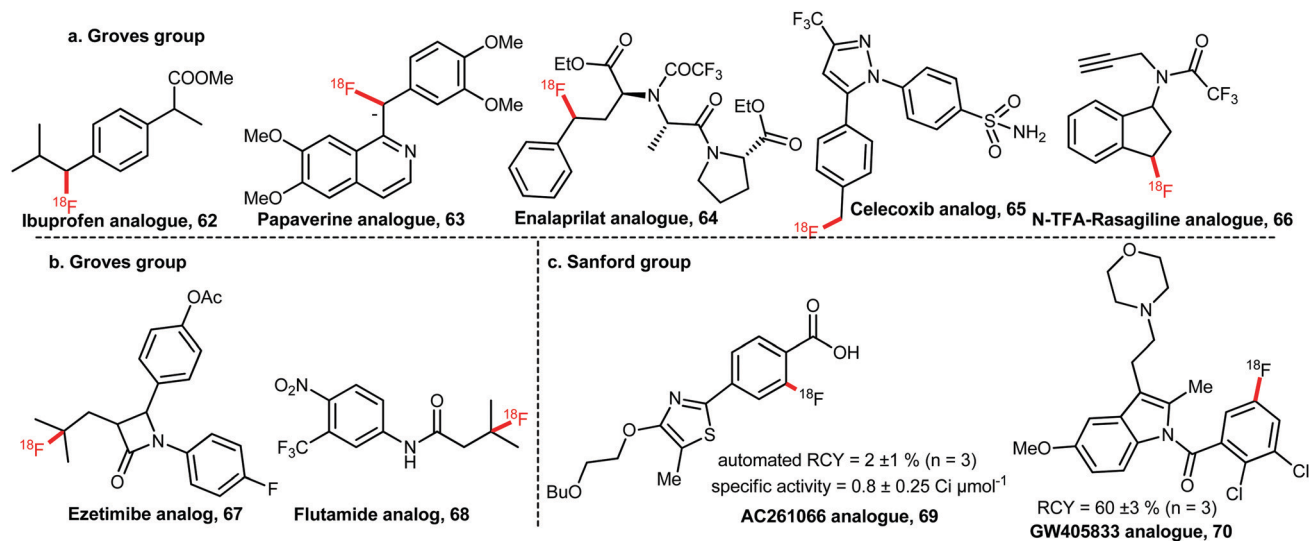
9.2 Application in neuroimaging

Fluorescence probes also find excellent applications in neuroscience.¹²⁴ Learning is one of the activities that are controlled and regulated by the nervous system and it is dependent on the plasticity of synaptic connections between neurons.¹²⁵ Obtaining information about signaling in individual synapses was a long-lasting problem in neuroscience.¹²⁶ This problem was solved by the Sames group by introducing a novel class of neuroimaging probes called fluorescent false neurotransmitters (FFNs) which enables optical imaging of neurotransmission in the brain.¹²⁷ A FFN is a fluorescent probe synthesized by mimicking a neurotransmitter which gives information about the activity changes in individual synapses during different levels of neuronal activity by examining the release of this fluorescence neurotransmitter at individual synapses. They developed Pt- or Au-catalysed conditions for intramolecular alkyne hydroarylation with arene C–H bonds to construct highly fluorescent amino coumarins (Scheme 12).¹²⁸ These mild catalytic methods directly afforded a library of FFN probes with a variety of functional groups in the amino coumarin core (**60**, **61**) which made it easier to tune the fluorescence properties and the ability to function as substrates for relevant protein targets.

9.3 ¹⁸F labelling for positron emission tomography (PET) imaging

Positron (β⁺) emission tomography (PET) is a non-invasive technique for the *in vivo* 3D imaging of physiological structures and biochemical pathways.¹²⁹ It has extensive applications

Scheme 12 Synthesis of fluorescent false neurotransmitters (FFNs) *via* intramolecular alkyne hydroarylation with arene C–H bonds.



Scheme 13 C(sp³)-H/C(sp²)-H radio-fluorination for the synthesis of radiolabelled drug analogues.

in cardiology, clinical oncology, neurology and basic biomedical research.¹³⁰ In addition to applications for diagnosis of diseases, PET imaging can also provide important information regarding potentially limiting side effects because of off-target binding.¹³¹ Out of all PET radioisotopes ¹⁸F has gained high interest for its favorable physical and nuclear characteristics, which include a high positron decay ratio (97%), a short half-life (109.7 min) and a low positron energy (max. 0.635 MeV).¹³² Hence, the methodology for the late-stage introduction of short-lived ¹⁸F atoms is in high demand. The Groves group has made a significant progress towards the development of step economic methods for ¹⁸F labeling through the direct C-H bonds of the parent molecules. They accomplished C(sp³)-H radio-fluorination efficiently at the benzylic as well as unactivated C-H bonds of a variety of drug or drug-like molecules (62–68, Scheme 13a and b) using Mn-catalysts.¹³³

The Sanford group has made a significant contribution in the field of C-H radio-fluorination chemistry. They developed Cu-catalysed C(sp²)-H radio-fluorination of 8-aminoquinoline protected benzoic acids using K¹⁸F as a radio-fluoride source (Scheme 13c).¹³⁴ The method was applicable to the synthesis of the RARβ2 agonist [¹⁸F]AC261066 69 with a high specific radioactivity dose. Then the same group reported an excellent method for the *meta*-selective C(sp²)-H radio-fluorination of arenes or heteroarenes without the need of any directing group.¹³⁵ This method involves Ir-catalysed borylation, followed by Cu-catalyzed coupling to provide the radio-fluorinated product with a good radiochemical yield (RCY) (Scheme 13c). Using this method, they synthesized a radio-fluorinated analogue of GW405833 70 (cannabinoid receptor 2 partial agonist) with a 60 ± 3% RCY.

10. Bioconjugation through C-H activation

Bioconjugation is a technique to staple a biomolecule or molecule of interest (MoI) with molecular probes through biorthogonal

reactions. Although there is a plethora of organic transformations that have been developed and practiced in pharmaceutical industries,¹³⁶ but only a few chemical reactions have been designated as biorthogonal reactions in chemical biology applications.¹³⁷ This is attributed to the fact that most of the organic reactions require toxic organic solvents, high reaction temperatures, nonaerobic conditions and other stoichiometric additives, which are detrimental for the sensitive biomolecules. Furthermore, bioconjugation of proteins may involve different difficulties to attach a fluorescent dye or antibody conjugate in a site-specific manner.¹³⁸ A copper-catalyzed azide-alkyne cycloaddition reaction or commonly called the “click” reaction developed by the Sharpless group is an elegant concept for bioconjugation (Scheme 14a).¹³⁹ Owing to the toxicity of copper metal to biomolecules, a strain-promoted cycloaddition reaction between cyclooctyne and azide was developed by the Bertozzi group.¹⁴⁰ Even more recently, the application of the ultraviolet light promoted cycloaddition reaction between tetrazole and alkene has received special attention due to better spatio-temporal control.¹⁴¹ However, the introduction of the requisite functionality such as azides, alkynes, tetrazoles, aldehydes, or alkenes, is extremely difficult for complex drugs or natural products. Conventionally, it requires multistep synthesis to introduce the functional building block. Furthermore, perturbation of lead molecules through structural modifications may alter the biological activity. Hence, direct bioconjugation through C-H activation is an attractive strategy. This technique is particularly useful for affinity- and activity-based protein profiling to identify the biological target and mechanism of action of a drug molecule.

10.1 Pull-down experiment for target identification

Small molecule inhibitors tend to inhibit multiple cellular targets and do not possess the type of exquisite cellular specificity. Hence, cell-based protein profiling is a crucial step to determine the off-target interactions.¹⁴² A very careful but deliberate design

of the original structure is essential so that necessary handles are installed into the backbone with minimum perturbation of the original structure; therefore, the pharmacokinetic and biological properties will not be altered drastically. Molecular docking is helpful to estimate the change in potential binding sites. A schematic presentation of cell-based target identification is shown in Fig. 3a. An alkyne tether and a photoaffinity probe are attached to the main core. This is incubated into the cell for sufficient time to reach equilibrium. Presumably, by this time the small molecular probe will bind non-covalently with its protein target. Then the cell is irradiated with UV light ($\lambda_{\text{max}} = 560 \text{ nm}$) to generate a reactive intermediate. It will bind with native proteins covalently. After that an *in situ* click reaction with biotin or fluorophore attached azide is performed. The protein-bound affinity probe is then pulled down with streptavidin beads washed with buffer solutions and run in an SDS-PAGE. After washing SDS-PAGE the respective bands are collected and analyzed by LCMS/MS.

A recent application of C–H amination for the simultaneous structure–activity studies and arming of eupalmerin acetate for the identification of cellular targets was demonstrated by the Romo group.¹⁴³ The late-stage allylic C–H amination reaction of an alkyne **72** on eupalmerin acetate **71** was performed using the rhodium catalyst developed by the Du Bois group (Fig. 3b).¹⁴⁴

Subsequently, it was treated in HL-60 cells, homogenized and conjugated to rhodamine-azide under copper-catalyzed azide–alkyne cycloaddition conditions, separated by SDS–polyacrylamide gel electrophoresis and visualized by in-gel fluorescence scanning. The protein target was identified *via* competitive ABPP-SILAC (activity-based protein profiling-stable isotope labeling by amino acids in cell culture) and mass spectrometric analysis. It was observed that the pulled-down proteins are typically over-expressed in cancer cells (Fig. 3b).

Azide linkers are highly desirable for bioconjugation reactions. The Baran group developed a general C–H functionalization method for tagging through azidoalkylation of several natural products and pharmaceuticals (Scheme 14b).¹⁴⁵ They were able to introduce the tag into unactivated C–H bonds in bioactive heteroarenes using sodium (difluoroalkylazido)sulfonate **73** (DAAS-Na) as an azidoalkyl transferring agent to synthesize the analogues (**74–76** and 16 more). This powerful reaction for native chemical tagging occurs efficiently in an aqueous medium and in the absence of protecting groups. Then they applied these synthesized azide-linked bioactive compounds for bioconjugation *via* copper-free strain promoted azide–alkyne cycloaddition with a dibenzylazacyclooctyne-containing monoclonal antibody **77**, affording the drug–antibody conjugate **78**.

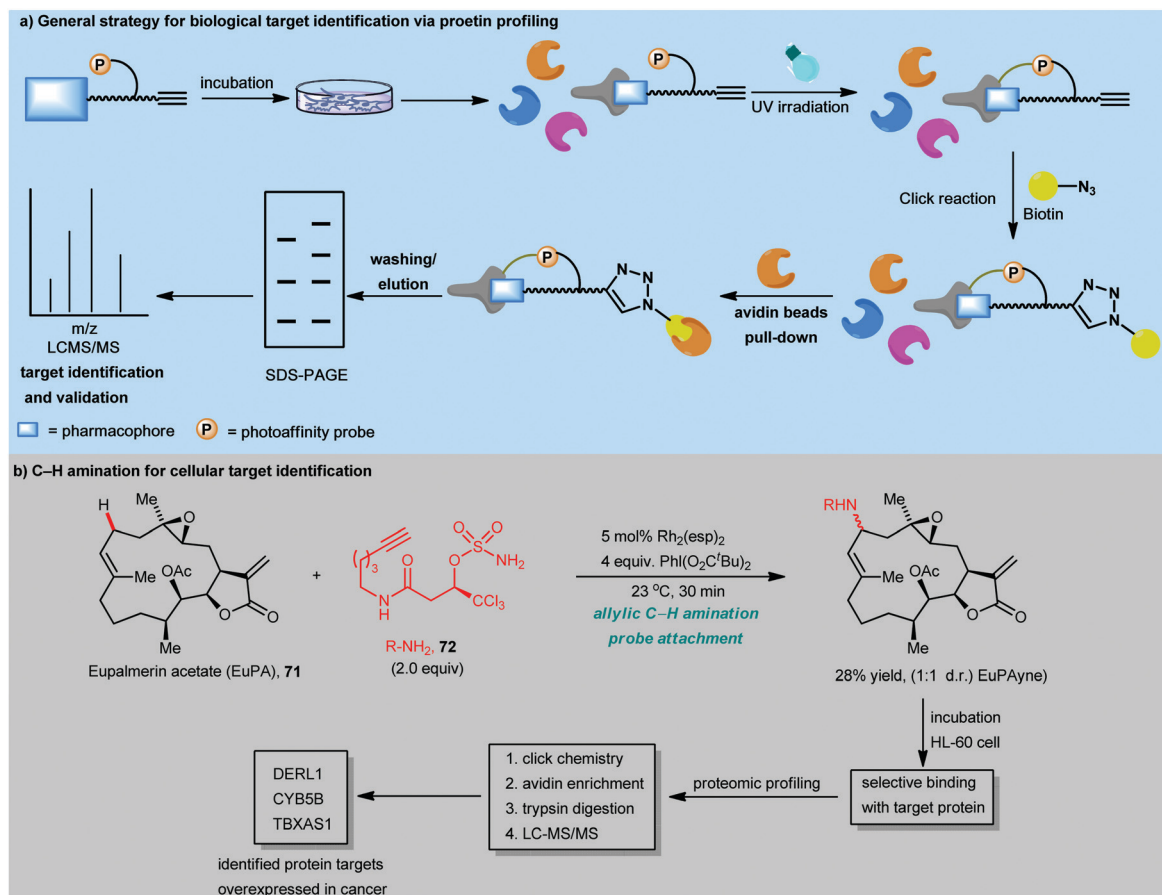
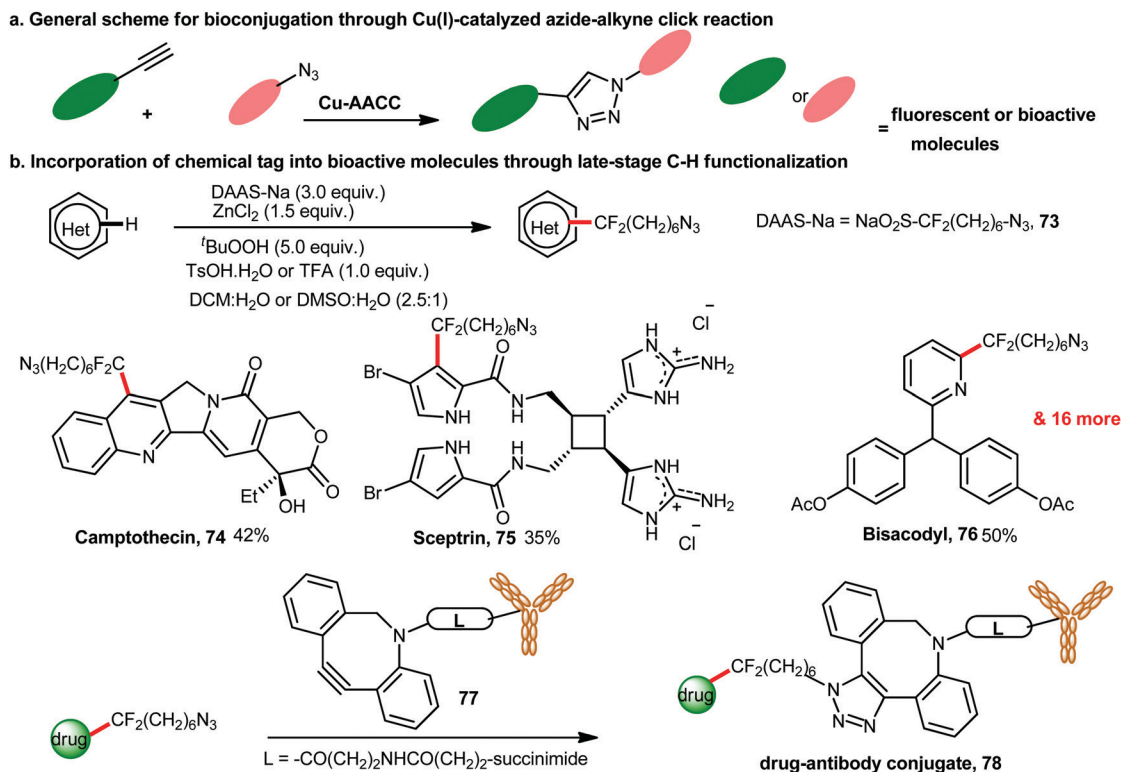


Fig. 3 (a) General strategy for biological target identification through protein profiling. (b) C–H amination for cellular target identification.



Scheme 14 (a) General scheme for bioconjugation through the CuAAC reaction. (b) Incorporation of a chemical tag into bioactive molecules through late-stage C-H functionalization.

11. Drug-metabolite synthesis through C-H oxidation

Metabolism of drugs in the body is a complex biotransformation process where drugs are transformed into different molecules (metabolites) by various metabolizing enzymes. A clear understanding of drug metabolism helps to optimize lead compounds with optimal PK/PD properties, identify a better lead from the active metabolites, minimize toxicity by reactive or toxic metabolites and for a comparative study of preclinical metabolism in animals including humans.¹⁴⁶ As the metabolites are produced after the metabolism of drugs, different functional parameters such as biological activity, clearance rates and toxicity are altered.¹⁴⁷ Therefore, rapid identification and scale-up synthesis of drug metabolites is necessary to facilitate the drug discovery cycle and guide the selection of clinical candidates. Drug metabolism in the human body is carried out by many enzymes of the cytochrome family which are mainly present in the liver.¹⁴⁸ But these enzymes generate a broad range of metabolites and also in very little amounts. Isolation of these drug metabolites from the biological system is a tedious and time-consuming process. This problem was solved to some extent using the biotransformation approach, that is, *in vitro* oxidation of drugs using cytochrome P450 monooxygenases (CYPs).¹⁴⁹ But this biotransformation limits their broad industrial use and practical impact due to the functional complexity, low activity and limited stability of these enzymes. The Sames group developed the transformation (metal-catalysed oxidation in a laboratory) approach as a complementary

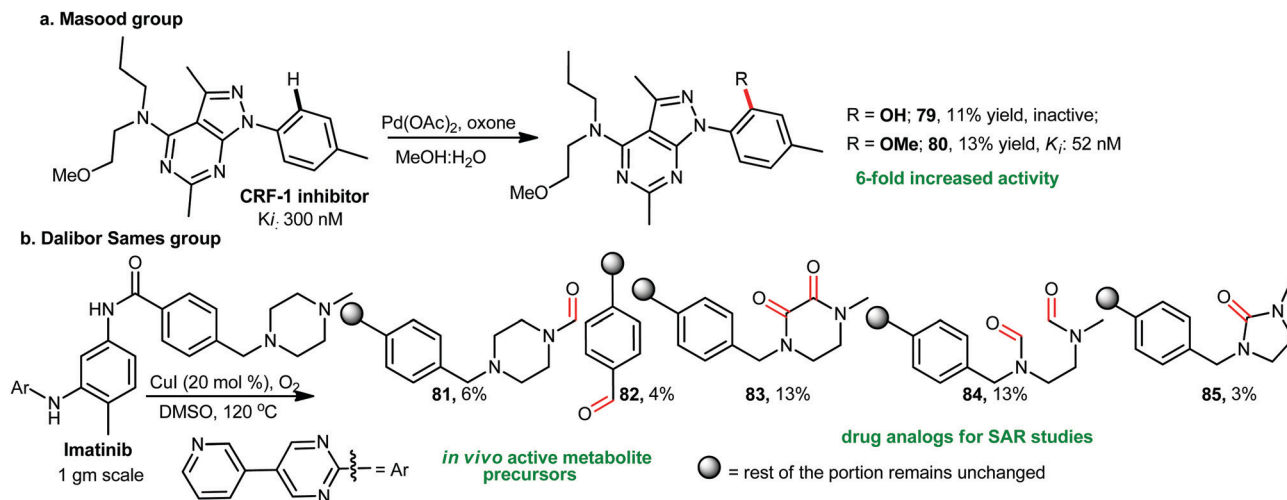
method to synthesize drug metabolites.¹⁵⁰ The modern C-H oxidation reaction can generate a wide range of drug metabolites with a suitable catalyst that can mimic CYPs.¹⁵¹ Here, a medicinal chemist can play an important role either (1) by optimizing suitable catalytic conditions or (2) by the development of a biomimetic catalyst for the metabolite synthesis through late-stage C-H oxidation of drug molecules.

11.1 Drug metabolite synthesis under optimized chemical reaction conditions

The Masood group reported the $\text{Pd}(\text{OAc})_2/\text{oxone}$ combination for the hydroxylation of the corticotropin-releasing factor-1 (CRF-1) receptor inhibitor which produced two metabolites (**79–80**, Scheme 15a), of which the first one was inactive and the latter was six times more active than the parent drug.¹⁵² The Sames group reported oxidation of the anticancer drug Imatinib by copper/ O_2 combination which produces five compounds, of which two were *in vivo* active metabolite precursors (**81–82**) and three were new drug analogues (**83–85**, Scheme 15b).¹⁵⁰

11.2 Drug metabolite synthesis with biomimetic catalysts

Monensin A (**86**), an important natural product, selectively complexes and transports sodium cations across lipid membranes and displays a variety of biological properties.¹⁵³ The Does Assis group evaluated the Jacobsen catalyst as a cytochrome P450 biomimetic model to investigate the oxidative metabolism of Monensin A.¹⁵⁴ Two metabolites **87** and **88** were obtained by the oxidation of the Jacobsen catalyst which were exactly the same

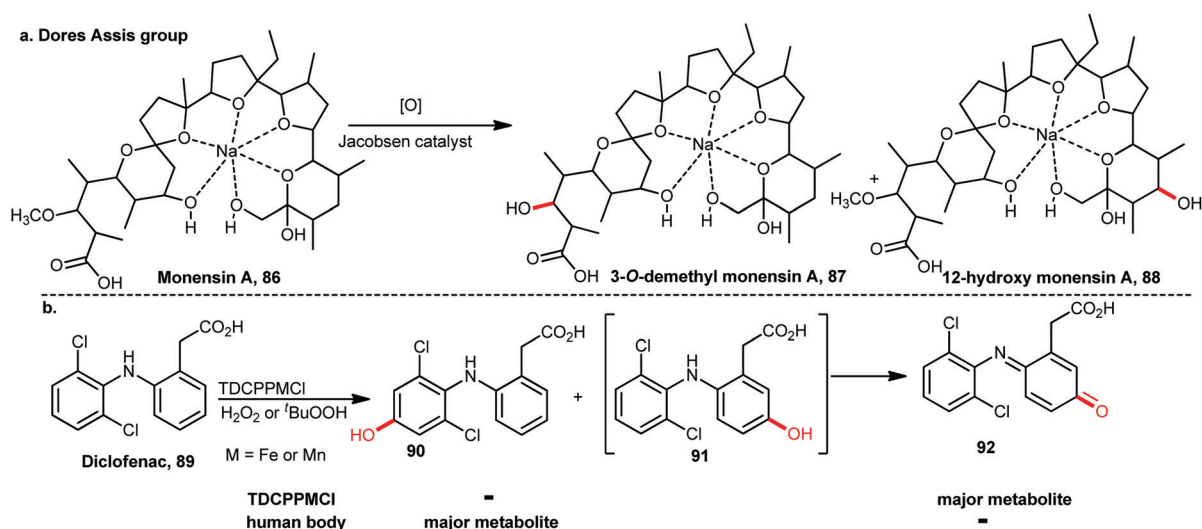


Scheme 15 Drug metabolite synthesis through Cu- or Pd-catalyzed C–H oxidation reactions.

metabolites obtained *in vivo* (Scheme 16a). This result implies that a biomimetic chemical catalyst has excellent potential for metabolite synthesis which inspires medicinal chemists to design and synthesis of biomimetic catalysts. Continuous efforts have also been devoted to the design and synthesis of biomimetic chemical catalysts that surrogate the heme-containing active center of CYP for more than three decades. A significant amount of work on drug metabolite synthesis using biomimetic chemical catalysts has been done by different groups which are reviewed by Jean Bernadou *et al.* and Lohmann *et al.*¹⁵⁵ As a representative example, we will discuss metal porphyrin-catalyzed oxidation of Diclofenac **89**. Using the Fe- or Mn-porphyrin catalyst Diclofenac underwent aromatic C(sp²)–H oxidation to generate two metabolites **90** and **91** (Scheme 16b). The latter one being susceptible to further oxidation was converted to **92**. In this chemotransformation, compound **92** is the major metabolite, whereas in the biological oxidation process **90** is obtained as the major metabolite.

12. Late-stage C–H functionalization of drug molecules

Current drug discovery mainly relies on identifying the leads and rapidly synthesizing a library of their analogues for modulating key pharmacological properties.¹⁵⁶ A well-established method to generate a vast library of analogues rapidly is diversification of the lead pharmacophore through late-stage functionalization (LSF).¹⁵⁷ Thus, LSF has a role in facilitating the development of structure–activity relationship (SAR) studies, on-target potency, selectivity optimization, ADME studies and improvement of physical properties such as solubility and stability. Therefore, it is considered as an integrated part of many drug-development programs today.¹⁵⁸ The C–H functionalization strategy offers an excellent alternative over conventional methods for this late-stage diversification where medicinal chemists can functionalize a selective C–H bond keeping many other functional groups



Scheme 16 Drug metabolite synthesis through C–H oxidation reactions using bio-mimetic chemical catalysts.

intact which are often necessary for biological activity.¹⁵⁹ However, late-stage functionalization of a complex molecule containing nitrogen or sulfur atoms is a daunting challenge due to the strong coordination with metal catalysts, which can lead to catalyst poisoning or C–H functionalization at an undesired location.¹⁶⁰ As an illustrative example, the Yu group overcame this problem associated with performing C–H functionalization reactions on a complex heterocyclic motif by using a simple *N*-methoxy amide group.¹⁶¹ It worked both as a directing group and as an anionic ligand that generates reactive PdX₂ *in situ*. Due to this preferential binding mode, the PdX₂ species is localized near the target C–H bond, avoiding interference from any nitrogen or sulfur atoms present in the molecule. This is conceptually a major advancement towards the late-stage functionalization of a heterocyclic molecule and complex natural products. This concept was further demonstrated with the inexpensive cobalt catalyst for the C–H functionalization of strongly coordinating nitrogen heterocycles, including pyrimidines, oxazolines, pyrazoles, pyridines, *etc.*¹⁶²

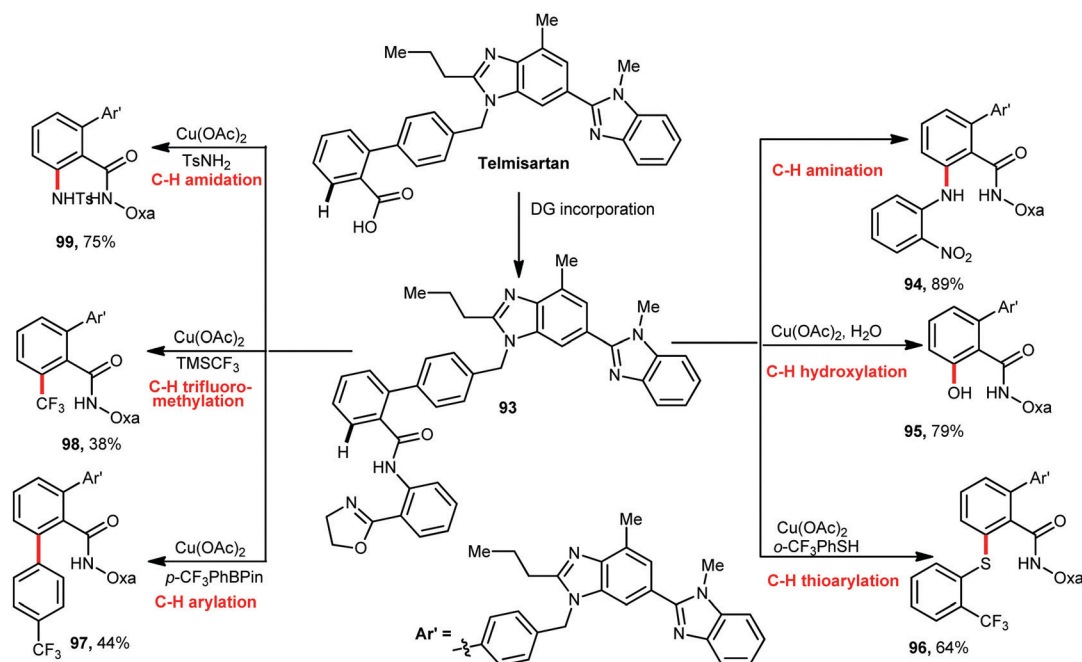
In 2017, the Yu group demonstrated copper-mediated late-stage diversification of Telmisartan (an angiotensin II receptor antagonist used to treat diabetic kidney disease, high blood pressure and heart failure)¹⁶³ amide **93**. Diversification was accomplished by six copper-mediated late-stage C–H functionalization reactions, namely, amination (**94**), hydroxylation (**95**), thioarylation (**96**), arylation (**97**), trifluoromethylation (**98**) and amidation (**99**), as shown in Scheme 17.¹⁶⁴

C–H functionalization reactions were also applied for the late-stage diversification of artemisinin (**100** or **101**) by several research groups,¹⁶⁵ *e.g.* analogues **102–105**, as summarized in Scheme 18. In addition, there is an array of examples of late-stage single C–H functionalization reactions for incorporating

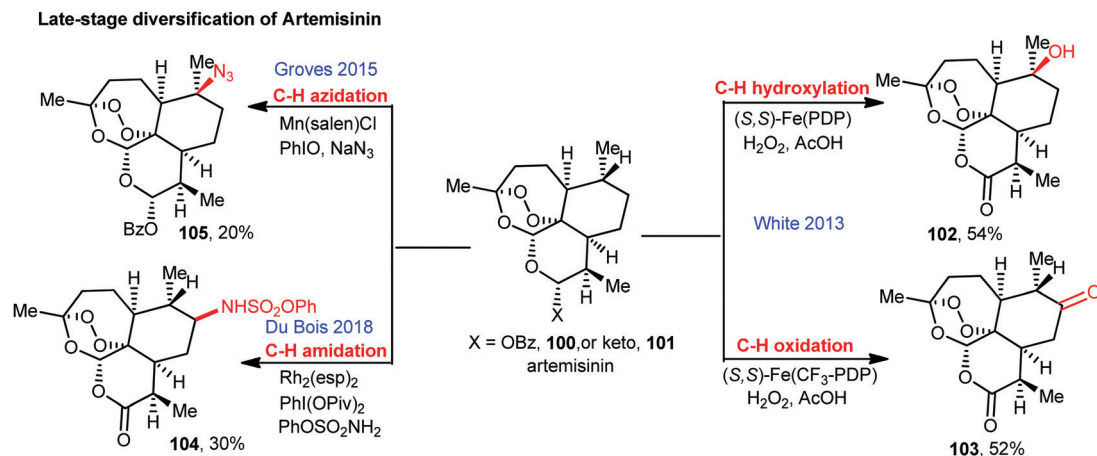
the desired functional group into various drug or drug-like molecules.¹⁶⁶

13. DNA encoded library development through C–H activation

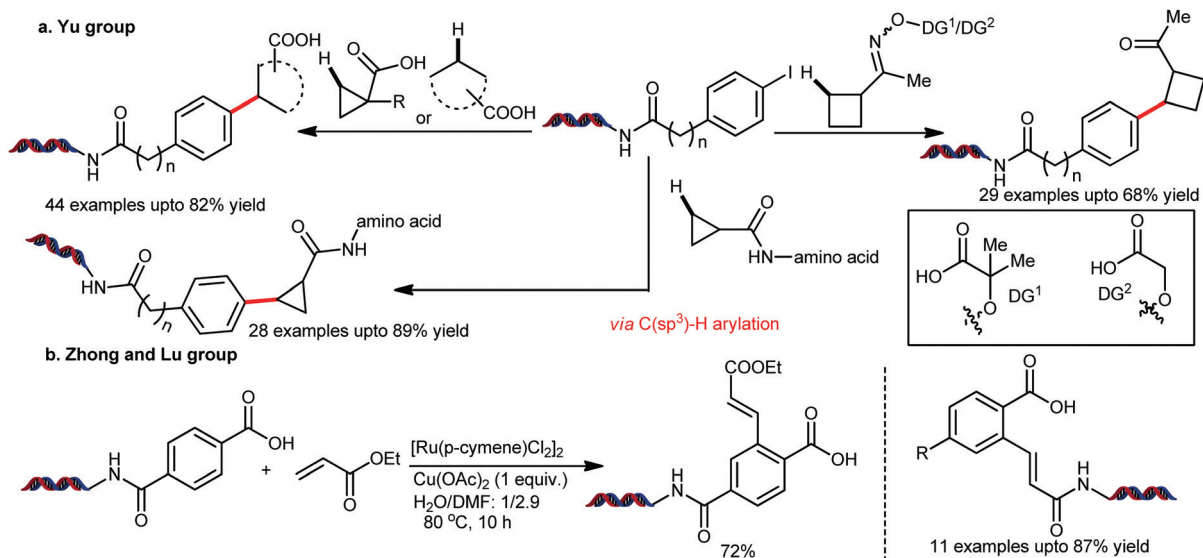
DNA-Encoded chemical libraries (DELs) represent an advanced screening platform that makes it possible to screen trillions of compounds in a single test tube.¹⁶⁷ Pharmaceutical companies are increasingly using this technology for the rapid identification of a hit molecule. Hence, integration of C–H activation technologies for the synthesis of DNA-encoded libraries is emerging. However, it poses several challenges such as the C–H activation chemistry should be feasible in water; secondly, nucleotides within DNA should not poison the transition metal catalysts; and thirdly the reaction should proceed at extremely low concentrations.¹⁶⁸ Through careful optimization, the Yu group developed a palladium-catalyzed C–H arylation of cyclobutane rings with DNA-bound aryl iodide to access rapid molecular diversity for the drug discovery program.¹⁶⁹ One of the striking advantages of this methodology was that it introduced three-dimensional sp³ character into DNA-encoded libraries. Furthermore, chiral amino acids, cyclopropane and heterocycles were also compatible (Scheme 19a). In another report, the Zhong and Lu group accomplished a DNA-compatible sp² C–H activation reaction between DNA-conjugated acrylamides and aromatic acids in buffer conditions using the ruthenium(II) catalyst (Scheme 19b).¹⁷⁰ The pendant carboxylic acid can be further functionalized for combinatorial library preparation. This DNA encoded library synthesis strategy has the potential for rapid generation of structural complexity and



Scheme 17 Late-stage diversification of Telmisartan via Cu-catalyzed C–H functionalizations.



Scheme 18 Late-stage diversification of artemisinin via C–H functionalization reactions.



Scheme 19 Synthesis of a DNA-encoded library via C–H activation.

diversity in a modular manner to accelerate the drug discovery program.

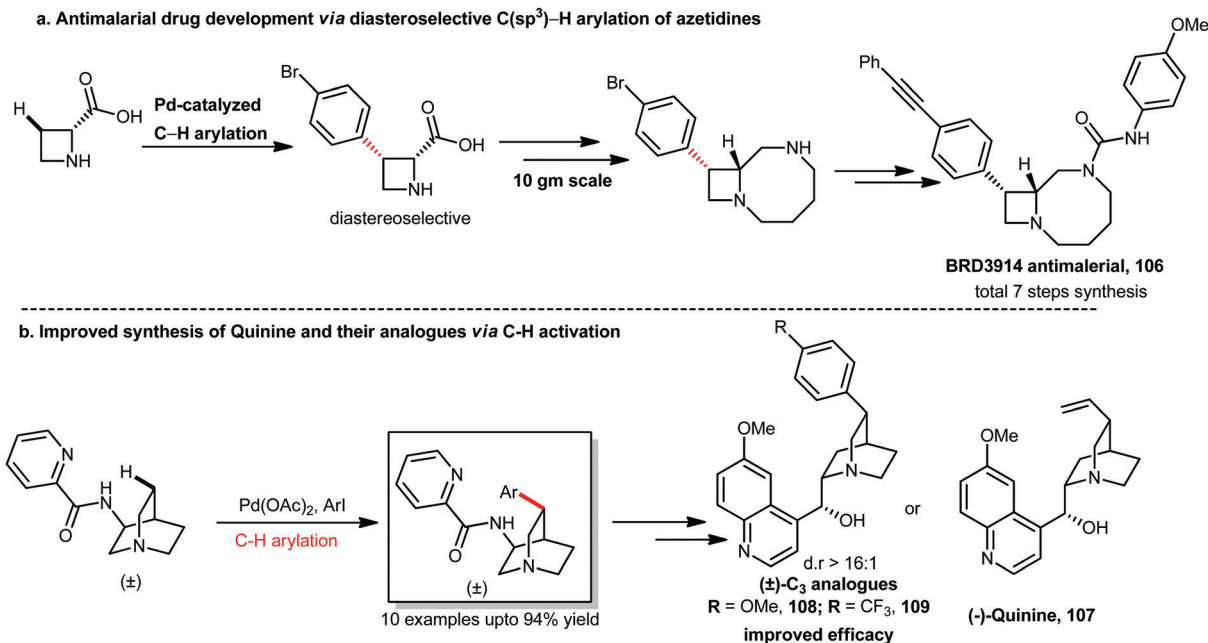
14. Case studies of drug/drug-like molecule synthesis via C–H activation

14.1 Application in antimalarial drugs

According to WHO, more than 4 000 000 people die of malaria infection each year. So countless efforts have been dedicated in recent years for the synthesis of antimalarial drugs to reduce the number of deaths from malaria worldwide.¹⁷¹ Artemisinin-based combination therapy (ACT) is the best available treatment, especially for *P. falciparum* malaria. In this technique, artemisinin derivatives (e.g. dihydroartemisinin, artesunate, artemether, etc.) are combined with different classes of drugs such as lumefantrine, mefloquine, sulfadoxine/pyrimethamine, chlorproguanil/dapsone

and many more for rapid action.¹⁷² In spite of the good curative effects of ACT, one problem associated with this therapy is that the clearance of malaria parasites is delayed by 3 days in South-East Asian countries.¹⁷³ Improvement of ACT can be achieved either by the synthesis of better artemisinin derivatives or by diversifying the partner drug (see Scheme 18).

After identifying BRD7929 (2*S*,3*R*,4*R*) as a new antimalarial that acts by inhibiting phenylalanyl-tRNA synthetase,¹⁷⁴ the Schreiber group reported the synthesis of another analogue, BRD3914 (**106**, Scheme 20a).¹⁷⁵ Initially, they developed an 8-aminoquinoline DG directed highly regio- and stereoselective C(sp³)-H arylation of azetidines using the Pd-catalyst, which gave a library of synthetically useful carboxylic acid core compounds. Incorporating this arylation method to synthesize the compound BRD3914, they were able to get the compound in only 7 steps over the known 14-step synthesis which included a stereoselective cyclization step. Their biological studies indicated that



Scheme 20 Synthesis of antimalarials via C–H functionalization reactions.

this compound was able to cure *P. falciparum* infection in a mouse model after giving four doses orally.

The Maulide group reported a Pd-catalyzed, directed C(sp³)-H arylation of quinine and its derivatives with better antimalarial activity. This method allowed the synthesis of four compounds, natural (–)-quinine, unnatural (+)-quinine and two analogues having aryl substitution at the C₃ position.¹⁷⁶ The first enantioselective synthesis of (–)-quinine was done by the Stork group in a 14-step reaction sequence.¹⁷⁷ The Maulide group reported the synthesis of (–)-quinine **107** in 10 steps including the C(sp³)-H arylation and they also synthesized (+)-quinine, an unnatural enantiomer, following the same reaction sequence with only changing the starting enantiomer of 3-amino quinuclidine which was not reported earlier. Using picolinamide, directing group C(sp³)-H arylation took place with complete regio- and stereoselectivity (Scheme 20b). After testing the antimalarial activity *in vitro*, they observed that although the activity of (+)-quinine against *P. falciparum* is inferior than that of (–)-quinine, the two novel C₃-aryl analogues (**108**, **109**) showed improved activity.

14.2 Application in antibiotics

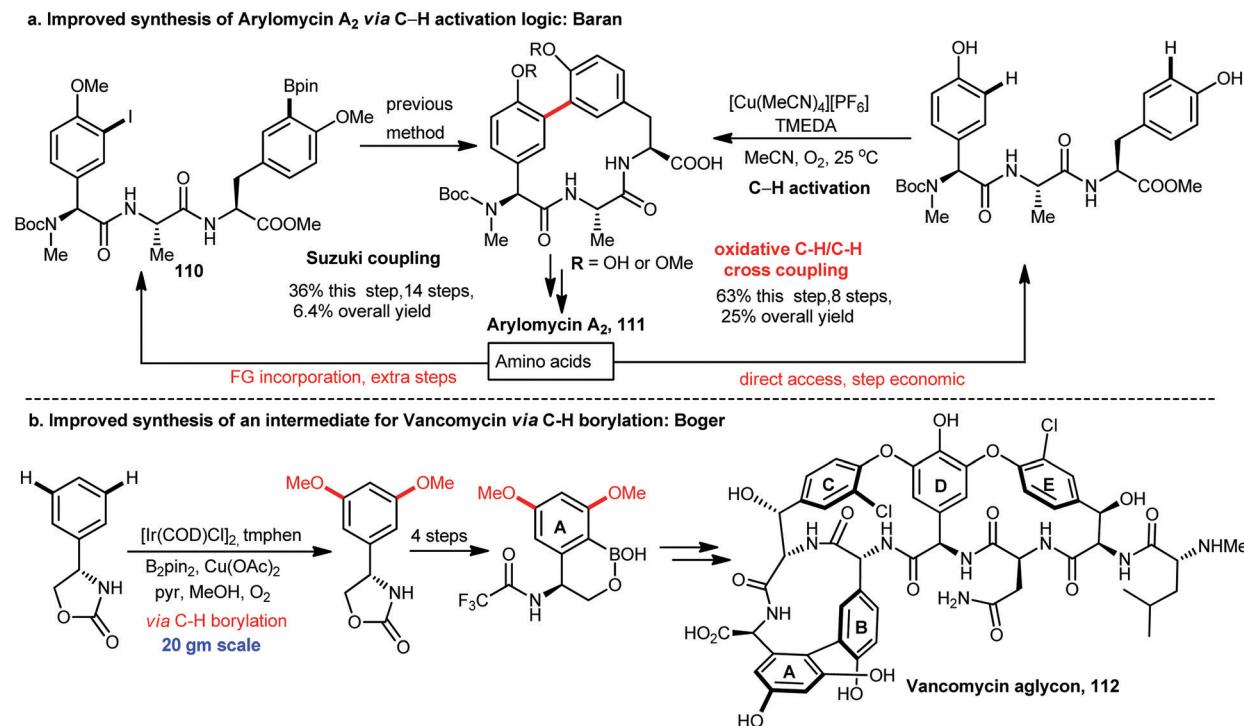
Arylomycins are an important class of antibacterial natural products.¹⁷⁸ They are made up of a lipophilic tail linked to a 14-membered macrocycle through a biaryl-bridge. The main challenge for the synthesis of these compounds was associated with the macrocyclic core formation. The total synthesis of arylomycins was first reported by the Romesberg group.¹⁷⁹ The problems of this route were that Suzuki–Miyaura coupling used for the macrocyclisation was very low-yielding even with the use of 20 mol% of Pd catalyst and the requirement of extensive pre-functionalizations of the amino acids to obtain **110**. This method used 14 steps to obtain the macrocycle with an overall

yield of 6.4%. Then Romesberg and Baran together developed a simplified route enabled by a Cu-mediated oxidative C–H/C–H coupling.¹⁸⁰ This operationally simple macrocyclization was performed on a gram scale. Using this strategy arylomycin A₂ **111** was achieved in 8 steps with a 25% overall yield (Scheme 21a).

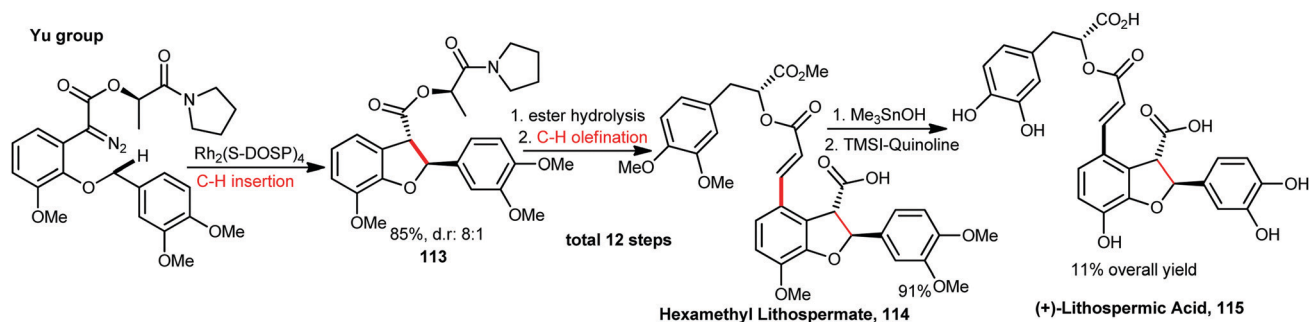
Vancomycin is one of the most important antibiotics to treat deadly Gram-positive bacterial infections.¹⁸¹ The best-known total synthesis of Vancomycin was reported by the Boger group.¹⁸² Vancomycin aglycon (Vancomycin without the disaccharide part) **112** was synthesized in 17 steps with a 5% overall yield. They used one-pot Ir-catalyzed di-C–H borylation, followed by a Cu-catalyzed methoxylation reaction that was easily performed in more than 20 g (Scheme 21b). This strategy afforded an improved route for ring A. Excellent kinetic diastereoselectivity was achieved. Glycosylation of vancomycin aglycon using the enzymatic method in two steps afforded Vancomycin. Hence, after this 19-step reaction sequence, Vancomycin was obtained in a 3.7% overall yield.

14.3 Application in anti-HIV drug synthesis

(+)-Lithospermic acid **115** has been reported to exhibit potent nontoxic activity against HIV by inhibiting HIV-1 integrase.¹⁸³ A total synthesis of (+)-lithospermic acid was achieved by the Ellman and Bergman group where they have included C–H activation in a 10-step reaction sequence and the overall yield was 5.9%.¹⁸⁴ Then in 2011, the Yu group also developed a total synthesis route that used two C–H activation reactions (Scheme 22).¹⁸⁵ One was Rh-catalysed C–H insertion which provided a *trans*-dihydrobenzofuran moiety **113** in 85% yield (d.r. 8:1) and the other one was Pd-catalysed intermolecular C–H alkenylation at a very late stage which afforded hexamethyl lithospermate **114** in 91% yield. It was a 12-step synthesis with an 11% overall yield.



Scheme 21 Improved synthesis of antibiotics via C–H activation.



Scheme 22 Improved synthesis of (+)-lithospermic acid via C–H activation.

15. Conclusions and outlook

Despite the inherent complex, expensive, time-consuming, inter-disciplinary nature and stringent regulation, speed of development is a critical parameter in today's drug discovery. Hence, adaptation of synthetic, computational, bioanalytical, automation techniques is important to accelerate the program. C–H activation is the latest technology added into an organic chemist's toolbox and an impressive array of C–H functionalization methodologies has been developed in the last few decades. Academic research of many synthetic chemistry labs to overcome challenges has been realized from concept development to successful applications. This technique offers a novel disconnection strategy to access privileged medicinal scaffolds unimaginably. Hence, rapid synthesis of heterocycles and late-stage modification of functional molecules can be achieved. Realizing the tremendous potential, the medicinal chemistry community in academic and

industrial sectors has readily adopted this technology in the drug discovery program. Particularly, the synthesis of small quantities of structural analogues for structure–activity relationship (SAR) studies in the lead optimization step and late-stage attachment of molecular probes (fluorescent, radioatom, affinity) for protein profiling using this technique is remarkable. Still, many challenges need to be overcome to exploit the full potential of C–H functionalization in medicinal chemistry and drug discovery. Despite significant research in the past, the mechanism of C–H activation in various substrates is not well-understood, which warrants further investigation for chemo-, regio- and stereoselective transformation of a complex molecule. Due to the higher energy barrier for C–H bond cleavage (85–115 kcal mol⁻¹), harsh reaction conditions and stoichiometric metal additives, strong bases are used which may lead to decomposition or racemization of the sophisticated lead molecule. Hence, the development of an efficient catalytic system to perform the reaction under

ambient conditions is important. Furthermore, the development of biorthogonal C–H functionalization reactions in aqueous medium is extremely important for the late-stage bioconjugation of molecular probes with minimum perturbation of the lead molecule. In the discovery phase, scalable synthesis of the lead molecule for pharmacological studies and finally large-scale processes for marketing is still a bottleneck of C–H activation chemistry. These issues have been partially resolved by the advent of photoredox chemistry, single electron transfer (SET) reactions, organo- and biocatalytic protocols, and electrochemical and microfluidic synthesis. A symbiotic collaboration between academic and industrial researchers is essential for the feedback-based constant improvement of this field. Indeed, working in an interdisciplinary field with smart colleagues to transform methodology to medicine or bench to bedside is a privileged experience. We anticipate that C–H activation will pave the way for the development of theranostic molecules having therapeutic and diagnostic efficacy in the near future.

Author contributions

All authors wrote the manuscript.

Conflicts of interest

There are no conflicts to declare.

Acknowledgements

This work was supported by the DST, SERB, Govt. of India, through Extra Mural Research grant no. EMR/2014/000469. HMB thanks the CSIR for her fellowship.

Notes and references

- D. J. Stewart, A. A. Stewart, P. Wheatley-Price, G. Batist, H. M. Kantarjian, J. Schiller, M. Clemons, J.-P. Bradford, L. Gillespie and R. Kurzrock, *Cancer Med.*, 2018, **7**, 1824–1836.
- (a) G. Sliwoski, S. Kothiwale, J. Meiler and E. W. Lowe, *Pharmacol. Rev.*, 2014, **66**, 334; (b) D. Paul, G. Sanap, S. Shenoy, D. Kalyane, K. Kalia and R. K. Tekade, *Drug Discovery Today*, 2021, **26**, 80–93.
- (a) D. C. Blakemore, L. Castro, I. Churcher, D. C. Rees, A. W. Thomas, D. M. Wilson and A. Wood, *Nat. Chem.*, 2018, **10**, 383–394; (b) J. G. Lombardino and J. A. Lowe, *Nat. Rev. Drug Discovery*, 2004, **3**, 853–862.
- D. G. Brown and J. Boström, *J. Med. Chem.*, 2016, **59**, 4443–4458.
- X. Chen, K. M. Engle, D.-H. Wang and J.-Q. Yu, *Angew. Chem., Int. Ed.*, 2009, **48**, 5094–5115.
- C. Sambigioglio, D. Schönbauer, R. Blicke, T. Dao-Huy, G. Pototschnig, P. Schaaf, T. Wiesinger, M. F. Zia, J. Wencel-Delord, T. Besset, B. U. W. Maes and M. Schnürch, *Chem. Soc. Rev.*, 2018, **47**, 6603–6743.
- (a) M. Ghosh and S. De Sarkar, *Asian J. Org. Chem.*, 2018, **7**, 1236–1255; (b) J. Yang, *Org. Biomol. Chem.*, 2015, **13**, 1930–1941; (c) I. Franzoni and C. Mazet, *Org. Biomol. Chem.*, 2014, **12**, 233–241; (d) M. Brochetta, T. Borsari, S. Bag, S. Jana, S. Maiti, A. Porta, D. B. Werz, G. Zanonni and D. Maiti, *Chem. – Eur. J.*, 2019, **25**, 10323–10327; (e) S. Guin, P. Dolui, X. Zhang, S. Paul, V. K. Singh, S. Pradhan, H. B. Chandrashekar, S. S. Anjana, R. S. Paton and D. Maiti, *Angew. Chem., Int. Ed.*, 2019, **58**, 5633–5638; (f) S. Bag, R. Jayarajan, U. Dutta, R. Chowdhury, R. Mondal and D. Maiti, *Angew. Chem., Int. Ed.*, 2017, **56**, 12538–12542; (g) A. Maji, B. Bhaskararao, S. Singha, R. B. Sunoj and D. Maiti, *Chem. Sci.*, 2016, **7**, 3147–3153.
- (a) J. I. Higham and J. A. Bull, *Org. Biomol. Chem.*, 2020, **18**, 7291–7315; (b) G. Rani, V. Luxami and K. Paul, *Chem. Commun.*, 2020, **56**, 12479–12521.
- T. Dalton, T. Faber and F. Glorius, *ACS Cent. Sci.*, 2021, **7**, 245–261.
- (a) C. K. Prier, D. A. Rankic and D. W. C. MacMillan, *Chem. Rev.*, 2013, **113**, 5322–5363; (b) Q. Qin, H. Jiang, Z. Hu, D. Ren and S. Yu, *Chem. Rev.*, 2017, **17**, 754–774.
- (a) S. Santoro, F. Ferlin, L. Ackermann and L. Vaccaro, *Chem. Soc. Rev.*, 2019, **48**, 2767–2782; (b) S. Govaerts, A. Nyuchev and T. Noel, *J. Flow Chem.*, 2020, **10**, 13–71.
- A. Polamarasetty, R. Kakularam Kumar and R. Pallu, *Curr. Med. Chem.*, 2012, **19**, 3763–3778.
- X. Wang, K. Song, L. Li and L. Chen, *Curr. Top. Med. Chem.*, 2018, **18**, 998–1006.
- (a) P. Kirsch, A. M. Hartman, A. K. H. Hirsch and M. Empting, *Molecules*, 2019, **24**, 4309; (b) Q. Li, *Front. Mol. Biosci.*, 2020, **7**, 180.
- H. Fang, B. Peng, S. Y. Ong, Q. Wu, L. Li and S. Q. Yao, *Chem. Sci.*, 2021, **12**, 8288–8310.
- (a) M. M. Heravi and V. Zadsirjan, *RSC Adv.*, 2020, **10**, 44247–44311; (b) N. Kerru, L. Gummidi, S. Maddila, K. K. Gangu and S. B. Jonnalagadda, *Molecules*, 2020, **25**, 1909.
- E. Vitaku, D. T. Smith and J. T. Njardarson, *J. Med. Chem.*, 2014, **57**, 10257–10274.
- (a) N. Kudo, M. Perseghini and G. C. Fu, *Angew. Chem., Int. Ed.*, 2006, **45**, 1282–1284; (b) M. A. Düfert, K. L. Billingsley and S. L. Buchwald, *J. Am. Chem. Soc.*, 2013, **135**, 12877–12885; (c) I. Nakamura and Y. Yamamoto, *Chem. Rev.*, 2004, **104**, 2127–2198.
- (a) A. Baccalini, G. Faita, G. Zanonni and D. Maiti, *Chem. – Eur. J.*, 2020, **26**, 9749–9783; (b) G. Meng, H.-Y. Niu, G.-R. Qu, J. S. Fossey, J.-P. Li and H.-M. Guo, *Chem. Commun.*, 2012, **48**, 9601–9603; (c) M. Zhang, Q. Wang, Y. Peng, Z. Chen, C. Wan, J. Chen, Y. Zhao, R. Zhang and A. Q. Zhang, *Chem. Commun.*, 2019, **55**, 13048–13065.
- (a) M. O. Tischler, M. B. Tóth and Z. Novák, *Chem. Rev.*, 2017, **17**, 184–199; (b) R. Das, G. S. Kumar and M. Kapur, *Eur. J. Org. Chem.*, 2017, 5439–5459; (c) B. K. Singh and R. Jana, *J. Org. Chem.*, 2016, **81**, 831–841; (d) B. K. Singh, A. Polley and R. Jana, *J. Org. Chem.*, 2016, **81**, 4295–4303; (e) B. K. Singh, G. Bairy and R. Jana, *ChemistrySelect*, 2017, **2**, 9227–9232; (f) A. Polley, K. Varalaxmi and R. Jana, *ACS Omega*, 2018, **3**, 14503–14516; (g) H. M. Begam, R. Choudhury, A. Behera and R. Jana, *Org. Lett.*, 2019, **21**, 4651–4656.
- A. E. Shilov and G. B. Shul'pin, *Chem. Rev.*, 1997, **97**, 2879–2932.
- T. V. Sravanthi and S. L. Manju, *Eur. J. Pharm. Sci.*, 2016, **91**, 1–10.
- (a) H. Zhu, S. Zhao, Y. Zhou, C. Li and H. Liu, *Catalysts*, 2020, **10**, 1253; (b) T. Guo, F. Huang, L. Yu and Z. Yu, *Tetrahedron Lett.*, 2015, **56**, 296–302; (c) S. Agasti, A. Dey and D. Maiti, *Chem. Commun.*, 2017, **53**, 6544–6556.
- R. J. Sundberg, *Indoles*, Academic Press, San Diego, 1996.
- (a) W. Yu, Y. Du and K. Zhao, *Org. Lett.*, 2009, **11**, 2417–2420; (b) J. S. S. Neto and G. Zeni, *Org. Chem. Front.*, 2020, **7**, 155–210.
- (a) M. K. Manna, S. K. Bhunia and R. Jana, *Chem. Commun.*, 2017, **53**, 6906–6909; (b) M. K. Manna, G. Bairy and R. Jana, *J. Org. Chem.*, 2018, **83**, 8390–8400.
- E. Dinda, S. K. Bhunia and R. Jana, *Curr. Org. Chem.*, 2020, **24**, 2612–2633.
- (a) A. H. Sandtorv, *Adv. Synth. Catal.*, 2015, **357**, 2403–2435; (b) J. A. Leitch, Y. Bhonoah and C. G. Frost, *ACS Catal.*, 2017, **7**, 5618–5627; (c) J. Wen and Z. Shi, *Acc. Chem. Res.*, 2021, **54**, 1723–1736.
- D. A. Horton, G. T. Bourne and M. L. Smythe, *Chem. Rev.*, 2003, **103**, 893–930.
- (a) B. Schmidt and B. Schieffer, *J. Med. Chem.*, 2003, **46**, 2261–2270; (b) M. Ojima, H. Igata, M. Tanaka, H. Sakamoto, T. Kuroita, Y. Kohara, K. Kubo, H. Fuse, Y. Imura, K. Kusumoto and H. Nagaya, *J. Pharmacol. Exp. Ther.*, 2011, **336**, 801–808.
- F. Bellina and R. Rossi, *Chem. Rev.*, 2010, **110**, 1082–1146.
- (a) M. Seki, *ACS Catal.*, 2011, **1**, 607–610; (b) L. Ackermann, *Org. Process Res. Dev.*, 2015, **19**, 260–269.
- R. J. Phipps and M. J. Gaunt, *Science*, 2009, **323**, 1593.
- (a) A. P. Honeycutt and J. M. Hoover, *ACS Catal.*, 2017, **7**, 4597–4601; (b) B. Liu, Z.-Z. Zhang, X. Li and B.-F. Shi, *Org. Chem. Front.*, 2016, **3**, 897–900.
- I. B. Seiple, S. Su, R. A. Rodriguez, R. Gianatassio, Y. Fujiwara, A. L. Sobel and P. S. Baran, *J. Am. Chem. Soc.*, 2010, **132**, 13194–13196.
- M. Simonetti, D. M. Cannas, X. Just-Baringo, I. J. Vitorica-Yrezabal and I. Larrosa, *Nat. Chem.*, 2018, **10**, 724–731.

- 37 S. G. Ouellet, A. Roy, C. Molinaro, R. Angelaud, J.-F. Marcoux, P. D. O'Shea and I. W. Davies, *J. Org. Chem.*, 2011, **76**, 1436–1439.
- 38 I.-L. Tsai, F.-P. Lee, C.-C. Wu, C.-Y. Duh, T. Ishikawa, J.-J. Chen, Y.-C. Chen, H. Seki and I.-S. Chen, *Planta Med.*, 2005, **71**, 535–542.
- 39 W. R. Gutekunst and P. S. Baran, *J. Am. Chem. Soc.*, 2011, **133**, 19076–19079.
- 40 B. S. Kadu, *Catal. Sci. Technol.*, 2021, **11**, 1186–1221.
- 41 A. Ros, R. Fernández and J. M. Lassaletta, *Chem. Soc. Rev.*, 2014, **43**, 3229–3243.
- 42 (a) I. A. I. Mkhaliid, J. H. Barnard, T. B. Marder, J. M. Murphy and J. F. Hartwig, *Chem. Rev.*, 2010, **110**, 890–931; (b) B. Ghaffari, S. M. Preshlock, D. L. Plattner, R. J. Staples, P. E. Maligres, S. W. Krska, R. E. Maleczka and M. R. Smith, *J. Am. Chem. Soc.*, 2014, **136**, 14345–14348; (c) S. M. Preshlock, B. Ghaffari, P. E. Maligres, S. W. Krska, R. E. Maleczka and M. R. Smith, *J. Am. Chem. Soc.*, 2013, **135**, 7572–7582; (d) J. Chaturvedi, C. Haldar, R. Bisht, G. Pandey and B. Chattopadhyay, *J. Am. Chem. Soc.*, 2021, **143**, 7604–7611; (e) M. E. Hoque, M. M. M. Hassan and B. Chattopadhyay, *J. Am. Chem. Soc.*, 2021, **143**, 5022–5037.
- 43 (a) H.-L. Li, M. Kanai and Y. Kuninobu, *Org. Lett.*, 2017, **19**, 5944–5947; (b) I. Sasaki, T. Amou, H. Ito and T. Ishiyama, *Org. Biomol. Chem.*, 2014, **12**, 2041–2044; (c) J. Zeng, M. Naito, T. Torigoe, M. Yamanaka and Y. Kuninobu, *Org. Lett.*, 2020, **22**, 3485–3489.
- 44 (a) T. Ishiyama, J. Takagi, J. F. Hartwig and N. Miyaara, *Angew. Chem., Int. Ed.*, 2002, **41**, 3056–3058; (b) Y. Kuninobu, H. Ida, M. Nishi and M. Kanai, *Nat. Chem.*, 2015, **7**, 712–717.
- 45 L.-C. Campeau, Q. Chen, D. Gauvreau, M. Girardin, K. Belyk, P. Maligres, G. Zhou, C. Gu, W. Zhang, L. Tan and P. D. O'Shea, *Org. Process Res. Dev.*, 2016, **20**, 1476–1481.
- 46 (a) S. Omura, Y. Iwai, A. Hirano, A. Nakagawa, J. Awaya, H. Tsuchiya, Y. Takahashi and R. Masuma, *J. Antibiot.*, 1977, **30**, 275–282; (b) M. I. Davis, J. P. Hunt, S. Herrgard, P. Ciceri, L. M. Wodicka, G. Pallares, M. Hocker, D. K. Treiber and P. P. Zarrinkar, *Nat. Biotechnol.*, 2011, **29**, 1046–1051.
- 47 L. Prade, R. A. Engh, A. Girod, V. Kinzel, R. Huber and D. Bossemeyer, *Structure*, 1997, **5**, 1627–1637.
- 48 K. M. Gayler, K. Kong, K. Reisenauer, J. H. Taube and J. L. Wood, *ACS Med. Chem. Lett.*, 2020, **11**, 2441–2445.
- 49 M. A. Larsen and J. F. Hartwig, *J. Am. Chem. Soc.*, 2014, **136**, 4287–4299.
- 50 C. Cheng and J. F. Hartwig, *J. Am. Chem. Soc.*, 2015, **137**, 592–595.
- 51 B. B. Fredholm, I. J. Ap, K. A. Jacobson, K. N. Klotz and J. Linden, *Pharmacol. Rev.*, 2001, **53**, 527–552.
- 52 M. M. Littleton, A. D. Campbell, A. Clarke, M. Dow, G. Ensor, M. C. Evans, A. Herring, B. A. Jackson, L. V. Jackson, S. Karlsson, D. J. Klauber, D. H. Legg, K. W. Leslie, Š. Moravčík, C. D. Parsons, T. O. Ronson and R. E. Meadows, *Org. Process Res. Dev.*, 2019, **23**, 1407–1419.
- 53 (a) X. Wang, T. Nitanda, M. Shi, M. Okamoto, T. Furukawa, Y. Sugimoto, S.-i. Akiyama and M. Baba, *Biochem. Pharmacol.*, 2004, **68**, 1363–1370; (b) S. K. Rabindran, D. D. Ross, L. A. Doyle, W. Yang and L. M. Greenberger, *Cancer Res.*, 2000, **60**, 47–50.
- 54 Y. Feng, D. Holte, J. Zoller, S. Umemiya, L. R. Simke and P. S. Baran, *J. Am. Chem. Soc.*, 2015, **137**, 10160–10163.
- 55 A. Modak, T. Patra, R. Chowdhury, S. Raul and D. Maiti, *Organometallics*, 2017, **36**, 2418–2423.
- 56 (a) J. C. Lewis, P. S. Coelho and F. H. Arnold, *Chem. Soc. Rev.*, 2011, **40**, 2003–2021; (b) J. Dong, E. Fernández-Fueyo, F. Hollmann, C. E. Paul, M. Pesic, S. Schmidt, Y. Wang, S. Younes and W. Zhang, *Angew. Chem., Int. Ed.*, 2018, **57**, 9238–9261.
- 57 (a) S. H. Cho, J. Y. Kim, J. Kwak and S. Chang, *Chem. Soc. Rev.*, 2011, **40**, 5068–5083; (b) M. C. Bagley, J. W. Dale, E. A. Merritt and X. Xiong, *Chem. Rev.*, 2005, **105**, 685–714.
- 58 (a) J. Bariwal and E. Van der Eycken, *Chem. Soc. Rev.*, 2013, **42**, 9283–9303; (b) J. Rayadurgam, S. Sana, M. Sasikumar and Q. Gu, *Org. Chem. Front.*, 2021, **8**, 384–414.
- 59 M. M. Heravi and V. Zadsirjan, *RSC Adv.*, 2020, **10**, 44247–44311.
- 60 D. Jelić and R. Antolović, *Antibiotics*, 2016, **5**, 29.
- 61 H. Lin and D. Sun, *Org. Prep. Proced. Int.*, 2013, **45**, 341–394.
- 62 (a) M. M. Heravi, Z. Kheilkordi, V. Zadsirjan, M. Heydari and M. Malmir, *J. Organometal. Chem.*, 2018, **861**, 17–104; (b) P. Ruiz-Castillo and S. L. Buchwald, *Chem. Rev.*, 2016, **116**, 12564–12649.
- 63 J.-Q. Chen, J.-H. Li and Z.-B. Dong, *Adv. Synth. Catal.*, 2020, **362**, 3311–3331.
- 64 (a) Y. Park, Y. Kim and S. Chang, *Chem. Rev.*, 2017, **117**, 9247–9301; (b) D. Hazeldard, P.-A. Nocquet and P. Compain, *Org. Chem. Front.*, 2017, **4**, 2500–2521; (c) M.-L. Louillat and F. W. Patureau, *Chem. Soc. Rev.*, 2014, **43**, 901–910; (d) K. Shin, H. Kim and S. Chang, *Acc. Chem. Res.*, 2015, **48**, 1040–1052.
- 65 (a) Q. Michaudel, D. Thevenet and P. S. Baran, *J. Am. Chem. Soc.*, 2012, **134**, 2547–2550; (b) G.-X. Li, C. A. Morales-Rivera, F. Gao, Y. Wang, G. He, P. Liu and G. Chen, *Chem. Sci.*, 2017, **8**, 7180–7185; (c) T. Shen and T. H. Lambert, *J. Am. Chem. Soc.*, 2021, **143**, 8597–8602.
- 66 A. McNally, B. Haffemayer, B. S. L. Collins and M. J. Gaunt, *Nature*, 2014, **510**, 129–133.
- 67 D. Willcox, B. G. N. Chappell, K. F. Hogg, J. Calleja, A. P. Smalley and M. J. Gaunt, *Science*, 2016, **354**, 851–857.
- 68 (a) M. Nappi, C. He, W. G. Whitehurst, B. G. N. Chappell and M. J. Gaunt, *Angew. Chem., Int. Ed.*, 2018, **57**, 3178–3182; (b) G. He, Y. Zhao, S. Zhang, C. Lu and G. Chen, *J. Am. Chem. Soc.*, 2012, **134**, 3–6.
- 69 B. J. Stokes, H. Dong, B. E. Leslie, A. L. Pumphrey and T. G. Driver, *J. Am. Chem. Soc.*, 2007, **129**, 7500–7501.
- 70 T.-S. Mei, D. Leow, H. Xiao, B. N. Laforteza and J.-Q. Yu, *Org. Lett.*, 2013, **15**, 3058–3061.
- 71 M. Yang, B. Su, Y. Wang, K. Chen, X. Jiang, Y.-F. Zhang, X.-S. Zhang, G. Chen, Y. Cheng, Z. Cao, Q.-Y. Guo, L. Wang and Z.-J. Shi, *Nat. Commun.*, 2014, **5**, 4707.
- 72 (a) K. Takahashi, D. Yamaguchi, J. Ishihara and S. Hatakeyama, *Org. Lett.*, 2012, **14**, 1644–1647; (b) A. L. Pumphrey, H. Dong and T. G. Driver, *Angew. Chem., Int. Ed.*, 2012, **51**, 5920–5923; (c) J. Du Bois, *Org. Process Res. Dev.*, 2011, **15**, 758–762.
- 73 J. J. Fleming, M. D. McReynolds and J. Du Bois, *J. Am. Chem. Soc.*, 2007, **129**, 9964–9975.
- 74 S. Purser, P. R. Moore, S. Swallow and V. Gouverneur, *Chem. Soc. Rev.*, 2008, **37**, 320–330.
- 75 P. Shah and A. D. Westwell, *J. Enzyme Inhib. Med. Chem.*, 2007, **22**, 527–540.
- 76 M. Inoue, Y. Sumii and N. Shibata, *ACS Omega*, 2020, **5**, 10633–10640.
- 77 (a) J. R. Brandt, E. Lee, G. B. Boursalian and T. Ritter, *Chem. Sci.*, 2014, **5**, 169–179; (b) J. Miao, K. Yang, M. Kurek and H. Ge, *Org. Lett.*, 2015, **17**, 3738–3741.
- 78 T. Truong, K. Klimovica and O. Daugulis, *J. Am. Chem. Soc.*, 2013, **135**, 9342–9345.
- 79 X. Yang, T. Wu, R. J. Phipps and F. D. Toste, *Chem. Rev.*, 2015, **115**, 826–870.
- 80 H. Lee, J. Börgel and T. Ritter, *Angew. Chem., Int. Ed.*, 2017, **56**, 6966–6969.
- 81 (a) W. Liu, X. Huang, M.-J. Cheng, R. J. Nielsen, W. A. Goddard and J. T. Groves, *Science*, 2012, **337**, 1322; (b) G. Li, A. K. Dilger, P. T. Cheng, W. R. Ewing and J. T. Groves, *Angew. Chem., Int. Ed.*, 2018, **57**, 1251–1255.
- 82 (a) Z. Deng, Z. Zhao, G. He and G. Chen, *Org. Lett.*, 2021, **23**, 3631–3635; (b) J. Li, J. Chen, R. Sang, W.-S. Ham, M. B. Plutschack, F. Berger, S. Chhabra, A. Schnegg, C. Genicot and T. Ritter, *Nat. Chem.*, 2020, **12**, 56–62.
- 83 (a) R. Szpera, D. F. J. Moseley, L. B. Smith, A. J. Sterling and V. Gouverneur, *Angew. Chem., Int. Ed.*, 2019, **58**, 14824–14848; (b) A. Lin, C. B. Huehls and J. Yang, *Org. Chem. Front.*, 2014, **1**, 434–438; (c) Q. Cheng and T. Ritter, *Trends Chem.*, 2019, **1**, 461–470.
- 84 S.-J. Lou, Q. Chen, Y.-F. Wang, D.-Q. Xu, X.-H. Du, J.-Q. He, Y.-J. Mao and Z.-Y. Xu, *ACS Catal.*, 2015, **5**, 2846–2849.
- 85 L. Wu, P. Chen and G. Liu, *Org. Lett.*, 2016, **18**, 960–963.
- 86 J. Y. Sun, H. Yang, S. Miao, J. P. Li, S. W. Wang, M. Z. Zhu, Y. H. Xie, J. B. Wang, Z. Liu and Q. Yang, *Phytomedicine*, 2009, **16**, 1070–1074.
- 87 J. Y. Sun, M. Z. Zhu, S. W. Wang, S. Miao, Y. H. Xie and J. B. Wang, *Phytomedicine*, 2007, **14**, 353–359.
- 88 Y. Takaya, H. Tasaka, T. Chiba, K. Uwai, M.-a. Tanitsu, H.-S. Kim, Y. Wataya, M. Miura, M. Takeshita and Y. Oshima, *J. Med. Chem.*, 1999, **42**, 3163–3166.
- 89 (a) C. D. Sessler, M. Rahm, S. Becker, J. M. Goldberg, F. Wang and S. J. Lippard, *J. Am. Chem. Soc.*, 2017, **139**, 9325–9332; (b) J. A. Erickson and J. I. McLoughlin, *J. Org. Chem.*, 1995, **60**, 1626–1631.
- 90 X. Zeng, W. Yan, M. Paeth, S. B. Zacate, P.-H. Hong, Y. Wang, D. Yang, K. Yang, T. Yan, C. Song, Z. Cao, M.-J. Cheng and W. Liu, *J. Am. Chem. Soc.*, 2019, **141**, 19941–19949.
- 91 C. Yuan, L. Zhu, C. Chen, X. Chen, Y. Yang, Y. Lan and Y. Zhao, *Nat. Commun.*, 2018, **9**, 1189.

- 92 S.-Q. Zhu, Y.-L. Liu, H. Li, X.-H. Xu and F.-L. Qing, *J. Am. Chem. Soc.*, 2018, **140**, 11613–11617.
- 93 Y.-J. Mao, B.-X. Wang, Q.-Z. Wu, K. Zhou, S.-J. Lou and D.-Q. Xu, *Chem. Commun.*, 2019, **55**, 2019–2022.
- 94 (a) G.-b. Li, C. Zhang, C. Song and Y.-d. Ma, *Beilstein J. Org. Chem.*, 2018, **14**, 155–181; (b) Y. Kunitobu and T. Torigoe, *Bull. Chem. Soc.*, 2020, **94**, 532–541; (c) J. B. I. Sap, C. F. Meyer, N. J. W. Straathof, N. Iwumene, C. W. am Ende, A. A. Trabanco and V. Gouverneur, *Chem. Soc. Rev.*, 2021, **50**, 8214–8247.
- 95 (a) Y. Fujiwara, J. A. Dixon, F. O'Hara, E. D. Funder, D. D. Dixon, R. A. Rodriguez, R. D. Baxter, B. Herlé, N. Sach, M. R. Collins, Y. Ishihara and P. S. Baran, *Nature*, 2012, **492**, 95–99; (b) Y. Ji, T. Brueckl, R. D. Baxter, Y. Fujiwara, I. B. Seiple, S. Su, D. G. Blackmond and P. S. Baran, *Proc. Natl. Acad. Sci. U. S. A.*, 2011, **108**, 14411–14415.
- 96 E. A. Meucci, S. N. Nguyen, N. M. Camasso, E. Chong, A. Ariafard, A. J. Canty and M. S. Sanford, *J. Am. Chem. Soc.*, 2019, **141**, 12872–12879.
- 97 S. Guo, D. I. AbuSalim and S. P. Cook, *J. Am. Chem. Soc.*, 2018, **140**, 12378–12382.
- 98 M. Paeth, W. Carson, J.-H. Luo, D. Tierney, Z. Cao, M.-J. Cheng and W. Liu, *Chem. – Eur. J.*, 2018, **24**, 11559–11563.
- 99 H. Xiao, Z. Liu, H. Shen, B. Zhang, L. Zhu and C. Li, *Chem*, 2019, **5**, 940–949.
- 100 (a) E. J. Barreiro, A. E. Kümmerle and C. A. M. Fraga, *Chem. Rev.*, 2011, **111**, 5215–5246; (b) S. Sun and J. Fu, *Bioorg. Med. Chem. Lett.*, 2018, **28**, 3283–3289.
- 101 (a) H. Schönherr and T. Cernak, *Angew. Chem., Int. Ed.*, 2013, **52**, 12256–12267; (b) D. Aynetdinova, M. C. Callens, H. B. Hicks, C. Y. X. Poh, B. D. A. Shennan, A. M. Boyd, Z. H. Lim, J. A. Leitch and D. J. Dixon, *Chem. Soc. Rev.*, 2021, **50**, 5517–5563.
- 102 B. R. Rosen, L. R. Simke, P. S. Thuy-Boun, D. D. Dixon, J.-Q. Yu and P. S. Baran, *Angew. Chem., Int. Ed.*, 2013, **52**, 7317–7320.
- 103 S. D. Friis, M. J. Johansson and L. Ackermann, *Nat. Chem.*, 2020, **12**, 511–519.
- 104 E. Weis, M. A. Hayes, M. J. Johansson and B. Martín-Matute, *iScience*, 2021, **24**, 102467.
- 105 D.-H. Wang, M. Wasa, R. Giri and J.-Q. Yu, *J. Am. Chem. Soc.*, 2008, **130**, 7190–7191.
- 106 (a) K. J. Culhane, Y. Liu, Y. Cai and E. C. Y. Yan, *Front. Pharmacol.*, 2015, **6**, 264; (b) L. T. Williams, R. Snyderman, M. C. Pike and R. J. Lefkowitz, *Proc. Natl. Acad. Sci. U. S. A.*, 1977, **74**, 1204; (c) S.-J. Kim, J. Xiao, J. Wan, P. Cohen and K. Yen, *J. Physiol.*, 2017, **595**, 6613–6621.
- 107 (a) P. Davide, T. Nikos, B. Alberto and P. Maurizio, *Mini-Rev. Med. Chem.*, 2004, **4**, 805–814; (b) W. Li, F. Separovic, N. M. O'Brien-Simpson and J. D. Wade, *Chem. Soc. Rev.*, 2021, **50**, 4932–4973.
- 108 (a) G. Zhang, S. Zheng, H. Liu and P. R. Chen, *Chem. Soc. Rev.*, 2015, **44**, 3405–3417; (b) Y. Takaoka, A. Ojida and I. Hamachi, *Angew. Chem., Int. Ed.*, 2013, **52**, 4088–4106.
- 109 A. C. Lee, J. L. Harris, K. K. Khanna and J.-H. Hong, *Int. J. Mol. Sci.*, 2019, **20**, 2383.
- 110 D. J. Craik, D. P. Fairlie, S. Liras and D. Price, *Chem. Biol. Drug Des.*, 2013, **81**, 136–147.
- 111 (a) G. H. Bird, N. Madani, A. F. Perry, A. M. Princiotta, J. G. Supko, X. He, E. Gavathiotis, J. G. Sodroski and L. D. Walensky, *Proc. Natl. Acad. Sci. U. S. A.*, 2010, **107**, 14093; (b) E. M. Driggers, S. P. Hale, J. Lee and N. K. Terrett, *Nat. Rev. Drug Discovery*, 2008, **7**, 608–624; (c) Z. Szewczuk, B. F. Gibbs, S. Y. Yue, E. O. Purisima and Y. Konishi, *Biochemistry*, 1992, **31**, 9132–9140.
- 112 A. F. M. Noisier and M. A. Brimble, *Chem. Rev.*, 2014, **114**, 8775–8806.
- 113 (a) H.-R. Tong, B. Li, G. Li, G. He and G. Chen, *CCS Chem.*, 2020, **2**, 1797–1820; (b) X. Lu, S.-J. He, W.-M. Cheng and J. Shi, *Chin. Chem. Lett.*, 2018, **29**, 1001–1008; (c) S. Sengupta and G. Mehta, *Tetrahedron Lett.*, 2017, **58**, 1357–1372.
- 114 S. Sengupta and G. Mehta, *Org. Biomol. Chem.*, 2020, **18**, 1851–1876.
- 115 L. Mendive-Tapia, S. Preciado, J. Garcia, R. Ramón, N. Kielland, F. Albericio and R. Lavilla, *Nat. Commun.*, 2015, **6**, 7160.
- 116 J. Tang, Y. He, H. Chen, W. Sheng and H. Wang, *Chem. Sci.*, 2017, **8**, 4565–4570.
- 117 E. Hausteina and P. Schwiller, *HFSP J.*, 2007, **1**, 169–180.
- 118 M. Vendrell, D. Zhai, J. C. Er and Y.-T. Chang, *Chem. Rev.*, 2012, **112**, 4391–4420.
- 119 G. Lukinavičius, K. Umezawa, N. Olivier, A. Honigmann, G. Yang, T. Plass, V. Mueller, L. Reymond, I. R. Corréa Jr, Z.-G. Luo, C. Schultz, E. A. Lemke, P. Heppenstall, C. Eggeling, S. Manley and K. Johnsson, *Nat. Chem.*, 2013, **5**, 132–139.
- 120 Y. Cheng, G. Li, Y. Liu, Y. Shi, G. Gao, D. Wu, J. Lan and J. You, *J. Am. Chem. Soc.*, 2016, **138**, 4730–4738.
- 121 X. Yang, L. Jiang, M. Yang, H. Zhang, J. Lan, F. Zhou, X. Chen, D. Wu and J. You, *J. Org. Chem.*, 2018, **83**, 9538–9546.
- 122 M. Virelli, W. Wang, R. Kuniyil, J. Wu, G. Zanoni, A. Fernandez, J. Scott, M. Vendrell and L. Ackermann, *Chem. – Eur. J.*, 2019, **25**, 12712–12718.
- 123 Y.-Y. Fan, X.-H. Gao and J.-M. Yue, *Sci. China: Chem.*, 2016, **59**, 1126–1141.
- 124 (a) E. H. Kim, G. Chin, G. Rong, K. E. Poskanzer and H. A. Clark, *Acc. Chem. Res.*, 2018, **51**, 1023–1032; (b) J. W. Taraska and W. N. Zagotta, *Neuron*, 2010, **66**, 170–189.
- 125 A. Ramirez and M. R. Arbuckle, *Biol. Psychiatry*, 2016, **80**, e73–e75.
- 126 (a) W. J. Betz and G. S. Bewick, *Science*, 1992, **255**, 200; (b) G. Miesenböck, D. A. De Angelis and J. E. Rothman, *Nature*, 1998, **394**, 192–195; (c) V. N. Murthy, T. J. Sejnowski and C. F. Stevens, *Neuron*, 1997, **18**, 599–612.
- 127 N. G. Gubernator, H. Zhang, R. G. W. Staal, E. V. Mosharov, D. B. Pereira, M. Yue, V. Balsanek, P. A. Vadola, B. Mukherjee, R. H. Edwards, D. Sulzer and D. Sames, *Science*, 2009, **324**, 1441.
- 128 P. A. Vadola and D. Sames, *J. Org. Chem.*, 2012, **77**, 7804–7814.
- 129 P. W. Miller, N. J. Long, R. Vilar and A. D. Gee, *Angew. Chem., Int. Ed.*, 2008, **47**, 8998–9033.
- 130 S. M. Ametamey, M. Honer and P. A. Schubiger, *Chem. Rev.*, 2008, **108**, 1501–1516.
- 131 J. Orit and C. Xiaoyuan, *Curr. Top. Med. Chem.*, 2010, **10**, 1048–1059.
- 132 O. Jacobson, D. O. Kiesewetter and X. Chen, *Bioconjugate Chem.*, 2015, **26**, 1–18.
- 133 (a) X. Huang, W. Liu, H. Ren, R. Neelamegam, J. M. Hooker and J. T. Groves, *J. Am. Chem. Soc.*, 2014, **136**, 6842–6845; (b) W. Liu, X. Huang, M. S. Placzek, S. W. Kraska, P. McQuade, J. M. Hooker and J. T. Groves, *Chem. Sci.*, 2018, **9**, 1168–1172.
- 134 S. J. Lee, K. J. Makaravage, A. F. Brooks, P. J. H. Scott and M. S. Sanford, *Angew. Chem., Int. Ed.*, 2019, **58**, 3119–3122.
- 135 J. S. Wright, L. S. Sharninghausen, S. Preshlock, A. F. Brooks, M. S. Sanford and P. J. H. Scott, *J. Am. Chem. Soc.*, 2021, **143**, 6915–6921.
- 136 (a) P. Farkaš and S. Bystrický, *Chem. Pap.*, 2010, **64**, 683–695; (b) J. M. J. M. Ravasco, H. Faustino, A. Trindade and P. M. P. Gois, *Chem. – Eur. J.*, 2019, **25**, 43–59.
- 137 (a) R. K. V. Lim and Q. Lin, *Chem. Commun.*, 2010, **46**, 1589–1600; (b) K. Lang and J. W. Chin, *ACS Chem. Biol.*, 2014, **9**, 16–20.
- 138 N. Stephanopoulos and M. B. Francis, *Nat. Chem. Biol.*, 2011, **7**, 876–884.
- 139 H. C. Kolb, M. G. Finn and K. B. Sharpless, *Angew. Chem., Int. Ed.*, 2001, **40**, 2004–2021.
- 140 (a) J. C. Jewett, E. M. Sletten and C. R. Bertozzi, *J. Am. Chem. Soc.*, 2010, **132**, 3688–3690; (b) C. G. Gordon, J. L. Mackey, J. C. Jewett, E. M. Sletten, K. N. Houk and C. R. Bertozzi, *J. Am. Chem. Soc.*, 2012, **134**, 9199–9208.
- 141 (a) A. Herner and Q. Lin, *Top. Curr. Chem.*, 2015, **374**, 1; (b) K. Singh, C. J. Fennell, E. A. Coutusias, R. Latifi, S. Hartson and J. D. Weaver, *Chem*, 2018, **4**, 124–137.
- 142 X. Chen, Y. Wang, N. Ma, J. Tian, Y. Shao, B. Zhu, Y. K. Wong, Z. Liang, C. Zou and J. Wang, *Sig. Transduct. Targeted Ther.*, 2020, **5**, 72.
- 143 J. Li, J. S. Cisar, C.-Y. Zhou, B. Vera, H. Williams, A. D. Rodriguez, B. F. Cravatt and D. Romo, *Nat. Chem.*, 2013, **5**, 510–517.
- 144 D. N. Zalatan and J. Du Bois, *J. Am. Chem. Soc.*, 2009, **131**, 7558–7559.
- 145 Q. Zhou, J. Gui, C.-M. Pan, E. Albone, X. Cheng, E. M. Suh, L. Grasso, Y. Ishihara and P. S. Baran, *J. Am. Chem. Soc.*, 2013, **135**, 12994–12997.
- 146 (a) Z. Zhoupeng, Z. Mingshe and T. Wei, *Curr. Pharm. Des.*, 2009, **15**, 2220–2235; (b) L. G. Yengi, L. Leung and J. Kao, *Pharm. Res.*, 2007, **24**, 842.
- 147 B. K. Park, A. Boobis, S. Clarke, C. E. P. Goldring, D. Jones, J. G. Kenna, C. Lambert, H. G. Lavery, D. J. Naisbitt, S. Nelson, D. A. Nicoll-Griffith, R. S. Obach, P. Routledge, D. A. Smith, D. J. Tweedie, N. Vermeulen, D. P. Williams, I. D. Wilson and T. A. Baillie, *Nat. Rev. Drug Discovery*, 2011, **10**, 292–306.
- 148 L. C. Wienkers and T. G. Heath, *Nat. Rev. Drug Discovery*, 2005, **4**, 825–833.

- 149 (a) F. P. Guengerich, *Nat. Rev. Drug Discovery*, 2002, **1**, 359–366; (b) K. P. Cusack, H. F. Koolman, U. E. W. Lange, H. M. Peltier, I. Piel and A. Vasudevan, *Bioorg. Med. Chem. Lett.*, 2013, **23**, 5471–5483.
- 150 J. Genovino, S. Lütz, D. Sames and B. B. Touré, *J. Am. Chem. Soc.*, 2013, **135**, 12346–12352.
- 151 J. Genovino, D. Sames, L. G. Hamann and B. B. Touré, *Angew. Chem., Int. Ed.*, 2016, **55**, 14218–14238.
- 152 M. A. Masood, M. Bazin, M. E. Bunnage, A. Calabrese, M. Cox, S.-A. Fancy, E. Farrant, D. W. Pearce, M. Perez, L. Hitzel and T. Peakman, *Bioorg. Med. Chem. Lett.*, 2012, **22**, 1255–1262.
- 153 A. Huczynski, J. Stefańska, P. Przybylski, B. Brzezinski and F. Bartl, *Bioorg. Med. Chem. Lett.*, 2008, **18**, 2585–2589.
- 154 B. A. Rocha, A. R. M. de Oliveira, M. Pazin, D. J. Dorta, A. P. N. Rodrigues, A. A. Berretta, A. P. F. Peti, L. A. B. de Moraes, N. P. Lopes, S. Pospíšil, P. J. Gates and M. d. D. Assis, *BioMed Res. Int.*, 2014, **2014**, 152102.
- 155 (a) J. Bernadou and B. Meunier, *Adv. Synth. Catal.*, 2004, **346**, 171–184; (b) W. Lohmann and U. Karst, *Anal. Bioanal. Chem.*, 2008, **391**, 79–96.
- 156 (a) S. L. Schreiber, *Nature*, 2009, **457**, 153–154; (b) R. E. Dolle, B. L. Bourdonnec, K. Worm, G. A. Morales, C. J. Thomas and W. Zhang, *J. Comb. Chem.*, 2010, **12**, 765–806.
- 157 B. Hong, T. Luo and X. Lei, *ACS Cent. Sci.*, 2020, **6**, 622–635.
- 158 M. Moir, J. J. Danon, T. A. Reekie and M. Kassiou, *Expert Opin. Drug Discovery*, 2019, **14**, 1137–1149.
- 159 (a) T. Cernak, K. D. Dykstra, S. Tyagarajan, P. Vachal and S. W. Kraska, *Chem. Soc. Rev.*, 2016, **45**, 546–576; (b) L. Guillemard, N. Kaplaneris, L. Ackermann and M. J. Johansson, *Nat. Rev. Chem.*, 2021, **5**, 522–545.
- 160 (a) M. C. Bryan, B. Dillon, L. G. Hamann, G. J. Hughes, M. E. Kopach, E. A. Peterson, M. Pourashraf, I. Raheem, P. Richardson, D. Richter and H. F. Sneddon, *J. Med. Chem.*, 2013, **56**, 6007–6021; (b) N. A. Meanwell, *Chem. Res. Toxicol.*, 2011, **24**, 1420–1456.
- 161 Y.-J. Liu, H. Xu, W.-J. Kong, M. Shang, H.-X. Dai and J.-Q. Yu, *Nature*, 2014, **515**, 389–393.
- 162 H. Wang, M. M. Lorion and L. Ackermann, *Angew. Chem., Int. Ed.*, 2016, **55**, 10386–10390.
- 163 (a) U. J. Ries, G. Mihm, B. Narr, K. M. Hasselbach, H. Wittneben, M. Entzeroth, J. C. A. van Meel, W. Wienen and N. H. Huel, *J. Med. Chem.*, 1993, **36**, 4040–4051; (b) S. C. Benson, H. A. Pershadsingh, C. I. Ho, A. Chittiboyina, P. Desai, M. Pravenec, N. Qi, J. Wang, M. A. Avery and T. W. Kurtz, *Hypertension*, 2004, **43**, 993–1002.
- 164 (a) M. Shang, M.-M. Wang, T. G. Saint-Denis, M.-H. Li, H.-X. Dai and J.-Q. Yu, *Angew. Chem., Int. Ed.*, 2017, **56**, 5317–5321; (b) M. Shang, S.-Z. Sun, H.-L. Wang, B. N. Laforteza, H.-X. Dai and J.-Q. Yu, *Angew. Chem., Int. Ed.*, 2014, **53**, 10439–10442.
- 165 (a) P. E. Gormisky and M. C. White, *J. Am. Chem. Soc.*, 2013, **135**, 14052–14055; (b) N. D. Chiappini, J. B. C. Mack and J. Du Bois, *Angew. Chem., Int. Ed.*, 2018, **57**, 4956–4959; (c) X. Huang, T. M. Bergsten and J. T. Groves, *J. Am. Chem. Soc.*, 2015, **137**, 5300–5303.
- 166 (a) V. Müller, R. Weck, V. Derdau and L. Ackermann, *ChemCatChem*, 2020, **12**, 100–104; (b) A. Sharma and J. F. Hartwig, *Nature*, 2015, **517**, 600–604; (c) T. Nanjo, E. C. de Lucca and M. C. White, *J. Am. Chem. Soc.*, 2017, **139**, 14586–14591; (d) J. R. Clark, K. Feng, A. Sookezian and M. C. White, *Nat. Chem.*, 2018, **10**, 583–591; (e) S. Porey, X. Zhang, S. Bhowmick, V. Kumar Singh, S. Guin, R. S. Paton and D. Maiti, *J. Am. Chem. Soc.*, 2020, **142**, 3762–3774; (f) S. Agasti, B. Mondal, T. K. Achar, S. K. Sinha, A. Sarala Suseelan, K. J. Szabo, F. Schoenebeck and D. Maiti, *ACS Catal.*, 2019, **9**, 9606–9613; (g) S. Bag, M. Petzold, A. Sur, S. Bhowmick, D. B. Werz and D. Maiti, *Chem. – Eur. J.*, 2019, **25**, 9433–9437.
- 167 M. Song and G. T. Hwang, *J. Med. Chem.*, 2020, **63**, 6578–6599.
- 168 M. L. Malone and B. M. Paegel, *ACS Comb. Sci.*, 2016, **18**, 182–187.
- 169 Z. Fan, S. Zhao, T. Liu, P.-X. Shen, Z.-N. Cui, Z. Zhuang, Q. Shao, J. S. Chen, A. S. Ratnayake, M. E. Flanagan, D. K. Kölmel, D. W. Piotrowski, P. Richardson and J.-Q. Yu, *Chem. Sci.*, 2020, **11**, 12282–12288.
- 170 X. Wang, H. Sun, J. Liu, D. Dai, M. Zhang, H. Zhou, W. Zhong and X. Lu, *Org. Lett.*, 2018, **20**, 4764–4768.
- 171 E. G. Tse, M. Korsik and M. H. Todd, *Malar. J.*, 2019, **18**, 93.
- 172 J. Pousibet-Puerto, J. Salas-Coronas, A. Sánchez-Crespo, M. A. Molina-Arrebola, M. J. Soriano-Pérez, M. J. Giménez-López, J. Vázquez-Villegas and M. T. Cabezas-Fernández, *Malar. J.*, 2016, **15**, 339.
- 173 H.-N. Lyu, N. Ma, Y. Meng, X. Zhang, Y.-K. Wong, C. Xu, F. Liao, T. Jiang, Y. Tu and J. Wang, *Nat. Prod. Rep.*, 2021, **38**, 1243–1250.
- 174 N. Kato, E. Comer, T. Sakata-Kato, A. Sharma, M. Sharma, M. Maetani, J. Bastien, N. M. Brancucci, J. A. Bittker, V. Corey, D. Clarke, E. R. Derbyshire, G. L. Dornan, S. Duffy, F. Catteruccia, J. C. Clardy, Koolen, T. A. Lewis, P. S. Lui, A. K. Lukens, E. Lund, S. March, E. Meibalan, B. C. Meier, J. A. McPhail, B. Mitasev, E. L. Moss, M. Sayes, Y. Van Gessel, M. J. Wawer, T. Yoshinaga, A.-M. Zeeman, V. M. Avery, S. N. Bhatia, J. E. Burke, F. Catteruccia, J. C. Clardy, P. A. Clemons, K. J. Dechering, J. R. Duvall, M. A. Foley, F. Gusovsky, C. H. M. Kocken, M. Marti, M. L. Morningstar, B. Munoz, D. E. Neafsey, A. Sharma, E. A. Winzler, D. F. Wirth, C. A. Scherer and S. L. Schreiber, *Nature*, 2016, **538**, 344–349.
- 175 M. Maetani, J. Zoller, B. Melillo, O. Verho, N. Kato, J. Pu, E. Comer and S. L. Schreiber, *J. Am. Chem. Soc.*, 2017, **139**, 11300–11306.
- 176 D. H. O'Donovan, P. Aillard, M. Berger, A. de la Torre, D. Petkova, C. Knittl-Frank, D. Geerdink, M. Kaiser and N. Maulide, *Angew. Chem., Int. Ed.*, 2018, **57**, 10737–10741.
- 177 G. Stork, D. Niu, A. Fujimoto, E. R. Koft, J. M. Balkovec, J. R. Tata and G. R. Dake, *J. Am. Chem. Soc.*, 2001, **123**, 3239–3242.
- 178 J. Schimana, K. Gebhardt, A. Hölzel, D. G. Schmid, R. Süßmuth, J. Müller, R. Pukall and H. P. Fiedler, *J. Antibiot.*, 2002, **55**, 565–570.
- 179 T. C. Roberts, P. A. Smith, R. T. Cirz and F. E. Romesberg, *J. Am. Chem. Soc.*, 2007, **129**, 15830–15838.
- 180 D. S. Peters, F. E. Romesberg and P. S. Baran, *J. Am. Chem. Soc.*, 2018, **140**, 2072–2075.
- 181 D. Kahne, C. Leimkuhler, W. Lu and C. Walsh, *Chem. Rev.*, 2005, **105**, 425–448.
- 182 M. J. Moore, S. Qu, C. Tan, Y. Cai, Y. Mogi, D. Jamin Keith and D. L. Boger, *J. Am. Chem. Soc.*, 2020, **142**, 16039–16050.
- 183 I. S. Abd-Elazem, H. S. Chen, R. B. Bates and R. C. C. Huang, *Antiviral Res.*, 2002, **55**, 91–106.
- 184 S. J. O'Malley, K. L. Tan, A. Watzke, R. G. Bergman and J. A. Ellman, *J. Am. Chem. Soc.*, 2005, **127**, 13496–13497.
- 185 D.-H. Wang and J.-Q. Yu, *J. Am. Chem. Soc.*, 2011, **133**, 5767–5769.